



Sn, Ge and Al compounds stabilized by bis-amidine, bis-sulfonimidamide, and Schiff base ligands : synthesis and reactivity

Alejandra Acuna Riveros

► To cite this version:

Alejandra Acuna Riveros. Sn, Ge and Al compounds stabilized by bis-amidine, bis-sulfonimidamide, and Schiff base ligands : synthesis and reactivity. *Catalysis*. Université Paul Sabatier - Toulouse III; Pontificia universidad católica de Chile (Santiago de Chile), 2023. English. NNT : 2023TOU30114 . tel-04266277

HAL Id: tel-04266277

<https://theses.hal.science/tel-04266277>

Submitted on 31 Oct 2023

HAL is a multi-disciplinary open access archive for the deposit and dissemination of scientific research documents, whether they are published or not. The documents may come from teaching and research institutions in France or abroad, or from public or private research centers.

L'archive ouverte pluridisciplinaire **HAL**, est destinée au dépôt et à la diffusion de documents scientifiques de niveau recherche, publiés ou non, émanant des établissements d'enseignement et de recherche français ou étrangers, des laboratoires publics ou privés.



Toulouse Midi-Pyrénées

THÈSE

**En vue de l'obtention du
DOCTORAT DE L'UNIVERSITÉ DE TOULOUSE
Délivrée par l'Université Toulouse 3 - Paul Sabatier**

Cotutelle internationale: Pontificia Universidad Católica de Chile

**Présentée et soutenue par
Alejandra ACUÑA RIVEROS**

Le 5 juillet 2023

Composés Sn, Ge et Al stabilisés par des ligands bis-amidine, bis-sulfonimidamide et base de Schiff : synthèse et réactivité

Ecole doctorale : **SDM - SCIENCES DE LA MATIERE - Toulouse**

Spécialité : **Chimie Moléculaire**

Unité de recherche :

LHFA - Laboratoire Hétérochimie Fondamentale et Appliquée

Thèse dirigée par
David MADEC et René ROJAS

Jury

M. Fernando GODOY, Rapporteur

M. Alan CABRERA, Examinateur

M. Eric BENOIST, Examinateur

M. David MADEC, Directeur de thèse

M. René ROJAS, Co-directeur de thèse

Mme Gina PECCHI, Présidente

ACKNOWLEDGMENTS

“La vida es como una escultura que moldeas mientras cometes errores y aprendes de ellos”.

Kim Namjoon

AGRADECIMIENTOS

Quisiera agradecer a los miembros del jurado y comisión de tesis Profesores Dra. Gina Pecchi, Dr. Fernando Godoy, Dr. Alan Cabrera y Dr. Eric Benoist por aceptar ser parte del jurado, corregir el manuscrito, brindarme comentarios y consejos durante todo el periodo de realización de esta tesis.

Esta tesis se realizó en un programa de doctorado en cotutela entre la Pontificia Universidad Católica de Chile y el laboratorio Hétérochimie Fondamentale et Appliquée (LHFA) en la Universidad Paul Sabatier de Toulouse bajo la dirección de los profesores René Rojas y David Madec. Quiero agradecer al profesor René primero por aceptarme en su grupo de investigación, guiarme en todo este proceso de estudiante de doctorado, dándome consejos y nuevas ideas para esta tesis, y por sobre todo por siempre darme nuevas oportunidades para aprender y crecer académicamente, como también en la confianza que deposita en mí. Quiero agradecer a David por su guía en este trabajo de tesis, por siempre tener disposición y disponibilidad para discutir los RMN y los resultados, por siempre brindarme nuevas ideas, alentarme a seguir nuevas rutas si los resultados no eran los esperados. Gracias David por hacer que mi estadía de casi dos años en LHFA fuera tan agradable, por todo el conocimiento, consejo, y por las oportunidades dadas.

Agradezco a Antoine Baceiredo, Tsuyoshi Kato y Eddy Maerten por todas las discusiones de resultados, por los consejos e ideas que dieron para esta tesis, como también para mis presentaciones. Agradezco las reuniones semanales de discusión de resultados, que me hicieron ser mas meticulosa y critica.

Quiero agradecer a Sonia por todos los análisis de difracción de rayos X que realizo para esta tesis, por siempre tener disponibilidad para medir y responder mis preguntas, como también por hacer milagros cuando le llevaba los cristales pequeños (o no muy bonito) y aun así lograba hacer la medición.

Quiero dar las gracias a los miembros permanentes de LHFA. Gracias Florence y Miguel por toda la ayuda en cuanto a trámites administrativos. Gracias a Olivier Volpato, Olivier Thillaye du Boullay, Julien, Isabelle, Saloua, Romaric, Christian y Mathieu por siempre tener disponibilidad para ayudar y responder preguntas. Quiero agradecer a las personas de MHT, Marc, Pierre, Claude y Caroline que gracias a ellos pude obtener los análisis de RMN.

Quiero agradecer a todos los miembros antiguos y los presentes del laboratorio de Química organometálica y catálisis. Agradezco en particular a Yersica, que cuando llegue al laboratorio me enseñó a trabajar con cloruros de imidoilo, ligandos amidinas y catálisis, que son parte importante de este trabajo, por tener disponibilidad a ayudar, incluso cuando ya no estaba en el lab. Agradezco a Tania y Marjorie por recibirme e incluirme tan bien en el laboratorio, por todos los almuerzos y por todas las salidas fuera del lab, son momentos que recuerdo y extraño con mucho cariño, valoro que hayamos podido formar una amistad. Quiero dar las gracias a Daniela y Fernando que en esta última etapa de mis estudios de doctorado han sido de gran apoyo, en cuanto a química como también emocional, ya que en momentos de estrés y ansiedad cada salida, cada piscola y cada momento de distracción fue de gran ayuda, agradezco poder haber compartido y conocerlos más en el encuentro en Olmué y en la casa de Fernando en Rapel, espero que cumplamos la promesa y nos vemos de nuevo en Colombia!

También quiero agradecer a todos los miembros del equipo ECOIH del laboratorio LHFA, fue un placer compartir y trabajar con ustedes durante mi estadía en Toulouse. Quisiera agradecer primero a Cynthia, quien fue la persona que me recibió, mostro y me enseñó los primeros tres meses en el laboratorio, fue muy agradable trabajar contigo y muchas gracias por todo lo que me enseñaste sobre trabajar con metalilenos, como también por todas las recomendaciones de cosas cotidianas de vivir en Toulouse. Quiero agradecer a Manuel por su ayuda y consejos de cristalización, pero por sobre todo por su simpatía. Agradezco a Shintaro por su disposición a ayudar y responder mis dudas. Agradezco a Aymeric y Ugo con quienes compartí oficina y laboratorio durante toda mi estadía en Toulouse, tal vez no soy la persona más habladora y sociable con la que han compartido, y por lo mismo no les dije cuando estuve allá, pero agradezco profundamente toda la ayuda que me dieron, enseñándome y aconsejándome sobre la manipulación del laboratorio, siempre respondieron mi preguntas y dudas e incluso por enseñarme un poquito de francés (et voilà). Limiao muchas gracias por ser tan amable, fue un agrado compartir oficina contigo. Y agradezco a Nasrina, compartir contigo fue realmente una experiencia genial y enriquecedora, obviamente siempre estuviste dispuesta a dar consejos sobre química, pero lo que más valoro fue poder encontrar una amiga, agradezco el haber pasado un momento que usualmente paso con mi familia como la navidad contigo y con José, hicieron que no fuera un momento triste. También recuerdo con mucho cariño nuestros viajes y aventuras por Suiza y Barcelona, espero que nos volvamos a encontrar y podamos seguir visitando nuevos lugares juntas.

José, mi gran amigo José, hemos trabajado juntos en ambos laboratorios ya por varios años, por lo que es mucho lo que quiero agradecerte. Tal vez eres uno de mis amigos mas distinto a mi en cuanto a pensamiento, ideas y gustos, pero por lo mismo gracias por darme la oportunidad de conocerte y compartir contigo. José realmente fuiste de gran apoyo durante mi estadía en Toulouse, fue una gran alegría cuando llegaste, ya que a veces estaba pasando por momentos tristes por extrañar a mi familia, pero ver una cara amiga después de un tiempo, el poder hablar en chileno, reírnos de estupideces que tal vez otros no entendían, las noches de completos y piscolas hizo que todo fuera más llevadero. Por eso y mucho más, muchas gracias.

El laboratorio LHFA es muy grande por lo que es difícil nombrarlos a todos sin olvidar a nadie, pero agradezco a todos los miembros de los diferentes equipos, SYMAC, SHEN, COP, LPBP y KISS. Agradezco en particular a Alejandro, Rosa, Nereida, Daniel y Avisek por todos los gratos momentos vividos dentro y fuera del laboratorio.

Quiero destacar la ayuda y apoyo de Marco durante todos mis estudios de doctorado, desde que entramos estudiamos e hicimos los trabajos juntos, por lo que de compañeros pasamos a ser amigos. Gracias por recibirme en Regensburg, mostrarme la ciudad y pasar una muy buena semana de vacaciones contigo.

Agradezco profunda e infinitamente a mi familia por su apoyo constante e incondicional, por siempre alentarme a nuevos desafíos, a cumplir mis metas, y por creer en mí, sin ellos no hubiera sido capaz de culminar esta etapa. A mis padres, Carlos y Edith, por el ejemplo de perseverancia y constancia que los caracteriza y que me han otorgado siempre, por el valor mostrado para salir adelante y no rendirse, y por supuesto por su completo amor. A mis hermanas Cindy, Mitzy y Karla por ser mis ejemplos a seguir, por su cariño y porque sé que puedo contar con ellas en todo momento. Gracias porque a pesar de que estuve lejos un tiempo, nunca me sentí sola.

Finalmente, a las entidades que financiaron este proyecto doctoral, a través de becas y proyectos. Estos son: a la Pontificia Universidad Católica de Chile, Dirección de Doctorado de la Vicerrectoría de Investigación (VRI). A ANID a través de la beca de doctorado nacional 2019 N° 21190209. A FONDECYT por medio del proyecto N° 1200748, y al programa de cooperación ECOS sud – CONICYT.

RESUME DE THESES

RESUME DE THESES

Cette thèse porte sur la synthèse et l'étude de nouveaux composés de l'étain, du germanium et de l'aluminium stabilisés avec trois familles différentes de ligands : des bis-amidines, des bis-sulfonimidamides et des bases de Schiff.

Le premier chapitre de cette thèse est principalement consacré à introduire les différents types de ligands étudiés, ainsi que les différents composés de l'étain, du germanium et de l'aluminium (Sn, Ge et Al). Dans ce chapitre sont exposés et rassemblés des principaux éléments bibliographiques sur les voies de synthèse, la réactivité et les propriétés de ces différents systèmes au travers d'exemples représentatifs ou récemment publiés.

D'un côté, nous avons les métallylènes qui sont les analogues lourds des carbènes, où le carbone central est remplacé par un atome de silicium, de germanium, d'étain ou de plomb. Nous nous focalisons plus particulièrement dans cette thèse sur les stannylènes et les germylènes. La valence de l'atome central des métallylènes est de deux, l'état fondamental est singulet, contrairement au cas des carbènes, où l'état fondamental est triplet (Schéma 1). Les métallylènes à l'état fondamental singulet ont donc une orbitale p vacante et une paire d'électrons dans l'orbitale s.

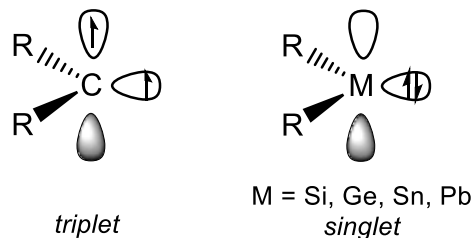


Schéma 1. Différence entre les états fondamentaux des carbènes et des métallylènes.

En raison de leur réactivité importante, il peut être difficile d'isoler les métallylènes en tant que composés stables dans des conditions ambiantes, car ils présentent généralement une réactivité extrêmement élevée au travers d'autres molécules mais aussi sur eux-mêmes, en formant des dimères. Ainsi, afin d'isoler les métallylènes sous leur forme monomérique, la stabilisation de l'orbitale p vacante réactive peut être réalisée de façon thermodynamique et/ou cinétique. Ainsi des ligands bis-amidines et bis-sulfonimidamides ont été choisis au cours de ce travail de thèse pour stabiliser les

germylènes et stannylènes, grâce à la possibilité de délocalisation 4π de ces ligands et de la modification aisée de leurs substituants. Différents types de réactivités possibles de ces nouveaux métallylènes sont ensuite exposés et discutés, tels que la polymérisation d'esters cyclique, des réactions d'oxydation, d'addition oxydative, de transmétallation ainsi que le transfert de ligands.

D'autre part, dans ce chapitre d'introduction, sont abordés les complexes d'aluminium. L'aluminium est le métal le plus abondant de la croûte terrestre et son coût de production est faible. L'aluminium est un métal du groupe 13 du tableau périodique, avec une configuration électronique externe $3s^23p^1$. Les propriétés et caractéristiques liées à la réactivité des réactifs de l'aluminium (III) dérivent généralement de leur forte acidité de Lewis, permettant ainsi leur utilisation comme catalyseurs.

Des complexes d'aluminium (III) sont donc envisagés au cours de ce travail avec des ligands bis-amidines et des bases de Schiff. Ces ligands permettent de stabiliser des complexes d'aluminium qui présentent une bonne activité en tant que catalyseurs pour l'obtention de carbonates cycliques à partir d'époxydes et de CO_2 .

Le deuxième chapitre de cette thèse définit les hypothèses et les objectifs.

Les hypothèses sont les suivantes :

La synthèse de ligands bis-amidines et bis-sulfonimidamides avec un espaceur dans leur structure permettra la stabilisation de germylènes et de stannylènes permettant la polymérisation d'esters cycliques et l'activation de petites molécules.

L'utilisation de ligands bis-amidines avec un espaceur naphthalène rigide permettra d'utiliser des complexes d'aluminium pentacoordonnés comme catalyseurs pour obtenir des carbonates cycliques à partir de CO_2 et d'époxydes. L'incorporation d'iodure dans la sphère de coordination des complexes d'aluminium avec des ligands bis-amidines permettra d'obtenir des systèmes à un composant sans utiliser de cocatalyseur pour activer le CO_2 avec des époxydes.

L'incorporation du fragment ferrocényle dans les ligands des bases de Schiff permettra la génération de complexes bimétalliques dans lesquels la réactivité de l'aluminium peut être

influencée électroniquement et stériquement afin d'obtenir des systèmes catalytiques plus efficaces et plus actifs vis-à-vis de l'activation du CO₂.

Cette thèse a deux objectifs principaux :

1. Synthétiser et caractériser de nouveaux métallylènes stables du germanium et de l'étain avec des ligands bis-amidines et bis-sulfonimidamides et évaluer leur potentiel catalytique dans la polymérisation d'esters cycliques et l'activation et la transformation de petites molécules.
2. Synthétiser et caractériser de nouveaux complexes d'aluminium incorporant des ligands bis-amidines et des bases de Schiff dérivés du ferrocène et évaluer leur potentiel catalytique dans l'activation du CO₂ avec des époxydes.

Le chapitre trois consiste en la partie expérimentale, décrivant la synthèse et la caractérisation des différents ligands, des complexes correspondants et les produits de réactivité.

Le quatrième chapitre présente les résultats obtenus et leur discussion. ce chapitre commence par la synthèse de trois ligands de type bis-amidines, où le 1,8-diaminonaphtalène a été utilisé comme plate-forme planaire conformationnellement rigide entre les deux groupes amidines (Schéma 2). Pour la synthèse de L₁, la procédure est basée sur celle rapportée précédemment pour notre groupe au Chili, par réaction de condensation du 1,8-diaminonaphtalène avec 2 équivalents de chlorure de N-(2,6-diméthylphényl)acétimidoyle. Le composé L₁ a été isolé sous forme de cristaux orange avec un rendement de 74 %. Pour la synthèse de L₂ et L₃, la procédure suivie est celle rapportée par Trifonov *et al.* avec quelques modifications. Le chlorure de N,N'-(naphtalène-1,8-diyl)bis(2,2-diméthylpropanimidoyle) a réagi avec deux équivalents de l'amine correspondante (2,6-diméthylaniline ou *p*-toluidine). L₂ a été obtenu sous forme de cristaux jaune avec 64 % de rendement et L₃ sous forme de cristaux jaune avec un rendement de 63 %. Les ligands ont été caractérisés par spectrométrie de masse (MS), spectroscopie RMN (¹H et ¹³C) et spectroscopie infrarouge (IR).

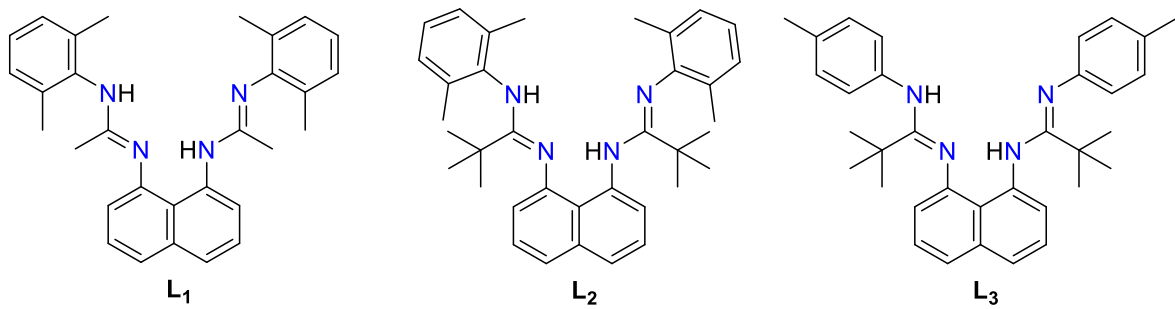


Schéma 2. Ligands bis-amidine synthétisés (**L₁**, **L₂** et **L₃**).

Une fois les ligands bis-amidines synthétisés, la synthèse des stannylènes et des germylènes a été réalisée au moyen d'une réaction de protonolyse. Dans le cas du stannylène, le ligand bis-amidine correspondant a réagi avec un équivalent de Sn(HMDS)₂ dans du THF sec à 60 °C pendant 3 h (Schéma 3). **L₁Sn** a été isolé sous la forme d'un solide brun pâle avec un rendement de 77 %. La formation de **L₁Sn** a été confirmée par RMN ¹H, ¹³C, ¹¹⁹Sn, spectrométrie de masse et par diffraction des rayons X. La structure moléculaire indique un centre étain tétracoordonné avec une géométrie pyramidale à base carrée.

En ce qui concerne la caractérisation du composé **L₂Sn**, aucune donnée spectroscopique RMN en solution n'a pu être obtenue, de part une solubilité négligeable dans les solvants organiques courants une fois cristallisé. Néanmoins, la structure aux rayons X de **L₂Sn** a été obtenue sous la forme d'un composé dimérique. **L₂Sn** a été isolé sous forme de cristaux jaune avec un rendement de 44 %.

L₃Sn a été isolé sous la forme d'un solide jaune avec un rendement de 61 %. La structure de **L₃Sn** a été déterminée par RMN ¹H, ¹³C, ¹¹⁹Sn et spectrométrie de masse.

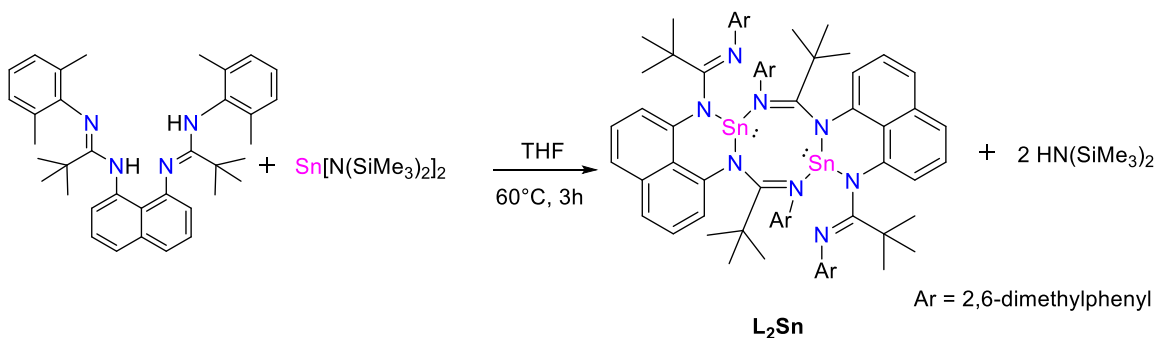
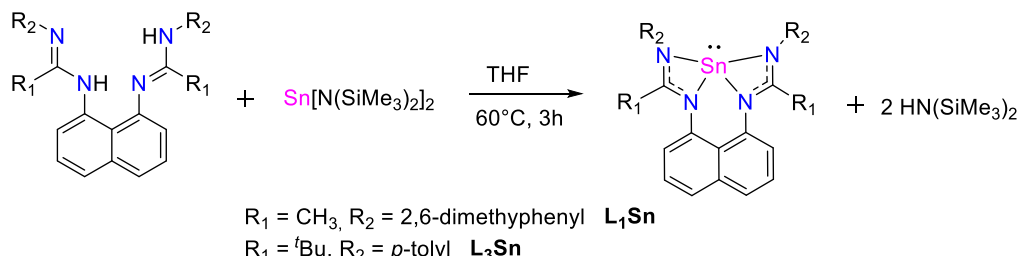


Schéma 3. Synthèse de $\mathbf{L}_{1-3}\mathbf{Sn}$.

Les germylènes ont été synthétisés par réaction de protonolyse avec $\text{Ge}(\text{HMDS})_2$ par analogie avec les résultats obtenus pour les stannylènes (Scheme 4) dans le THF à 60 °C pendant 3 heures de réaction. Cependant, dans ces conditions, seul $\mathbf{L}_1\mathbf{Ge}$ a été obtenu sous forme de dimère. Ce dimère cristallise dans le milieu réactionnel et est obtenu sous forme de cristaux jaune avec un rendement de 42 %. $\mathbf{L}_1\mathbf{Ge}$ présente une solubilité négligeable dans les solvants usuels une fois cristallisés, de sorte que les données spectroscopiques n'ont pas pu être obtenues en solution. La synthèse de $\mathbf{L}_2\mathbf{Ge}$ et $\mathbf{L}_3\mathbf{Ge}$ a été réalisée dans des conditions plus fortes, en utilisant le toluène comme solvant afin de chauffer la réaction à 120 °C pendant 48 h. $\mathbf{L}_2\mathbf{Ge}$ a été isolé sous forme de cristaux jaune avec un rendement de 52 %. Ce composé a été caractérisé par RMN ^1H et ^{13}C et par diffraction des rayons X. En solution, le composé $\mathbf{L}_2\mathbf{Ge}$ montre que le germanium est tétracoordonné mais à l'état solide, la structure cristalline montre que l'atome de germanium est tricoordonné. En ce qui concerne $\mathbf{L}_3\mathbf{Ge}$, il n'a pas été possible malheureusement d'isoler l'espèce en raison de sa trop forte solubilité dans les solvants non polaires et polaires, provoquant un lavage au cours du processus de purification et pas de possibilité de cristallisation.

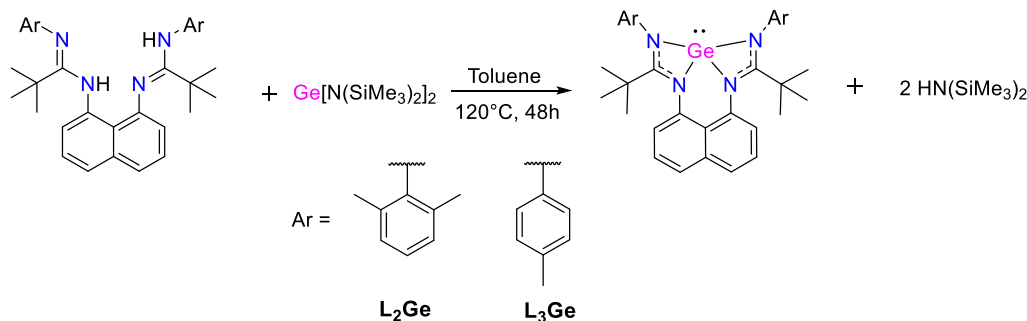
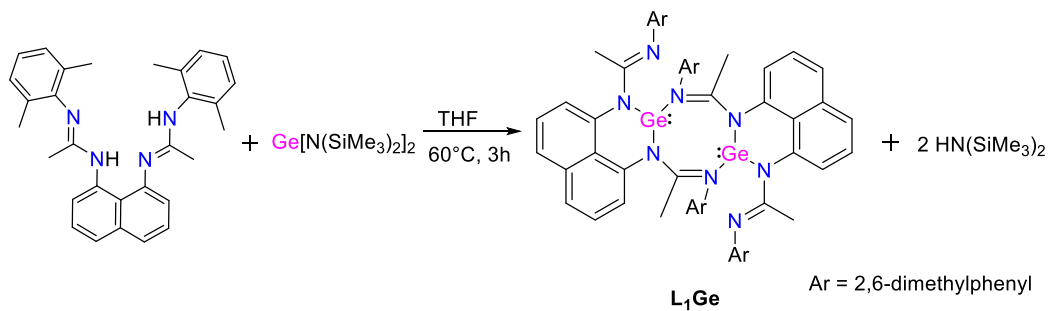


Schéma 4. Synthèse de L_{1-3}Ge .

Le schéma 5 présente un récapitulatif global des stannylènes et germylènes obtenus par rapport à chaque ligand.

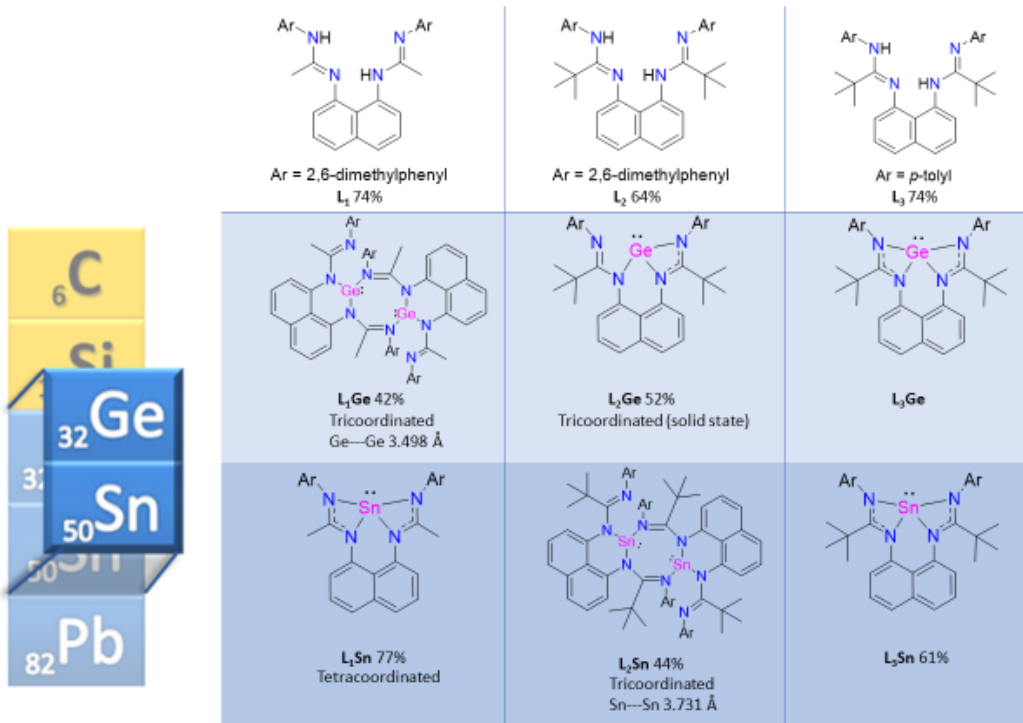


Schéma 5. Récapitulatif des stannylènes et germylènes obtenus.

Parce qu'il existe une grande variété d'études utilisant des stannylènes et des germylènes comme catalyseurs pour la polymérisation d'esters cycliques, **L₁Sn**, qui a été obtenu avec le rendement le plus élevé et qu'il a été entièrement caractérisé, a été testé pour la polymérisation de l'ε-caprolactone (Schème 6).

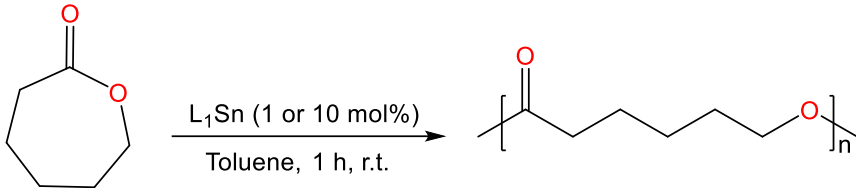


Schéma 6. **L₁Sn** comme catalyseur pour la polymérisation de l'ε-caprolactone.

Les conditions de réaction et les conversions obtenues sont présentées dans le tableau 1. Malgré les conversions élevées, il a été déterminé qu'il n'était pas possible d'obtenir le polymère correspondant, mais simplement des oligomères.

Tableau 1. Condition et activité pour la polymérisation de l'ε-caprolactone.

Entry ^a	Catalyst (mol%)	t (h)	T (°C)	Conversion (%) ^b
1	L ₁ (1.0%)	1	23	0
2	L ₁ Sn (10.0%)	1	25	>99
3	L ₁ Sn (1.0%)	1	27	>99

^a Les réactions ont été réalisées dans du toluène sec et dégazé (2 mL) sous argon en présence d'ε-caprolactone (8,76 mmol).

^b Déterminé par analyse RMN ¹H en comparant l'intégration du signal du polymère avec le monomère.

D'autres tests de réactivité ont été effectués avec le composé **L₁Sn**, d'abord afin d'activer de petites molécules, cependant **L₁Sn** s'est révélé inactif avec l'éthylène, NH₃, CO₂ et H₂, malgré les multiples conditions évaluées, telles que l'augmentation de la température, de la pression ou du temps de réaction. Cependant, lorsqu'il est exposé à N₂O, qui réagit comme un agent oxydant, **L₁Sn** présente une activité, et un amidinate-stannoxyane dimérique **1a** (Schema 7) a été obtenu sous forme de cristaux incolores avec un rendement de 46 %. Ce composé a été caractérisé par RMN ¹H, ¹³C et ¹¹⁹Sn, spectrométrie de masse et par diffraction des rayons X.

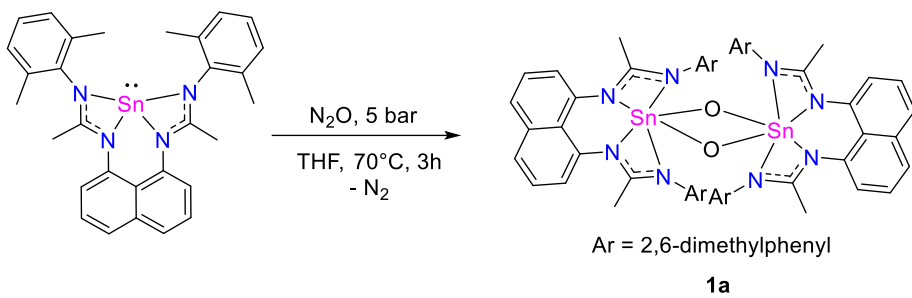


Schéma 7. Synthèse de **1a**.

A partir de ce résultat, nous avons essayé une autre réaction d'oxydation avec du soufre élémentaire (Schéma 8), permettant d'isoler un analogue soufré du produit obtenu précédemment. **1b** a été caractérisé par RMN ^1H , ^{13}C et ^{119}Sn , spectrométrie de masse et par diffraction des rayons X.

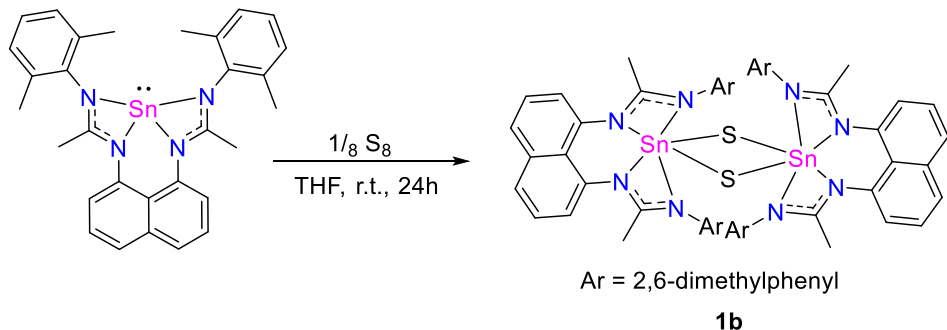


Schéma 8. Synthèse de **1b**.

En complément des réactions d'oxydation, nous avons étudié les réactions d'addition oxydative. **1a** réagit avec le disulfure de p-tolyle et la 3,5-di-tert-butyl-ortho-quinone (Schéma 9). Les produits correspondants ont été caractérisés par RMN ^1H , ^{13}C et ^{119}Sn et spectrométrie de masse. Dans le cas de **2a**, il a également été possible d'obtenir la structure cristalline.

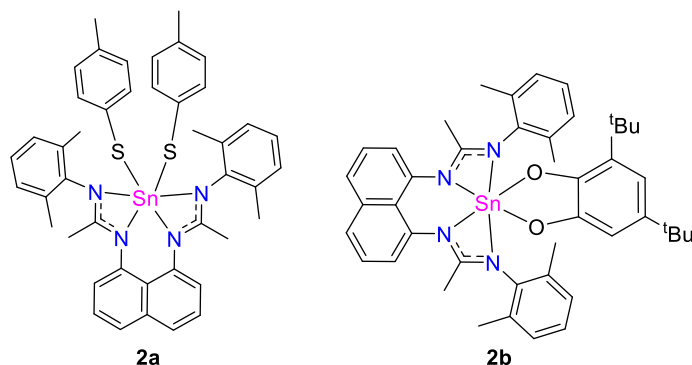


Schéma 9. Composés **2a** et **2b** synthétisés.

Les métallylènes sont décrits comme de puissants ligands donneurs d'électrons, principalement si des groupes donneurs les stabilisent. Par conséquent, les métallylènes peuvent potentiellement être utilisés comme ligands pour coordonner les métaux de transition. Les ligands stannylènes peuvent généralement fonctionner comme donneurs ou accepteurs de paires d'électrons (types Z) dans les complexes de métaux de transition. Stimulés par ces propriétés, une tentative a été faite pour utiliser le stannylène **L₁Sn** comme ligand pour coordonner les métaux de transition. Cependant malgré l'utilisation de différents substrats avec différents métaux tels que Pd, Pt, Ni, Rh, Co, Cu et Au, il a été impossible d'obtenir une coordination chimique, malgré l'évolution des conditions de synthèse telles que la nature du solvant, le temps de réaction et le chauffage du mélange réactionnel.

En continuant avec les propriétés de coordination chimique, les silylènes et les germylènes peuvent coordonner les éléments du groupe 14 à l'état d'oxydation II en raison de la capacité de don d'électrons de la paire libre de ces derniers dans les orbitales p vacantes des métallylènes. En conséquence, **L₁Sn** a été placé en réaction avec un équivalent de GeCl₂·dioxane dans du THF à température ambiante. Après 15 minutes, un solide cristallin jaune s'est formé (Schéma 10). La RMN ¹¹⁹Sn a montré une résonance à -214,0 ppm, en accord avec la formation de SnCl₂. Le solide cristallin obtenu a été analysé par RMN et a été caractérisé comme le composé dimérique **L₁Ge**, indiquant ainsi une réaction de transmétallation.

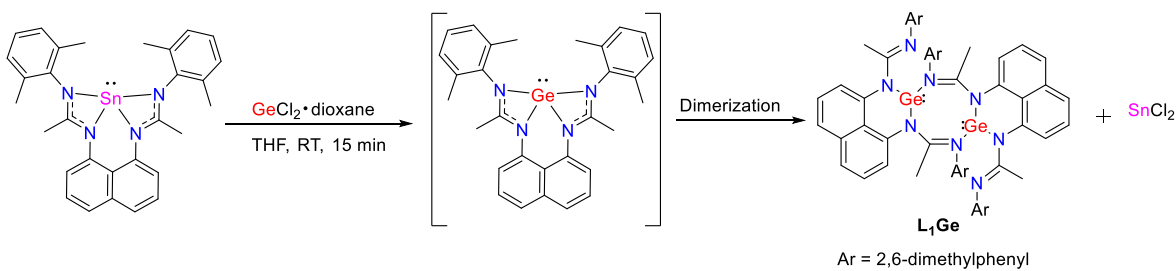


Schéma 10. Synthèse de **L₁Ge** par réaction de transmétallation.

À la recherche d'un éventail plus large de réactions de transmétallation, des substrats halogénés du groupe 13, tels que AlCl₃ et GaCl₃ (schéma 11), ont été étudiés avec **L₁Sn**. Dans les deux cas, des réactions de transmétallation ont bien été observées, libérant du SnCl₂ comme sous-produit, comme le montre la RMN ¹¹⁹Sn. Dans les deux cas, la formation d'un composé pentacoordonné est observée. Les composés **3a** et **3b** ont été caractérisés par RMN ¹H et ¹³C. Dans le cas de **3b**, la structure cristalline a également été obtenue.

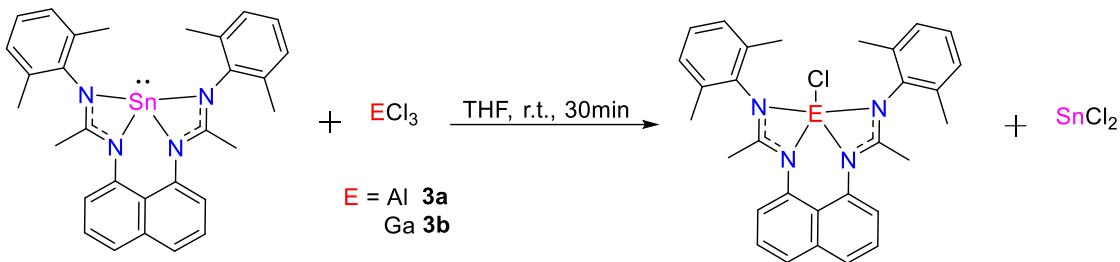


Schéma 11. Synthèse de **3a** et **3b**.

Pour finaliser les tests de réactivité du composé **L₁Sn**, des réactions de transfert ou d'échange de ligands ont été réalisées avec PCl_3 et PhPCl_2 (Schème 12), les deux produits ont été caractérisés par RMN ^1H , ^{13}C et ^{31}P , spectrométrie de masse et par diffraction des rayons X.

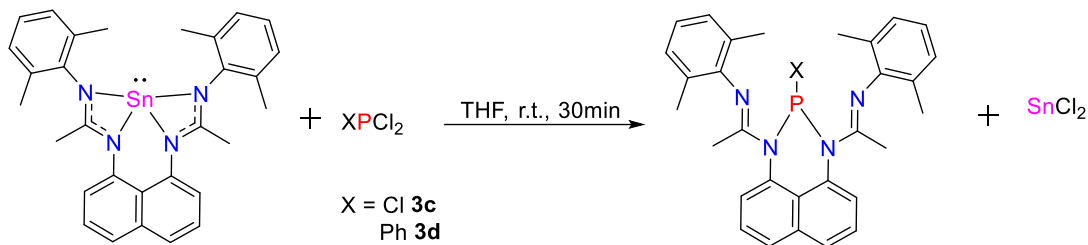


Schéma 12. Synthèse de **3c** et **3d**.

En conclusion de ces résultats, le stannylène **L₁Sn** présente une réactivité en oxydation, en addition oxydative, en transmétallation et en transfert de ligand. Le schéma 13 résume les composés obtenus à partir de **L₁Sn**.

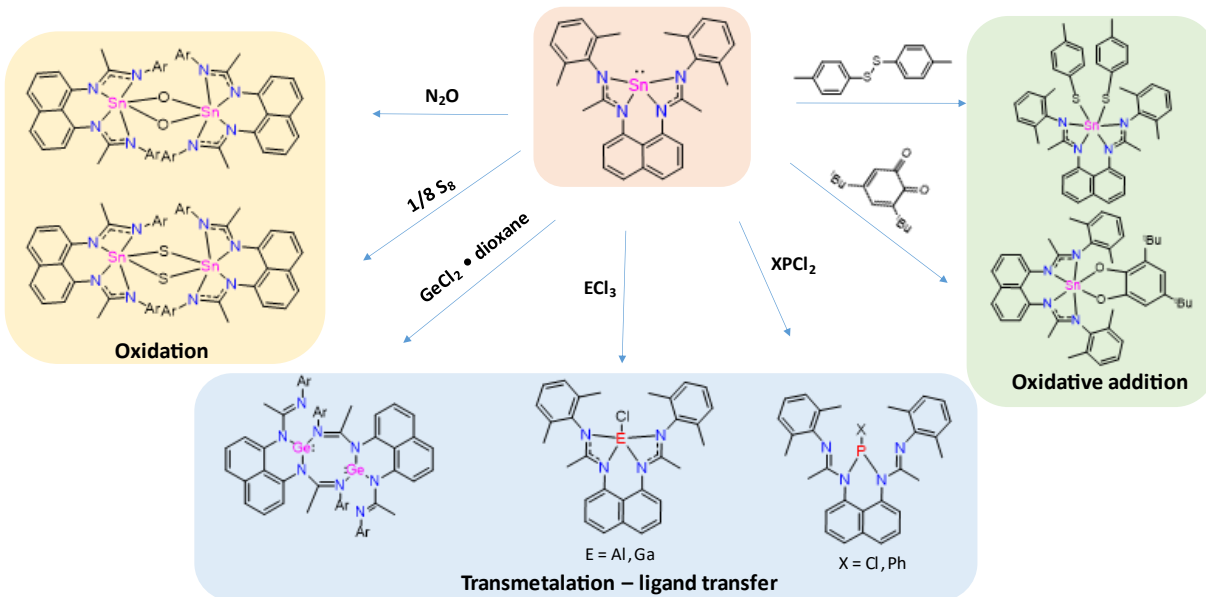


Schéma 13. Composés obtenus à partir de $\mathbf{L}_1\mathbf{Sn}$ et type de réactivité.

D'autre part, il a été proposé dans cette thèse de synthétiser des complexes d'aluminium (III) avec des ligands bis-amidines. Dans un premier temps il s'agissait d'obtenir des complexes pentacoordinés avec les ligands \mathbf{L}_2 et \mathbf{L}_3 , analogues au composé précédemment rapporté par notre groupe avec le ligand \mathbf{L}_1 , mais il n'a pas été possible de les obtenir, en raison de l'effet stérique que possèdent les groupements tert-butyles. Au lieu de cela, des complexes bimétalliques ont été obtenus lorsque le ligand correspondant est mis à réagir avec deux équivalents de triméthylaluminium (Scheme 14). Dans les deux cas, les produits ont été caractérisés par RMN ^1H et ^{13}C , et dans le cas de $\mathbf{L}_2\mathbf{Al}_2$ par diffraction des rayons X.

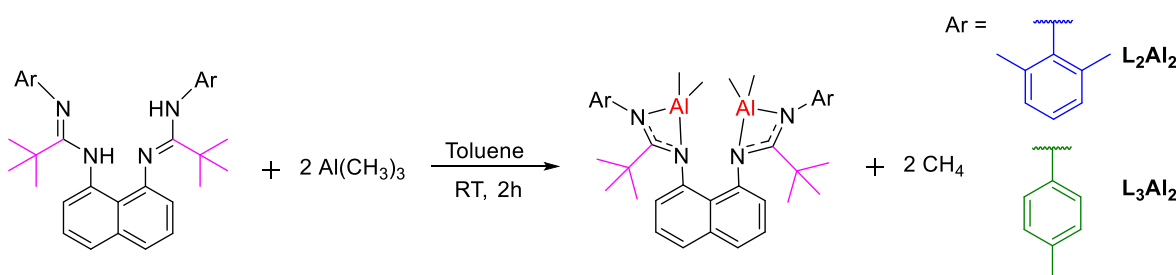


Schéma 14. Synthèse de $\mathbf{L}_2\mathbf{Al}_2$ et $\mathbf{L}_3\mathbf{Al}_2$.

Pour synthétiser des systèmes mono-composants actifs pour former des carbonates cycliques à partir de CO_2 et d'époxydes, et sans avoir besoin d'utiliser un cocatalyseur, il est proposé dans ce travail de remplacer les groupements méthyle liés à l'aluminium par des iodures pour avoir le nucléophile nécessaire dans le cycle catalytique dans le même système. Par conséquent, la réaction entre L_2Al_2 et Bi_3 est effectuée dans le benzène à température ambiante pendant 1 h (Schema 15). Des cristaux jaune ont été obtenus avec un rendement de 91 % (composé $\text{L}_2\text{Al}_2\text{I}_4$). La réaction attendue consiste à dissocier le radical méthyle de l'atome d'aluminium, à former une nouvelle liaison Al-I, et à générer $\text{B}(\text{CH}_3)_2\text{I}$ comme sous-produit. Cette même réaction a été testée à partir du composé L_3Al_2 , sans résultat.

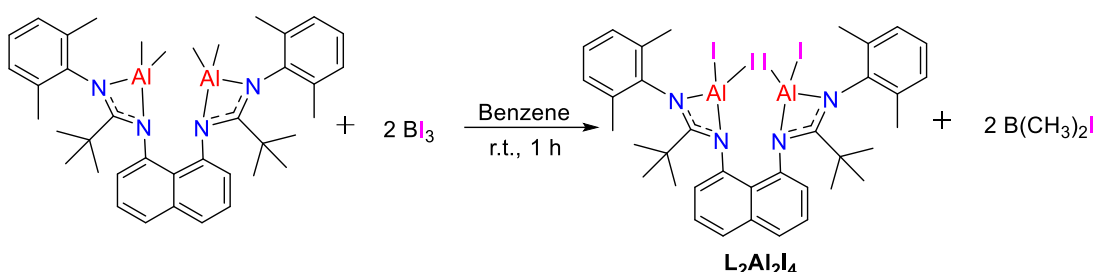
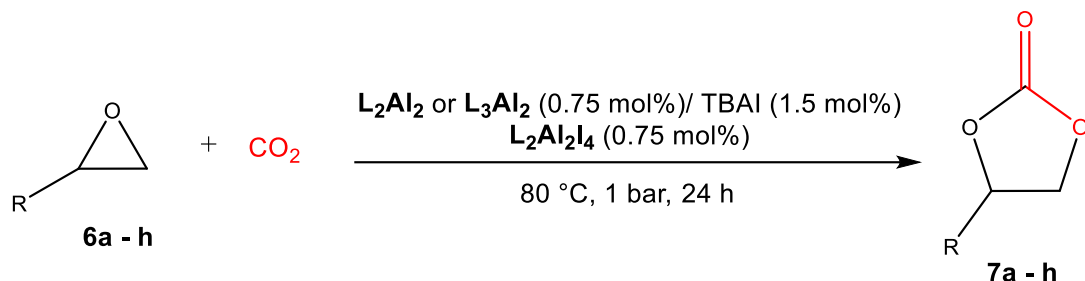


Schéma 15. Synthèse de $\text{L}_2\text{Al}_2\text{I}_4$.

Après avoir préparé et caractérisé les complexes L_2Al_2 , L_3Al_2 et $\text{L}_2\text{Al}_2\text{I}_4$, nous avons exploré leur utilisation potentielle comme catalyseurs pour la préparation d'une gamme de carbonates cycliques (**7a - h**) à partir de leurs époxydes correspondants (**6a - h**) et de CO_2 . Les conversions des essais catalytiques sont présentées dans le tableau 2.

Tableau 2. Conversions des carbonates cycliques 7a-h utilisant les catalyseurs L_2Al_2 , L_3Al_2 et $\text{L}_2\text{Al}_2\text{I}_4$.



Entry	Epoxides	L_2Al_2 conv (%) ^a	L_3Al_2 conv (%) ^a	$\text{L}_2\text{Al}_2\text{I}_4$ conv (%) ^a
1	6a (R = Ph)	90	91	0
2	6b (R = n-Bu)	94	95	0
3	6c (R = CH ₂ Cl)	97	93	0
4	6d (R = CH ₂ OPh)	79	90	0
5	6e (R = 4-ClC ₆ H ₄)	90	62	0
6	6f (R = 4-BrC ₆ H ₄)	74	71	0
7	6g (R = 4-FC ₆ H ₄)	92	92	0
8	6h (R = CH ₂ OCH ₂ (CF ₂) ₃ CHF ₂)	84	56	0

^a Déterminé par spectroscopie RMN ¹H du mélange réactionnel brut.

Les réactions ont été réalisées à 80 °C et 1 bar de pression de CO₂ pendant 24 h en utilisant une combinaison de 0,75 % molaire de complexes L_2Al_2 ou L_3Al_2 et 1,5 % molaire de TBAI comme cocatalyseur, tandis que seulement 0,75 % molaire du mono-composant comme catalyseur $\text{L}_2\text{Al}_2\text{I}_4$ a été utilisés dans des conditions sans solvant. Fait intéressant, aucun polycarbonate linéaire n'a été obtenu dans ces conditions de réaction, et les substrats époxydes ont généralement montré une sélectivité envers la formation de carbonates cycliques. En général, les catalyseurs L_2Al_2 et L_3Al_2 ont permis obtention de rendements modérés à excellents pour la préparation de carbonates cycliques. Le système catalytique mixte (catalyseur/TBAI) est réactif vis-à-vis de la formation d'une grande variété de carbonates cycliques fonctionnalisés avec des groupes alkyles, aryle, halogénure et éther, ce qui démontre que les composés L_2Al_2 et L_3Al_2 ont une large portée et sont sélectifs pour les formations de carbonate cyclique.

Malheureusement, le complexe $\mathbf{L}_2\mathbf{Al}_2\mathbf{I}_4$ n'a pas montré d'activité catalytique en tant que système à un composant pour tous les époxydes testés. Le manque d'activité catalytique peut s'expliquer par le fait qu'il présente une distance de liaison Al-I plus courte (2,485 Å) que les autres systèmes à un composant rapportés pour notre groupe (2,553 Å) avec \mathbf{L}_1 comme ligand et l'aluminium pentacoordonné, ce qui rend difficile la libération d'iodure pour agir comme un nucléophile dans le mécanisme de réaction pour ouvrir le cycle époxyde.

L'un des objectifs de ce projet a aussi été de synthétiser des ligands bis-sulfonimidamides avec un espaceur dans leur structure et d'utiliser ces ligands pour stabiliser les métallylènes (Schéma 16). Mais il n'a pas été possible d'obtenir ces ligands et de mener à bien cette partie du projet.

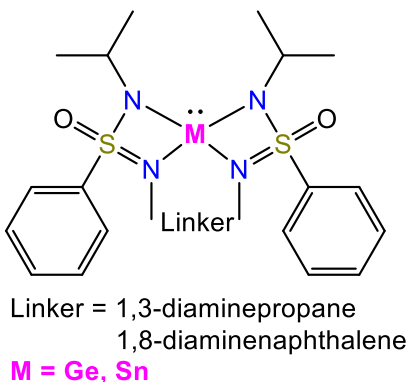


Schéma 16. Métallylènes proposés avec des ligands bis-sulfonimidamide.

Enfin, les ligands de base de Schiff sont faciles à synthétiser et, comme indiqué dans l'introduction, ces systèmes, lorsqu'ils sont coordonnés avec des métaux de transition ou du groupe 13 présentent de bons résultats en catalyse. D'autre part, le ferrocène est un squelette intéressant et utile et a été utilisé dans la conception d'une grande variété de ligands, en raison de ses propriétés électroniques et stériques.

Les composés **4a** et **4b** ont été obtenus par réaction de 1,1'-(4,6-dihydroxy-1,3-phénylène)biséthanone et de deux équivalents de ferrocénylamine dans du toluène sec au reflux pendant 24h (Schéma 17). Les deux composés sont obtenus à partir du même mélange, puis séparés par extraction de **4a** dans CH_2Cl_2 . **4a** est un composé bis-azométhine symétrique obtenu sous forme de cristaux violet avec un rendement de 70 %, et **4b** est une azométhine unique asymétrique obtenue sous forme de cristaux rouge avec un rendement de 26 %. Ces composés ont été entièrement caractérisés par RMN, spectrométrie de masse et diffraction des rayons X.

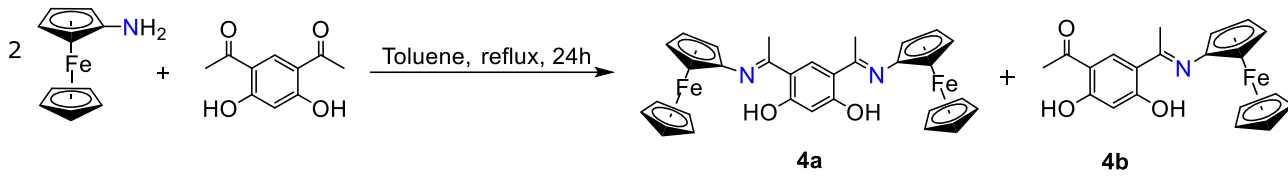


Schéma 17. Synthèse de **4a** et **4b**.

Le complexe d'aluminium **5a** a été synthétisé par une réaction de protonolyse entre le ligand **4a** et deux équivalents de Al(CH₃)₃ (Schéma 18). Le complexe **5a** a été obtenu sous la forme d'un solide rouge avec un rendement de 95 %. La formation du complexe bis-aluminium correspondant est mise en évidence par RMN ¹H et ¹³C.

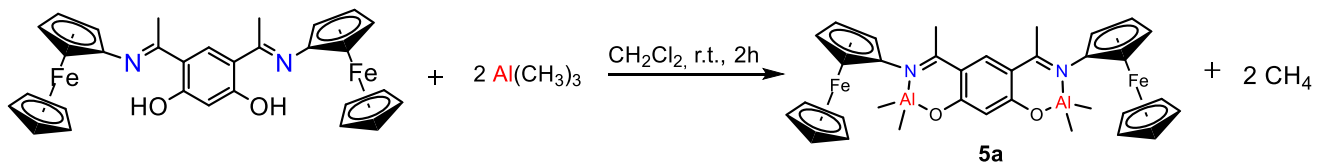


Schéma 18. Synthèse de **5a**.

Après avoir préparé le complexe bis-aluminium **5a**, nous avons décidé de nous concentrer sur l'exploration de son utilisation comme catalyseur pour la formation de carbonates cycliques. Dans un premier temps, l'oxyde de styrène a été sélectionné comme substrat modèle pour étudier l'activité catalytique du complexe **5a**. Les réactions ont été réalisées à 80 °C et 1 bar de pression de CO₂ pendant 24 h dans des conditions sans solvant en utilisant 0,5 à 1,5 % molaire de catalyseur **5a** et 1,0 à 3,0 % molaire d'iodure de tétrabutylammonium (Bu₄NI). Le résultat catalytique est présenté dans le tableau 3. Malheureusement, le complexe présente une faible activité catalytique par rapport aux autres complexes d'aluminium.

Tableau 3. Tests préliminaires de réactivité du complexe d'aluminium **5a** pour la synthèse de styrène carbonate^a.

Ent.	Cat.	Cocat. (mol%)	amt of cat. (mol%) ^b	T (°C)	t (h)	Conversion (%)
1	5a	TBAI 1.0	0.5	80	24	18
2	5a	TBAI 2.0	1.0	80	24	39
3	5a	TBAI 3.0	1.5	80	24	48

^aL'oxyde de styrène est utilisé pour toutes les entrées.

^bLe pourcentage est calculé en fonction de la quantité d'époxyde ajoutée (1,7 mmol).

En conclusion, différents stannylènes et germylènes ont été synthétisés avec des ligands bis-amidines à squelette naphtalène rigide par une réaction de protonolyse entre le ligand et Sn(HMDS)₂ ou Ge(HMDS)₂. **L₁Sn** et **L₃Sn** sont obtenus en tant qu'espèces monomériques, et la structure aux rayons X de **L₁Sn** a montré que l'atome d'étain est tétracoordonné et présente une géométrie pyramidale à base carrée. **L₂Sn** est obtenu sous forme d'espèce dimérique. D'autre part, le germylène **L₁Ge** a été obtenu sous la forme d'une espèce dimérique qui présente l'atome de germanium avec une géométrie pyramidale trigonale. **L₂Ge** et **L₃Ge** sont des espèces monomériques et la structure aux rayons X de **L₂Ge** a montré que l'atome de germanium est tricoordonné avec une géométrie pyramidale trigonale.

Les métallylènes ont été utilisés comme catalyseurs dans les réactions de polymérisation d'esters cycliques mais n'ont pas montré la réactivité souhaitée. Cependant, le stannylène **L₁Sn** a présenté une réactivité vis-à-vis de réactions d'oxydation, d'addition oxydante, et de transmétallation ou de transfert de ligands.

D'autre part, il a été possible de synthétiser de nouveaux complexes bis-aluminium avec un ligand bis-amidine à pont naphtalène rigide. Ces complexes bis-aluminium ont été testés comme catalyseurs pour l'obtention de carbonates cycliques à partir d'époxydes et de CO₂, avec une conversion de modérée à excellente. De même, il a été possible d'obtenir un nouveau complexe d'aluminium en utilisant le même ligand bis-amidine mais en incorporant des iodures dans sa structure afin de l'utiliser comme catalyseur mono-composant. Néanmoins cette nouvelle génération de complexes n'a pas présenté d'activité catalytique.

Un ligand de base de Schiff dérivé du ferrocène a aussi été synthétisé, ainsi que le complexe d'aluminium correspondant. Ce complexe présente une faible activité catalytique pour la formation de carbonates cycliques à partir d'époxydes et de CO₂.

INDEX

INDEX

RESUME DE THESES.....	8
INDEX	25
INDEX OF TABLES.....	29
INDEX OF FIGURES.....	30
INDEX OF SCHEMES.....	32
ABBREVIATIONS	34
ABSTRACT.....	35
RESUMEN.....	36
CHAPTER I: INTRODUCTION	37
1. General Introduction	38
1.1 Amidine ligands.....	39
1.2 Sulfonimidamide ligands	43
1.3 Schiff base ligands	45
2. Metallylenes.....	46
2.1 General aspects of Metallylenes	46
2.2 Amidine ligands stabilized metallylenes	49
2.3. Sulfonimidamide ligands stabilized metallylenes	53
2.4. Metallylenes reactivity	54
2.4.1. General aspects of the metallylenes reactivity	54
2.4.2. Metallylenes reactivity: polymerization of cyclic esters.....	55
2.4.3. Metallylenes reactivity: oxidation	55
2.4.4. Metallylenes reactivity: oxidative addition.....	57
2.4.5. Metallylenes reactivity: transmetalation – ligand transfer reactions	57
3. Aluminum complexes	59
3.1 General aspects of aluminum complexes	59
2.3 Aluminum complexes with amidine ligands	60
2.4 Aluminum complexes with Schiff base ligands	61
2.5 Aluminum complexes reactivity.....	61
2.5.1 Aluminum complexes reactivity: catalysis to obtaining cyclic carbonates from CO ₂ and epoxides	61
3. Project proposal	66
CHAPTER II: HYPOTHESIS AND GOALS.....	68

HYPOTHESIS.....	69
GOALS	70
1. Main goals.....	70
2. Specific goals.....	70
CHAPTER III: EXPERIMENTAL PART	71
General procedures.....	72
Characterization	72
1. Preparation of the precursors required for the synthesis of bis-amidine ligands	72
1.1. Synthesis of the precursor <i>N</i> -(2,6-dimethylphenyl)acetimidoyl chloride	72
1.2. Synthesis of the precursor <i>N,N</i> -(naphthalene-1,8-diyl)bis(2,2-dimethylpropanimidoyl chloride).....	73
2. Synthesis and characterization of bis-amidine ligands.....	74
2.1. Synthesis of L ₁	74
2.2. Synthesis of L ₂ and L ₃	75
3. Synthesis and characterization of stannylenes stabilized by bis-amidine ligands	76
3.1. Synthesis of L ₁ Sn	76
3.2. Synthesis of L ₂ Sn	77
3.3. Synthesis of L ₃ Sn	77
4. Synthesis and characterization of germylenes stabilized by bis-amidine ligands	78
4.1. Synthesis of L ₁ Ge.....	78
4.2. Synthesis general of L ₂ Ge and L ₃ Ge	79
5. Metallylenes reactivity	80
5.1. Metallylenes reactivity: polymerization of ε-caprolactone.....	80
5.1.1. General procedure for ε-caprolactone polymerization tests.....	80
5.2. Metallylenes reactivity: oxidation	80
5.2.1. Synthesis of 1a - Reaction of L ₁ Sn with N ₂ O	80
5.2.2. Synthesis of 1b - Reaction of L ₁ Sn with S ₈	81
5.3. Metallylenes reactivity: oxidative addition	82
5.3.1. Synthesis of 2a - Reaction of L ₁ Sn with disulfide	82
5.3.2. Synthesis of 2b - Reaction of L ₁ Sn with ortho-quinone	83
5.4. Metallylenes reactivity: transmetalation	84
5.4.1. Synthesis of L ₁ Ge - Reaction of L ₁ Sn with GeCl ₂ •(dioxane)	84
5.4.2. Synthesis of 3a and 3b - Reaction of L ₁ Sn with AlCl ₃ and GaCl ₃	84
5.4.3. Synthesis of 3c and 3d - Reaction of L ₁ Sn with PCl ₃ and PhPCl ₂	85

6. Synthesis and characterization of aluminum complexes stabilized by bis-amidine ligands (L₁)	86
6.1. Synthesis of L₂Al₂.....	86
6.2. Synthesis of L₂Al₂I₄.....	87
6.3. Synthesis of L₃Al₂.....	88
7. Synthesis of Schiff base ligand derived from ferrocene.....	88
7.1 Synthesis of ligands symmetrical bis-azomethine 4a and unsymmetrical single azomethine 4b.....	88
8. Synthesis and characterization of bis-aluminum complex stabilized by Schiff ligand derived from ferrocene (5a).....	89
9. Aluminum complexes reactivity: catalysis to obtaining cyclic carbonates.....	90
9.1. General procedure for the synthesis of Cyclic Carbonates at 1 bar Pressure.....	90
CHAPTER IV: RESULTS AND DISCUSSIONS	91
1. Synthesis of the bis-amidine ligands.	92
2. Synthesis of stannylenes stabilized by bis-amidine ligands.	95
3. Synthesis of germylenes stabilized by bis-amidine ligands.	101
4. Metallylenes reactivity	106
5. Synthesis of aluminum complexes stabilized by bis-amidine ligands.....	118
6. Aluminum complexes stabilized by bis-amidine reactivity: catalysis to obtaining cyclic carbonates.....	121
7. Synthetic routes tested to obtain bis-sulfonimidamide ligands.	125
8. Synthesis of Schiff base ligand derived from ferrocene.....	127
9. Synthesis of bis-aluminum complex stabilized by Schiff ligand derived from ferrocene (5a).	129
10. Aluminum complex 5a reactivity: catalysis to obtaining cyclic carbonates.....	130
CHAPTER V: CONCLUSION	131
REFERENCES	133
ANNEXES	141

INDEX OF TABLES

Table 1. Main resonances in ^1H and ^{13}C NMR of the ligands obtained (L_1 , L_2 and L_3) and yields	94
Table 2. Main resonances in ^1H , ^{13}C and ^{119}Sn NMR of the stannylenes obtained (L_1Sn , L_2Sn and L_3Sn) and yields	99
Table 3. Main resonances in ^1H and ^{13}C NMR of the germylenes obtained (L_1Ge , L_2Ge and L_3Ge) and yields	104
Table 4. Condition and activity for polymerization of ϵ -caprolactone	107
Table 5. TOF of 7a-h cyclic carbonates using the catalysts L_2Al_2 , L_3Al_2 and $\text{L}_2\text{Al}_2\text{I}_4$	122
Table 6. Preliminary tests reactivity of the aluminum complex 5a for the synthesis of styrene carbonate ^a	130

INDEX OF FIGURES

Figure 1. General structure of amidine (1), amidinate (2) and amidinium (3).....	40
Figure 2. Examples of bis-amidines 4 and 5	42
Figure 3. Examples of sulfonimidamides 12 and 13	44
Figure 4. Difference between the ground states of carbenes and metallylenes.....	46
Figure 5. Thermodynamic stabilization of metallylenes.....	48
Figure 6. Kinetic stabilization of metallylenes.....	48
Figure 7. Coordination modes of substituents with heteroatoms in the side chains.....	49
Figure 8. Examples of bis-germylenes and bis-stannylenes with bis-amidine ligands with a bridge.....	52
Figure 9. Stannylenes applied in polymerization (ϵ -caprolactone and lactide).....	55
Figure 10. Oxidation products of metallylenes with chalcogens.....	56
Figure 11. Oxidative addition products of metallylenes.....	57
Figure 12. Structure of organic carbonates: cyclic a , linear b , and polycarbonates c	62
Figure 13. Active aluminum catalysts in the synthesis of cyclic carbonates.....	64
Figure 14. Singlet-component aluminum catalyst for the synthesis of cyclic carbonates.....	65
Figure 15. Aluminum amidinate complexes.....	66
Figure 16. ^1H NMR of L ₁	93
Figure 17. ^1H NMR of L ₁ Sn before purification.....	96
Figure 18. Molecular structure of L ₁ Sn (hydrogens are omitted for clarity).....	97
Figure 19. Molecular structure of L ₂ Sn (hydrogens are omitted for clarity).....	98
Figure 20. Molecular structure of L ₁ Ge (hydrogens are omitted for clarity).....	102
Figure 21. Molecular structure of L ₂ Ge (hydrogens are omitted for clarity).....	103
Figure 22. Molecular structure of 1a (hydrogens are omitted for clarity).....	108
Figure 23. Molecular structure of 1b (hydrogens are omitted for clarity).....	109
Figure 24. ^1H NMR of 2a	111
Figure 25. Molecular structure of 2a (hydrogens are omitted for clarity).....	111
Figure 26. ^1H NMR of 2b	112
Figure 27. ^1H NMR of 3a	115
Figure 28. Molecular structure of 3b (hydrogens are omitted for clarity).....	115
Figure 29. Molecular structures of 3c and 3d (hydrogens are omitted for clarity).....	117
Figure 30. Molecular structures of L ₂ Al ₂ (hydrogens are omitted for clarity).....	119
Figure 31. Molecular structures of L ₂ Al ₂ I ₄ (hydrogens are omitted for clarity).....	120
Figure 32. ^1H NMR of 4a and 4b	128

Figure 33. Molecular structures of **4a** and **4b**.....129

INDEX OF SCHEMES

Scheme 1. Isomeric and tautomeric forms for tri-substituted amidines	41
Scheme 2. Synthesis of amidines	41
Scheme 3. Synthesis of bis-amidines	42
Scheme 4. Structure of sulfonimidamides	43
Scheme 5. Synthesis of sulfonimidamides	44
Scheme 6. Synthesis general of Schiff base ligands	45
Scheme 7. General pathways for the synthesis of metallylenes	47
Scheme 8. First amidinatogermylenes	50
Scheme 9. Example of bis-amidinatogermylene	50
Scheme 10. First amidinatostannylenes	51
Scheme 11. Triimido sulfur phosphanyl metallylenes	53
Scheme 12. Diimidatosulfinate metallylenes	53
Scheme 13. Metallylenes stabilized by sulfonimidamides ligands	54
Scheme 14. Examples of transmetalation – ligand transfer reactions with metallylenes	58
Scheme 15. Examples of mono-amidinato and bis-amidinato aluminum complexes.....	60
Scheme 16. Synthesis of cyclic carbonates.....	62
Scheme 17. General proposal.....	67
Scheme 18. Synthesis of <i>N</i> -(2,6-dimethylphenyl)acetimidoyl chloride.....	72
Scheme 19. Synthesis of <i>N,N</i> -(naphthalene-1,8-diyl)bis(2,2-dimethylpropanimidoyl chloride).73	73
Scheme 20. Synthesis of L₁	74
Scheme 21. Synthesis of L₂ and L₃	75
Scheme 22. Synthesis of L₁Sn	76
Scheme 23. Synthesis of L₂Sn	77
Scheme 24. Synthesis of L₃Sn	77
Scheme 25. Synthesis of L₁Ge	78
Scheme 26. Synthesis of L₂Ge and L₃Ge	79
Scheme 27. Synthesis of 1a	80
Scheme 28. Synthesis of 1b	81
Scheme 29. Synthesis of 2a	82
Scheme 30. Synthesis of 2b	83
Scheme 31. Synthesis of L₁Ge via transmetalation.....	84
Scheme 32. Synthesis of 3a and 3b	84
Scheme 33. Synthesis of 3c and 3d	85

Scheme 34. Synthesis of L_2Al_2	86
Scheme 35. Synthesis of $\text{L}_2\text{Al}_2\text{I}_4$	87
Scheme 36. Synthesis of L_3Al_2	88
Scheme 37. Synthesis of 4a and 4b	88
Scheme 38. Synthesis of 5a	89
Scheme 39. Synthesis of L_1	93
Scheme 40. Synthesis of L_2 and L_3	94
Scheme 41. Synthesis of L_{1-3}Sn	96
Scheme 42. Synthesis of L_1Sn by deprotonation of the ligand.....	98
Scheme 43. Synthetic routes to obtain L_2Sn	100
Scheme 44. Synthetic routes to obtain L_3Sn	101
Scheme 45. Synthesis of L_{1-3}Ge	102
Scheme 46. Summary of the stannylenes and germynes obtained.....	105
Scheme 47. L_1Sn as catalyst for the polymerization of ϵ -caprolactone.....	106
Scheme 48. Synthesis of 1a	108
Scheme 49. Synthetic route to obtain 1b	109
Scheme 50. Synthesis of 2a	110
Scheme 51. Synthesis of 2b	112
Scheme 52. Example of coordination chemistry of an amidinatogermylene with group 14 elements.....	113
Scheme 53. Synthesis of L_1Ge by transmetalation reaction.....	113
Scheme 54. Synthesis of 3a and 3b	114
Scheme 55. Synthesis of 3c and 3d	116
Scheme 56. Compounds obtained from L_1Sn and the type of reactivity.....	117
Scheme 57. Synthesis of L_2Al_2	118
Scheme 58. Synthesis of $\text{L}_2\text{Al}_2\text{I}_4$	120
Scheme 59. Synthesis of cyclic carbonates.....	121
Scheme 60. General mechanism proposed for the synthesis of cyclic carbonates catalyzed by binary systems.....	124
Scheme 61. Route 1 tested for the synthesis of bis-sulfonimidamides using <i>N,N</i> -(propane-1,3-diy) dibenzenesulfonamide as a precursor.....	126
Scheme 62. Route 2 tested for the synthesis of bis-sulfonimidamides using <i>N</i> -isopropylbenzenesulfonamide as a precursor.....	127
Scheme 63. Synthesis of 3a and 3b	128
Scheme 64. Synthesis of 5a	129

ABBREVIATIONS

PE = polyethylene

PET = polyethylene terephthalate

ROP = ring-opening polymerization

Cp* = cyclopentadienyl

Cy = cyclohexyl

ⁱPr = isopropyl

^tBu = tert-butyl

HMDS = Bis(trimethylsilyl)amine

Dip = 2,6-diisopropylphenyl

TBAI = tetrabutylammonium iodide

TOF = turn over frequency

ABSTRACT

Considering the current problems related to the environment that affect our planet, such as the greenhouse effect, global warming, and the accumulation of plastic waste produced by the emission of gases such as CO₂ into the atmosphere and the indiscriminate use of plastics, strategies are necessary to reduce these problems. One of these is to develop catalytic systems through the synthesis of new compounds to use contaminants such as CO₂, CO, CH₄, etc. to obtain new compounds with added value.

Therefore, in this thesis project, germylenes and stannylenes were synthesized with bis-amidine ligands with a rigid naphthalene bridge. These systems were used as catalysts in cyclic ester polymerization reactions but did not show the desired reactivity. However, to understand and know the properties of these new compounds and their reactivity, they were also tested against oxidation, oxidative addition, coordination, and transmetalation type reactions.

On the other hand, it was possible to synthesize new bis-aluminum complexes with bis-amidine ligand with a rigid naphthalene bridge, which were tested as a catalyst for obtaining cyclic carbonates from epoxides and CO₂, which presented moderate to excellent conversion. Likewise, it was possible to obtain an aluminum complex using the same bis-amidine ligand but incorporating iodides in its structure to use it as a one-component catalyst, but unfortunately it did not present catalytic activity.

A Schiff base ligand derived from ferrocene was synthesized with its respective aluminum complex, which presented low catalytic activity for obtaining cyclic carbonates from epoxides and CO₂.

Despite the bis-sulfonimidamide ligands that contain a bridge in their structure, it was impossible to obtain them despite multiple tests.

RESUMEN

Teniendo en cuenta los problemas actuales relacionados con el medio ambientales que afectan a nuestro planeta, como el efecto invernadero, el calentamiento global y la acumulación de residuos plásticos, producidos por la emisión de gases como CO₂ a la atmósfera y el uso indiscriminado de plásticos, es necesario estrategias para disminuir estos problemas, y una de estas es desarrollar sistemas catalíticos mediante la síntesis de nuevos compuestos, para así usar los contaminantes como CO₂, CO, CH₄, etc. para obtener nuevos compuestos con valor agregado.

Por lo tanto, en este proyecto de tesis se sintetizaron germilenos y estanilenos con ligandos bis-amidinas con un puente rígido de naftaleno. Estos sistemas fueron usados como catalizadores en reacciones de polimerización de esteres cílicos, pero no presentaron la reactividad deseada. Sin embargo, para entender y saber las propiedades de estos nuevos compuestos y la reactividad que poseen es que de igual manera se probaron frente a reacciones del tipo oxidación, adición oxidativa, coordinación y transmetalación.

Por otra parte, fue posible sintetizar nuevos complejos bis-aluminio con ligando bis-amidinas con un puente rígido de naftaleno, los cuales fueron testeado como catalizador para la obtención de carbonatos cílicos a partir de epóxidos y CO₂, que presentaron de moderada a excelente conversión. Asimismo, fue posible obtener un complejo de aluminio usando el mismo ligando bis-amidina, pero incorporando yoduros en su estructura para utilizarlo como un catalizador de un componente, pero desafortunadamente no presento actividad catalítica.

Se sintetizo un ligando base de Schiff derivado de ferroceno, con su respectivo complejo de aluminio, el cual presentó baja actividad catalítica para la obtención de carbonatos cílicos a partir de epóxidos y CO₂.

En cuanto a los ligandos bis-sulfonimidamida que contengan un puente en su estructura, a pesar de las múltiples pruebas, no fue posible obtenerlos.

CHAPTER I: INTRODUCTION

INTRODUCTION

1. General Introduction

Due to humanity's growing and constant development, we face various environmental problems, one of the most relevant being the indiscriminate production of certain gases, such as N₂O and CO₂, generated by industrial growth¹. The greenhouse effect is an environmental problem directly related to the climate change observed in recent decades, caused by the accumulation of gases in the atmosphere, mainly CH₄, N₂O, and CO₂². Although these gases exist naturally in the atmosphere, human actions and primarily industrial processes have altered the natural balance of these gases³. On the other hand, the problem of environmental pollution is also caused by the substantial accumulation of plastic waste, which results in the contamination of soils, watercourses, and oceans⁴. Plastics are polymeric materials, the main ones being polyethylene (PE) and polyethylene terephthalate (PET), which are widely used due to their excellent physical and chemical properties but are harmful to the environment since they are not biodegradable⁵.

Due to the above, the scientific community has not remained oblivious to environmental problems, carrying out studies and scientific advances, such as catalytic reactions, obtaining new materials, or the use of pollutants to generate compounds of more excellent commercial value. Therefore, environmental problems can be addressed in the following way:

- a. Reduce CO₂ emissions: the existing problem with this gas can be approached in three ways. The first and the most efficient way is to reduce the production of CO₂ by replacing energy generation via fossil fuels with renewable energies⁶. Second, the way to capture the CO₂ currently emitted into the environment has been studied, using different types of porous materials capable of interacting physically or chemically with this gas to maintain it as part of its structure⁷. On the other hand, the interest in using CO₂ as a carbon source in chemical reactions, however, should be considered the high thermodynamic stability that CO₂ presents, having a considerable energy barrier, which is a drawback when it comes to using it directly. Different methods are being designed to overcome this energy barrier, specifically catalytic methods, and thus be able to use CO₂ as a raw material in industrial processes⁸.
- b. New environmentally friendly materials: research has been carried out to replace non-biodegradable materials by obtaining synthetic materials with similar physical properties. One of the most studied systems is lactones, organic compounds of the cyclic ester type,

which through a ring-opening polymerization (ROP) process, it is feasible to obtain biodegradable polymers⁹.

These two lines of research that seek to mitigate environmental pollution can be carried out by synthesizing new compounds or complexes used as catalysts. When synthesizing new complexes, we must consider their design, the ligand being the first step, where this ligand must be able to bind to the corresponding metal and confer desirable properties to the resulting complexes. Ligands can be simple, like ammonia, with a single pair of electrons to bind to the metal, or larger and more complex, with more functionalities. Aspects to consider when designing or choosing a ligand are: the steric bulk of the ligand, the addition of sterically encumbering groups that can block off the metal ion, limiting its binding to that which is desired; the electronic character of the ligand, the σ and π donation or acceptance by a ligand can affect the geometry of the complex as well as its spin state, which can be used to tailor the binding and reactivity at the metal center; electron-withdrawing or donation ligands impact the electronic character of the metal, making it electron-rich or electron-poor, respectively, this can affect the resulting complexes making them more or less likely to react; incorporating functionality into the ligand that can interact with the metal in a stabilizing or destabilizing manner¹⁰. Consequently, a constant demand for new ligand systems that support catalytically active metal centers places continual pressure on the organometallic and coordination chemistry to develop evermore elaborate compounds for use in this context.

1.1 Amidine ligands

Amidines are nitrogen analogs of carboxylic acids, with a central sp^2 -hybridized carbon atom in which an imine and one amine group are bonded (**1**, Figure 1). Structurally, they correspond to the amine equivalent of carboxylic esters (carboxylic acid imidates)¹¹. Amidines have been employed as ligands for numerous metallic and semimetallic elements throughout the periodic table. This combination of nitrogen-based functionalities leads to many substitutions of the CN_2 framework, which adjusts the steric and electronic properties of this ligand, one of the more attractive characteristics of these compounds as ligands. Another characteristic of amidine ligands is their high basicity, whose pK_a value is 5-12¹². The most extended applications of these compounds as ligands are centered around the corresponding negatively charged amidinate ion (**2**, Figure 1), also exists a considerable amount of work on the application of cationic amidinium (**3**, Figure 1), particularly concerning their anion binding properties¹³.

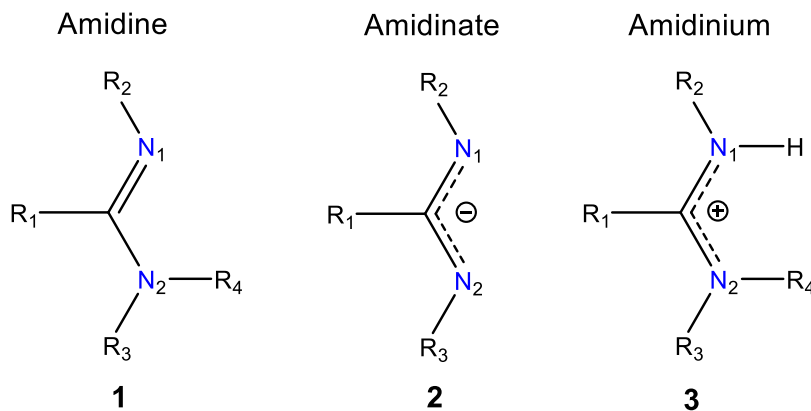


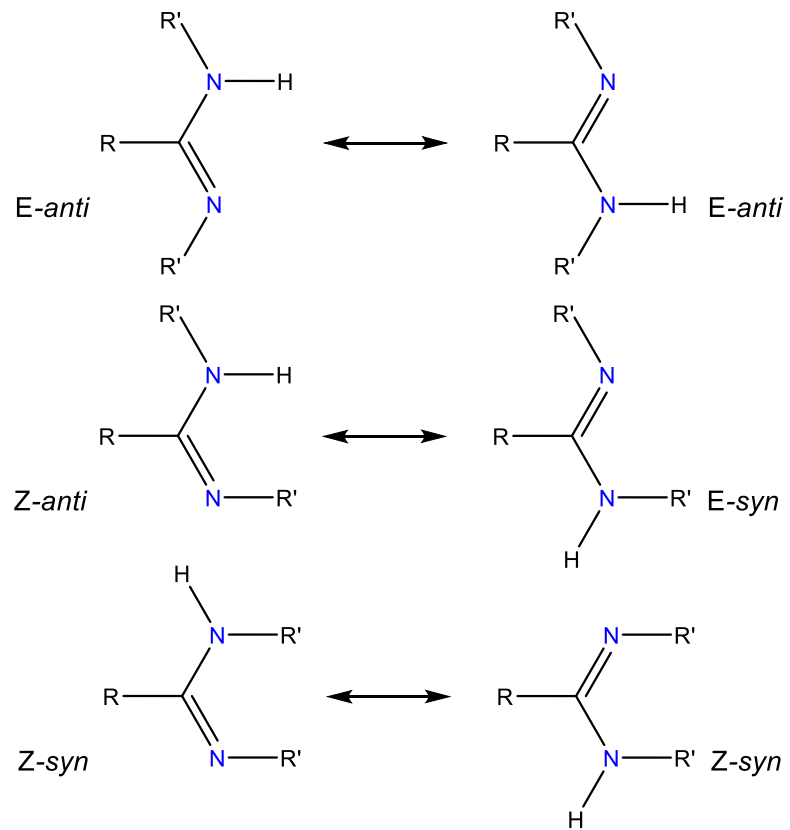
Figure 1. General structure of amidine (**1**), amidinate (**2**) and amidinium (**3**).

Non-symmetric amidines exist as different isomers depending on the position of the substituents relative to each other for the double bond; furthermore, in the case where a secondary amino group is present, different tautomers are also generated (Scheme 1)^{13,14}. These different forms are essential when considering how such compounds interact with metal centers.

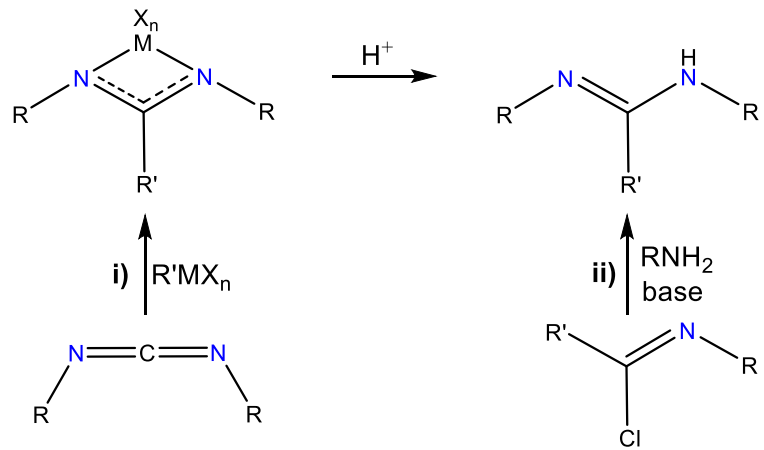
The most used routes to synthesize amidines are i) a carbodiimide, $\text{RN}=\text{C}=\text{NR}$, react with an organometallic compound (Scheme 2). This route offers the advantage of generating amidines containing a large number of carbon-based N - and N -substituents, limited only by the carbodiimide source; ii) via imidoyl chloride with amines (Scheme 2), this methodology allows the sequential addition of nitrogen substituents, affording not only bulky derivatives but also permits access to asymmetric systems containing different N -substituents^{13,15}.

In recent years the trend with the amidinate ligands was to develop systems bulkier and sterically hindered to stabilize more range of metal centers and control the geometry of the active metal center via rigid coordination, being a bridged bis-amidine a good alternative.

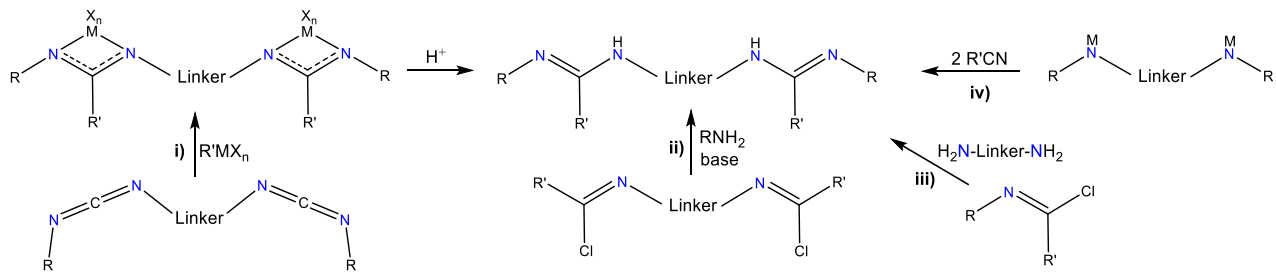
Bis-amidines can be divided into two classes according to how the two amidine units are connected: through the nitrogen atom or the backbone-base carbon atom. N -bridged bis-amidine are in general accessible on the four routes depicted in Scheme 3: i) treatment of a bis(carbodiimide) with organometallic compounds, synthesis via ii) bis-(imidoyl chloride)s, and iii) imidoyl chlorides or iv) by the addition of nitriles to metallated secondary diamines¹⁶.



Scheme 1. Isomeric and tautomeric forms for tri-substituted amidines.



Scheme 2. Synthesis of amidines.



Scheme 3. Synthesis of bis-amidines.

The use of imidoyl chlorides and bis(imidoylchloride)s is the most general approach towards the synthesis of *N*-bridged bis-amidines and this method has also been used to synthesize the first report example back in the 1930s. Most of the synthetic protocols make use of bis(imidoylchloride)s and primary amines (route ii, Scheme 3), whereas there is only limited precedence for routes starting from imidoyl chlorides and primary diamines (route iii, Scheme 3)¹⁶.

In recent years our group has reported two *N*-bridged bis-amidine ligands, where the linkers are benzidine (**4**, Figure 2)¹⁷ and 1,8-diaminonaphthalene (**5**, Figure 2)¹⁸, with yields of 80 and 76%, respectively. These ligands were synthesized via route ii, where one equivalent of the corresponding diamine reacts with two equivalents of imidoyl chloride. In both cases, these reactions are carried out in toluene, reflux, and in the presence of a base. These ligands were used to obtain catalytically active aluminum complexes for forming cyclic carbonates from epoxides and CO₂¹⁷⁻¹⁹, which will be described in greater detail in section 3.2.

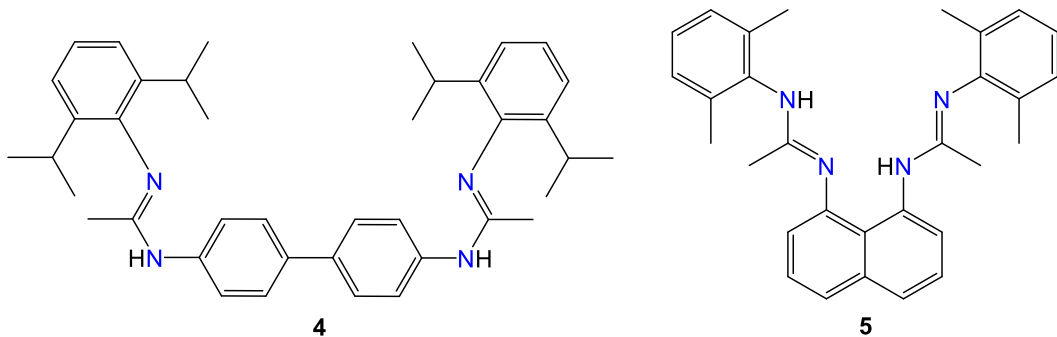
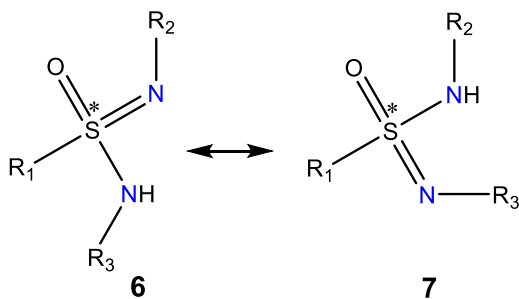


Figure 2. Examples of bis-amidines **4** and **5**.

1.2 Sulfonimidamide ligands

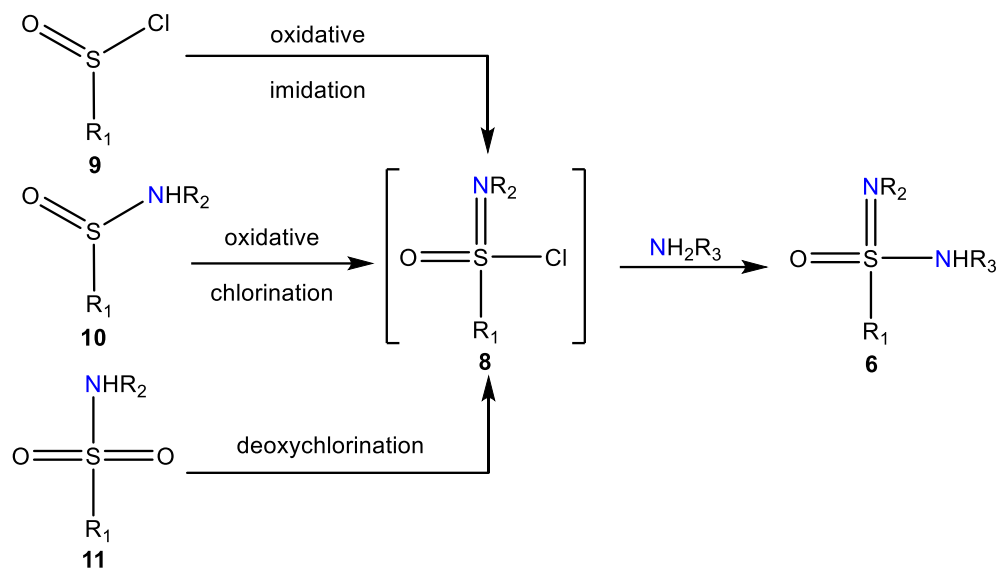
Sulfonimidamides (**6**, Scheme 4) are the aza-analogs of sulfonamides, with a hexavalent sulfur atom, where one of the sulfonamide oxygen atoms has been replaced by a nitrogen atom. This replacement provides a new class of compounds, generates a new stereogenic sulfur center, and offers the possibility of introducing extra structural diversity around the widely used sulfonamide functional group. When the amide is primary or secondary, the sulfonimidamide undergoes tautomerism due to the exchange of a proton between the amide and the imine group, and the relative stability of the tautomers depends on the nature of substituents present as R₂ and R₃ (**7**, Scheme 4)^{20,21}. Sulfonimidamides have been less studied than their sulfonamide analogs in their applications, mainly studied for the design and synthesis of possible drugs and agrochemicals. However, there are also studies where they have been used as chiral ligands for coordinating metals and as catalysts^{20,22}.



Scheme 4. Structure of sulfonimidamides.

Since the synthesis of sulfonimidamides was first reported by Levchenko *et al.* in 1960, numerous methods have been developed to obtain these compounds, with sulfonimidoyl chlorides (**8**, Scheme 5) as a key intermediate which upon nucleophilic substitution with amine provided the corresponding sulfonimidamides²⁰. There are three routes to obtain the sulfonimidoyl chloride intermediate. First, the direct transformation of sulfinyl chloride (**9**, Scheme 5) into sulfonimidoyl chloride via oxidative imidation using various N-chloro compounds like chloramine; sulfinamides (**10**, Scheme 5) may also provide sulfonimidoyl chlorides via oxidative chlorination using chlorinating agents like chlorine; a direct conversion of readily available mono N-substituted sulfonamides (**11**, Scheme 5) into sulfonimidoyl chlorides via deoxychlorination employing PCl₅ as chlorinating agent²⁰. In recent years this last method has been searching of new chlorinating agents. For example, Roy *et al.* developed a new chlorinating agent, triphenyldichlorophosphorane (Ph₃PCl₂)²³, which showed better activity than PCl₅. Also, Chen *et*

al. and Gibson *et al.* applied the same agent in only a one-pot procedure to convert silyl-protected sulfonamides to sulfonimidamides²⁴.



Scheme 5. Synthesis of sulfonimidamides.

In recent years our group synthesized two sulfonimidamide ligands, following the one-pot procedure of Chen *et al.*, via deoxychlorination from sulfonamides where the N-isopropylbenzenesulfonamide reacts with Ph_3PCl_2 like a chlorinating agent to form a sulfonimidoyl chloride, which is substituted by the addition of isopropylamine (**12**, Figure 3) or mesitylamine (**13**, Figure 3) to form the corresponding sulfonimidamides²⁵.

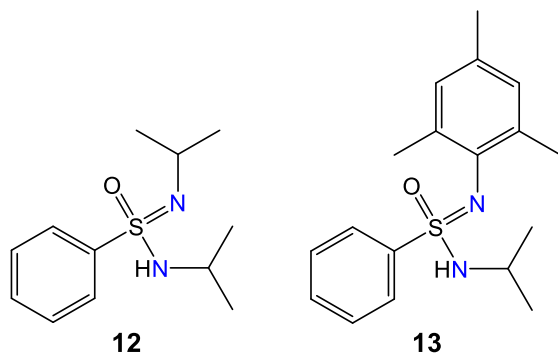
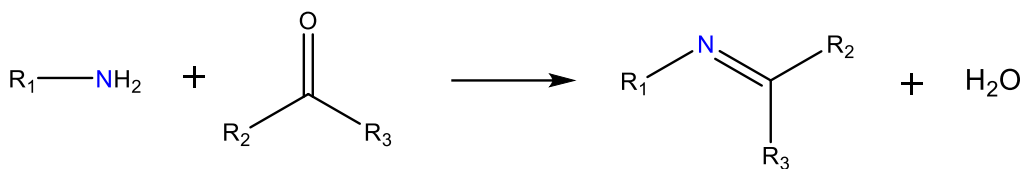


Figure 3. Examples of sulfonimidamides **12** and **13**.

1.3 Schiff base ligands

Schiff base, named after Hugo Schiff, is a nitrogen analog of an aldehyde or ketone in which the carbonyl group has been replaced by an imine or azomethine group. These bases Schiff are formed when any primary amine reacts with an aldehyde or ketone under specific conditions. Schiff base ligands are easily synthesized and form complexes with almost all metal ions. Over the past years, there have been many reports on their applications in biology, including antibacterial, antifungal, anticancer, antiviral activity, and as a catalyst in several reactions such as polymerization reactions, reduction of thionyl chloride, oxidation of organic compounds, reduction of ketones, aldol reaction and more^{26,27}.

The first preparation of imines was reported in 1864 by Schiff²⁶. Since then, a variety of methods for the synthesis of imines have been described. The classical synthesis reported by Schiff implies the condensation of a carbonyl compound with an amine under azeotropic distillation (Scheme 6). Molecular sieves are then used to remove altogether water formed in the system. In the 1990s, an in-situ method for water elimination was developed, using dehydrating solvents^{26–28}. In 2004, Chakraborti *et al*²⁹ showed that the efficiency of these methods is dependent on the use of highly electrophilic carbonyl compounds and strongly nucleophilic amines, for they proposed the use of substances that function as Brönsted-Lowry or Lewis acids to activate the carbonyl group of aldehydes, catalyze the nucleophilic attack by amines, and dehydrate the system, eliminating water as the final step. To this day, different techniques and methods are still being sought to synthesize these compounds, such as solvent-free/clay/microwave irradiation and solid-state synthesis.



Scheme 6. Synthesis general of Schiff base ligands.

2. Metallylenes

2.1 General aspects of Metallylenes

Metallylenes are the heavier analogs of carbenes R_2C : where the central carbon is replaced with silicon, germanium, tin, or lead. The chemistry of carbene has been widely explored and well understood. However, much attention is now being paid to the metallylenes. Metallylenes having many similarities and differences with carbenes, might have numerous applications in fundamental and applied chemistry. The valency of the central atom of the heavier carbene analogs is two. That is, its oxidation state is $M^{(II)}$, and its stability increases as the principal quantum number (n) increases ($Pb > Sn > Ge > Si$). Dichloroplumbylene and dichlorostannylene ($PbCl_2$ and $SnCl_2$, respectively) are stable ionic compounds. However, these dihalides exist as polymers or ion pairs in solution and solid states. The dichlorogermylene complex ($GeCl_2 \bullet (\text{dioxane})$) is also stable and isolable, whereas the dihalosilylenes are barely isolable compounds^{30,31}.

Compared to carbenes, metallylenes have a low ability to form hybrid orbitals and prefer the $(ns)^2(np)^2$ valence electron configuration in their divalent species. The ground state of the heavier metallylenes is singlet, unlike the case of carbenes, where the ground state is a triplet (Figure 4). Metallylenes have a vacant p-orbital and a lone pair of electrons in the singlet ground state. The lone pair in their valance orbital is expected to be inert due to its high s-character. At the same time, the presence of a vacant p-orbital makes them highly reactive since six valence electrons are less than the eight electrons of the “octet rule”^{30,31}.

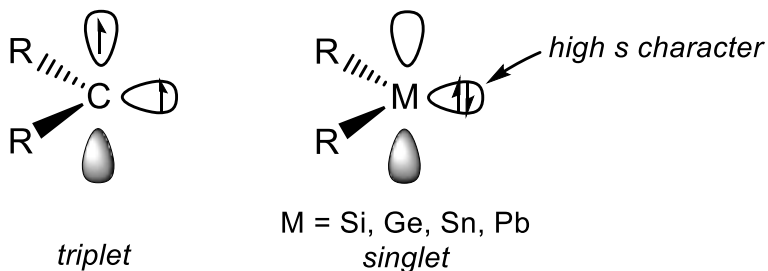
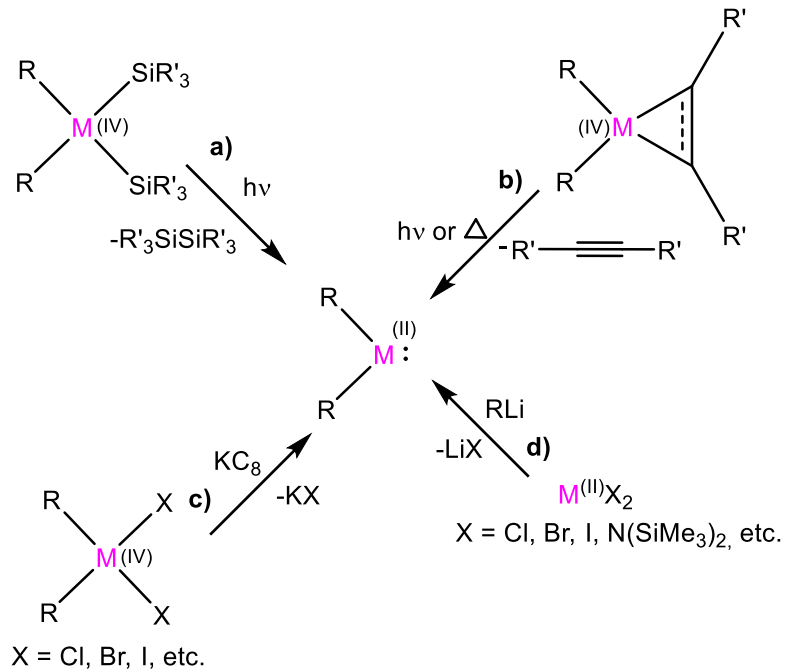


Figure 4. Difference between the ground states of carbenes and metallylenes.

There are two general routes to obtain metallylenes, which are: i) the reduction of $M^{(IV)}$ species as the precursors; ii) the substitution of $M^{(II)}$ species as a dihalides precursor of $M^{(II)}$ species with organometallic ligands such as ArLi/RLi as the nucleophile. In the case of the reduction of R_4M

to forming the corresponding metallylene, there are various options of reaction, such as the photochemical reductive elimination of a disilene from $(R_2M(SiR'_3)_2$ (route a, Scheme 7), the thermal and/or photochemical reductive elimination of an olefin or an alkyne from the three-membered ring systems metalliranes or metallirenes (route b, Scheme 7) and the reduction of the corresponding dihalides, R_2MX_2 , using reagents such as lithium naphthalenide and KC_8 (route c, Scheme 7). In the case of the method of substitution of a dihalide precursor of $M^{(II)}$ species (route d, Scheme 7) is more applicable for germanium, tin, and lead. There are few examples in the case of Si since $SiCl_2$ as starting material is challenging to isolate and handle^{30–32}.

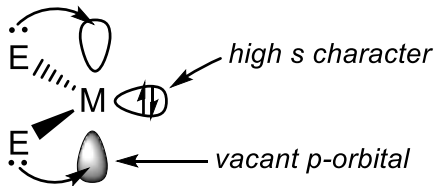
Due to its high reactivity, it might be challenging to isolate metallylenes as stable compounds under ambient conditions since they generally exhibit extremely high reactivity toward other molecules as well as themselves, forming dimers.



Scheme 7. General pathways for the synthesis of metallylenes.

For the above, to isolate metallylenes in their monomeric form, stabilization of the reactive vacant p-orbital is required by thermodynamic and/or kinetic methods. The stabilization by thermodynamics consists of the effect of electron-donating substituents linked to the central divalent atom, where electron density transfer takes place from the ligand into the empty p-orbitals, compensating their electron deficiency through, for example, the coordinating Cp^* ligands, and the inclusion of heteroatoms such as N, O, and P (Figure 5). The stabilization by

kinetic resides in using bulky organic substituents, where the ligands can sterically block the self-dimerization and the access to the vacant p-orbital (Figure 6)³¹. Likewise, metallylenes are stabilized in kinetic and thermodynamic ways, where bulky substituents are incorporated into heteroatoms.



M = Si, Ge, Sn, Pb
E = N, O, P, Cp* ligand, etc.

Figure 5. Thermodynamic stabilization of metallylenes.

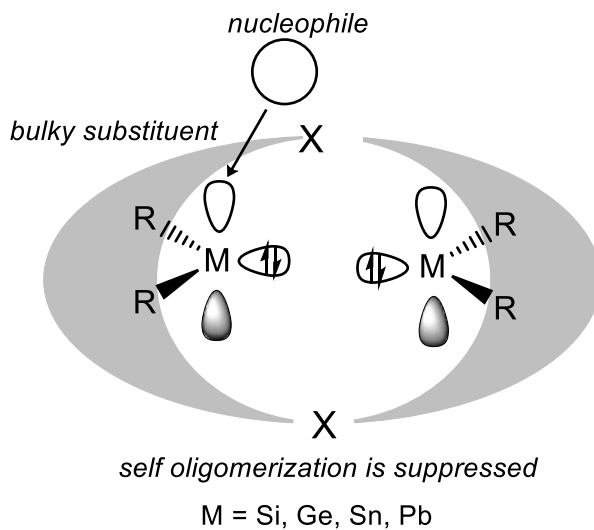


Figure 6. Kinetic stabilization of metallylenes.

The stabilization of metallylenes using heteroatoms is very effective. It is carried out through the coordination of these elements and by introducing delocalized, monoanionic bidentate ligands. In metallylenes, how the heteroatoms coordinate to the central atom of group 14 is essential. They can have a coordination number three (**a**, Figure 7), where a ligand and a substituent coordinate. Another way includes the coordination of two ligands where the coordination number is four (**b**, Figure 7) and where there are also two ligands but the coordination number is three because steric hindrance prevents the ligand from binding at the second site (**c**, Figure 7)³¹. The

stability of the metallylenes is enhanced by electronic delocalization that gives enough electron to avoid dimerization of the central atom without using sometimes bulky substituents.

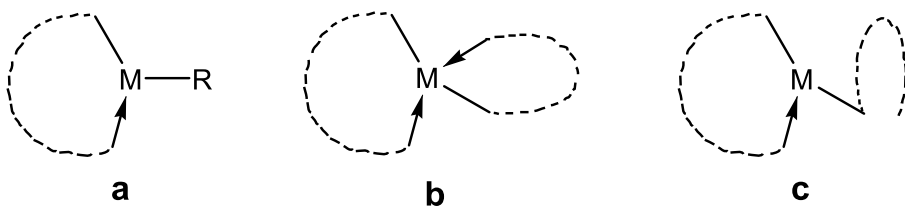


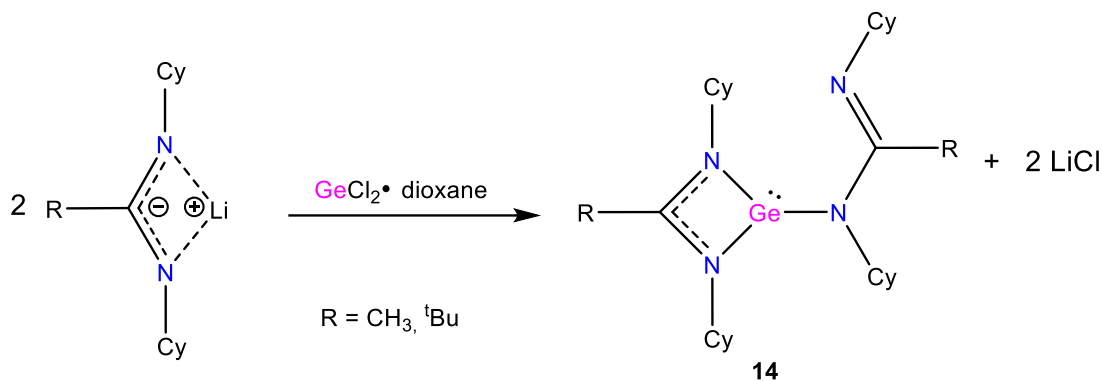
Figure 7. Coordination modes of substituents with heteroatoms in the side chains.

Amidine and sulfonimidamide are monoanionic bidentate ligands when deprotonated, giving a 4π delocalization system to stabilize metallylenes. In the following sections, examples of this type of stabilization will be given, mainly for the stabilization of germylenes and stannylenes.

2.2 Amidine ligands stabilized metallylenes

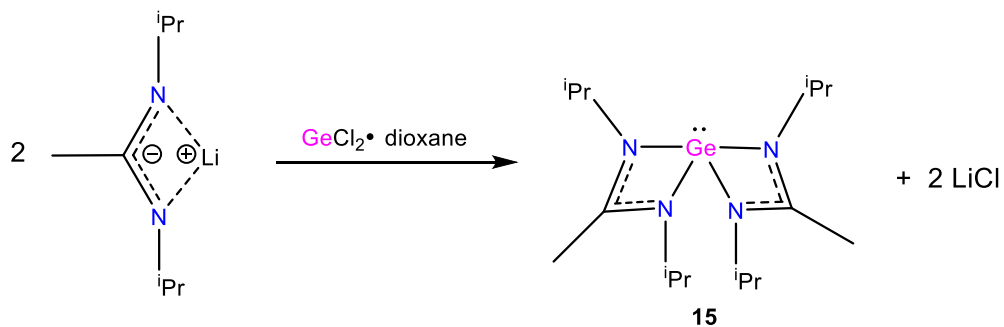
The amidinates are monoanionic ligands forming planar four-membered rings with $\text{Ge}^{(\text{II})}$ and $\text{Sn}^{(\text{III})}$. The resulting structures can have the coordination shown in Figure 7, two amidinate chelate rings or one ligand. The decisive parameter as to which structure will be realized by the complex seems to be the steric demand of the substituent on nitrogen³³.

The first amidinatogermylenes were published by Richeson *et al.* in 1997, $[\text{CH}_3\text{C}(\text{NCy})_2]_2\text{Ge}$ and $[{}^{\text{t}}\text{BuC}(\text{NCy})_2]_2\text{Ge}$, which were both prepared through substitution reaction (metathetical reaction) between $\text{GeCl}_2 \bullet (\text{dioxane})$ and the respective lithium amidinates (Scheme 8). The coordination geometry around germanium is distorted tetrahedral, with one of the vertices occupied by a lone pair of electrons. Both molecules exhibit one chelating and one monodentate (dangling) amidinate ligand³⁴.



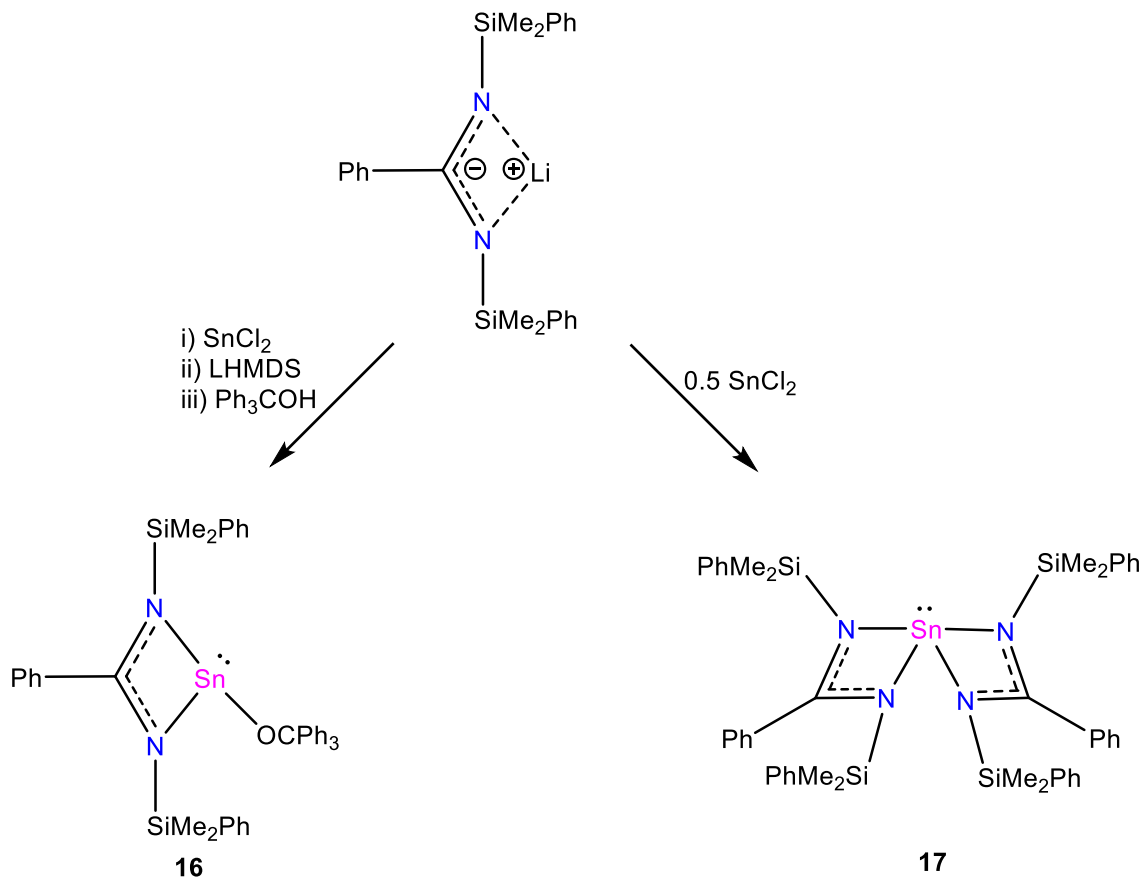
Scheme 8. First amidinatogermylenes.

Using the same synthetic method, Karsch *et al.* reported a bis-amidinatogermylene, [CH₃C(NPr)₂]₂Ge, but in this case with the two chelating amidinate ligands, due to the substituents on the nitrogens that allowed this structure (Scheme 9)³⁵.



Scheme 9. Example of bis-amidinatogermylene.

Regarding tin, the first amidinatostannylenes were published by Tolman *et al.* in 2002, using an N-silylated benzamidinate ligand, where monomeric Sn^(II) alkoxide complexes of bulky amidinate ligands and the corresponding bis-amidinate compounds were synthesized. Through the reaction of 1 or 0.5 equivalents of tin dichloride and the corresponding lithium amidinate. For the case of obtaining the alkoxide, the corresponding amidinatostannylene monomer was reacted with LiHMDS and alcohol (Scheme 10)³⁶.



Scheme 10. First amidinatostannylenes.

Germynes and stannylenes stabilized by amidine ligands, such as those presented above, have been and continue to be studied since the first examples were obtained. However, it is only in recent years that metallylenes with bis-amidine ligands connected by a bridge have begun to be studied, with few reported examples (Figure 8). In these bis-amidine ligands, the bridge can be connected in two ways, where the bridge is made through one of the nitrogens of the amidine, $\text{RNC(R')N-linker-NC(R')NR}$, or through the central carbon of the amidine, $(\text{RN})_2\text{C-linker-C(NR)}_2$. Jones *et al.* in 2020 reported bis-stannylenes and bis-germylenes with two 2,6-diisopropylphenyl (Dip) substituted bis-amidines ligands with bridges 1,4-phenylene (**I**, Figure 8) and 1,4-cyclohexylene (**II**, Figure 8) connected via the central carbon of the amidine, which had unsuccessful results to be used as precursors to obtain dinuclear metal (**I**) complexes or polymers by reduction³⁷. In 2021, Jones *et al.* reported again bis-germylene and bis-stannylene with 2,6-diisopropylphenyl substituted bis-amidine ligand with a dibenzofurandiyl bridged (**III**, Figure 8) connected via the central carbon of the amidine. These compounds were tried to obtain the reduction product, but it was not possible³⁸. In the same year, Kretschmer *et al.* reported another example of bis-amidine's 1,4-bis(phenyl)benzene bridge (**IV**, Figure 8) through the central carbon. In this case, bis stannylenes and bis germylenes were also obtained. The x-ray

analysis structure showed that in bis-germylene, two chloride ligands are directed toward each other, but in the bis-stannylenes are directed away from each other³⁹. To the best of our knowledge, the only reported example where a bis-germylene was obtained with a bis-amidine ligand connected to the bridge through one of the amidine nitrogens is the one reported by Jones *et al.* where the bridge is 1,3-phenylene (**V**, Figure 8). Attempts to reduce the bis-germylene to a dinuclear (**I**) specie was largely unsuccessful³⁸. It is worth mentioning that until now, there are only examples where bis-metallylene species are obtained from bridged bis-amidines. However, no systems have been reported in which the two amidine groups are coordinated to a central germanium and tin atom.

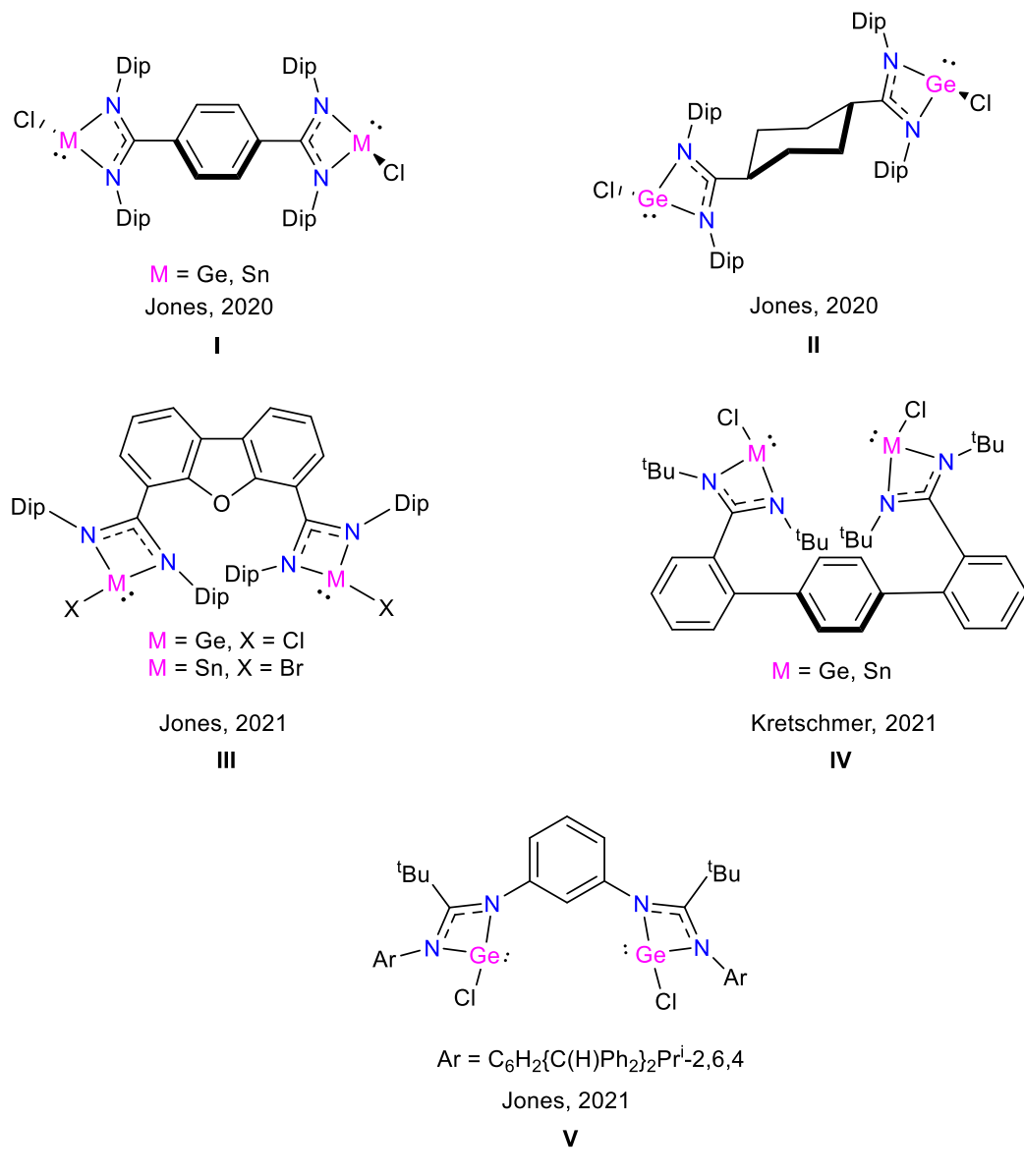
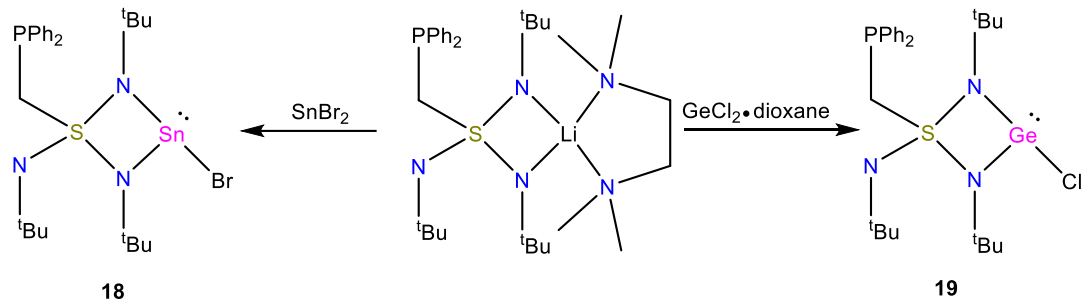


Figure 8. Examples of bis-germylenes and bis-stannylenes with bis-amidine ligands with a bridge.

2.3. Sulfonimidamide ligands stabilized metallylenes

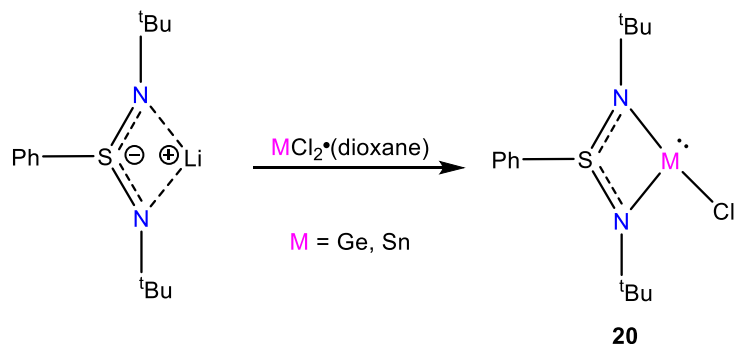
A family of monoanionic ligands with 4π delocalization that has been less studied for the stabilization of metallylenes are the sulfonimidamides, which also have a chiral center, which could form asymmetric metallylenes.

Regarding examples of stannylenes and germynes stabilized with sulfur ligands (NSN-type), we can mention the one reported by Stalke *et al.* in 2015, where they synthesized a novel triimido sulfur (VI) phosphanyl ligand for the stabilization of germynes and stannylenes (Scheme 11). The metallylenes were obtained by substitution of the corresponding dihalogenometallylene and characterized by X-ray crystallography. The design of this ligand with a free phosphine arm could be used for potential bidentate coordination with the metallylene lone pair⁴⁰.



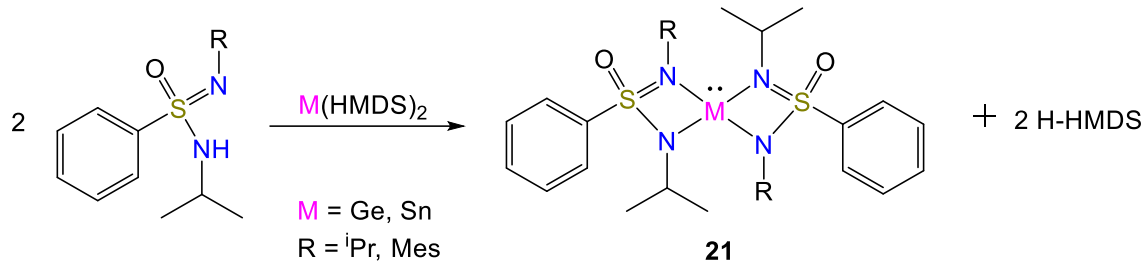
Scheme 11. Triimido sulfur phosphanyl metallylenes.

In 2018 Nakata *et al.* reported stannylenes and germynes stabilized with a diimidosulfinate ligand (Scheme 12). These compounds were obtained by reaction of the lithium salt of N,N'-di-tert-butylidiosulfinate having a phenyl group on the sulfur atom with $\text{MCl}_2 \cdot (\text{dioxane})$ ($\text{E} = \text{Ge}, \text{Sn}$). The crystalline states showed that the diimidosulfinate ligands chelate to the metal center to form slightly hinged four-membered rings⁴¹.



Scheme 12. Diimidosulfinate metallylenes.

In recent years our group reported homoleptic germylenes and stannylenes stabilized by sulfonimidamide ligands (Scheme 13). These compounds were obtained through a protonolysis reaction of the corresponding sulfonimidamide ligand and $M(HMDS)_2$ ($M = Ge, Sn$). The X-ray structures showed different bond lengths for Ge-N or Sn-N interatomic distances. However, a fast exchange is observed by 1H NMR spectroscopy at room temperature. These results lead to classify these metallylenes as 4π delocalized stabilized systems²⁵.



Scheme 13. Metallylenes stabilized by sulfonimidamides ligands.

2.4. Metallylenes reactivity

2.4.1. General aspects of the metallylenes reactivity

The metallylenes have a diverse range of reported reactivities that can be roughly categorized into five types: i) insertion, ii) cycloaddition, iii) reduction, iv) oxidation, and v) coordination reactions. This diverse range of reactions is due to the initial formation of a Lewis acid-base complex between the metallylene and the reagent with the metallylene acting as a Lewis acid with high electrophilicity. As discussed above, heavy carbene analogs in their singlet states feature two reactive sites, the vacant p-orbital and the lone pair of electrons, manifesting nucleophilic (Lewis base) and electrophilic (Lewis acid) behavior. However, the lone pair is expected to be relatively “inert” as a nucleophile since it exhibits a high **s** character due to its $(ns)^2(np)^2$ valence electron configuration. On the other hand, due to the 6 valance electrons and the octet rules, the vacant p-orbital should make the metallylenes highly electrophilic. Thus, almost all the metallylene reactivity can be initiated by the nucleophilic reaction of the reagents toward the vacant p-orbital^{31,32}.

2.4.2. Metallylenes reactivity: polymerization of cyclic esters

Lately, one of the fastest-growing branches of modern chemistry has been the synthesis of biodegradable polymers (in particular, polylactide, polyglycolide, poly- ϵ -caprolactone, and their copolymers) and new materials on their basis. The main method for industrial production of these compounds is the ring-opening polymerization (ROP) of cyclic esters, in which tin bis(octanoate) ($\text{Sn}(\text{oct})_2$) is used as the initiator. The search for new organic and new initiators based on electron-deficient metal complexes is continued. For this, metallylenes continue to attract particular attention as derivatives potentially valuable for the initiation of polymerization (Figure 9)⁴².

Considering the work of Kricheldorf *et al.* in 1995 about the influence and mechanism of $\text{Sn}(\text{oct})_2$ in the polymerization of L-lactide⁴³ and also that N-heterocyclic carbenes were reported to be efficient catalysts for high molecular weight linear PLA and PCL it is that interest has been put in using stannylenes for the polymerization of cyclic esters^{36,44,45}.

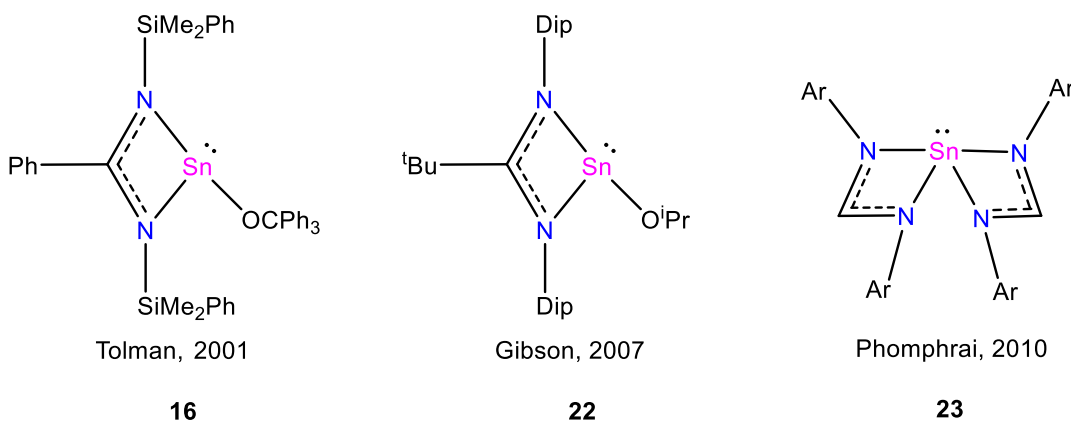


Figure 9. Stannylenes applied in polymerization (ϵ -caprolactone and lactide).

2.4.3. Metallylenes reactivity: oxidation

The reaction of metallylenes leading to the formation of the corresponding tetravalent species is an oxidation reaction. Since the oxidation number of the central group 14 element is changed from E^{II} to E^{IV} during the reaction, here we will focus on chalcogenation (O, S, Se, Te) reactions of the metallylenes. In these reactions, the nucleophilic oxidant acts as an oxidant toward the vacant p-orbital of the metallylene. Thus, the lone pairs of the chalcogen can react with the vacant p-orbital of the metallylenes³¹.

There are reports of metallylenes stabilized with amidine ligands that form oxidation products with chalcogens (Figure 10), such as the one reported by Richeson *et al.* in 1997, where amidinatogermylene react with styrene sulfide and Se to give heavier ketone analog of Ge (**24**, Figure 10), the structure studied showed a tetrahedral geometry for the Ge atom³⁴. Later, in 1999 Richeson *et al.* reported that an amidinatostannylene did not form a heavier ketone when react with propylene sulfide, obtaining a dimeric bridging sulfide complex (**25**, Figure 10)⁴⁶. Růžička *et al.* reported a dimeric amidinato-stannoxygen (**26**, Figure 10) obtained from a homoleptic amidinatostannylene with oxygen gas. Also, they mention that the same amidinatostannylene did not show reactivity against elemental sulfur, benzaldehyde, 1-phenylethanone, and small molecules like CO₂ or acetylene, probably due to their insufficient oxidizing strength⁴⁷.

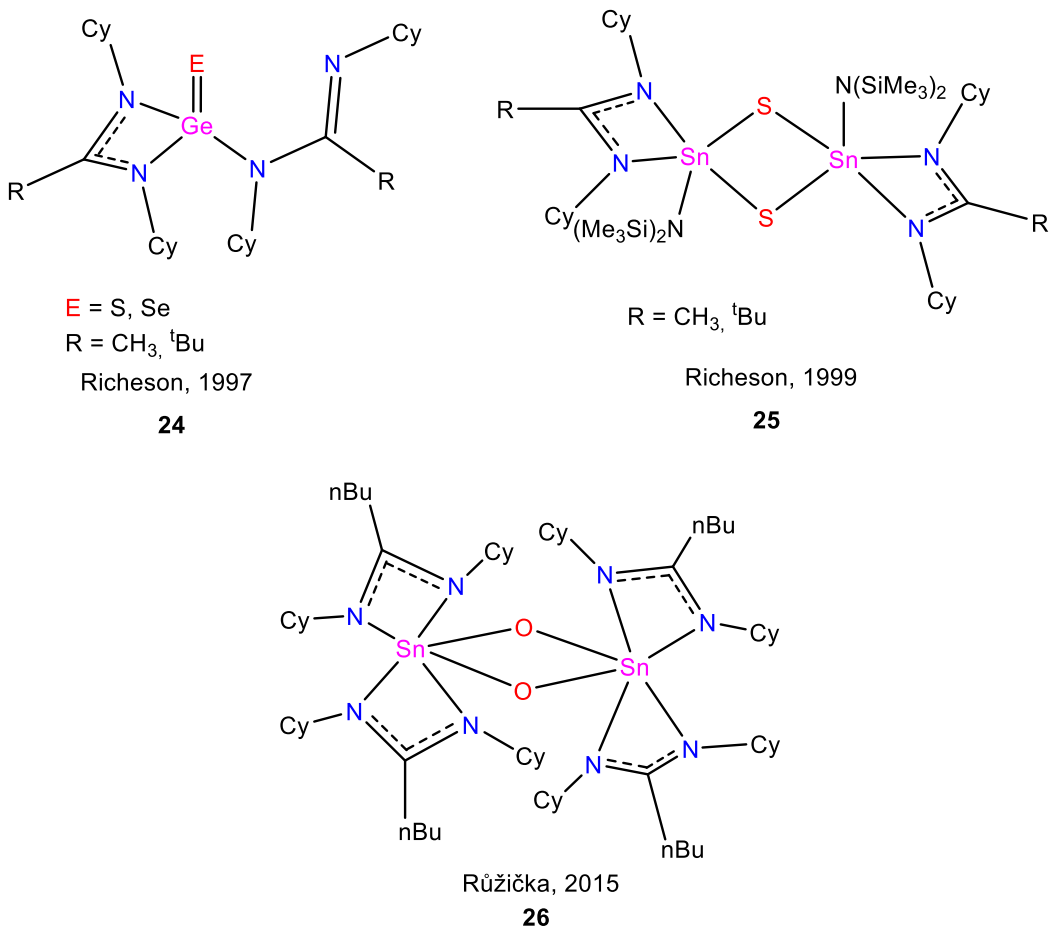


Figure 10. Oxidation products of metallylenes with chalcogens.

2.4.4. Metallylenes reactivity: oxidative addition

Since metallylenes show interesting reactivity in oxidation reactions with chalcogens, the oxidative addition reactions that metallylenes can present have also been studied. In 2000, Richeson *et al.* reported that oxidative addition of diphenyl disulfide and diphenyl diselenide occurs rapidly to amidinatogermylenes. The products of these reactions result from the cleavage of the chalcogen-chalcogen bond and the formation of the corresponding bis-(phenylchalcogenolate)M^{IV} complexes (**27**, Figure 11) in high yields⁴⁸. As oxidative addition reactions that metallylenes present, we can also mention a work reported by our group corresponding to a cycloaddition reaction between a bis-sulfonyl O,C,O-chelated-germylene and stannylenes and 3,5-di-tert-butylorthoquinone led to cycloaddition products (**28**, Figure 11)⁴⁹.

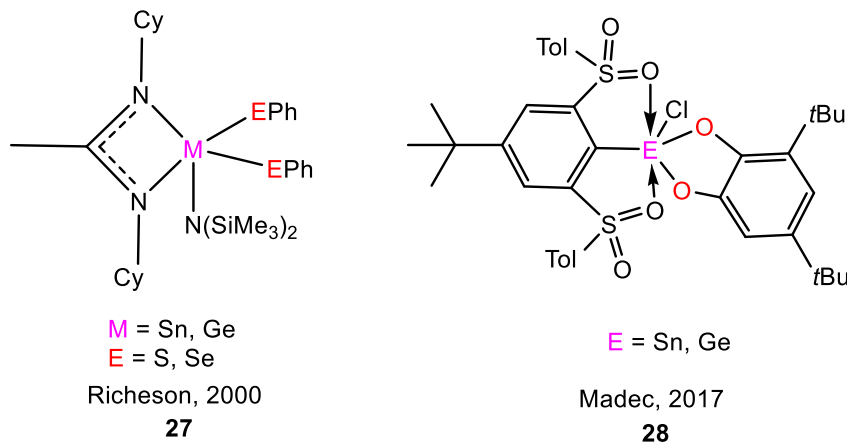


Figure 11. Oxidative addition products of metallylenes.

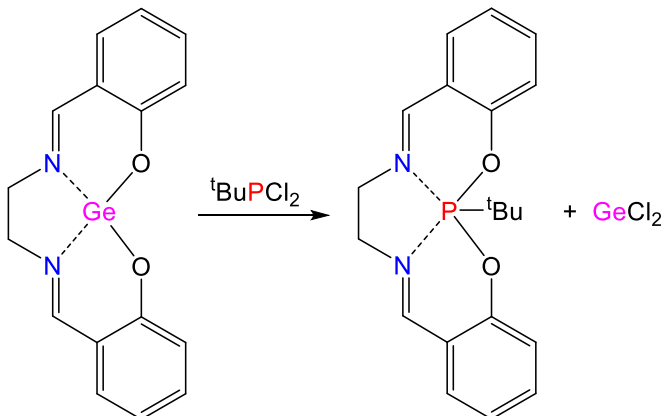
2.4.5. Metallylenes reactivity: transmetalation – ligand transfer reactions

Some reports show that metallylenes are used to obtain group 13, 14, and 15 complexes, which have halogens. Metallylenes react with the corresponding halides containing main group substrates by a reaction of transmetalation or ligand transfer. The most frequent synthetic route to obtain halogenated complexes of groups 13, 14, and 15 is through the relatively straightforward reaction of the appropriate halide with the ligand. However, often side reactions resulting from the presence of HX (X = halogen) byproducts are observed. So, the use of metallylenes is an alternative route⁵⁰.

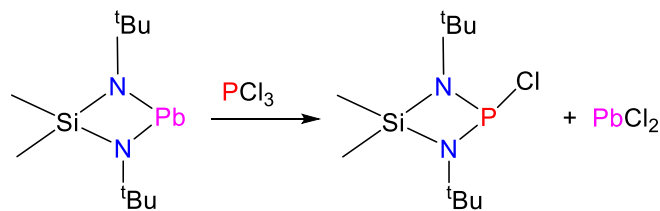
Barrau *et al.* reported a stannylene stabilized by a Salen ligand that react with $t\text{BuPCl}_2$ to obtain the corresponding phosphonite through a ligand transfer or exchange reaction (**a**, Scheme 14). Veith *et al.* reported that PCl_3 react with a cyclic diazaplumbylene by a ligand exchange reaction

to give PbCl_2 and a P-chloro-1,3,λ³,4-diazaphosphasiletidine, which had been previously accessible only by a much more cumbersome route (**b**, Scheme 14)^{51,52}. Sen *et al.* reported a transmetalation reaction between a germylene stabilized by a nacnac ligand with a picolyl functionality, and AlCl_3 to give GeCl_2 and the corresponding transmetalated product (**c**, Scheme 14)⁵³.

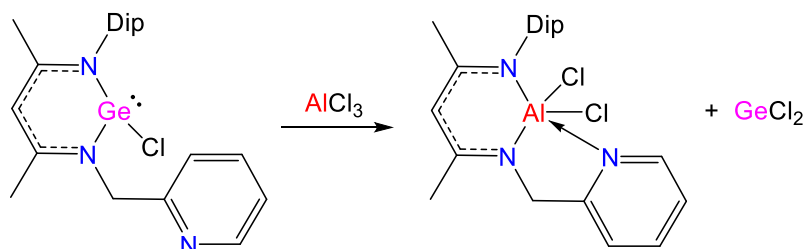
a) Barrau, 2000



b) Veith, 1984



c) Sen, 2020



Scheme 14. Examples of transmetalation – ligand transfer reactions with metallylenes.

3. Aluminum complexes

3.1 General aspects of aluminum complexes

Aluminum is the most abundant metal in the earth's crust⁵⁴ and has low production costs⁵⁵. Aluminum is a metal of group 13 of the periodic table, with an external electronic configuration $3s^23p^1$. It usually occurs in trivalent form, adopting a trigonal planar geometry with sp^2 hybridization⁵⁶. However, the aluminum center can adopt various geometries according to its coordination number through the subsequent coordination of electron-pair donor ligands.

Alkyl aluminum-type compounds, such as trimethylaluminum, represent an approximation to the role of aluminum in organometallic chemistry and have been extensively studied, expanding their scope in catalytic applications and even in materials science⁵⁷. These compounds, like Al^(III) by itself, have a high oxophilicity, which leads to the disadvantage of being highly unstable in air and humidity; they exhibit pyrophoricity, that is, they ignite at room temperature in the presence of oxygen, in addition to the fact that they react violently with water. They must be handled under controlled conditions, under an inert atmosphere (N₂ or Ar), and in the total absence of humidity.

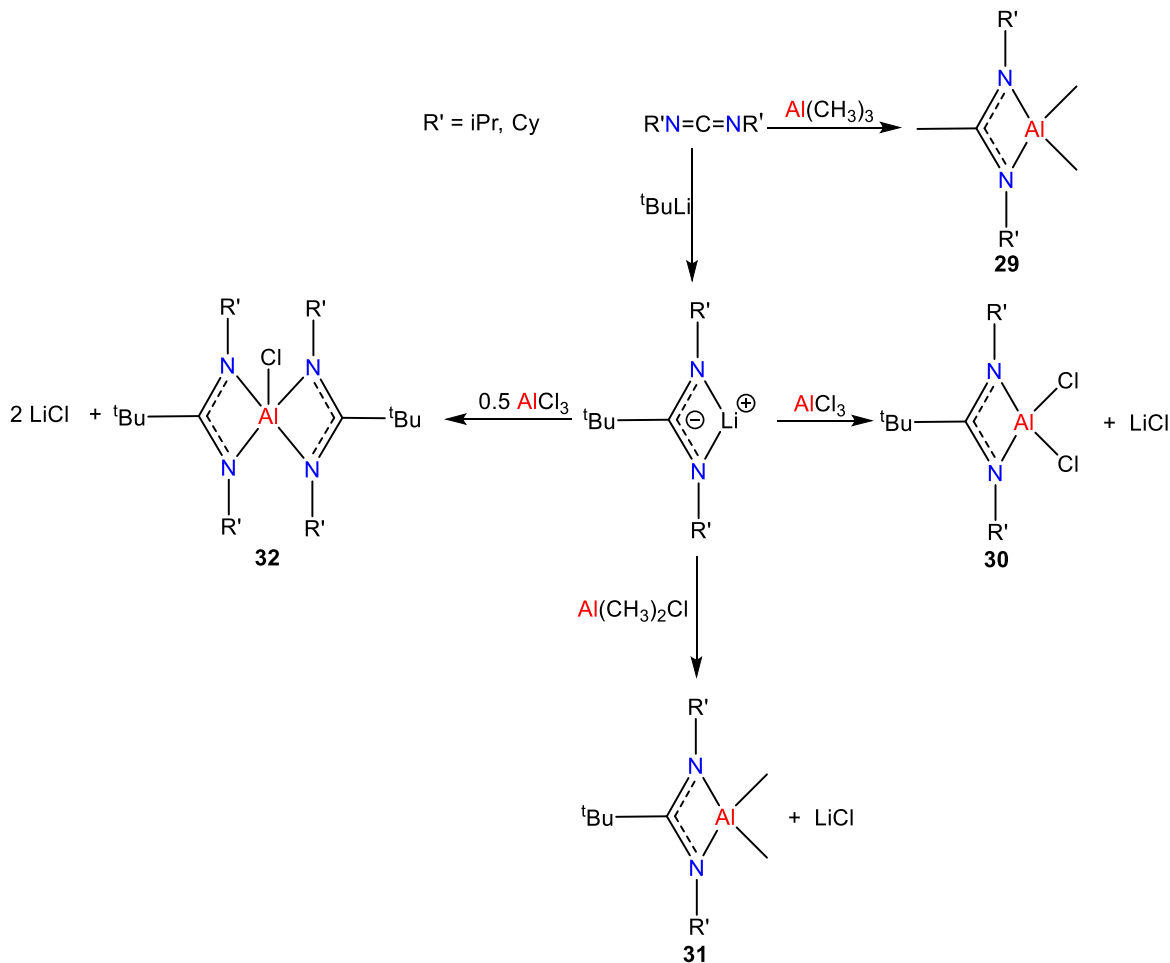
The properties and characteristics related to the reactivity of aluminum (III) reagents generally derive from the high Lewis acidity of the organoaluminum compounds. This property allows the formation of complexes through covalent or coordination bonds; the latter originated when the acidic species Al–R reacts with a Lewis base, with a pair of electrons available to occupy the empty orbitals around the aluminum atom^{56–58}.

The coordination of ligands to the aluminum center affects its traditional planar trigonal geometry, giving rise to new geometric arrangements depending on the number of species attached to the aluminum atom. Tetracoordinate aluminum species generally adopt a tetrahedral geometry; the pentacoordinate species, depending on the nature of the ligand(s), can be arranged as a trigonal bipyramidal or a square-based pyramid; hexacoordinate species adopt octahedral geometry⁵⁶. Considering that the alkyl ligands bonded to the aluminum center are relatively labile and the Al–C bond polarity makes it easy to synthesize derivatives of these by substituting one or more alkyl, thus transforming them into excellent precursors for obtaining aluminum complexes with more elaborate ligands⁵⁸.

2.3 Aluminum complexes with amidine ligands

Aluminum complexes stabilized by amidine ligands have been extensively studied, and these compounds appear in diverse applications as catalysts. Generally, aluminum complexes with amidines as a ligand can be formed by several different mechanisms. The most common synthetic method is a salt metathesis reaction between a lithium amidinate and an aluminum halide. Also, it is common to use a carbodiimide insertion into an aluminum alkyl bond, for the synthesis of the aluminum complexes. As well reaction of the parent amidine with an aluminum alkyl is a facile method of amidinate formation if the parent amidine is available⁵⁹.

Jordan *et al.* described the synthesis and structures of an extensive set of mono-amidinato aluminum dichlorides and dialkyls complexes (**29**, **30**, and **31**, Scheme 15) and bis-amidinato aluminum chlorides complexes (**32**, Scheme 14). These complexes were made by a salt metathesis reaction and a carbodiimide insertion into an aluminum alkyl bond⁶⁰.



Scheme 15. Examples of mono-amidinato and bis-amidinato aluminum complexes.

2.4 Aluminum complexes with Schiff base ligands

Schiff base ligands being easy to synthesize, form complexes with almost all metal ions. Schiff base complexes of transition metal ions are efficient catalysts in homogeneous and heterogeneous reactions. However, to reduce costs regarding the use of transition metals, it was seen in different reports that the use of Schiff base ligands with non-transitions metals such as aluminum gives good results in catalysis, mainly in olefin polymerization, and obtaining polycarbonates as well as cyclic carbonates. The Salen-type Schiff base ligands are (an OH group is added to their structure) the most promising in this field²⁸. Salen complexes with aluminum will be discussed in the following section due to their reactivity toward forming cyclic carbonates.

2.5 Aluminum complexes reactivity

2.5.1 Aluminum complexes reactivity: catalysis to obtaining cyclic carbonates from CO₂ and epoxides

Using CO₂ as an abundant, renewable, and cheap source for industrial chemical production would reduce atmospheric emissions of this gas. It would contribute to remedying the greenhouse effect^{61,62}. However, the activation and utilization of CO₂ remain problematic because it is the most oxidized form of carbon, leading to high thermodynamic stability⁶³. Consequently, few chemical processes use carbon dioxide as a raw material due to its low reactivity. Among the uses for CO₂ at an industrial level are the synthesis of urea and salicylic acid, which acts as a starting reagent. However, these processes contribution to reducing CO₂ emissions is minimal. The chemical industry uses less than 1 % of total CO₂ emissions, so more chemical reuse processes are required to transform the CO₂ into other value-added products⁶⁴.

Recently, there has been a vast development in the field of CO₂ catalysis, leading to various organic compounds or intermediates such as polycarbonates^{65,66}, carboxylated hetero-arenes⁶⁷, amides⁶⁸, and isocyanates⁶⁹, among others.

Thus, inserting CO₂ to obtain low-energy molecules, such as carbonates, is a potentially significant transformation to reduce CO₂ emissions. Carbonates can be classified into inorganic carbonates if they have a metal, and organic carbonates, which in turn can be divided into cyclic

carbonates **a**, linear carbonates **b**, and polycarbonates **c** (Figure 12)⁶², the most important being cyclic carbonates and polycarbonates.

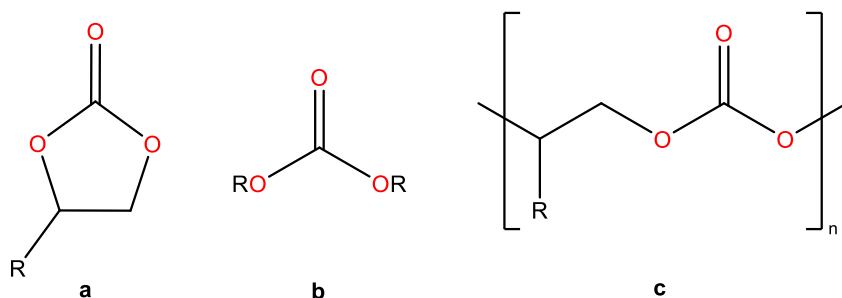
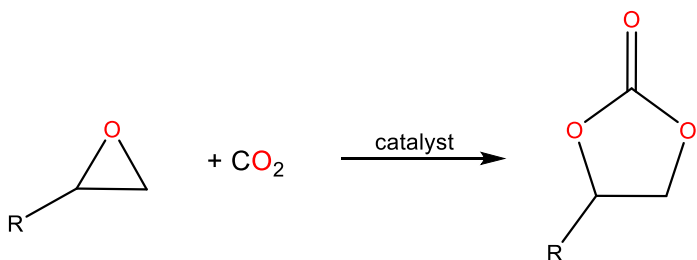


Figure 12. Structure of organic carbonates: cyclic **a**, linear **b**, and polycarbonates **c**.

In recent years, numerous studies have been carried out on synthesizing organic carbonates by catalytic addition of CO₂ to constrained geometry heterocyclics, such as epoxides and oxetanes, to contribute to reusing CO₂, associated with economic benefits since the synthesis of these carbonates has always been marketed^{70,71}. Cyclic carbonates are used as solvents for electrolytes in lithium-ion batteries⁷², as polar aprotic solvents⁷³, and as intermediates in synthesizing other small molecules⁷⁴ and polymers⁷⁵. Cyclic carbonates can be obtained through reactions between epoxides and CO₂ using different organometallic complexes as catalysts (Scheme 16). In the catalytic process, systems formed by the combination of Lewis acids and nucleophiles are needed. The metal center acts as the Lewis acid activating the epoxide, and a cocatalyst that supplies a halide acts as a nucleophile, causing the opening of the ring^{70,71}.



Scheme 16. Synthesis of cyclic carbonates.

Commercially, the synthesis of cyclic carbonates has been carried out by a catalytic process at high temperatures and pressures (100-200 °C and 20-100 bar) for more than 50 years, where quaternary ammonium salts (R₄NX) are used as catalysts⁷⁶. Given the high energy consumption of this process, it is necessary to develop new efficient catalysts so that the synthesis of cyclic carbonates can be carried out at room temperature and low CO₂ pressure since, in this way, the

cost of industrial-scale production. Following this, in the last decade, different research groups have actively worked on the development of efficient catalysts for this process, including organometallic complexes of Zn(II), Mg(II), Fe(III), Cr(III), Co(III) and Al(III), among other metals and organocatalysts⁷¹. In recent years, due to the great interest in this field, catalytic systems are sought that combine low or no toxicity of the metal used and cost that is valid for a wide range of substrates and that present high activity under mild reaction conditions, aluminum-based catalysts being one of those that have shown the most excellent catalytic activity in cyclic carbonate synthesis processes⁷¹.

The most representative aluminum compounds with catalytic activity in the synthesis of cyclic carbonates are shown in Figure 13, where SALEN-type (**33**) and ACEN-type (**34**) bimetallic systems stand out, developed by North *et al.*^{77–80}. These aluminum complexes are the most active catalysts to date in the synthesis of cyclic carbonates from terminal epoxides and carbon dioxide, in combination with tetrabutylammonium bromide (Bu₄NBr) as cocatalysts at room temperature and one bar of CO₂ pressure. Another system to highlight is the one developed in 1983 by Inoue *et al.*, which consists of an AlOMe (TPP) complex (**35**), which can quickly and reversibly trap CO₂ at room temperature, the carbon dioxide being trapped sufficiently active to react with an epoxide under ambient conditions to produce the corresponding cyclic carbonates⁸¹. Another catalyst that has drawn attention is the aluminum complex based on aminotriphenolate (**36**), which, together with the cocatalyst Bu₄NI, achieves the complete conversion of 1-hexene oxide into the corresponding cyclic carbonate at 90 °C, 10 bar CO₂ in two hours⁸². Furthermore, this system is active for various terminal epoxides and disubstituted epoxides (at higher temperatures and pressures).

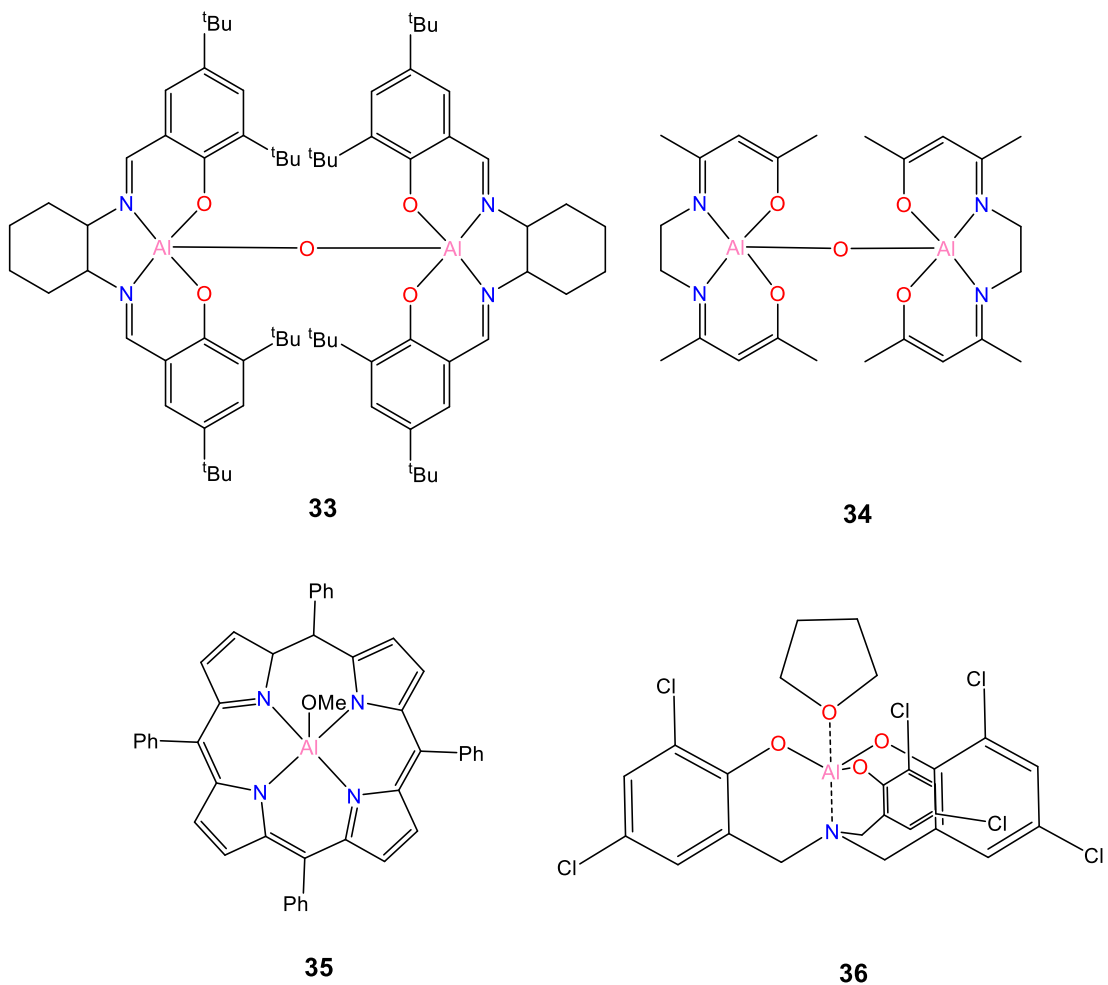


Figure 13. Active aluminum catalysts in the synthesis of cyclic carbonates.

Single-component aluminum catalysts have been designed to integrate catalyst and cocatalyst into a single system (Figure 14). Daresbourg *et al.* reported the synthesis of a one-component aluminum SALEN-type catalyst (**37**, Figure 14), which is active in synthesizing cyclic carbonates from epoxides and CO₂, where low CO₂ pressures are used⁸³. However, higher temperatures are required at 120 °C to achieve considerable activities. In contrast, the catalyst reported by North *et al.* (**38**, Fig. 14), also a SALEN-type singlet-component, is highly active in forming cyclic carbonates at 25 °C and 1 bar of CO₂ pressure⁸⁴.

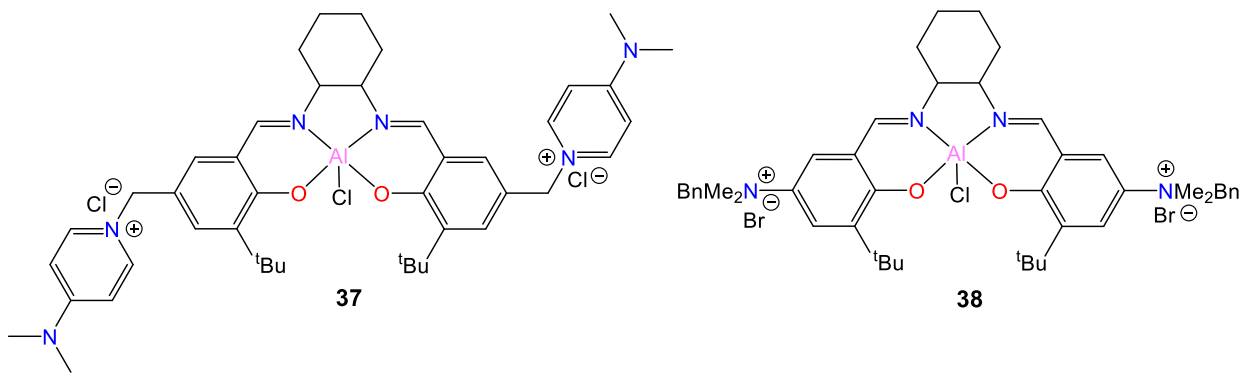


Figure 14. Singlet-component aluminum catalyst for the synthesis of cyclic carbonates.

On the other hand, in recent years, our research group has reported a series of aluminum amidinate complexes as catalysts for synthesizing cyclic carbonates from CO₂ and epoxides. Among which, symmetric aluminum bimetallic complexes stand out (**39**, Figure 15), which in the presence of tetrabutylammonium iodide as a co-catalyst, an excellent catalytic activity is obtained (conversions between 62-100%) being these the first aluminum amidinate catalysts to be developed for the synthesis of cyclic carbonates from epoxides and CO₂¹⁹. Aluminum complex bi- and tri-metal amidinate systems were also reported (Figure 15, **40** and **41** respectively), which presented catalytic activity at 50 ° C and 1 bar of CO₂ pressure in the absence of solvent for the formation of cyclic carbonates from epoxides terminals and CO₂⁸⁵. In 2021, a pentacoordinate amidinate iodide aluminum complex (**42**, Figure 15) was reported, one of the first examples of a non-zwitterionic aluminum complex used as a neutral single-component for obtaining cyclic carbonate, which presented catalytic activity at 80 ° C and 1 bar of CO₂ and without co-catalyst¹⁸.

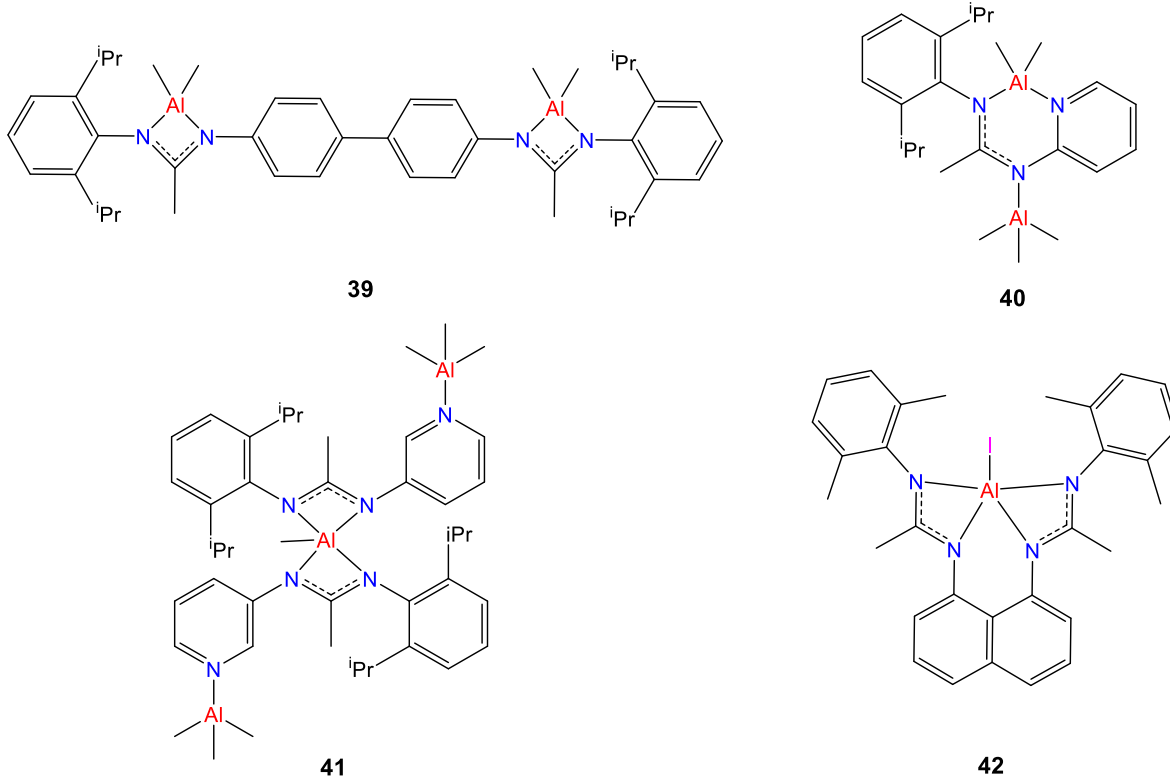
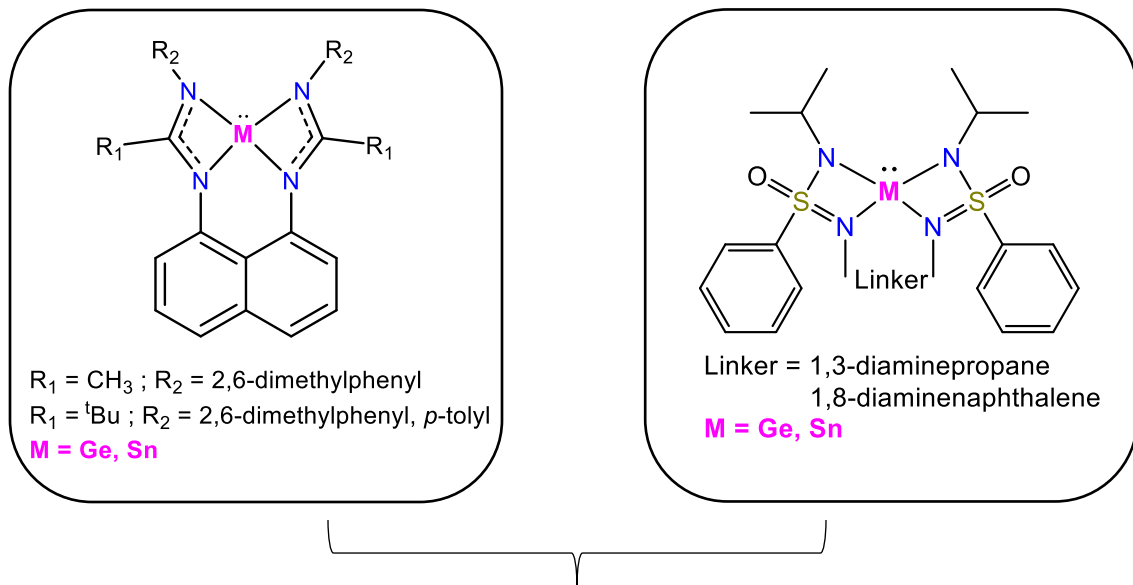


Figure 15. Aluminum amidinate complexes.

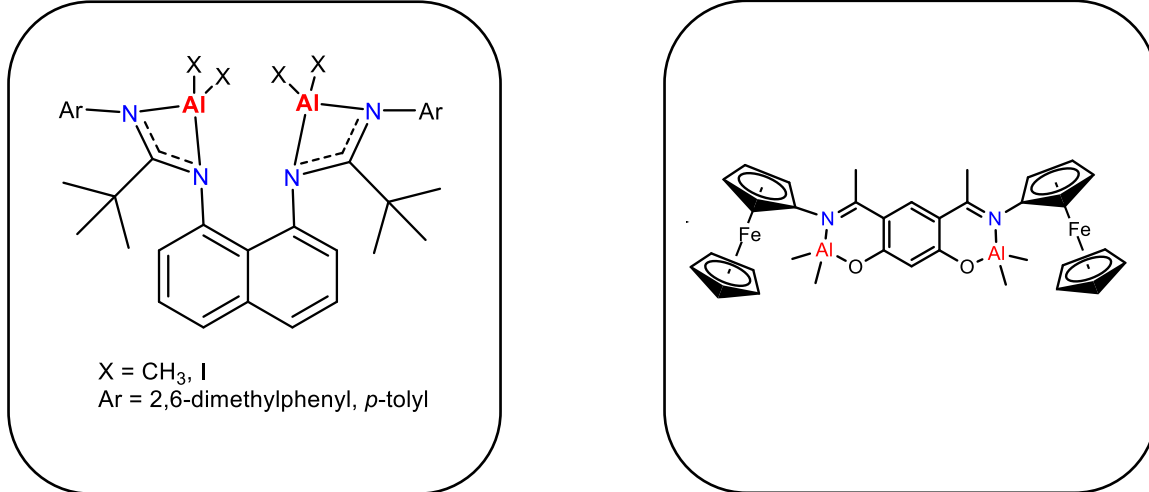
3. Project proposal

Considering recent events, the current state of development in this area, and knowing the environmental problems that affect our planet, such as the greenhouse effect, global warming, and the accumulation of plastic waste, this thesis project proposes to achieve catalysts that can be used in catalytic reactions and thus contribute to diminishing the problems mentioned above as well to continuing to study and develop catalytic systems that allow more active, efficient, and selective processes. This proposal will first be carried out by synthesizing stable germylenes and stannylenes with bis amidine and bis sulfonimidamide ligands and thus evaluating their catalytic potential in the polymerization of cyclic esters. Furthermore, these synthesized metallylenes' reactivity in oxidation, oxidative addition, chemical coordination, and transmetalation will be explored. On the other hand, the synthesis of aluminum complexes with bis-amidine and Schiff base ligands will be carried out to study the catalytic potential for transforming CO₂ with epoxides to cyclic carbonates.



Catalytic systems for polymerization of cyclic esters and small molecule activation

Catalytic systems for obtaining cyclic carbonates



Scheme 17. General proposal.

CHAPTER II: HYPOTHESIS AND GOALS

HYPOTHESIS

The synthesis of bis-amidines and bis-sulfonimidamide ligands with a linker in their structure will allow the stabilization of germynes and stannylenes to be used for the polymerization of cyclic esters and the activation of small molecules.

Using bis-amidine ligands with a rigid naphthalene linker will allow pentacoordinated aluminum complexes to be used as catalysts to obtain cyclic carbonates from CO₂ and epoxides. Incorporating iodide in the coordination sphere of the aluminum complexes with bis-amidine ligands will achieve one-component systems without using a cocatalyst to activate CO₂ with epoxides.

Incorporating the ferrocenyl fragment in Schiff bases ligands will allow obtaining bimetallic complexes where the reactivity of Al can be influenced electronically and sterically so that more efficient and active catalytic systems can be obtained towards the activation of CO₂.

GOALS

1. Main goals

Synthesize and characterize new stable germanium and tin metallylenes with bis-amidines and bis-sulfonimidamide ligands and evaluate their catalytic potential in the polymerization of cyclic esters and the activation and transformation of small molecules.

Synthesize and characterize new one-component aluminum complexes with bis-amidines and Schiff bases ligands derived from ferrocene and evaluate their catalytic potential in the activation of CO₂ with epoxides.

2. Specific goals

1. To synthesize and characterize bis-amidine and bis-sulfonimidamide ligands with various spacers in their structure.
2. To synthesize and characterize Schiff Base ligands derived from ferrocene.
3. To synthesize and characterize Al complexes with the bis-amidine, and Schiff base ligands obtained.
4. To obtain one-component systems, incorporate the iodide ligand into the Al complexes obtained.
5. To synthesize and characterize germylenes and stannylenes of bis amidines, and bis sulfonimidamides.
6. To evaluate the catalytic activity of Al complexes obtained towards transforming CO₂ to cyclic carbonates.
7. To evaluate the catalytic activity of metallylenes obtained towards the polymerization of cyclic esters.
8. To evaluate the reactivity of metallylenes in oxidation, oxidative addition, chemical coordination and transmetalation reactions.

CHAPTER III: EXPERIMENTAL PART

EXPERIMENTAL PART

General procedures

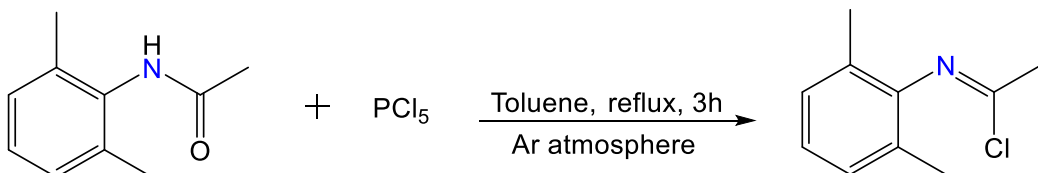
All manipulations were performed under an inert atmosphere of argon or nitrogen using standard Schlenk-line and glovebox techniques. Dry, oxygen-free solvents were employed. All reagents were obtained from commercial suppliers unless otherwise stated. *N*-(2,6-dimethylphenyl)acetamide¹⁴ and *N,N*-(naphthalene-1,8-diyl)bis(2,2-dimethylpropanamide)⁸⁶ were prepared according to published procedures.

Characterization

NMR spectra were recorded with the following spectrometers for ¹H, ¹³C, ¹¹⁹Sn, ²⁷Al, and ³¹P: Bruker Avance II 300MHz, Avance III HD 400 MHz, and Avance I and II 500 MHz spectrometers. The chemical shift has been counted positively verse the low field and expressed in part per million (ppm). The following abbreviations and combinations are used: br, broad; s, singlet; d, doublet; t, triplet; q, quartet; m, multiplet. ¹H and ¹³C resonance signals were attributed through 2D COSY, HSQC, and HMBC experiments. The mass spectroscopy analysis was done using three techniques, direct chemical ionization (DCI-CH₄) methods and recorded on a GCT Premier Waters mass spectrometer; electrospray ionization (ESI), recorded on a Waters Xevo G2 Q-TOF mass spectrometer; and a Maldi micro-MX micro-Mass in a pyrene matrix (ratio product/matrix:1/100). Melting points were measured with a capillary Electrothermal Stuart SMP40 apparatus, and samples were prepared in the glovebox before the analysis. IR spectra were measured on a ThermoNicolet 6700, Nexus and recovered in solid state (KBr).

1. Preparation of the precursors required for the synthesis of bis-amidine ligands

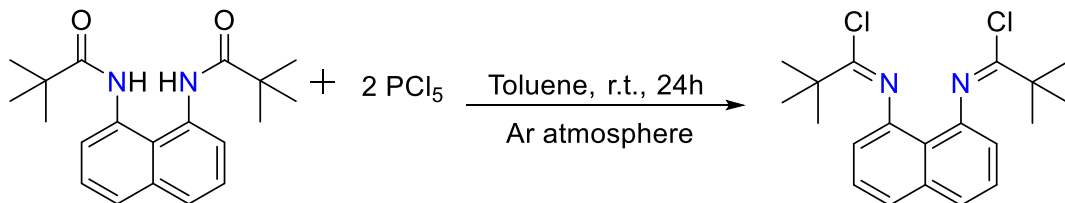
1.1. Synthesis of the precursor *N*-(2,6-dimethylphenyl)acetimidoyl chloride



Scheme 18. Synthesis of *N*-(2,6-dimethylphenyl)acetimidoyl chloride.

The general procedure for obtaining imidoyl chloride is followed¹⁴. PCl_5 (7.0 g, 43 mmol) was added to a solution of *N*-(2,6-dimethylphenyl)acetamide (9.8 g, 47.2 mmol) in dry toluene (40 mL), and the mixture was refluxed for 3 h under an Ar atmosphere. After the reaction time, the solution is allowed to cool to room temperature. Then, toluene was removed under reduced pressure, and the resulting mixture is distilled between 90 and 110 °C. The product is a colorless liquid (6.5 g, 35.6 mmol, 82 %). $^1\text{H NMR}$ (CDCl_3 , 400 MHz): δ 7.04 (d, $J_{\text{HH}} = 7.34$ Hz, 2H, C_6H_3), 6.98 (t, $J_{\text{HH}} = 7.34$ Hz, 1H, C_6H_3), 2.64 (s, 3H, CH_3), 2.08 (s, 6H, CH_3). $^{13}\text{C}\{^1\text{H}\} \text{NMR}$ (CDCl_3 , 100 MHz): δ 145.19 (C=N), 135.17 ($\text{C}_6\text{H}_{3\text{ipso}}$), 127.85 ($\text{C}_6\text{H}_{3\text{ipso}}$), 126.77 (C_6H_3), 124.47 (C_6H_3), 29.00 (CH_3) 17.77 (CH_3).

1.2. Synthesis of the precursor *N,N*-(naphthalene-1,8-diyl)bis(2,2-dimethylpropanimidoyl chloride)

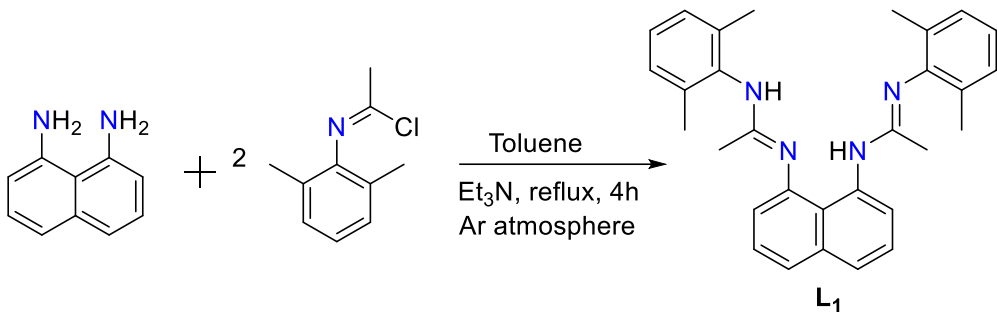


Scheme 19. Synthesis of *N,N*-(naphthalene-1,8-diyl)bis(2,2-dimethylpropanimidoyl chloride).

The procedure of Trifonov *et al.* was followed with some modifications⁸⁶. PCl_5 (6.7 g, 0.032 mol) was added to a solution of *N,N*-(naphthalene-1,8-diyl)bis(2,2-dimethylpropanamide) (5.0 g, 0.015 mol) in toluene (70 mL) to give a green solution, which was stirred at room temperature for 24 h. The solution was filtered, the volatiles were removed in vacuo at room temperature, and the solid residual was extracted with pentane (2 x 30 mL). The pentane extracts were filtered and dried in vacuo at room temperature. A pale-yellow solid was obtained (5.1 g, 0.014 mol, 94 %). $^1\text{H NMR}$ (CDCl_3 , 300 MHz): δ 7.66 (dd, $J_{\text{HH}} = 8.4, 1.1$ Hz, 2H, C_{10}H_6), 7.40 (dd, $J_{\text{HH}} = 8.2, 7.4$ Hz, 2H, C_{10}H_6), 6.63 (dd, $J_{\text{HH}} = 7.4, 1.1$ Hz, 2H, C_{10}H_6), 1.45 (s, 18H, $\text{C}(\text{CH}_3)_3$).

2. Synthesis and characterization of bis-amidine ligands

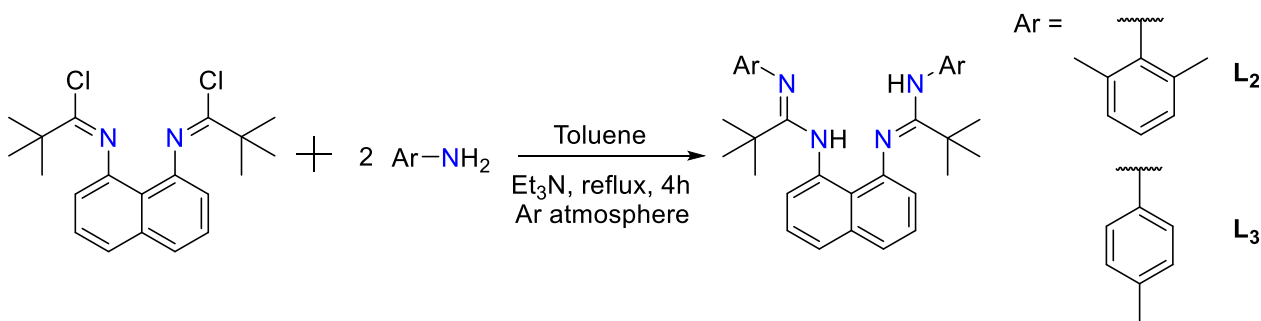
2.1. Synthesis of L₁



Scheme 20. Synthesis of L₁.

The procedure previously reported by our group was followed¹⁸. N-(2,6-dimethylphenyl)acetimidoyl chloride (1.2 g, 6.3 mmol) was added to a solution of 1,8-diaminonaphthalene (500 mg, 3.16 mmol) and Et₃N (0.7 g, 6.3 mmol) in 40 mL of toluene. The reaction was stirred for 4 h under reflux. All volatiles were removed under vacuum. The solid residue was taken up in 30 mL of Et₂O and washed with 15 mL of a saturated solution of Na₂CO₃. Then the organic layer was washed with water (3 x 20 mL) and dried over Na₂SO₄. After that, solvent was removed, and the crude product was recrystallized with CH₂Cl₂/pentane (1:2) to give orange crystals (1.04 g, 2.3 mmol, 74 %). **Melting point:** 136 – 141 °C (decomposition). **¹H NMR** (DMSO-d₆, 400 MHz): δ 11.14 (s, 1H, NH), 8.98 (d, J_{HH} = 7.4 Hz, 1H, C₁₀H₆), 8.78 (s, 1H, NH), 7.45 (d, J_{HH} = 8.0 Hz, 1H, C₁₀H₆), 7.37-7.19 (m, 3H, C₁₀H₆), 7.07-6.93 (m, 5H, C₁₀H₆, C₆H₃), 6.84-6.70 (m, 2H, C₆H₃), 2.30 (s, 6H, CH₃), 2.14 (s, 3H, CH₃), 1.90 (s, 6H, CH₃), 0.85 (s, 3H, CH₃). **¹³C{¹H} NMR** (DMSO-d₆, 100 MHz): δ 156.54 (C=N), 151.84 (C=N), 148.54 (aryl, C_(C6H3)), 146.60 (aryl, C), 138.88 (aryl, C), 136.22 (aryl,C), 135.51 (aryl, C_(C6H3)), 134.60 (aryl, C), 128.18 (aryl, CH_(C6H3)), 127.60 (aryl, CH_(C6H3)), 126.78 (aryl, C), 125.70 (aryl, C), 122.78 (aryl, CH_(C10H6)), 121.21 (aryl, CH_(C6H3)), 120.51 (aryl, CH_(C10H6)), 118.28 (aryl, CH_(C6H3)), 113.06 (aryl, CH_(C10H6)), 18.74 (CH₃), 18.02 (CH₃), 17.82 (CH₃), 17.60 (CH₃). **IR** (KBr, cm⁻¹): 3367 (vNH), 1628 (vC=N). **HRMS** (DCI-CH₄) m/z: 449.2697 ([M + 1]⁺) calcd for C₃₀H₃₃N₄ ([M + 1]⁺) 449.2705.

2.2 Synthesis of L₂ and L₃



Scheme 21. Synthesis of L₂ and L₃.

The procedure of Trifonov *et al.* was followed with some modifications⁸⁶. The corresponding amine (2,6-dimethylaniline (670 mg, 5.6 mmol) for L₂ and *p*-toluidine (591 mg, 5.6 mmol) for L₃) was added to a solution of *N,N'*-(naphthalene-1,8-diyl)bis(2,2-dimethylpropanimidoyl chloride) (1 g, 2.8 mmol) in toluene (50 mL). Then Et₃N (559 mg, 5.6 mmol) was added to the mixture. The reaction was stirred for 4 h under reflux. All volatiles were removed under vacuum. The solid residue was taken up in 40 mL of Et₂O and washed with 25 mL of a saturated solution of Na₂CO₃. Then the organic layer was washed with water (3 x 30 mL) and dried over Na₂SO₄. After that, solvent was removed, and the crude product was recrystallized with CH₂Cl₂/pentane (1:2).

L₂: Yellow crystals were obtained (950 mg, 1.8 mmol, 64 %). **Melting point:** 180 – 183 °C. **¹H NMR** (DMSO-d₆, 500 MHz): δ 9.42 (s, 1H, NH), 8.19 (s, 1H, NH), 6.75-6.57 (m, 6H, aryl), 6.52-6.32 (m, 5H, aryl), 6.20-6.15 (m, 1H, aryl), 2.21 (s, 3H, CH₃), 2.15 (s, 3H, CH₃), 1.88 (s, 3H, CH₃), 1.84 (s, 1H, CH₃), 1.50 (s, 9H, C(CH₃)₃), 1.40 (s, 9H, C(CH₃)₃). **¹³C{¹H} NMR** (DMSO-d₆, 125 MHz): δ 163.76 (C=N), 158.81 (C=N), 146.61 (aryl, C), 137.69 (aryl, C), 136.41 (aryl, C), 134.64 (aryl, C), 127.30 (aryl, CH), 125.11 (Aryl, CH), 123.71 (aryl, CH), 123.63 (aryl, CH), 122.54 (aryl, CH), 121.75 (aryl, CH), 121.03 (aryl, CH), 119.30 (aryl, CH), 116.51 (aryl, C), 115.82 (aryl, CH), 111.50 (aryl, CH), 29.02 (C(CH₃)₃), 28.69 (C(CH₃)₃), 18.48 (CH₃), 18.16 (CH₃), 17.85 (CH₃). **IR** (KBr, cm⁻¹): 3361 (vNH), 1671 (vC=N). **HRMS** (DCI-CH₄) m/z: 531.3491 ([M]⁺) calcd for C₃₆H₄₃N₄ ([M]⁺) 531.3488.

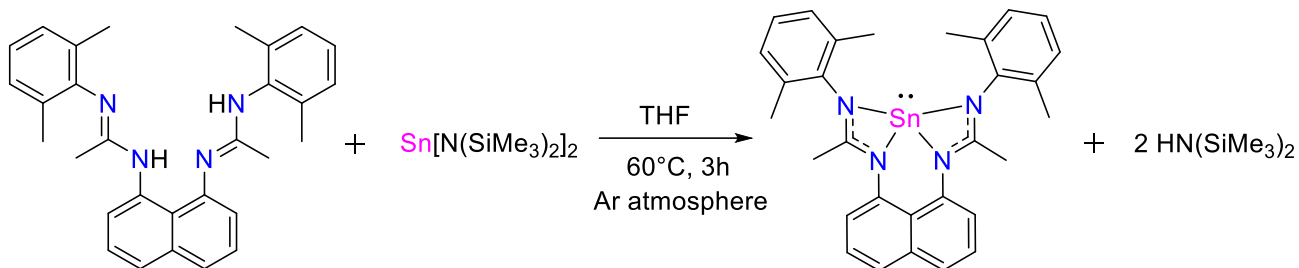
L₃: Yellow crystals were obtained (890 mg, 1.8 mmol, 63 %). **Melting point:** 116 – 122 °C. **¹H NMR** (DMSO-d₆, 500 MHz): δ 9.43 (s, 1H, NH), 8.50 (s, 1H, NH), 7.26 (d, J_{HH} = 6.5 Hz, 1H, aryl), 6.94 (d, J_{HH} = 7.9 Hz, 1H, aryl), 6.88-6.83 (m, 3H, aryl), 6.80 (d, J_{HH} = 8.0 Hz, 3H, aryl), 6.66 (d, J_{HH} = 8.1 Hz, 2H, aryl), 6.58-6.51 (m, 2H, aryl), 6.32-6.20 (m, 2H, aryl), 2.05 (s, 3H, CH₃), 2.01 (s, 3H, CH₃), 1.38 (s, 9H, C(CH₃)₃), 1.23 (s, 9H, C(CH₃)₃). **¹³C{¹H} NMR** (DMSO-d₆, 125 MHz): δ

161.35 (C=N), 160.69 (C=N), 147.20 (aryl, C), 146.55 (aryl, C), 138.60 (aryl, C), 137.20 (aryl, C), 135.57 (aryl, C), 131.25 (aryl, C), 130.42 (aryl, C), 128.74 (aryl, CH), 127.99 (aryl, CH), 127.66 (aryl, CH), 124.83 (aryl, CH), 121.40 (aryl, CH), 120.91 (aryl, CH), 119.77 (aryl, CH), 116.49 (aryl, C), 114.76 (aryl, CH), 28.79 (C(CH₃)₃), 28.28 (C(CH₃)₃), 20.29 (CH₃). **IR** (KBr, cm⁻¹): 3373 (vNH), 1623 (vC=N). **HRMS** (CDI-CH₄) m/z: 504.33 ([M]⁺) calcd for C₃₄H₄₀N₄ ([M]⁺) 504.3253.

3. Synthesis and characterization of stannylenes stabilized by bis-amidine ligands

For the synthesis of the stannylenes, reported procedures for metallylenes were followed^{44,45,87}, but modifying them was to have the best synthetic conditions for the bis-amidine ligands with a rigid naphthalene bridge.

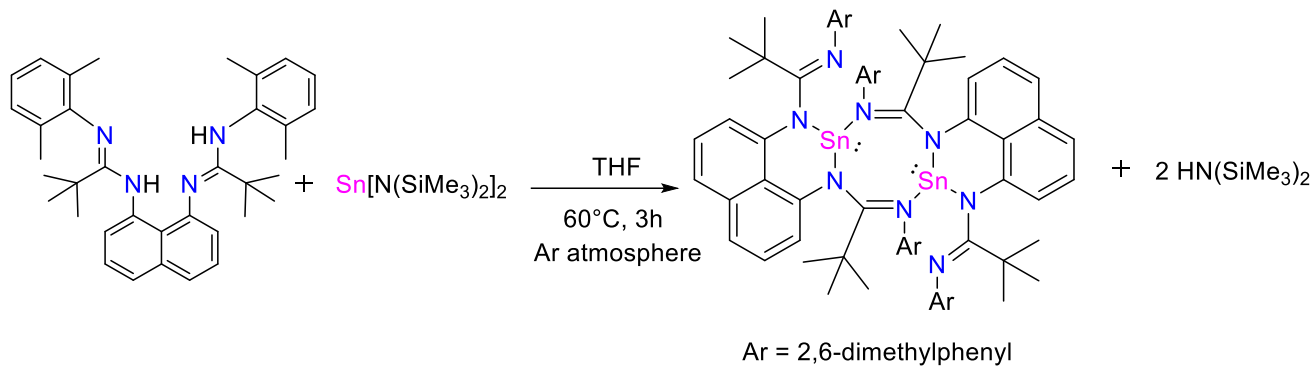
3.1. Synthesis of L₁Sn



Scheme 22. Synthesis of L₁Sn.

THF (5 mL) was added to SnCl₂ (42.3 mg, 0.22 mmol) and K[N(SiMe₃)₂]₂ (89 mg, 0.45 mmol) in a pressure NMR tube inside the glovebox. The mixture was stirred for 30 minutes at room temperature. After this time, a white precipitate was observed. The mixture was filtered, and the solution was added to L₁ (100 mg, 0.22 mmol). Then the resulting solution was stirred at 60 °C for 3 h. After all the volatiles were removed and the solid residual was washed with pentane (3 x 5 mL). The pale-brown solid was recrystallized from pentane at -30 °C. Colorless crystals were obtained (97 mg, 0.17 mmol, 77 %). **Melting point:** 202 °C (decomposition). **¹H NMR** (THF-d₈, 500 MHz): δ 7.42 (dd, J_{HH} = 8.2, 1.1 Hz, 2H, C₁₀H₆), 7.31-7.27 (m, 2H, C₁₀H₆), 7.07 (dd, J_{HH} = 7.5, 1.1 Hz, 2H, C₁₀H₆), 6.96 (d, J_{HH} = 7.4 Hz, 4H, C₆H₃), 6.83 (t, J_{HH} = 7.5 Hz, 2H, C₆H₃), 2.18 (s, 12H, CH₃), 1.97 (s, 6H, CH₃). **¹³C{¹H} NMR** (THF-d₈, 125 MHz): δ 169.03 (NCN), 145.35 (C₆H₃ipso), 144.50 (C₁₀H₆ipso), 138.63 (C₁₀H₆ipso), 134.42 (C₆H₃ipso), 128.84 (C₆H₃), 126.37 (C₁₀H₆), 124.78 (C₆H₃), 123.44 (C₁₀H₆), 119.80 (C₁₀H₆), 20.03 (CH₃), 17.87 (CH₃). **¹¹⁹Sn{¹H} NMR** (THF-d₈, 186 MHz): δ -276.71. **HRMS** (CDI-CH₄) m/z: 565.1518 ([M]⁺) calcd for C₃₀H₃₀N₄ ([M]⁺) 565.1512, 449.27 ([M - Sn]⁺).

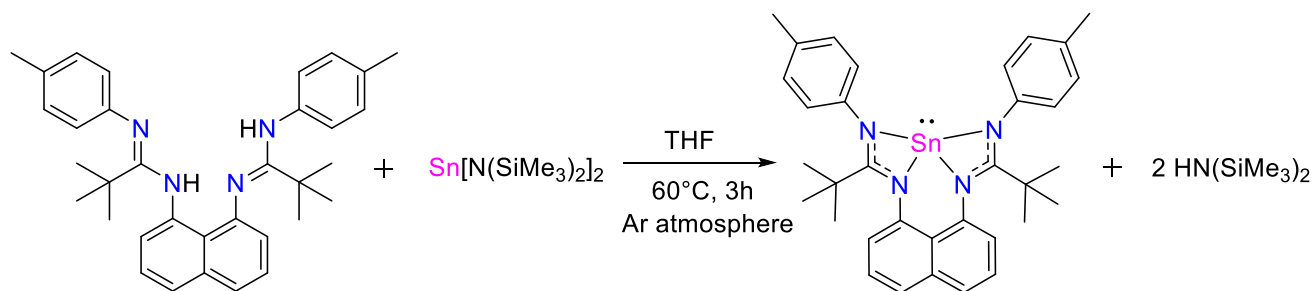
3.2. Synthesis of L₂Sn



Scheme 23. Synthesis of L₂Sn.

THF (5 mL) was added to SnCl₂ (35.6 mg, 0.19 mmol) and K[N(SiMe₃)₂]₂ (75 mg, 0.38 mmol) in a pressure NMR tube inside the glovebox. The mixture was stirred for 30 minutes at room temperature. After this time, a white precipitate was observed. The mixture was filtered, and the solution was added to L₂ (100 mg, 0.19 mmol). Then the resulting solution was stirred at 60 °C for 3 h. Yellow crystals were observed and separated from the solution by filtration. After the crystals were washed with pentane (3 x 2 mL). Yellow crystals were obtained (132 mg, 0.083 mmol, 44 %). **Melting point:** 243 °C (decomposition). **MS** (Maldi-TOF) m/z: 649.3 ([M/2, monomer]⁺). Meaningful solution state spectroscopic data for the compound could not be obtained for the compound as it shows negligible solubility in normal non-coordinating deuterated solvents once crystallized.

3.3. Synthesis of L₃Sn



Scheme 24. Synthesis of L₃Sn.

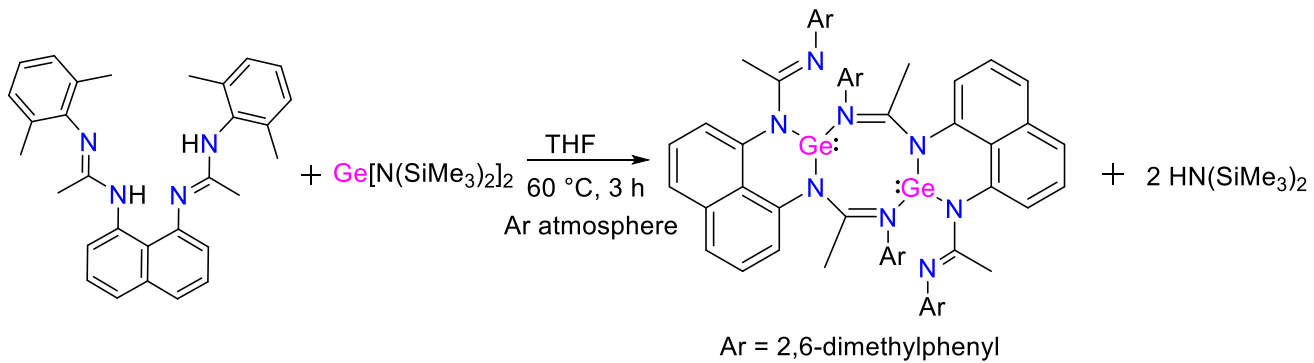
THF (5 mL) was added to SnCl₂ (38 mg, 0.20 mmol) and K[N(SiMe₃)₂]₂ (79 mg, 0.40 mmol) in a pressure NMR tube inside the glovebox. The mixture was stirred for 30 minutes at room

temperature. After this time, a white precipitate was observed. The mixture was filtered, and the solution was added to **L**₃ (100 mg, 0.20 mmol). Then the resulting solution was stirred at 60 °C for 3 h. After all the volatiles were removed and the solid residual was washed with pentane (3 x 5 mL). A yellow solid was obtained (76 mg, 0.12 mmol, 61 %). **Melting point:** 189 °C (decomposition). ¹**H NMR** (THF-d₈, 400 MHz): δ 7.38 (d, *J*_{HH} = 7.5 Hz, 2H, C₁₀H₆), 7.24-7.19 (m, 2H, C₁₀H₆), 7.09 (d, *J*_{HH} = 7.1 Hz, 2H, C₁₀H₆), 7.05 (d, *J*_{HH} = 8.0 Hz, 4H, C₆H₄), 6.97 (d, *J*_{HH} = 8.2 Hz, 4H, C₆H₄), 2.29 (s, 6H, CH₃), 1.30 (s, 18H, C(CH₃)₃). ¹³**C{¹H} NMR** (THF-d₈, 125 MHz): δ 177.53 (NCN), 146.67 (C₆H_{4ipso}), 145.74 (C₁₀H_{6ipso}), 138.36 (C₁₀H_{6ipso}), 132.96 (C₆H_{4ipso}), 130.40 (C₆H₄), 126.28 (C₁₀H₆), 124.95 (C₆H₄), 123.36 (C₁₀H₆), 121.33 (C₁₀H₆), 43.65 (C(CH₃)₃), 31.85 (C(CH₃)₃), 21.04 (CH₃). ¹¹⁹**Sn{¹H} NMR** (THF-d₈, 186 MHz): δ -254.87. **MS** (Maldi-TOF) m/z: 621.2 ([M]⁺), 503.4 ([M - Sn]⁺).

4. Synthesis and characterization of germynes stabilized by bis-amidine ligands

For the synthesis of the germynes, reported procedures for metallylenes were followed^{44,45,87}, but modifying them was to have the best synthetic conditions for the bis-amidine ligands with a rigid naphthalene bridge.

4.1. Synthesis of L₁Ge

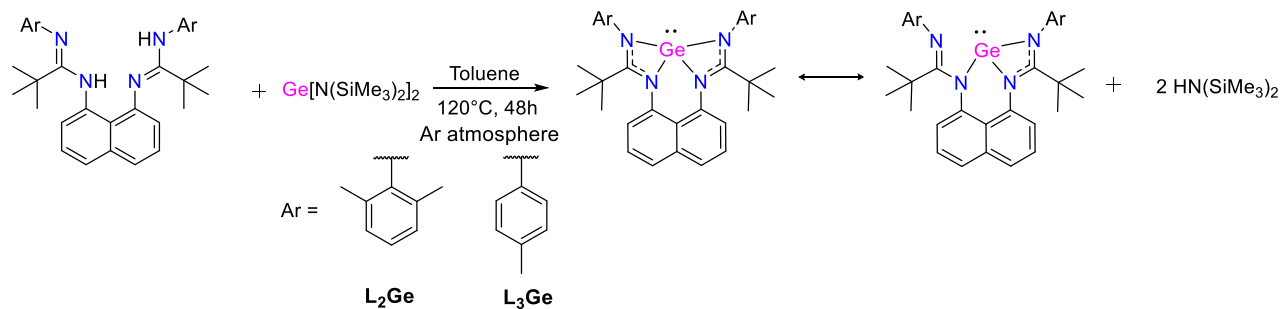


Scheme 25. Synthesis of L₁Ge.

THF (5 mL) was added to GeCl₂•(dioxane) (51.7 mg, 0.22 mmol) and K[N(SiMe₃)₂] (89 mg, 0.45 mmol) in a pressure NMR tube inside the glovebox. The mixture was stirred for 30 minutes at room temperature. After this time, a white precipitate was observed. The mixture was filtered, and the solution was added to **L**₁ (100 mg, 0.22 mmol). Then the resulting solution was stirred at 60 °C for 3 h. Yellow crystals were observed and separated from the solution by filtration. After the crystals were washed with pentane (3 x 2 mL). Yellow crystals were obtained (97 mg, 0.093

mmol, 42 %). **Melting point:** 259 °C (decomposition). **MS** (Maldi-TOF) m/z: 519.14 ([M/2, monomer]⁺). Meaningful solution state spectroscopic data for the compound could not be obtained for the compound as it shows negligible solubility in normal non-coordinating deuterated solvents once crystallized.

4.2. Synthesis general of L₂Ge and L₃Ge



Scheme 26. Synthesis of L_2Ge and L_3Ge .

L₂Ge: Toluene (5 mL) was added to GeCl_2 •(dioxane) (26 mg, 0.11 mmol) and $\text{K}[\text{N}(\text{SiMe}_3)_2]_2$ (44 mg, 0.22 mmol) in a pressure NMR tube inside the glovebox. The mixture was stirred for 1 h at room temperature. After this time, a white precipitate was observed. The mixture was filtered, and the solution was added to L_2 (60 mg, 0.11 mmol). Then the resulting solution was stirred at 120 °C for 48 h. After all the volatiles were removed and the solid residual was washed with pentane (3 x 5 mL). The yellow solid was recrystallized from pentane at -30 °C. Yellow crystals were obtained (35 mg, 0.058 mmol, 52 %). **Melting point:** 199 °C (decomposition). **¹H NMR** (C_6D_6 , 300 MHz): δ 6.98-6.91 (m, 2H, C_{10}H_6), 6.89-6.81 (m, 2H, C_{10}H_6), 6.62 (d, $J_{\text{HH}} = 7.7$ Hz, 4H, C_6H_3), 6.47-6.40 (m, 2H, C_6H_3), 6.33 (d, $J_{\text{HH}} = 6.3$ Hz, 2H, C_{10}H_6), 2.18 (s, 12H, CH_3), 1.60 (s, 18H, $\text{C}(\text{CH}_3)_3$). **¹³C{¹H} NMR** (C_6D_6 , 125 MHz): δ 170.95 (NCN), 151.81 ($\text{C}_6\text{H}_{3\text{ipso}}$), 148.81 ($\text{C}_{10}\text{H}_{6\text{ipso}}$), 139.68 ($\text{C}_{10}\text{H}_{6\text{ipso}}$), 138.54 ($\text{C}_6\text{H}_{3\text{ipso}}$), 128.35 (C_6H_3), 126.31 (C_{10}H_6), 120.36 (C_6H_3), 114.90 (C_{10}H_6), 108.76 (C_{10}H_6), 41.87 ($\text{C}(\text{CH}_3)_3$), 30.60 ($\text{C}(\text{CH}_3)_3$), 19.68 (CH_3).

L₃Ge: Toluene (5 mL) was added to GeCl_2 •(dioxane) (28 mg, 0.12 mmol) and $\text{K}[\text{N}(\text{SiMe}_3)_2]_2$ (48 mg, 0.24 mmol) in a pressure NMR tube inside the glovebox. The mixture was stirred for 1 h at room temperature. After this time, a white precipitate was observed. The mixture was filtered, and the solution was added to L_3 (60 mg, 0.12 mmol). Then the resulting solution was stirred at 120 °C for 48 h. After all the volatiles were removed and a yellow solid residual was obtained. Despite multiple attempts to purify the resulting solid, it was not possible. **¹H NMR** (C_6D_6 , 300

MHz): δ 7.10-7.06 (m, 2H, C₁₀H₆), 7.06-7.02 (m, 2H, C₁₀H₆), 7.02-6.96 (m, 2H, C₁₀H₆), 6.91 (d, J_{HH} = 8.2 Hz, 4H, C₆H₄), 6.71 (d, J_{HH} = 7.8 Hz, 4H, C₆H₄), 1.45 (s, 6H, CH₃), 1.23 (s, 18H, C(CH₃)₃).

5. Metallylenes reactivity

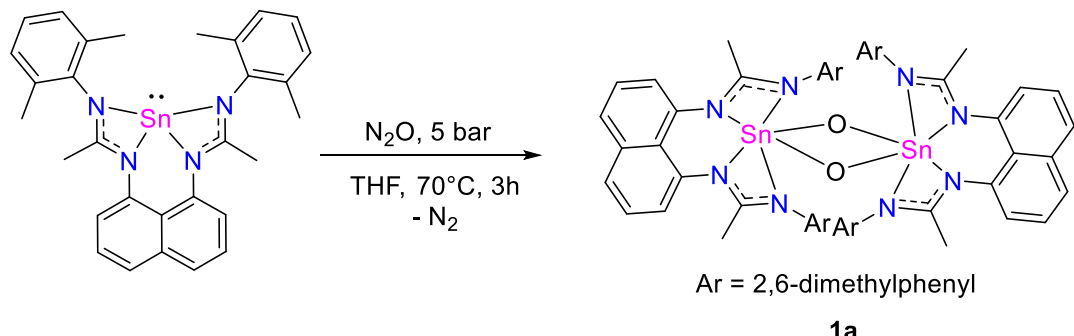
5.1. Metallylenes reactivity: polymerization of ϵ -caprolactone

5.1.1. General procedure for ϵ -caprolactone polymerization tests

In a Schlenk tube, catalyst was dissolved in toluene (2 mL) and stirred for 10 min. Then ϵ -caprolactone (1 g, 8.76 mmol) was added and the mixture stirred at the indicated temperature for the desire time. Aliquots (0.2 mL) were dissolved in CDCl₃ (0.4 mL) with a small amount of benzoic acid and conversions were determined by ¹H NMR analysis. Then the mixture was treated at the end of reaction by addition of benzoic acid. The mixture was then evaporated and CH₂Cl₂ was added. The solution was cooled with liquid nitrogen and methanol was added dropwise to try to precipitate the polymer, but in all the case an oil was obtained.

5.2. Metallylenes reactivity: oxidation

5.2.1. Synthesis of 1a - Reaction of L₁Sn with N₂O

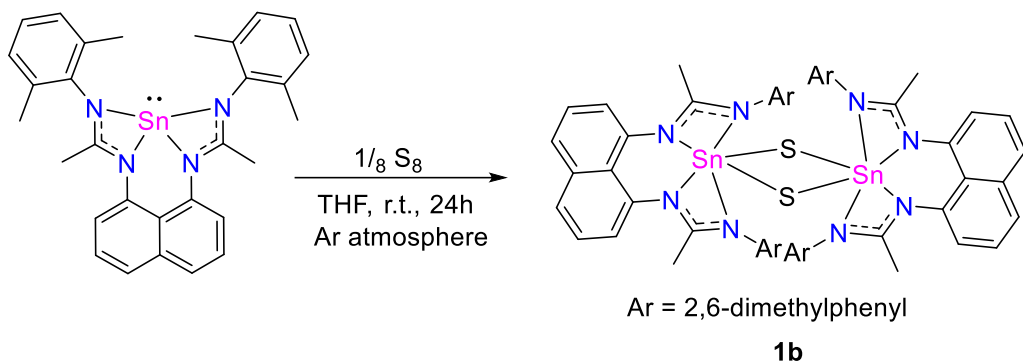


Scheme 27. Synthesis of 1a.

In a pressure NMR tube, a THF (0.4 mL) solution of L₁Sn (30 mg, 0.053 mmol) was exposed to 5 bar of N₂O. The reaction was monitored by NMR and proceeded quantitatively after 3 h at 70 °C. Colorless crystals were observed and separated from the solution by filtration. After the crystals were washed with pentane (3 x 2 mL). Colorless crystals were obtained (32 mg, 0.024 mmol, 46 %). **Melting point:** 204 °C. ¹H NMR (THF-d₈, 500 MHz): δ 7.42 (d, J_{HH} = 6.4 Hz, 4H,

C_{10}H_6), 7.26 (t, $J_{\text{HH}} = 7.8$ Hz, 4H, C_{10}H_6), 7.13 (d, $J_{\text{HH}} = 6.8$ Hz, 4H, C_{10}H_6), 7.01 (s, 4H, C_6H_3), 6.92-6.83 (m, 8H, C_6H_3), 2.07 (s, 12H, CH_3), 1.85 (s, 12H, CH_3), 1.76 (s, 12H, CH_3). $^{13}\text{C}\{\text{H}\}$ NMR (THF-d₈, 125 MHz): δ 168.70 (NCN), 143.64 ($\text{C}_6\text{H}_{3\text{ipso}}$), 142.68 ($\text{C}_{10}\text{H}_{6\text{ipso}}$), 138.50 ($\text{C}_{10}\text{H}_{6\text{ipso}}$), 136.98 ($\text{C}_{10}\text{H}_{6\text{ipso}}$), 135.26 ($\text{C}_6\text{H}_{3\text{ipso}}$), 128.74 (C_6H_3), 128.31 (C_6H_3), 126.26 (C_{10}H_6), 125.69 (C_6H_3), 124.81 (C_{10}H_6), 120.59 (C_{10}H_6), 19.81 (CH_3), 19.03 (CH_3), 15.76 (CH_3). $^{119}\text{Sn}\{\text{H}\}$ NMR (THF-d₈, 186 MHz): δ -494.50. MS (Maldi-TOF) m/z: 1161.26 ([M]⁺), 583.13 ([M/2, monomer]⁺).

5.2.2. Synthesis of 1b - Reaction of L₁Sn with S₈

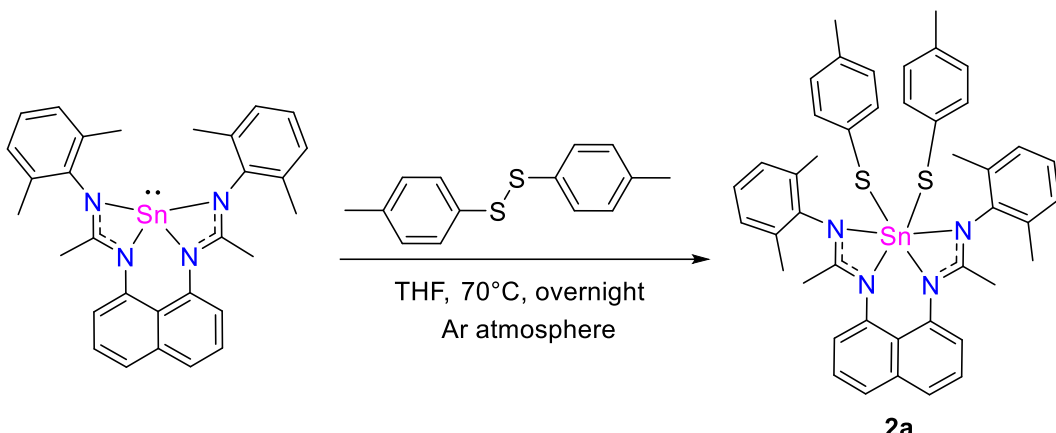


Scheme 28. Synthesis of **1b**.

THF (0.4 mL) was added to **L₁Sn** (50 mg, 0.088 mmol) and S₈ (2.8 mg, 0.011 mmol) in a pressure NMR tube. The mixture was stirred for 24 h at room temperature. After the solvent was removed and the solid residual was washed with pentane (3 x 0.5 mL). The pale-yellow solid was recrystallized from THF at -30 °C. Pale-yellow crystals were obtained (42 mg, 0.045 mmol, 51 %). **Melting point:** 229 °C (decomposition). ^1H NMR (THF-d₈, 300 MHz): δ 7.40 (d, $J_{\text{HH}} = 7.5$ Hz, 4H, C_{10}H_6), 7.22 (t, $J_{\text{HH}} = 7.8$ Hz, 4H, C_{10}H_6), 7.11-7.02 (m, 4H, C_{10}H_6), 6.93 (s, 12H, C_6H_3), 2.11 (br s, 24H, CH_3), 1.75 (s, 12H, CH_3). $^{13}\text{C}\{\text{H}\}$ NMR (THF-d₈, 125 MHz): δ 167.43 (NCN), 142.70 ($\text{C}_{10}\text{H}_{6\text{ipso}}$), 138.23 ($\text{C}_{10}\text{H}_{6\text{ipso}}$), 135.88 ($\text{C}_6\text{H}_{3\text{ipso}}$), 128.79 (C_6H_3), 126.43 (C_{10}H_6), 125.72 (C_6H_3), 124.85 (C_{10}H_6), 121.55 (C_{10}H_6), 19.70 (CH_3), 16.44 (CH_3). $^{119}\text{Sn}\{\text{H}\}$ NMR (THF-d₈, 186 MHz): δ -647.99. MS (Maldi-TOF) m/z: 1193.10 ([M]⁺), 597.04 ([M/2, monomer]⁺).

5.3. Metallylenes reactivity: oxidative addition

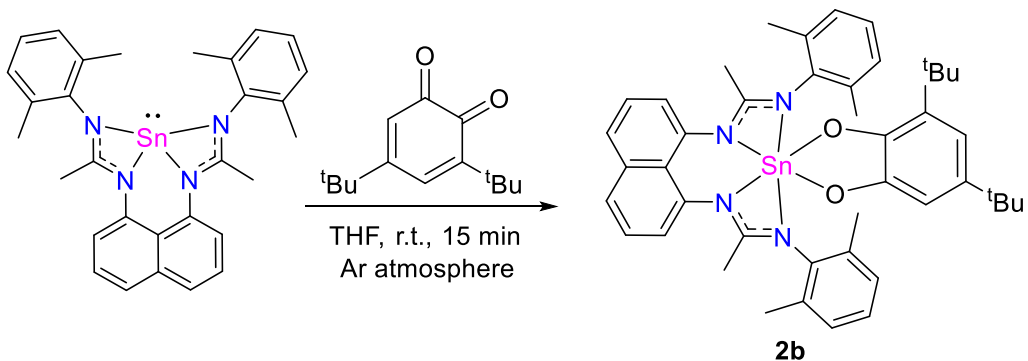
5.3.1. Synthesis of 2a - Reaction of L₁Sn with disulfide



Scheme 29. Synthesis of **2a**.

THF (0.4 mL) was added to **L₁Sn** (40 mg, 0.071 mmol) and *p*-tolyldisulfide (17 mg, 0.071 mmol) in a pressure NMR tube. The mixture was stirred overnight at 70°C. After the solvent was removed and the solid residual was washed with pentane (3 x 0.5 mL). The pale-brown solid was recrystallized from pentane at -30 °C. Pale-brown crystals were obtained (41 mg, 0.051 mmol, 51 %). **Melting point:** 199 °C. **¹H NMR** (THF-d₈, 500 MHz): δ 7.40 (dd, *J*_{HH} = 8.1, 1.1 Hz, 2H, C₁₀H₆), 7.25-7.21 (m, 2H, C₁₀H₆), 7.17 (dd, *J*_{HH} = 7.5, 1.2 Hz, 2H, C₁₀H₆), 7.05-6.96 (m, 6H, C₆H₃), 6.63 (d, *J*_{HH} = 8.1 Hz, 4H, C₆H₄), 6.44 (d, *J*_{HH} = 7.9 Hz, 4H, C₆H₄), 2.19 (s, 12H, CH₃), 2.09 (s, Sn satellite: *J*_{HSn} = 7.3 Hz, 6H, CH₃), 1.79 (s, Sn satellite: *J*_{HSn} = 2.4 Hz, 6H, C₆H₃). **¹³C{¹H} NMR** (THF-d₈, 125 MHz): δ 168.82 (NCN), 143.78 (Sn satellite: *J*_{CSn} = 5.2 Hz, C₁₀H_{6ipso}), 143.31 (Sn satellite: *J*_{CSn} = 7.2 Hz, C₆H₃), 138.36 (Sn satellite: *J*_{CSn} = 3.3 Hz, C₁₀H_{6ipso}), 136.11 (Sn satellite: *J*_{CSn} = 12.8 Hz, C₆H₄), 135.62 (Sn satellite: *J*_{CSn} = 3.1 Hz, C₆H₃), 135.54 (C₆H_{4ipso}), 131.44 (C₆H_{4ipso}), 129.18 (C₆H₃), 128.97 (Sn satellite: *J*_{CSn} = 6.6 Hz, C₆H₄), 127.57 (C₁₀H_{6ipso}), 126.42 (C₁₀H₆), 126.45 (C₆H₃), 125.22 (C₁₀H₆), 121.12 (Sn satellite: *J*_{CSn} = 11.2 Hz, C₁₀H₆), 21.14 (CH₃), 19.89 (CH₃), 16.42 (Sn satellite: *J*_{CSn} = 21.40 Hz, CH₃). **¹¹⁹Sn{¹H} NMR** (THF-d₈, 186 MHz): δ -456.70. **MS** (Maldi-TOF) m/z: 687.13 ([M – S(tolyl)]⁺), 565.05 ([M – 2 S(tolyl)]⁺).

5.3.2. Synthesis of 2b - Reaction of L₁Sn with ortho-quinone

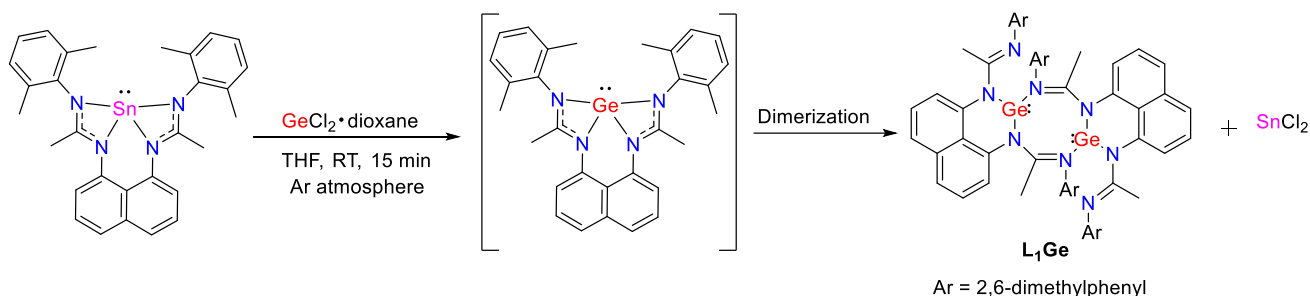


Scheme 30. Synthesis of **2b**.

THF (0.4 mL) was added to **L₁Sn** (30 mg, 0.053 mmol) and 3,5-di-tert-butyl-o-benzoquinone (12 mg, 0.053 mmol) in a pressure NMR tube. The mixture was stirred for 15 minutes at room temperature. After the solvent was removed and the solid residual was washed with pentane (3 x 0.5 mL). A white solid was obtained (43 mg, 0.051 mmol, 96 %). **Melting point:** 240 °C (decomposition). **¹H NMR** (THF-d₈, 500 MHz): δ 7.65-7.62 (m, 2H, C₁₀H₆), 7.44-7.39 (m, 4H, C₁₀H₆), 6.98-6.92 (m, 6H, C₆H₃), 6.57 (d, J_{HH} = 2.4 Hz, 1H, C₆H₂), 6.39 (d, J_{HH} = 2.4 Hz, 1H, C₆H₂), 2.08 (s, 12H, CH₃), 2.00 (s, Sn satellite: J_{HSn} = 3.5 Hz, 6H, CH₃), 1.16 (s, 9H, C(CH₃)₃), 1.06 (s, 9H, C(CH₃)₃). **¹³C{¹H} NMR** (THF-d₈, 125 MHz): δ 171.64 (NCN), 151.28 (Sn satellite: J_{CSn} = 5.1 Hz, C₆H_{2ipso}), 147.12 (Sn satellite: J_{CSn} = 3.3 Hz, C₆H_{2ipso}), 142.03 (Sn satellite: J_{CSn} = 3.9 Hz, C₁₀H_{6ipso}), 140.91 (Sn satellite: J_{CSn} = 7.5 Hz, C₆H_{3ipso}), 138.70 (C₆H_{2ipso}), 138.55 (C₁₀H_{6ipso}), 136.08 (C₆H_{3ipso}), 134.10 (C₆H_{2ipso}), 129.09 (C₆H₃), 127.10 (C₆H₃), 126.75 (C₁₀H₆), 126.15 (C₁₀H_{6ipso}), 126.05 (C₁₀H₆), 121.21 (Sn satellite: J_{CSn} = 11.6 Hz, C₁₀H₆), 111.50 (C₆H₂), 110.27 (Sn satellite: J_{CSn} = 40.2 Hz, C₆H₂), 35.33 (C(CH₃)₃), 34.87 (C(CH₃)₃), 32.44 (C(CH₃)₃), 30.16 (C(CH₃)₃), 19.12 (CH₃), 15.49 (Sn satellite: J_{CSn} = 33.7 Hz, CH₃). **¹¹⁹Sn{¹H} NMR** (THF-d₈, 186 MHz): δ -512.16. **HRMS** (DCI-CH₄) m/z: 786.2988 ([M]⁺) calcd for C₄₄H₅₀N₄O₂Sn ([M]⁺) 786.2956.

5.4. Metallylenes reactivity: transmetalation

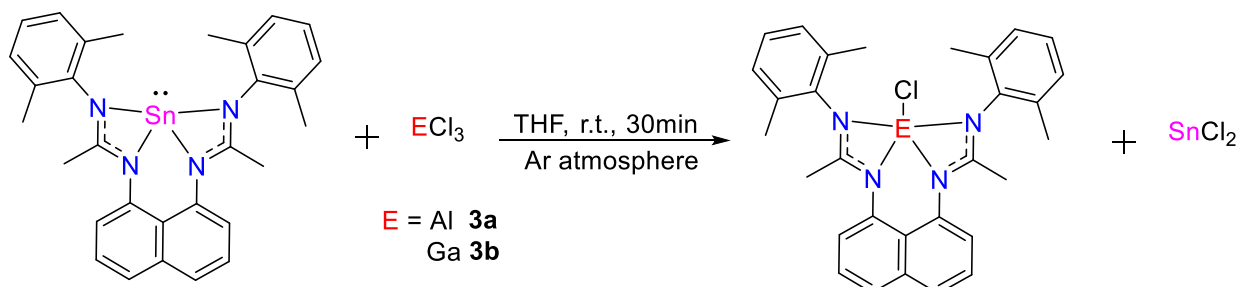
5.4.1. Synthesis of $\mathbf{L}_1\mathbf{Ge}$ - Reaction of $\mathbf{L}_1\mathbf{Sn}$ with $\mathbf{GeCl}_2\bullet(\text{dioxane})$



Scheme 31. Synthesis of $\mathbf{L}_1\mathbf{Ge}$ via transmetalation.

THF (0.4 mL) was added to $\mathbf{L}_1\mathbf{Sn}$ (30 mg, 0.053 mmol) and $\mathbf{GeCl}_2\bullet(\text{dioxane})$ (12 mg, 0.053 mmol) in a vial. The mixture was stirred for 15 minutes at room temperature. A yellow precipitate was observed and separated from the solution by filtration. After the solid was washed with pentane (3×2 mL). A yellow solid was obtained (55 mg, 0.047 mmol, 88 %). Characterization in section 4.1.

5.4.2. Synthesis of $\mathbf{3a}$ and $\mathbf{3b}$ - Reaction of $\mathbf{L}_1\mathbf{Sn}$ with \mathbf{AlCl}_3 and \mathbf{GaCl}_3



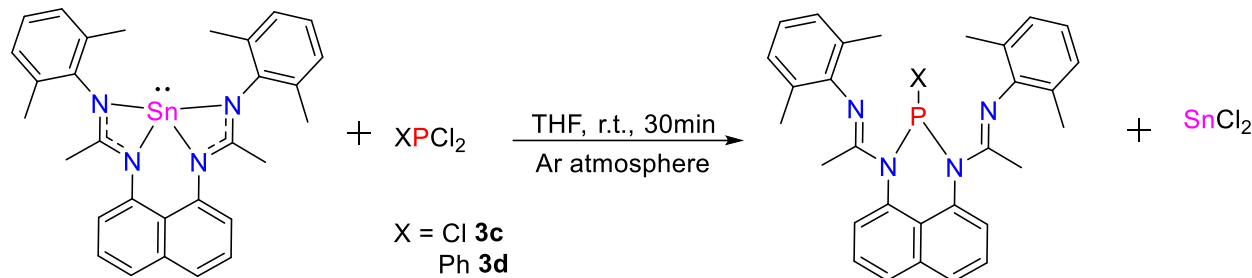
Scheme 32. Synthesis of $\mathbf{3a}$ and $\mathbf{3b}$.

3a: THF (1 mL) was added to $\mathbf{L}_1\mathbf{Sn}$ (60.0 mg, 0.11 mmol) and \mathbf{AlCl}_3 (14.2 mg, 0.11 mmol) in a vial. The mixture was stirred for 30 minutes at room temperature. After the solvent was removed and the solid residual was washed with pentane (3×0.5 mL). A white solid was obtained (48 mg, 0.093 mmol, 85 %). **Melting point:** 124 °C. **$^1\text{H NMR}$** (THF-d_8 , 500 MHz): δ 7.46 (dd, $J_{\text{HH}} = 8.3, 1.1$ Hz, 2H, C_{10}H_6), 7.35-7.31 (m, 2H, C_{10}H_6), 7.24 (dd, $J_{\text{HH}} = 7.5, 1.2$ Hz, 2H, C_{10}H_6), 7.02-

6.90 (m, 6H, C₆H₃), 2.33 (s, 6H, CH₃), 2.13 (s, 6H, CH₃), 1.90 (s, 6H, CH₃). ¹³C{¹H} NMR (THF-d₈, 125 MHz): δ 176.45 (NCN), 141.87 (C₁₀H_{6ipso}), 141.80 (C₁₀H_{6ipso}), 140.58 (C₆H_{3ipso}), 138.39 (C₁₀H_{6ipso}), 135.82 (C₆H_{3ipso}), 135.12 (C₆H_{3ipso}), 129.42 (C₆H₃), 128.78 (C₆H₃), 126.58 (C₁₀H₆), 126.23 (C₆H₃), 124.12 (C₁₀H₆), 123.89 (C₁₀H_{6ipso}), 117.80 (C₁₀H₆), 19.95 (CH₃), 19.31 (CH₃), 15.59 (CH₃). ²⁷Al{¹H} NMR (THF-d₈, 130 MHz): δ 69.44.

3b: THF (1 mL) was added to **L₁Sn** (60.0 mg, 0.11 mmol) and GaCl₃ (18.6 mg, 0.11 mmol) in a vial. The mixture was stirred for 30 minutes at room temperature. After the solvent was removed and the solid residual was washed with pentane (3 x 0.5 mL). The white solid was recrystallized from pentane at -30 °C. Colorless crystals were obtained (54 mg, 0.098 mmol, 88 %). **Melting point:** 209 °C (decomposition). ¹H NMR (THF-d₈, 500 MHz): δ 7.46 (dd, J_{HH} = 8.3, 1.1 Hz, 2H, C₁₀H₆), 7.34-7.30 (m, 2H, C₁₀H₆), 7.20 (dd, J_{HH} = 7.5, 1.2 Hz, 2H, C₁₀H₆), 7.03-6.90 (m, 6H, C₆H₃), 2.34 (s, 6H, CH₃), 2.12 (s, 6H, CH₃), 1.98 (s, 6H, CH₃). ¹³C{¹H} NMR (THF-d₈, 125 MHz): δ 172.26 (NCN), 142.89 (C₁₀H_{6ipso}), 141.93 (C₆H_{3ipso}), 138.58 (C₁₀H_{6ipso}), 136.09 (C₆H_{3ipso}), 135.47 (C₆H_{3ipso}), 128.84 (C₆H₃), 126.40 (C₁₀H₆), 126.40 (C₆H₃), 124.34 (C₁₀H₆), 123.11 (C₁₀H_{6ipso}), 118.35 (C₁₀H₆), 19.77 (CH₃), 15.08 (CH₃). **MS** (Maldi-TOF) m/z: 551.06 ([M]⁺), 517.04 ([M - Cl]⁺), 449.10 ([M - GaCl]⁺).

5.4.3. Synthesis of **3c** and **3d** - Reaction of **L₁Sn** with PCl₃ and PhPCl₂



Scheme 33. Synthesis of **3c** and **3d**.

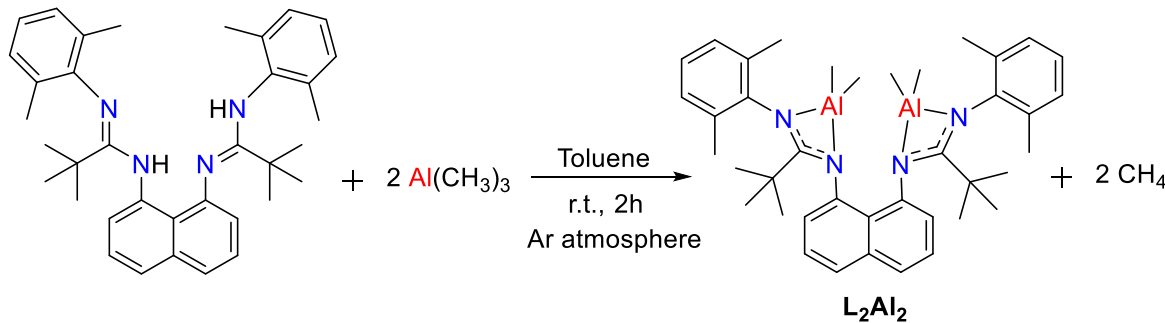
3c: PCl₃ (24.3 mg, 0.18 mmol) was added to a solution of **L₁Sn** (100 mg, 0.18 mmol) in THF (2 mL). The mixture was stirred for 30 minutes at room temperature. After the solvent was removed and the solid residual was washed with pentane (3 x 0.5 mL). The white solid was recrystallized from pentane at -30 °C. Colorless crystals were obtained (75 mg, 0.15 mmol, 81%). **Melting point:** 213 °C (decomposition). ¹H NMR (THF-d₈, 400 MHz): δ 7.62 (d, J_{HH} = 7.9 Hz, 2H, C₁₀H₆), 7.50-7.44 (m, 2H, C₁₀H₆), 7.09-7.00 (m, 4H, C₆H₃), 6.92-6.85 (m, 4H, C₁₀H₆, C₆H₃), 2.24 (s, 6H, CH₃), 2.15 (s, 6H, CH₃), 2.05 (s, 3H, CH₃), 2.04 (s, 3H, CH₃). ¹³C{¹H} NMR (THF-d₈, 100 MHz):

δ 158.83 (d, J_{CP} = 18.8 Hz, NCN), 147.60 (C_6H_{3ipso}), 136.60 ($C_{10}H_{6ipso}$), 135.29 (d, J_{CP} = 4.3 Hz, $C_{10}H_{6ipso}$), 128.95 (d, J_{CP} = 2.6 Hz, C_6H_3), 127.50 ($C_{10}H_6$), 127.26 (C_6H_{3ipso}), 124.47 ($C_{10}H_6$), 124.11 (C_6H_3), 119.96 ($C_{10}H_{6ipso}$), 117.26 ($C_{10}H_6$), 19.28 (CH_3), 18.90 (d, J_{CP} = 6.9 Hz, CH_3), 18.59 (CH_3). $^{31}P\{^1H\}$ NMR (THF-d₈, 161 MHz): δ 77.10. MS (Maldi-TOF) m/z: 477.4 ([M – Cl]⁺).

3d: PhPCl₂ (32.2 mg, 0.18 mmol) was added to a solution of **L₁Sn** (100 mg, 0.18 mmol) in THF (2 mL). The mixture was stirred for 30 minutes at room temperature. After the solvent was removed and the solid residual was washed with pentane (3 x 0.5 mL). The white solid was recrystallized from pentane at -30 °C. Colorless crystals were obtained (77 mg, 0.14 mmol, 77 %). **Melting point:** 210 °C (decomposition). 1H NMR (THF-d₈, 500 MHz): δ 7.66-7.61 (m, 2H, C_6H_5), 7.41-7.38 (m, 2H, $C_{10}H_6$), 7.34-7.30 (m, 2H, $C_{10}H_6$), 7.09-6.97 (m, 9H, $C_{10}H_6$, C_6H_3 , C_6H_5), 6.86 (C_6H_3), 2.32 (s, 6H, CH_3), 2.22 (s, 6H, CH_3), 2.10 (overlapped, 6H, CH_3). $^{13}C\{^1H\}$ NMR (THF-d₈, 125 MHz): δ 160.78 (d, J_{CP} = 19.0 Hz, NCN), 148.62 (C_6H_{3ipso}), 141.36 (d, J_{CP} = 24.1 Hz, C_6H_{5ipso}), 137.45 (d, J_{CP} = 3.9 Hz, $C_{10}H_{6ipso}$), 136.48 ($C_{10}H_{6ipso}$), 131.68 (d, J_{CP} = 16.4 Hz, C_6H_5), 129.11 (d, J_{CP} = 1.4 Hz, C_6H_5), 128.91 (C_6H_3), 128.78 (C_6H_3), 128.61 (d, J_{CP} = 2.9 Hz, C_6H_5), 127.55 (C_6H_{3ipso}), 127.48 (C_6H_{3ipso}), 126.61 ($C_{10}H_6$), 124.06 ($C_{10}H_6$), 123.60 (C_6H_3), 120.53 ($C_{10}H_{6ipso}$), 118.95 ($C_{10}H_6$), 19.25 (CH_3), 19.22 (CH_3), 19.10 (d, J_{CP} = 5.0 Hz, CH_3), 18.91 (CH_3). $^{31}P\{^1H\}$ NMR (THF-d₈, 202 MHz): δ 58.45. MS (Maldi-TOF) m/z: 555.3 ([M]⁺).

6. Synthesis and characterization of aluminum complexes stabilized by bis-amidine ligands (**L₁**)

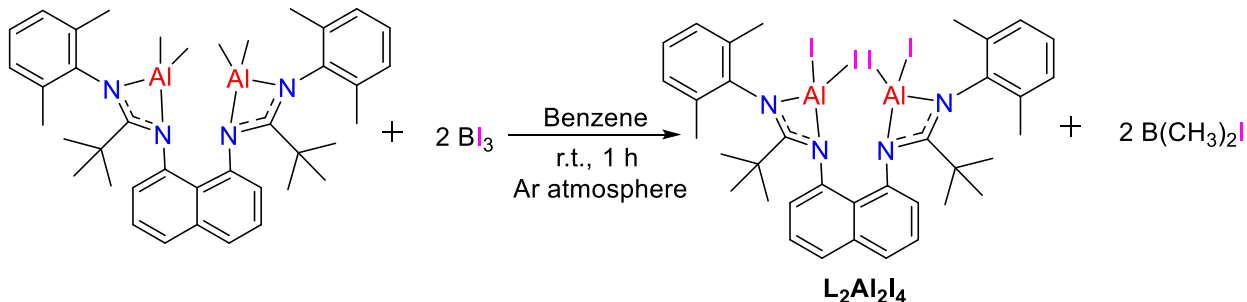
6.1. Synthesis of **L₂Al₂**



Scheme 34. Synthesis of **L₂Al₂**.

A 2 M solution of $\text{Al}(\text{CH}_3)_3$ in heptane (1.9 mL, 3.8 mmol) was added to a solution of **L₁** (1.0 g, 1.9 mmol) in toluene (20 mL) in a Schlenk. The mixture was stirred for 2 h at room temperature. After the solvent was removed and the solid residual was washed with pentane (5 x 10 mL). The orange solid was recrystallized from pentane at -30 °C. Orange crystals were obtained (1.07 g, 1.7 mmol, 83 %). **Melting point:** 200 °C. **¹H NMR** (C_6D_6 , 500 MHz): δ 7.44 (dd, $J_{\text{HH}} = 8.1, 1.0$ Hz, 2H, C_{10}H_6), 7.18-7.16 (overlapped, 2H, C_{10}H_6), 7.11-7.07 (m, 2H, C_{10}H_6), 7.00-6.91 (m, 6H, C_6H_3), 2.55 (s, 6H, CH_3), 2.52 (s, 6H, CH_3), 0.95 ($\text{C}(\text{CH}_3)_3$), -0.02 ($\text{CH}_3\text{-Al}$), -0.33 ($\text{CH}_3\text{-Al}$). **¹³C{¹H} NMR** (C_6D_6 , 125 MHz): δ 186.91 (NCN), 144.61 ($\text{C}_{10}\text{H}_{6\text{ipso}}$), 142.43 ($\text{C}_6\text{H}_{3\text{ipso}}$), 137.94 ($\text{C}_{10}\text{H}_{6\text{ipso}}$), 133.91 ($\text{C}_6\text{H}_{3\text{ipso}}$), 132.77 ($\text{C}_6\text{H}_{3\text{ipso}}$), 128.95 (C_6H_3), 128.73 (C_6H_3), 127.11 ($\text{C}_{10}\text{H}_{6\text{ipso}}$), 126.63 (C_{10}H_6), 126.55 (C_{10}H_6), 125.73 (C_{10}H_6), 125.09 (C_{10}H_6), 41.26 ($\text{C}(\text{CH}_3)_3$), 29.84 ($\text{C}(\text{CH}_3)_3$), 20.69 (CH_3), 20.49 (CH_3), -5.41 ($\text{CH}_3\text{-Al}$), -9.16 ($\text{CH}_3\text{-Al}$). **²⁷Al{¹H} NMR** (C_6D_6 , 130 MHz): δ 66.88. **MS** (Maldi-TOF) m/z: 643.21 ([M]⁺), 629.17 ([M - CH_3]⁺), 615.16 ([M - 2(CH_3)]⁺).

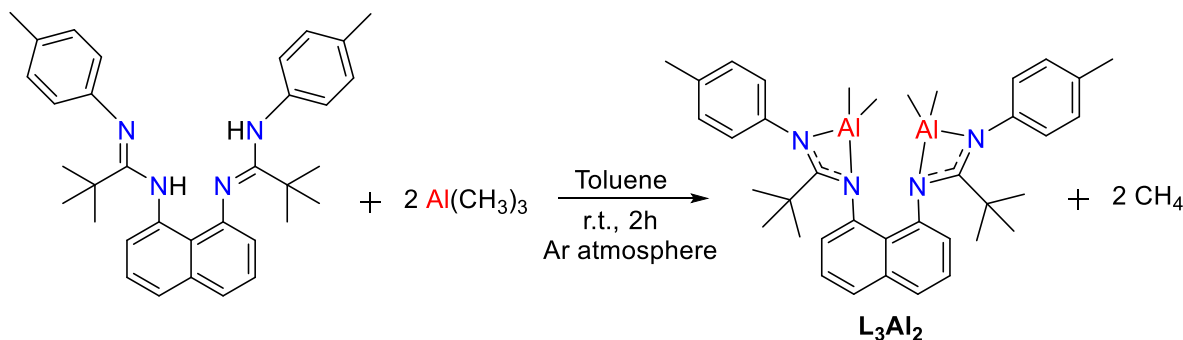
6.2. Synthesis of $\text{L}_2\text{Al}_2\text{I}_4$



Scheme 35. Synthesis of $\text{L}_2\text{Al}_2\text{I}_4$.

Benzene (10 mL) was added to L_2Al_2 (200.0 mg, 0.31 mmol) and BI_3 (243.0 mg, 0.62 mmol) in a Schlenk. The mixture was stirred for 1 h at room temperature, and a white precipitate was observed. After the solvent was removed and the solid residual was washed with pentane (3 x 5 mL). The white solid was recrystallized from benzene at room temperature. Yellow crystals were obtained (307.0 mg, 0.281 mmol, 91 %). **Melting point:** 203 °C (decomposition). **¹H NMR** (C_6D_6 , 300 MHz): δ 7.48-7.39 (m, 4H, C_{10}H_6), 7.07-7.02 (m, 2H, C_{10}H_6), 6.93-6.83 (m, 6H, C_6H_3), 2.83 (s, 6H, CH_3), 2.70 (s, 6H, CH_3), 0.95 (s, 18H, $\text{C}(\text{CH}_3)_3$). **MS** (Maldi-TOF) m/z: 583.3 ([M - 4I]⁺).

6.3. Synthesis of L_3Al_2

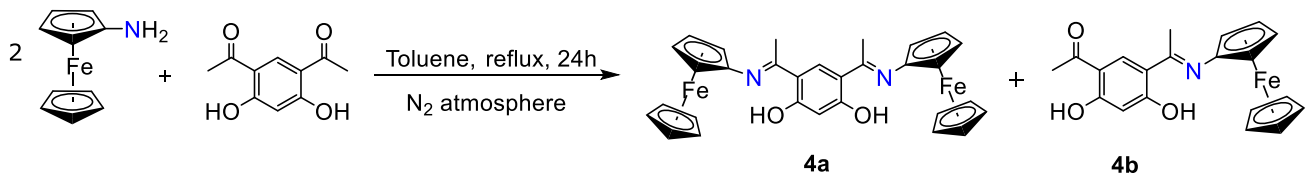


Scheme 36. Synthesis of L_3Al_2 .

A 2 M solution of $\text{Al}(\text{CH}_3)_3$ in heptane (0.6 mL, 1.2 mmol) was added to a solution of L_3Al_2 (300 mg, 0.60 mmol) in toluene (6 mL) in a Schlenk. The mixture was stirred for 2 h at room temperature. After the solvent was removed and the solid residual was washed with pentane (5 x 10mL). A yellow solid was obtained (295.0 mg, 0.48 mmol, 79 %). **Melting point:** 221 °C. **$^1\text{H NMR}$** (CDCl_3 , 300 MHz): δ 7.63 (d, $J_{\text{HH}} = 8.2$ Hz, 2H, C_{10}H_6), 7.32 (t, $J_{\text{HH}} = 7.7$ Hz, 2H, C_{10}H_6), 7.16 (s, 8H, C_6H_4), 6.99 (d, $J_{\text{HH}} = 7.3$ Hz, 2H, C_{10}H_6), 2.36 (s, 6H, CH_3), 0.89 (s, 18H, $\text{C}(\text{CH}_3)_3$), -0.33 (s, 6H, $\text{CH}_3\text{-Al}$), -0.75 (s, 6H, $\text{CH}_3\text{-Al}$). **$^{13}\text{C}\{\text{H}\}$ NMR** (C_6D_6 , 125 MHz): δ 183.85 (NCN), 143.72 ($\text{C}_{10}\text{H}_{6\text{ipso}}$), 142.67 ($\text{C}_6\text{H}_{4\text{ipso}}$), 137.10 ($\text{C}_{10}\text{H}_{6\text{ipso}}$), 134.66 ($\text{C}_6\text{H}_{4\text{ipso}}$), 129.92 (C_6H_4), 126.40 (C_{10}H_6), 126.10 (C_{10}H_6), 125.22 (C_{10}H_6), 41.20 ($\text{C}(\text{CH}_3)_3$), 30.98 ($\text{C}(\text{CH}_3)_3$), 20.88 (CH_3), -7.90 ($\text{CH}_3\text{-Al}$), -10.86 ($\text{CH}_3\text{-Al}$).

7. Synthesis of Schiff base ligand derived from ferrocene.

7.1 Synthesis of ligands symmetrical bis-azomethine **4a** and unsymmetrical single azomethine **4b**



Scheme 37. Synthesis of **4a** and **4b**.

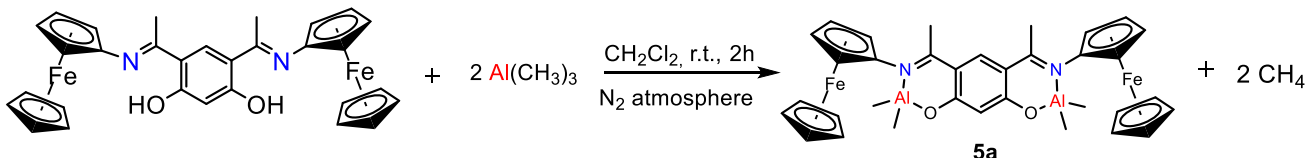
The Schiff base ligands were prepared by the addition of ferrocenylamine (2 eq.) (500 mg, 2.49 mmol) and 1,1'-(4,6-dihydroxy-1,3-phenylene)bisethanone (1 eq.) (241.7 mg, 1.245 mmol) in dry toluene (20 mL). The solution was refluxed for 24 h under a nitrogen atmosphere. After this time,

the solvent was removed under vacuum. The solid obtained contains a mixture of symmetrical bis-azomethine (**4a**) and unsymmetrical single azomethine (**4b**) (by TLC and ^1H NMR). These ligands were separated by dissolving **4a** in CH_2Cl_2 , and **4b** remains as a red precipitate. Finally, both solids obtained after solvent evaporation were purified by crystallization from $\text{CH}_2\text{Cl}_2/\text{hexane}$ (1:5) at -18 °C. For **4a** purple crystals were obtained (490 mg, 70 %) and for **4b** red crystals were obtained (120 mg, 26 %).

4a: ^1H NMR (400 MHz, CDCl_3 , 298K) $\delta/\text{ppm} = 16.92$ (s, 2H, OH), 7.72 (s, 1H, C_6H_2), 6.46 (s, 1H, C_6H_2), 4.36 (s, 4H, C_5H_4), 4.25 (s, 10H, C_5H_5), 4.20 (s, 4H, C_5H_4), 2.37 (s, 6H, CH_3). $^{13}\text{C}\{^1\text{H}\}$ NMR (100 MHz, CDCl_3 , 298K) $\delta/\text{ppm} = 169.27$ (C=N), 130.31 (C_6H_2), 112.55 ($\text{C}_6\text{H}_{2\text{ipso}}$), 105.94 (C_6H_2), 99.04 ($\text{C}_6\text{H}_{2\text{ipso}}$), 69.98 (C_5H_5), 66.62 (C_5H_4), 65.05 (C_5H_4), 16.19 (CH_3). HRMS (DCI- CH_4) m/z: 560.2489 ([M] $^+$) calcd for $\text{C}_{30}\text{H}_{28}\text{Fe}_2\text{N}_2\text{O}_2$ ([M] $^+$) 560.2356.

4b: ^1H NMR (400 MHz, CDCl_3 , 298K) $\delta/\text{ppm} = 17.54$ (s, 1H, OH), 12.74 (s, 1H, OH), 7.95 (s, 1H, C_6H_2), 6.40 (s, 1H, C_6H_2), 4.40 (s, 2H, C_5H_4), 4.26 (s, 7H, C_5H_4 , C_5H_5), 2.58 (s, 3H, CH_3), 2.42 (s, 3H, CH_3). $^{13}\text{C}\{^1\text{H}\}$ NMR (100 MHz, CDCl_3 , 298K) $\delta/\text{ppm} = 201.79$ (C=O), 166.66 (C=N), 133.51 (C_6H_2), 113.12 ($\text{C}_6\text{H}_{2\text{ipso}}$), 112.52 ($\text{C}_6\text{H}_{2\text{ipso}}$), 105.41 (C_6H_2), 99.99 ($\text{C}_6\text{H}_{2\text{ipso}}$), 97.18 ($\text{C}_6\text{H}_{2\text{ipso}}$), 69.95 (C_5H_5), 66.92 (C_5H_4), 65.11 (C_5H_4), 22.89 ($\text{CH}_3\text{-C=O}$), 16.04 ($\text{CH}_3\text{-C=N}$). HRMS (DCI- CH_4) m/z: 377.2178 ([M] $^+$) calcd for $\text{C}_{20}\text{H}_{19}\text{FeNO}_3$ ([M] $^+$) 377.2167.

8. Synthesis and characterization of bis-aluminum complex stabilized by Schiff ligand derived from ferrocene (**5a**)



Scheme 38. Synthesis of **5a**.

A solution of $\text{Al}(\text{CH}_3)_3$ (25.8 mg, 0.358 mmol) in dichloromethane was drop by drop added to a solution of **1a** (100 mg, 0.178 mmol) in dichloromethane. The reaction mixture was stirred for 2 hours at room temperature. All volatiles were removed under vacuum and the solid was washed with hexane. A red solid was obtained (114 mg, 95 %). ^1H NMR (400 MHz, CDCl_3 , 298K) $\delta/\text{ppm} = 7.88$ (s, 1H, C_6H_2), 6.30 (s, 1H, C_6H_2), 4.34 (s, 14H, C_5H_4 , C_5H_5), 4.17 (s, 4H, C_5H_4), 2.53 (s, 6H, CH_3), -0.64 (s, 12H, $\text{CH}_3\text{-Al}$). $^{13}\text{C}\{^1\text{H}\}$ NMR (100 MHz, CDCl_3 , 298K) $\delta/\text{ppm} = 169.39$ (C=N),

136.86 (C_6H_2), 116.11 (C_6H_{2ipso}), 111.95 (C_6H_2), 101.22 (C_6H_{2ipso}), 70.36 (C_5H_5), 66.55 (C_5H_4), 65.68 (C_5H_4), 20.98 (CH_3), -8.80 ($CH_3\text{-Al}$).

9. Aluminum complexes reactivity: catalysis to obtaining cyclic carbonates

9.1. General procedure for the synthesis of Cyclic Carbonates at 1 bar Pressure.

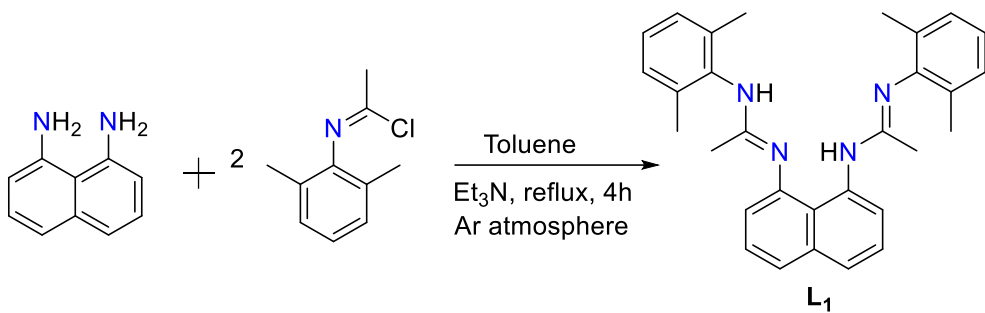
An epoxide (210 mg, 1.7 mmol), catalyst (L_2Al_2 , L_3Al_2 , $L_2Al_2I_4$ and **5a**) and TBAI (tetrabutylammonium iodide) or catalyst $L_2Al_2I_4$ were placed in individual glass reaction tubes with a magnetic stirrer bar in a multipoint reactor. The reaction mixture was stirred at 80 °C and 1 bar of CO_2 pressure for 24 h. The conversion of epoxide to cyclic carbonate was then determined by analysis of a sample by 1H NMR spectroscopy.

CHAPTER IV: RESULTS AND DISCUSSIONS

RESULTS AND DISCUSSIONS

1. Synthesis of the bis-amidine ligands.

1,8-diaminonaphthalene was used as a platform for all the synthesis of bis-amidine ligands containing a conformationally rigid planar linker between the two amidine groups. For **L₁** synthesis, the procedure was based on the previously reported for our group¹⁸, by reaction of 1,8-diaminonaphthalene with 2 equivalents of *N*-(2,6-dimethylphenyl)acetimidoyl chloride and Et₃N in dry toluene under reflux (Scheme 39). After the appropriate workup, compound **L₁** was isolated as orange crystals in 74 % yield. The ligand **L₁** was characterized by mass spectroscopy (MS), NMR spectroscopy (¹H and ¹³C), and Infrared spectroscopy (IR). They coincide with what was previously reported by our group¹⁸. In the ¹H NMR spectrum of this ligand (Figure 16), two resonances at 11.14 and 8.78 ppm are assigned to the NH groups, as previously observed for other bis-amidine ligands^{17,86}. The low field shift of one of these resonances (11.14 ppm) arises due to the formation of an intramolecular hydrogen bond between the NH and the nitrogen atom of the amidine moiety. The large size of the 2,6-dimethylphenyl substituent attached to the amidine group exerts steric hindrance for that it makes it difficult for the remaining hydrogen to form a hydrogen bond with the opposite nitrogen atom. The signal at 8.78 ppm attributed to the NH proton not forming a hydrogen bond agrees with the shift observed for hydrogens of amidine groups in molecules of a similar nature^{19,85}. In the aromatic region, it is observed that the integration of these signals is consistent with the expected number of hydrogen atoms. It is interesting to observe the appearance of a doublet at 8.98 ppm, well above the aromatic region of the spectrum. This doublet corresponds to hydrogen in the ortho position in the naphthalene fragment, for the amidine group, which is unshielded due to the change in electronic density caused by hydrogen bond type interaction. In the aliphatic region of the ¹H NMR spectrum, four high-intensity signals are observed in this region; the signals that appear at 2.14 ppm and 0.85 ppm, both integrating for 3 hydrogens, correspond to the -CH₃ of the amidine group. The singlets, at 2.30 ppm and 1.90 ppm, integrate for 6 hydrogens each, corresponding to the 2,6-dimethylphenyl fragments. The differentiation of these signals shows that the molecule, at least in solution, presents stable non-symmetrical conformations, for which the electronic environment of the methyl protons is different for each -CH₃; additionally, the existence of the hydrogen bond, as mentioned earlier, has consequences on the electronic density around the methyls of the amidine groups, which would explain the significant separation in chemical shift of the two signals corresponding to these. Concerning to ¹³C NMR spectrum, two resonances at 156.54 and 151.84 are assigned to C=N groups of the amidines, which confirm that the molecule in solution is non-symmetrical.



Scheme 39. Synthesis of **L₁**.

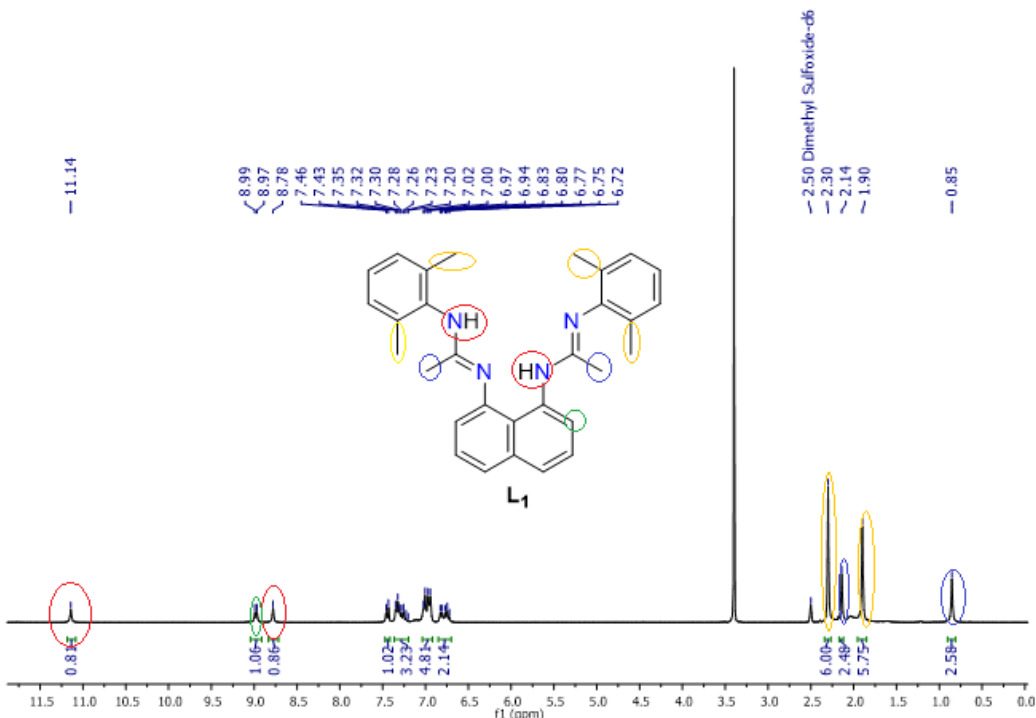
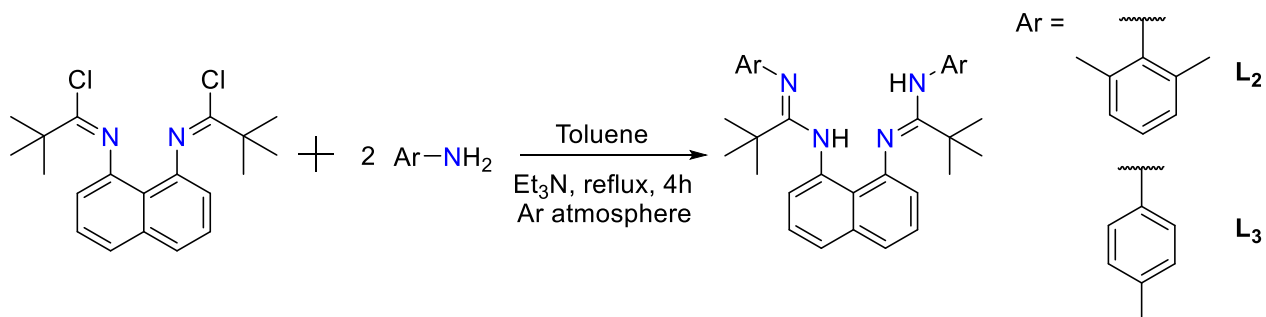


Figure 16. ¹H NMR of **L₁**.

For **L₂** and **L₃** synthesis, the followed procedure was one reported by Trifonov *et al.* with some modifications⁸⁶. *N,N*-(naphthalene-1,8-diyl)bis(2,2-dimethylpropanimidoyl chloride reacted with two equivalents of the corresponding amine and Et₃N in dry toluene under reflux for 4 h (Scheme 40). The modifications were the use of toluene as a solvent and reduced reflux time. These modifications made it possible to obtain a similar yield in less time. **L₂** was obtained as yellow crystals in 64 % yield and **L₃** as yellow crystals in 63 % yield. In **L₂** and **L₃**, the ¹H NMR spectrum also presents two signals for the NH group (9.42 and 8.18 ppm for **L₂**; 9.43 and 8.50 ppm for **L₃**) similar to that observed with **L₁**. Therefore, these ligands present in solution non-symmetrical structure, which was confirmed with ¹³C NMR. In both cases, it was possible to observe two different C=N groups (163.76 and 158.81 ppm for **L₂**; 161.35 and 160.69 ppm for **L₃**). The ¹H

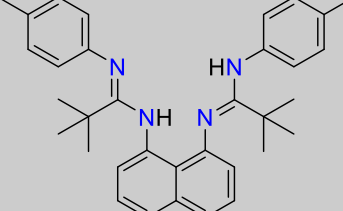
NMR of **L**₂ showed that in the aromatic region, the integration of these signals was coherent with the expected number of hydrogen atoms; and showed four different singlet signals that integrate for 3 hydrogens for each -CH₃ of the 2,6-dimethylphenyl fragments and two singlets that integrate for 9 hydrogens corresponding to the ^tbutyl group of the amidine. The ¹H NMR of **L**₃ showed the resonances corresponding to the -CH₃ of the para-tolyl fragments, which are two singlets at 2.05 and 2.01 ppm that integrate 3 hydrogens. Also, it was observed that two singlets correspond to the ^tbutyl group in the amidine. Table 1 summarizes the main ¹H and ¹³C NMR resonances of all synthesized bis-amidine ligands, as well as the respective yield.



Scheme 40. Synthesis of **L**₂ and **L**₃.

Table 1. Main resonances in ¹H and ¹³C NMR of the ligands obtained (**L**₁, **L**₂ and **L**₃) and yields.

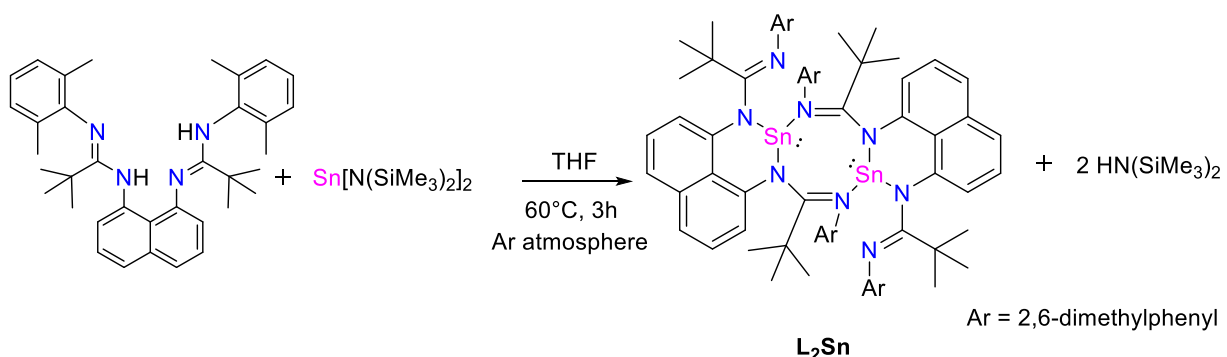
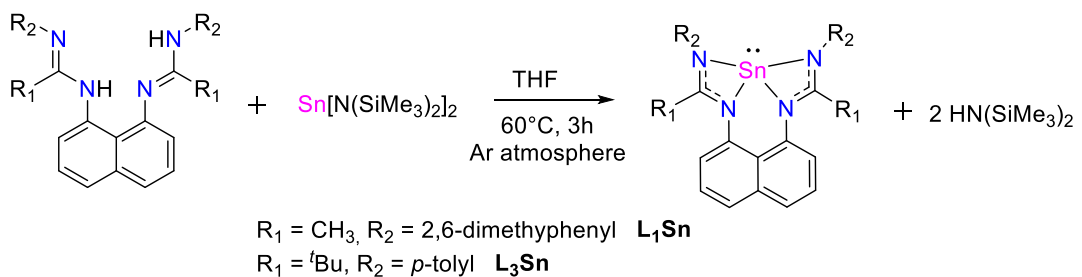
Ligand	Structure	¹ H NMR (ppm) ^a	¹³ C NMR (ppm) ^a	% Yield
L ₁		-NH 11.14, 8.78 CH ₃ -C=N 2.14, 0.85 CH ₃ -Ar 2.30, 1.90	N-C=N 156.54, 151.84 CH ₃ -C=N 17.82, 17.60	74
L ₂		-NH 9.42, 8.19 ^t butyl 1.50, 1.40 CH ₃ -Ar 2.21, 2.15, 1.88, 1.84	N-C=N 163.76, 158.81 -C(CH ₃) ₃ 29.02, 28.69	64

L ₃		-NH 9.43, 8.50 'butyl 1.38, 1.23 CH ₃ -Ar 2.05, 2.01	N-C=N 161.35, 160.69 -C(CH ₃) ₃ 28.79, 28.28	63
----------------	---	--	--	----

^a DMSO-d₆ as solvent.

2. Synthesis of stannylenes stabilized by bis-amidine ligands.

The synthesis of the stannylenes was carried out by a protonolysis reaction due to the large variety of reported and the simplicity of the procedure^{44,45,87}. The corresponding bis-amidine ligand reacted with one equivalent of Sn(HMDS)₂ in dry THF at 60 °C for 3 h (Scheme 41). **L₁Sn** was isolated as a pale-brown solid in 77 % yield. The formation of **L₁Sn** was confirmed by ¹H, ¹³C, ¹¹⁹Sn NMR, and mass spectroscopy. ¹H NMR spectrum showed a singlet that integrates for 6 hydrogens corresponding to the -CH₃ of amidine and a singlet that integrate for 12 hydrogens corresponding to -CH₃ of the 2,6-dimethylphenyl fragments (Figure 17). These indicated the symmetrical coordination of the tin center on the ¹H NMR. It is worth mentioning that the NH signals of the **L₁** ligand disappeared, confirming the obtaining of **L₁Sn**. In addition, before isolating the **L₁Sn** compound, it was possible to observe in ¹H NMR the signal corresponding to H-HMDS at 0.11 ppm as a by-product (Figure 17), which was later removed by vacuum and with pentane washes. ¹³C NMR spectrum showed the characteristic signal for the NCN at 169.03 ppm, like other amidinatostannylenes previously reported^{36,45,88}. The tetracoordinated nature of tin was observed in the ¹¹⁹Sn NMR spectrum with a resonance at -276.71 ppm, like stannylenes stabilized with tetracoordinate bis-amidine ligands⁴⁴.



Scheme 41. Synthesis of $\mathbf{L}_{1-3}\mathbf{Sn}$.

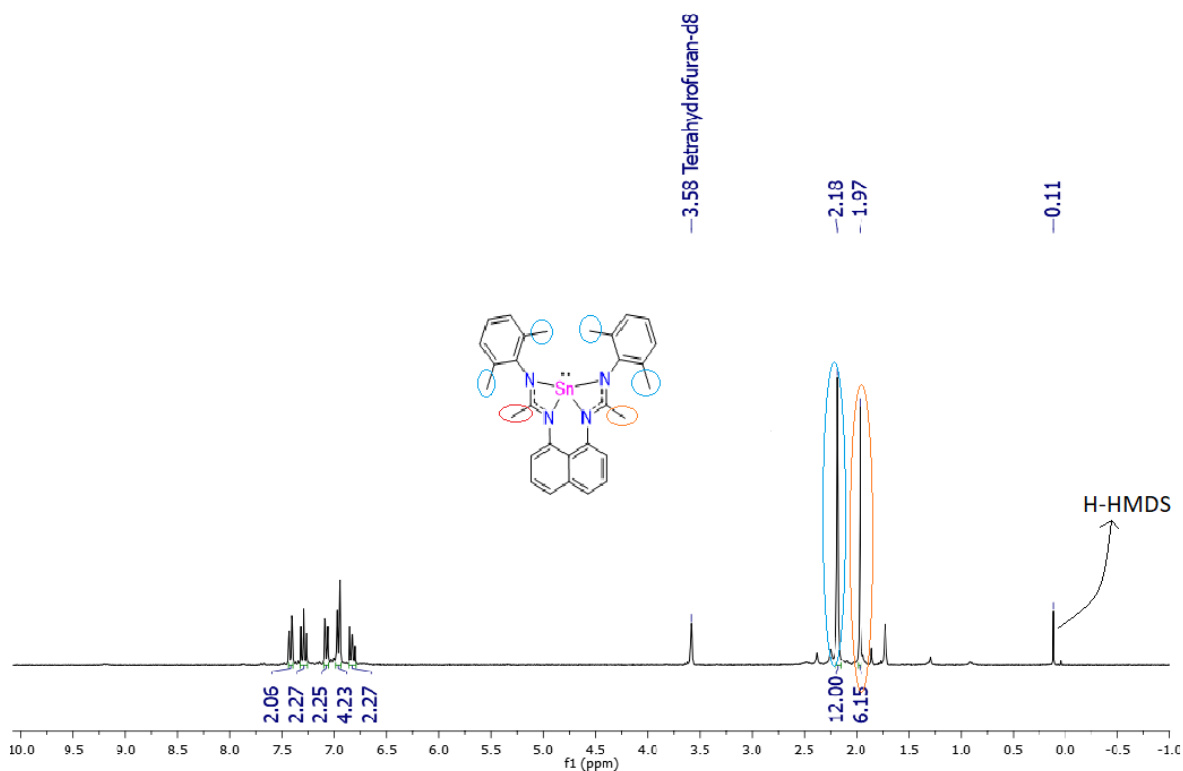


Figure 17. ^1H NMR of $\mathbf{L}_1\mathbf{Sn}$ before purification.

Stannylene **L₁Sn** was characterized crystallographically (Figure 18). The molecular structure indicates a four-coordinate tin center with a square-based pyramidal geometry. The Sn atom is at the top of the pyramid and four nitrogen atoms are at the base. This geometry has been seen in a few reports of stannylenes with unbridged bis-amidine ligands⁴⁵. The position of the lone-pair electrons above the Sn atom is clear evidence. The anionic charge on the ligand is delocalized over the amidinate groups in the ligand as shown by the symmetric bonding pattern within the core ($N(1)-C(11) = 1.326(3)$, $N(2)-C(11) = 1.328(3)$ Å; $N(1)-Sn = 2.2435(17)$, $N(2)-Sn = 2.3327(17)$ Å). The tin center is coplanar with the amidinate groups. The acute N–Sn–N angles of 57.38° and 57.74° are comparable to values previously recorded for Sn^(II) amidinate complexes^{44,88}.

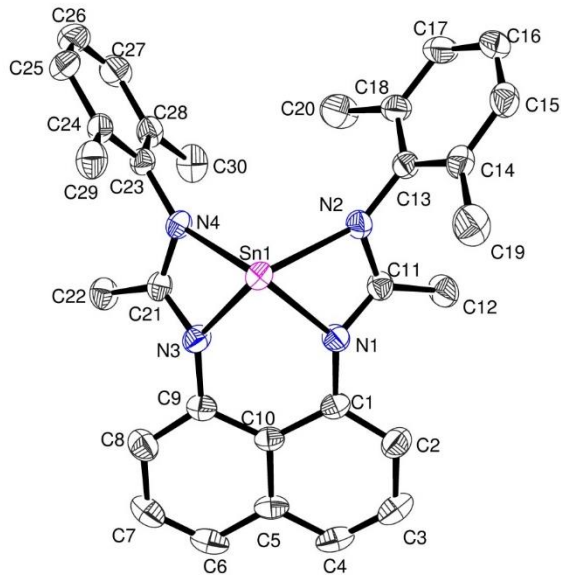
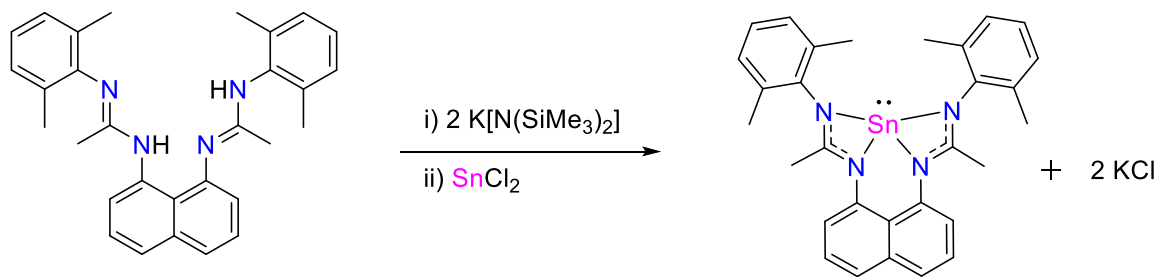


Figure 18. Molecular structure of **L₁Sn** (hydrogens are omitted for clarity). Thermal ellipsoids are shown with 50 % probability.

The stannylene **L₁Sn** can also be synthesized by deprotonating the ligand with KHMDS and then adding two equivalents of $SnCl_2$ (Scheme 42). This synthetic route was not chosen since the deprotonated ligand must be isolated to continue with the next step, which makes this procedure less direct and takes more time.



Scheme 42. Synthesis of **L₁Sn** by deprotonation of the ligand.

L₂Sn was isolated as yellow crystals in 44 % yield. The obtaining of a dimer **L₂Sn**, could be explained by a highly steric hindrance in the ligand, exerted by the 2,6-dimethylphenyl and the *t*-butyl groups, which prevent ordering a tetracoordinate tin center.

Regarding the characterization of compound **L₂Sn**, no solution state NMR spectroscopic data could be obtained for **L₂Sn**, as it has negligible solubility in common organic solvents once crystallized. Nevertheless, the X-ray structure of **L₂Sn** was obtained as a dimeric compound (Figure 19). Each of its Sn centers has a trigonal pyramidal geometry with two lone pairs pointing away from each other and with an Sn-Sn distance of 3.731 Å. Interestingly, the tin atoms are coordinated to both nitrogens directly linked to the naphthalene core and, at the same time, coordinated to one of the nitrogen from another bis-amidinate ligand, without coordination to the NCN amidine fragment.

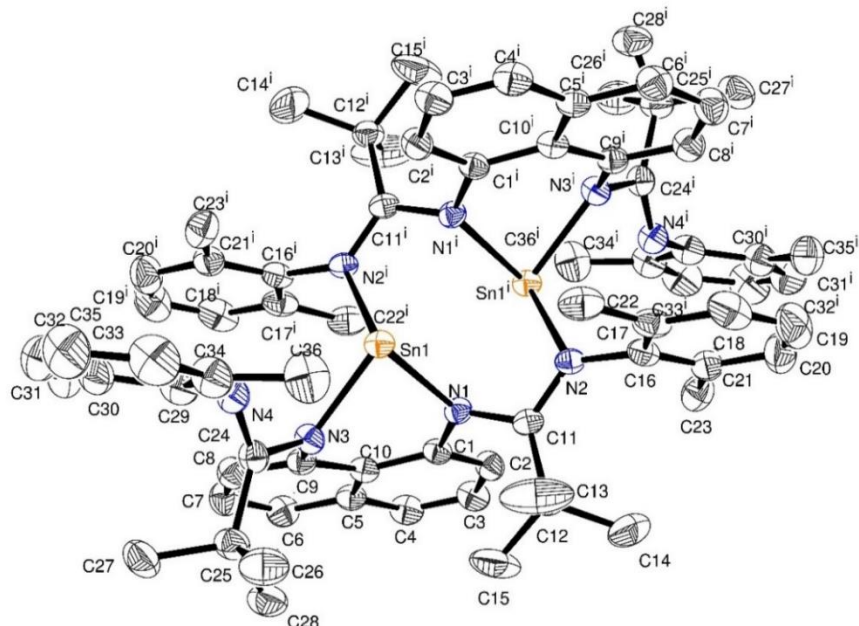


Figure 19. Molecular structure of **L₂Sn** (hydrogens are omitted for clarity). Thermal ellipsoids are shown with 50 % probability.

L₃Sn was isolated as a yellow solid in 61 % yield. The structure of **L₃Sn** was determined by means of ¹H, ¹³C, ¹¹⁹Sn NMR, and mass spectroscopy. ¹H NMR spectrum showed a singlet that integrates for 18 hydrogens corresponding to the ^tbutyl of amidine and a singlet that integrate for 6 hydrogens corresponding to -CH₃ of the *para*-tolyl fragments. These indicated the symmetrical coordination of the tin center on the ¹H NMR. Similarly, as with **L₁Sn**, before isolating the **L₃Sn** compound, it was possible to observe in ¹H NMR the signal corresponding to H-HMDS at 0.11 ppm as a by-product, which was later removed by vacuum and with pentane washes. ¹³C NMR spectrum showed the characteristic signal for the NCN at 177.53 ppm. ¹¹⁹Sn NMR spectrum with a resonance at -254.87 ppm showed that tin is tetracoordinated. Table 2 summarizes the main ¹H, ¹³C and ¹¹⁹Sn NMR resonances of all synthesized stannylenes stabilized by bis-amidine ligands with a rigid naphthalene backbone, as well as the respective yield.

Table 2. Main resonances in ¹H, ¹³C and ¹¹⁹Sn NMR of the stannylenes obtained (**L₁Sn**, **L₂Sn** and **L₃Sn**) and yields.

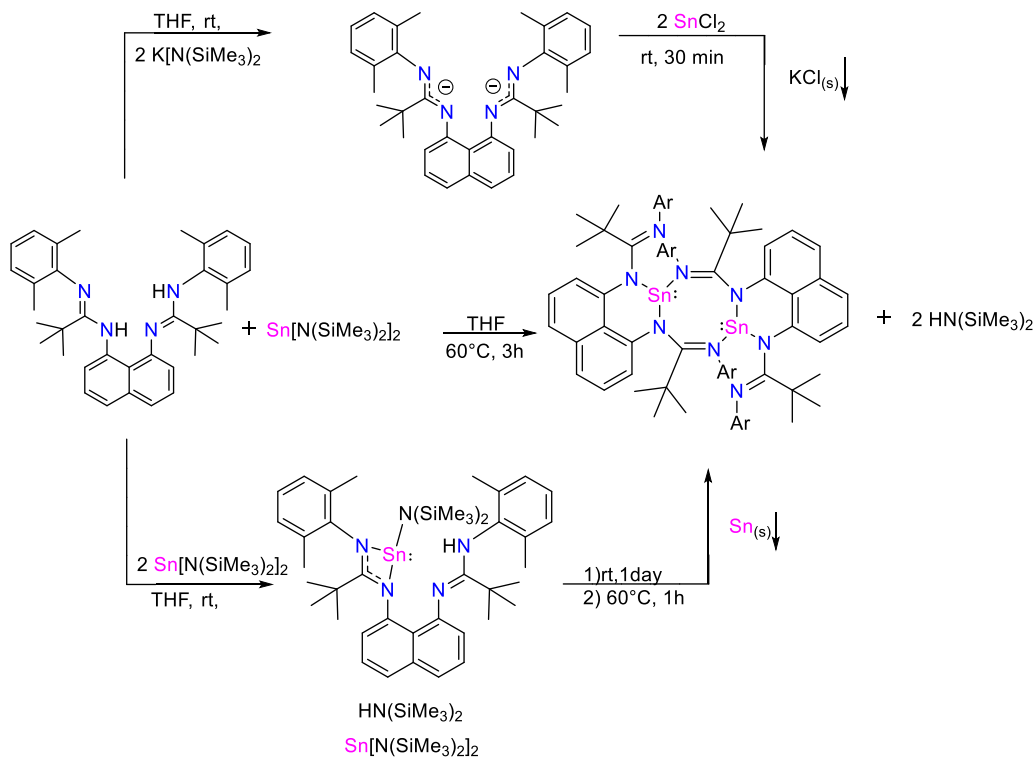
Compound	Structure	¹ H NMR (ppm) ^a	¹³ C NMR (ppm) ^a	¹¹⁹ Sn NMR (ppm) ^a	% Yield
L ₁ Sn		CH ₃ -C=N 1.97 CH ₃ -Ar 2.18	NCN 169.03 CH ₃ -C=N 20.03 CH ₃ -Ar 17.87	-276.71	77
L ₂ Sn ^b		-	-	-	44
L ₃ Sn		^t butyl 1.30 CH ₃ -Ar 2.29	NCN 177.53 - C(CH ₃) ₃ 31.85 CH ₃ -Ar 21.04	-254.87	61

^a THF-d₈ as solvent.

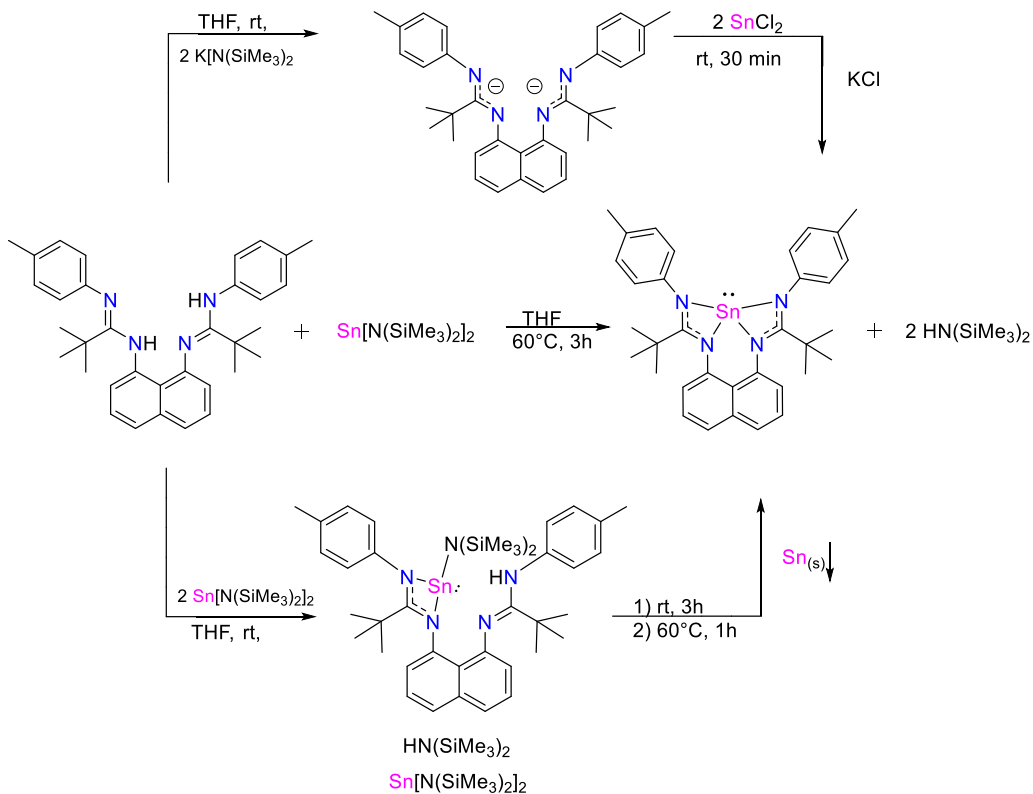
^b Compound insoluble in common organic solvents.

On the other hand, to obtain bis-stannylene systems from the same bis-amidine ligands with a

naphthalene bridge, two tests were carried out for the synthesis: i) to the deprotonated ligand (**L**₂ and **L**₃) were added two equivalents of SnCl₂, observing in the ¹H and ¹¹⁹Sn NMR the formation of **L**₂**Sn** and **L**₃**Sn**, the same products obtained by addition of one equivalent of Sn(HMDS)₂. Also, the formation of a white precipitate that correspond to KCl is observed; ii) reaction of one equivalent of the ligand (**L**₂ and **L**₃) with two equivalents of Sn(HMDS)₂. In this case, an intermediate with the tin coordinated to one of the amidines was observed, slowly migrating to the corresponding stannylenes **L**₂**Sn** or **L**₃**Sn**. Besides, H-HMDS and a black solid were obtained like by-products with Sn⁰ as the residue. Schemes 43 depict the route with **L**₂ and Scheme 44 with **L**₃. In summary, the most stable species are formed despite the stoichiometric ratios used, corresponding to the dimer **L**₂**Sn** and the tetradentate **L**₃**Sn**.



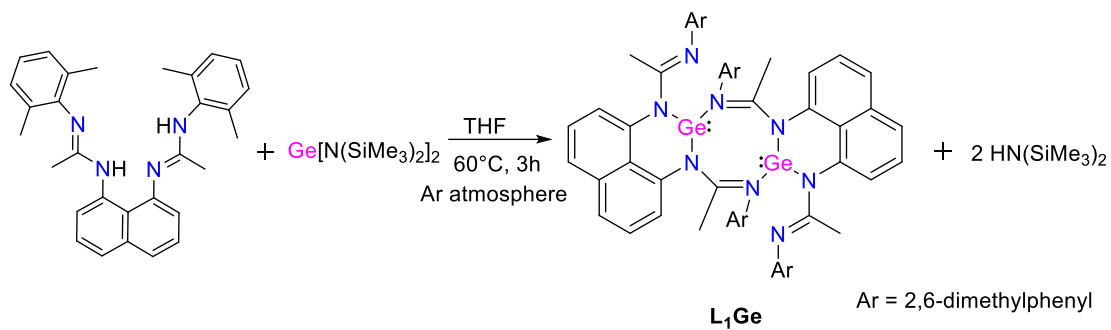
Scheme 43. Synthetic routes to obtain **L**₂**Sn**.



Scheme 44. Synthetic routes to obtain $\mathbf{L}_3\mathbf{Sn}$.

3. Synthesis of germynes stabilized by bis-amidine ligands.

The germynes were synthesized through the protonolysis reaction with $\text{Ge}(\text{HMDS})_2$ due to the good results obtained for the stannylenes. When trying to carry out the reactions to obtain stabilized germynes with bis-amidine ligands under the same conditions as the stannylenes, that is, THF, 60 °C and 3 hours of reaction. However, under these conditions only $\mathbf{L}_1\mathbf{Ge}$ was obtained as a dimer (Scheme 45). This dimer crystallizes in the reaction medium and is obtained as yellow crystals in 42 % yield. $\mathbf{L}_1\mathbf{Ge}$ is negligibly soluble once crystallized, so spectroscopic data could not be obtained in solution. The X-ray structure of $\mathbf{L}_1\mathbf{Ge}$ showed that each of its Ge centers has a trigonal pyramidal geometry with two lone pairs pointing away from each other (Figure 20). The Ge–Ge separation in the compound is 3.498 Å. The germanium atoms are coordinated in the same way as for the dimer obtained above for tin ($\mathbf{L}_2\mathbf{Sn}$), to the two nitrogens directly linked to the naphthalene linker and at the same time coordinated to nitrogen from another bis-amidine ligand. Therefore, the germanium atoms are not coordinated in the NCN amidine group.



Scheme 45. Synthesis of **L₁₋₃Ge**.

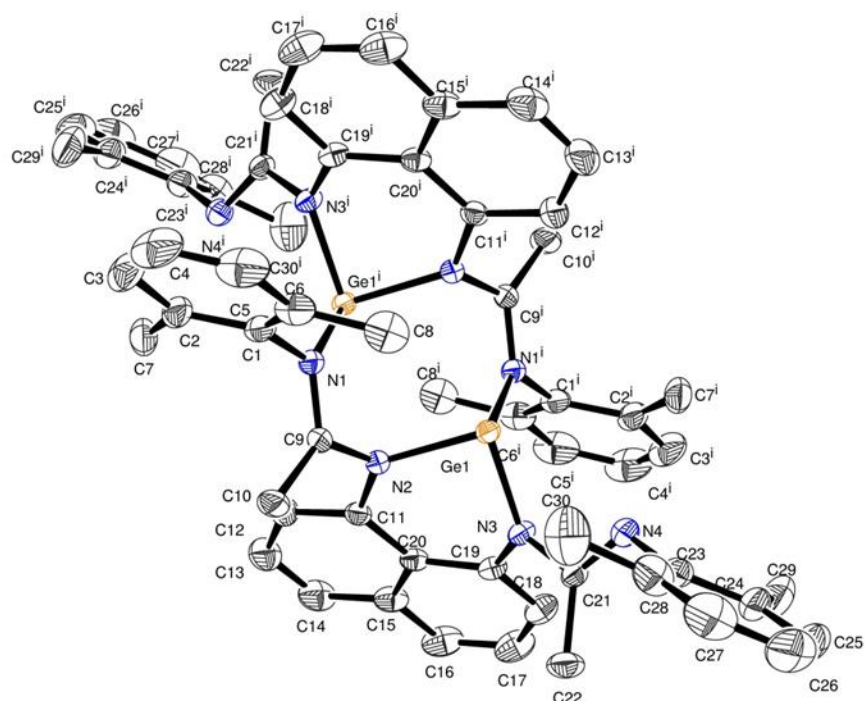


Figure 20. Molecular structure of **L₁Ge** (hydrogens are omitted for clarity). Thermal ellipsoids are shown with 50 % probability.

The synthesis of **L₂Ge** and **L₃Ge** was carried out under stronger conditions, using toluene as a solvent to heat the reaction at 120 °C for 48 h (Scheme 45). **L₂Ge** was isolated as yellow crystals in 52 %. This compound was characterized by ¹H and ¹³C NMR at room temperature. ¹H NMR spectrum showed a singlet that integrates for 18 hydrogens corresponding to the ⁴butyl of amidine and a singlet that integrate for 12 hydrogens corresponding to -CH₃ of the 2,6-dimethylphenyl group. In addition, the ¹³C NMR spectrum showed the characteristic signal for the NCN at 170.95 ppm. These indicated the tetracoordinated and symmetrical coordination of the germanium center in the solution state. However, the X-ray structure of **L₂Ge** showed that in the solid state, the germanium atom is tricoordinated, with a distorted trigonal pyramidal geometry. Here, the coordination is through the nitrogen atoms bonded to the naphthalene, and one of the nitrogen atoms of the amidine, leaving dangling the remaining nitrogen atom (Figure 21). The N-C distances within the amidinate NCN fragments of the compound **L₂Ge** strongly indicate an electronic delocalization over those fragments. Due to the bulky nature of the ⁴butyl substituents on the central carbon of the amidines, these are placed in opposite directions to each other, distorting the naphthalene rings. Regarding **L₃Ge**, unfortunately, it was not possible to isolate the specie due to its high solubility in non-polar and polar solvents, causing washing and unavailable to crystallization. Table 3 summarizes the synthesized germylenes stabilized by bis-amidine ligands with a rigid naphthalene backbone, as well as the respective yield.

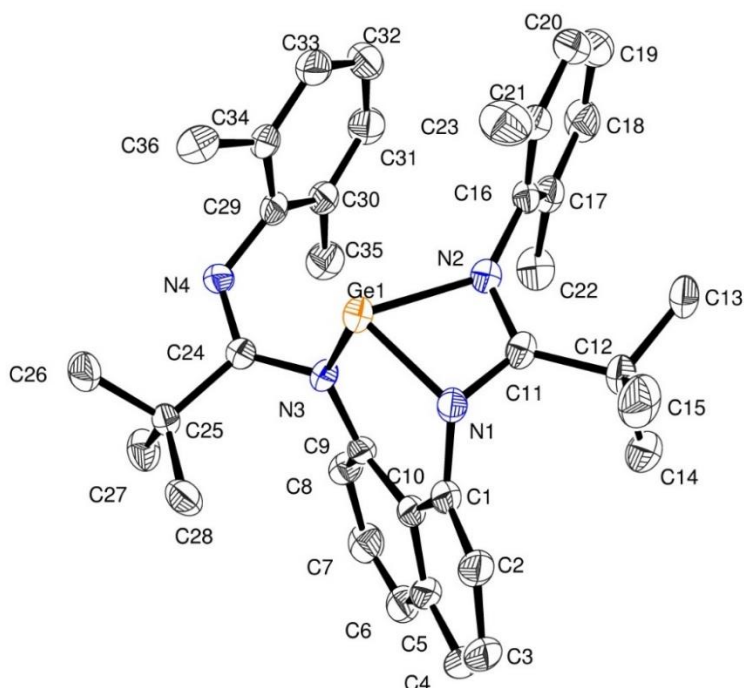
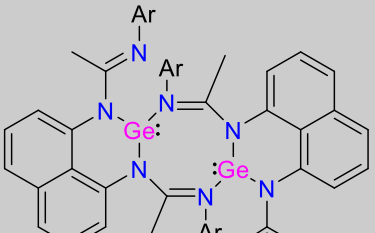
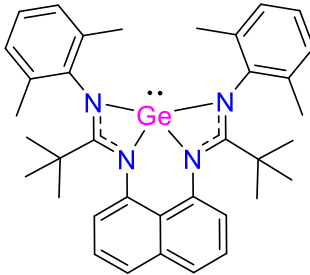
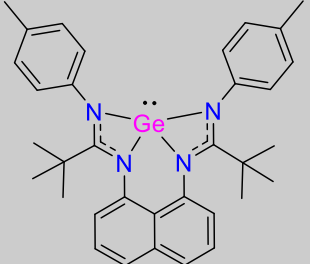


Figure 21. Molecular structure of **L₂Ge** (hydrogens are omitted for clarity). Thermal ellipsoids are shown with 50 % probability.

Table 3. Main resonances in ^1H and ^{13}C NMR of the germylenes obtained (**L₁Ge**, **L₂Ge** and **L₃Ge**) and yields.

Compound	Structure	^1H NMR (ppm) ^a	^{13}C NMR (ppm) ^a	% Yield
L₁Ge^b	 $\text{Ar} = 2,6\text{-dimethylphenyl}$	-	-	42
L₂Ge		$^t\text{butyl}$ 1.60 $\text{CH}_3\text{-Ar}$ 2.18	NCN 170.95 - $\text{C}(\text{CH}_3)_3$ 30.60 $\text{CH}_3\text{-Ar}$ 19.68	52
L₃Ge^c		$^t\text{butyl}$ 1.23 $\text{CH}_3\text{-Ar}$ 1.45	-	-

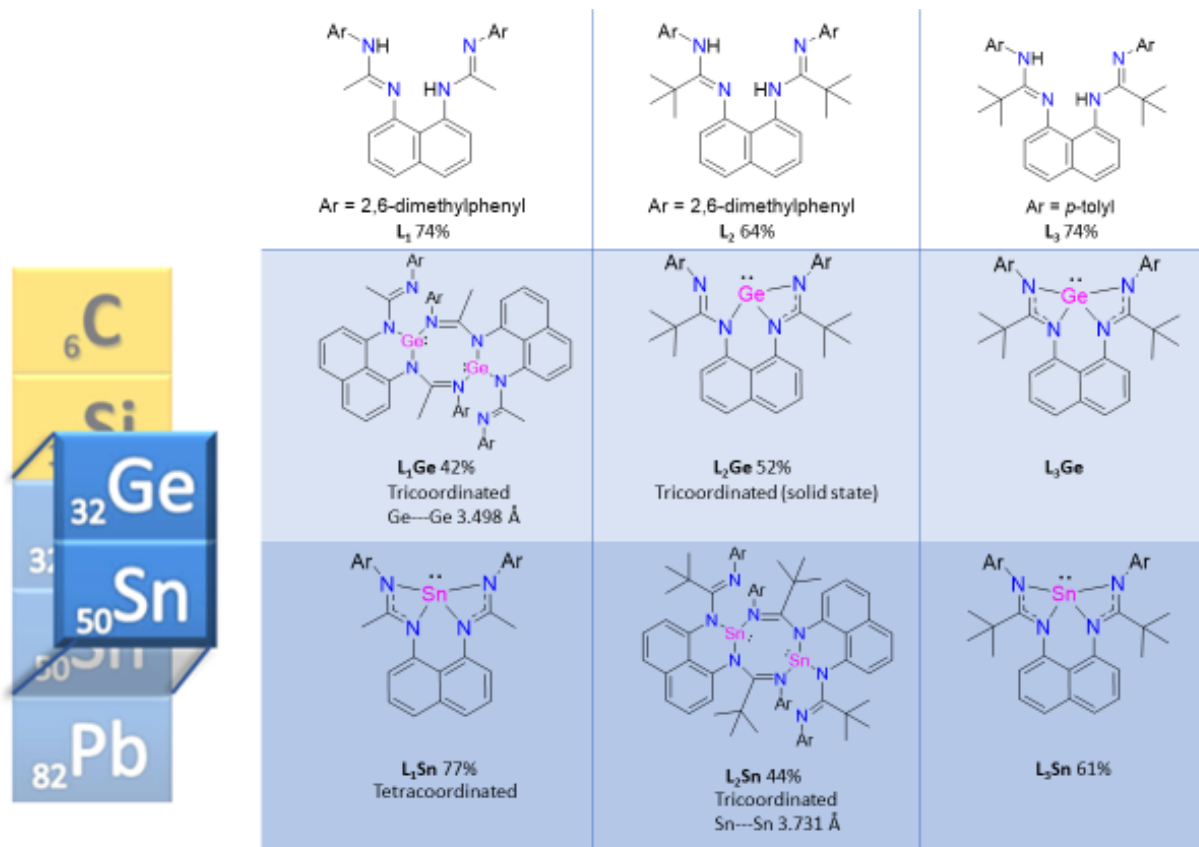
^a C_6D_6 as solvent.

^b Compound insoluble in common organic solvents.

^c Unpurified compound.

Scheme 46 shows a global summary of the stannylenes and germylenes obtained with respect to each ligand. For the **L₁** ligand, a difference in the structure between germylene and stannylene is observed, obtaining a dimer (**L₁Ge**) with the tricoordinated germanium atoms. In contrast, for the tin derivative, a tetracoordinated monomer is obtained (**L₁Sn**). This structural difference may be due to the size of the central atoms, with germanium being smaller than tin, favoring the formation of a dimer. For the **L₂** ligand, the opposite is observed. A dimer for stannylene (**L₂Sn**) and a monomer for germylene (**L₂Ge**) are obtained. This difference can be explained again by the size of the central atoms, but in this case, changing the methyl substituent for $^t\text{butyl}$ on the central carbon of the amidine for **L₂** produces that by having a more voluminous group, tin, which

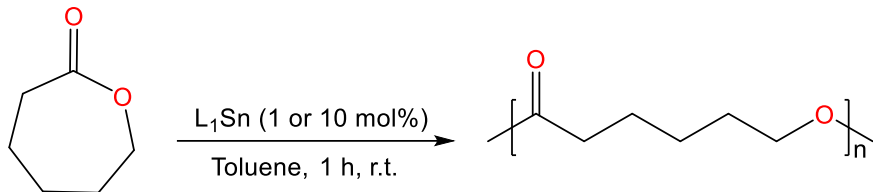
is a larger form the dimer, instead, the germanium compound is a monomer, which in the solid state appears as tricoordinated. The distance between the central atoms in the dimers, observing a greater distance between Sn--Sn. For ligand L_3 , it is observed by NMR that in both cases, a monomer with germanium and tin is obtained, so having a less bulky aromatic substituent such as *p*-tolyl in the nitrogens favors the obtaining of tetracoordinated species.



Scheme 46. Summary of the stannylenes and germlylenes obtained.

4. Metallylenes reactivity

Until today several studies have been reported that show that stannylenes are reactive toward the polymerization of cyclic esters^{36,44,45,89–92}. Mainly stannylenes are used as catalysts and initiators of the polymerization of lactones. Due to this background, this project proposed using the synthesized stannylenes as catalysts for the polymerization of cyclic esters (Scheme 47), specifically ϵ -caprolactone, and thus obtain a biodegradable polymer.



Scheme 47. **L₁Sn** as catalyst for the polymerization of ϵ -caprolactone.

The tests were carried out following reported procedures, and the stannylene **L₁Sn** was tested (Scheme 46). The reaction conditions and the conversions obtained are presented in Table 4. The synthesis conditions were using 10 mol% of **L₁Sn**, 1 h at room temperature, after that time, an aliquot was taken, and the conversion was analyzed through ¹H NMR. Under these conditions, the conversion was major than 99 %, and it was decided to terminate the reaction by adding benzoic acid and then trying to precipitate the polymer formed by adding methanol. Only oil was obtained despite multiple attempts to obtain a precipitate by adding cold methanol or cooling the reaction mixture. This result indicates that the desired polymer was not formed but could be the formation of oligomers. Then the test was repeated, but this time using a smaller quantity of stannylene **L₁Sn** (1 mol%), and the same conditions of 1 h at room temperature were used. Again, a conversion major than 99 % was obtained. However, it was not possible to isolate a polymer obtaining an oil, which indicates that the **L₁Sn** compound is active against ϵ -caprolactone but reacts quickly. Hence, there is no control of polymerization under the tested conditions. In the same way, a test was made with the ligand **L₁**, obtaining as a result by ¹H NMR that this compound does not present activity, and the catalytic activity previously tested with **L₁Sn** comes from the tin compound.

Table 4. Condition and activity for polymerization of ϵ -caprolactone.

Entry ^a	Catalyst (mol%)	t (h)	T (°C)	Conversion (%) ^b
1	L ₁ (1.0%)	1	23	0
2	L ₁ Sn (10.0%)	1	25	>99
3	L ₁ Sn (1.0%)	1	27	>99

^a The reactions were carried out in dry and degassed toluene (2 mL) under argon in presence of ϵ -caprolactone (8.76 mmol).

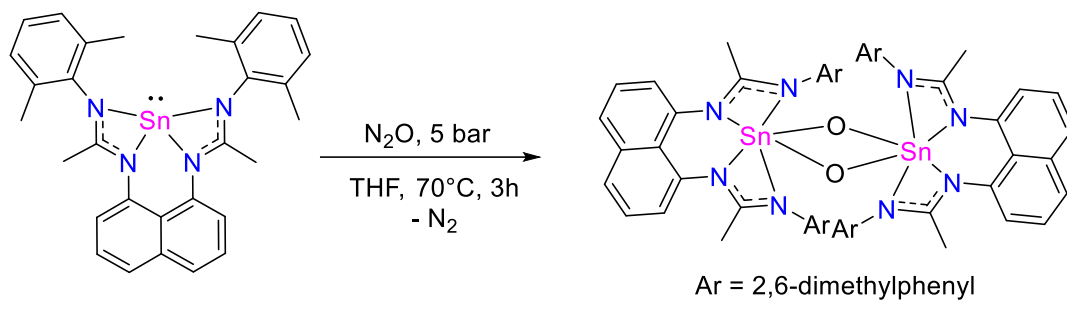
^b Determined by ¹H NMR analysis by comparing the integration of the signal of the polymer with the monomer.

Due to the unexpected results of the stannylenes against polymerization, it was proposed to investigate the type of reactivity that metallylenes stabilized by bis-amidine ligands with a rigid naphthalene bridge have against a series of different substrates. The tests were carried out mainly with the stannylene L₁Sn, due to its easy production and good synthesis yield.

The first reactivity tested was the activation of small molecules, but L₁Sn was not active against ethylene, NH₃, CO₂, and H₂, despite the multiple conditions evaluated, such as increasing the temperature, time, and pressure.

However, when exposed to N₂O, which reacts as an oxidizing agent, L₁Sn presents activity. The reaction was carried out in THF, 3 h at 70 °C, and 5 bars of N₂O (Scheme 48) and monitored by ¹H and ¹¹⁹Sn NMR. After the complete disappearance of the L₁Sn resonances, the formation of crystals in the reaction medium was observed, which were separated and washed with pentane. A dimeric amidinate-stannoxane **1a** was obtained as colorless crystals in 46 % yield. Compound **1a** is moderately soluble in THF, and due to its dimeric form, the signals in ¹H NMR are broadened. Therefore, the coupling of signals in the aromatic region cannot be clearly seen, but the integration is as expected. In the aliphatic region, two broad singlets, which integrate 12 hydrogens at 2.07 and 1.85 ppm, correspond to the -CH₃ of the 2,6-dimethylphenyl fragment. In addition, another resonance that integrates 12 hydrogens at 1.76 ppm corresponds to the -CH₃ of the amidine groups. The characteristic signal of the C_{ipso} atom of the amidinate group in the ¹³C NMR spectrum resonates at 168.70 ppm. The ¹¹⁹Sn chemical shift at -494.50 ppm was observed, consistent with another stannoxane⁴⁷. The X-ray structure obtained for **1a** showed a dinuclear specie with hexa-coordinated tin atoms (Figure 22), in a distorted pseudo-octahedral geometry with a central planar Sn₂O₂ ring. The O–Sn distances (~2.000 Å), Sn–Sn contact (2.978 Å), and O–Sn–O angles (84.01°) are in the range of other dimeric tin amidinate-stannoxane

reported⁴⁷. Also, the values of N-Sn distances and C_{ipso}-Sn interactions (~2.69 Å) are similar to those observed in the literature.⁴⁷.



Scheme 48. Synthesis of **1a**.

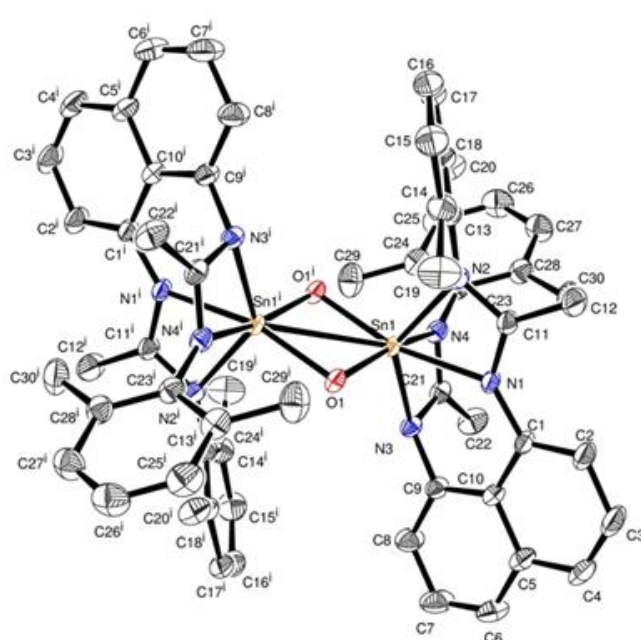
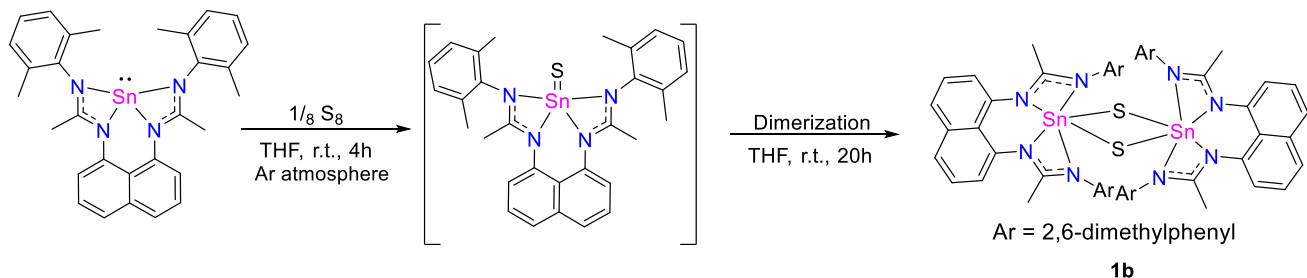


Figure 22. Molecular structure of **1a** (hydrogens are omitted for clarity). Thermal ellipsoids are shown with 50 % probability.

With this result, we tried another oxidation reaction with elemental sulfur due to the various reports that stannylenes can react with chalcogenides^{34,41,46,48,93,94}. The reaction was carried out at room temperature (Scheme 49) and monitored by ¹H and ¹¹⁹Sn NMR. In the ¹H NMR, a mixture of new signals and starting material in the first 4 h were observed. In ¹¹⁹Sn NMR, the resonance of the **L₁Sn** and a new one at -371 ppm were seen, which evolved to a single one at -647 ppm after 24 h. After purifying the crude by crystallization, pale-yellow crystals in 51% yield were obtained, and single crystals suitable for XRD were isolated. The molecular structure showed

compound **1b** as a dimeric compound, analog to **1a** but with Sn_2S_2 ring. Also, the tin atoms in the central planar Sn_2S_2 ring appear in a distorted pseudo-octahedral geometry (Figure 23). The S-Sn distances are $\sim 2.400 \text{ \AA}$, and Sn-Sn contact is 3.385 \AA , longer than observed in the analogs with oxygen due to the size of the sulfur atom.



Scheme 49. Synthetic route to obtain **1b**.

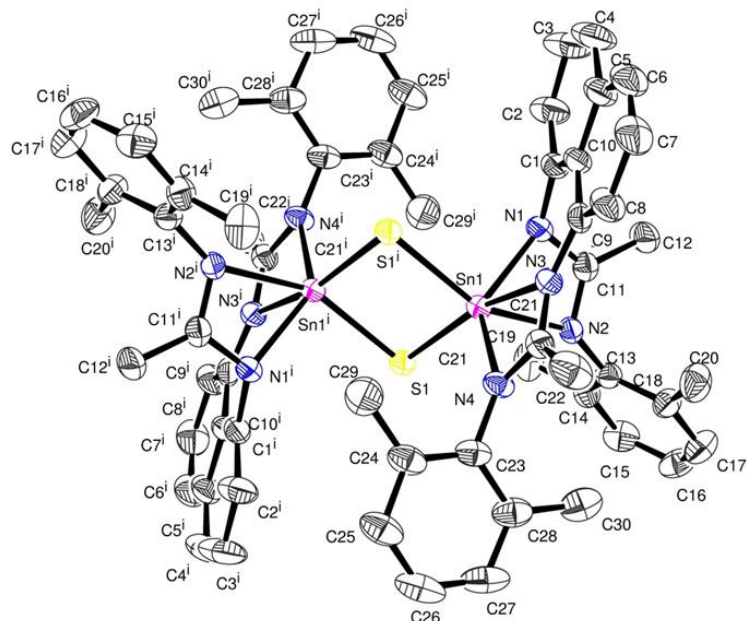
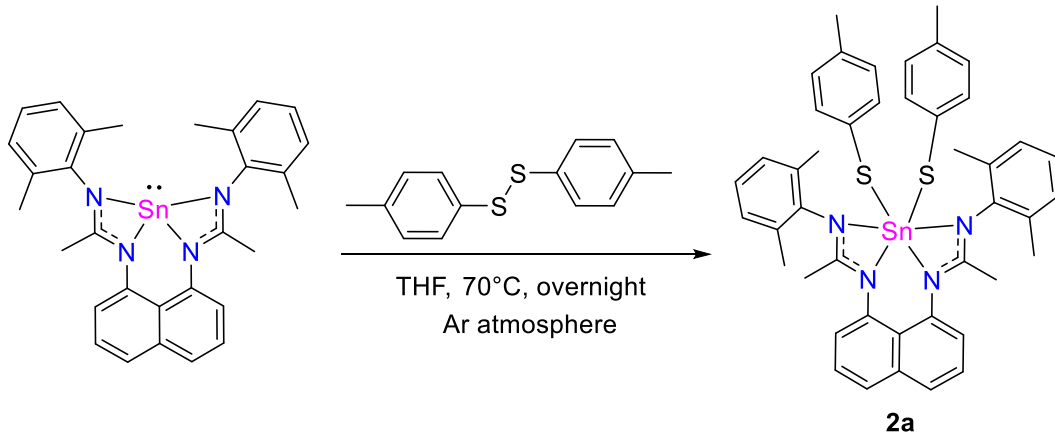


Figure 23. Molecular structure of **1b** (hydrogens are omitted for clarity). Thermal ellipsoids are shown with 50 % probability.

In addition, compound **1b** was characterized through NMR. The signals in ^1H NMR are broadened due to the dimeric form of the compound. The aliphatic region in the ^1H NMR showed two broad resonances as singlets. Moreover, one integrates 24 hydrogens at 2.11 ppm , corresponding to the 2,6-dimethylphenyl fragment, and another integrates 12 hydrogens at 1.75 ppm , corresponding to $-\text{CH}_3$ of the amidine groups. The characteristic signal of the NCN fragment

in ^{13}C NMR is 167.43 ppm. The ^{119}Sn chemical shift at -647.99 ppm is unexpected because it is at a very high field. Unfortunately, to our knowledge, other similar dimeric compounds with an Sn_2S_2 ring do not report the ^{119}Sn NMR. However, a similar dimeric compound with a Sn_2Se_2 ring and bis-guanidine ligands shows a resonance and a high field in the ^{119}Sn NMR at -779.00 ppm. Based on the XRD and ^{119}Sn NMR data, it is proposed that the first signal obtained at -371 ppm corresponds to the monomeric specie with a double bond $\text{Sn}=\text{S}$. However, this compound is unstable, and the dimerization occurs to give the more stable dimeric compound **1b** (see Scheme 48).

After oxidation reactions, we studied oxidative addition reactions with **L₁Sn**. The first evaluation was in the presence of *p*-tolyl disulfide in THF at 70 °C overnight (Scheme 50). An oxidative addition reaction occurs with the cleavage of the S-S bond and the tin's insertion, forming product **2a**. The most apparent change in the ^1H NMR for the product of this reaction is the appearance of aromatic signals and the singlet in the aliphatic region corresponding to the *p*-tolyl fragment (Figure 24). ^{119}Sn NMR showed a singlet at -456.70 ppm, consistent with a hexacoordinated tin. Besides, a crystallographic study was performed, revealing a monomeric $\text{Sn}^{(\text{IV})}$ specie in a distorted octahedral coordination sphere that included the four nitrogen atoms of the two chelating amidinate anions and the two *p*-tolyl sulfur fragments (Figure 25). The equivalence of the C-N bond lengths within NCN frameworks and their magnitudes (range from 1.301 to 1.361 Å) indicate that the π electrons within the ligands are delocalized.



Scheme 50. Synthesis of **2a**.

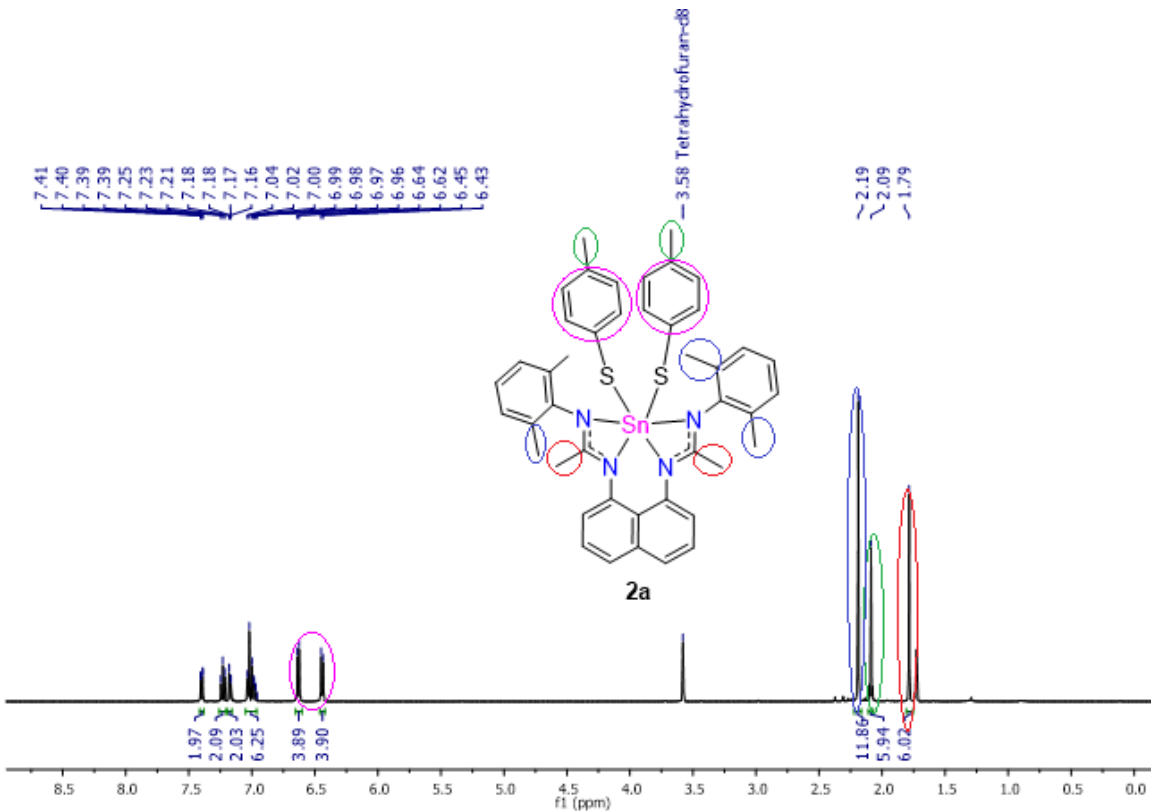


Figure 24. ^1H NMR of **2a**.

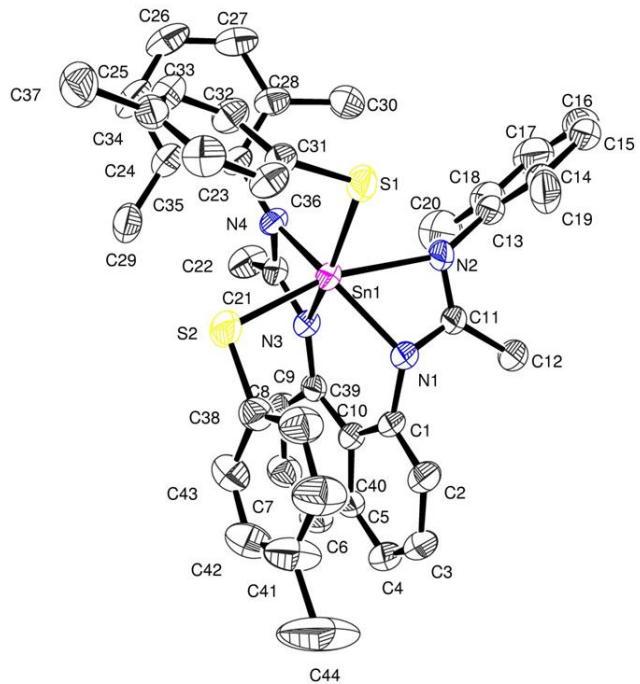
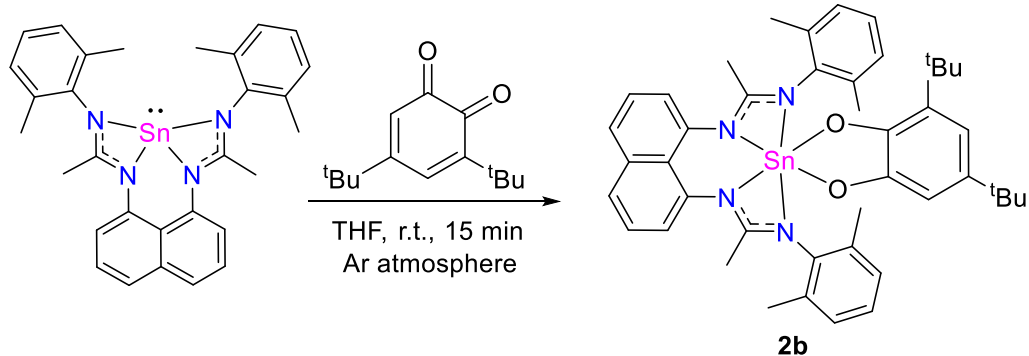


Figure 25. Molecular structure of **2a** (hydrogens are omitted for clarity). Thermal ellipsoids are shown with 50 % probability.

The second oxidative addition reaction was carried out between **L₁Sn** and 3,5-di-*tert*-butyl-ortho-quinone, leading to a cycloaddition product **2b** (Scheme 51). ¹H NMR analysis performed on compound **2b** in solution revealed the characteristic signals of the quinone group in the aromatic region, doublets at 6.57 and 6.39 ppm ($J_{HH} = 2.4$ Hz), and two singlets corresponding to the ⁴Bu in the aliphatic area. Also, the signal corresponds to the amidine -CH₃ as a singlet that integrates 6 hydrogens was observed (Figure 26). The ¹³C NMR spectrum showed the specific signals for all the carbon atoms. The ¹¹⁹Sn NMR showed a singlet at -512.16 ppm, corresponding to a cycloaddition product. The mass analysis (DCI/CH₄) spectrum exhibits a peak at 786.29, which corresponds to [M]⁺ of compound **2b**, evidencing its formation.



Scheme 51. Synthesis of **2b**.

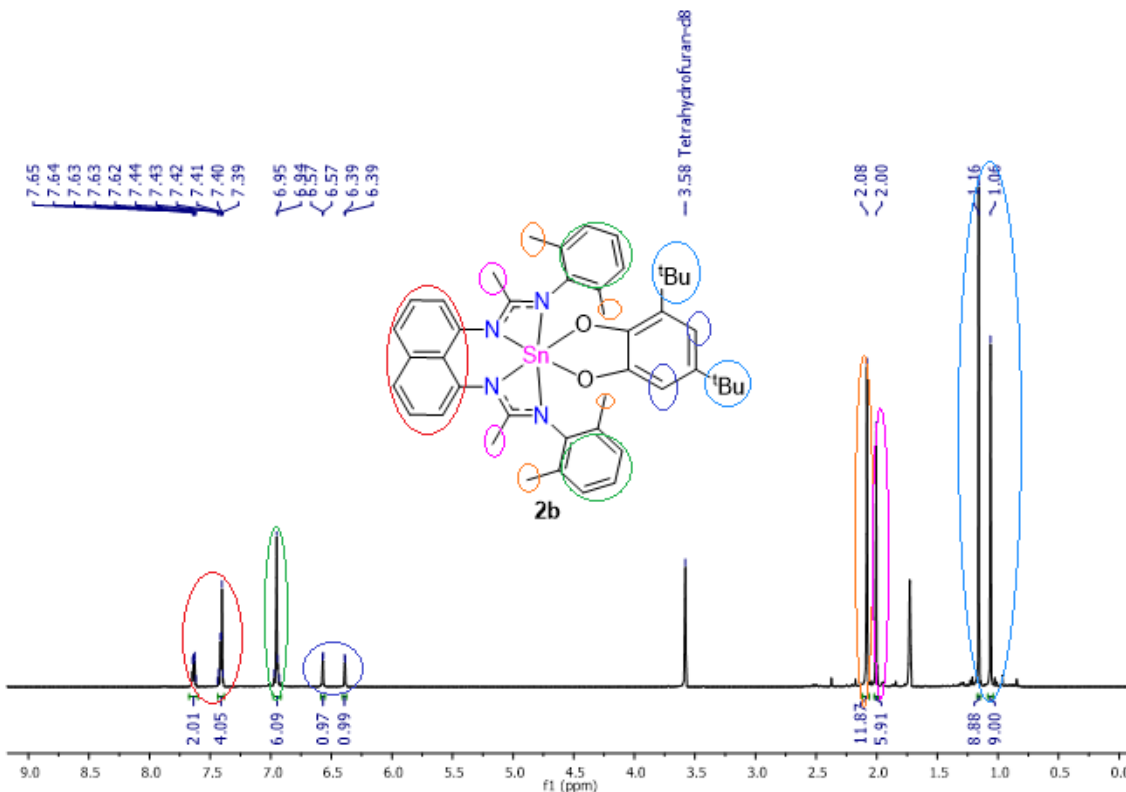
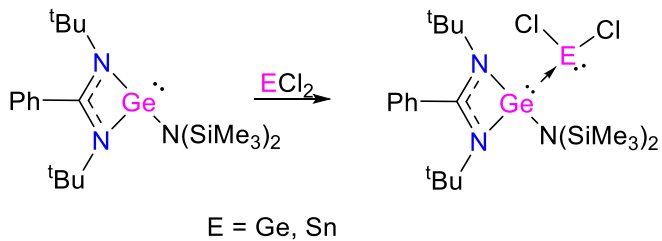


Figure 26. ¹H NMR of **2b**.

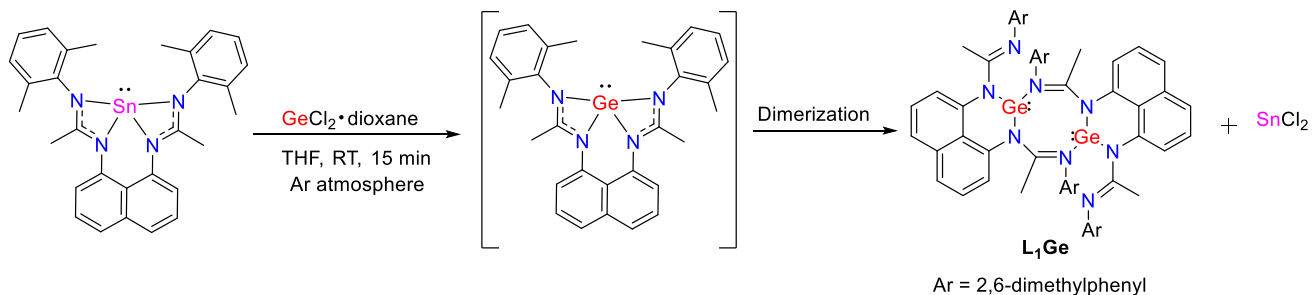
Metallylenes have been recognized as strong electron-donating ligands, mainly if donor groups stabilize them. Therefore, metallylenes can be used like ligands to coordinate transition metals. Some of their transition metal complexes have already demonstrated high efficiency in various catalytic reactions⁹⁵. Stannylene ligands can generally function as electron-pair donors or acceptors (Z-types) in transition metal complexes⁹⁶. Stimulated by the above facts, an attempt was made to use the stannylene **L₁Sn** as a ligand to coordinate transition metals. Despite using different substrates with different metals such as Pd, Pt, Ni, Rh, Co, Cu, and Au, it was impossible to obtain chemical coordination, despite changing synthesis conditions such as solvents, time, and heating of the reaction mixture.

Continuing with chemical coordination, silylenes and germylenes coordinate group 14 elements in the oxidation state II due to the latter's lone pair electrons donation ability into the vacant p orbitals of metallylenes. As reported by So *et al.*, an amidinatogermylene forms a heteronuclear adduct with GeCl₂ and SnCl₂ (Scheme 52)⁹⁷.



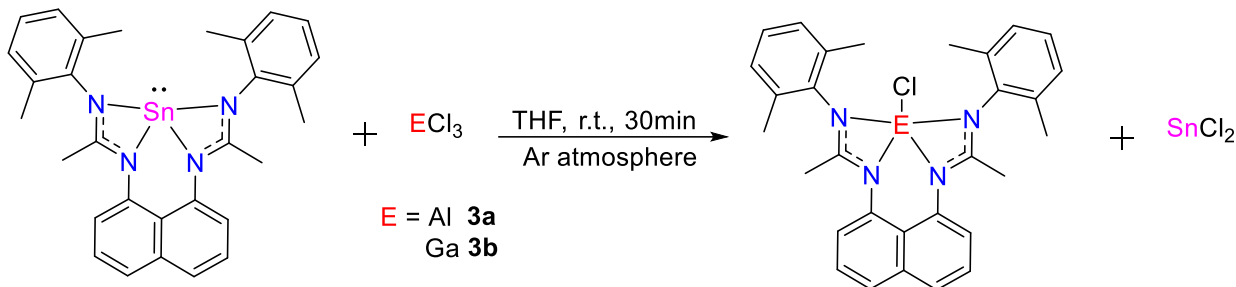
Scheme 52. Example of coordination chemistry of an amidinatogermylene with group 14 elements.

Accordingly, **L₁Sn** was mixed with GeCl₂(dioxane) in THF at room temperature. After 15 min, a yellow crystalline solid was formed (Scheme 53). The ¹¹⁹Sn NMR showed a resonance at -214.00 ppm, in agreement with the formation of SnCl₂. The crystalline solid obtained was analyzed by NMR and corresponded to the dimeric compound **L₁Ge**, indicating a transmetalation reaction.



Scheme 53. Synthesis of **L₁Ge** by transmetalation reaction.

Looking for a broader scope of reactions, group 13 halogenated substrates, such as AlCl_3 and GaCl_3 (Scheme 54), were studied with L_1Sn . In both cases, transmetalation reactions are observed, forming SnCl_2 as a by-product, as seen in the ^{119}Sn NMR. L_1Sn reacted with AlCl_3 quickly in THF at room temperature for 30 min to give a white solid with 83 % yield (**3a**) (Scheme 54), characterized by ^1H and ^{13}C NMR. The ^1H NMR showed, in the aromatic region the expected resonances and integrals. Also, in the aliphatic area, three singlets are observed that integrate each one 6 hydrogens, with resonances at 2.33 and 1.90 ppm corresponding to 2,6-dimethylphenyl fragments and with a signal at 2.13 related to $-\text{CH}_3$ in the amidine (Figure 27). In the ^{13}C NMR, the typical characteristic signal for NCN was observed at 176.45 ppm. A single resonance for this group indicates equivalent carbons and, added to the symmetry rigidity of the ^1H and ^{13}C NMR, suggests that the aluminum atom is pentacoordinate between the four nitrogens of the amidines and one chlorine atom. In addition, L_1Sn reacted with GaCl_3 under the same conditions as AlCl_3 giving the transmetalation product **3b** with an 88 % yield. NMR studies showed a similar pattern as the one exhibited for **3a**. The structure of **3b** was corroborated by crystallographic studies (Figure 28), where gallium is pentacoordinated with a distorted square-based pyramidal geometry. The Ga–Cl bond has a length of 2.183 Å, and the Ga–N distances are similar to the previously reported aluminum pentacoordinated complexes with L_1 .¹⁸



Scheme 54. Synthesis of **3a** and **3b**.

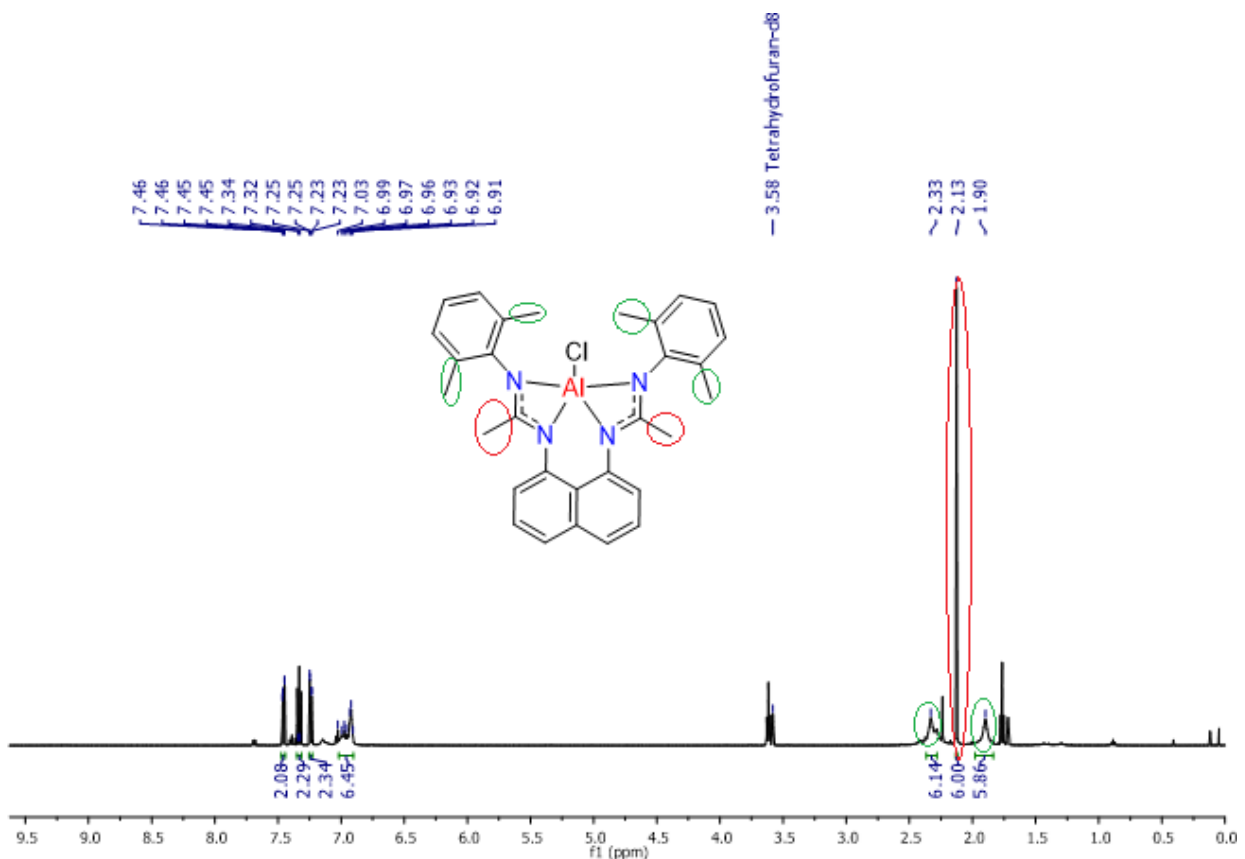


Figure 27. ^1H NMR of **3a**.

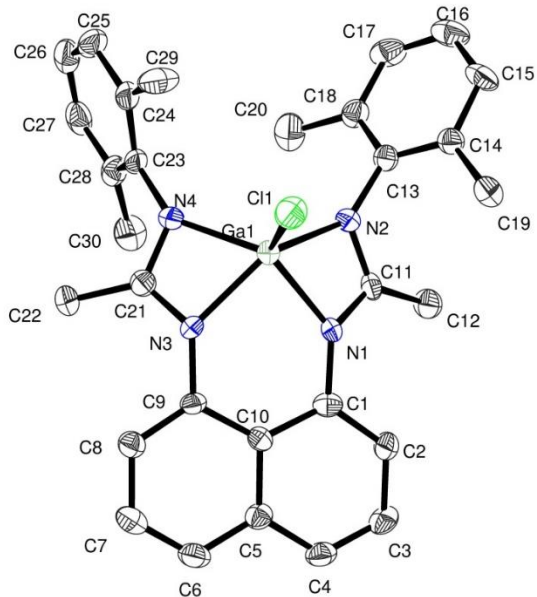
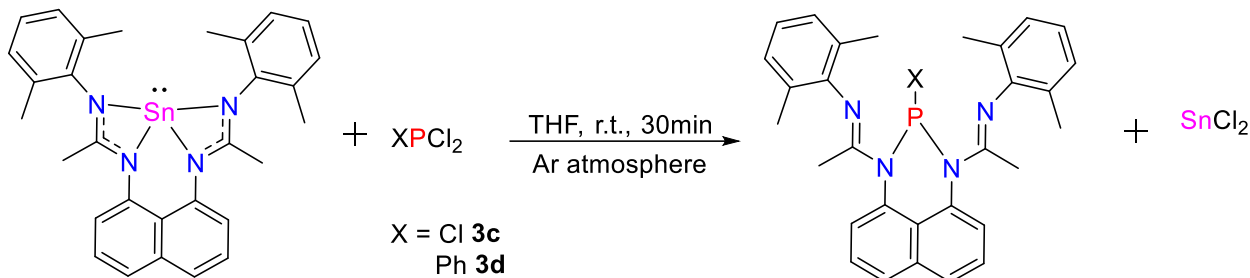


Figure 28. Molecular structure of **3b** (hydrogens are omitted for clarity). Thermal ellipsoids are shown with 50 % probability.

Finally, exchange reactions were studied between **L₁Sn** and PCl₃ or PhPCl₂ (Scheme 55) in THF as solvent for 30 min at room temperature. As before, in the ¹¹⁹Sn NMR, the formation of SnCl₂ as a by-product, and the respective products **3c** (reaction with PCl₃) and **3d** (reaction with PhPCl₂) were observed, which were characterized by ¹H, ¹³C, and ³¹P NMR, MS spectroscopy and X-ray diffraction. For **3c**, the ¹H NMR spectrum showed in the aliphatic region, four singlets: at 2.24 and 2.15 ppm, with an integration of 6 hydrogens corresponding to the 2,6-dimethylphenyl fragments and at 2.05 and 2.04 slightly overlapping with an integration of 3 hydrogens, corresponding to the -CH₃ of the amidine. These data indicate a not symmetric behavior of these groups distributed in a non-equivalent space. This trend is also observed in **3d**. The signals in ³¹P NMR 77.10 ppm for **3c** and 58.45 ppm for **3d** correspond to a +3 oxidation state tricoordinated phosphorus. The X-ray structures confirmed the tricoordinated phosphorus in **3c** and **3d** (Figure 29). These phosphorus atoms are bonded to the nitrogen atoms directly linked to naphthalene and complete the coordination sphere with a Cl ligand in the case of **3c** and a phenyl group for **3d**. Therefore, remaining nitrogen atom of the amidines are dangling. The phosphorus in both cases has a trigonal pyramidal geometry. The distances C7-N2 for **3c** and C11-N2 for **3d** are shorter than for C7-N1 and C11-N1, respectively. This indicates that there is no delocalization in the NCN fragments. These new compounds are promising pincer ligands with amidines and phosphorus atom functionalities.



Scheme 55. Synthesis of **3c** and **3d**.

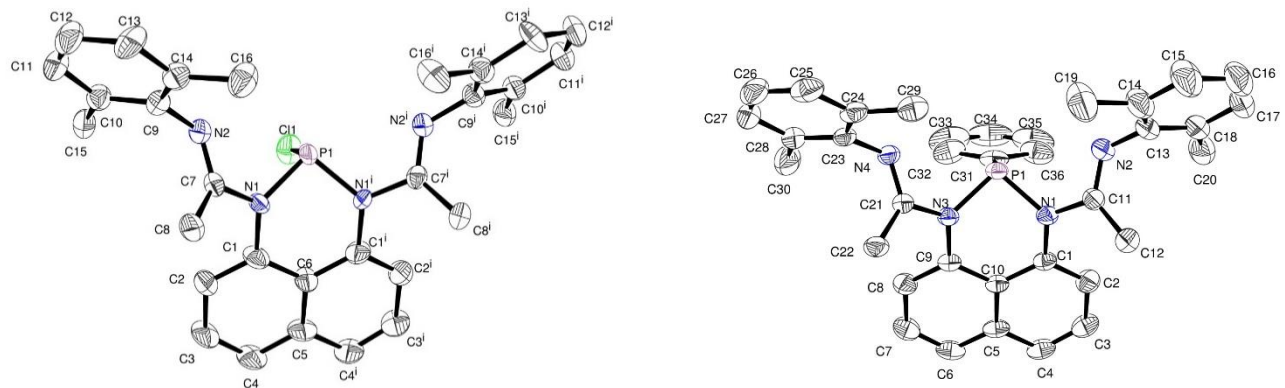
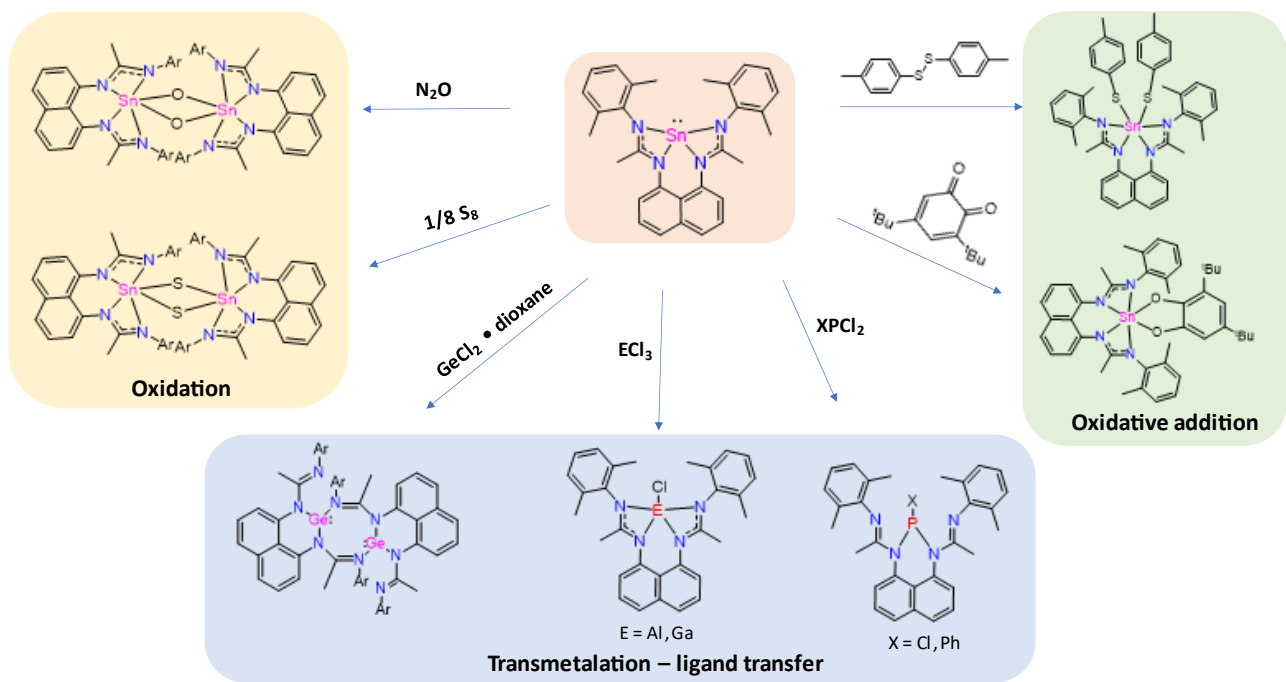


Figure 29. Molecular structures of **3c** and **3d** (hydrogens are omitted for clarity). Thermal ellipsoids are shown with 50 % probability.

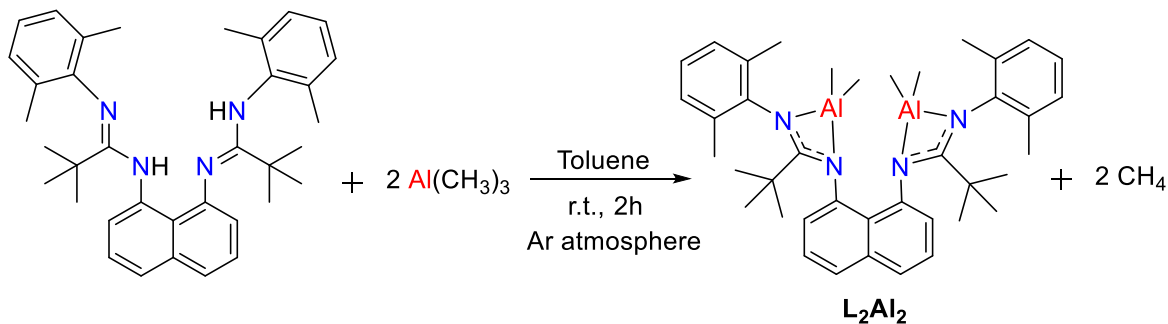
According to the above, stannylenes **L₁Sn** presents reactivity against oxidation, oxidative addition, transmetalation, and ligand transfer. Scheme 56 summarizes the compounds obtained from **L₁Sn**.



Scheme 56. Compounds obtained from **L₁Sn** and the type of reactivity.

5. Synthesis of aluminum complexes stabilized by bis-amidine ligands.

The bis-aluminum complex L_2Al_2 was synthesized through a protonolysis reaction between ligand L_2 and two equivalents of $\text{Al}(\text{CH}_3)_3$ (Scheme 57). In the reaction medium, the generation of CH_4 is observed as bubbles as $\text{Al}(\text{CH}_3)_3$ is added. The L_2Al_2 complex was obtained as orange crystals in 83 % yield. The formation of the corresponding bis-aluminum complexes was corroborated by NMR spectroscopy and XRD. ^1H NMR showed two signals in the negative region (-0.02 and -0.33 ppm) that integrate each one at 6 hydrogens, which indicates that each aluminum atom is tetracoordinated with one amidine ligand and two CH_3 ligands in its structure. Also, the disappearance of the NH signals observed in the ligand. In addition, it was possible to observe these characteristic signals of the CH_3 bonded to Al in ^{13}C NMR, observing two signals at -5.41 and -9.16 ppm. The crystalline structure confirmed that the aluminum atoms are tetracoordinated with a distorted tetrahedral geometry, similar to other aluminum tetracoordinated complexes with amidine ligands (Figure 30)^{85,98}. The indistinguishable bond distances of N-C in the NCN unit and almost equal bond distances N-Al proved the formation of delocalized systems.



Scheme 57. Synthesis of L_2Al_2 .

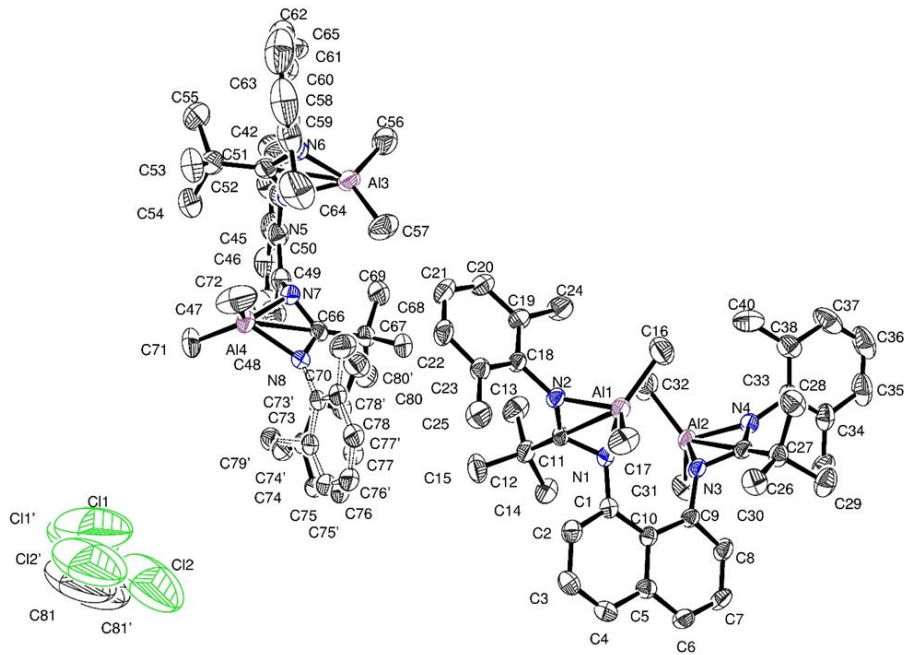
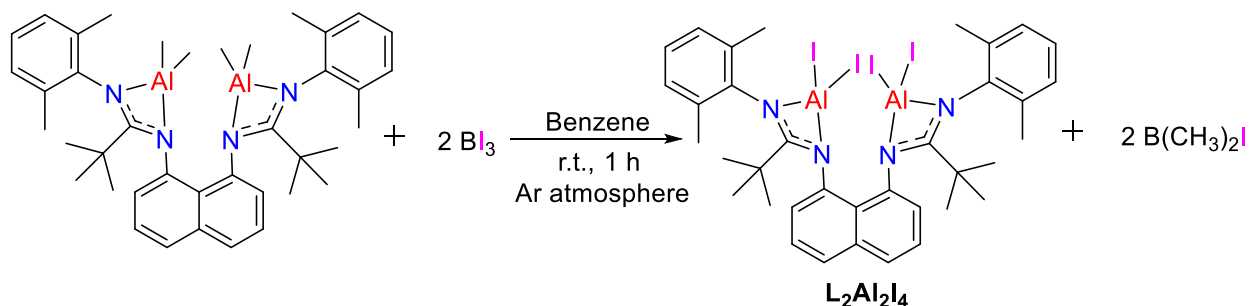


Figure 30. Molecular structures of L_2Al_2 (hydrogens are omitted for clarity). Thermal ellipsoids are shown with 50 % probability.

To synthesize one-component systems that are active for forming cyclic carbonates from CO_2 and epoxides, and without the need to use a cocatalyst, it is proposed in this work to replace the methyl groups bonded to the aluminum with iodides to have the necessary nucleophile in the catalytic cycle in the same system. Therefore, the reaction between L_2Al_2 and Bi_3 is carried out in benzene at room temperature for 1 h (Scheme 58). Yellow crystals were obtained in 91 % yield (compound $\text{L}_2\text{Al}_2\text{I}_4$). The expected reaction consists of dissociating the methyl radical from the aluminum atom, forming a new Al–I bond, and generating $\text{B}(\text{CH}_3)_2\text{I}$ as a byproduct. The evident disappearance of the signals in the negative zone in the ^1H NMR spectrum indicates that the substitution of methyls by iodines occurred. Furthermore, this was corroborated by obtaining the crystalline structure (Figure 31). The aluminum atoms exhibit a distorted tetrahedral geometry. All the bond distances corresponding to the nitrogen atoms coordinated to the aluminum atoms are shorter than the analogous distances in complex L_2Al_2 . Although it is a minimal difference, it shows that the substitution of the $-\text{CH}_3$ ligand attached to the aluminum atom by iodide results in an alteration in the electronic density positioned on the aluminum atom and, therefore, on the strength and length of the other bonds. The iodine atom, being more electronegative than carbon, shifts the electron density of the bond toward itself more strongly than the methyl group, leaving the aluminum center more electron deficient and consequently shortening the bonds of other ligands bonded to him. This phenomenon is consistent with what

was observed by other aluminum complexes^{18,99}.



Scheme 58. Synthesis of **L₂Al₂I₄**.

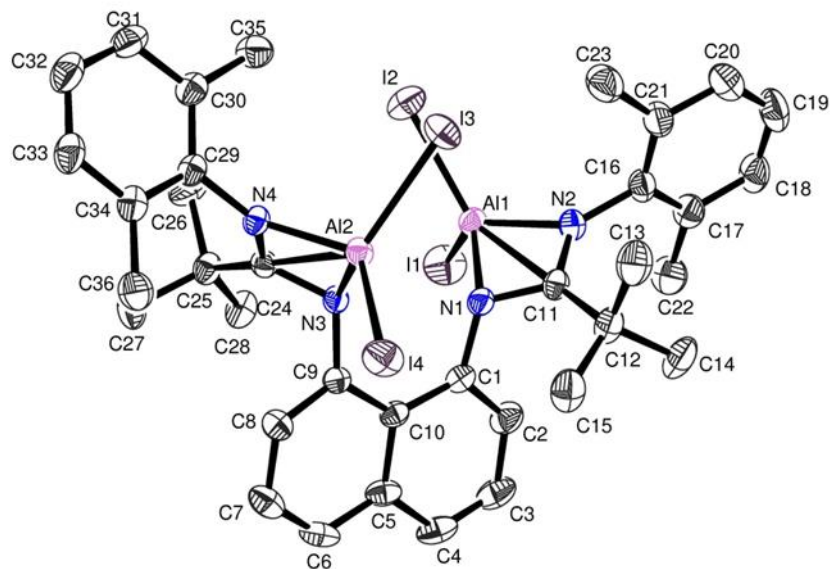


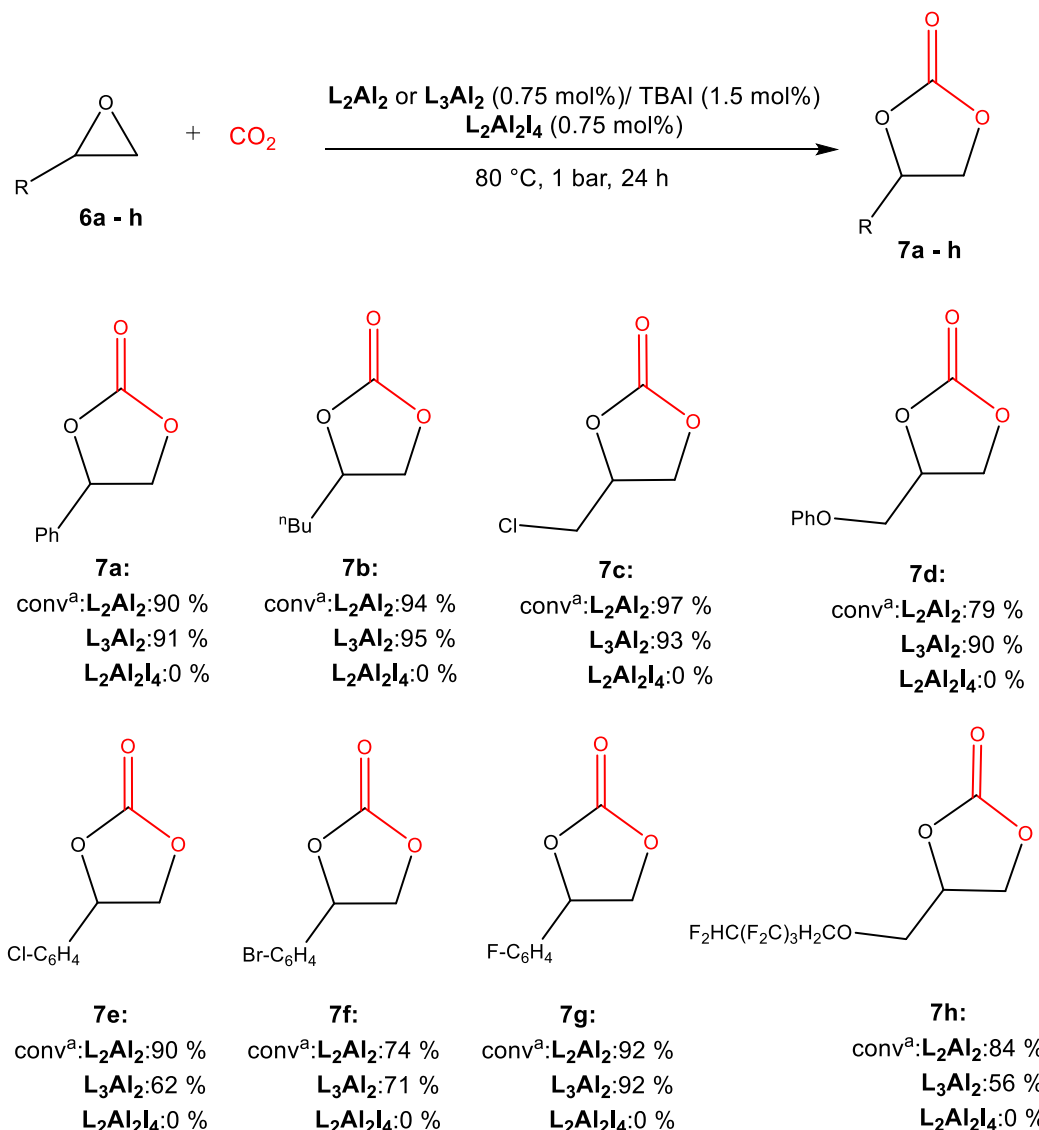
Figure 31. Molecular structures of **L₂Al₂I₄** (hydrogens are omitted for clarity). Thermal ellipsoids are shown with 50 % probability.

In the same way, a bis-aluminum complex was synthesized with the ligand **L₃** to give a yellow solid in 79 % yield (**L₃Al₂**). Obtaining the complex **L₃Al₂** was evidenced through the disappearance of the NH in the ligand by ¹H NMR spectrum and the appearance of two signals in the negative region of the spectrum at -0.33 and -0.75 ppm that integrate each one at 6 hydrogens, similar pattern as the one exhibited for **L₂Al₂**. This indicates that each aluminum atom is tetracoordinated. It was also tried to replace the methyls attached to the aluminum atoms with iodine to obtain one-component systems for catalysis, but it was not possible. This is because the complex formed is too sensitive and unstable. When the reaction is carried out on an NMR scale, it is possible to observe the product in ¹H NMR but keep the reaction at a low

temperature. Once it is brought to room temperature to purify, it decomposes. This is because the *p*-tolyl group is not large enough to stabilize the aluminum atom compared to the L_2AL_2 complex.

6. Aluminum complexes stabilized by bis-amidine reactivity: catalysis to obtaining cyclic carbonates.

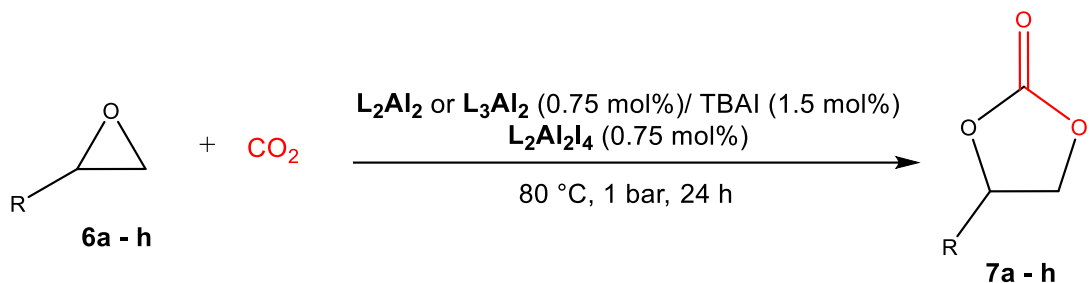
Having prepared and characterized complexes L_2Al_2 , L_3Al_2 and $\text{L}_2\text{Al}_2\text{I}_4$, we explored their potential use as catalysts for the preparation of a range of cyclic carbonates (*7a - h*) from their corresponding epoxides (*6a - h*) and CO_2 (Scheme 59). The conversions of the catalytic runs are shown in Scheme 59 and Table 5 shows the TOF values.



^a Determined by ^1H NMR spectroscopy of the crude reaction mixture.

Scheme 59. Synthesis of cyclic carbonates.

Table 5. TOF of 7a-h cyclic carbonates using the catalysts **L₂Al₂**, **L₃Al₂** and **L₂Al₂I₄**.



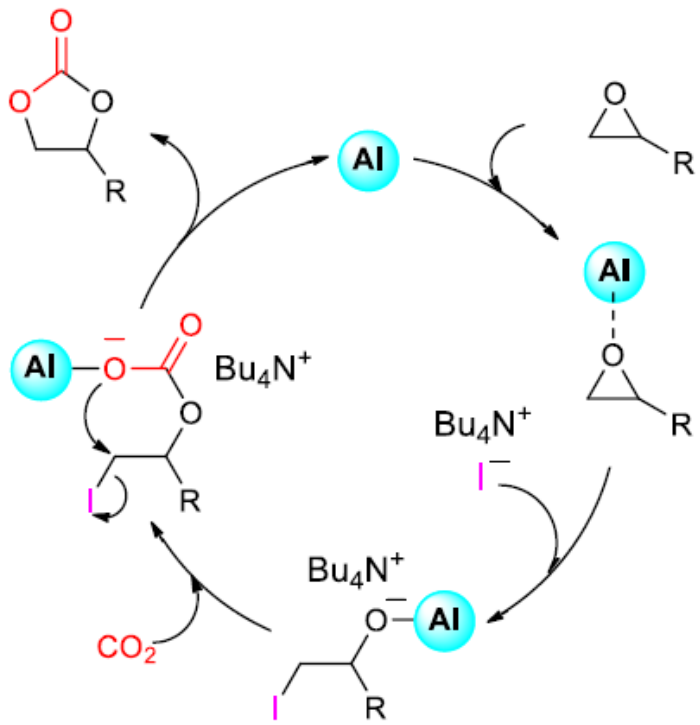
Entry	Epoxides	L ₂ Al ₂ TOF (h ⁻¹)	L ₃ Al ₂ TOF (h ⁻¹)
1	6a (R = Ph)	5.00	5.06
2	6b (R = n-Bu)	5.22	5.28
3	6c (R = CH ₂ Cl)	5.39	5.17
4	6d (R = CH ₂ OPh)	4.43	5.05
5	6e (R = 4-ClC ₆ H ₄)	5.02	3.46
6	6f (R = 4-BrC ₆ H ₄)	4.12	3.96
7	6g (R = 4-FC ₆ H ₄)	5.10	5.10
8	6h (R = CH ₂ OCH ₂ (CF ₂) ₃ CHF ₂)	4.67	3.11

The reactions were carried out at 80 °C and 1 bar of CO₂ pressure for 24 h employing a combination of 0.75 mol% of complexes **L₂Al₂** or **L₃Al₂** and 1.5 mol% of TBAI as a cocatalyst, while only 0.75 mol% of the one-component catalyst **L₂Al₂I₄** were used under solvent-free conditions. Interestingly, no polycarbonates were obtained under these reaction conditions as expected, since these epoxide substrates generally showed selectivity toward cyclic carbonate formation^{18,19,77–79,81,82,85,100}. In general, catalysts **L₂Al₂** and **L₃Al₂** achieved moderate to excellent yields for the preparation of cyclic carbonates (Scheme 59). The mixed catalytic system (catalyst/TBAI) was reactive toward the formation of a wide variety of cyclic carbonates functionalized with alkyl, aryl, halide, and ether groups, which demonstrates that compounds **L₂Al₂** and **L₃Al₂** has a broad scope and is selective for cyclic carbonate formation. In addition, the efficiency of these complexes as catalysts is demonstrated by the TOF (turn over frequency) values (Table 5), which are higher compared to other similar systems reported⁸⁵.

It is worth mentioning that the tetrabutylammonium iodide is directly chosen as a cocatalyst because, in previously reported studies^{18,19,77,78,85}, it demonstrates being the cocatalyst that leads to the highest conversions in analogous systems, in addition to allowing the use of lower catalyst charges; probably because the iodide ion can act as a good nucleophile for epoxide ring opening, and as a good leaving group in the cyclic carbonate formation step. To choose the working temperature, an optimization is proposed starting from high temperatures, to ensure good conversions from epoxy to carbonate. The temperature would be decreased whenever conversions above 99% are obtained, until all the values obtained are below this number. When carrying out a first test at 80 °C, conversions below the mentioned value are obtained, knowing that a lower reaction temperature will result in lower conversions, related to the kinetic implications of this system, we choose to set the temperature at 80 °C. The amount of catalyst was chosen due to previous studies reported for similar systems¹⁸.

It is worth noting, regardless of the good conversions obtained and the relatively mild reaction conditions ($p = 1$ bar, $< 100^\circ\text{C}$), catalysts $\mathbf{L}_2\text{Al}_2$ and $\mathbf{L}_3\text{Al}_2$ presents a moderately lower activity with respect to other aluminum amidinate type catalysts with alkyl ligands, which, in many cases, are capable of reaching similar conversions with a lower temperature and/or shorter reaction times⁸⁵.

A plausible mechanism of this reaction when it is catalyzed by binary systems (catalyst/cocatalyst) (Scheme 60) is widely studied and generally accepted. It consists of a first adduct-type coordination of one of the free electronic pairs on the oxygen atom in the epoxide, with the metal center. This coordination shifts the electron density of the epoxide group toward the oxygen atom, increasing the electrophilicity of the carbon atoms in the cycle. In the second stage, an iodide ion, coming from a cocatalyst molecule (TBAI) found in the reaction medium, acts as a nucleophile, attacking the carbon atom with less steric hindrance; the displacement of the pair of electrons that formed the C–O bond towards the oxygen atom leads to the opening of the epoxide and the formation of a formal Al–O bond. Once the epoxide has been opened, a CO_2 molecule is inserted into the Al–O bond, producing a charge shift that ends with a formal negative charge on one of the oxygen atoms. The latter, in turn, acts as a nucleophile and attacks the carbon atom that supports the iodide, the iodide dissociates from the molecule, and a five-membered cycle is formed corresponding to the cyclic carbonate, which is immediately released from the center of the catalyst.



Scheme 60. General mechanism proposed for the synthesis of cyclic carbonates catalyzed by binary systems.

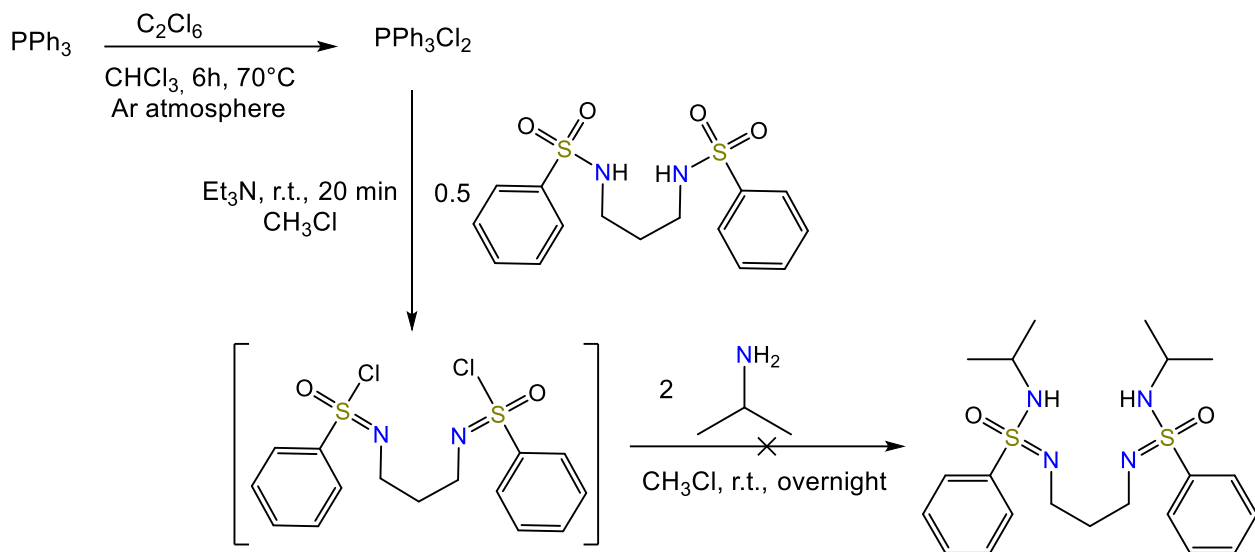
Unfortunately, the L₂Al₂I₄ complex did not show catalytic activity as a one-component system for all epoxides tested. The lack of catalytic activity can be explained because it presents a shorter Al-I bond (2.485 Å) distance than other reported one-component system reported for our group (2.553 Å) with L₁ as a ligand and the aluminum pentacoordinated¹⁸ (42, Figure 15), making it challenging to release iodide to act as a nucleophile in the reaction mechanism to open the epoxide ring. Besides, it is important to mention that the compound with an aluminum pentacoordinated is one of the rare examples of non-zwitterionic single component catalysts, and to date there are no examples of tetracoordinated aluminum complexes with two iodide ligands in their structure that are used as one-component catalysts. Therefore, the L₂Al₂I₄ complex is too stable to release all four iodine atoms.

7. Synthetic routes tested to obtain bis-sulfonimidamide ligands.

One of the objectives of this project is to synthesize bis-sulfonimidamide ligands with a spacer in their structure and use these ligands to stabilize metallylenes. It is proposed to stabilize metallylenes with bis-sulfonimidamide ligands because our group reported a few years ago, in a good manner, stannylenes and germynes stabilized with sulfonimidamide ligands, which presented promising reactivity for obtaining polycaprolactone²⁵. So, to continue studying these systems, it was proposed to synthesize bis-sulfonimidamide ligands with rigid linkers such as naphthalene or more flexible linkers such as propane. The general synthetic route that was tested consist in one reported by Chen *et al.*²⁴, as well as the synthetic route that our group previously followed²⁵ to synthesize sulfonimidamide ligands with a one-pot procedure via deoxychlorination from sulfonamides, using as chlorinating agent Ph₃PCl₂ to form a sulfonimidoyl chloride, that after reacting with a corresponding amine.

The first procedure tested consist in using a bis-sulfonamide as a precursor with a linker propane in its structure (Scheme 61). The details of the procedure are as follows:

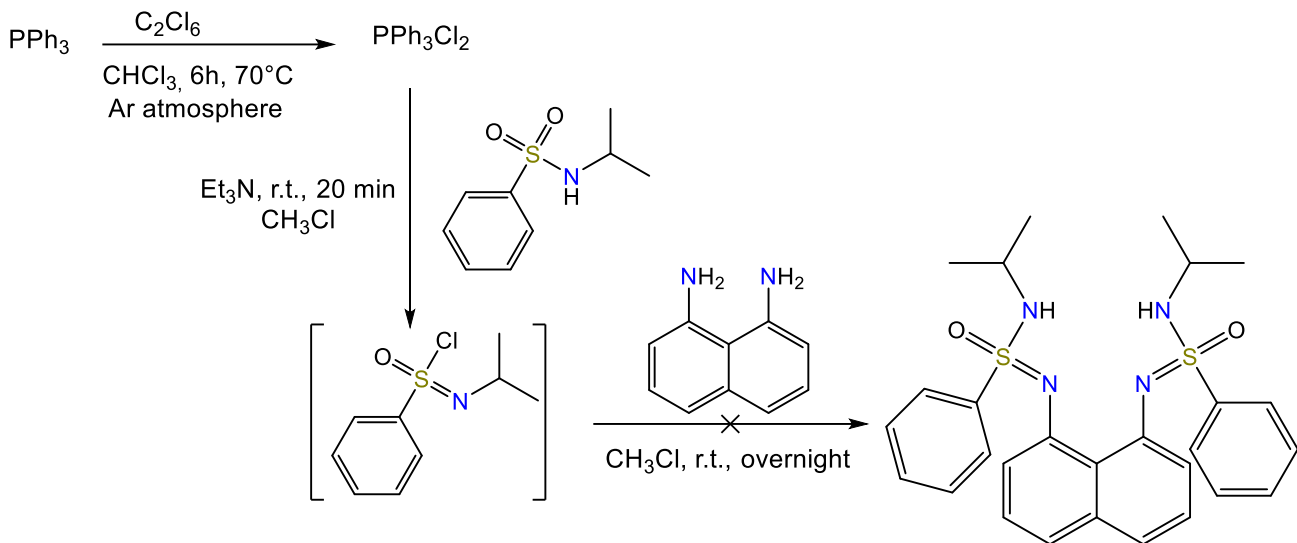
Procedure 1: CHCl₃ was added to hexachloroethane (281 mg, 1.2 mmol) and triphenylphosphine (311 mg, 1.2 mmol) at room temperature. The solution was heated at reflux for 6 h. Then, the mixture was allowed to return at room temperature, and Et₃N (171 mg, 1.7 mmol) was added. The mixture was stirred for 30 minutes at room temperature. N,N'-(propane-1,3-diyl)dibenzenesulfonamide (200 mg, 0.6 mmol) was dissolved in CHCl₃ and added to the mixture. Finally, after stirring the mixture for 30 minutes at room temperature, isopropylamine (200 mg, 3.4 mmol) was added, and the solution was stirred overnight at room temperature. The solvent was removed under reduced pressure.



Scheme 61. Route 1 tested for the synthesis of bis-sulfonimidamides using *N,N*-(propane-1,3-diyl)dibenzenesulfonamide as a precursor.

The second procedure tested consist in using a sulfonamide as a precursor and then incorporate the naphthalene linker by means of la 1,8-diaminenaphthalene (Scheme 62). The details of the procedure are as follows:

Procedure 2: CHCl_3 was added to hexachloroethane (261 mg, 1.1 mmol) and triphenylphosphine (290 mg, 1.1 mmol) at room temperature. The solution was heated at reflux for 6 h. Then, the mixture was allowed to return at room temperature, and Et_3N (152 mg, 1.5 mmol) was added. The mixture was stirred for 30 minutes at room temperature. N -isopropylbenzenesulfonamide (200 mg, 1.0 mmol) was dissolved in CHCl_3 and added to the mixture. Finally, after stirring the mixture for 30 minutes at room temperature, 1,8-diaminenaphthalene (238 mg, 1.5 mmol) was added, and the solution was stirred overnight at room temperature. The solvent was removed under reduced pressure.



Scheme 62. Route 2 tested for the synthesis of bis-sulfonimidamides using N-isopropylbenzenesulfonamide as a precursor.

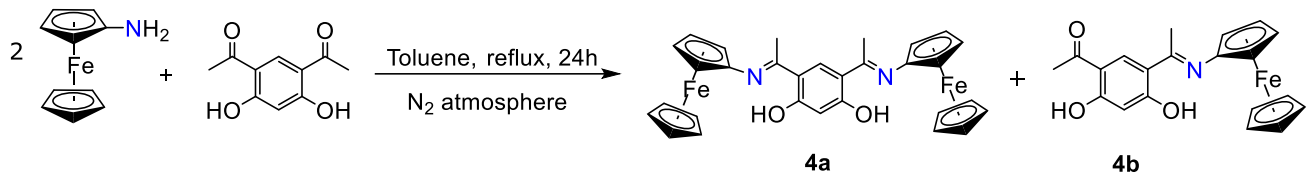
Unfortunately, despite multiple attempts, the bis-sulfonimidamide ligands could not be obtained, usually obtaining unreacted starting precursors, despite changing reaction conditions such as solvents, time, and temperature.

8. Synthesis of Schiff base ligand derived from ferrocene.

The Schiff base ligands are easy to synthesize and also, as stated in the introduction, these systems when coordinated with transition metals or group 13 present good results in catalysis. On the other hand, ferrocene is an interesting and useful backbone and has been employed in the design of a large variety of ligands, due to its electronic and steric properties.

Compounds **4a** and **4b** were obtained by the reaction of 1,1'-(4,6-dihydroxy-1,3-phenylene)bisethanone and two equivalents of ferrocenylamine in dry toluene under reflux for 24 h (Scheme 63). Both compounds are obtained in the same mixture, separated by extracting **4a** in CH_2Cl_2 . **4a** is a symmetrical bis-azomethine compound obtained as purple crystals in 70 % yield, and **4b** is an unsymmetrical single azomethine obtained as red crystals in 26 %. For **4a**, the ^1H NMR shows a signal at a low field at 16.92 ppm corresponding to the OH. In the aromatic region, two singlets that integrate 1 hydrogen each are observed, consistent with what was

expected. Around ~4 ppm of the characteristic signals of the ferrocenyl fragment. In the aliphatic region, a signal integrates for 6 hydrogens corresponding to the CH_3 (Figure 32). ^{13}C NMR shows the characteristic signal for the $\text{C}=\text{N}$ imino group at 169.27 ppm. For **4b**, the ^1H NMR shows two signals at a low field at 17.54 and 12.74 ppm corresponding to the OH. In the aromatic region, two singlets that integrate 1 hydrogen each are observed, consistent with what was expected. Around ~4 ppm of the characteristic signals of the ferrocenyl fragment. In the aliphatic region, two singlets integrate for 3 hydrogens, each corresponding to the CH_3 (Figure 32). ^{13}C NMR shows the characteristic signal for the $\text{C}=\text{N}$ imino group at 166.66 ppm and the resonance corresponding to $\text{C}=\text{O}$ at 201.79 ppm. Obtaining the crystalline structure confirms these two compounds' synthesis (Figure 26).



Scheme 63. Synthesis of **4a** and **4b**.

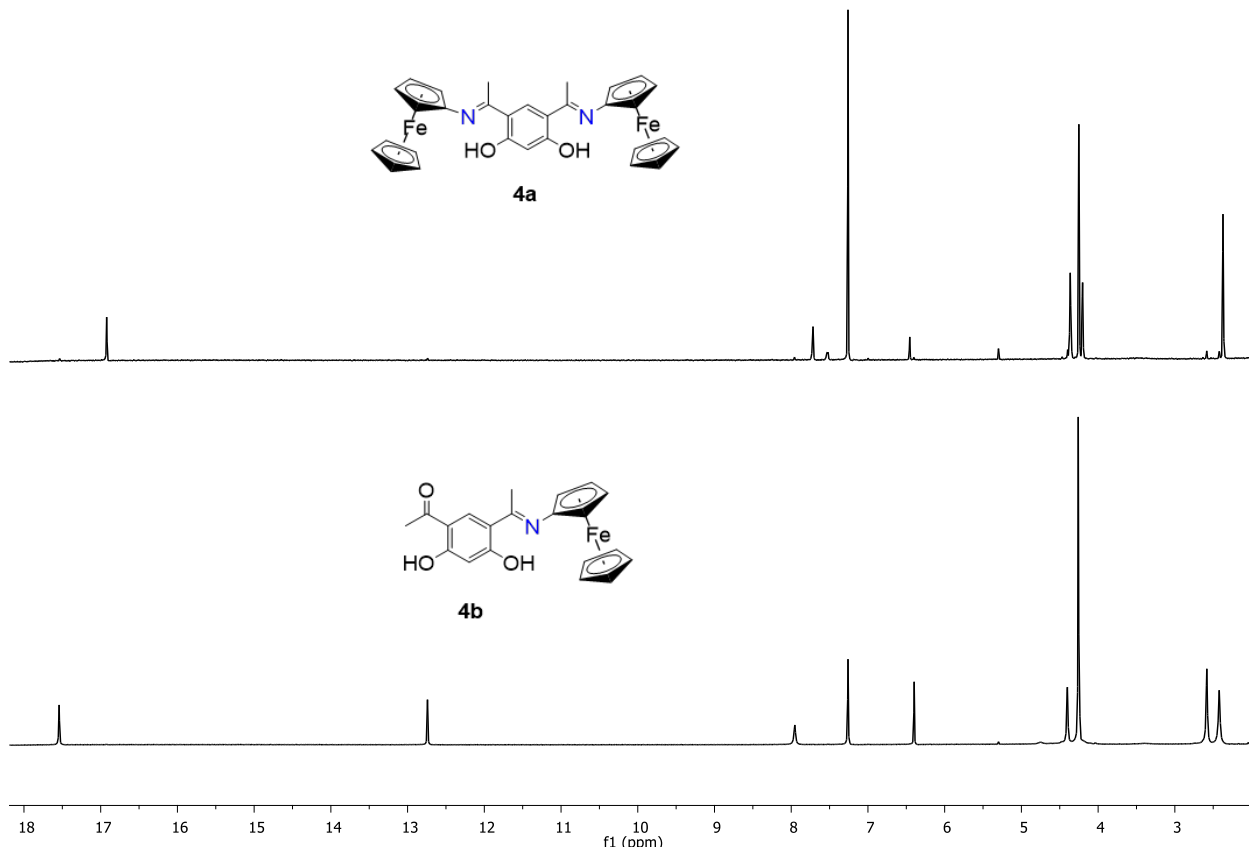


Figure 32. ^1H NMR of **4a** and **4b**.

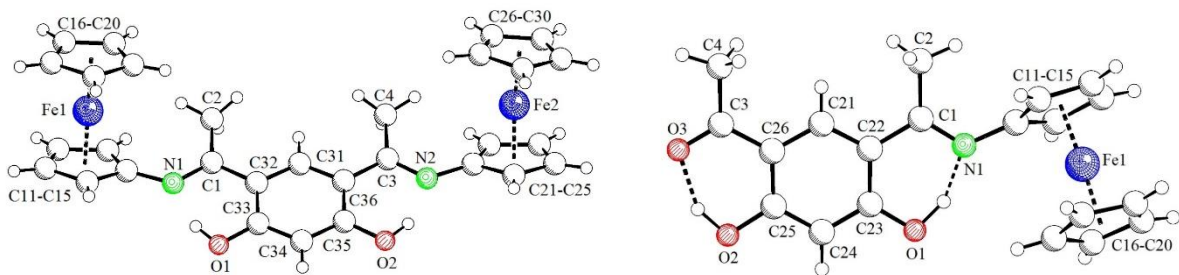
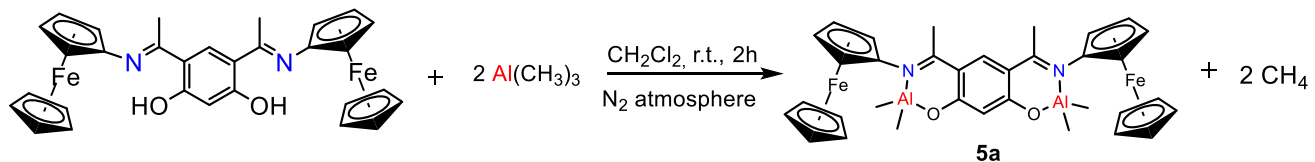


Figure 33. Molecular structures of **4a** and **4b**. Thermal ellipsoids are shown with 50 % probability.

9. Synthesis of bis-aluminum complex stabilized by Schiff ligand derived from ferrocene (**5a**).

The aluminum complex **5a** was synthesized through a protonolysis reaction between the ligand **4a** and two equivalents of $\text{Al}(\text{CH}_3)_3$ (Scheme 64). **5a** complex was obtained as a red solid in 95 % yield. The formation of the corresponding bis-aluminum complex is evidenced by ^1H NMR that showed one singlet in the negative region at -0.64 ppm that integrates at 12 hydrogens, which indicates the coordination of two aluminum atoms in the ligands and each one is tetracoordinated. In addition, the disappearance of the OH signals observed in the ligand. Also, it was possible to observe these characteristic signals of the CH_3 bonded to Al in ^{13}C NMR, observing a signal at -8.80 ppm.



Scheme 64. Synthesis of **5a**.

To obtain a one-component system, an attempt was made to replace the methyls bonded to the aluminum with iodides, but despite the attempts, it was not possible to obtain it. The substitution was not possible due to a possible redox reaction between the iodine and the ferrocenyl fragment.

10. Aluminum complex 5a reactivity: catalysis to obtaining cyclic carbonates.

Having prepared the bis-aluminum complex **5a**, we decided to focus on exploring their use as a catalyst for forming cyclic carbonates. Firstly, styrene oxide was selected as a model substrate to study the catalytic activity of complex **5a**. The reactions were performed at 80 °C and 1 bar of CO₂ pressure for 24 h under solvent-free conditions using 0.5-1.5 mol% of catalyst **5a** and 1.0-3.0 mol% of tetrabutylammonium iodide (Bu₄NI) as a cocatalyst, based on other previous work in which the ammonium salt was found to be the best nucleophile. The catalytic result is shown in Table 6. Unfortunately, the complex presents low catalytic activity compared to other aluminum complexes.

Table 6. Preliminary tests reactivity of the aluminum complex **5a** for the synthesis of styrene carbonate^a.

Ent.	Cat.	Cocat. (mol%)	amt of cat. (mol%) ^b	T (°C)	t (h)	Conversion (%)
1	5a	TBAI 1.0	0.5	80	24	18
2	5a	TBAI 2.0	1.0	80	24	39
3	5a	TBAI 3.0	1.5	80	24	48

^aStyrene oxide is used for all entries.

^bThe percentage is calculated based on the amount of epoxide added (1,7 mmol).

CHAPTER V: CONCLUSION

CONCLUSION

In conclusion, stannylenes and germylenes were synthesized with bis-amidine ligands with a rigid naphthalene backbone by a protonolysis reaction between the respective ligand and Sn(HMDS)₂ or Ge(HMDS)₂. L₁Sn and L₃Sn are obtained as monomeric species, where the X-ray structure of L₁Sn showed that the tin atom is tetracoordinated and presents a square-based pyramidal geometry. L₂Sn is obtained as a dimeric species. On the other hand, the germylene L₁Ge was obtained as a dimeric species that presents the germanium atom with a trigonal pyramidal geometry. L₂Ge and L₃Ge are monomeric species, and the X-ray structure of L₂Ge showed that the germanium atom is tricoordinate with a trigonal pyramidal geometry.

Metallylenes were used as catalysts in cyclic ester polymerization reactions but did not show the desired reactivity. However, stannylene L₁Sn presented reactivity against oxidation reactions, generating the product amidinate-stannoxyane (1a) and its analog with sulfur (1b); oxidative addition, generating the product 2a due to the insertion of tin in the S-S bond of *para*-tolyl disulfide, as well as generating a cycloaddition product (2b) from a quinone; and transmetalation-transfer of ligands, when stannylene L₁Sn reacts with different halogenated substrates such as AlCl₃, GaCl₃, PCl₃, and PhPCl₂.

On the other hand, it was possible to synthesize new bis-aluminum complexes with bis-amidine ligand with a rigid naphthalene bridge, which were tested as a catalyst for obtaining cyclic carbonates from epoxides and CO₂, which presented moderate to excellent conversion. Likewise, it was possible to obtain an aluminum complex using the same bis-amidine ligand but incorporating iodides in its structure to use it as a one-component catalyst, but unfortunately it did not present catalytic activity.

A Schiff base ligand derived from ferrocene was synthesized with its respective aluminum complex, which presented low catalytic activity for obtaining cyclic carbonates from epoxides and CO₂.

Despite the bis-sulfonimidamide ligands that contain a bridge in their structure, it was impossible to obtain them despite multiple tests.

REFERENCES

REFERENCES

- (1) Hallegatte, S.; Rogelj, J.; Allen, M.; Clarke, L.; Edenhofer, O.; Field, C. B.; Friedlingstein, P.; van Kesteren, L.; Knutti, R.; Mach, K. J.; Mastrandrea, M.; Michel, A.; Minx, J.; Oppenheimer, M.; Plattner, G.-K.; Riahi, K.; Schaeffer, M.; Stocker, T. F.; van Vuuren, D. P. Mapping the Climate Change Challenge. *Nature Clim Change* **2016**, *6* (7), 663–668. <https://doi.org/10.1038/nclimate3057>.
- (2) Anderson, T. R.; Hawkins, E.; Jones, P. D. CO₂, the Greenhouse Effect and Global Warming: From the Pioneering Work of Arrhenius and Callendar to Today's Earth System Models. *Endeavour* **2016**, *40* (3), 178–187. <https://doi.org/10.1016/j.endeavour.2016.07.002>.
- (3) Grimm, N. B.; Groffman, P.; Staudinger, M.; Tallis, H. Climate Change Impacts on Ecosystems and Ecosystem Services in the United States: Process and Prospects for Sustained Assessment. *Climatic Change* **2016**, *135* (1), 97–109. <https://doi.org/10.1007/s10584-015-1547-3>.
- (4) Wilcox, C.; Mallos, N. J.; Leonard, G. H.; Rodriguez, A.; Hardesty, B. D. Using Expert Elicitation to Estimate the Impacts of Plastic Pollution on Marine Wildlife. *Marine Policy* **2016**, *65*, 107–114. <https://doi.org/10.1016/j.marpol.2015.10.014>.
- (5) Welden, N. A. Chapter 8 - The Environmental Impacts of Plastic Pollution. In *Plastic Waste and Recycling*; Letcher, T. M., Ed.; Academic Press, 2020; pp 195–222. <https://doi.org/10.1016/B978-0-12-817880-5.00008-6>.
- (6) Kåberger, T. Progress of Renewable Electricity Replacing Fossil Fuels. *Global Energy Interconnection* **2018**, *1* (1), 48–52. <https://doi.org/10.14171/j.2096-5117.gei.2018.01.006>.
- (7) Burghaus, U. Chapter 2 - Surface Science Studies of Carbon Dioxide Chemistry. In *New and Future Developments in Catalysis*; Suib, S. L., Ed.; Elsevier: Amsterdam, 2013; pp 27–47. <https://doi.org/10.1016/B978-0-444-53882-6.00003-6>.
- (8) Fujita, S.; Yoshida, H.; Liu, R.; Arai, M. Chapter 5 - Catalytic Transformation of CO₂ into Value-Added Organic Chemicals. In *New and Future Developments in Catalysis*; Suib, S. L., Ed.; Elsevier: Amsterdam, 2013; pp 149–169. <https://doi.org/10.1016/B978-0-444-53882-6.00006-1>.
- (9) Albertsson, A.-C.; Varma, I. K. Recent Developments in Ring Opening Polymerization of Lactones for Biomedical Applications. *Biomacromolecules* **2003**, *4* (6), 1466–1486. <https://doi.org/10.1021/bm034247a>.
- (10) Elsevier, C. J.; Reedijk, J.; Walton, P. H.; Ward, M. D. Ligand Design in Coordination Chemistry: Approaches to New Catalysts, New Materials, and a More Sustainable Environment. *Dalton Trans.* **2003**, No. 10, 1869–1880. <https://doi.org/10.1039/B303975G>.
- (11) Quek, J. Y.; Davis, T. P.; Lowe, A. B. Amidine Functionality as a Stimulus-Responsive Building Block. *Chem. Soc. Rev.* **2013**, *42* (17), 7326–7334. <https://doi.org/10.1039/C3CS60065C>.
- (12) Aly, A. A.; El-Din, A. M. N. Functionality of Amidines and Amidrazones. *Arkivoc* **2008**, *2008* (1), 153–194. <https://doi.org/10.3998/ark.5550190.0009.106>.
- (13) Coles, M. P. Application of Neutral Amidines and Guanidines in Coordination Chemistry. *Dalton Trans.* **2006**, No. 8, 985–1001. <https://doi.org/10.1039/B515490A>.
- (14) Boéré, R. T.; Klassen, V.; Wolmershäuser, G. Synthesis of Some Very Bulky N,N'-Disubstituted Amidines and Initial Studies of Their Coordination Chemistry†. *J. Chem. Soc., Dalton Trans.* **1998**, No. 24, 4147–4154. <https://doi.org/10.1039/A805548C>.
- (15) Dunn, P. J. Amidines and N-Substituted Amidines. *ChemInform* **2005**, *36* (26). <https://doi.org/10.1002/chin.200526223>.
- (16) Kretschmer, R. Ligands with Two Monoanionic N,N-Binding Sites: Synthesis and Coordination Chemistry. *Chemistry – A European Journal* **2020**, *26* (10), 2099–2119. <https://doi.org/10.1002/chem.201903442>.
- (17) Osorio Meléndez, D.; Castro-Osma, J. A.; Lara-Sánchez, A.; Rojas, R. S.; Otero, A. Ring-Opening Polymerization and Copolymerization of Cyclic Esters Catalyzed by Amidinate

- Aluminum Complexes. *Journal of Polymer Science Part A: Polymer Chemistry* **2017**, *55* (14), 2397–2407. <https://doi.org/10.1002/pola.28629>.
- (18) Saltarini, S.; Villegas-Escobar, N.; Martínez, J.; Daniliuc, C. G.; Matute, R. A.; Gade, L. H.; Rojas, R. S. Toward a Neutral Single-Component Amidinate Iodide Aluminum Catalyst for the CO₂ Fixation into Cyclic Carbonates. *Inorg. Chem.* **2021**, *60* (2), 1172–1182. <https://doi.org/10.1021/acs.inorgchem.0c03290>.
- (19) Meléndez, D. O.; Lara-Sánchez, A.; Martínez, J.; Wu, X.; Otero, A.; Castro-Osma, J. A.; North, M.; Rojas, R. S. Amidinate Aluminium Complexes as Catalysts for Carbon Dioxide Fixation into Cyclic Carbonates. *ChemCatChem* **2018**, *10* (10), 2271–2277. <https://doi.org/10.1002/cctc.201702014>.
- (20) Nandi, G. C.; Arvidsson, P. I. Sulfonimidamides: Synthesis and Applications in Preparative Organic Chemistry. *Advanced Synthesis & Catalysis* **2018**, *360* (16), 2976–3001. <https://doi.org/10.1002/adsc.201800273>.
- (21) Chinthakindi, P. K.; Naicker, T.; Thota, N.; Govender, T.; Kruger, H. G.; Arvidsson, P. I. Sulfonimidamides in Medicinal and Agricultural Chemistry. *Angewandte Chemie International Edition* **2017**, *56* (15), 4100–4109. <https://doi.org/10.1002/anie.201610456>.
- (22) Bremerich, M.; Conrads, C. M.; Langletz, T.; Bolm, C. Additions to N-Sulfinylamines as an Approach for the Metal-Free Synthesis of Sulfonimidamides: O-Benzotriazolyl Sulfonimidates as Activated Intermediates. *Angewandte Chemie* **2019**, *131* (52), 19190–19196. <https://doi.org/10.1002/ange.201911075>.
- (23) Roy, A. K. Novel Synthesis of Sulfonimidoyl Halides and Sulfonimidates from N-Silylated Sulfonamides and Dihalophosphoranes. *J. Am. Chem. Soc.* **1993**, *115* (7), 2598–2603. <https://doi.org/10.1021/ja00060a008>.
- (24) Chen, Y.; Gibson, J. A Convenient Synthetic Route to Sulfonimidamides from Sulfonamides. *RSC Adv.* **2014**, *5* (6), 4171–4174. <https://doi.org/10.1039/C4RA14056G>.
- (25) Lentz, N. Metallylene-Sulfur Compounds : Synthesis, Characterization and Applications in Coordination and Catalysis. These de doctorat, Toulouse 3, 2018. <https://www.theses.fr/2018TOU30274> (accessed 2022-09-20).
- (26) Abu-Dief, A. M.; Mohamed, I. M. A. A Review on Versatile Applications of Transition Metal Complexes Incorporating Schiff Bases. *Beni-Suef University Journal of Basic and Applied Sciences* **2015**, *4* (2), 119–133. <https://doi.org/10.1016/j.bjbas.2015.05.004>.
- (27) da Silva, C. M.; da Silva, D. L.; Modolo, L. V.; Alves, R. B.; de Resende, M. A.; Martins, C. V. B.; de Fátima, Â. Schiff Bases: A Short Review of Their Antimicrobial Activities. *Journal of Advanced Research* **2011**, *2* (1), 1–8. <https://doi.org/10.1016/j.jare.2010.05.004>.
- (28) Gupta, K. C.; Sutar, A. K. Catalytic Activities of Schiff Base Transition Metal Complexes. *Coordination Chemistry Reviews* **2008**, *252* (12), 1420–1450. <https://doi.org/10.1016/j.ccr.2007.09.005>.
- (29) Chakraborti, A. K.; Bhagat, S.; Rudrawar, S. Magnesium Perchlorate as an Efficient Catalyst for the Synthesis of Imines and Phenylhydrazones. *Tetrahedron Letters* **2004**, *45* (41), 7641–7644. <https://doi.org/10.1016/j.tetlet.2004.08.097>.
- (30) Dasgupta, R.; Khan, S. Chapter Three - N-Heterocyclic Germynes and Stannylenes: Synthesis, Reactivity and Catalytic Application in a Nutshell. In *Advances in Organometallic Chemistry*; Pérez, P. J., Ed.; Academic Press, 2020; Vol. 74, pp 105–152. <https://doi.org/10.1016/bs.adomc.2020.04.001>.
- (31) Mizuhata, Y.; Sasamori, T.; Tokitoh, N. Stable Heavier Carbene Analogues. *Chem. Rev.* **2009**, *109* (8), 3479–3511. <https://doi.org/10.1021/cr900093s>.
- (32) Lee, V. Ya.; Sekiguchi, A. *Organometallic Compounds of Low-Coordinate Si, Ge, Sn and Pb: From Phantom Species to Stable Compounds*, 1st ed.; Wiley, 2010. <https://doi.org/10.1002/9780470669266>.
- (33) Kühl, O. N-Heterocyclic Germynes and Related Compounds. *Coordination Chemistry Reviews* **2004**, *248* (5), 411–427. <https://doi.org/10.1016/j.ccr.2003.12.004>.

- (34) Foley, S. R.; Bensimon, C.; Richeson, D. S. Facile Formation of Rare Terminal Chalcogenido Germanium Complexes with Alkylamidinates as Supporting Ligands. *J. Am. Chem. Soc.* **1997**, *119* (43), 10359–10363. <https://doi.org/10.1021/ja9719891>.
- (35) Karsch, H. H.; Schlüter, P. A.; Reisky, M. Bis(Amidinate) Complexes of Silicon and Germanium. *European Journal of Inorganic Chemistry* **1998**, *1998* (4), 433–436. [https://doi.org/10.1002/\(SICI\)1099-0682\(199804\)1998:4<433::AID-EJIC433>3.0.CO;2-P](https://doi.org/10.1002/(SICI)1099-0682(199804)1998:4<433::AID-EJIC433>3.0.CO;2-P).
- (36) Aubrecht, K. B.; Hillmyer, M. A.; Tolman, W. B. Polymerization of Lactide by Monomeric Sn(II) Alkoxide Complexes. *Macromolecules* **2002**, *35* (3), 644–650. <https://doi.org/10.1021/ma011873w>.
- (37) Garg, P.; Dange, D.; Jones, C. S- and p-Block Dinuclear Metal(Loid) Complexes Bearing 1,4-Phenylene and 1,4-Cyclohexylene Bridged Bis(Amidinate) Ligands. *European Journal of Inorganic Chemistry* **2020**, *2020* (42), 4037–4044. <https://doi.org/10.1002/ejic.202000737>.
- (38) Garg, P.; Dange, D.; Jones, C. Bulky Arene-Bridged Bis(Amide) and Bis(Amidinate) Complexes of Germanium(II) and Tin(II). *Dalton Trans.* **2021**, *50* (26), 9118–9122. <https://doi.org/10.1039/D1DT01642C>.
- (39) Dehmel, M.; Wünsche, M. A.; Görls, H.; Kretschmer, R. Dinuclear Chlorotetrylenes of Silicon, Germanium, and Tin Based on a Backbone-Bridged Bis(Amidine). *European Journal of Inorganic Chemistry* **2021**, *2021* (46), 4806–4811. <https://doi.org/10.1002/ejic.202100692>.
- (40) Carl, E.; Stalke, D. Germanium(II) and Tin(II) Halide Complexes Containing the Triimido Sulfur(VI) Phosphanyl Ligand. *European Journal of Inorganic Chemistry* **2015**, *2015* (12), 2052–2056. <https://doi.org/10.1002/ejic.201500074>.
- (41) Nakata, N.; Hosoda, N.; Takahashi, S.; Ishii, A. Chlorogermylenes and -Stannylenes Stabilized by Diimidatosulfinate Ligands: Synthesis, Structures, and Reactivity. *Dalton Trans.* **2018**, *47* (2), 481–490. <https://doi.org/10.1039/C7DT04390B>.
- (42) Karlov, S. S.; Zaitseva, G. S.; Egorov, M. P. Tetrylenes Based on Tri- and Tetradentate ONO-, NNO-, NNN-, and ONNO-Type Ligands: Synthesis, Structure, and Reactivity. *Russ Chem Bull* **2019**, *68* (6), 1129–1142. <https://doi.org/10.1007/s11172-019-2532-1>.
- (43) Kricheldorf, H. R.; Kreiser-Saunders, I.; Boettcher, C. Polylactones: 31. Sn(II)Octoate-Initiated Polymerization of L-Lactide: A Mechanistic Study. *Polymer* **1995**, *36* (6), 1253–1259. [https://doi.org/10.1016/0032-3861\(95\)93928-F](https://doi.org/10.1016/0032-3861(95)93928-F).
- (44) Nimitsiriwat, N.; Gibson, V. C.; Marshall, E. L.; White, A. J. P.; Dale, S. H.; Elsegood, M. R. J. Tert-Butylamidinate Tin(II) Complexes: High Activity, Single-Site Initiators for the Controlled Production of Polylactide. *Dalton Trans.* **2007**, No. 39, 4464. <https://doi.org/10.1039/b706663e>.
- (45) Phomphrai, K.; Pongchan-o, C.; Thumrongpatanaraks, W.; Sangtrirutnugul, P.; Kongsaeree, P.; Pohmakotr, M. Synthesis of High-Molecular-Weight Poly(*e*-Caprolactone) Catalyzed by Highly Active Bis(Amidinate) Tin(II) Complexes. *Dalton Trans.* **2011**, *40* (10), 2157–2159. <https://doi.org/10.1039/C0DT01050B>.
- (46) Foley, S. R.; Yap, G. P. A.; Richeson, D. S. Formation of Novel Tetrasulfido Tin Complexes and Their Ability To Catalyze the Cyclotrimerization of Aryl Isocyanates. *Organometallics* **1999**, *18* (23), 4700–4705. <https://doi.org/10.1021/om990405w>.
- (47) Chlupatý, T.; Růžičková, Z.; Horáček, M.; Alonso, M.; De Proft, F.; Kampová, H.; Brus, J.; Růžička, A. Oxidative Additions of Homoleptic Tin(II) Amidinate. *Organometallics* **2015**, *34* (3), 606–615. <https://doi.org/10.1021/om501074m>.
- (48) Foley, S. R.; Yap, G. P. A.; Richeson, D. S. Oxidative Addition to M(II) (M = Ge, Sn) Amidinate Complexes: Routes to Group 14 Chalcogenolates with Hypervalent Coordination Environments. *J. Chem. Soc., Dalton Trans.* **2000**, No. 10, 1663–1668. <https://doi.org/10.1039/a909228e>.
- (49) Deak, N.; Moraru, I.-T.; Saffon-Merceron, N.; Madec, D.; Nemes, G. Reactivity of Bis(Sulfonyl) O,C,O-Chelated Metallylenes in Cycloaddition with Ortho-Benzoquinone: An Experimental and Computational Study. *European Journal of Inorganic Chemistry* **2017**, *2017* (36), 4214–4220. <https://doi.org/10.1002/ejic.201700756>.

- (50) Agustin, D.; Rima, G.; Gornitzka, H.; Barrau, J. Ligand Transfer Reactions between Schiff Base Divalent Group 14 Element Species and Titanium, Nickel, Boron, and Phosphorus Halides. *Organometallics* **2000**, 19 (21), 4276–4282. <https://doi.org/10.1021/om000426m>.
- (51) Veith, M.; Grosser, M.; Huch, V. Cyclische Diazastannylene. XIX. Zur Reaktion eines Bis(amino)germylens, -stannylens und -plumbylens mit Phosphortrichlorid und 2, 3-Dimethyl-1, 3-butadien. *Zeitschrift für anorganische und allgemeine Chemie* **1984**, 513 (6), 89–102. <https://doi.org/10.1002/zaac.19845130610>.
- (52) West, J. K.; Stahl, L. Reactions of Germynes and Stannylenes with Halo(Hydrocarbyl)- and Chloro(Amino)Phosphines: Oxidative Addition versus Ligand Transfer. *Inorg. Chem.* **2017**, 56 (21), 12728–12738. <https://doi.org/10.1021/acs.inorgchem.7b01275>.
- (53) Pahar, S.; Swamy, V. S. V. S. N.; Das, T.; Gonnade, R. G.; Vanka, K.; Sen, S. S. Access to Diverse Germynes and a Six-Membered Dialane with a Flexible β -Diketiminate. *Chem. Commun.* **2020**, 56 (79), 11871–11874. <https://doi.org/10.1039/D0CC05202G>.
- (54) Bag, P.; Weetman, C.; Inoue, S. Experimental Realisation of Elusive Multiple-Bonded Aluminium Compounds: A New Horizon in Aluminium Chemistry. *Angewandte Chemie International Edition* **2018**, 57 (44), 14394–14413. <https://doi.org/10.1002/anie.201803900>.
- (55) Atwood, D. A.; Yearwood, B. C. The Future of Aluminum Chemistry. *Journal of Organometallic Chemistry* **2000**, 600 (1), 186–197. [https://doi.org/10.1016/S0022-328X\(00\)00147-9](https://doi.org/10.1016/S0022-328X(00)00147-9).
- (56) Saito, S. Aluminum in Organic Synthesis. In *Main Group Metals in Organic Synthesis*; John Wiley & Sons, Ltd, 2004; pp 189–306. <https://doi.org/10.1002/3527602607.ch6>.
- (57) Saito, S. 9.06 - Aluminum. In *Comprehensive Organometallic Chemistry III*; Mingos, D. M. P., Crabtree, R. H., Eds.; Elsevier: Oxford, 2007; pp 245–296. <https://doi.org/10.1016/B0-08-045047-4/00113-8>.
- (58) Mitra, A.; Atwood, D. A. 3.06 - Aluminum Organometallics. In *Comprehensive Organometallic Chemistry III*; Mingos, D. M. P., Crabtree, R. H., Eds.; Elsevier: Oxford, 2007; pp 265–285. <https://doi.org/10.1016/B0-08-045047-4/00047-9>.
- (59) Brazeau, A. L.; Wang, Z.; Rowley, C. N.; Barry, S. T. Synthesis and Thermolysis of Aluminum Amidinates: A Ligand-Exchange Route for New Mixed-Ligand Systems. *Inorg. Chem.* **2006**, 45 (5), 2276–2281. <https://doi.org/10.1021/ic051856d>.
- (60) Coles, M. P.; Swenson, D. C.; Jordan, R. F.; Young, V. G. Synthesis and Structures of Mono- and Bis(Amidinate) Complexes of Aluminum. *Organometallics* **1997**, 16 (24), 5183–5194. <https://doi.org/10.1021/om9706323>.
- (61) Aresta, M.; Dibenedetto, A. Utilisation of CO₂ as a Chemical Feedstock: Opportunities and Challenges. *Dalton Trans.* **2007**, No. 28, 2975–2992. <https://doi.org/10.1039/B700658F>.
- (62) Plasseraud, L. Carbon Dioxide as Chemical Feedstock. Edited by Michele Aresta. *ChemSusChem* **2010**, 3 (5), 631–632. <https://doi.org/10.1002/cssc.201000097>.
- (63) Sakakura, T.; Choi, J.-C.; Yasuda, H. Transformation of Carbon Dioxide. *Chem. Rev.* **2007**, 107 (6), 2365–2387. <https://doi.org/10.1021/cr068357u>.
- (64) Aresta, M.; Dibenedetto, A.; Angelini, A. Catalysis for the Valorization of Exhaust Carbon: From CO₂ to Chemicals, Materials, and Fuels. Technological Use of CO₂. *Chem. Rev.* **2014**, 114 (3), 1709–1742. <https://doi.org/10.1021/cr4002758>.
- (65) Klaus, S.; Lehenmeier, M. W.; Herdtweck, E.; Deglmann, P.; Ott, A. K.; Rieger, B. Mechanistic Insights into Heterogeneous Zinc Dicarboxylates and Theoretical Considerations for CO₂–Epoxide Copolymerization. *J. Am. Chem. Soc.* **2011**, 133 (33), 13151–13161. <https://doi.org/10.1021/ja204481w>.
- (66) Nakano, K.; Hashimoto, S.; Nozaki, K. Bimetallic Mechanism Operating in the Copolymerization of Propylene Oxide with Carbon Dioxide Catalyzed by Cobalt–Salen Complexes. *Chem. Sci.* **2010**, 1 (3), 369–373. <https://doi.org/10.1039/C0SC00220H>.
- (67) Mizuno, H.; Takaya, J.; Iwasawa, N. Rhodium(I)-Catalyzed Direct Carboxylation of Arenes with CO₂ via Chelation-Assisted C–H Bond Activation. *J. Am. Chem. Soc.* **2011**, 133 (5), 1251–1253. <https://doi.org/10.1021/ja109097z>.

- (68) Das Neves Gomes, C.; Jacquet, O.; Villiers, C.; Thuéry, P.; Ephritikhine, M.; Cantat, T. A Diagonal Approach to Chemical Recycling of Carbon Dioxide: Organocatalytic Transformation for the Reductive Functionalization of CO₂. *Angewandte Chemie International Edition* **2012**, 51 (1), 187–190. <https://doi.org/10.1002/anie.201105516>.
- (69) Gao, J.; Li, H.; Zhang, Y.; Fei, W. Non-Phosgene Synthesis of Isocyanates Based on CO₂: Synthesis of Methyl N-Phenyl Carbamate through Coupling Route with Lead Compound Catalysts. *Catalysis Today* **2009**, 148 (3), 378–382. <https://doi.org/10.1016/j.cattod.2009.07.069>.
- (70) Comerford, J. W.; Ingram, I. D. V.; North, M.; Wu, X. Sustainable Metal-Based Catalysts for the Synthesis of Cyclic Carbonates Containing Five-Membered Rings. *Green Chem.* **2015**, 17 (4), 1966–1987. <https://doi.org/10.1039/C4GC01719F>.
- (71) Martín, C.; Fiorani, G.; Kleij, A. W. Recent Advances in the Catalytic Preparation of Cyclic Organic Carbonates. *ACS Catal.* **2015**, 5 (2), 1353–1370. <https://doi.org/10.1021/cs5018997>.
- (72) Aravindan, V.; Gnanaraj, J.; Madhavi, S.; Liu, H.-K. Lithium-Ion Conducting Electrolyte Salts for Lithium Batteries. *Chemistry – A European Journal* **2011**, 17 (51), 14326–14346. <https://doi.org/10.1002/chem.201101486>.
- (73) North, M.; Omedes-Pujol, M. Kinetics and Mechanism of Vanadium Catalysed Asymmetric Cyanohydrin Synthesis in Propylene Carbonate. *Beilstein J. Org. Chem.* **2010**, 6, 1043–1055. <https://doi.org/10.3762/bjoc.6.119>.
- (74) Souza, L. F. S.; Ferreira, P. R. R.; de Medeiros, J. L.; Alves, R. M. B.; Araújo, O. Q. F. Production of DMC from CO₂ via Indirect Route: Technical–Economical–Environmental Assessment and Analysis. *ACS Sustainable Chem. Eng.* **2014**, 2 (1), 62–69. <https://doi.org/10.1021/sc400279n>.
- (75) Fleischer, M.; Blattmann, H.; Mülhaupt, R. Glycerol-, Pentaerythritol- and Trimethylopropane-Based Polyurethanes and Their Cellulose Carbonate Composites Prepared via the Non-Isocyanate Route with Catalytic Carbon Dioxide Fixation. *Green Chem.* **2013**, 15 (4), 934–942. <https://doi.org/10.1039/C3GC00078H>.
- (76) Peppel, W. J. Preparation and Properties of the Alkylene Carbonates. *Ind. Eng. Chem.* **1958**, 50 (5), 767–770. <https://doi.org/10.1021/ie50581a030>.
- (77) Meléndez, J.; North, M.; Pasquale, R. Synthesis of Cyclic Carbonates from Atmospheric Pressure Carbon Dioxide Using Exceptionally Active Aluminium(Salen) Complexes as Catalysts. *European Journal of Inorganic Chemistry* **2007**, 2007 (21), 3323–3326. <https://doi.org/10.1002/ejic.200700521>.
- (78) North, M.; Pasquale, R. Mechanism of Cyclic Carbonate Synthesis from Epoxides and CO₂. *Angewandte Chemie International Edition* **2009**, 48 (16), 2946–2948. <https://doi.org/10.1002/anie.200805451>.
- (79) Clegg, W.; Harrington, R. W.; North, M.; Pasquale, R. Cyclic Carbonate Synthesis Catalysed by Bimetallic Aluminium–Salen Complexes. *Chemistry – A European Journal* **2010**, 16 (23), 6828–6843. <https://doi.org/10.1002/chem.201000030>.
- (80) Castro-Osma, J. A.; North, M.; Wu, X. Synthesis of Cyclic Carbonates Catalysed by Chromium and Aluminium Salphen Complexes. *Chemistry – A European Journal* **2016**, 22 (6), 2100–2107. <https://doi.org/10.1002/chem.201504305>.
- (81) Aida, T.; Inoue, S. Activation of Carbon Dioxide with Aluminum Porphyrin and Reaction with Epoxide. Studies on (Tetraphenylporphinato)Aluminum Alkoxide Having a Long Oxyalkylene Chain as the Alkoxide Group. *J. Am. Chem. Soc.* **1983**, 105 (5), 1304–1309. <https://doi.org/10.1021/ja00343a038>.
- (82) Whiteoak, C. J.; Kielland, N.; Laserna, V.; Escudero-Adán, E. C.; Martin, E.; Kleij, A. W. A Powerful Aluminum Catalyst for the Synthesis of Highly Functional Organic Carbonates. *J. Am. Chem. Soc.* **2013**, 135 (4), 1228–1231. <https://doi.org/10.1021/ja311053h>.
- (83) Tian, D.; Liu, B.; Gan, Q.; Li, H.; Darensbourg, Donald. J. Formation of Cyclic Carbonates from Carbon Dioxide and Epoxides Coupling Reactions Efficiently Catalyzed by Robust, Recyclable One-Component Aluminum-Salen Complexes. *ACS Catal.* **2012**, 2 (9), 2029–2035. <https://doi.org/10.1021/cs300462r>.

- (84) Rulev, Y. A.; Gugkaeva, Z.; Maleev, V. I.; North, M.; Belokon, Y. N. Robust Bifunctional Aluminium–Salen Catalysts for the Preparation of Cyclic Carbonates from Carbon Dioxide and Epoxides. *Beilstein J. Org. Chem.* **2015**, 11 (1), 1614–1623. <https://doi.org/10.3762/bjoc.11.176>.
- (85) Rios Yepes, Y.; Quintero, C.; Osorio Meléndez, D.; Daniliuc, C. G.; Martínez, J.; Rojas, R. S. Cyclic Carbonates from CO₂ and Epoxides Catalyzed by Tetra- and Pentacoordinate Amidinate Aluminum Complexes. *Organometallics* **2019**, 38 (2), 469–478. <https://doi.org/10.1021/acs.organomet.8b00795>.
- (86) Yakovenko, M. V.; Cherkasov, A. V.; Fukin, G. K.; Cui, D.; Trifonov, A. A. Lanthanide Complexes Coordinated by a Dianionic Bis(Amidinate) Ligand with a Rigid Naphthalene Linker. *Eur. J. Inorg. Chem.* **2010**, 2010 (21), 3290–3298. <https://doi.org/10.1002/ejic.201000330>.
- (87) Bestgen, S.; Rees, N. H.; Goicoechea, J. M. Flexible and Versatile Pincer-Type PGeP and PSnP Ligand Frameworks. *Organometallics* **2018**, 37 (21), 4147–4155. <https://doi.org/10.1021/acs.organomet.8b00698>.
- (88) Foley, S. R.; Zhou, Y.; Yap, G. P. A.; Richeson, D. S. Synthesis of M^{II} [N(SiMe₃)₂][Me₃SiNC(^tBu)NSiMe₃] (M = Sn, Ge) from Amidinate Precursors: Active Catalysts for Phenyl Isocyanate Cyclization. *Inorg. Chem.* **2000**, 39 (5), 924–929. <https://doi.org/10.1021/ic991004b>.
- (89) Qi, C.-Y.; Wang, Z.-X. Synthesis and Characterization of Aluminum(III) and Tin(II) Complexes Supported by Diiminophosphinate Ligands and Their Application in Ring-Opening Polymerization Catalysis of ε-Caprolactone. *J. Polym. Sci. A Polym. Chem.* **2006**, 44 (15), 4621–4631. <https://doi.org/10.1002/pola.21561>.
- (90) Mankaev, B. N.; Zaitsev, K. V.; Timashova, V. S.; Zaitseva, G. S.; Egorov, M. P.; Karlov, S. S. Tetrylenes Based on 1,10-Phenanthroline-Containing Diol: The Synthesis and Application as Initiators of ε-Caprolactone Polymerization. *Russ Chem Bull* **2018**, 67 (3), 542–547. <https://doi.org/10.1007/s11172-018-2108-5>.
- (91) Mankaev, B. N.; Zaitsev, K. V.; Zaitseva, G. S.; Churakov, A. V.; Egorov, M. P.; Karlov, S. S. Sterically Hindered Tetrylenes Based on New 1,10-Phenanthroline-Containing Diols: Initiators for ε-Caprolactone Polymerization. *Russ Chem Bull* **2019**, 68 (2), 380–388. <https://doi.org/10.1007/s11172-019-2396-4>.
- (92) Mankaev, B. N.; Zaitsev, K. V.; Kuchuk, E. A.; Vershinina, M. V.; Zaitseva, G. S.; Egorov, M. P.; Karlov, S. S. New Tetrylenes Based on Substituted Diethylenetriamines: Synthesis and Use as Initiators for ε-Caprolactone Polymerization. *Russ Chem Bull* **2019**, 68 (2), 389–393. <https://doi.org/10.1007/s11172-019-2397-3>.
- (93) Ahmet, I. Y.; Hill, M. S.; Raithby, P. R.; Johnson, A. L. Tin Guanidinato Complexes: Oxidative Control of Sn, SnS, SnSe and SnTe Thin Film Deposition. *Dalton Trans.* **2018**, 47 (14), 5031–5048. <https://doi.org/10.1039/C8DT00773J>.
- (94) Guthardt, R.; Bachmann, D.; Bruhn, C.; Siemeling, U. Oxidation Reactions of the N-Heterocyclic Stannylenes [o-C₆H₄(NSiBuMe₂)₂]Sn and [Fe(H₅-C₅H₄-NSiBuMe₂)₂Sn] with Sulfur, Selenium, and Diphenyl Diselenide. *Zeitschrift für anorganische und allgemeine Chemie* **2020**, 646 (13), 761–768. <https://doi.org/10.1002/zaac.201900335>.
- (95) Cabeza, J. A.; García-Álvarez, P.; Laglera-Gándara, C. J.; Pérez-Carreño, E. Phosphane-Functionalized Heavier Tetrylenes: Synthesis of Silylene- and Germylene-Decorated Phosphanes and Their Reactions with Group 10 Metal Complexes. *Dalton Trans.* **2020**, 49 (24), 8331–8339. <https://doi.org/10.1039/D0DT01727B>.
- (96) Krebs, K. M.; Freitag, S.; Maudrich, J.-J.; Schubert, H.; Sirsch, P.; Wesemann, L. Coordination Chemistry of Stannylene-Based Lewis Pairs – Insertion into M–Cl and M–C Bonds. From Base Stabilized Stannylene to Bidentate Ligands. *Dalton Trans.* **2018**, 47 (1), 83–95. <https://doi.org/10.1039/C7DT04044J>.
- (97) Shan, Y.-L.; Leong, B.-X.; Xi, H.-W.; Ganguly, R.; Li, Y.; Lim, K. H.; So, C.-W. Reactivity of an Amidinato Silylene and Germylene toward Germanium(II), Tin(II) and Lead(II) Halides. *Dalton Trans.* **2017**, 46 (11), 3642–3648. <https://doi.org/10.1039/C7DT00051K>.
- (98) Rios Yépes, Y.; Martínez, J.; Rangel Sánchez, H.; Quintero, C.; Ortega-Alfaro, M. C.; López-Cortés, J. G.; Daniliuc, C. G.; Antíñolo, A.; Ramos, A.; Rojas, R. S. Aluminum Complexes with

- New Non-Symmetric Ferrocenyl Amidine Ligands and Their Application in CO₂ Transformation into Cyclic Carbonates. *Dalton Trans.* **2020**, *49* (4), 1124–1134.
<https://doi.org/10.1039/C9DT03808F>.
- (99) Peddarao, T.; Baishya, A.; Hota, S. K.; Nembenna, S. Bimetallic Aluminum Alkyl and Iodide Complexes Stabilized by a Bulky Bis-Guanidinate Ligand. *J Chem Sci* **2018**, *130* (7), 97.
<https://doi.org/10.1007/s12039-018-1486-4>.
- (100) Meléndez, D. O.; Lara-Sánchez, A.; Martínez, J.; Wu, X.; Otero, A.; Castro-Osma, J. A.; North, M.; Rojas, R. S. Amidinate Aluminium Complexes as Catalysts for Carbon Dioxide Fixation into Cyclic Carbonates. *ChemCatChem* **2018**, *10* (10), 2271–2277.
<https://doi.org/10.1002/cctc.201702014>.

ANNEXES

ANNEXES

A1. Ligand L₁, ¹H and ¹³C NMR spectrum

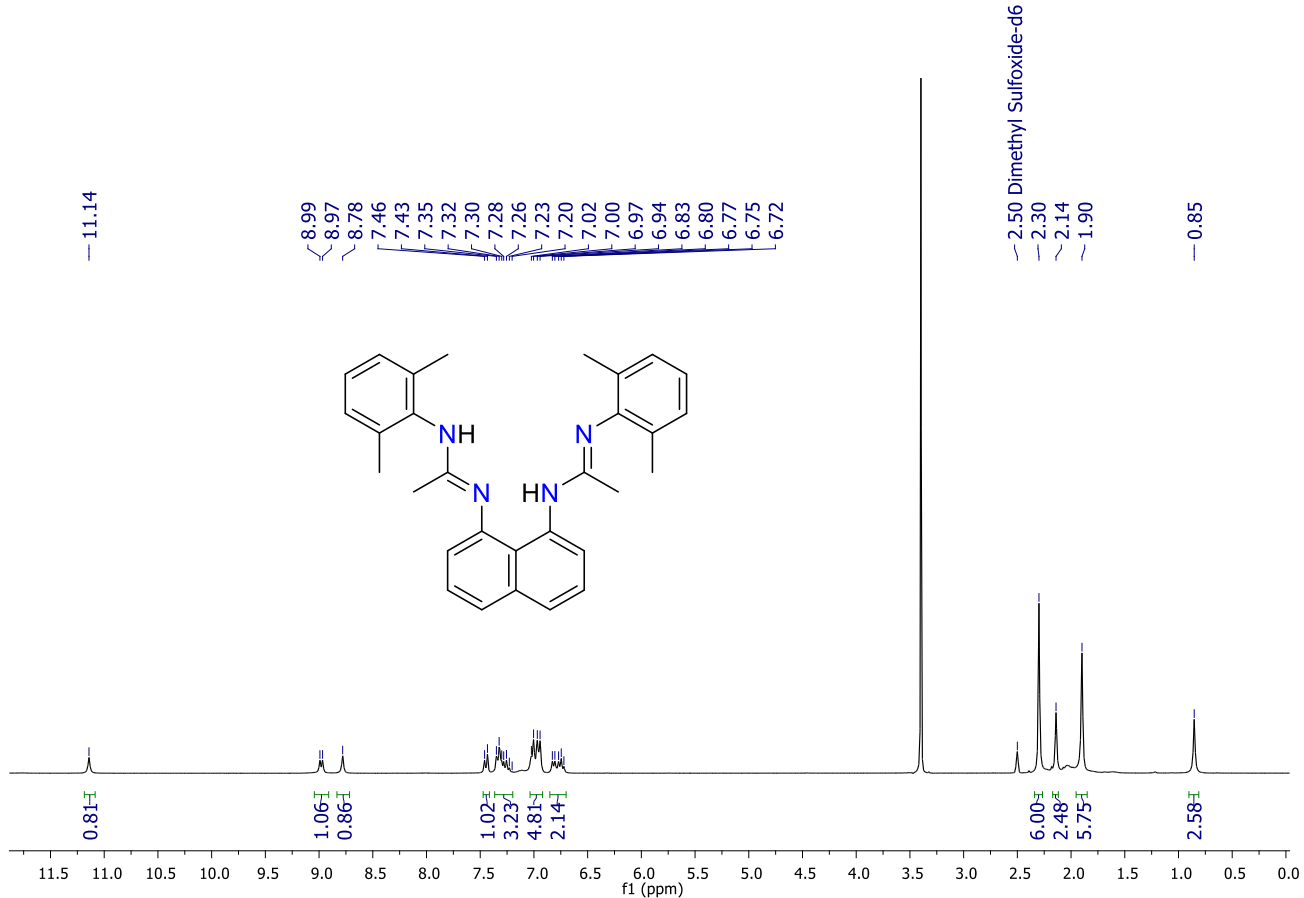


Figure S1. ¹H NMR of L₁.

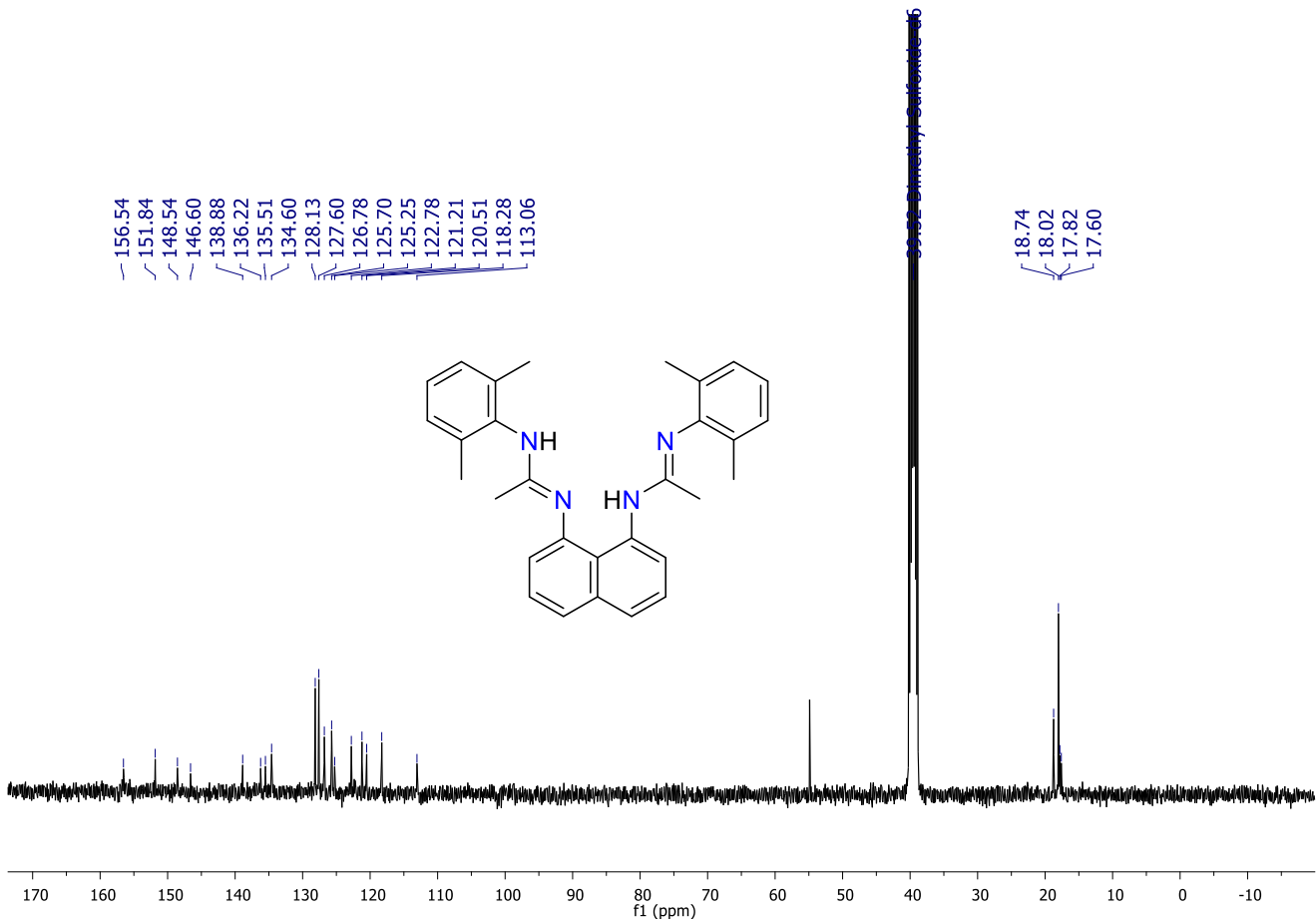


Figure S2. ^{13}C NMR of L_1 .

A2. Ligand L₂, ¹H and ¹³C NMR spectrum

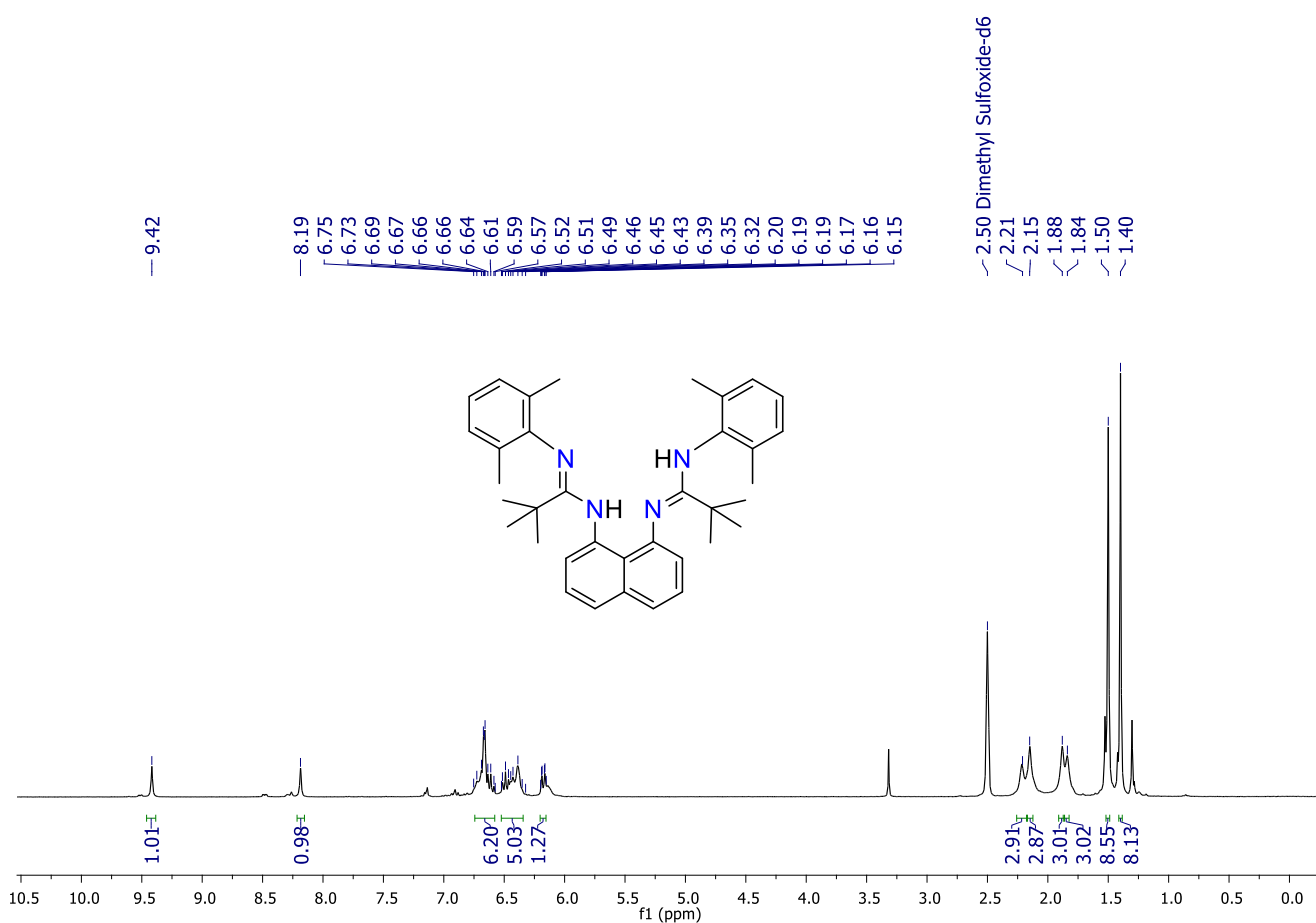


Figure S3. ¹H NMR of L₂.

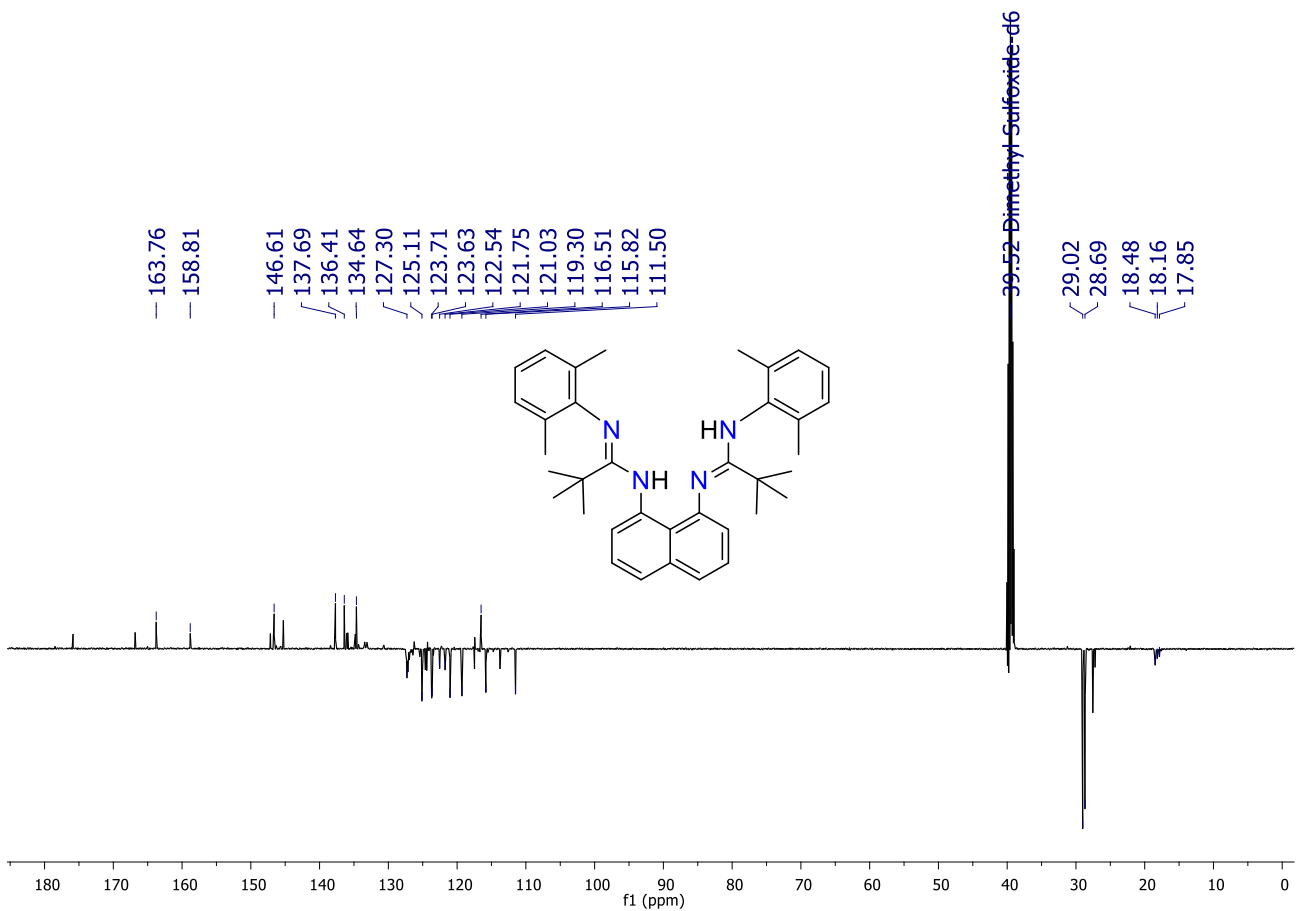


Figure S4. ^{13}C NMR of L_2 .

A3. Ligand L₃, ¹H and ¹³C NMR spectrum

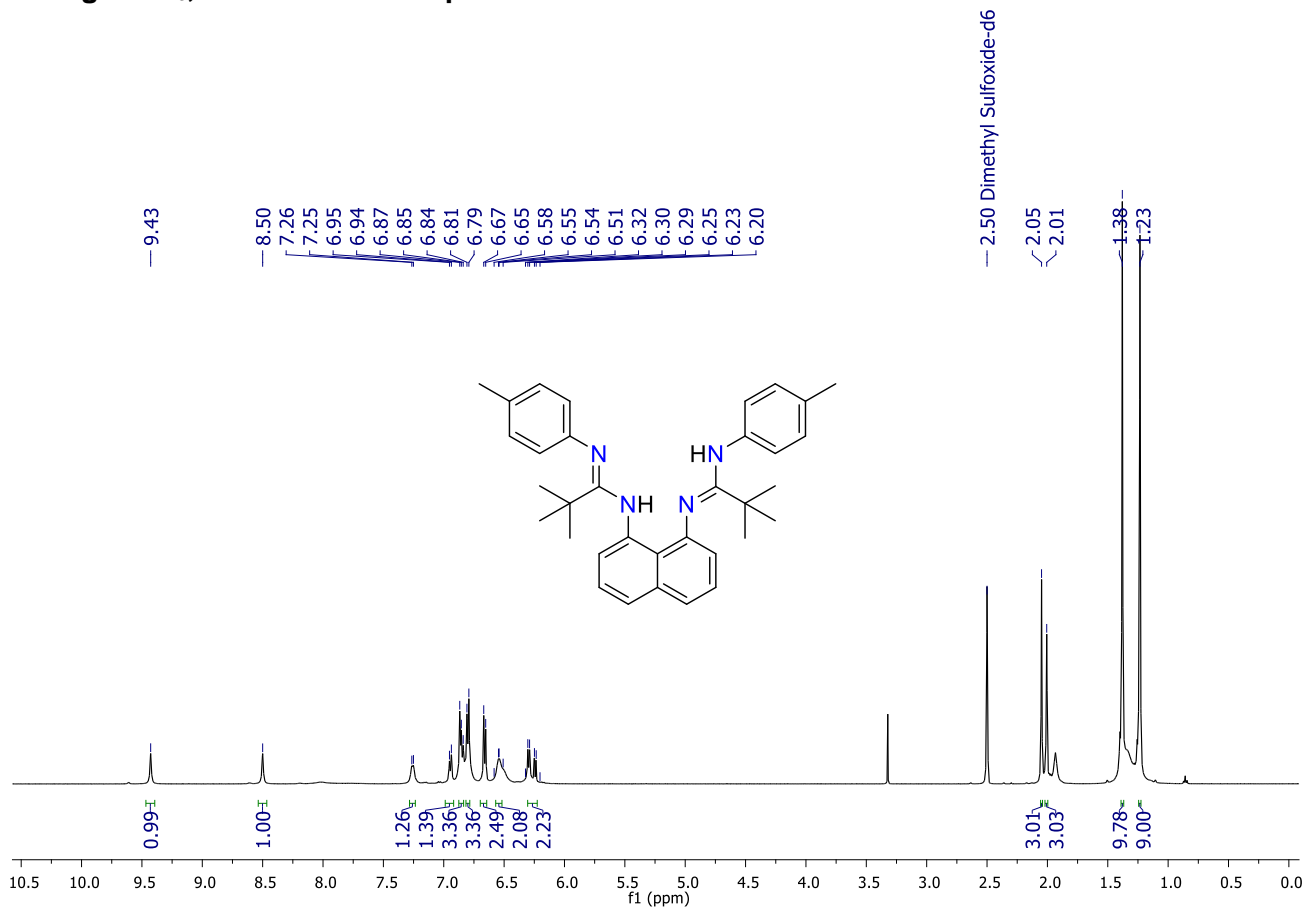


Figure S5. ¹H NMR of L₃.

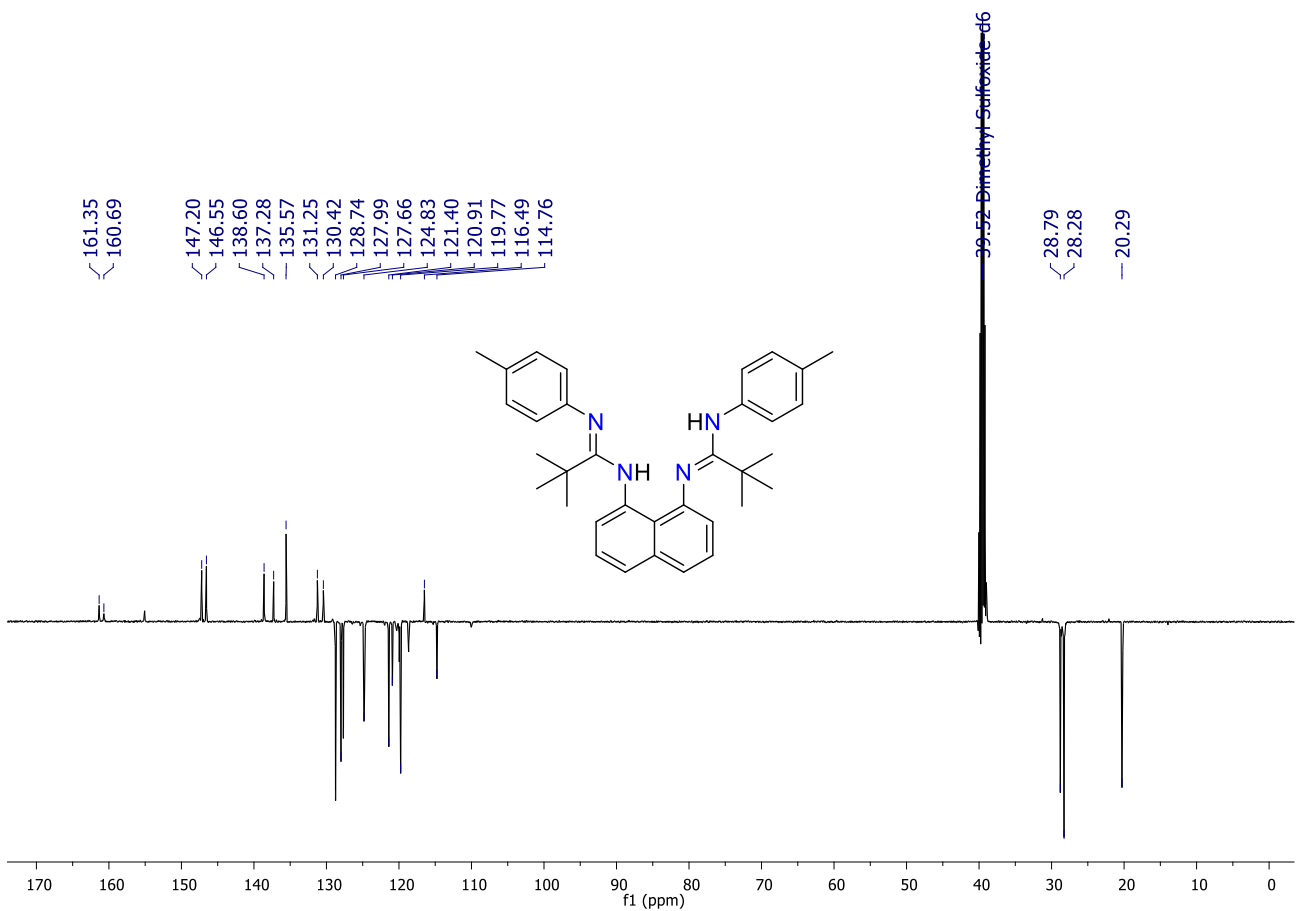


Figure S6. ^{13}C NMR of L_3 .

A4. L₁Sn, ¹H, ¹³C and ¹¹⁹Sn NMR spectrum

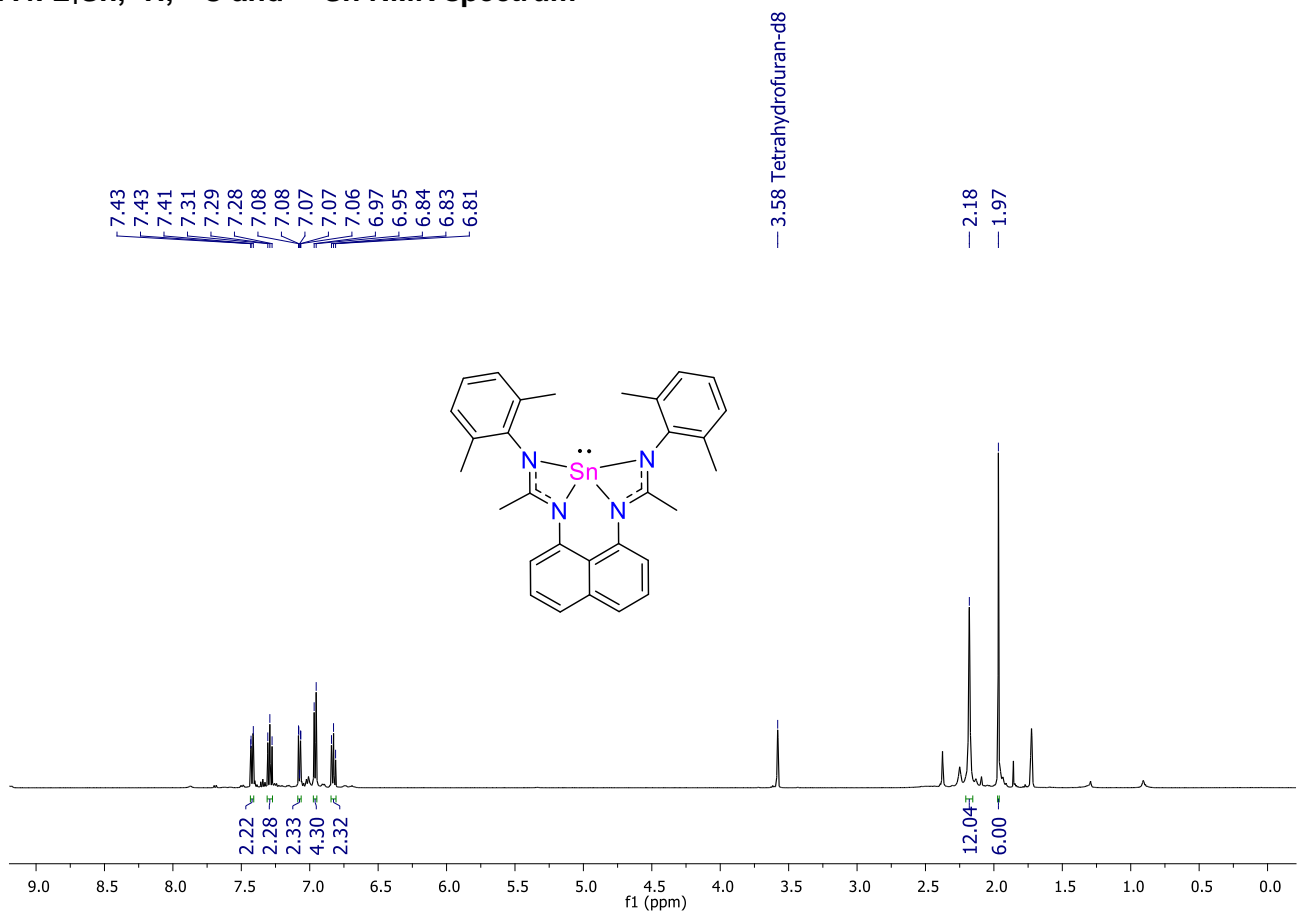


Figure S7. ¹H NMR of L₁Sn.

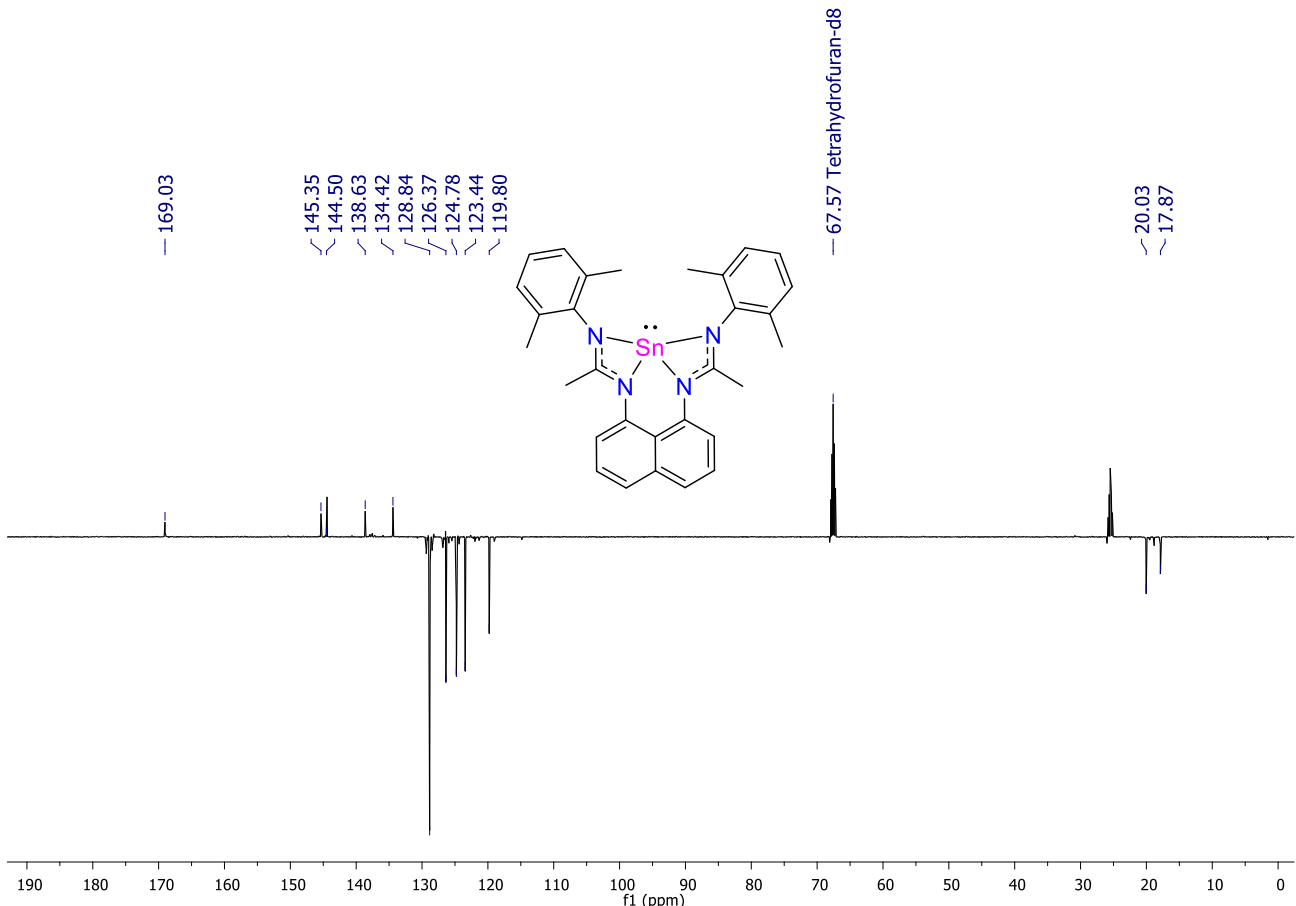


Figure S8. ^{13}C NMR of L_1Sn .

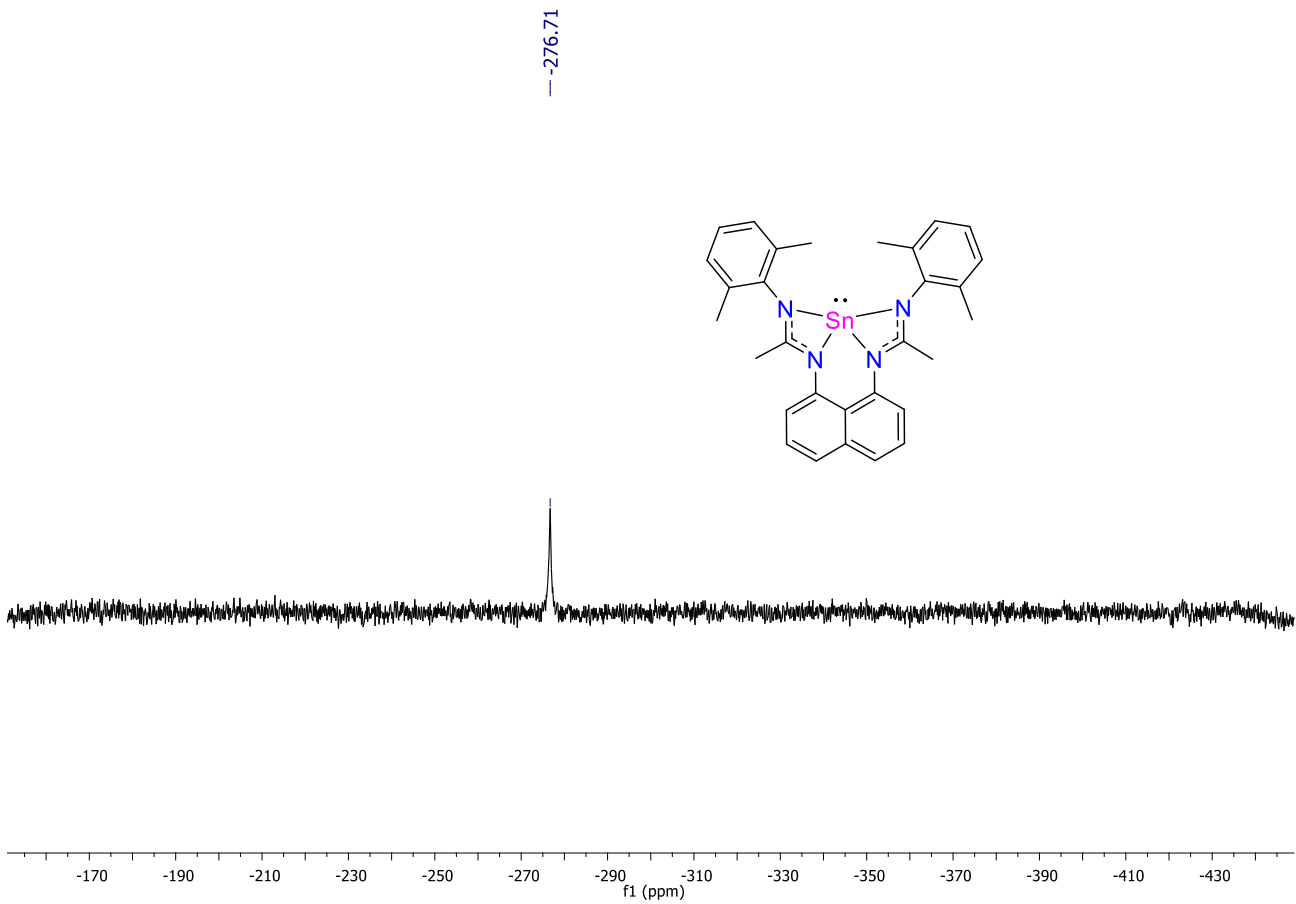


Figure S9. ^{119}Sn NMR of L_1Sn .

A5. L₃Sn, ¹H, ¹³C and ¹¹⁹Sn NMR spectrum

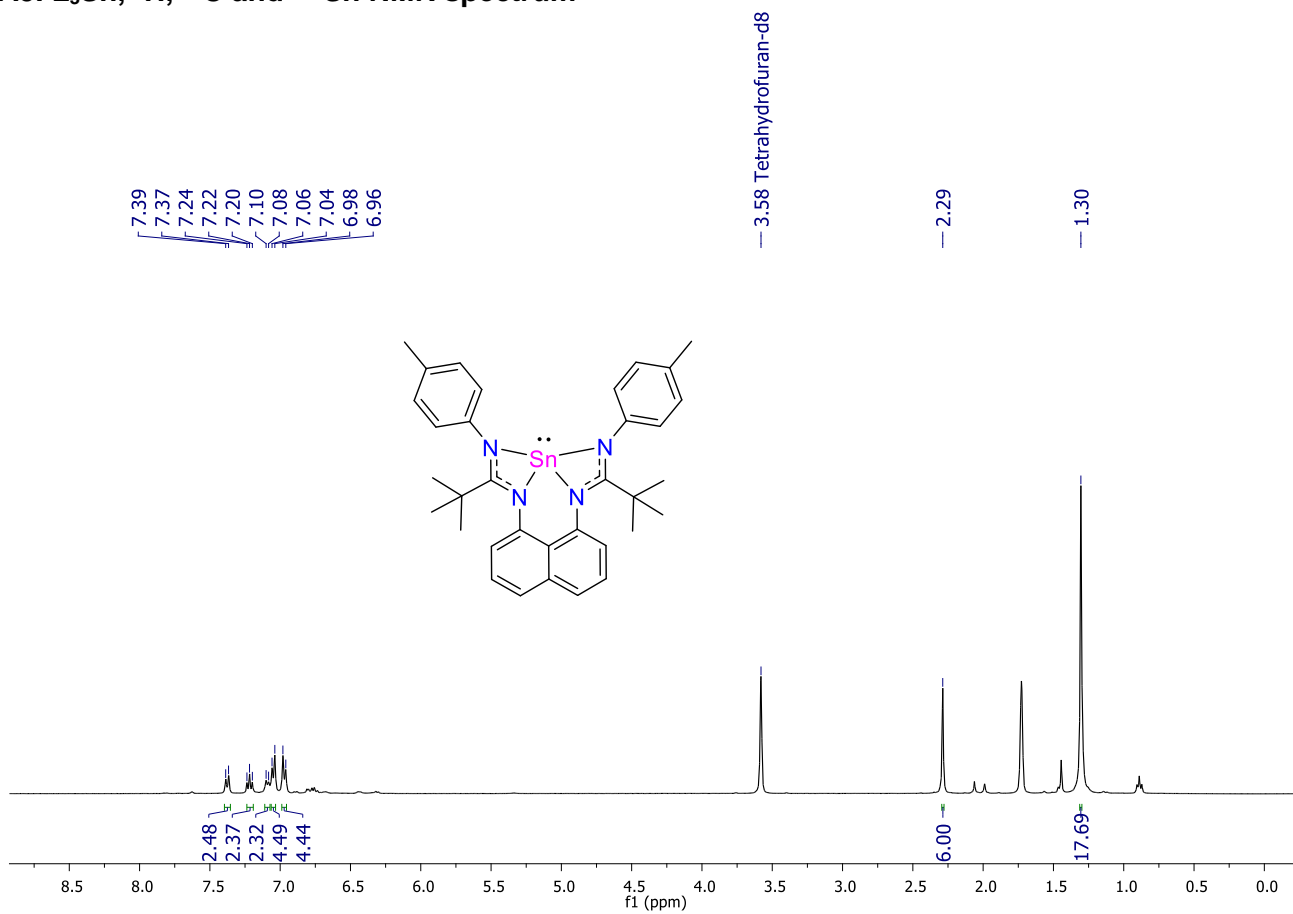


Figure S10. ¹H NMR of L₃Sn.

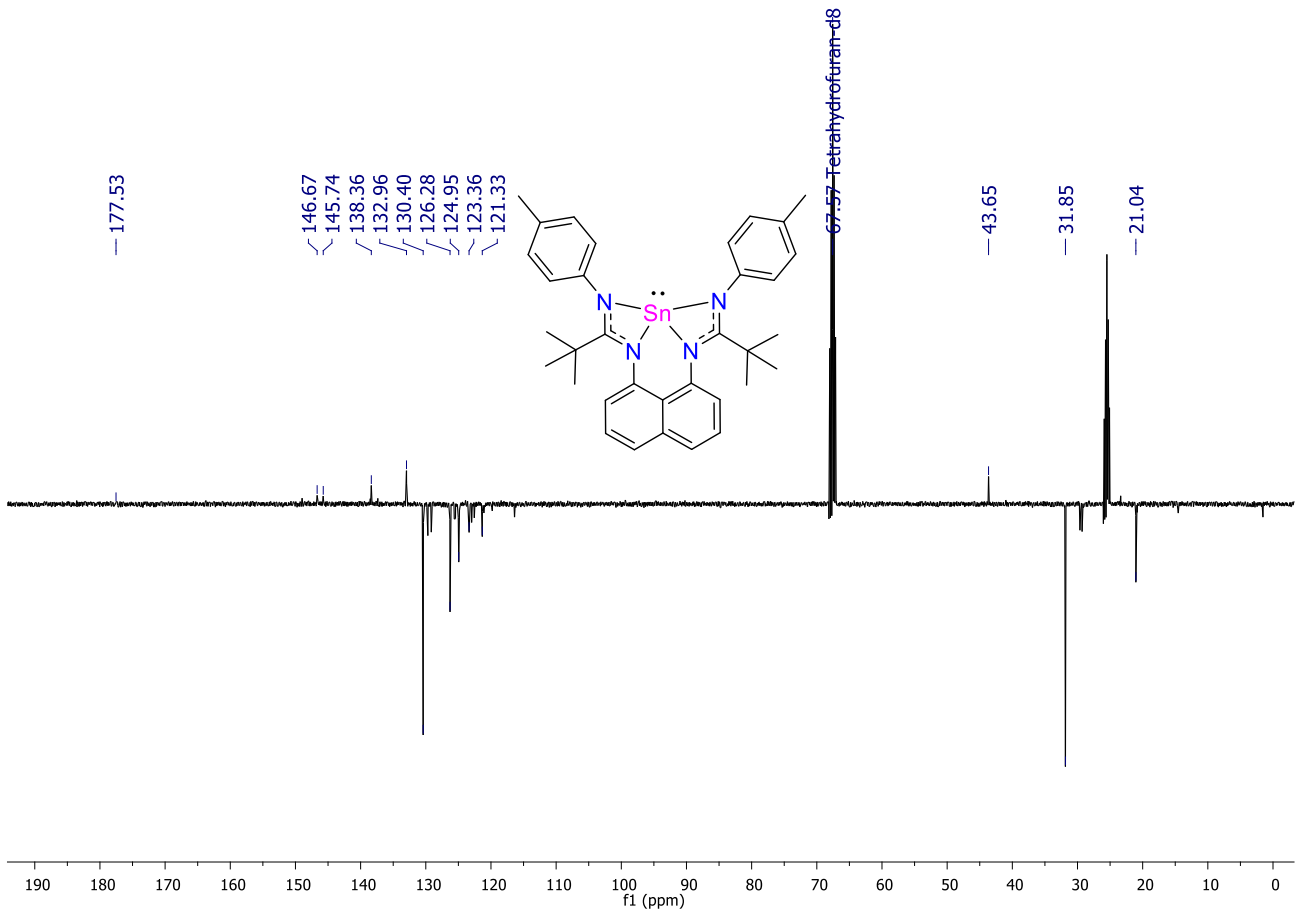


Figure S11. ^{13}C NMR of L_3Sn .

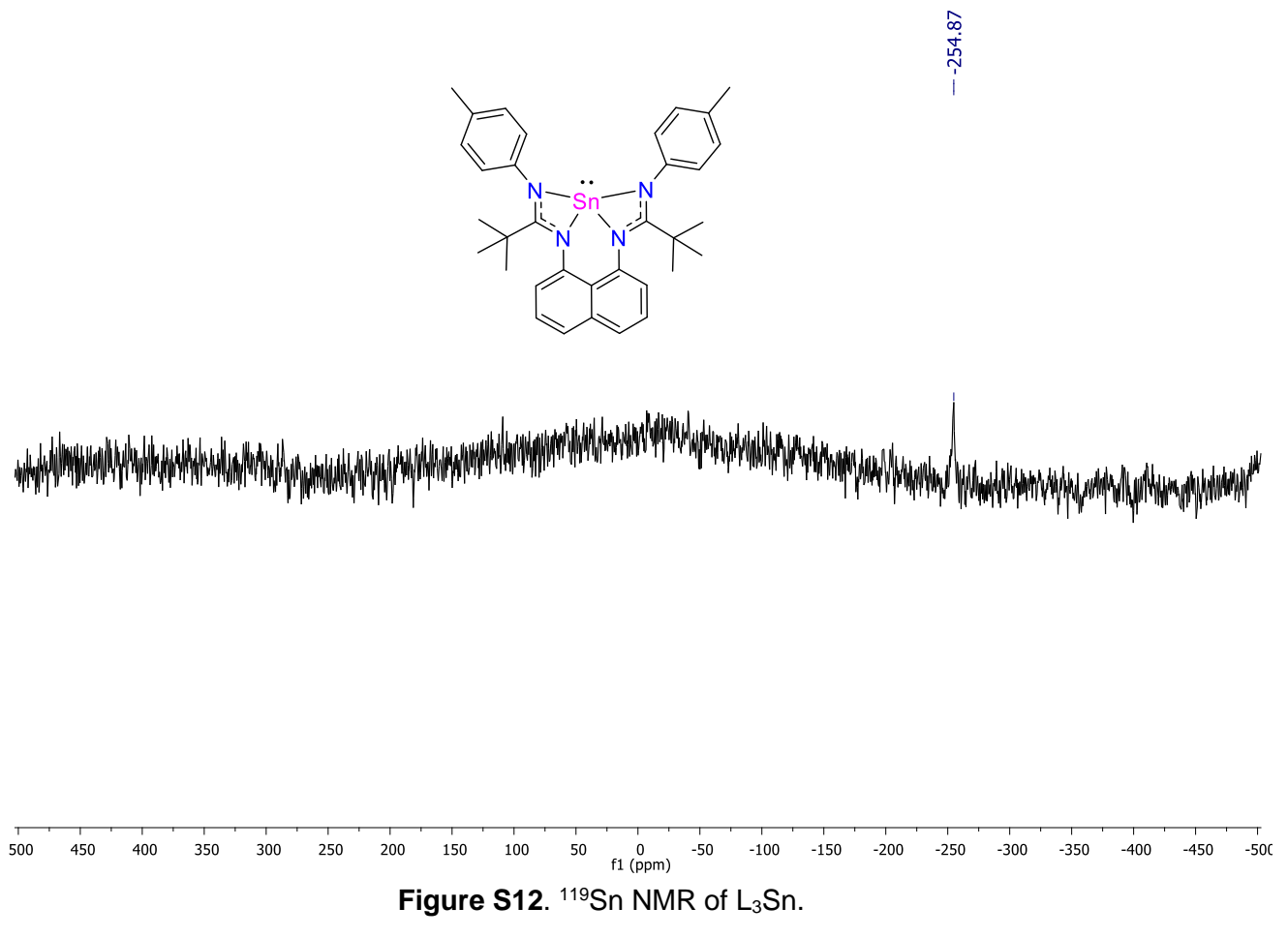


Figure S12. ^{119}Sn NMR of $L_3\text{Sn}$.

A6. L₂Ge, ¹H and ¹³C NMR spectrum

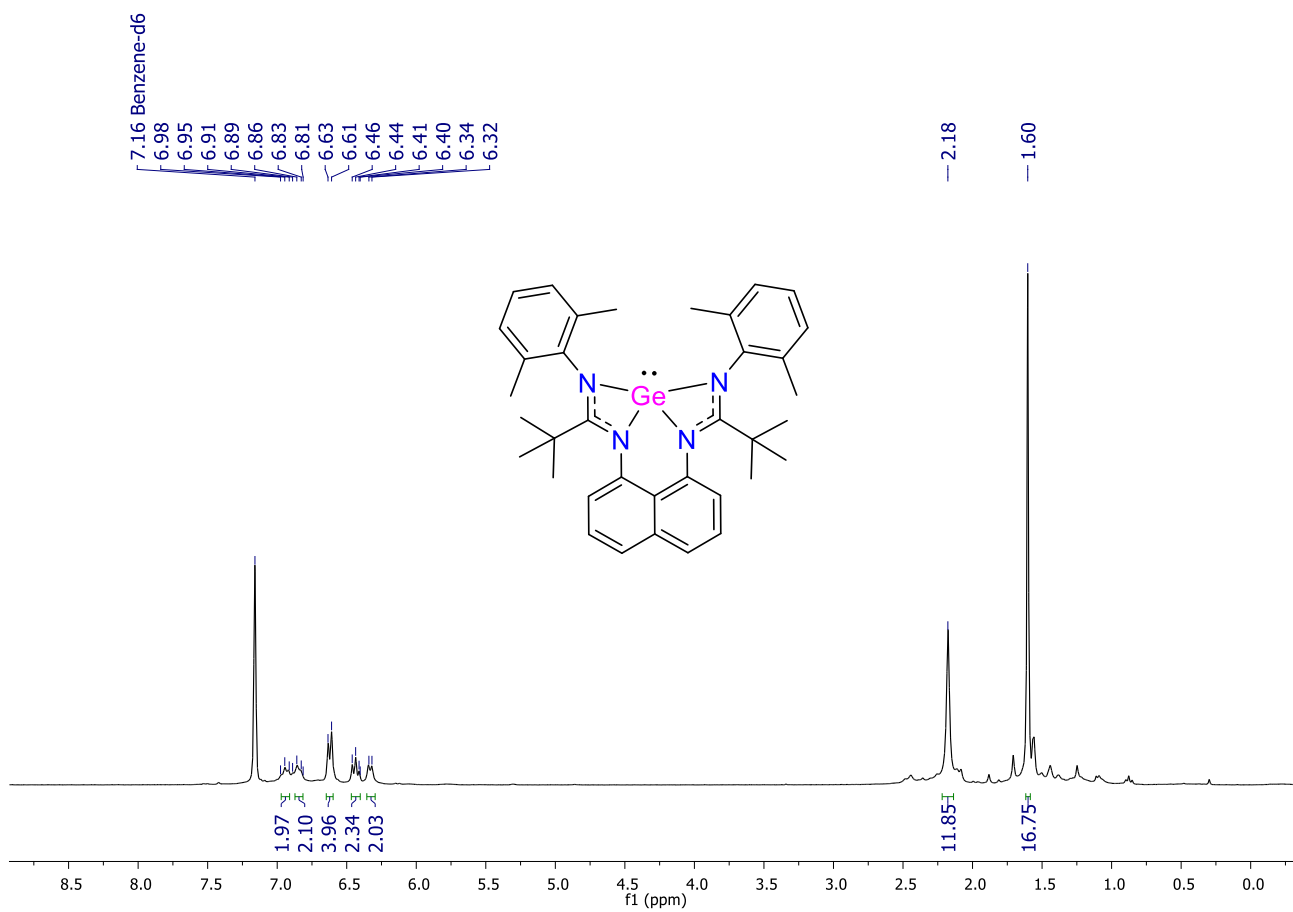


Figure S13. ¹H NMR of L₂Ge.

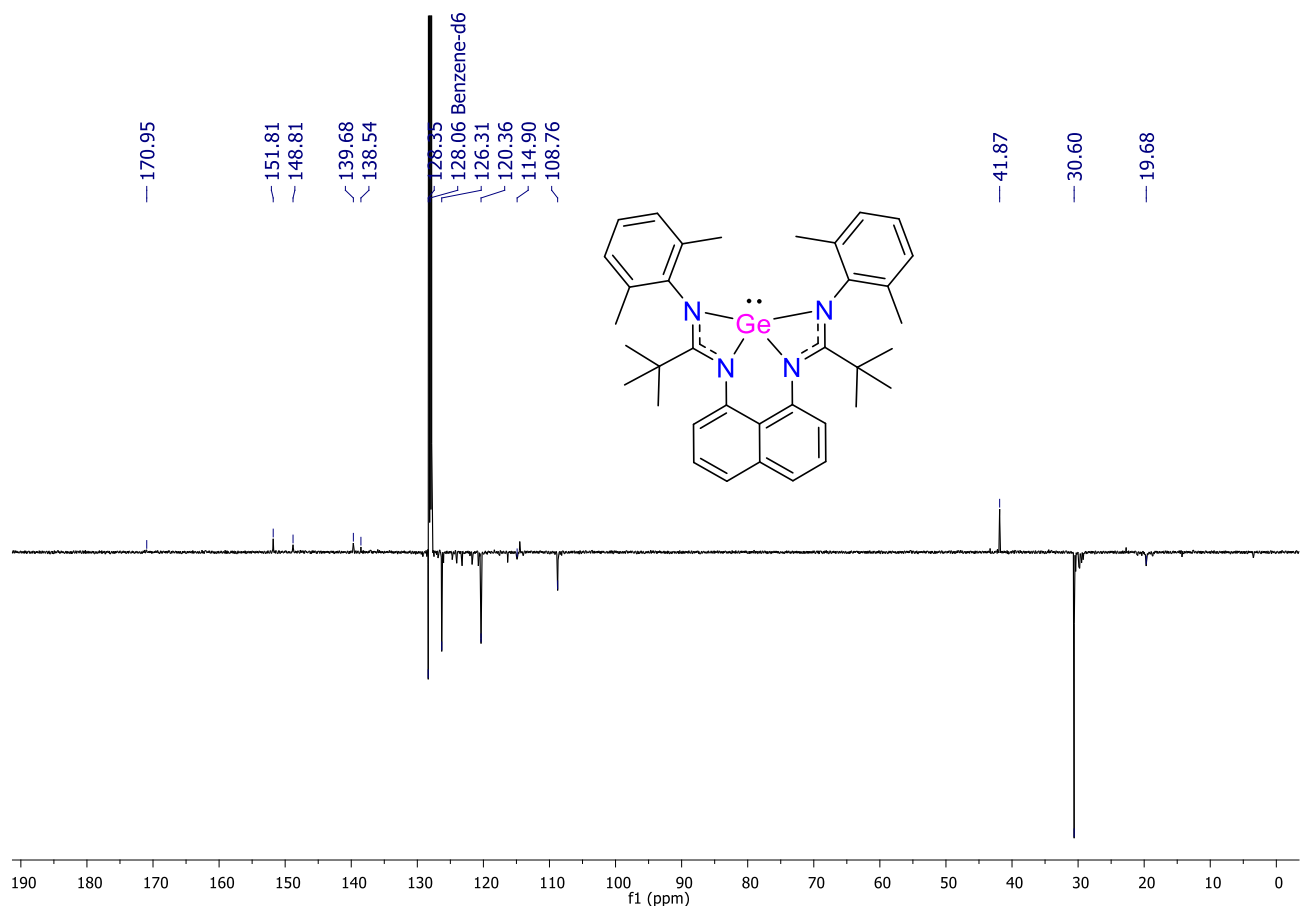


Figure S14. ^{13}C NMR of L_2Ge .

A7. 1a, ^1H , ^{13}C and ^{119}Sn NMR spectrum

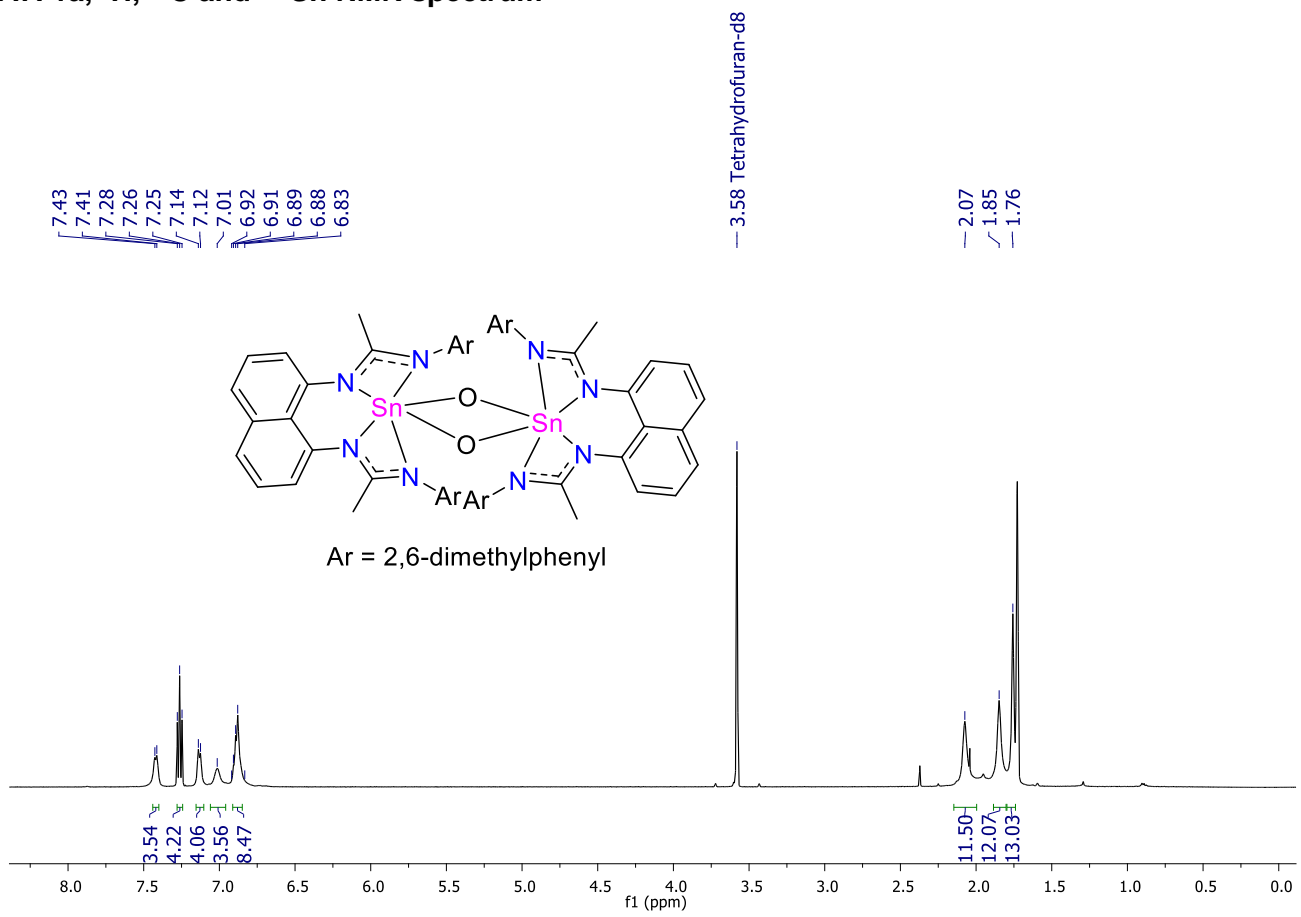


Figure S15. ^1H NMR of 1a.

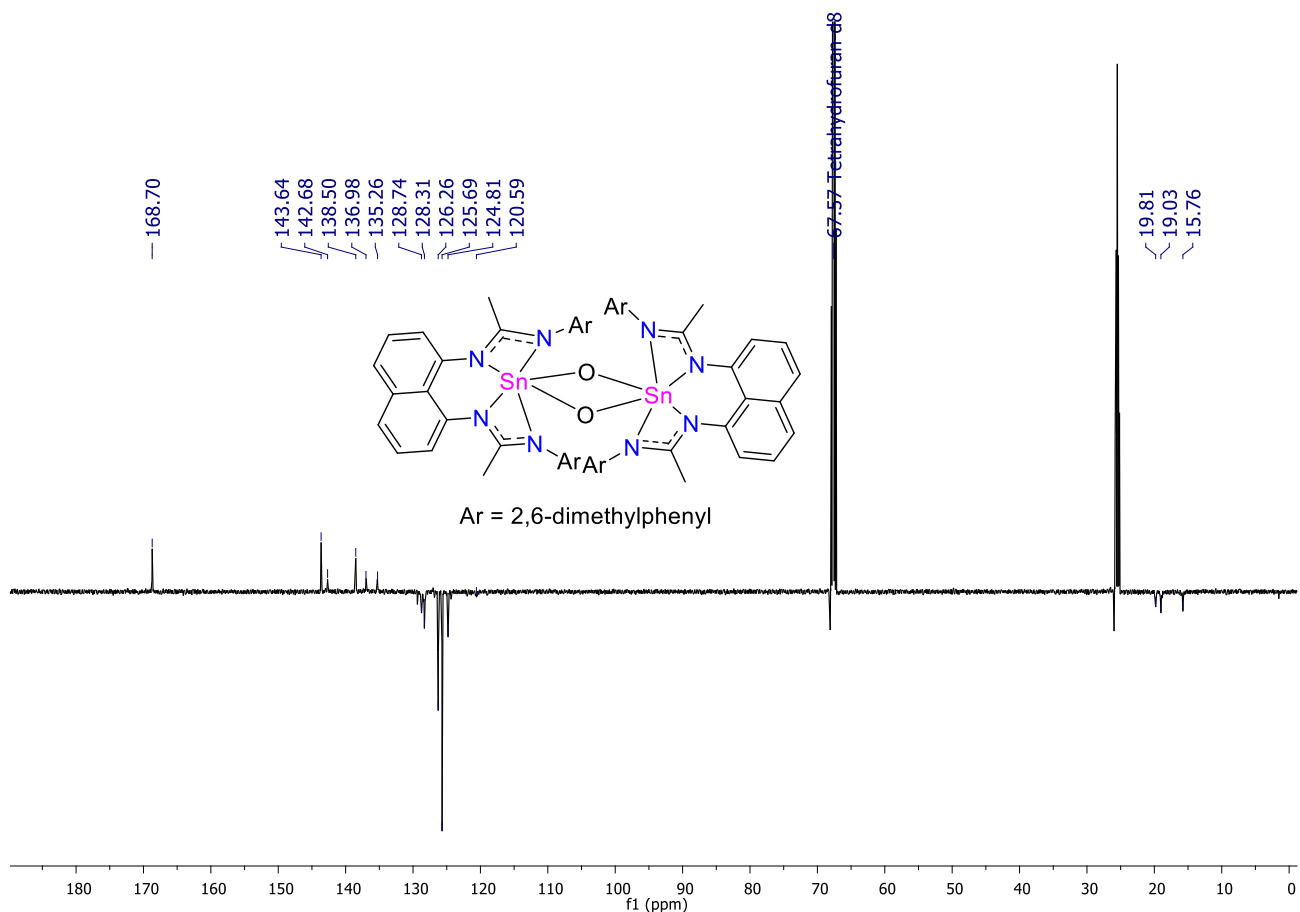


Figure S16. ^{13}C NMR of 1a.

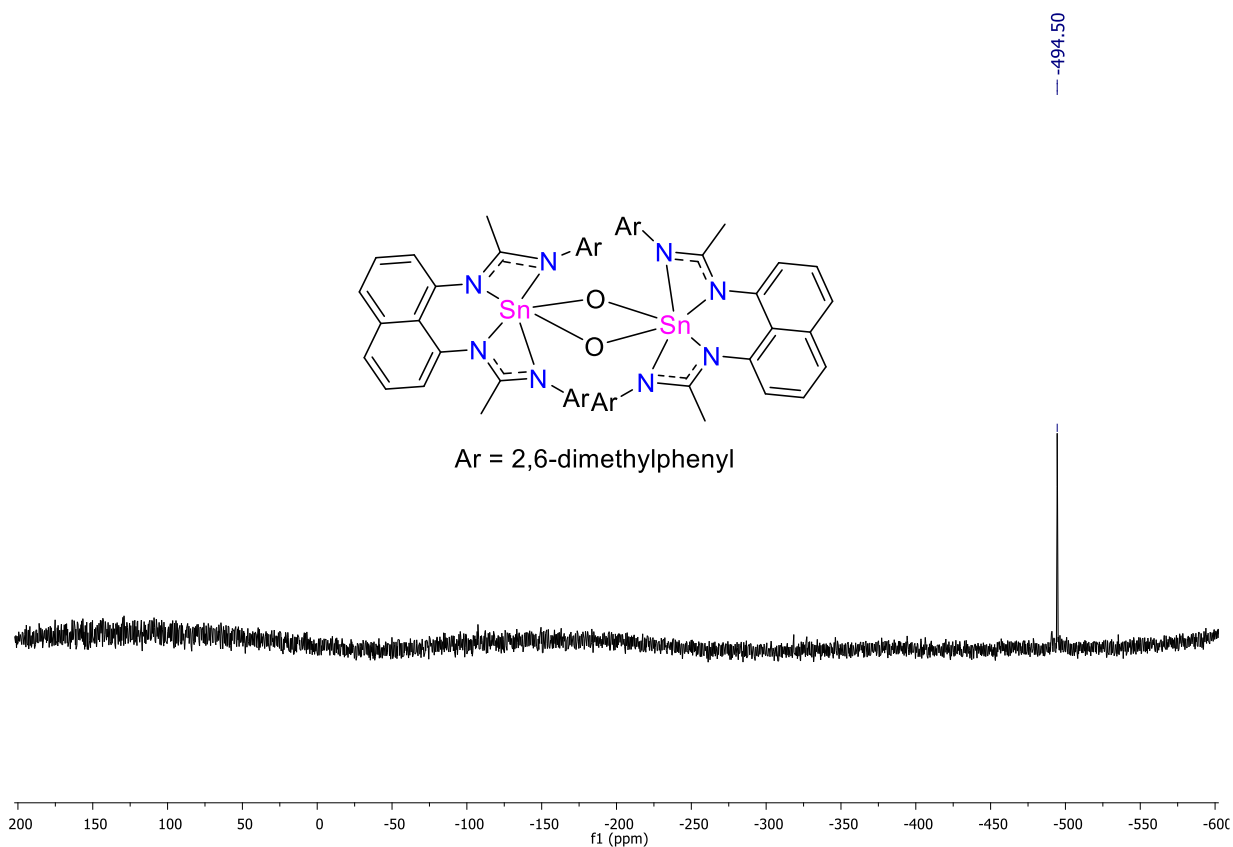


Figure S17. ^{119}Sn NMR of 1a.

A8. 1b, ^1H , ^{13}C and ^{119}Sn NMR spectrum

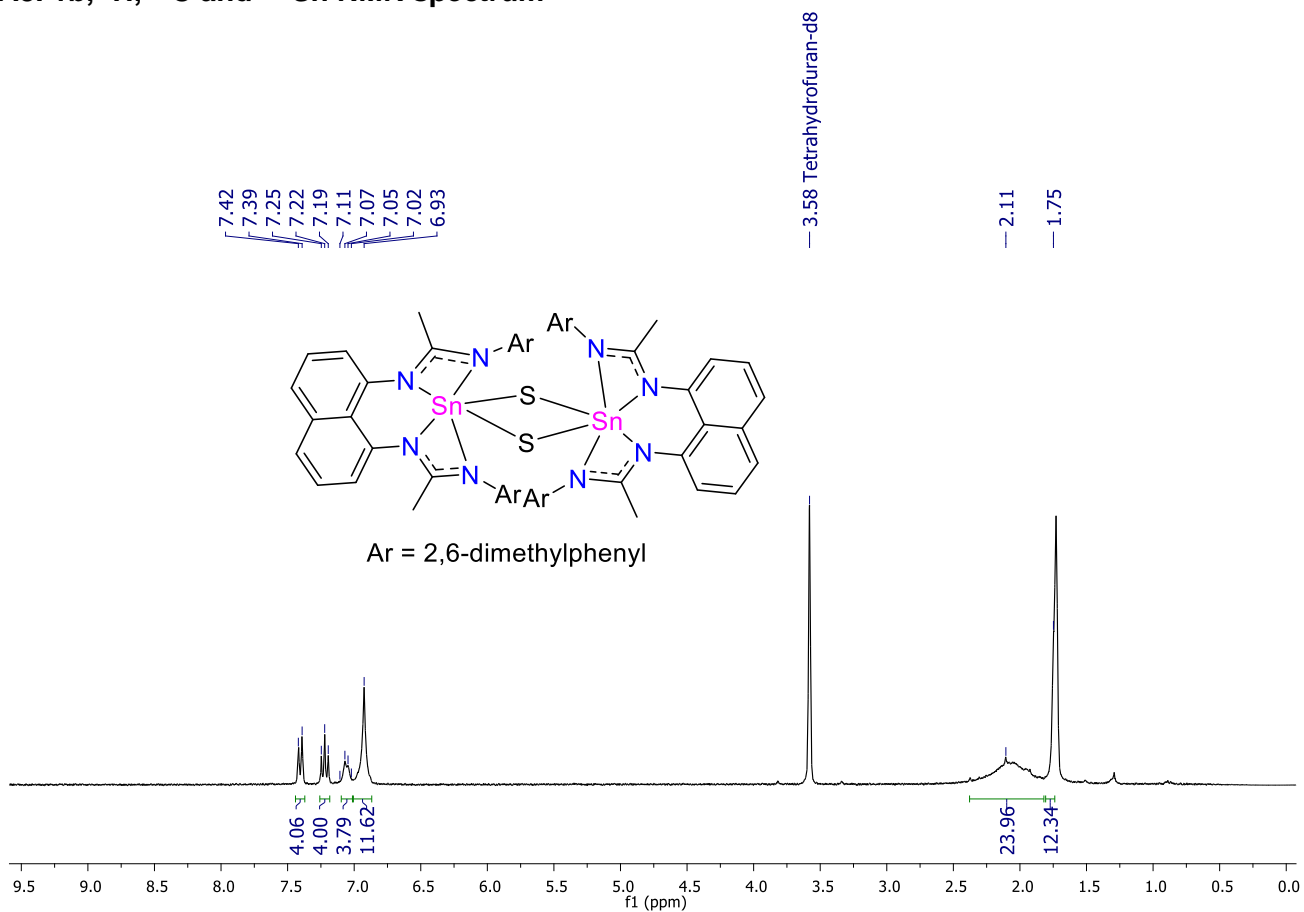


Figure S18. ^1H NMR of 1b.

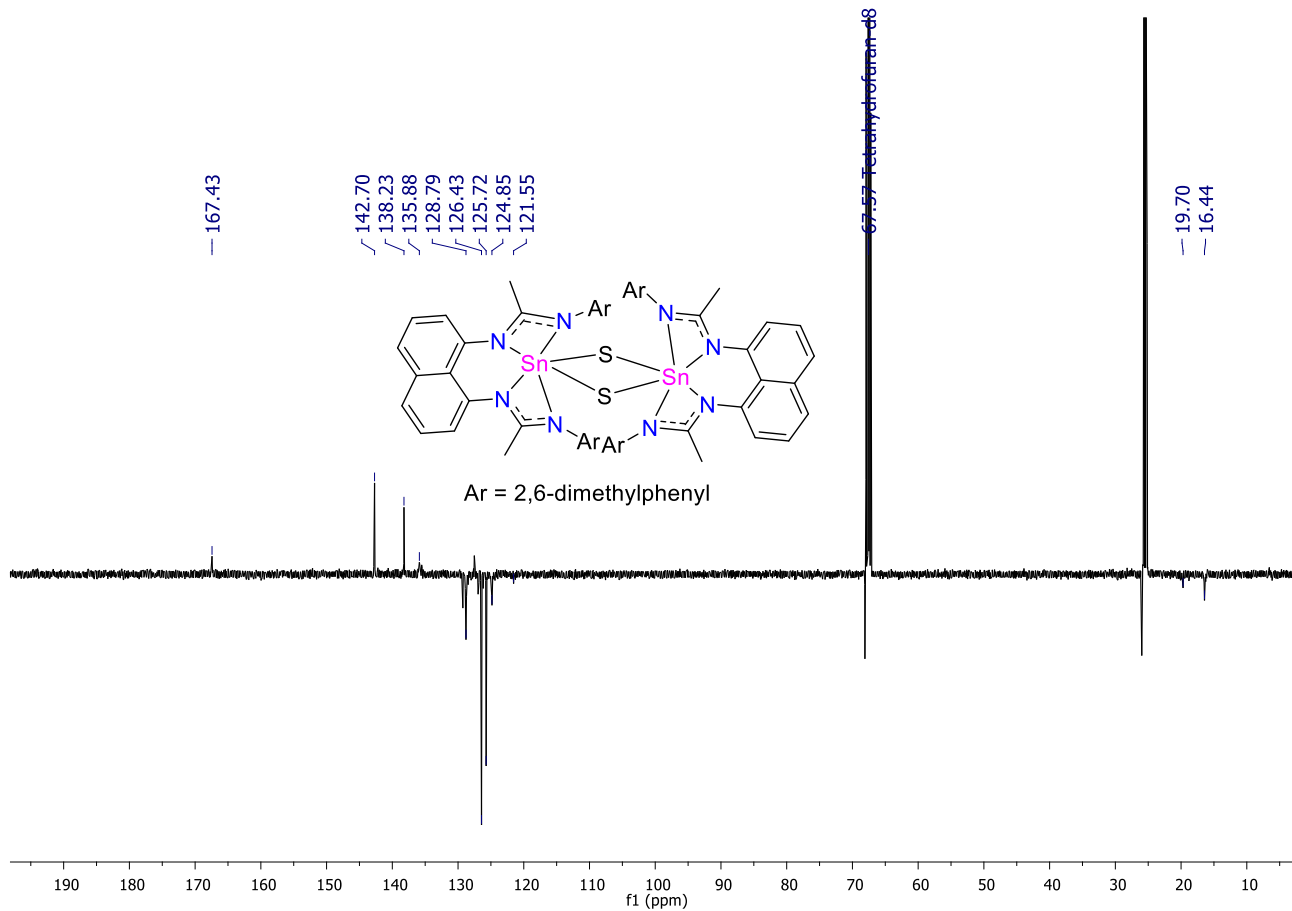


Figure S19. ^{13}C NMR of 1b.

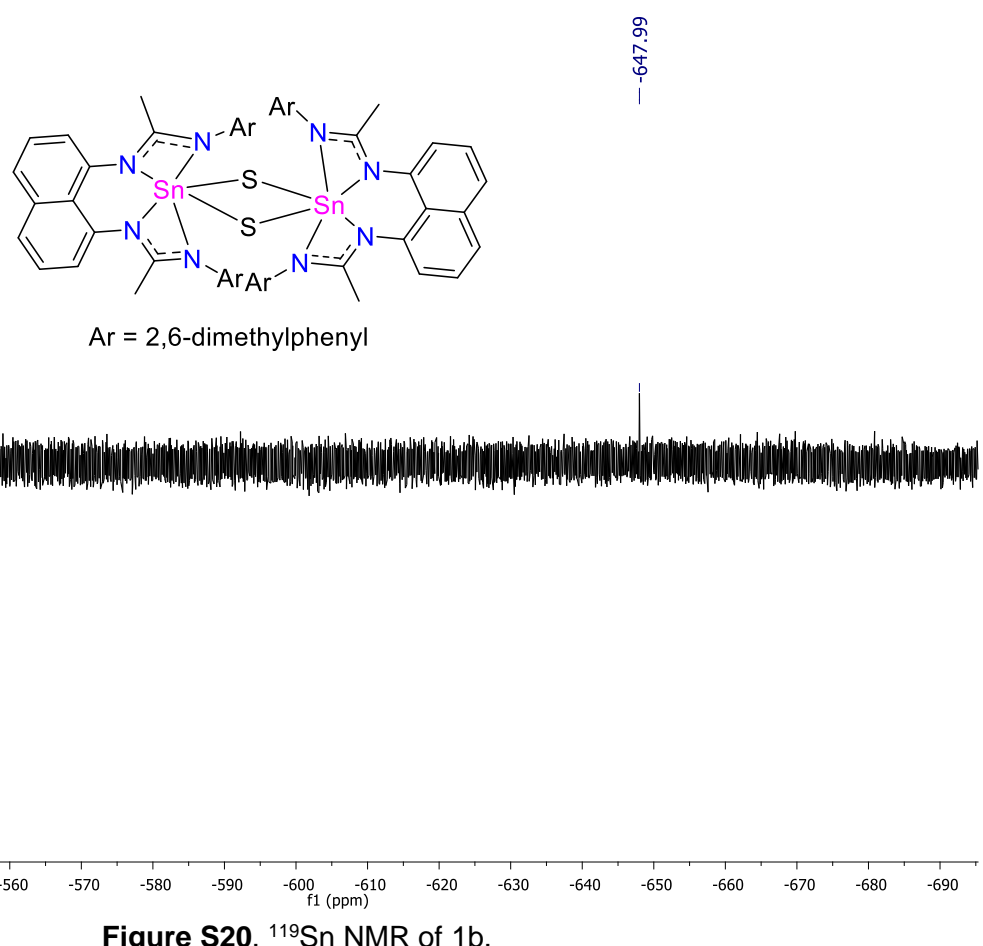


Figure S20. ^{119}Sn NMR of 1b.

A9. 2a, ^1H , ^{13}C and ^{119}Sn NMR spectrum

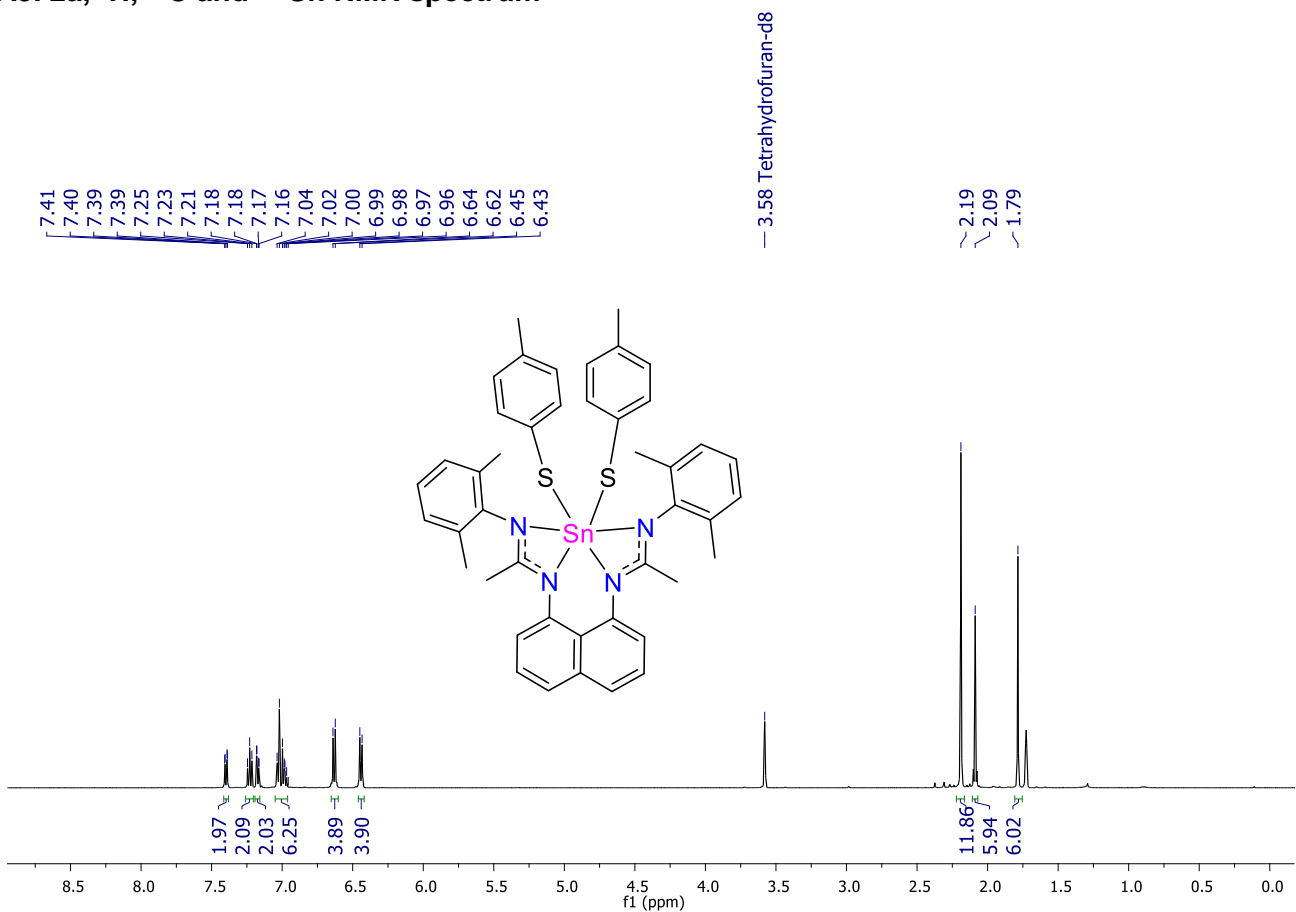


Figure S21. ^1H NMR of 2a.

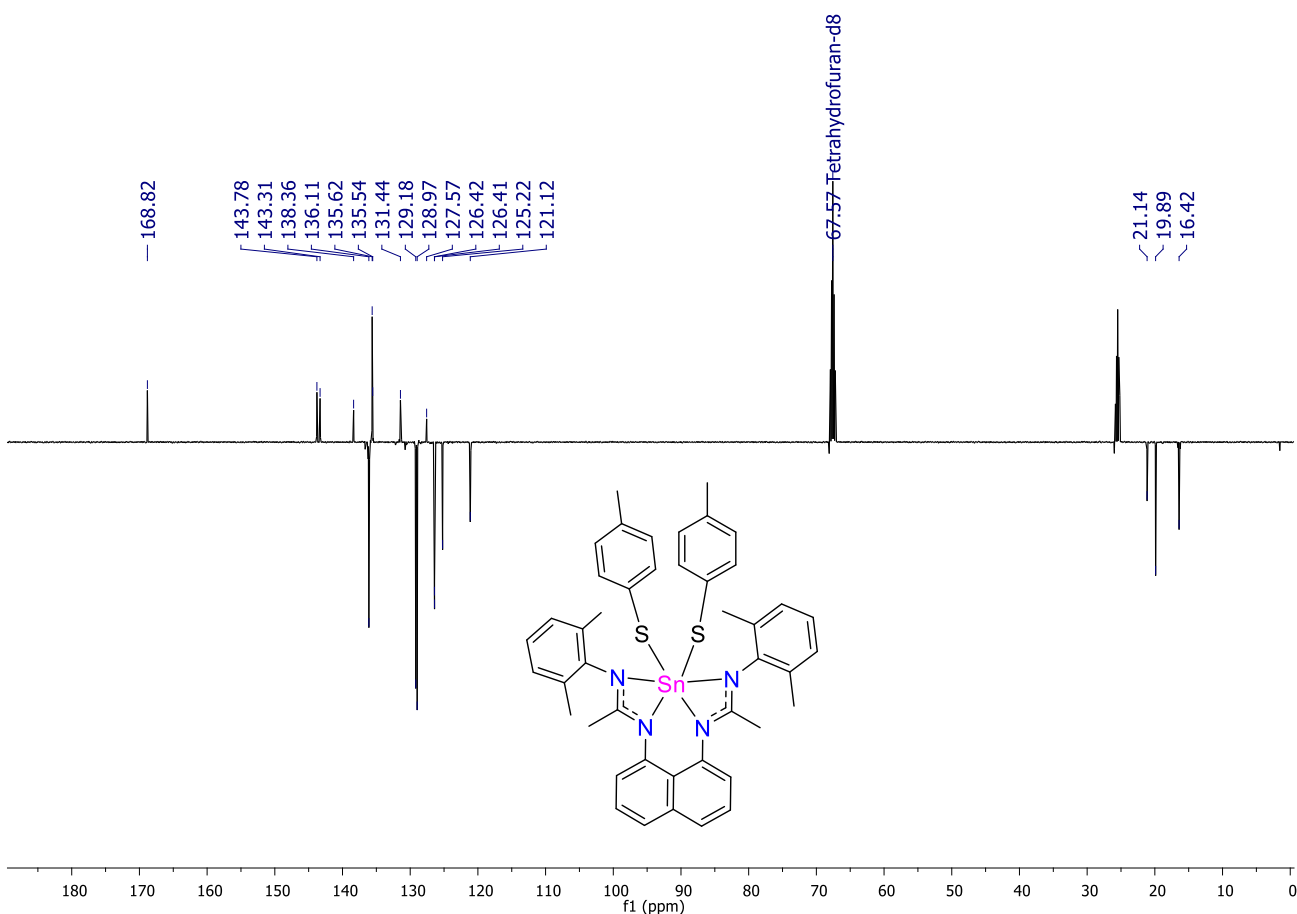


Figure S22. ^{13}C NMR of 2a.

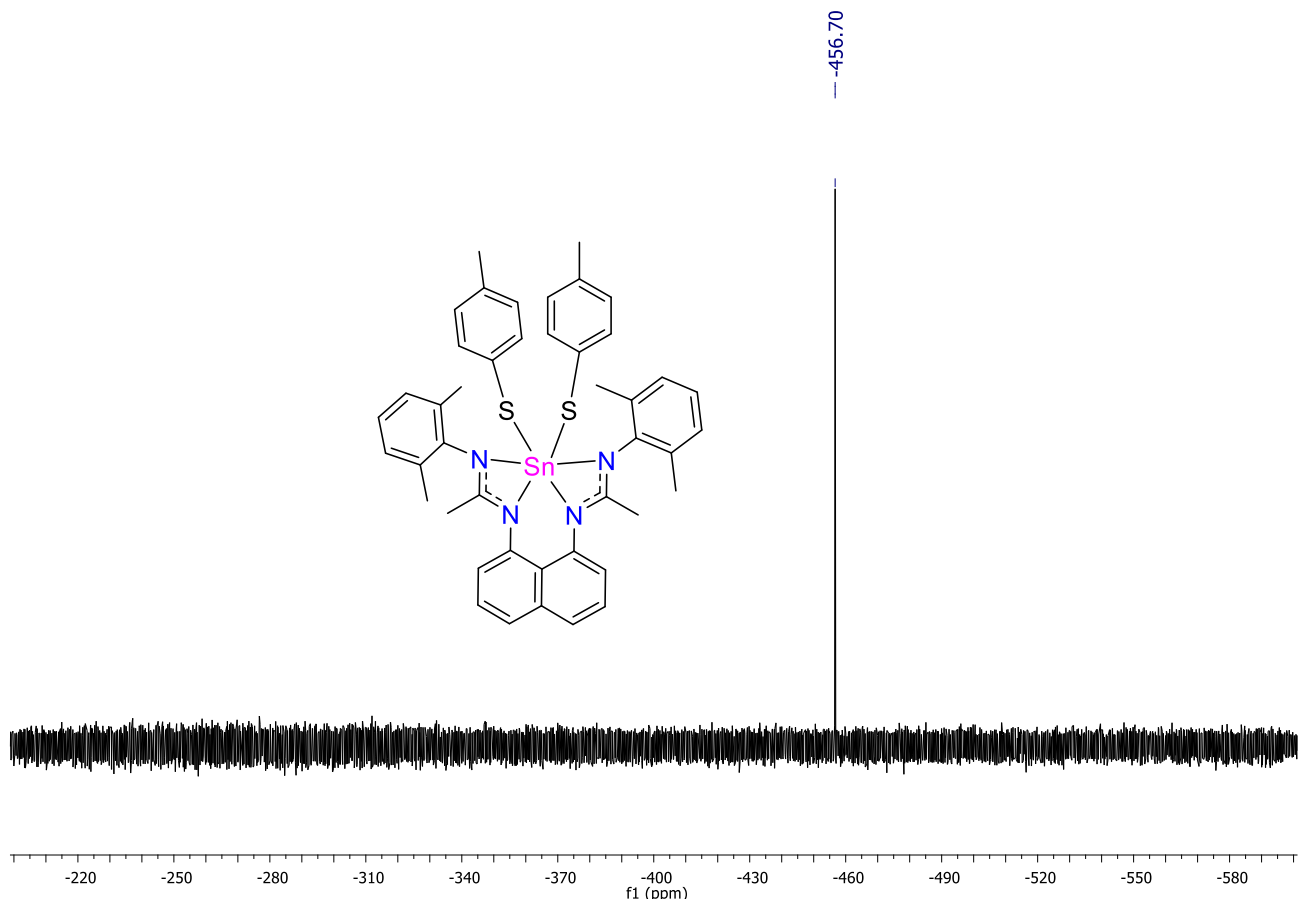


Figure S23. ^{119}Sn NMR of 2a.

A10. 2b, ^1H , ^{13}C and ^{119}Sn NMR spectrum

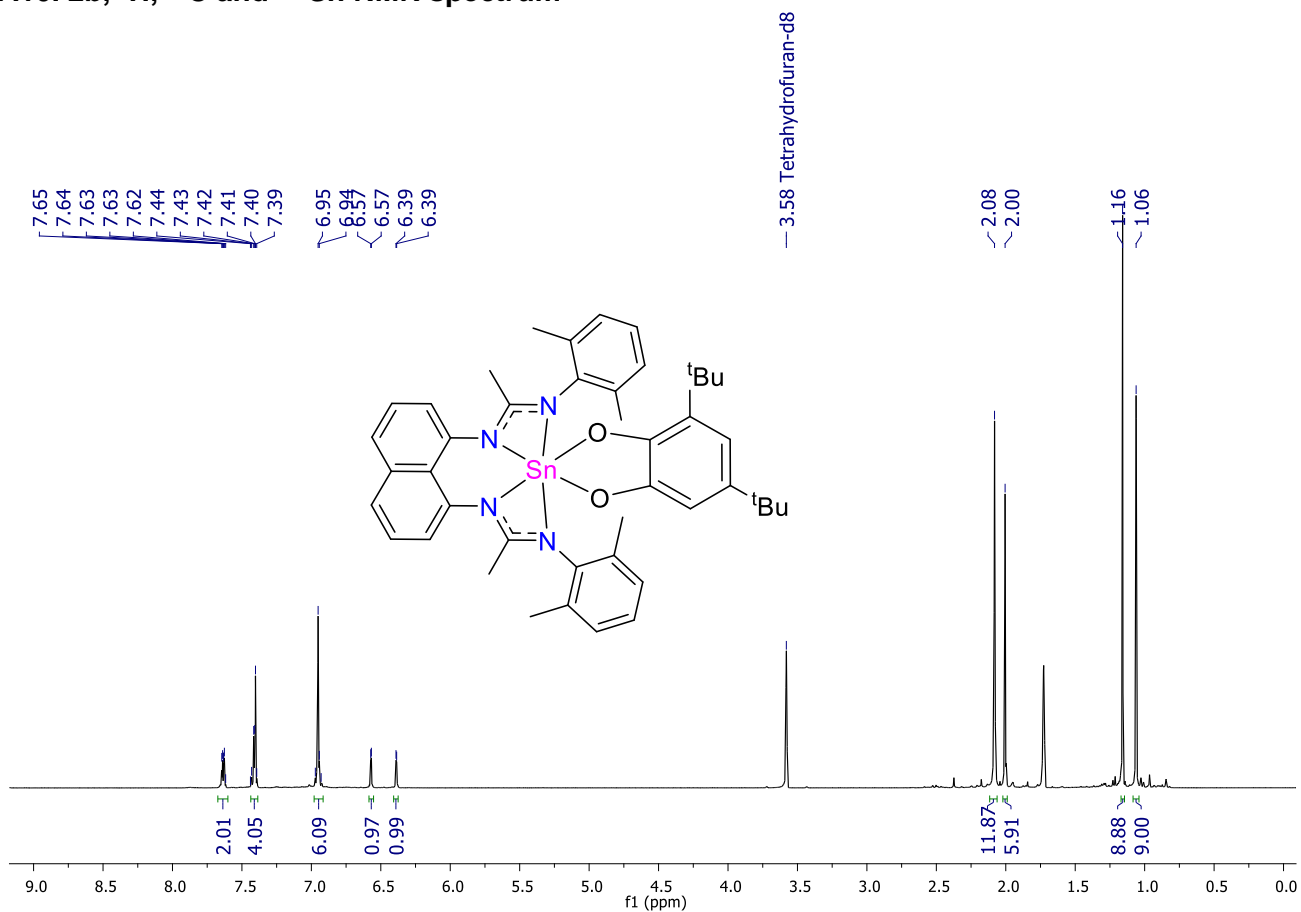


Figure S24. ^1H NMR of 2b.

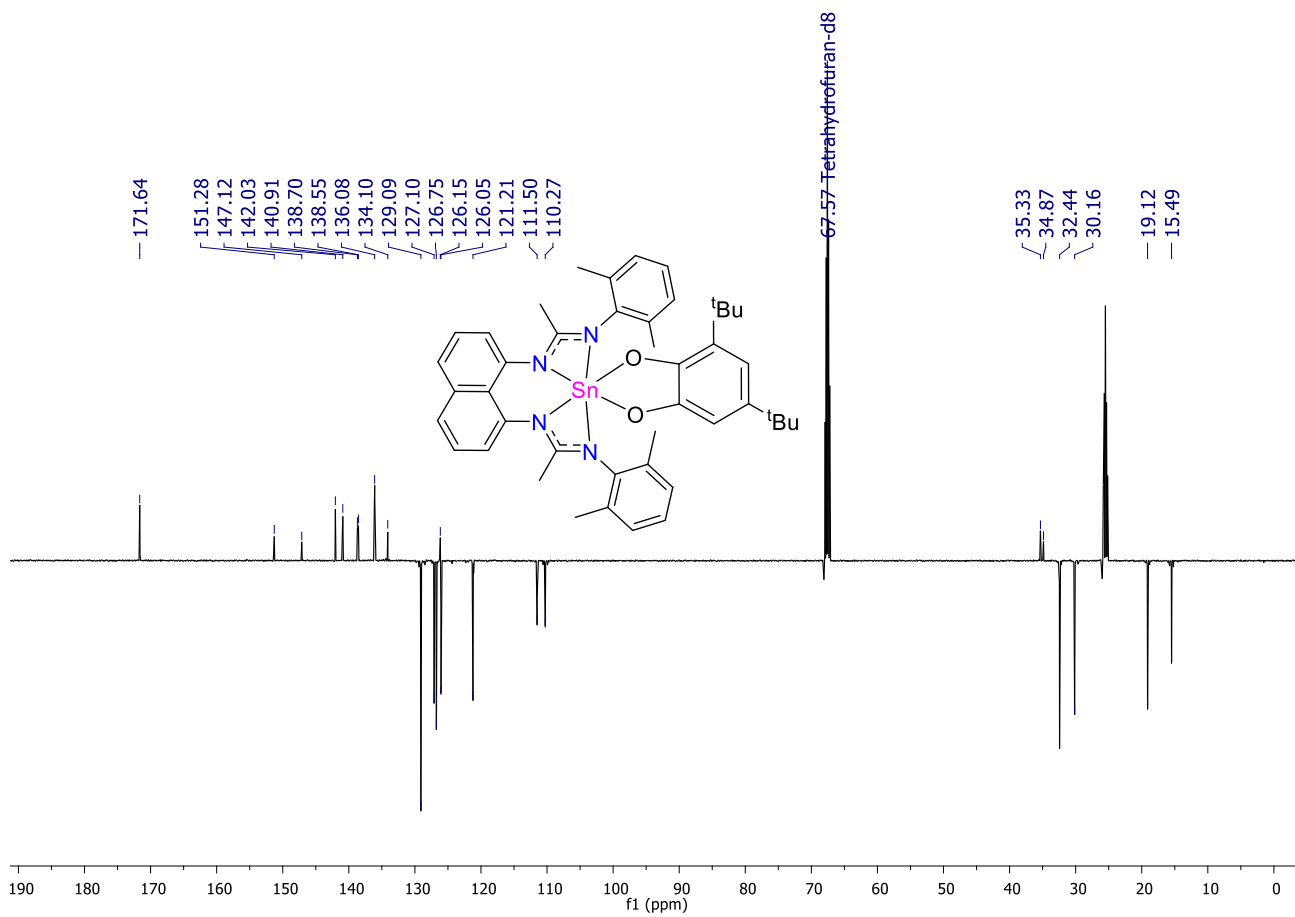


Figure S25. ^{13}C NMR of 2b.

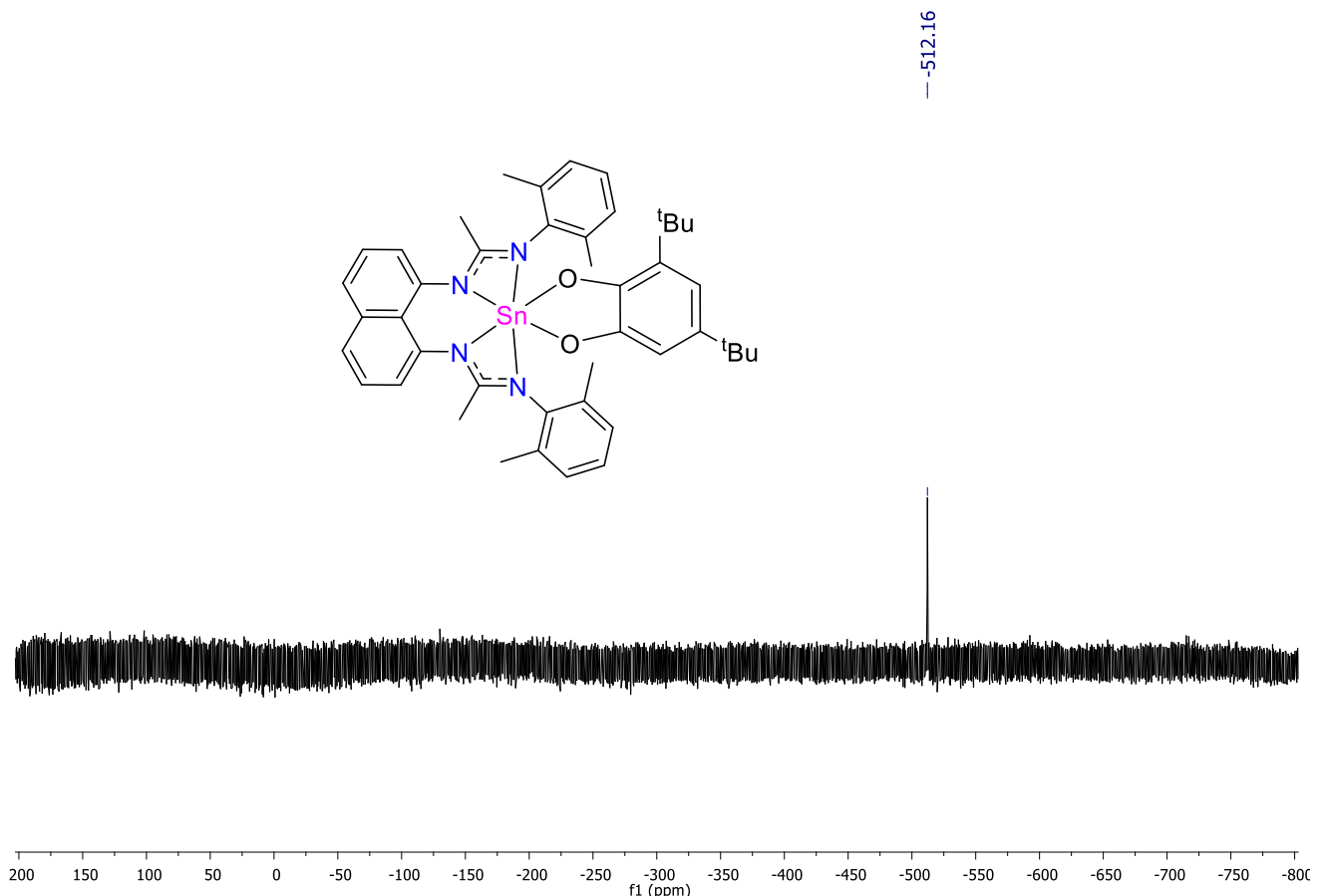


Figure S26. ^{119}Sn NMR of 2b.

A11. 3a, ^1H , ^{13}C and ^{27}Al NMR spectrum

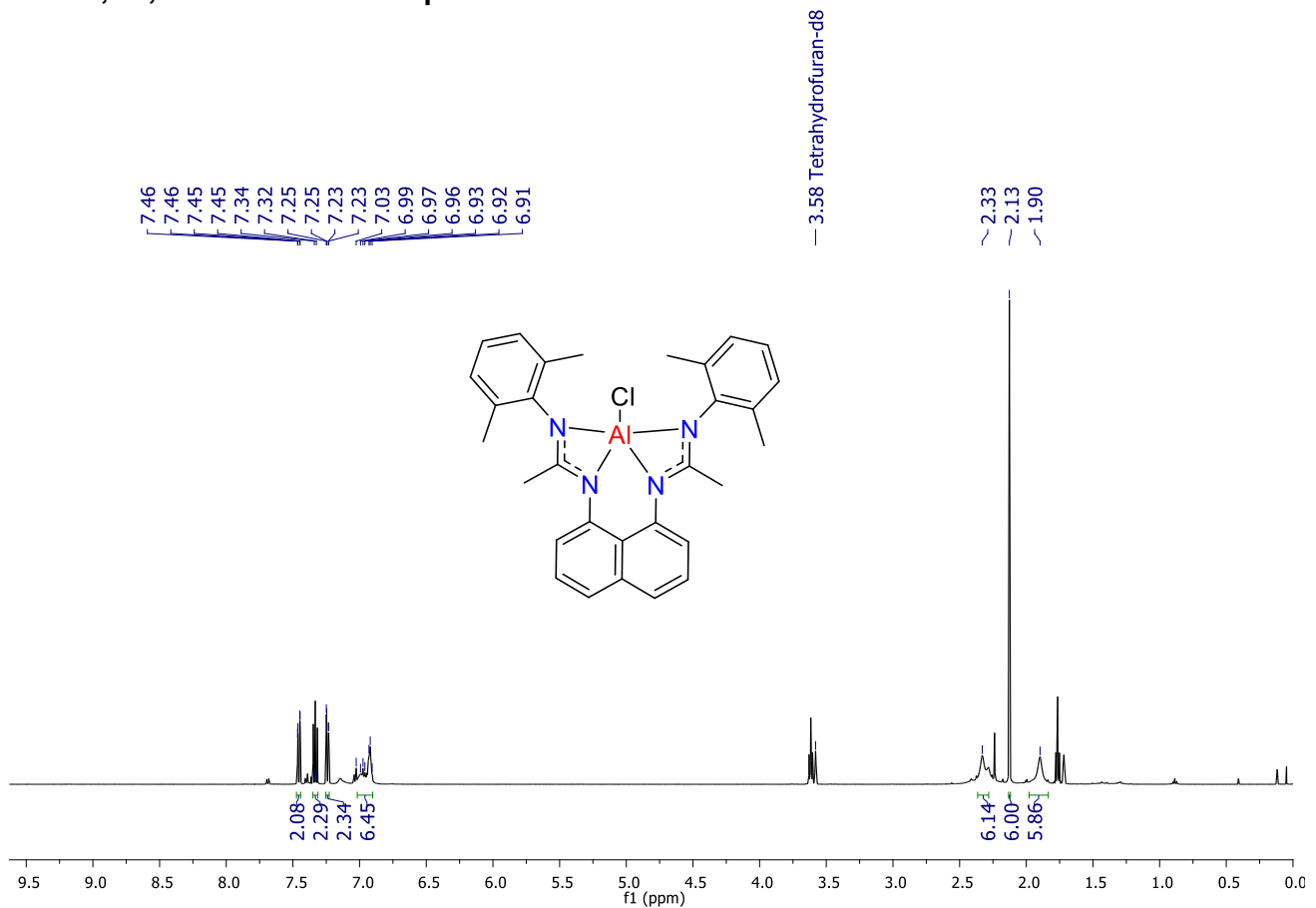


Figure S27. ^1H NMR of 3a.

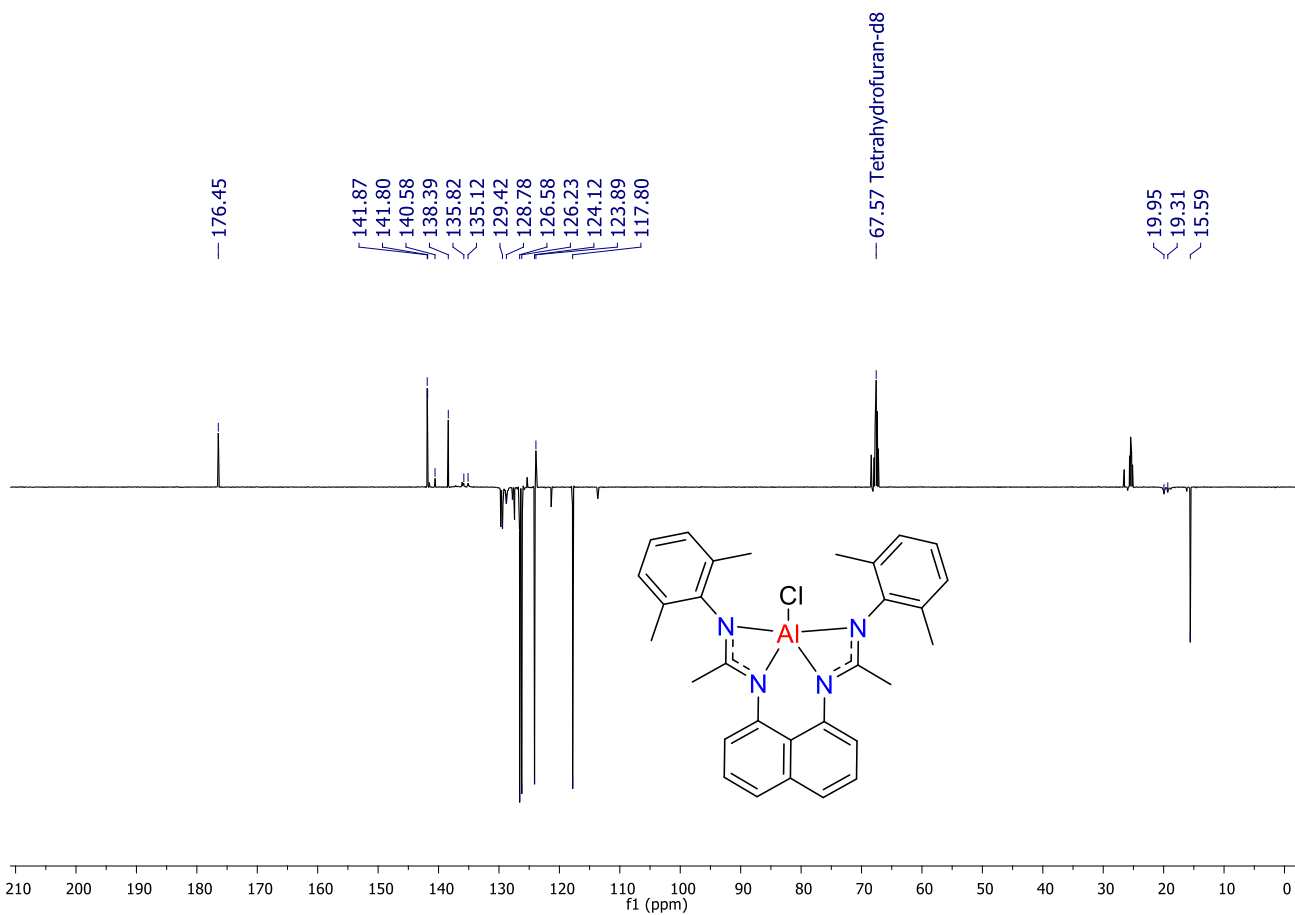


Figure S28. ^{13}C NMR of 3a.

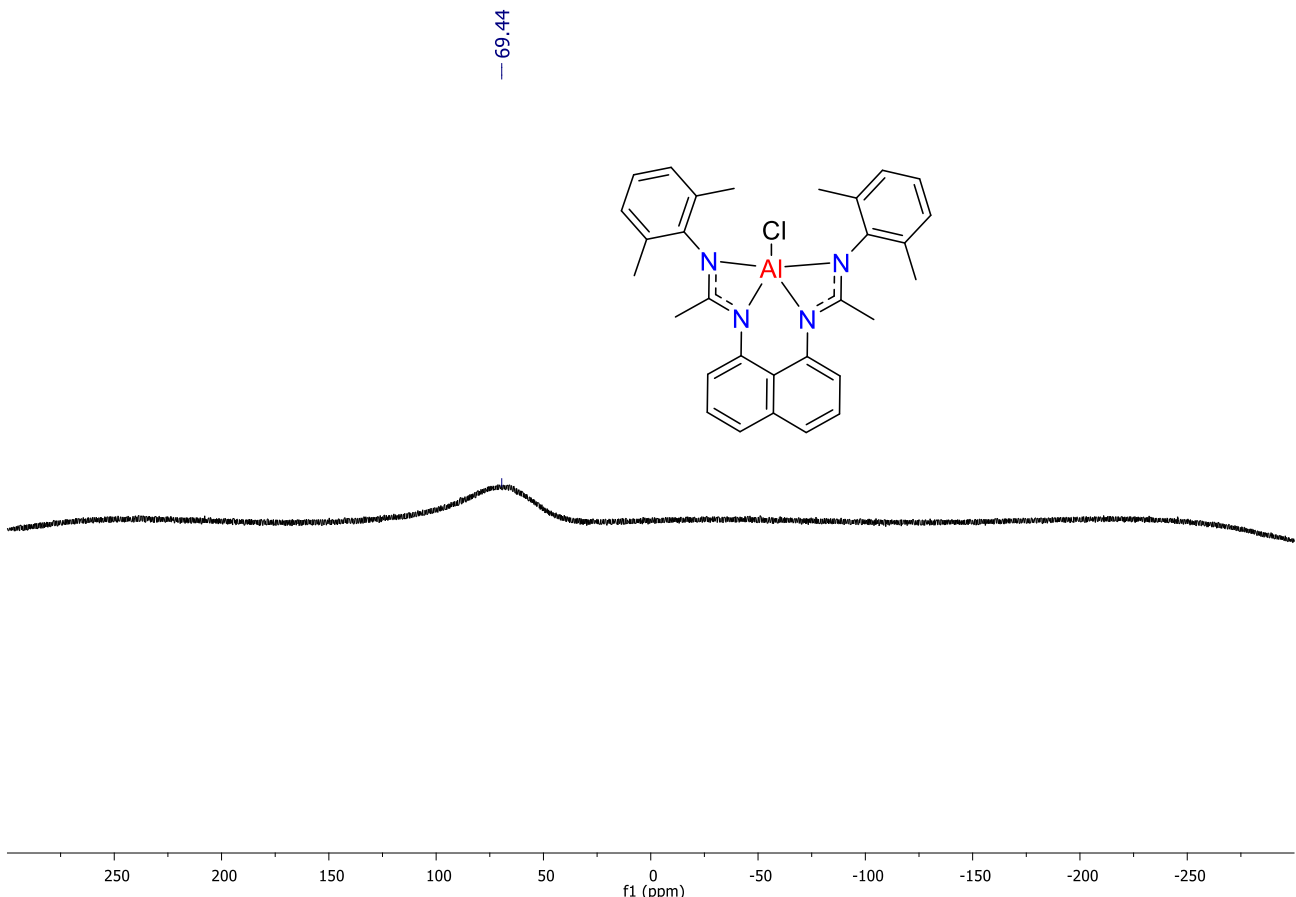


Figure S29. ^{27}Al NMR of 3a.

A12. 3b, ^1H , and ^{13}C NMR spectrum

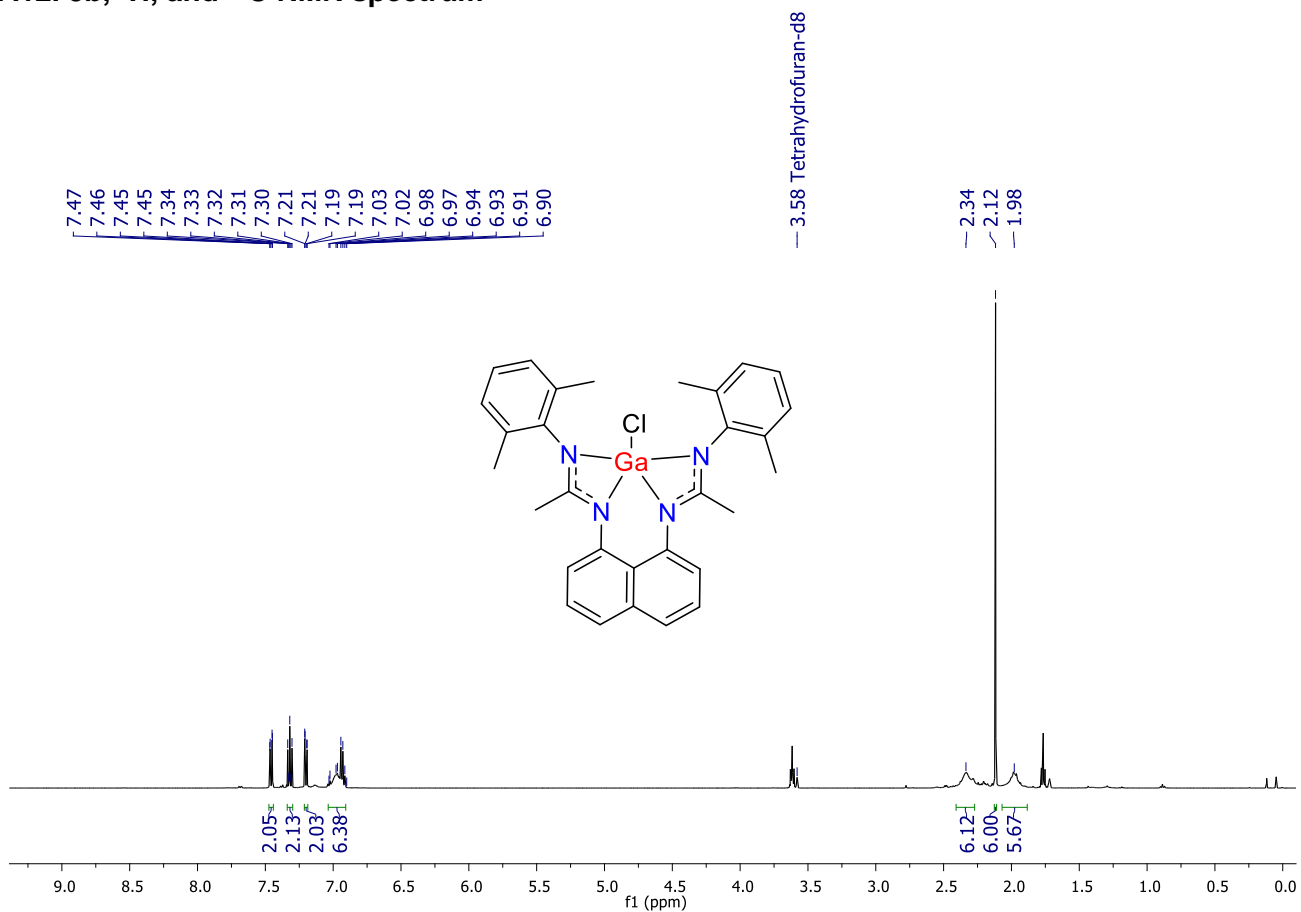


Figure S30. ^1H NMR of 3b.

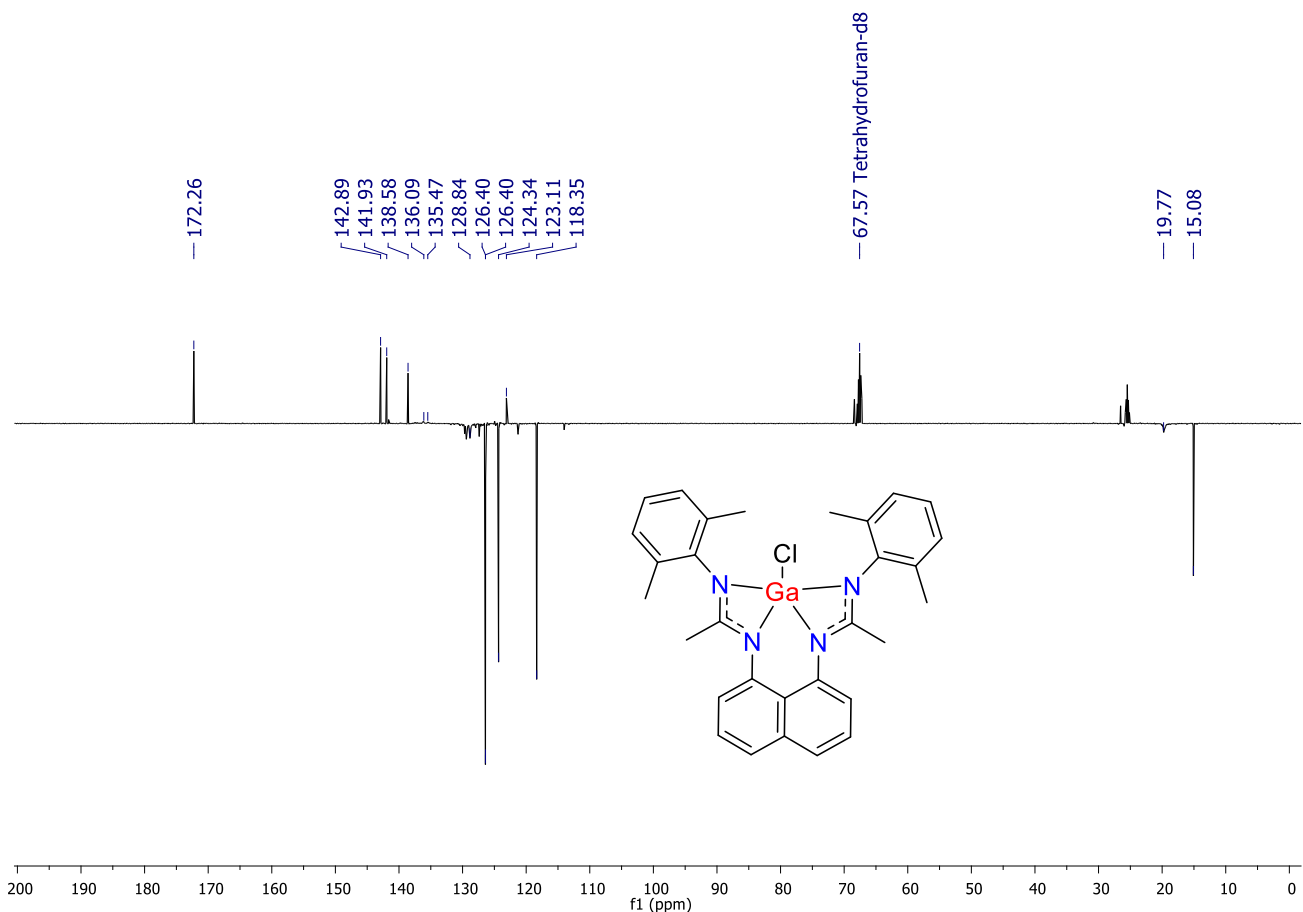


Figure S31. ^{13}C NMR of 3b.

A13. 3c, ^1H , ^{13}C and ^{31}P NMR spectrum

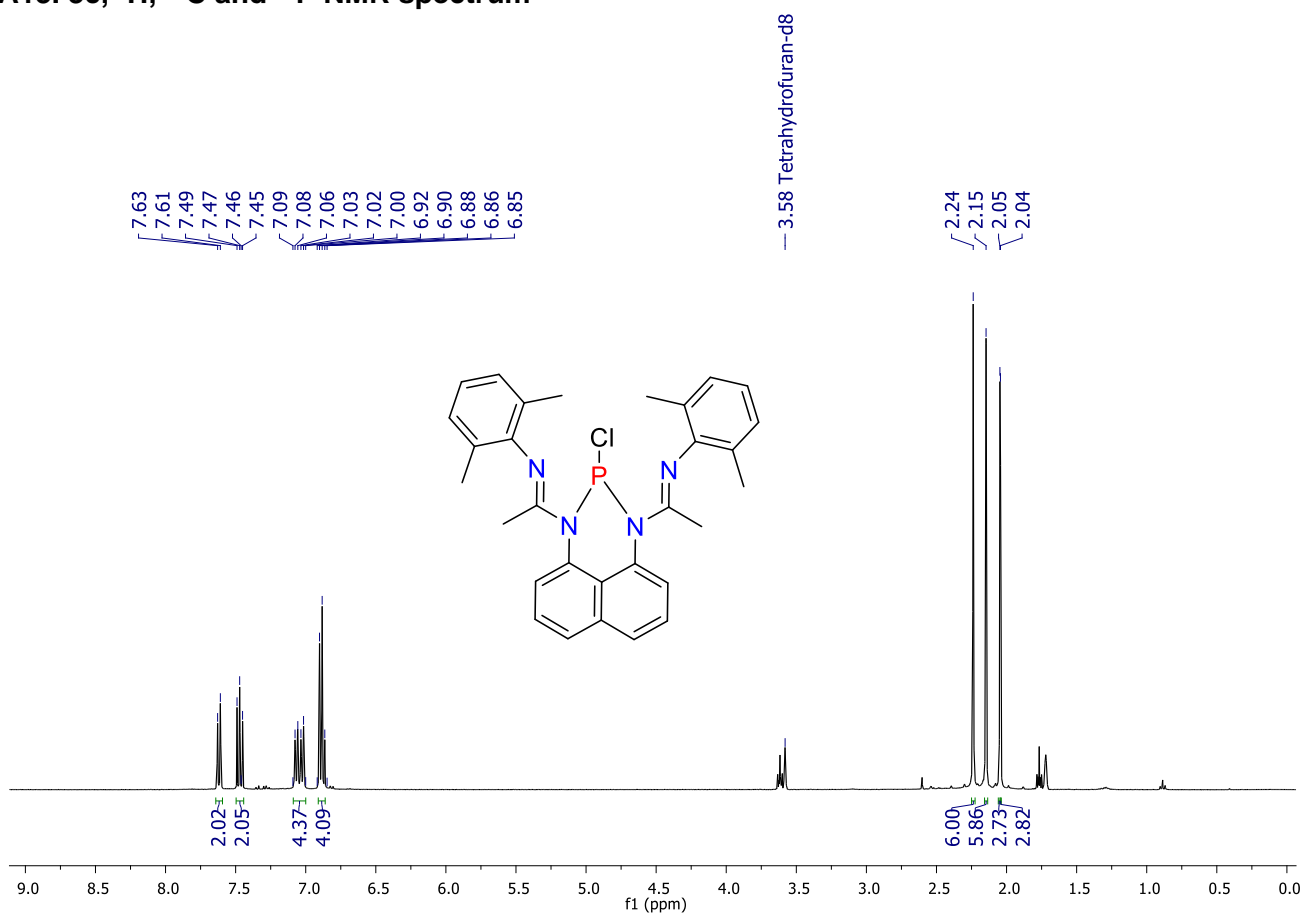


Figure S32. ^1H NMR of 3c.

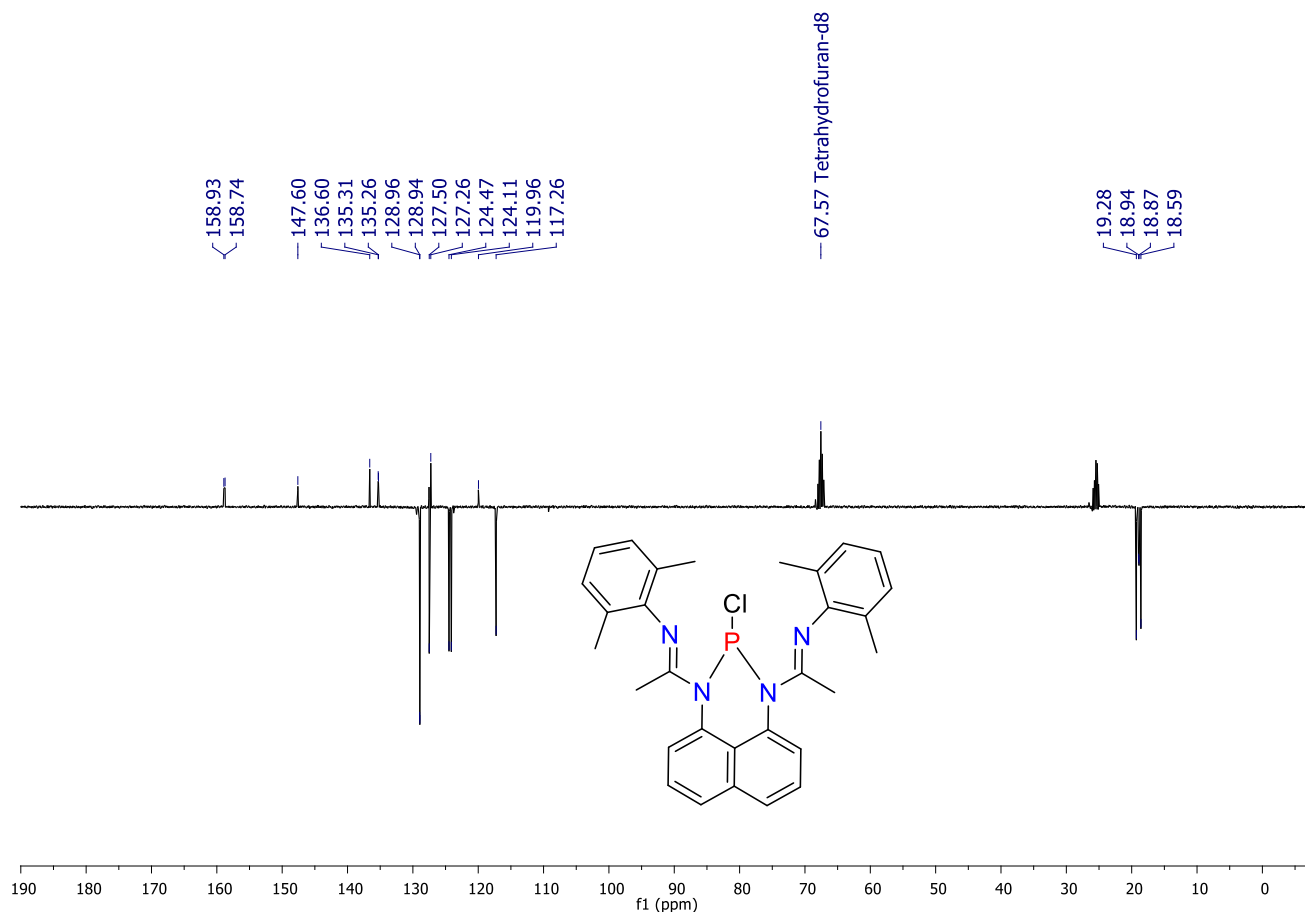


Figure S32. ^{13}C NMR of 3c.

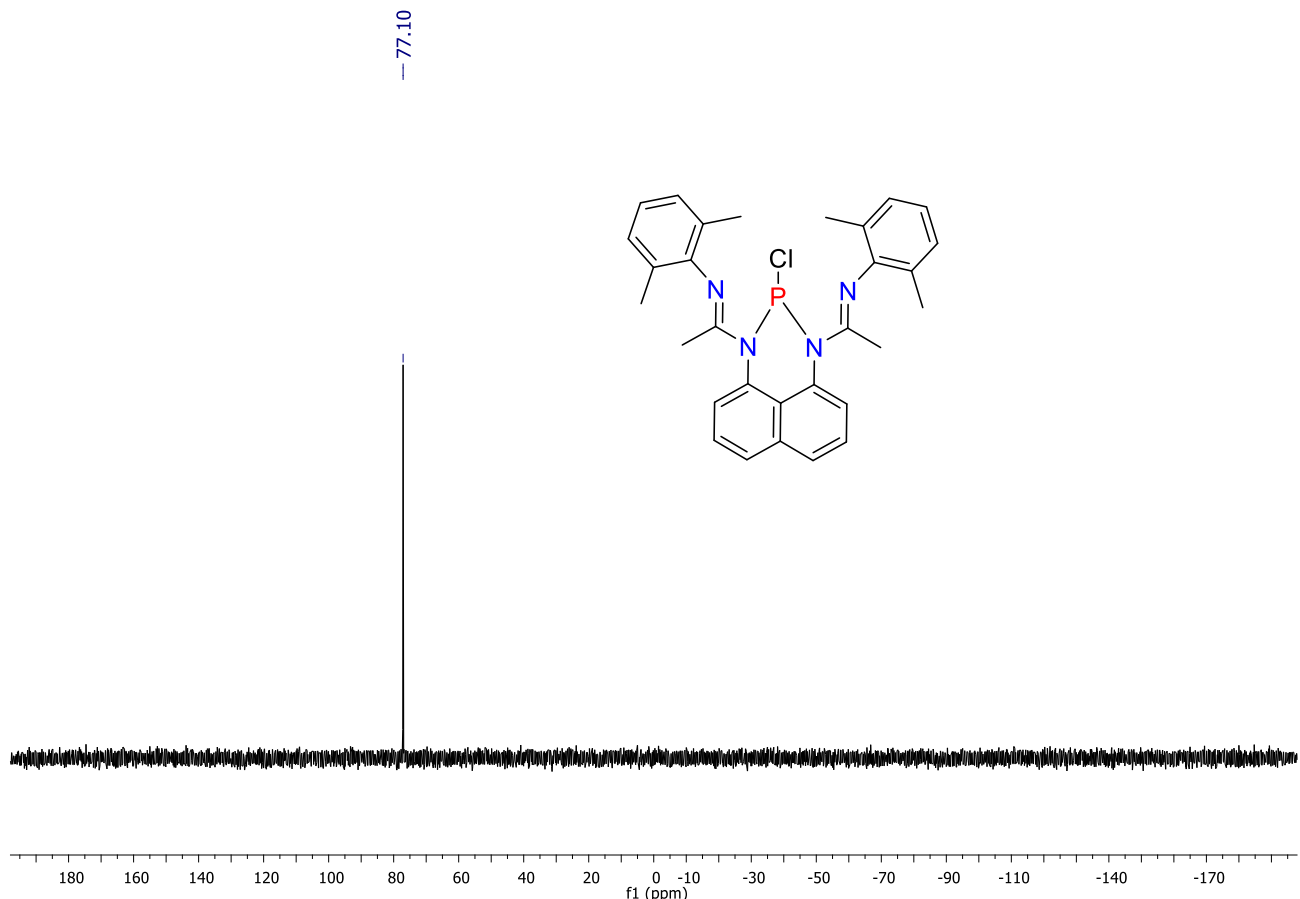


Figure S33. ^{31}P NMR of 3c.

A14. 3d, ^1H , ^{13}C and ^{31}P NMR spectrum

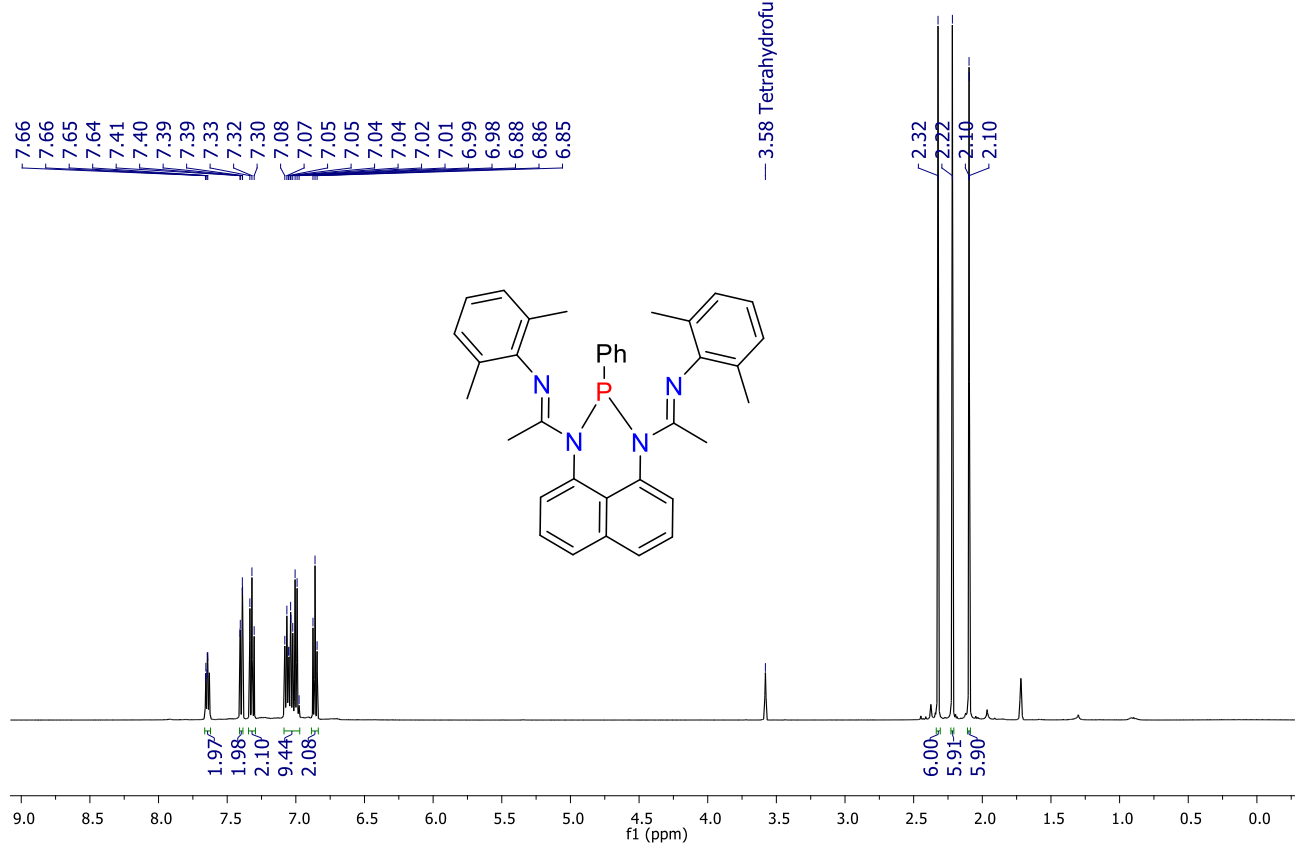


Figure S34. ^1H NMR of 3d.

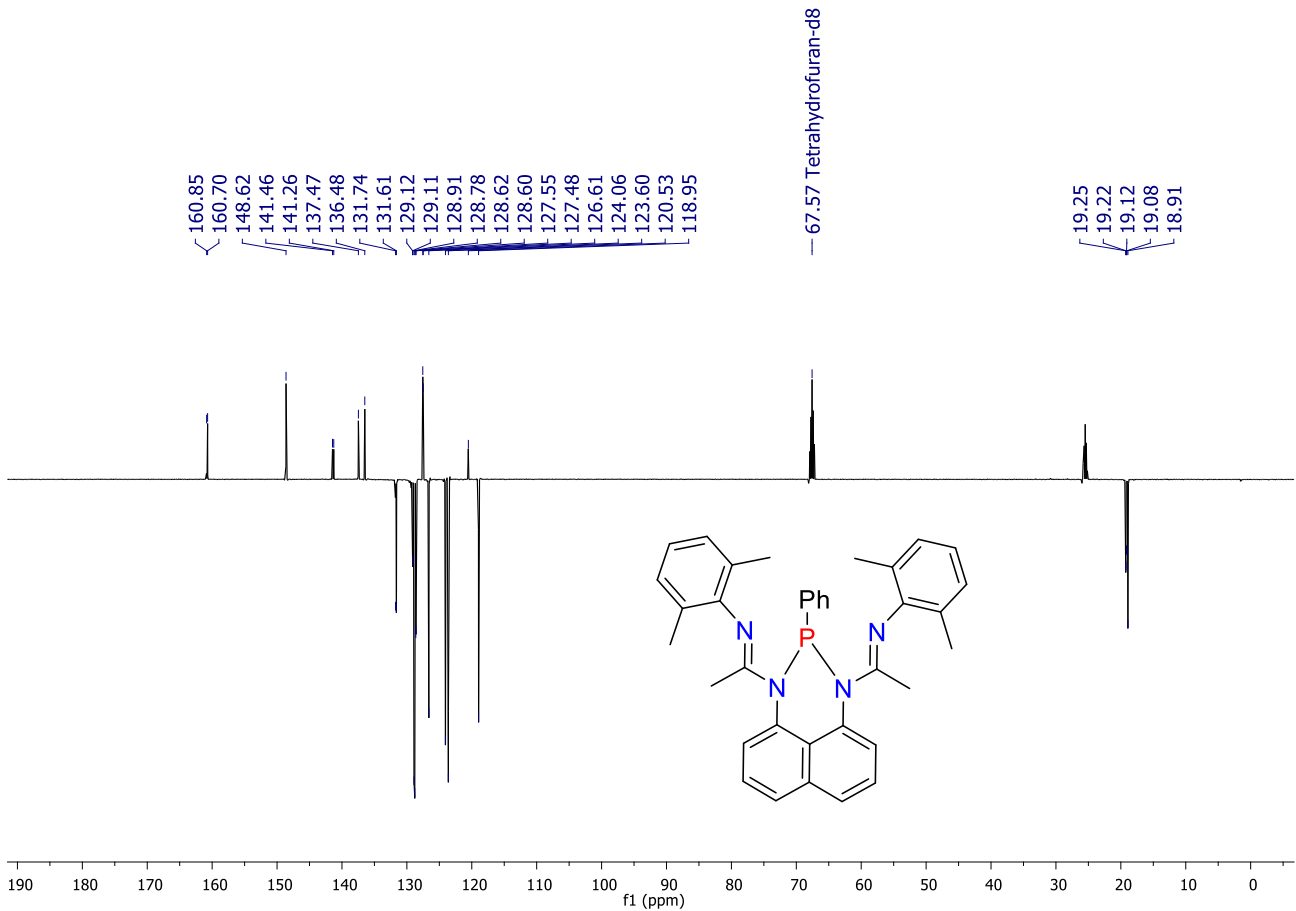


Figure S35. ^{13}C NMR of 3d.

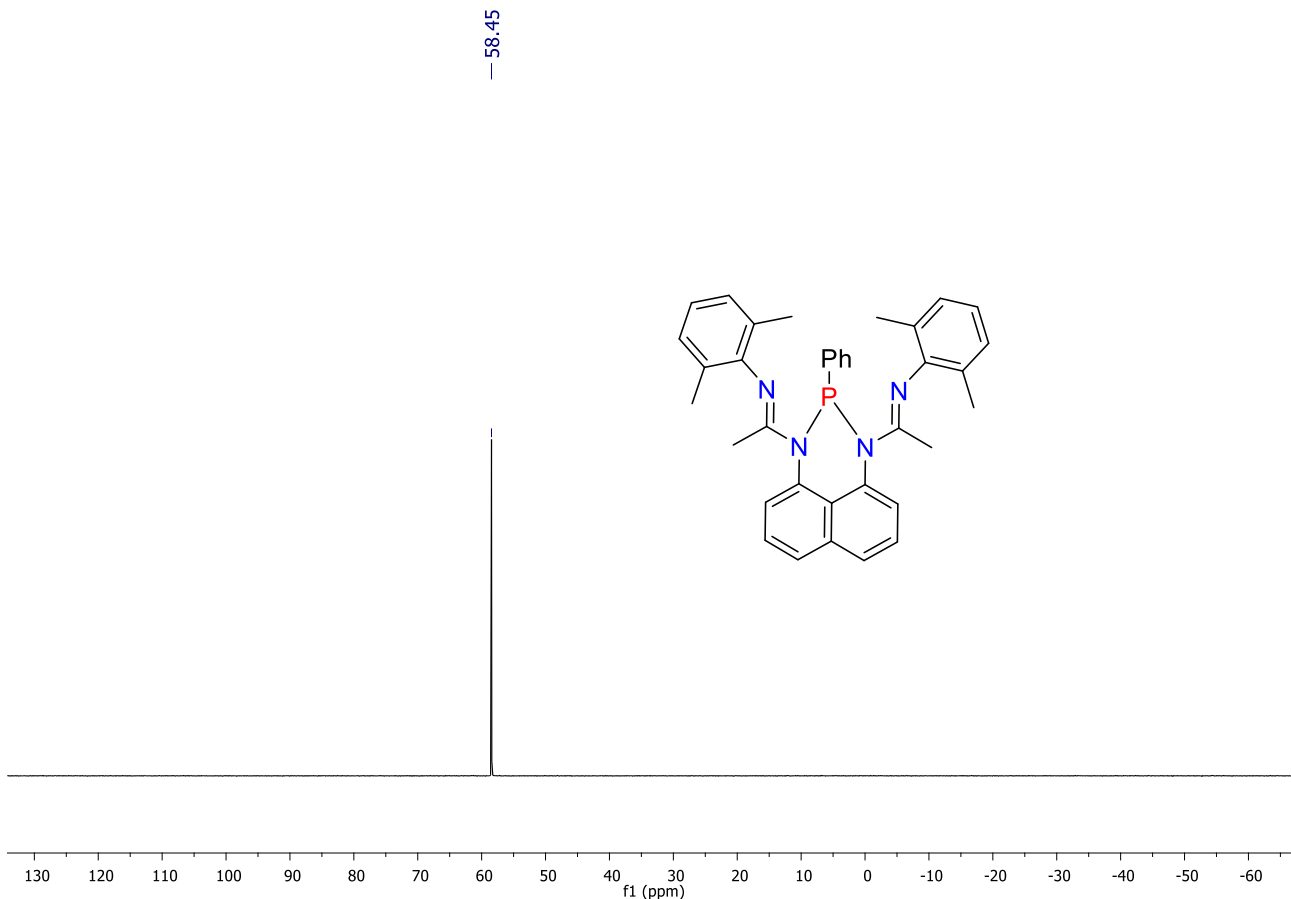


Figure S36. ^{31}P NMR of 3d.

A15. L_2Al_2 , ^1H , ^{13}C and ^{27}Al NMR spectrum

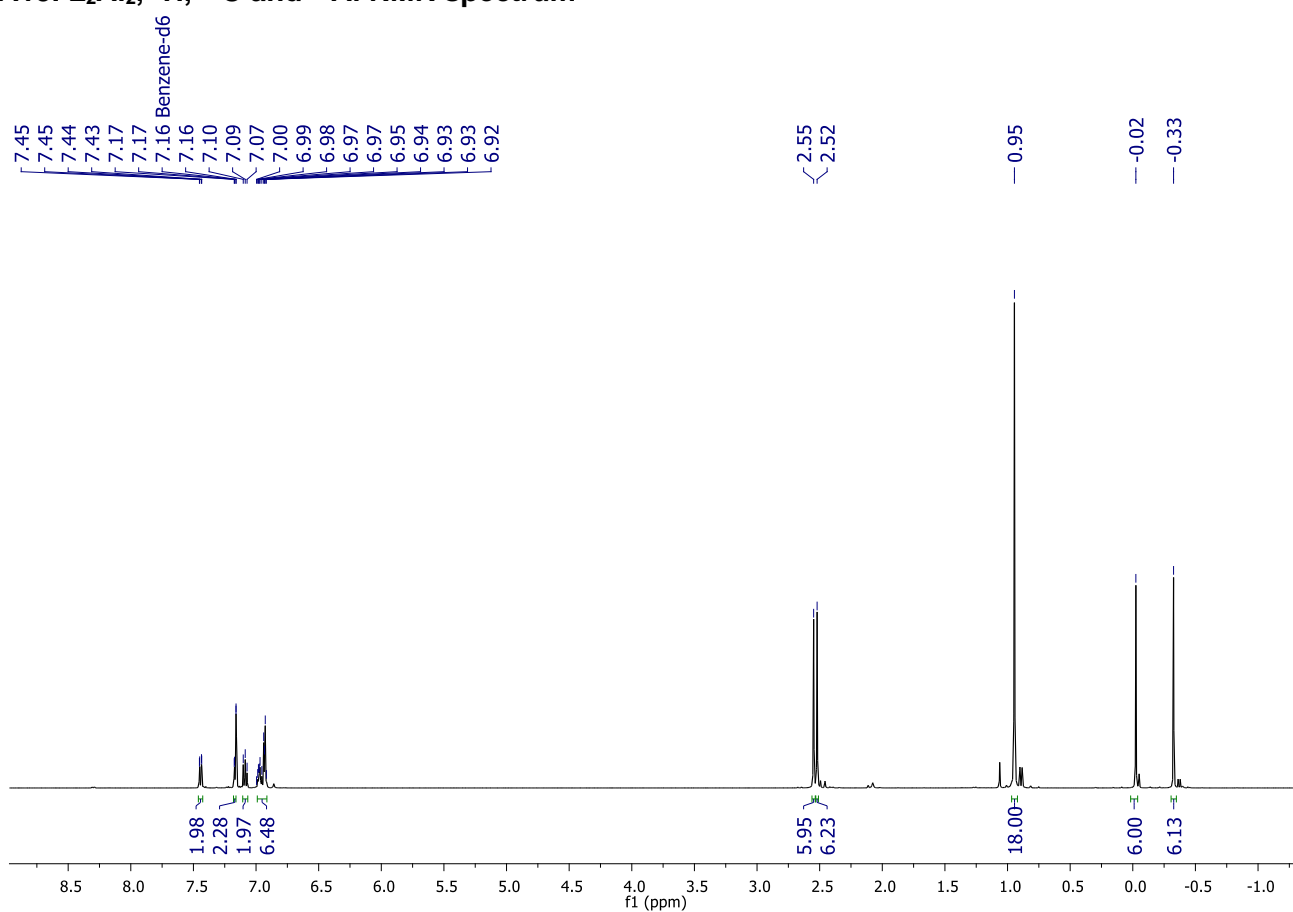


Figure S37. ^1H NMR of L_2Al_2 .

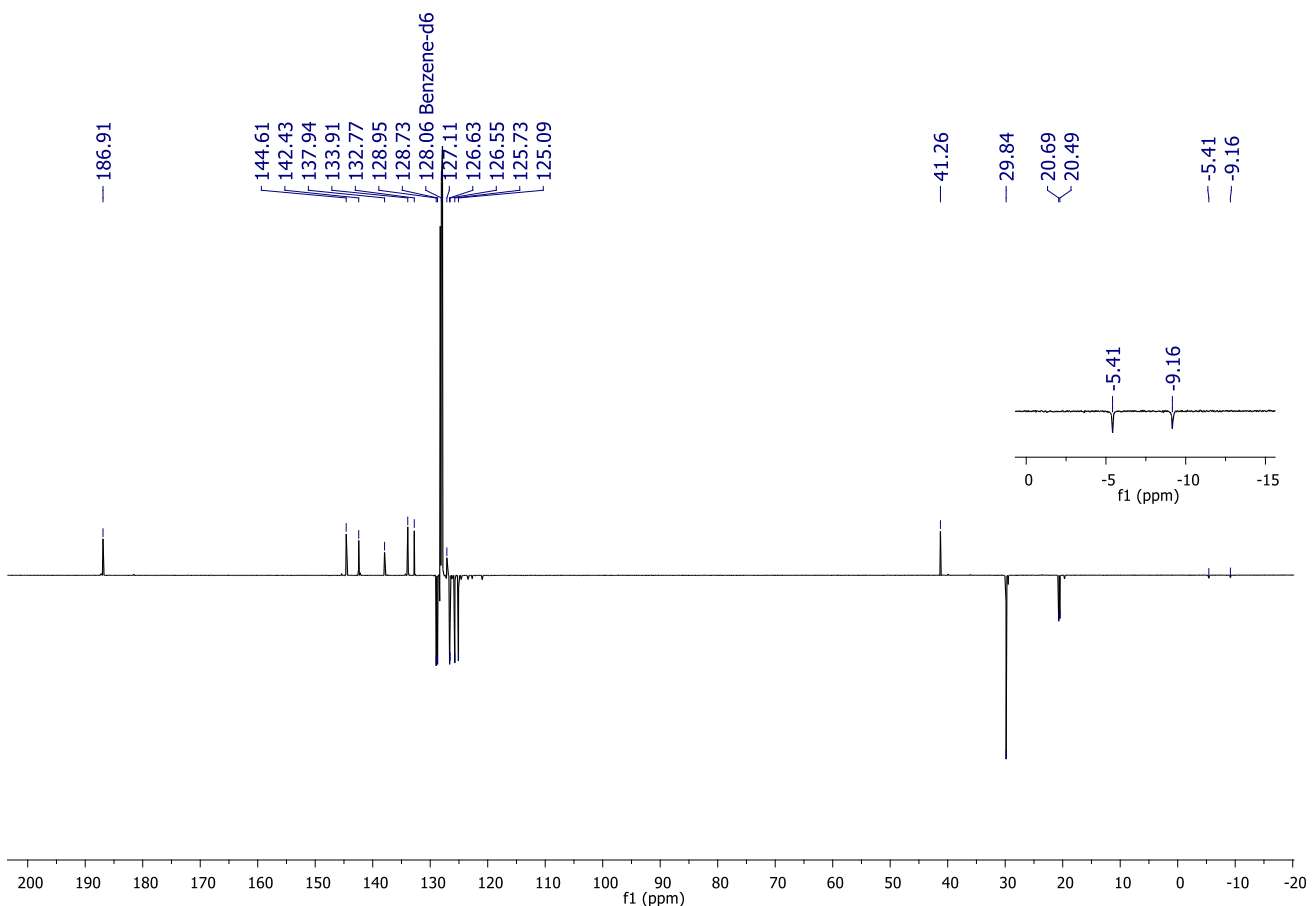


Figure S38. ^{13}C NMR of L_2Al_2 .

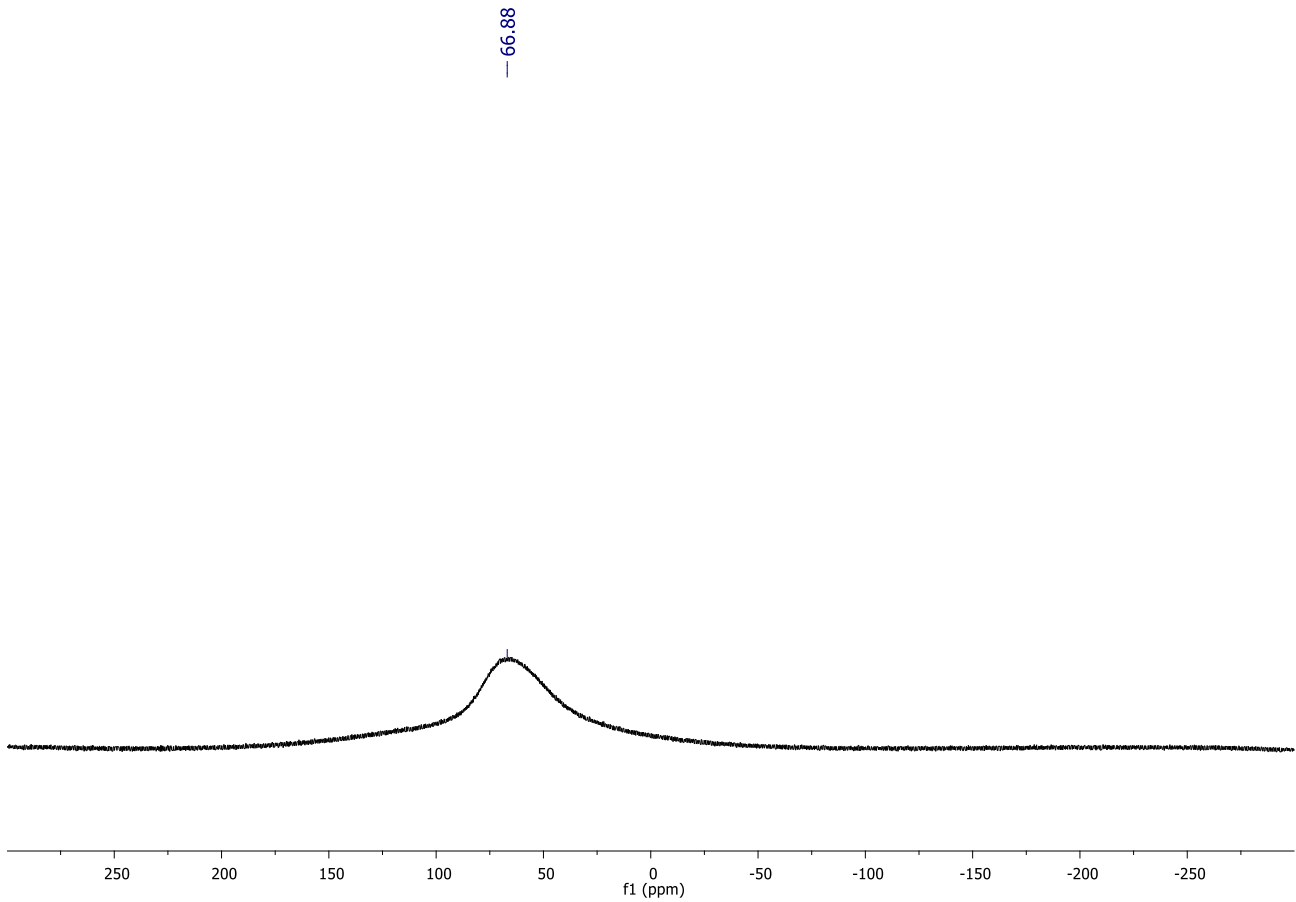


Figure S39. ^{27}Al NMR of L_2Al_2 .

A16. $\text{L}_2\text{Al}_2\text{I}_4$, ^1H NMR spectrum

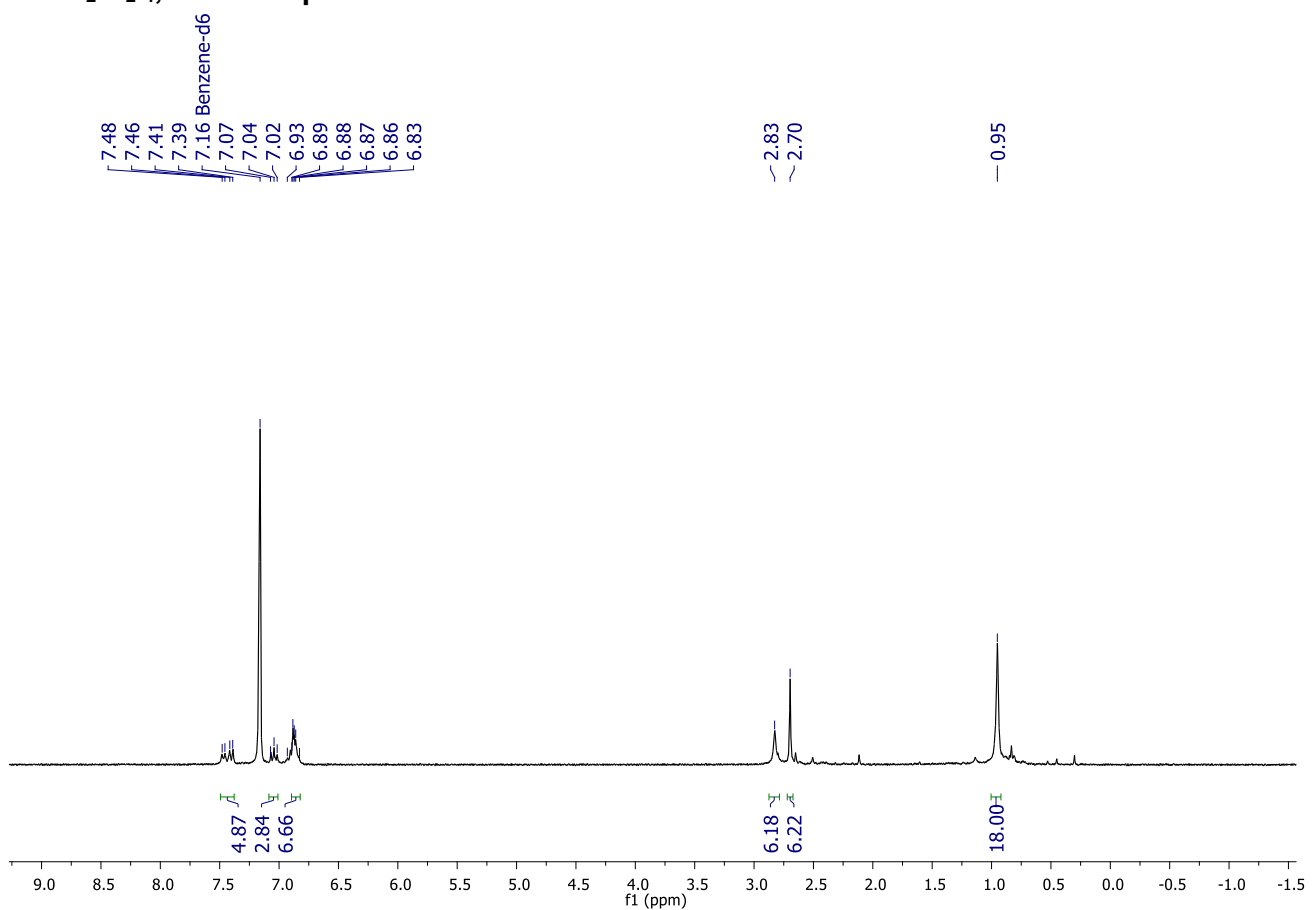


Figure S40. ^1H NMR of $\text{L}_2\text{Al}_2\text{I}_4$.

A17. L_3Al_2 , ^1H NMR spectrum

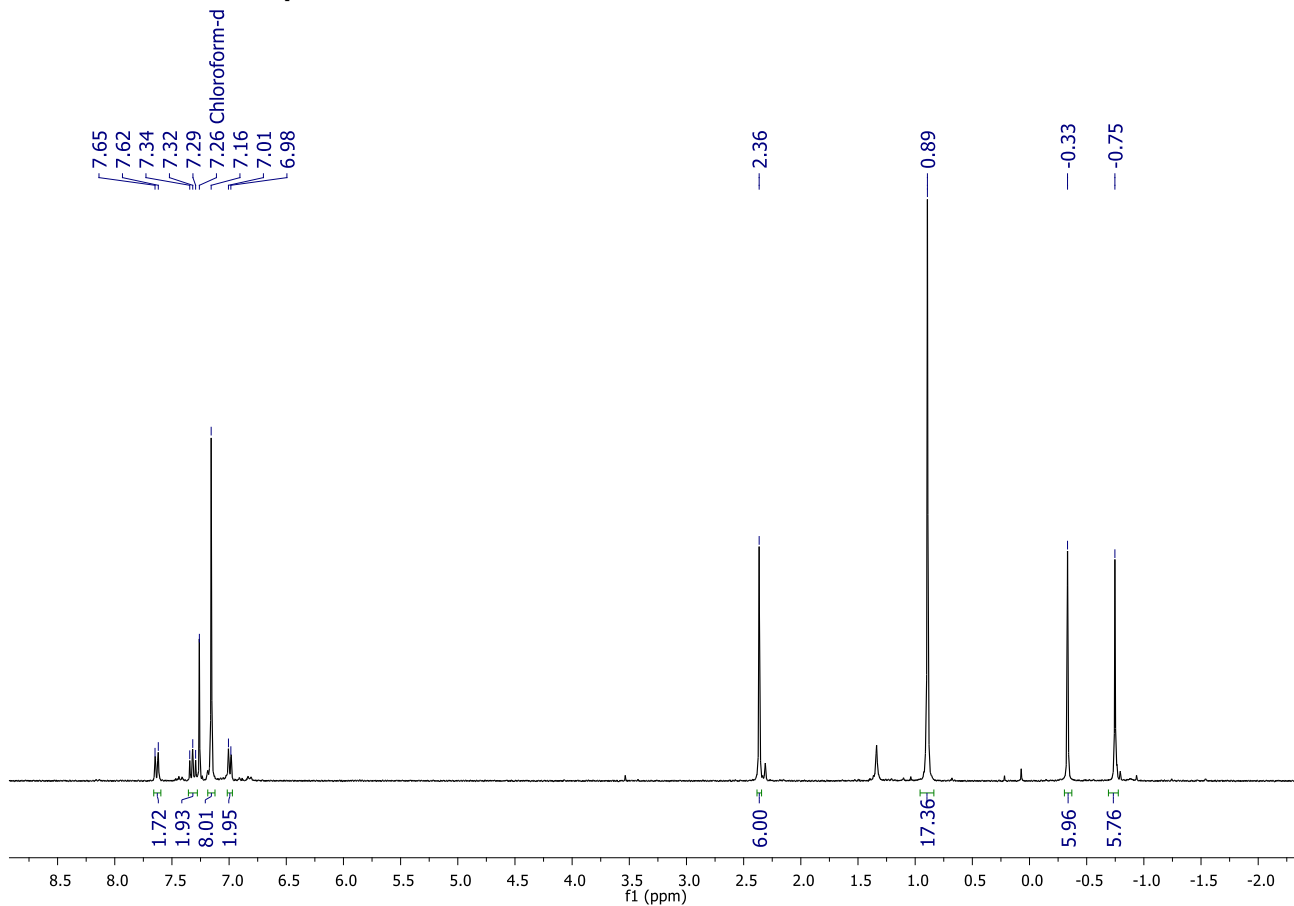


Figure S41. ^1H NMR of L_3Al_2 .

A18. 4a, ^1H and ^{13}C NMR spectrum

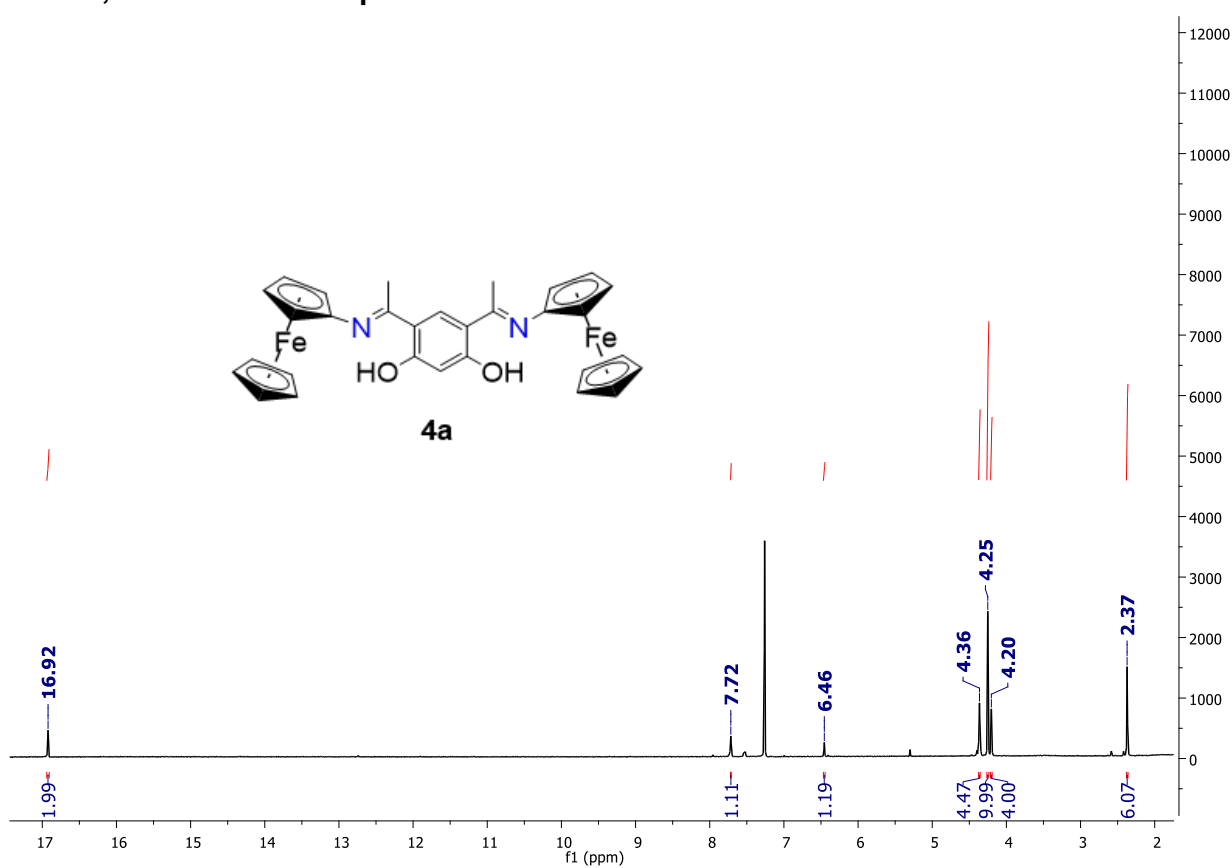


Figure S42. ^1H NMR of 4a.

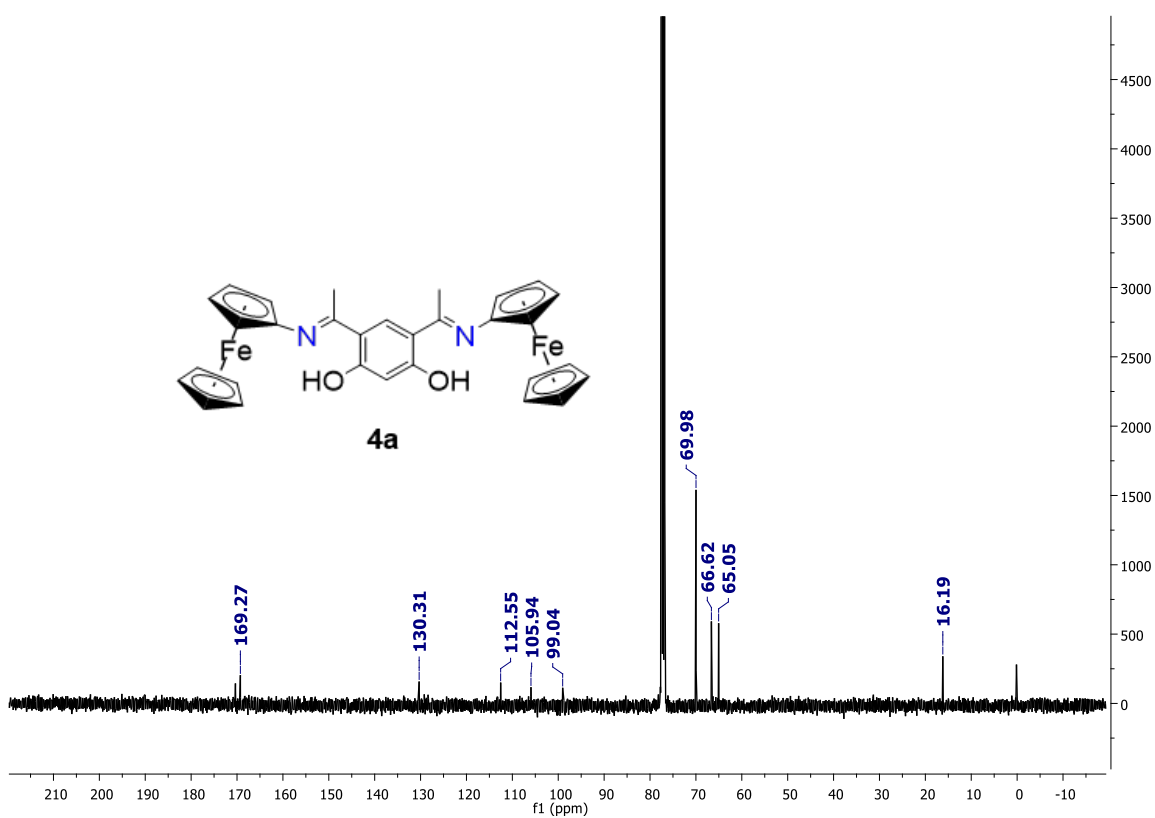


Figure S43. ¹³C NMR of 4a.

A19. 4b, ^1H and ^{13}C NMR spectrum

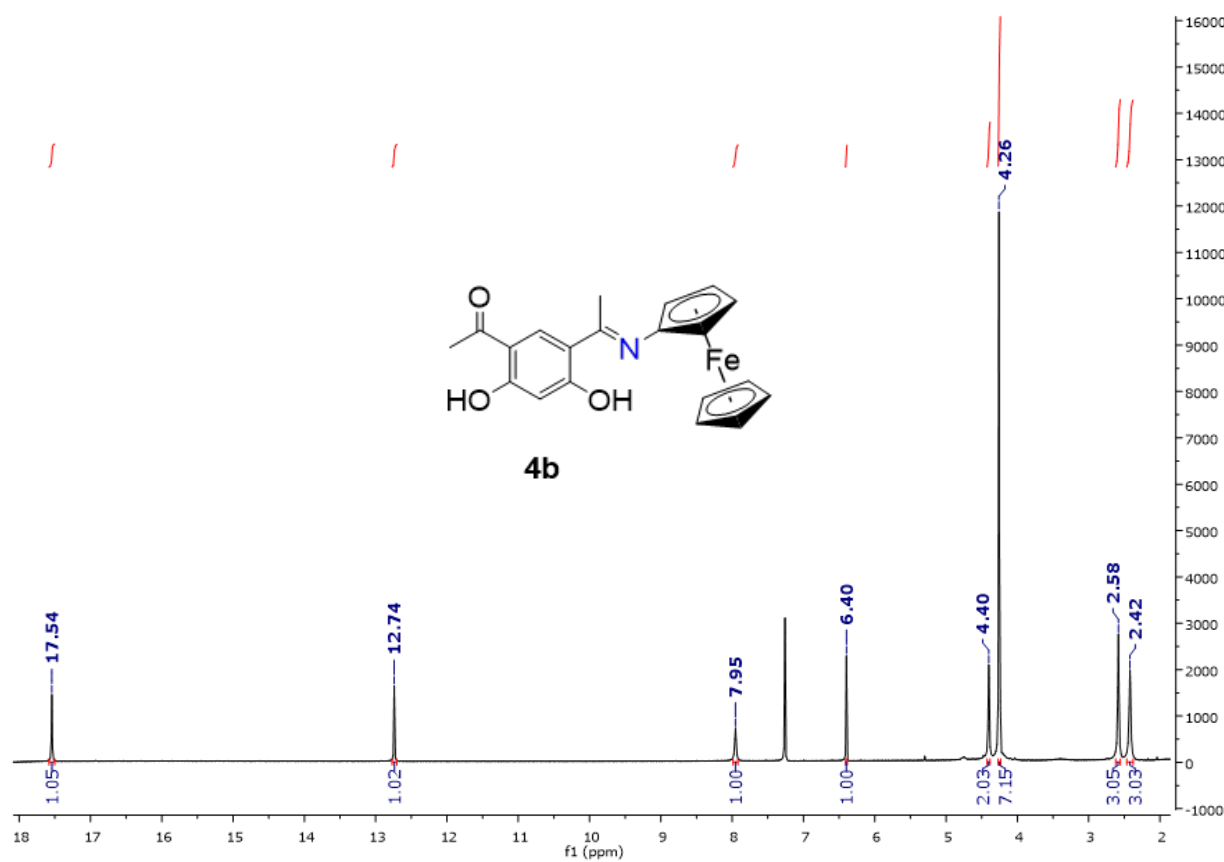


Figure S44. ^1H NMR of 4b.

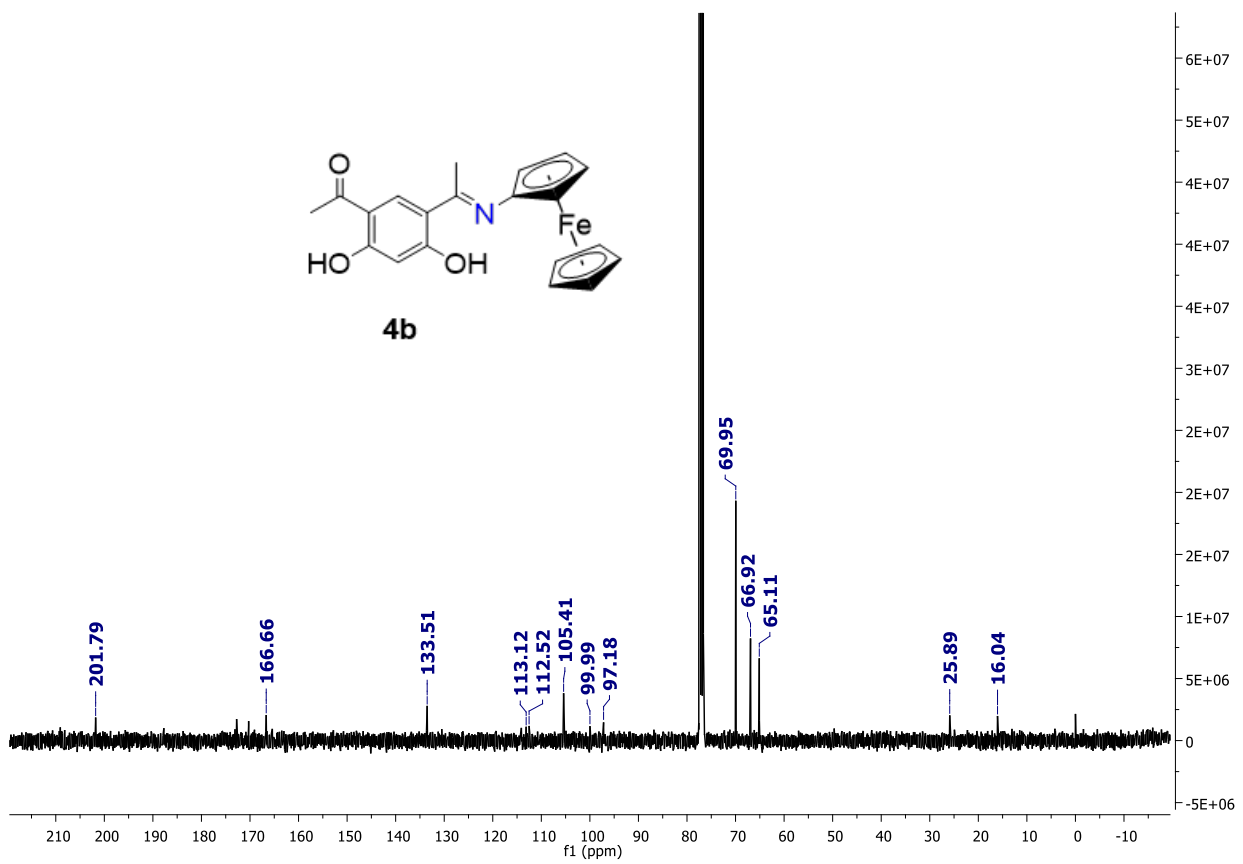


Figure S45. ^{13}C NMR of 4b.

A20. 5a, ^1H and ^{13}C NMR spectrum

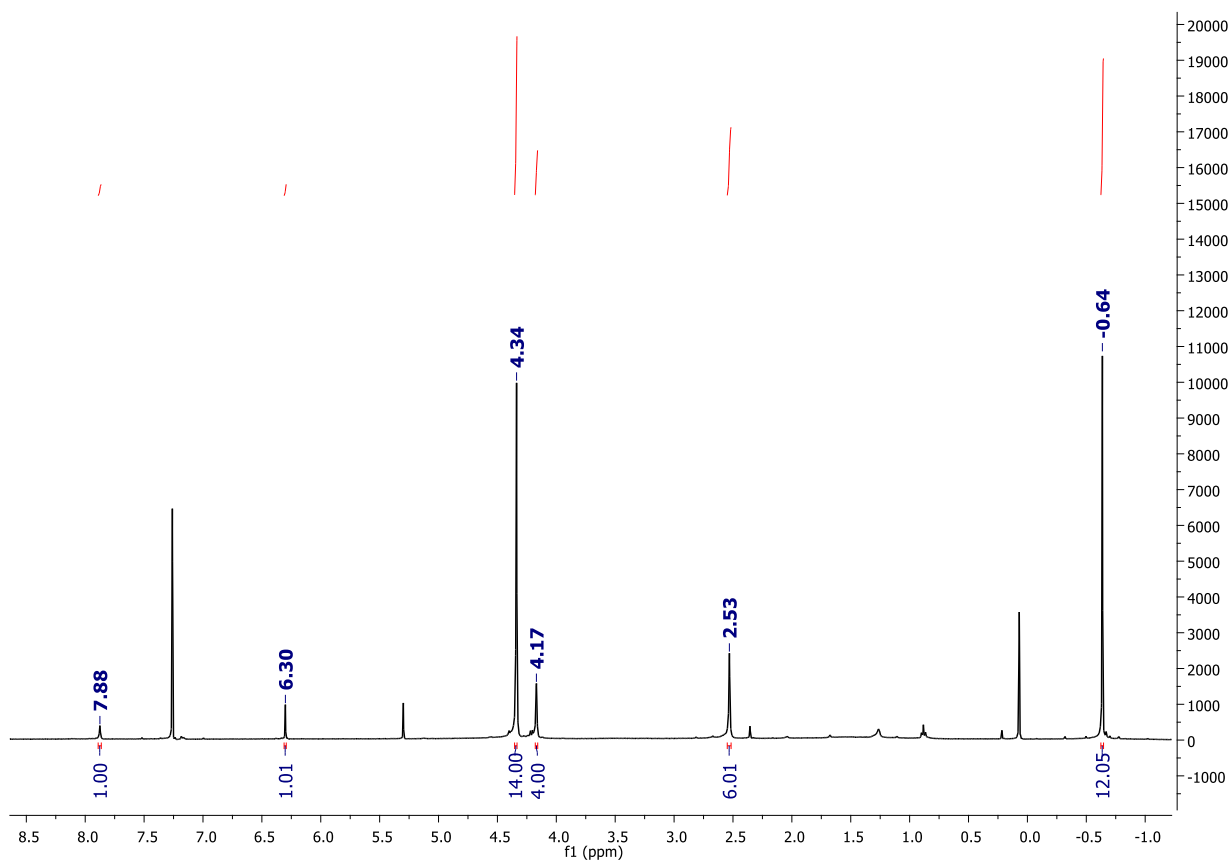


Figure S46. ^1H NMR of 5a.

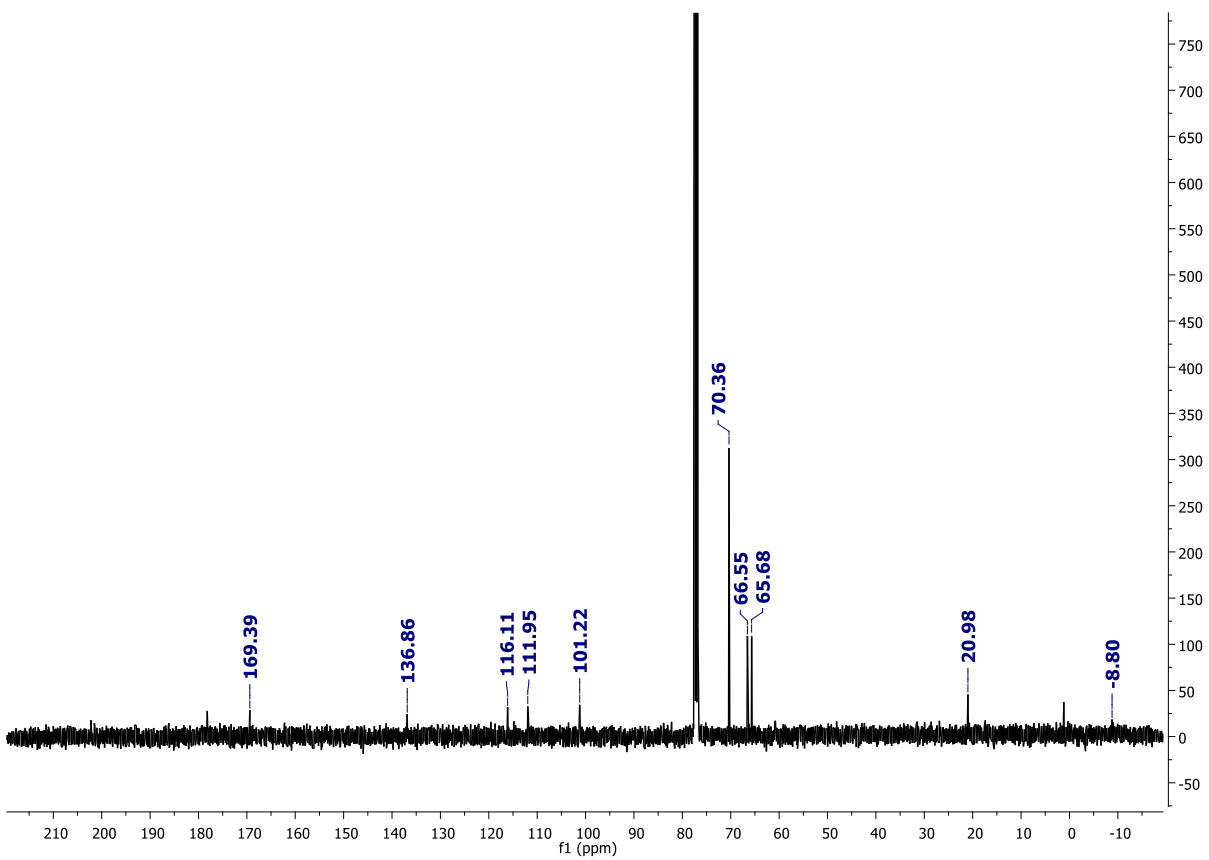


Figure S47. ^{13}C NMR of 5a.

A21. Crystal data and structure refinement of L₁Sn

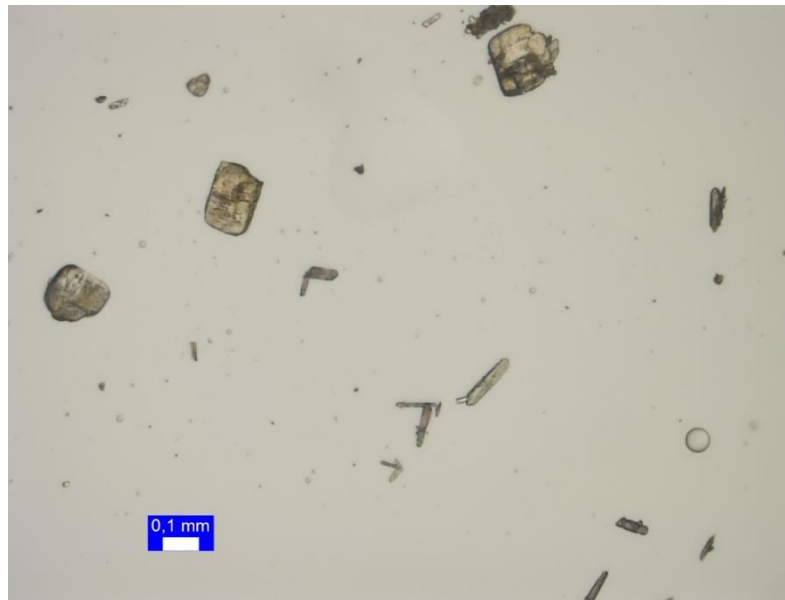


Figure S48. Sample of L₁Sn.

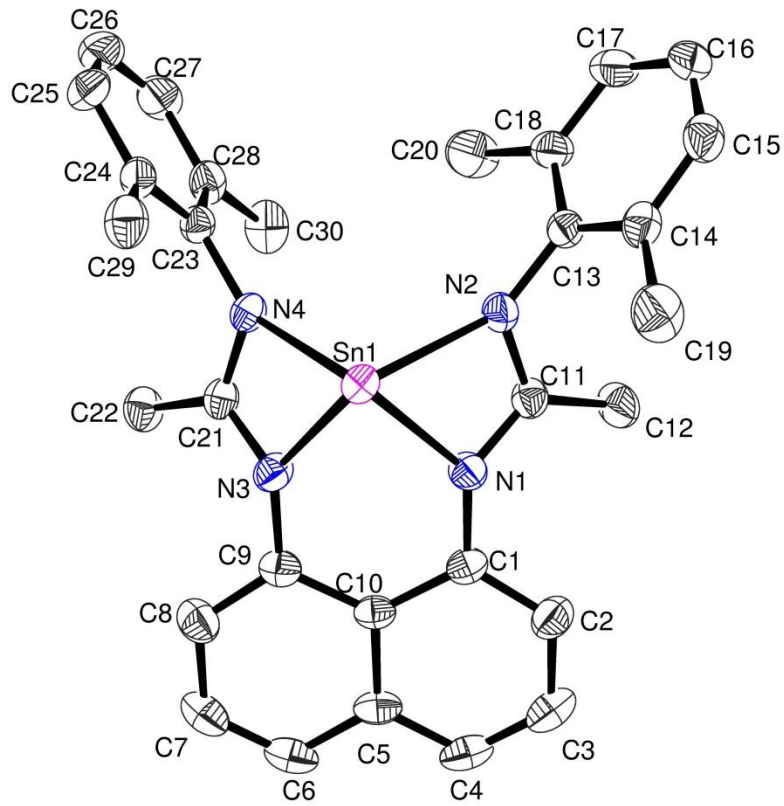


Figure S49. Asymmetric Unit of L_1Sn .

Table A1. Crystal data and structure refinement for L_1Sn .

Identification code	L_1Sn
Empirical formula	C ₃₀ H ₃₀ N ₄ Sn
Formula weight	565.29
Temperature	193(2) K
Wavelength	0.71073 Å
Crystal system, space group	Monoclinic, C 2/c
Unit cell dimensions	a = 20.6812(9) Å alpha = 90 deg. b = 12.6563(5) Å beta = 96.409(2) deg. c = 20.1577(8) Å gamma = 90 deg.
Volume	5243.3(4) Å ³
Z, Calculated density	8, 1.432 Mg/m ³
Absorption coefficient	1.000 mm ⁻¹
F(000)	2304
Crystal size	0.120 x 0.100 x 0.080 mm

Theta range for data collection	2.677 to 35.008 deg.
Limiting indices	-33<=h<=33, -20<=k<=19, -31<=l<=32
Reflections collected / unique	95894 / 11564 [R(int) = 0.0699]
Completeness to theta = 25.242	99.9 %
Refinement method	Full-matrix least-squares on F^2
Data / restraints / parameters	11564 / 0 / 322
Goodness-of-fit on F^2	1.029
Final R indices [$I > 2\sigma(I)$]	R1 = 0.0403, wR2 = 0.0747
R indices (all data)	R1 = 0.0784, wR2 = 0.0867
Largest diff. peak and hole	0.588 and -0.596 e. \AA^{-3}

Table A2. Atomic coordinates ($\times 10^4$) and equivalent isotropic displacement parameters ($\text{\AA}^2 \times 10^3$) for L₁Sn. U(eq) is defined as one third of the trace of the orthogonalized Uij tensor.

	x	y	z	U(eq)
Sn(1)	7150(1)	5482(1)	5806(1)	25(1)
N(4)	6571(1)	4738(1)	4870(1)	26(1)
C(6)	5812(1)	9560(2)	5074(1)	40(1)
N(2)	6556(1)	4643(1)	6572(1)	29(1)
C(13)	6597(1)	3738(2)	6994(1)	28(1)
C(14)	7039(1)	3723(2)	7579(1)	33(1)
C(5)	5874(1)	8979(2)	5682(1)	32(1)
N(1)	6434(1)	6341(1)	6368(1)	29(1)
C(12)	5794(1)	5558(2)	7243(1)	41(1)
C(15)	7088(1)	2815(2)	7967(1)	38(1)
C(7)	5987(1)	9129(2)	4508(1)	43(1)
C(22)	5955(1)	5806(2)	3973(1)	36(1)
N(3)	6518(1)	6438(1)	5071(1)	30(1)
C(4)	5690(1)	9446(2)	6268(1)	40(1)
C(16)	6706(1)	1946(2)	7796(1)	43(1)
C(10)	6121(1)	7917(2)	5698(1)	26(1)
C(25)	7039(1)	2465(2)	3872(1)	42(1)
C(18)	6225(1)	2845(2)	6807(1)	34(1)
C(24)	7087(1)	3392(2)	4248(1)	31(1)
C(9)	6281(1)	7478(2)	5077(1)	29(1)
C(21)	6347(1)	5667(2)	4640(1)	27(1)
C(19)	7462(1)	4663(2)	7776(1)	52(1)
C(29)	7736(1)	3935(2)	4402(1)	40(1)
C(11)	6272(1)	5533(2)	6734(1)	29(1)
C(17)	6282(1)	1959(2)	7220(1)	43(1)
C(8)	6228(1)	8093(2)	4507(1)	38(1)
C(3)	5764(1)	8922(2)	6856(1)	46(1)

C(28)	5926(1)	3267(2)	4352(1)	33(1)
C(26)	6453(2)	1946(2)	3740(1)	48(1)
C(2)	6022(1)	7892(2)	6893(1)	38(1)
C(23)	6524(1)	3800(2)	4482(1)	26(1)
C(1)	6179(1)	7367(2)	6331(1)	28(1)
C(27)	5905(1)	2334(2)	3978(1)	43(1)
C(20)	5777(1)	2848(2)	6164(1)	52(1)
C(30)	5309(1)	3669(2)	4599(1)	43(1)

Table A3. Bond lengths [Å] and angles [deg] for L₁Sn.

Sn(1)-N(3)	2.2232(17)
Sn(1)-N(1)	2.2435(17)
Sn(1)-N(4)	2.3181(16)
Sn(1)-N(2)	2.3327(17)
N(4)-C(21)	1.329(3)
N(4)-C(23)	1.420(2)
C(6)-C(7)	1.350(4)
C(6)-C(5)	1.422(3)
C(6)-H(6)	0.9500
N(2)-C(11)	1.328(3)
N(2)-C(13)	1.423(3)
C(13)-C(18)	1.395(3)
C(13)-C(14)	1.409(3)
C(14)-C(15)	1.387(3)
C(14)-C(19)	1.505(3)
C(5)-C(4)	1.410(3)
C(5)-C(10)	1.437(3)
N(1)-C(11)	1.326(3)
N(1)-C(1)	1.400(3)
C(12)-C(11)	1.503(3)
C(12)-H(12A)	0.9800
C(12)-H(12B)	0.9800
C(12)-H(12C)	0.9800
C(15)-C(16)	1.375(4)
C(15)-H(15)	0.9500
C(7)-C(8)	1.403(3)
C(7)-H(7)	0.9500
C(22)-C(21)	1.500(3)
C(22)-H(22A)	0.9800
C(22)-H(22B)	0.9800
C(22)-H(22C)	0.9800
N(3)-C(21)	1.328(3)
N(3)-C(9)	1.405(3)
C(4)-C(3)	1.352(4)
C(4)-H(4)	0.9500
C(16)-C(17)	1.375(4)
C(16)-H(16)	0.9500
C(10)-C(9)	1.442(3)

C(10)-C(1)	1.447(3)
C(25)-C(26)	1.379(4)
C(25)-C(24)	1.394(3)
C(25)-H(25)	0.9500
C(18)-C(17)	1.392(3)
C(18)-C(20)	1.507(3)
C(24)-C(23)	1.404(3)
C(24)-C(29)	1.509(3)
C(9)-C(8)	1.380(3)
C(19)-H(19A)	0.9800
C(19)-H(19B)	0.9800
C(19)-H(19C)	0.9800
C(29)-H(29A)	0.9800
C(29)-H(29B)	0.9800
C(29)-H(29C)	0.9800
C(17)-H(17)	0.9500
C(8)-H(8)	0.9500
C(3)-C(2)	1.408(3)
C(3)-H(3)	0.9500
C(28)-C(27)	1.399(3)
C(28)-C(23)	1.406(3)
C(28)-C(30)	1.509(3)
C(26)-C(27)	1.369(4)
C(26)-H(26)	0.9500
C(2)-C(1)	1.383(3)
C(2)-H(2)	0.9500
C(27)-H(27)	0.9500
C(20)-H(20A)	0.9800
C(20)-H(20B)	0.9800
C(20)-H(20C)	0.9800
C(30)-H(30A)	0.9800
C(30)-H(30B)	0.9800
C(30)-H(30C)	0.9800
N(3)-Sn(1)-N(1)	72.57(6)
N(3)-Sn(1)-N(4)	57.74(6)
N(1)-Sn(1)-N(4)	107.35(6)
N(3)-Sn(1)-N(2)	112.07(6)
N(1)-Sn(1)-N(2)	57.38(6)
N(4)-Sn(1)-N(2)	95.29(6)
C(21)-N(4)-C(23)	123.17(17)
C(21)-N(4)-Sn(1)	93.11(12)
C(23)-N(4)-Sn(1)	141.84(13)
C(7)-C(6)-C(5)	120.8(2)
C(7)-C(6)-H(6)	119.6
C(5)-C(6)-H(6)	119.6
C(11)-N(2)-C(13)	122.30(17)
C(11)-N(2)-Sn(1)	93.22(12)
C(13)-N(2)-Sn(1)	139.58(13)
C(18)-C(13)-C(14)	120.13(19)
C(18)-C(13)-N(2)	119.73(18)
C(14)-C(13)-N(2)	120.04(19)

C(15)-C(14)-C(13)	118.9(2)
C(15)-C(14)-C(19)	120.2(2)
C(13)-C(14)-C(19)	120.9(2)
C(4)-C(5)-C(6)	119.9(2)
C(4)-C(5)-C(10)	120.1(2)
C(6)-C(5)-C(10)	120.0(2)
C(11)-N(1)-C(1)	128.94(17)
C(11)-N(1)-Sn(1)	97.36(12)
C(1)-N(1)-Sn(1)	133.51(13)
C(11)-C(12)-H(12A)	109.5
C(11)-C(12)-H(12B)	109.5
H(12A)-C(12)-H(12B)	109.5
C(11)-C(12)-H(12C)	109.5
H(12A)-C(12)-H(12C)	109.5
H(12B)-C(12)-H(12C)	109.5
C(16)-C(15)-C(14)	121.1(2)
C(16)-C(15)-H(15)	119.4
C(14)-C(15)-H(15)	119.4
C(6)-C(7)-C(8)	120.5(2)
C(6)-C(7)-H(7)	119.8
C(8)-C(7)-H(7)	119.8
C(21)-C(22)-H(22A)	109.5
C(21)-C(22)-H(22B)	109.5
H(22A)-C(22)-H(22B)	109.5
C(21)-C(22)-H(22C)	109.5
H(22A)-C(22)-H(22C)	109.5
H(22B)-C(22)-H(22C)	109.5
C(21)-N(3)-C(9)	128.79(18)
C(21)-N(3)-Sn(1)	97.47(13)
C(9)-N(3)-Sn(1)	133.17(14)
C(3)-C(4)-C(5)	120.9(2)
C(3)-C(4)-H(4)	119.5
C(5)-C(4)-H(4)	119.5
C(17)-C(16)-C(15)	119.8(2)
C(17)-C(16)-H(16)	120.1
C(15)-C(16)-H(16)	120.1
C(5)-C(10)-C(9)	117.16(19)
C(5)-C(10)-C(1)	117.60(19)
C(9)-C(10)-C(1)	125.23(18)
C(26)-C(25)-C(24)	120.9(2)
C(26)-C(25)-H(25)	119.6
C(24)-C(25)-H(25)	119.6
C(17)-C(18)-C(13)	118.9(2)
C(17)-C(18)-C(20)	121.3(2)
C(13)-C(18)-C(20)	119.9(2)
C(25)-C(24)-C(23)	118.7(2)
C(25)-C(24)-C(29)	120.2(2)
C(23)-C(24)-C(29)	121.06(19)
C(8)-C(9)-N(3)	121.1(2)
C(8)-C(9)-C(10)	120.02(19)
N(3)-C(9)-C(10)	118.82(18)
N(3)-C(21)-N(4)	111.37(17)

N(3)-C(21)-C(22)	125.31(19)
N(4)-C(21)-C(22)	123.32(19)
C(14)-C(19)-H(19A)	109.5
C(14)-C(19)-H(19B)	109.5
H(19A)-C(19)-H(19B)	109.5
C(14)-C(19)-H(19C)	109.5
H(19A)-C(19)-H(19C)	109.5
H(19B)-C(19)-H(19C)	109.5
C(24)-C(29)-H(29A)	109.5
C(24)-C(29)-H(29B)	109.5
H(29A)-C(29)-H(29B)	109.5
C(24)-C(29)-H(29C)	109.5
H(29A)-C(29)-H(29C)	109.5
H(29B)-C(29)-H(29C)	109.5
N(1)-C(11)-N(2)	111.85(17)
N(1)-C(11)-C(12)	126.14(19)
N(2)-C(11)-C(12)	121.89(19)
C(16)-C(17)-C(18)	121.2(2)
C(16)-C(17)-H(17)	119.4
C(18)-C(17)-H(17)	119.4
C(9)-C(8)-C(7)	121.4(2)
C(9)-C(8)-H(8)	119.3
C(7)-C(8)-H(8)	119.3
C(4)-C(3)-C(2)	120.4(2)
C(4)-C(3)-H(3)	119.8
C(2)-C(3)-H(3)	119.8
C(27)-C(28)-C(23)	118.6(2)
C(27)-C(28)-C(30)	119.1(2)
C(23)-C(28)-C(30)	122.3(2)
C(27)-C(26)-C(25)	120.4(2)
C(27)-C(26)-H(26)	119.8
C(25)-C(26)-H(26)	119.8
C(1)-C(2)-C(3)	121.5(2)
C(1)-C(2)-H(2)	119.2
C(3)-C(2)-H(2)	119.2
C(24)-C(23)-C(28)	120.44(19)
C(24)-C(23)-N(4)	118.90(18)
C(28)-C(23)-N(4)	120.63(18)
C(2)-C(1)-N(1)	121.5(2)
C(2)-C(1)-C(10)	119.24(19)
N(1)-C(1)-C(10)	119.12(18)
C(26)-C(27)-C(28)	120.9(2)
C(26)-C(27)-H(27)	119.5
C(28)-C(27)-H(27)	119.5
C(18)-C(20)-H(20A)	109.5
C(18)-C(20)-H(20B)	109.5
H(20A)-C(20)-H(20B)	109.5
C(18)-C(20)-H(20C)	109.5
H(20A)-C(20)-H(20C)	109.5
H(20B)-C(20)-H(20C)	109.5
C(28)-C(30)-H(30A)	109.5
C(28)-C(30)-H(30B)	109.5

H(30A)-C(30)-H(30B)	109.5
C(28)-C(30)-H(30C)	109.5
H(30A)-C(30)-H(30C)	109.5
H(30B)-C(30)-H(30C)	109.5

Symmetry transformations used to generate equivalent atoms:

Table A4. Anisotropic displacement parameters ($\text{Å}^2 \times 10^3$) for L1Sn. The anisotropic displacement factor exponent takes the form: $-2 \pi^2 [h^2 a^* a^* U_{11} + \dots + 2 h k a^* b^* U_{12}]$

	U11	U22	U33	U23	U13	U12
Sn(1)	20(1)	28(1)	26(1)	-4(1)	1(1)	-1(1)
N(4)	24(1)	30(1)	24(1)	-4(1)	1(1)	0(1)
C(6)	33(1)	25(1)	61(2)	9(1)	2(1)	1(1)
N(2)	32(1)	30(1)	27(1)	2(1)	7(1)	2(1)
C(13)	29(1)	28(1)	27(1)	1(1)	7(1)	5(1)
C(14)	32(1)	40(1)	29(1)	-2(1)	6(1)	3(1)
C(5)	25(1)	23(1)	47(1)	-3(1)	0(1)	-2(1)
N(1)	28(1)	28(1)	30(1)	2(1)	6(1)	3(1)
C(12)	43(1)	42(1)	43(1)	8(1)	22(1)	10(1)
C(15)	40(1)	46(1)	29(1)	2(1)	1(1)	13(1)
C(7)	41(1)	38(1)	51(2)	17(1)	7(1)	1(1)
C(22)	35(1)	42(1)	29(1)	2(1)	-2(1)	2(1)
N(3)	32(1)	30(1)	29(1)	-4(1)	1(1)	5(1)
C(4)	38(1)	26(1)	56(1)	-12(1)	-2(1)	4(1)
C(16)	60(2)	33(1)	37(1)	7(1)	8(1)	16(1)
C(10)	21(1)	23(1)	35(1)	-2(1)	2(1)	-4(1)
C(25)	57(2)	36(1)	35(1)	-5(1)	10(1)	13(1)
C(18)	38(1)	28(1)	35(1)	0(1)	0(1)	2(1)
C(24)	36(1)	33(1)	25(1)	2(1)	6(1)	4(1)
C(9)	24(1)	27(1)	37(1)	1(1)	4(1)	-1(1)
C(21)	22(1)	34(1)	26(1)	-2(1)	5(1)	2(1)
C(19)	50(2)	59(2)	43(1)	0(1)	-9(1)	-14(1)
C(29)	32(1)	51(2)	39(1)	0(1)	11(1)	2(1)
C(11)	27(1)	32(1)	27(1)	1(1)	5(1)	4(1)
C(17)	58(2)	26(1)	45(1)	0(1)	0(1)	0(1)
C(8)	37(1)	39(1)	40(1)	8(1)	10(1)	2(1)
C(3)	48(1)	41(1)	48(1)	-19(1)	3(1)	3(1)
C(28)	35(1)	38(1)	25(1)	-1(1)	0(1)	-10(1)
C(26)	77(2)	32(1)	33(1)	-6(1)	-2(1)	-1(1)
C(2)	43(1)	37(1)	33(1)	-7(1)	1(1)	2(1)
C(23)	27(1)	28(1)	22(1)	-1(1)	1(1)	-1(1)
C(1)	24(1)	27(1)	33(1)	-4(1)	0(1)	-1(1)
C(27)	55(2)	37(1)	35(1)	-2(1)	-6(1)	-16(1)
C(20)	56(2)	45(1)	50(2)	1(1)	-16(1)	-6(1)
C(30)	27(1)	61(2)	41(1)	-1(1)	1(1)	-8(1)

A22. Crystal data and structure refinement of L₂Sn

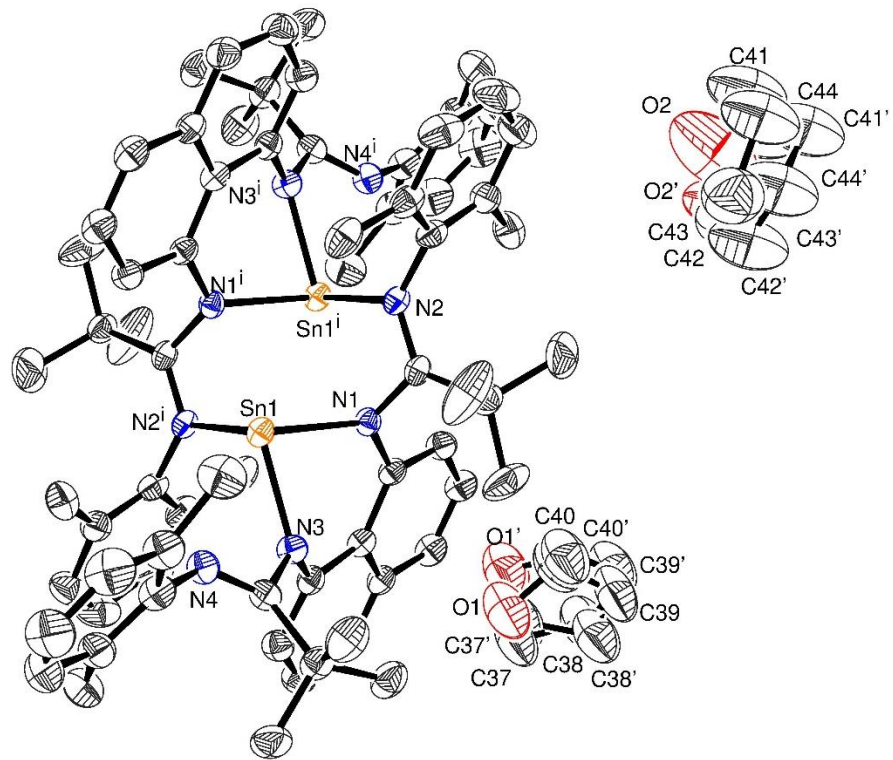


Figure S50. Asymmetric Unit of L₂Sn.

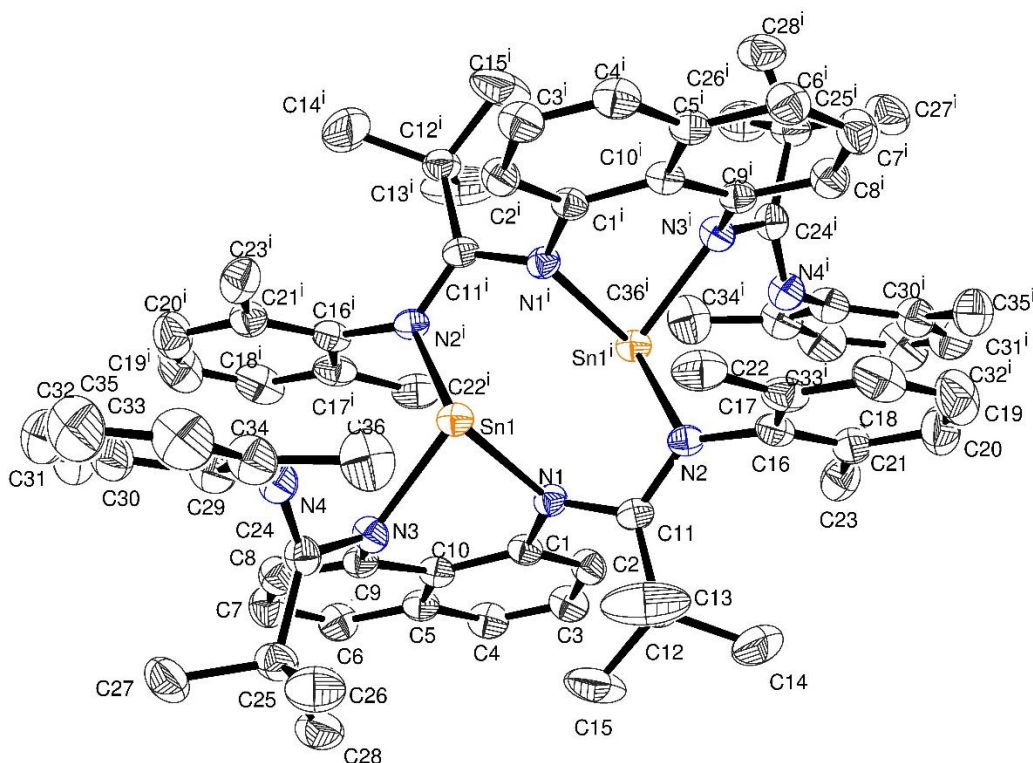


Figure S51. Compound L_2Sn .

Table A5. Crystal data and structure refinement for L_2Sn .

Identification code	L_2Sn
Empirical formula	$\text{C}_{72} \text{H}_{84} \text{N}_8 \text{Sn}_2, 4(\text{C}_4 \text{H}_8 \text{O})$
Formula weight	1587.31
Temperature	193(2) K
Wavelength	0.71073 Å
Crystal system, space group	Triclinic, P -1
Unit cell dimensions	$a = 11.2468(7)$ Å $\alpha = 86.510(2)$ deg. $b = 12.6512(7)$ Å $\beta = 78.588(2)$ deg. $c = 14.5050(9)$ Å $\gamma = 79.579(2)$ deg.
Volume	1989.0(2) Å ³
Z, Calculated density	1, 1.325 Mg/m ³
Absorption coefficient	0.683 mm ⁻¹
F(000)	832
Crystal size	0.080 x 0.060 x 0.040 mm
Theta range for data collection	3.327 to 29.622 deg.

Limiting indices	-15<=h<=15, -17<=k<=17, -20<=l<=20
Reflections collected / unique	75976 / 11128 [R(int) = 0.0936]
Completeness to theta = 25.242	99.4 %
Refinement method	Full-matrix least-squares on F^2
Data / restraints / parameters	11128 / 277 / 564
Goodness-of-fit on F^2	1.015
Final R indices [I>2sigma(I)]	R1 = 0.0461, wR2 = 0.1054
R indices (all data)	R1 = 0.0747, wR2 = 0.1209
Extinction coefficient	0.0126(10)
Largest diff. peak and hole	1.132 and -0.909 e.A^-3

Table A6. Atomic coordinates ($\times 10^4$) and equivalent isotropic displacement parameters ($\text{\AA}^2 \times 10^3$) for R102. U(eq) is defined as one third of the trace of the orthogonalized U_{ij} tensor.

	x	y	z	U(eq)
C(1)	7596(3)	5785(2)	4640(2)	25(1)
C(2)	7495(3)	5731(3)	3707(2)	31(1)
C(3)	6786(3)	6554(3)	3259(2)	35(1)
C(4)	6215(3)	7465(3)	3729(2)	34(1)
C(5)	6292(3)	7571(3)	4678(2)	28(1)
C(6)	5712(3)	8527(3)	5142(3)	36(1)
C(7)	5787(3)	8659(3)	6059(3)	39(1)
C(8)	6402(3)	7829(3)	6555(2)	34(1)
C(9)	6931(3)	6843(2)	6151(2)	27(1)
C(10)	6958(3)	6705(2)	5169(2)	25(1)
C(11)	8587(3)	3925(2)	4711(2)	24(1)
C(12)	7481(3)	3306(3)	4982(2)	32(1)
C(13)	7679(4)	2623(5)	5846(4)	80(2)
C(14)	7341(4)	2573(5)	4212(4)	79(2)
C(15)	6253(3)	4048(3)	5221(4)	65(1)
C(16)	10183(3)	2413(2)	4079(2)	30(1)
C(17)	10704(3)	1681(3)	4708(3)	35(1)
C(18)	11205(3)	642(3)	4407(3)	48(1)
C(19)	11215(4)	349(3)	3503(3)	56(1)
C(20)	10720(4)	1087(3)	2882(3)	47(1)
C(21)	10205(3)	2130(3)	3149(2)	35(1)
C(22)	10750(3)	1953(3)	5701(3)	42(1)
C(23)	9669(4)	2923(3)	2451(2)	42(1)
C(24)	7082(3)	5931(3)	7667(2)	29(1)
C(25)	5716(3)	5845(3)	8102(2)	35(1)
C(26)	5707(4)	4703(3)	8496(3)	53(1)
C(27)	5164(4)	6631(4)	8912(3)	49(1)

C(28)	4837(3)	6045(4)	7398(3)	45(1)
C(29)	8024(3)	5543(3)	9082(2)	36(1)
C(30)	7876(3)	6404(3)	9679(2)	40(1)
C(31)	8031(4)	6178(4)	10607(3)	51(1)
C(32)	8340(4)	5144(4)	10931(3)	61(1)
C(33)	8536(4)	4304(4)	10327(3)	55(1)
C(34)	8402(3)	4493(3)	9383(2)	42(1)
C(35)	7613(4)	7554(3)	9352(3)	49(1)
C(36)	8753(4)	3560(3)	8711(3)	54(1)
O(1)	4578(11)	9100(6)	2166(8)	109(2)
C(37)	4034(16)	9949(9)	1700(12)	105(3)
C(38)	3512(15)	9554(9)	922(11)	110(3)
C(39)	3615(14)	8390(9)	1182(10)	109(3)
C(40)	4680(20)	8175(9)	1660(20)	112(3)
O(1')	5176(17)	8998(13)	1611(15)	113(3)
C(37')	4250(20)	9830(16)	1450(20)	111(3)
C(38')	3190(20)	9323(18)	1210(20)	111(3)
C(39')	4020(20)	8359(17)	810(18)	109(3)
C(40')	4720(40)	8043(15)	1570(40)	110(3)
C(43)	7733(10)	41(8)	2503(7)	117(3)
C(42)	7580(11)	919(8)	1851(10)	121(4)
O(2)	8651(14)	719(8)	1069(7)	203(5)
C(41)	9022(13)	-427(9)	1098(8)	146(4)
C(44)	8468(11)	-823(8)	1925(8)	135(4)
C(43')	7380(60)	-270(30)	2190(30)	140(5)
C(42')	7010(60)	830(30)	2100(40)	140(6)
O(2')	7840(50)	1200(30)	1290(30)	142(6)
C(41')	8420(60)	220(40)	780(30)	143(5)
C(44')	7930(60)	-620(30)	1250(40)	141(5)
N(1)	8441(2)	4967(2)	4998(2)	24(1)
N(2)	9719(2)	3514(2)	4329(2)	25(1)
N(3)	7461(2)	6003(2)	6691(2)	27(1)
N(4)	7988(3)	5748(2)	8112(2)	31(1)
Sn(1)	9263(1)	5074(1)	6270(1)	25(1)

Table A7. Bond lengths [Å] and angles [deg] for R102.

C(1)-C(2)	1.387(4)
C(1)-N(1)	1.421(4)
C(1)-C(10)	1.431(4)
C(2)-C(3)	1.401(4)
C(2)-H(2)	0.9500
C(3)-C(4)	1.364(5)
C(3)-H(3)	0.9500
C(4)-C(5)	1.412(4)
C(4)-H(4)	0.9500
C(5)-C(6)	1.408(5)
C(5)-C(10)	1.444(4)
C(6)-C(7)	1.371(5)

C(6)-H(6)	0.9500
C(7)-C(8)	1.394(5)
C(7)-H(7)	0.9500
C(8)-C(9)	1.391(5)
C(8)-H(8)	0.9500
C(9)-N(3)	1.397(4)
C(9)-C(10)	1.440(4)
C(11)-N(2)	1.309(4)
C(11)-N(1)	1.378(4)
C(11)-C(12)	1.561(4)
C(12)-C(13)	1.508(5)
C(12)-C(15)	1.513(5)
C(12)-C(14)	1.543(6)
C(13)-H(13A)	0.9800
C(13)-H(13B)	0.9800
C(13)-H(13C)	0.9800
C(14)-H(14A)	0.9800
C(14)-H(14B)	0.9800
C(14)-H(14C)	0.9800
C(15)-H(15A)	0.9800
C(15)-H(15B)	0.9800
C(15)-H(15C)	0.9800
C(16)-C(17)	1.395(4)
C(16)-C(21)	1.410(5)
C(16)-N(2)	1.438(4)
C(17)-C(18)	1.393(5)
C(17)-C(22)	1.515(5)
C(18)-C(19)	1.381(6)
C(18)-H(18)	0.9500
C(19)-C(20)	1.379(6)
C(19)-H(19)	0.9500
C(20)-C(21)	1.386(5)
C(20)-H(20)	0.9500
C(21)-C(23)	1.515(5)
C(22)-H(22A)	0.9800
C(22)-H(22B)	0.9800
C(22)-H(22C)	0.9800
C(23)-H(23A)	0.9800
C(23)-H(23B)	0.9800
C(23)-H(23C)	0.9800
C(24)-N(4)	1.291(4)
C(24)-N(3)	1.398(4)
C(24)-C(25)	1.562(4)
C(25)-C(26)	1.522(5)
C(25)-C(28)	1.538(5)
C(25)-C(27)	1.544(5)
C(26)-H(26A)	0.9800
C(26)-H(26B)	0.9800
C(26)-H(26C)	0.9800
C(27)-H(27A)	0.9800
C(27)-H(27B)	0.9800
C(27)-H(27C)	0.9800
C(28)-H(28A)	0.9800
C(28)-H(28B)	0.9800
C(28)-H(28C)	0.9800

C(29)-C(34)	1.391(5)
C(29)-C(30)	1.398(5)
C(29)-N(4)	1.422(4)
C(30)-C(31)	1.397(5)
C(30)-C(35)	1.498(5)
C(31)-C(32)	1.370(6)
C(31)-H(31)	0.9500
C(32)-C(33)	1.377(6)
C(32)-H(32)	0.9500
C(33)-C(34)	1.408(5)
C(33)-H(33)	0.9500
C(34)-C(36)	1.523(6)
C(35)-H(35A)	0.9800
C(35)-H(35B)	0.9800
C(35)-H(35C)	0.9800
C(36)-H(36A)	0.9800
C(36)-H(36B)	0.9800
C(36)-H(36C)	0.9800
O(1)-C(37)	1.349(11)
O(1)-C(40)	1.395(14)
C(37)-C(38)	1.519(13)
C(37)-H(37A)	0.9900
C(37)-H(37B)	0.9900
C(38)-C(39)	1.486(14)
C(38)-H(38A)	0.9900
C(38)-H(38B)	0.9900
C(39)-C(40)	1.470(13)
C(39)-H(39A)	0.9900
C(39)-H(39B)	0.9900
C(40)-H(40A)	0.9900
C(40)-H(40B)	0.9900
O(1')-C(37')	1.385(15)
O(1')-C(40')	1.41(2)
C(37')-C(38')	1.557(18)
C(37')-H(37C)	0.9900
C(37')-H(37D)	0.9900
C(38')-C(39')	1.469(18)
C(38')-H(38C)	0.9900
C(38')-H(38D)	0.9900
C(39')-C(40')	1.466(18)
C(39')-H(39C)	0.9900
C(39')-H(39D)	0.9900
C(40')-H(40C)	0.9900
C(40')-H(40D)	0.9900
C(43)-C(42)	1.423(12)
C(43)-C(44)	1.446(13)
C(43)-H(43A)	0.9900
C(43)-H(43B)	0.9900
C(42)-O(2)	1.478(12)
C(42)-H(42A)	0.9900
C(42)-H(42B)	0.9900
O(2)-C(41)	1.435(12)
C(41)-C(44)	1.350(12)
C(41)-H(41A)	0.9900
C(41)-H(41B)	0.9900

C(44)-H(44A)	0.9900
C(44)-H(44B)	0.9900
C(43')-C(42')	1.389(18)
C(43')-C(44')	1.44(2)
C(43')-H(43C)	0.9900
C(43')-H(43D)	0.9900
C(42')-O(2')	1.454(19)
C(42')-H(42C)	0.9900
C(42')-H(42D)	0.9900
O(2')-C(41')	1.464(18)
C(41')-C(44')	1.374(18)
C(41')-H(41C)	0.9900
C(41')-H(41D)	0.9900
C(44')-H(44C)	0.9900
C(44')-H(44D)	0.9900
N(1)-Sn(1)	2.243(2)
N(2)-Sn(1)#1	2.327(2)
N(3)-Sn(1)	2.144(3)
C(2)-C(1)-N(1)	117.6(3)
C(2)-C(1)-C(10)	119.5(3)
N(1)-C(1)-C(10)	122.6(3)
C(1)-C(2)-C(3)	122.1(3)
C(1)-C(2)-H(2)	119.0
C(3)-C(2)-H(2)	119.0
C(4)-C(3)-C(2)	119.9(3)
C(4)-C(3)-H(3)	120.0
C(2)-C(3)-H(3)	120.0
C(3)-C(4)-C(5)	120.5(3)
C(3)-C(4)-H(4)	119.7
C(5)-C(4)-H(4)	119.7
C(6)-C(5)-C(4)	119.4(3)
C(6)-C(5)-C(10)	120.3(3)
C(4)-C(5)-C(10)	120.3(3)
C(7)-C(6)-C(5)	120.7(3)
C(7)-C(6)-H(6)	119.6
C(5)-C(6)-H(6)	119.6
C(6)-C(7)-C(8)	120.2(3)
C(6)-C(7)-H(7)	119.9
C(8)-C(7)-H(7)	119.9
C(9)-C(8)-C(7)	121.7(3)
C(9)-C(8)-H(8)	119.2
C(7)-C(8)-H(8)	119.2
C(8)-C(9)-N(3)	120.0(3)
C(8)-C(9)-C(10)	119.6(3)
N(3)-C(9)-C(10)	120.4(3)
C(1)-C(10)-C(9)	125.3(3)
C(1)-C(10)-C(5)	117.5(3)
C(9)-C(10)-C(5)	117.2(3)
N(2)-C(11)-N(1)	114.2(3)
N(2)-C(11)-C(12)	126.3(3)
N(1)-C(11)-C(12)	119.0(3)
C(13)-C(12)-C(15)	108.0(4)
C(13)-C(12)-C(14)	108.7(4)
C(15)-C(12)-C(14)	105.5(4)

C(13)-C(12)-C(11)	106.9(3)
C(15)-C(12)-C(11)	112.8(3)
C(14)-C(12)-C(11)	114.7(3)
C(12)-C(13)-H(13A)	109.5
C(12)-C(13)-H(13B)	109.5
H(13A)-C(13)-H(13B)	109.5
C(12)-C(13)-H(13C)	109.5
H(13A)-C(13)-H(13C)	109.5
H(13B)-C(13)-H(13C)	109.5
C(12)-C(14)-H(14A)	109.5
C(12)-C(14)-H(14B)	109.5
H(14A)-C(14)-H(14B)	109.5
C(12)-C(14)-H(14C)	109.5
H(14A)-C(14)-H(14C)	109.5
H(14B)-C(14)-H(14C)	109.5
C(12)-C(15)-H(15A)	109.5
C(12)-C(15)-H(15B)	109.5
H(15A)-C(15)-H(15B)	109.5
C(12)-C(15)-H(15C)	109.5
H(15A)-C(15)-H(15C)	109.5
H(15B)-C(15)-H(15C)	109.5
C(17)-C(16)-C(21)	121.3(3)
C(17)-C(16)-N(2)	120.7(3)
C(21)-C(16)-N(2)	117.7(3)
C(18)-C(17)-C(16)	118.2(3)
C(18)-C(17)-C(22)	118.2(3)
C(16)-C(17)-C(22)	123.6(3)
C(19)-C(18)-C(17)	121.1(4)
C(19)-C(18)-H(18)	119.4
C(17)-C(18)-H(18)	119.4
C(20)-C(19)-C(18)	120.1(4)
C(20)-C(19)-H(19)	120.0
C(18)-C(19)-H(19)	120.0
C(19)-C(20)-C(21)	121.0(4)
C(19)-C(20)-H(20)	119.5
C(21)-C(20)-H(20)	119.5
C(20)-C(21)-C(16)	118.3(3)
C(20)-C(21)-C(23)	119.8(3)
C(16)-C(21)-C(23)	121.9(3)
C(17)-C(22)-H(22A)	109.5
C(17)-C(22)-H(22B)	109.5
H(22A)-C(22)-H(22B)	109.5
C(17)-C(22)-H(22C)	109.5
H(22A)-C(22)-H(22C)	109.5
H(22B)-C(22)-H(22C)	109.5
C(21)-C(23)-H(23A)	109.5
C(21)-C(23)-H(23B)	109.5
H(23A)-C(23)-H(23B)	109.5
C(21)-C(23)-H(23C)	109.5
H(23A)-C(23)-H(23C)	109.5
H(23B)-C(23)-H(23C)	109.5
N(4)-C(24)-N(3)	113.1(3)
N(4)-C(24)-C(25)	125.5(3)
N(3)-C(24)-C(25)	120.2(3)
C(26)-C(25)-C(28)	107.2(3)

C(26)-C(25)-C(27)	108.4(3)
C(28)-C(25)-C(27)	106.9(3)
C(26)-C(25)-C(24)	107.2(3)
C(28)-C(25)-C(24)	114.6(3)
C(27)-C(25)-C(24)	112.4(3)
C(25)-C(26)-H(26A)	109.5
C(25)-C(26)-H(26B)	109.5
H(26A)-C(26)-H(26B)	109.5
C(25)-C(26)-H(26C)	109.5
H(26A)-C(26)-H(26C)	109.5
H(26B)-C(26)-H(26C)	109.5
C(25)-C(27)-H(27A)	109.5
C(25)-C(27)-H(27B)	109.5
H(27A)-C(27)-H(27B)	109.5
C(25)-C(27)-H(27C)	109.5
H(27A)-C(27)-H(27C)	109.5
H(27B)-C(27)-H(27C)	109.5
C(25)-C(28)-H(28A)	109.5
C(25)-C(28)-H(28B)	109.5
H(28A)-C(28)-H(28B)	109.5
C(25)-C(28)-H(28C)	109.5
H(28A)-C(28)-H(28C)	109.5
H(28B)-C(28)-H(28C)	109.5
C(34)-C(29)-C(30)	120.8(3)
C(34)-C(29)-N(4)	118.6(3)
C(30)-C(29)-N(4)	119.7(3)
C(31)-C(30)-C(29)	118.4(4)
C(31)-C(30)-C(35)	118.9(4)
C(29)-C(30)-C(35)	122.6(3)
C(32)-C(31)-C(30)	121.6(4)
C(32)-C(31)-H(31)	119.2
C(30)-C(31)-H(31)	119.2
C(31)-C(32)-C(33)	119.7(4)
C(31)-C(32)-H(32)	120.2
C(33)-C(32)-H(32)	120.2
C(32)-C(33)-C(34)	120.8(4)
C(32)-C(33)-H(33)	119.6
C(34)-C(33)-H(33)	119.6
C(29)-C(34)-C(33)	118.6(4)
C(29)-C(34)-C(36)	122.0(3)
C(33)-C(34)-C(36)	119.3(4)
C(30)-C(35)-H(35A)	109.5
C(30)-C(35)-H(35B)	109.5
H(35A)-C(35)-H(35B)	109.5
C(30)-C(35)-H(35C)	109.5
H(35A)-C(35)-H(35C)	109.5
H(35B)-C(35)-H(35C)	109.5
C(34)-C(36)-H(36A)	109.5
C(34)-C(36)-H(36B)	109.5
H(36A)-C(36)-H(36B)	109.5
C(34)-C(36)-H(36C)	109.5
H(36A)-C(36)-H(36C)	109.5
H(36B)-C(36)-H(36C)	109.5
C(37)-O(1)-C(40)	108.7(9)
O(1)-C(37)-C(38)	109.6(8)

O(1)-C(37)-H(37A)	109.7
C(38)-C(37)-H(37A)	109.7
O(1)-C(37)-H(37B)	109.7
C(38)-C(37)-H(37B)	109.7
H(37A)-C(37)-H(37B)	108.2
C(39)-C(38)-C(37)	100.4(10)
C(39)-C(38)-H(38A)	111.7
C(37)-C(38)-H(38A)	111.7
C(39)-C(38)-H(38B)	111.7
C(37)-C(38)-H(38B)	111.7
H(38A)-C(38)-H(38B)	109.5
C(40)-C(39)-C(38)	103.6(10)
C(40)-C(39)-H(39A)	111.0
C(38)-C(39)-H(39A)	111.0
C(40)-C(39)-H(39B)	111.0
C(38)-C(39)-H(39B)	111.0
H(39A)-C(39)-H(39B)	109.0
O(1)-C(40)-C(39)	104.5(11)
O(1)-C(40)-H(40A)	110.9
C(39)-C(40)-H(40A)	110.9
O(1)-C(40)-H(40B)	110.9
C(39)-C(40)-H(40B)	110.9
H(40A)-C(40)-H(40B)	108.9
C(37')-O(1')-C(40')	106.0(16)
O(1')-C(37')-C(38')	107.7(13)
O(1')-C(37')-H(37C)	110.2
C(38')-C(37')-H(37C)	110.2
O(1')-C(37')-H(37D)	110.2
C(38')-C(37')-H(37D)	110.2
H(37C)-C(37')-H(37D)	108.5
C(39')-C(38')-C(37')	93.6(15)
C(39')-C(38')-H(38C)	113.0
C(37')-C(38')-H(38C)	113.0
C(39')-C(38')-H(38D)	113.0
C(37')-C(38')-H(38D)	113.0
H(38C)-C(38')-H(38D)	110.4
C(40')-C(39')-C(38')	100.3(18)
C(40')-C(39')-H(39C)	111.7
C(38')-C(39')-H(39C)	111.7
C(40')-C(39')-H(39D)	111.7
C(38')-C(39')-H(39D)	111.7
H(39C)-C(39')-H(39D)	109.5
O(1')-C(40')-C(39')	99.1(18)
O(1')-C(40')-H(40C)	111.9
C(39')-C(40')-H(40C)	111.9
O(1')-C(40')-H(40D)	111.9
C(39')-C(40')-H(40D)	111.9
H(40C)-C(40')-H(40D)	109.6
C(42)-C(43)-C(44)	103.6(9)
C(42)-C(43)-H(43A)	111.0
C(44)-C(43)-H(43A)	111.0
C(42)-C(43)-H(43B)	111.0
C(44)-C(43)-H(43B)	111.0
H(43A)-C(43)-H(43B)	109.0
C(43)-C(42)-O(2)	106.2(8)

C(43)-C(42)-H(42A)	110.5
O(2)-C(42)-H(42A)	110.5
C(43)-C(42)-H(42B)	110.5
O(2)-C(42)-H(42B)	110.5
H(42A)-C(42)-H(42B)	108.7
C(41)-O(2)-C(42)	103.7(9)
C(44)-C(41)-O(2)	108.9(8)
C(44)-C(41)-H(41A)	109.9
O(2)-C(41)-H(41A)	109.9
C(44)-C(41)-H(41B)	109.9
O(2)-C(41)-H(41B)	109.9
H(41A)-C(41)-H(41B)	108.3
C(41)-C(44)-C(43)	110.4(8)
C(41)-C(44)-H(44A)	109.6
C(43)-C(44)-H(44A)	109.6
C(41)-C(44)-H(44B)	109.6
C(43)-C(44)-H(44B)	109.6
H(44A)-C(44)-H(44B)	108.1
C(42')-C(43')-C(44')	105(2)
C(42')-C(43')-H(43C)	110.7
C(44')-C(43')-H(43C)	110.7
C(42')-C(43')-H(43D)	110.7
C(44')-C(43')-H(43D)	110.7
H(43C)-C(43')-H(43D)	108.8
C(43')-C(42')-O(2')	107(2)
C(43')-C(42')-H(42C)	110.4
O(2')-C(42')-H(42C)	110.4
C(43')-C(42')-H(42D)	110.4
O(2')-C(42')-H(42D)	110.4
H(42C)-C(42')-H(42D)	108.6
C(42')-O(2')-C(41')	104(2)
C(44')-C(41')-O(2')	107.8(18)
C(44')-C(41')-H(41C)	110.1
O(2')-C(41')-H(41C)	110.2
C(44')-C(41')-H(41D)	110.2
O(2')-C(41')-H(41D)	110.2
H(41C)-C(41')-H(41D)	108.5
C(41')-C(44')-C(43')	106.7(19)
C(41')-C(44')-H(44C)	110.4
C(43')-C(44')-H(44C)	110.4
C(41')-C(44')-H(44D)	110.4
C(43')-C(44')-H(44D)	110.4
H(44C)-C(44')-H(44D)	108.6
C(11)-N(1)-C(1)	119.7(2)
C(11)-N(1)-Sn(1)	112.43(18)
C(1)-N(1)-Sn(1)	126.11(19)
C(11)-N(2)-C(16)	126.8(3)
C(11)-N(2)-Sn(1)#1	107.94(19)
C(16)-N(2)-Sn(1)#1	123.20(19)
C(9)-N(3)-C(24)	121.8(3)
C(9)-N(3)-Sn(1)	124.34(19)
C(24)-N(3)-Sn(1)	110.35(19)
C(24)-N(4)-C(29)	131.6(3)
N(3)-Sn(1)-N(1)	78.80(9)
N(3)-Sn(1)-N(2)#1	97.73(9)

Symmetry transformations used to generate equivalent atoms:
#1 -x+2,-y+1,-z+1

Table A8. Anisotropic displacement parameters ($\text{A}^2 \times 10^3$) for L_2Sn . The anisotropic displacement factor exponent takes the form: $-2 \pi^2 [h^2 a^{*2} U_{11} + \dots + 2 h k a^* b^* U_{12}]$

	U11	U22	U33	U23	U13	U12
C(1)	22(1)	29(2)	24(1)	3(1)	-6(1)	-3(1)
C(2)	30(2)	38(2)	24(2)	-1(1)	-6(1)	-2(1)
C(3)	33(2)	47(2)	24(2)	6(1)	-9(1)	-3(2)
C(4)	34(2)	40(2)	30(2)	10(1)	-12(1)	-3(1)
C(5)	25(2)	31(2)	29(2)	5(1)	-8(1)	-5(1)
C(6)	36(2)	31(2)	42(2)	4(1)	-13(2)	0(1)
C(7)	41(2)	32(2)	41(2)	-2(2)	-9(2)	0(2)
C(8)	35(2)	37(2)	29(2)	-1(1)	-6(1)	-5(1)
C(9)	25(1)	30(2)	26(1)	2(1)	-6(1)	-6(1)
C(10)	23(1)	28(2)	24(1)	6(1)	-4(1)	-5(1)
C(11)	24(1)	27(2)	24(1)	6(1)	-10(1)	-5(1)
C(12)	25(2)	33(2)	38(2)	0(1)	-5(1)	-7(1)
C(13)	51(3)	112(4)	85(4)	63(3)	-27(3)	-44(3)
C(14)	52(3)	103(4)	89(4)	-41(3)	8(3)	-46(3)
C(15)	26(2)	44(2)	117(4)	6(2)	6(2)	-10(2)
C(16)	22(1)	26(2)	39(2)	2(1)	-3(1)	-4(1)
C(17)	25(2)	30(2)	49(2)	9(1)	-5(1)	-7(1)
C(18)	38(2)	32(2)	65(3)	13(2)	0(2)	-3(2)
C(19)	58(3)	26(2)	75(3)	-4(2)	6(2)	-5(2)
C(20)	54(2)	36(2)	50(2)	-9(2)	3(2)	-12(2)
C(21)	30(2)	34(2)	39(2)	-3(1)	-1(1)	-10(1)
C(22)	35(2)	44(2)	50(2)	15(2)	-15(2)	-9(2)
C(23)	51(2)	43(2)	34(2)	-3(2)	-10(2)	-14(2)
C(24)	33(2)	30(2)	22(1)	1(1)	-2(1)	-6(1)
C(25)	30(2)	50(2)	26(2)	2(1)	-3(1)	-8(2)
C(26)	45(2)	58(3)	56(2)	13(2)	-5(2)	-20(2)
C(27)	37(2)	73(3)	33(2)	-10(2)	2(2)	-3(2)
C(28)	32(2)	69(3)	34(2)	1(2)	-4(2)	-13(2)
C(29)	33(2)	48(2)	25(2)	6(1)	-6(1)	-5(2)
C(30)	41(2)	50(2)	27(2)	-1(2)	-5(1)	-5(2)
C(31)	55(2)	75(3)	25(2)	-4(2)	-12(2)	-8(2)
C(32)	69(3)	86(3)	25(2)	7(2)	-17(2)	1(3)
C(33)	60(3)	66(3)	36(2)	18(2)	-16(2)	1(2)
C(34)	43(2)	52(2)	29(2)	7(2)	-6(2)	-5(2)
C(35)	56(2)	50(2)	40(2)	-6(2)	-7(2)	-8(2)
C(36)	66(3)	44(2)	48(2)	8(2)	-15(2)	1(2)
O(1)	152(5)	77(3)	112(5)	-14(4)	-65(4)	-7(4)
C(37)	145(6)	65(4)	119(6)	-22(4)	-58(5)	-9(4)

C(38)	148(6)	75(4)	117(6)	-9(4)	-63(5)	-2(4)
C(39)	151(6)	71(4)	121(6)	-20(4)	-64(5)	-15(4)
C(40)	149(5)	71(4)	122(6)	-8(4)	-56(5)	-3(4)
O(1')	145(6)	78(4)	128(6)	-15(5)	-57(5)	-14(4)
C(37')	151(6)	71(4)	123(7)	-16(5)	-59(5)	-10(4)
C(38')	147(6)	75(5)	119(7)	-19(5)	-60(5)	-1(5)
C(39')	149(6)	70(4)	118(7)	-21(5)	-56(5)	-4(5)
C(40')	148(6)	70(4)	122(6)	-13(5)	-56(5)	-7(5)
C(43)	113(8)	98(7)	134(9)	-3(6)	-9(6)	-15(6)
C(42)	111(9)	99(7)	150(11)	-4(8)	-26(8)	-8(6)
O(2)	331(16)	133(8)	126(7)	-4(6)	5(9)	-46(10)
C(41)	175(9)	118(7)	114(6)	-25(6)	27(6)	10(6)
C(44)	170(9)	106(6)	102(6)	-17(5)	13(6)	10(6)
C(43')	172(11)	115(9)	106(8)	-18(8)	16(8)	9(8)
C(42')	171(13)	116(10)	103(10)	-14(9)	17(10)	14(10)
O(2')	170(12)	118(9)	104(10)	-12(9)	17(10)	17(10)
C(41')	173(11)	117(9)	106(8)	-18(8)	17(8)	15(8)
C(44')	172(10)	116(8)	107(8)	-22(7)	18(8)	10(8)
N(1)	25(1)	27(1)	22(1)	0(1)	-7(1)	-5(1)
N(2)	22(1)	26(1)	26(1)	2(1)	-7(1)	-5(1)
N(3)	28(1)	33(1)	19(1)	3(1)	-5(1)	-3(1)
N(4)	35(2)	37(2)	21(1)	3(1)	-8(1)	-5(1)
Sn(1)	25(1)	28(1)	21(1)	4(1)	-7(1)	-5(1)

A23. Crystal data and structure refinement of L₁Ge

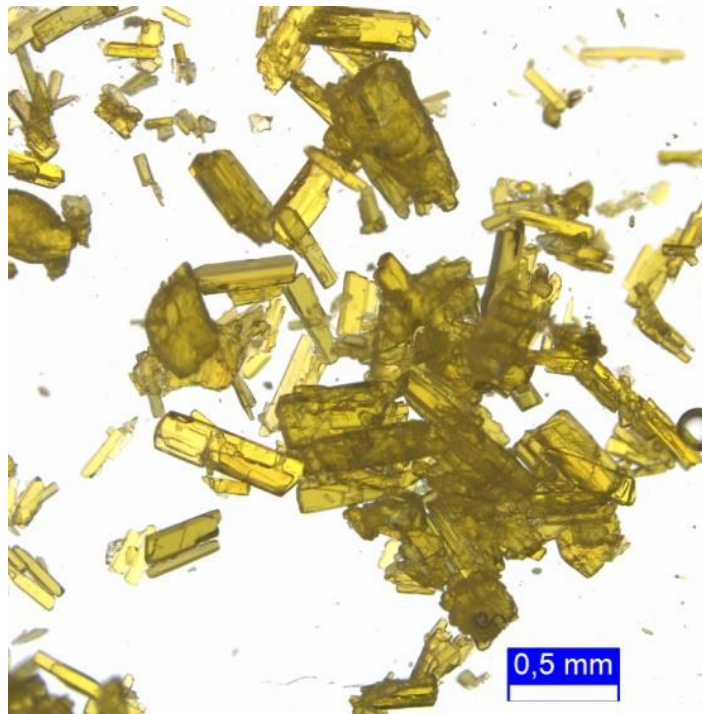


Figure S52. Sample of L₁Ge.

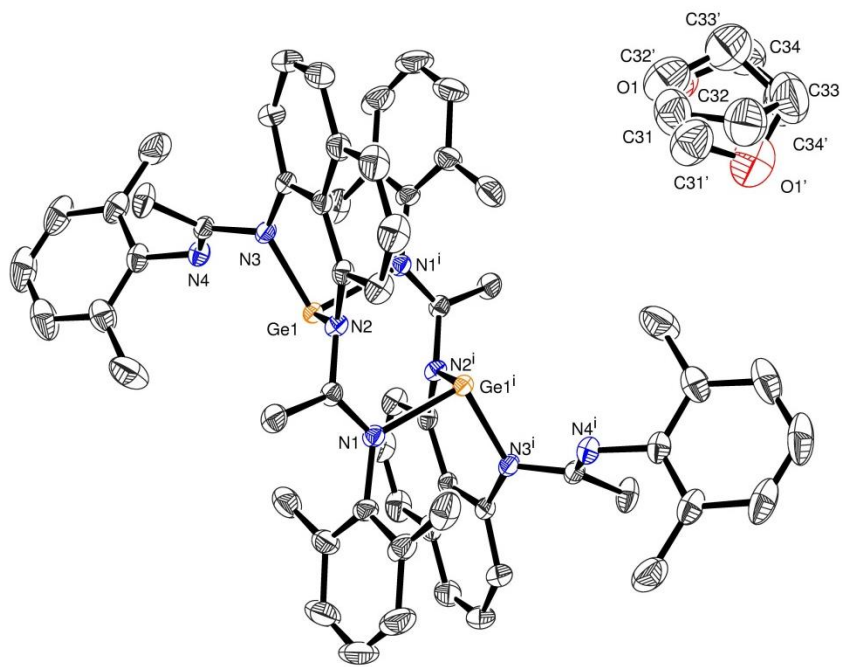


Figure S53. Asymmetric Unit [Symmetry code: (i) 1-x, 1-y, 1-z]

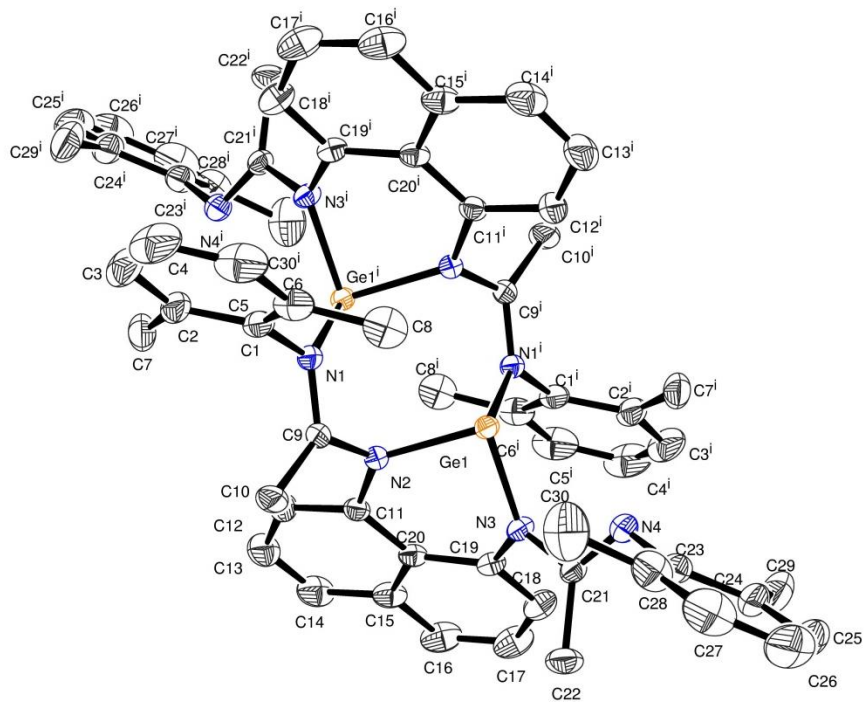


Figure S54. Compound [Symmetry code : (i) 1-x, 1-y, 1-z]

Table A9. Crystal data and structure refinement for L₁Ge.

Identification code	L ₁ Ge
Empirical formula	C ₆₀ H ₆₀ Ge ₂ N ₈ , 2(C ₄ H ₈ O)
Formula weight	1182.59
Temperature	193(2) K
Wavelength	0.71073 Å
Crystal system, space group	Triclinic, P -1
Unit cell dimensions	a = 9.1577(4) Å alpha = 65.967(2) deg. b = 12.9975(5) Å beta = 73.850(2) deg. c = 14.4975(5) Å gamma = 83.201(2) deg.
Volume	1513.79(11) Å ³
Z, Calculated density	1, 1.297 Mg/m ³
Absorption coefficient	1.044 mm ⁻¹
F(000)	620
Crystal size	0.200 x 0.080 x 0.060 mm
Theta range for data collection	2.874 to 34.433 deg.
Limiting indices	-14<=h<=14, -20<=k<=20, -23<=l<=21
Reflections collected / unique	62134 / 12689 [R(int) = 0.0398]
Completeness to theta = 25.242	99.5 %
Refinement method	Full-matrix least-squares on F ²
Data / restraints / parameters	12689 / 186 / 414
Goodness-of-fit on F ²	1.051
Final R indices [I>2sigma(I)]	R1 = 0.0381, wR2 = 0.0898
R indices (all data)	R1 = 0.0527, wR2 = 0.0964
Largest diff. peak and hole	0.674 and -0.468 e.Å ⁻³

Table A10. Atomic coordinates ($\times 10^4$) and equivalent isotropic displacement parameters ($\text{Å}^2 \times 10^3$) for L_1Ge . $U(\text{eq})$ is defined as one third of the trace of the orthogonalized U_{ij} tensor.

	x	y	z	$U(\text{eq})$
C(1)	5002(2)	4429(1)	7510(1)	26(1)
C(2)	5066(2)	3390(2)	8339(1)	35(1)
C(3)	4578(2)	3367(2)	9350(1)	51(1)
C(4)	4064(2)	4323(2)	9526(2)	59(1)
C(5)	4052(2)	5347(2)	8696(2)	50(1)
C(6)	4523(2)	5419(2)	7669(1)	33(1)
C(7)	5668(2)	2348(2)	8151(1)	42(1)
C(8)	4540(2)	6536(2)	6771(2)	40(1)
C(9)	6772(1)	4662(1)	5873(1)	20(1)
C(10)	8088(2)	4774(1)	6255(1)	30(1)
C(11)	8077(1)	4261(1)	4369(1)	21(1)
C(12)	8404(2)	3167(1)	4984(1)	30(1)
C(13)	9418(2)	2482(1)	4552(2)	39(1)
C(14)	10050(2)	2866(1)	3507(2)	38(1)
C(15)	9725(2)	3965(1)	2840(1)	29(1)
C(16)	10386(2)	4347(2)	1752(1)	39(1)
C(17)	10089(2)	5406(2)	1096(1)	40(1)
C(18)	9133(2)	6137(1)	1500(1)	31(1)
C(19)	8510(1)	5817(1)	2560(1)	22(1)
C(20)	8744(1)	4698(1)	3267(1)	21(1)
C(21)	8118(1)	7709(1)	2521(1)	21(1)
C(22)	9799(2)	7948(1)	2184(1)	35(1)
C(23)	7531(2)	9586(1)	2280(1)	28(1)
C(24)	7771(2)	10359(1)	1239(1)	36(1)
C(25)	8141(2)	11472(2)	1003(2)	52(1)
C(26)	8267(3)	11801(2)	1762(2)	60(1)
C(27)	7999(2)	11041(2)	2785(2)	55(1)
C(28)	7608(2)	9924(2)	3071(2)	39(1)
C(29)	7619(3)	9999(2)	413(1)	50(1)
C(30)	7269(3)	9095(2)	4187(2)	59(1)
O(1)	2910(4)	1766(2)	1930(2)	76(1)
C(31)	3761(5)	1192(4)	2702(4)	74(1)
C(32)	3318(5)	-47(4)	3259(4)	81(1)
C(33)	2147(10)	-147(6)	2799(5)	93(2)
C(34)	2378(5)	886(4)	1778(4)	79(1)
O(1')	2125(11)	254(9)	3602(7)	97(2)
C(31')	3548(13)	772(13)	3286(8)	78(2)
C(32')	3854(18)	1449(13)	2118(10)	81(2)
C(33')	3102(19)	812(15)	1777(10)	90(2)
C(34')	1980(30)	50(20)	2741(11)	88(3)
Ge(1)	5879(1)	6276(1)	4108(1)	18(1)
N(1)	5383(1)	4465(1)	6463(1)	20(1)
N(2)	6962(1)	4871(1)	4839(1)	20(1)
N(3)	7640(1)	6605(1)	2931(1)	21(1)

Table A11. Bond lengths [Å] and angles [deg] for AA-R34.

C(1)-C(6)	1.397(2)
C(1)-C(2)	1.403(2)
C(1)-N(1)	1.4419(16)
C(2)-C(3)	1.397(2)
C(2)-C(7)	1.502(3)
C(3)-C(4)	1.372(4)
C(3)-H(3)	0.9500
C(4)-C(5)	1.386(3)
C(4)-H(4)	0.9500
C(5)-C(6)	1.397(2)
C(5)-H(5)	0.9500
C(6)-C(8)	1.502(3)
C(7)-H(7A)	0.9800
C(7)-H(7B)	0.9800
C(7)-H(7C)	0.9800
C(8)-H(8A)	0.9800
C(8)-H(8B)	0.9800
C(8)-H(8C)	0.9800
C(9)-N(1)	1.3074(16)
C(9)-N(2)	1.3740(16)
C(9)-C(10)	1.5027(18)
C(10)-H(10A)	0.9800
C(10)-H(10B)	0.9800
C(10)-H(10C)	0.9800
C(11)-C(12)	1.3867(18)
C(11)-N(2)	1.4125(16)
C(11)-C(20)	1.4317(18)
C(12)-C(13)	1.408(2)
C(12)-H(12)	0.9500
C(13)-C(14)	1.358(3)
C(13)-H(13)	0.9500
C(14)-C(15)	1.414(2)
C(14)-H(14)	0.9500
C(15)-C(16)	1.416(2)
C(15)-C(20)	1.4373(18)
C(16)-C(17)	1.364(3)
C(16)-H(16)	0.9500
C(17)-C(18)	1.408(2)
C(17)-H(17)	0.9500
C(18)-C(19)	1.3815(18)
C(18)-H(18)	0.9500
C(19)-N(3)	1.4102(16)
C(19)-C(20)	1.4305(18)
C(21)-N(4)	1.2869(17)

C(21)-N(3)	1.3831(16)
C(21)-C(22)	1.5089(19)
C(22)-H(22A)	0.9800
C(22)-H(22B)	0.9800
C(22)-H(22C)	0.9800
C(23)-C(24)	1.402(2)
C(23)-C(28)	1.404(2)
C(23)-N(4)	1.4153(18)
C(24)-C(25)	1.406(2)
C(24)-C(29)	1.496(3)
C(25)-C(26)	1.368(4)
C(25)-H(25)	0.9500
C(26)-C(27)	1.377(4)
C(26)-H(26)	0.9500
C(27)-C(28)	1.400(3)
C(27)-H(27)	0.9500
C(28)-C(30)	1.502(3)
C(29)-H(29A)	0.9800
C(29)-H(29B)	0.9800
C(29)-H(29C)	0.9800
C(30)-H(30A)	0.9800
C(30)-H(30B)	0.9800
C(30)-H(30C)	0.9800
O(1)-C(34)	1.410(5)
O(1)-C(31)	1.443(5)
C(31)-C(32)	1.524(6)
C(31)-H(31A)	0.9900
C(31)-H(31B)	0.9900
C(32)-C(33)	1.454(8)
C(32)-H(32A)	0.9900
C(32)-H(32B)	0.9900
C(33)-C(34)	1.521(7)
C(33)-H(33A)	0.9900
C(33)-H(33B)	0.9900
C(34)-H(34A)	0.9900
C(34)-H(34B)	0.9900
O(1')-C(31')	1.410(9)
O(1')-C(34')	1.421(11)
C(31')-C(32')	1.517(10)
C(31')-H(31C)	0.9900
C(31')-H(31D)	0.9900
C(32')-C(33')	1.436(11)
C(32')-H(32C)	0.9900
C(32')-H(32D)	0.9900
C(33')-C(34')	1.517(10)
C(33')-H(33C)	0.9900
C(33')-H(33D)	0.9900
C(34')-H(34C)	0.9900
C(34')-H(34D)	0.9900
Ge(1)-N(3)	1.9332(10)
Ge(1)-N(2)	2.0048(10)
Ge(1)-N(1)#1	2.0961(11)

C(6)-C(1)-C(2)	122.28(14)
C(6)-C(1)-N(1)	118.95(13)
C(2)-C(1)-N(1)	118.71(14)
C(3)-C(2)-C(1)	117.35(18)
C(3)-C(2)-C(7)	121.06(16)
C(1)-C(2)-C(7)	121.57(14)
C(4)-C(3)-C(2)	121.36(19)
C(4)-C(3)-H(3)	119.3
C(2)-C(3)-H(3)	119.3
C(3)-C(4)-C(5)	120.39(17)
C(3)-C(4)-H(4)	119.8
C(5)-C(4)-H(4)	119.8
C(4)-C(5)-C(6)	120.7(2)
C(4)-C(5)-H(5)	119.7
C(6)-C(5)-H(5)	119.7
C(5)-C(6)-C(1)	117.91(17)
C(5)-C(6)-C(8)	120.38(17)
C(1)-C(6)-C(8)	121.70(13)
C(2)-C(7)-H(7A)	109.5
C(2)-C(7)-H(7B)	109.5
H(7A)-C(7)-H(7B)	109.5
C(2)-C(7)-H(7C)	109.5
H(7A)-C(7)-H(7C)	109.5
H(7B)-C(7)-H(7C)	109.5
C(6)-C(8)-H(8A)	109.5
C(6)-C(8)-H(8B)	109.5
H(8A)-C(8)-H(8B)	109.5
C(6)-C(8)-H(8C)	109.5
H(8A)-C(8)-H(8C)	109.5
H(8B)-C(8)-H(8C)	109.5
N(1)-C(9)-N(2)	116.31(11)
N(1)-C(9)-C(10)	123.05(12)
N(2)-C(9)-C(10)	120.36(11)
C(9)-C(10)-H(10A)	109.5
C(9)-C(10)-H(10B)	109.5
H(10A)-C(10)-H(10B)	109.5
C(9)-C(10)-H(10C)	109.5
H(10A)-C(10)-H(10C)	109.5
H(10B)-C(10)-H(10C)	109.5
C(12)-C(11)-N(2)	118.31(12)
C(12)-C(11)-C(20)	119.64(12)
N(2)-C(11)-C(20)	121.69(11)
C(11)-C(12)-C(13)	121.36(14)
C(11)-C(12)-H(12)	119.3
C(13)-C(12)-H(12)	119.3
C(14)-C(13)-C(12)	120.31(15)
C(14)-C(13)-H(13)	119.8
C(12)-C(13)-H(13)	119.8
C(13)-C(14)-C(15)	120.67(14)
C(13)-C(14)-H(14)	119.7
C(15)-C(14)-H(14)	119.7

C(14)-C(15)-C(16)	119.79(14)
C(14)-C(15)-C(20)	120.10(14)
C(16)-C(15)-C(20)	120.10(14)
C(17)-C(16)-C(15)	120.61(14)
C(17)-C(16)-H(16)	119.7
C(15)-C(16)-H(16)	119.7
C(16)-C(17)-C(18)	120.10(15)
C(16)-C(17)-H(17)	119.9
C(18)-C(17)-H(17)	119.9
C(19)-C(18)-C(17)	121.36(15)
C(19)-C(18)-H(18)	119.3
C(17)-C(18)-H(18)	119.3
C(18)-C(19)-N(3)	119.18(12)
C(18)-C(19)-C(20)	120.04(12)
N(3)-C(19)-C(20)	120.77(11)
C(19)-C(20)-C(11)	124.53(11)
C(19)-C(20)-C(15)	117.63(12)
C(11)-C(20)-C(15)	117.85(12)
N(4)-C(21)-N(3)	117.45(11)
N(4)-C(21)-C(22)	123.03(12)
N(3)-C(21)-C(22)	119.03(11)
C(21)-C(22)-H(22A)	109.5
C(21)-C(22)-H(22B)	109.5
H(22A)-C(22)-H(22B)	109.5
C(21)-C(22)-H(22C)	109.5
H(22A)-C(22)-H(22C)	109.5
H(22B)-C(22)-H(22C)	109.5
C(24)-C(23)-C(28)	121.00(14)
C(24)-C(23)-N(4)	119.86(14)
C(28)-C(23)-N(4)	118.97(14)
C(23)-C(24)-C(25)	118.11(18)
C(23)-C(24)-C(29)	120.42(14)
C(25)-C(24)-C(29)	121.47(17)
C(26)-C(25)-C(24)	121.3(2)
C(26)-C(25)-H(25)	119.3
C(24)-C(25)-H(25)	119.3
C(25)-C(26)-C(27)	120.03(17)
C(25)-C(26)-H(26)	120.0
C(27)-C(26)-H(26)	120.0
C(26)-C(27)-C(28)	121.3(2)
C(26)-C(27)-H(27)	119.4
C(28)-C(27)-H(27)	119.4
C(27)-C(28)-C(23)	118.17(19)
C(27)-C(28)-C(30)	121.82(19)
C(23)-C(28)-C(30)	120.01(16)
C(24)-C(29)-H(29A)	109.5
C(24)-C(29)-H(29B)	109.5
H(29A)-C(29)-H(29B)	109.5
C(24)-C(29)-H(29C)	109.5
H(29A)-C(29)-H(29C)	109.5
H(29B)-C(29)-H(29C)	109.5
C(28)-C(30)-H(30A)	109.5

C(28)-C(30)-H(30B)	109.5
H(30A)-C(30)-H(30B)	109.5
C(28)-C(30)-H(30C)	109.5
H(30A)-C(30)-H(30C)	109.5
H(30B)-C(30)-H(30C)	109.5
C(34)-O(1)-C(31)	103.9(3)
O(1)-C(31)-C(32)	109.8(3)
O(1)-C(31)-H(31A)	109.7
C(32)-C(31)-H(31A)	109.7
O(1)-C(31)-H(31B)	109.7
C(32)-C(31)-H(31B)	109.7
H(31A)-C(31)-H(31B)	108.2
C(33)-C(32)-C(31)	104.2(4)
C(33)-C(32)-H(32A)	110.9
C(31)-C(32)-H(32A)	110.9
C(33)-C(32)-H(32B)	110.9
C(31)-C(32)-H(32B)	110.9
H(32A)-C(32)-H(32B)	108.9
C(32)-C(33)-C(34)	103.8(4)
C(32)-C(33)-H(33A)	111.0
C(34)-C(33)-H(33A)	111.0
C(32)-C(33)-H(33B)	111.0
C(34)-C(33)-H(33B)	111.0
H(33A)-C(33)-H(33B)	109.0
O(1)-C(34)-C(33)	108.1(4)
O(1)-C(34)-H(34A)	110.1
C(33)-C(34)-H(34A)	110.1
O(1)-C(34)-H(34B)	110.1
C(33)-C(34)-H(34B)	110.1
H(34A)-C(34)-H(34B)	108.4
C(31')-O(1')-C(34')	106.1(9)
O(1')-C(31')-C(32')	106.7(8)
O(1')-C(31')-H(31C)	110.4
C(32')-C(31')-H(31C)	110.4
O(1')-C(31')-H(31D)	110.4
C(32')-C(31')-H(31D)	110.4
H(31C)-C(31')-H(31D)	108.6
C(33')-C(32')-C(31')	103.2(9)
C(33')-C(32')-H(32C)	111.1
C(31')-C(32')-H(32C)	111.1
C(33')-C(32')-H(32D)	111.1
C(31')-C(32')-H(32D)	111.1
H(32C)-C(32')-H(32D)	109.1
C(32')-C(33')-C(34')	106.5(9)
C(32')-C(33')-H(33C)	110.4
C(34')-C(33')-H(33C)	110.4
C(32')-C(33')-H(33D)	110.4
C(34')-C(33')-H(33D)	110.4
H(33C)-C(33')-H(33D)	108.6
O(1')-C(34')-C(33')	107.3(10)
O(1')-C(34')-H(34C)	110.3
C(33')-C(34')-H(34C)	110.2

O(1')-C(34')-H(34D)	110.2
C(33')-C(34')-H(34D)	110.2
H(34C)-C(34')-H(34D)	108.5
N(3)-Ge(1)-N(2)	87.48(4)
N(3)-Ge(1)-N(1)#1	95.69(4)
N(2)-Ge(1)-N(1)#1	96.79(4)
C(9)-N(1)-C(1)	121.22(11)
C(9)-N(1)-Ge(1)#1	110.44(8)
C(1)-N(1)-Ge(1)#1	125.38(8)
C(9)-N(2)-C(11)	119.28(10)
C(9)-N(2)-Ge(1)	112.38(8)
C(11)-N(2)-Ge(1)	126.95(8)
C(21)-N(3)-C(19)	120.24(10)
C(21)-N(3)-Ge(1)	113.24(8)
C(19)-N(3)-Ge(1)	126.15(8)
C(21)-N(4)-C(23)	119.68(12)

Symmetry transformations used to generate equivalent atoms: #1 -x+1,-y+1,-z+1

Table A12. Anisotropic displacement parameters ($\text{Å}^2 \times 10^3$) for L_1Ge . The anisotropic displacement factor exponent takes the form: $-2 \pi^2 [h^2 a^{*2} U_{11} + \dots + 2 h k a^* b^* U_{12}]$

	U11	U22	U33	U23	U13	U12
C(1)	20(1)	39(1)	19(1)	-11(1)	-4(1)	-6(1)
C(2)	29(1)	47(1)	22(1)	-3(1)	-9(1)	-11(1)
C(3)	46(1)	77(1)	20(1)	-5(1)	-9(1)	-20(1)
C(4)	48(1)	107(2)	26(1)	-32(1)	0(1)	-20(1)
C(5)	40(1)	84(2)	42(1)	-44(1)	-4(1)	-6(1)
C(6)	27(1)	49(1)	31(1)	-23(1)	-5(1)	-4(1)
C(7)	40(1)	36(1)	38(1)	4(1)	-20(1)	-7(1)
C(8)	44(1)	39(1)	48(1)	-28(1)	-12(1)	1(1)
C(9)	18(1)	22(1)	20(1)	-6(1)	-7(1)	-1(1)
C(10)	21(1)	42(1)	28(1)	-10(1)	-9(1)	-7(1)
C(11)	16(1)	21(1)	25(1)	-9(1)	-5(1)	-1(1)
C(12)	27(1)	23(1)	33(1)	-6(1)	-7(1)	3(1)
C(13)	34(1)	25(1)	52(1)	-12(1)	-11(1)	7(1)
C(14)	30(1)	29(1)	56(1)	-23(1)	-5(1)	6(1)
C(15)	23(1)	29(1)	38(1)	-20(1)	-1(1)	-2(1)
C(16)	35(1)	42(1)	43(1)	-29(1)	6(1)	-4(1)
C(17)	42(1)	46(1)	30(1)	-23(1)	8(1)	-9(1)
C(18)	34(1)	34(1)	23(1)	-12(1)	1(1)	-7(1)
C(19)	19(1)	24(1)	22(1)	-10(1)	-1(1)	-5(1)
C(20)	17(1)	22(1)	26(1)	-12(1)	-3(1)	-3(1)
C(21)	21(1)	20(1)	20(1)	-5(1)	-4(1)	-4(1)
C(22)	21(1)	28(1)	52(1)	-13(1)	-3(1)	-5(1)

C(23)	24(1)	21(1)	37(1)	-10(1)	-6(1)	-1(1)
C(24)	32(1)	23(1)	41(1)	-3(1)	-4(1)	-3(1)
C(25)	42(1)	23(1)	68(1)	-3(1)	-1(1)	-5(1)
C(26)	48(1)	26(1)	102(2)	-25(1)	-10(1)	-5(1)
C(27)	50(1)	41(1)	92(2)	-42(1)	-22(1)	4(1)
C(28)	39(1)	34(1)	54(1)	-23(1)	-17(1)	4(1)
C(29)	58(1)	43(1)	33(1)	1(1)	-8(1)	-10(1)
C(30)	85(2)	59(1)	49(1)	-29(1)	-31(1)	5(1)
O(1)	84(2)	59(1)	68(2)	-22(1)	6(1)	-3(1)
C(31)	57(2)	81(2)	99(3)	-45(2)	-21(2)	-9(2)
C(32)	65(2)	91(2)	92(2)	-37(2)	-24(2)	-8(2)
C(33)	82(3)	94(3)	124(3)	-60(2)	-23(2)	-19(3)
C(34)	67(2)	108(3)	78(2)	-51(2)	-21(2)	0(2)
O(1')	89(4)	88(4)	100(4)	-26(3)	-15(4)	-15(3)
C(31')	66(4)	89(5)	72(4)	-19(4)	-21(4)	-14(4)
C(32')	59(4)	93(4)	77(4)	-22(4)	-13(4)	-2(3)
C(33')	79(4)	96(4)	92(4)	-36(4)	-13(4)	-7(4)
C(34')	72(4)	84(5)	113(4)	-42(4)	-20(4)	-15(4)
Ge(1)	17(1)	17(1)	17(1)	-6(1)	-3(1)	-1(1)
N(1)	18(1)	22(1)	18(1)	-6(1)	-5(1)	-2(1)
N(2)	17(1)	21(1)	18(1)	-5(1)	-4(1)	0(1)
N(3)	20(1)	19(1)	20(1)	-6(1)	0(1)	-4(1)
N(4)	24(1)	20(1)	26(1)	-6(1)	-5(1)	-2(1)

A24. Crystal data and structure refinement of L₂Ge

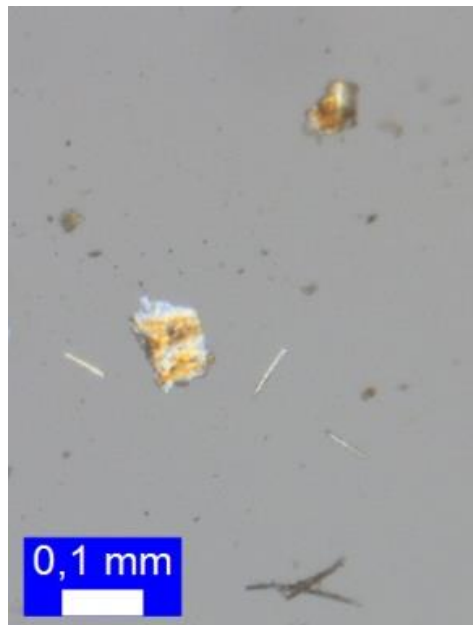


Figure S55. Sample of L₂Ge.

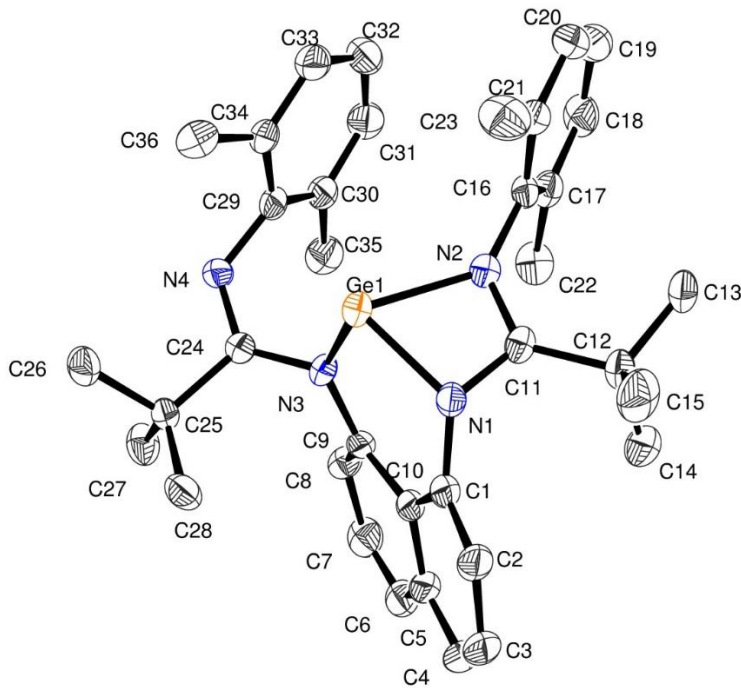


Figure S56. Asymmetric Unit of L_2Ge

Table A13. Crystal data and structure refinement for L_2Ge .

Identification code	L_2Ge
Empirical formula	$\text{C}_{36}\text{H}_{42}\text{GeN}_4$
Formula weight	603.35
Temperature	193(2) K
Wavelength	0.71073 Å
Crystal system, space group	Monoclinic, $\text{P} 21/n$
Unit cell dimensions	$a = 10.879(2)$ Å $\alpha = 90$ deg. $b = 14.307(2)$ Å $\beta = 97.332(6)$ deg. $c = 20.235(4)$ Å $\gamma = 90$ deg.
Volume	3123.7(10) Å ³
Z, Calculated density	4, 1.283 Mg/m ³
Absorption coefficient	1.011 mm ⁻¹
F(000)	1272
Crystal size	0.180 x 0.040 x 0.010 mm
Theta range for data collection	1.748 to 24.129 deg.
Limiting indices	-12 <= h <= 12, -14 <= k <= 16, -23 <= l <= 23
Reflections collected / unique	56977 / 4948 [$R(\text{int}) = 0.1415$]

Completeness to theta = 25.242	99.2 %
Refinement method	Full-matrix least-squares on F^2
Data / restraints / parameters	4948 / 0 / 380
Goodness-of-fit on F^2	1.051
Final R indices [I>2sigma(I)]	R1 = 0.0485, wR2 = 0.1040
R indices (all data)	R1 = 0.0920, wR2 = 0.1230
Largest diff. peak and hole	0.527 and -0.577 e.Å^-3

Table A14. Atomic coordinates (x 10^4) and equivalent isotropic displacement parameters (Å^2 x 10^3) for L₂Ge. U(eq) is defined as one third of the trace of the orthogonalized Uij tensor.

	x	y	z	U(eq)
C(1)	8505(4)	5352(3)	1746(2)	28(1)
C(2)	9492(4)	5021(3)	1465(2)	35(1)
C(3)	9754(4)	5372(3)	855(2)	44(1)
C(4)	9044(4)	6073(3)	543(2)	44(1)
C(5)	7952(4)	6386(3)	786(2)	34(1)
C(6)	7179(4)	7072(3)	447(2)	38(1)
C(7)	6102(5)	7309(3)	666(2)	39(1)
C(8)	5718(4)	6860(3)	1216(2)	30(1)
C(9)	6409(4)	6167(3)	1556(2)	24(1)
C(10)	7623(4)	5967(3)	1382(2)	28(1)
C(11)	8690(4)	5728(3)	2941(2)	25(1)
C(12)	10019(4)	6107(3)	3089(2)	31(1)
C(13)	10277(4)	6598(3)	3770(2)	40(1)
C(14)	10290(4)	6810(3)	2554(2)	44(1)
C(15)	10897(4)	5256(3)	3106(3)	49(1)
C(16)	7704(4)	6242(3)	3925(2)	25(1)
C(17)	7389(4)	7194(3)	3923(2)	31(1)
C(18)	7273(4)	7612(3)	4527(2)	40(1)
C(19)	7448(4)	7109(3)	5113(2)	45(1)
C(20)	7739(4)	6171(3)	5105(2)	41(1)
C(21)	7852(4)	5718(3)	4507(2)	31(1)
C(22)	7182(4)	7739(3)	3283(2)	40(1)
C(23)	8152(5)	4689(3)	4498(2)	48(1)
C(24)	4593(4)	5390(2)	1884(2)	21(1)
C(25)	4093(4)	4904(3)	1212(2)	26(1)
C(26)	3245(4)	4092(3)	1381(2)	38(1)
C(27)	3282(4)	5564(3)	745(2)	38(1)
C(28)	5124(4)	4488(3)	856(2)	37(1)
C(29)	4105(4)	5776(3)	2966(2)	28(1)
C(30)	4070(4)	6748(3)	3095(2)	31(1)
C(31)	4200(4)	7034(3)	3752(2)	40(1)
C(32)	4357(4)	6419(4)	4276(2)	43(1)

C(33)	4339(4)	5459(3)	4141(2)	38(1)
C(34)	4187(4)	5125(3)	3489(2)	29(1)
C(35)	3853(4)	7445(3)	2541(2)	42(1)
C(36)	4033(4)	4092(3)	3363(2)	41(1)
N(1)	8322(3)	5144(2)	2415(2)	26(1)
N(2)	7773(3)	5801(2)	3298(2)	24(1)
N(3)	5867(3)	5612(2)	2030(2)	24(1)
N(4)	3822(3)	5429(2)	2308(2)	26(1)
Ge(1)	6714(1)	4836(1)	2710(1)	25(1)

Table A15. Bond lengths [Å] and angles [deg] for L₂Ge.

C(1)-C(2)	1.362(6)
C(1)-N(1)	1.424(5)
C(1)-C(10)	1.435(6)
C(2)-C(3)	1.396(6)
C(2)-H(2)	0.9500
C(3)-C(4)	1.370(6)
C(3)-H(3)	0.9500
C(4)-C(5)	1.416(6)
C(4)-H(4)	0.9500
C(5)-C(6)	1.411(6)
C(5)-C(10)	1.431(6)
C(6)-C(7)	1.349(6)
C(6)-H(6)	0.9500
C(7)-C(8)	1.395(6)
C(7)-H(7)	0.9500
C(8)-C(9)	1.375(5)
C(8)-H(8)	0.9500
C(9)-N(3)	1.428(5)
C(9)-C(10)	1.439(5)
C(11)-N(2)	1.308(5)
C(11)-N(1)	1.374(5)
C(11)-C(12)	1.537(5)
C(12)-C(14)	1.534(6)
C(12)-C(13)	1.541(5)
C(12)-C(15)	1.545(6)
C(13)-H(13A)	0.9800
C(13)-H(13B)	0.9800
C(13)-H(13C)	0.9800
C(14)-H(14A)	0.9800
C(14)-H(14B)	0.9800
C(14)-H(14C)	0.9800
C(15)-H(15A)	0.9800
C(15)-H(15B)	0.9800
C(15)-H(15C)	0.9800
C(16)-C(21)	1.388(5)
C(16)-C(17)	1.404(5)
C(16)-N(2)	1.427(5)

C(17)-C(18)	1.381(6)
C(17)-C(22)	1.503(6)
C(18)-C(19)	1.379(6)
C(18)-H(18)	0.9500
C(19)-C(20)	1.380(6)
C(19)-H(19)	0.9500
C(20)-C(21)	1.392(6)
C(20)-H(20)	0.9500
C(21)-C(23)	1.508(6)
C(22)-H(22A)	0.9800
C(22)-H(22B)	0.9800
C(22)-H(22C)	0.9800
C(23)-H(23A)	0.9800
C(23)-H(23B)	0.9800
C(23)-H(23C)	0.9800
C(24)-N(4)	1.275(5)
C(24)-N(3)	1.417(5)
C(24)-C(25)	1.561(5)
C(25)-C(28)	1.530(6)
C(25)-C(27)	1.532(6)
C(25)-C(26)	1.548(5)
C(26)-H(26A)	0.9800
C(26)-H(26B)	0.9800
C(26)-H(26C)	0.9800
C(27)-H(27A)	0.9800
C(27)-H(27B)	0.9800
C(27)-H(27C)	0.9800
C(28)-H(28A)	0.9800
C(28)-H(28B)	0.9800
C(28)-H(28C)	0.9800
C(29)-C(34)	1.403(6)
C(29)-C(30)	1.417(6)
C(29)-N(4)	1.417(5)
C(30)-C(31)	1.380(6)
C(30)-C(35)	1.497(6)
C(31)-C(32)	1.372(6)
C(31)-H(31)	0.9500
C(32)-C(33)	1.400(6)
C(32)-H(32)	0.9500
C(33)-C(34)	1.392(6)
C(33)-H(33)	0.9500
C(34)-C(36)	1.506(6)
C(35)-H(35A)	0.9800
C(35)-H(35B)	0.9800
C(35)-H(35C)	0.9800
C(36)-H(36A)	0.9800
C(36)-H(36B)	0.9800
C(36)-H(36C)	0.9800
N(1)-Ge(1)	1.969(3)
N(2)-Ge(1)	2.073(3)
N(3)-Ge(1)	1.912(3)

C(2)-C(1)-N(1)	122.5(4)
C(2)-C(1)-C(10)	120.6(4)
N(1)-C(1)-C(10)	116.9(4)
C(1)-C(2)-C(3)	120.4(4)
C(1)-C(2)-H(2)	119.8
C(3)-C(2)-H(2)	119.8
C(4)-C(3)-C(2)	120.3(4)
C(4)-C(3)-H(3)	119.9
C(2)-C(3)-H(3)	119.9
C(3)-C(4)-C(5)	121.4(4)
C(3)-C(4)-H(4)	119.3
C(5)-C(4)-H(4)	119.3
C(6)-C(5)-C(4)	121.6(4)
C(6)-C(5)-C(10)	120.2(4)
C(4)-C(5)-C(10)	118.1(4)
C(7)-C(6)-C(5)	120.2(4)
C(7)-C(6)-H(6)	119.9
C(5)-C(6)-H(6)	119.9
C(6)-C(7)-C(8)	120.5(4)
C(6)-C(7)-H(7)	119.7
C(8)-C(7)-H(7)	119.7
C(9)-C(8)-C(7)	122.1(4)
C(9)-C(8)-H(8)	118.9
C(7)-C(8)-H(8)	118.9
C(8)-C(9)-N(3)	119.4(4)
C(8)-C(9)-C(10)	118.7(4)
N(3)-C(9)-C(10)	121.7(3)
C(5)-C(10)-C(1)	117.9(4)
C(5)-C(10)-C(9)	117.4(4)
C(1)-C(10)-C(9)	124.7(4)
N(2)-C(11)-N(1)	108.0(3)
N(2)-C(11)-C(12)	129.0(4)
N(1)-C(11)-C(12)	122.6(4)
C(14)-C(12)-C(11)	110.7(3)
C(14)-C(12)-C(13)	107.6(3)
C(11)-C(12)-C(13)	113.2(3)
C(14)-C(12)-C(15)	111.0(4)
C(11)-C(12)-C(15)	106.9(3)
C(13)-C(12)-C(15)	107.4(4)
C(12)-C(13)-H(13A)	109.5
C(12)-C(13)-H(13B)	109.5
H(13A)-C(13)-H(13B)	109.5
C(12)-C(13)-H(13C)	109.5
H(13A)-C(13)-H(13C)	109.5
H(13B)-C(13)-H(13C)	109.5
C(12)-C(14)-H(14A)	109.5
C(12)-C(14)-H(14B)	109.5
H(14A)-C(14)-H(14B)	109.5
C(12)-C(14)-H(14C)	109.5
H(14A)-C(14)-H(14C)	109.5
H(14B)-C(14)-H(14C)	109.5
C(12)-C(15)-H(15A)	109.5

C(12)-C(15)-H(15B)	109.5
H(15A)-C(15)-H(15B)	109.5
C(12)-C(15)-H(15C)	109.5
H(15A)-C(15)-H(15C)	109.5
H(15B)-C(15)-H(15C)	109.5
C(21)-C(16)-C(17)	121.9(4)
C(21)-C(16)-N(2)	120.1(3)
C(17)-C(16)-N(2)	117.8(3)
C(18)-C(17)-C(16)	117.9(4)
C(18)-C(17)-C(22)	121.1(4)
C(16)-C(17)-C(22)	121.0(4)
C(19)-C(18)-C(17)	121.1(4)
C(19)-C(18)-H(18)	119.5
C(17)-C(18)-H(18)	119.5
C(18)-C(19)-C(20)	120.3(4)
C(18)-C(19)-H(19)	119.8
C(20)-C(19)-H(19)	119.8
C(19)-C(20)-C(21)	120.6(4)
C(19)-C(20)-H(20)	119.7
C(21)-C(20)-H(20)	119.7
C(16)-C(21)-C(20)	118.2(4)
C(16)-C(21)-C(23)	121.3(4)
C(20)-C(21)-C(23)	120.5(4)
C(17)-C(22)-H(22A)	109.5
C(17)-C(22)-H(22B)	109.5
H(22A)-C(22)-H(22B)	109.5
C(17)-C(22)-H(22C)	109.5
H(22A)-C(22)-H(22C)	109.5
H(22B)-C(22)-H(22C)	109.5
C(21)-C(23)-H(23A)	109.5
C(21)-C(23)-H(23B)	109.5
H(23A)-C(23)-H(23B)	109.5
C(21)-C(23)-H(23C)	109.5
H(23A)-C(23)-H(23C)	109.5
H(23B)-C(23)-H(23C)	109.5
N(4)-C(24)-N(3)	124.0(3)
N(4)-C(24)-C(25)	114.8(3)
N(3)-C(24)-C(25)	120.3(3)
C(28)-C(25)-C(27)	110.4(3)
C(28)-C(25)-C(26)	107.8(3)
C(27)-C(25)-C(26)	106.6(3)
C(28)-C(25)-C(24)	112.8(3)
C(27)-C(25)-C(24)	111.8(3)
C(26)-C(25)-C(24)	107.0(3)
C(25)-C(26)-H(26A)	109.5
C(25)-C(26)-H(26B)	109.5
H(26A)-C(26)-H(26B)	109.5
C(25)-C(26)-H(26C)	109.5
H(26A)-C(26)-H(26C)	109.5
H(26B)-C(26)-H(26C)	109.5
C(25)-C(27)-H(27A)	109.5
C(25)-C(27)-H(27B)	109.5

H(27A)-C(27)-H(27B)	109.5
C(25)-C(27)-H(27C)	109.5
H(27A)-C(27)-H(27C)	109.5
H(27B)-C(27)-H(27C)	109.5
C(25)-C(28)-H(28A)	109.5
C(25)-C(28)-H(28B)	109.5
H(28A)-C(28)-H(28B)	109.5
C(25)-C(28)-H(28C)	109.5
H(28A)-C(28)-H(28C)	109.5
H(28B)-C(28)-H(28C)	109.5
C(34)-C(29)-C(30)	120.8(4)
C(34)-C(29)-N(4)	117.5(4)
C(30)-C(29)-N(4)	120.6(4)
C(31)-C(30)-C(29)	117.8(4)
C(31)-C(30)-C(35)	120.7(4)
C(29)-C(30)-C(35)	121.4(4)
C(32)-C(31)-C(30)	122.8(4)
C(32)-C(31)-H(31)	118.6
C(30)-C(31)-H(31)	118.6
C(31)-C(32)-C(33)	118.7(4)
C(31)-C(32)-H(32)	120.6
C(33)-C(32)-H(32)	120.6
C(34)-C(33)-C(32)	121.2(4)
C(34)-C(33)-H(33)	119.4
C(32)-C(33)-H(33)	119.4
C(33)-C(34)-C(29)	118.4(4)
C(33)-C(34)-C(36)	119.6(4)
C(29)-C(34)-C(36)	121.9(4)
C(30)-C(35)-H(35A)	109.5
C(30)-C(35)-H(35B)	109.5
H(35A)-C(35)-H(35B)	109.5
C(30)-C(35)-H(35C)	109.5
H(35A)-C(35)-H(35C)	109.5
H(35B)-C(35)-H(35C)	109.5
C(34)-C(36)-H(36A)	109.5
C(34)-C(36)-H(36B)	109.5
H(36A)-C(36)-H(36B)	109.5
C(34)-C(36)-H(36C)	109.5
H(36A)-C(36)-H(36C)	109.5
H(36B)-C(36)-H(36C)	109.5
C(11)-N(1)-C(1)	123.2(3)
C(11)-N(1)-Ge(1)	94.7(2)
C(1)-N(1)-Ge(1)	125.0(3)
C(11)-N(2)-C(16)	131.0(3)
C(11)-N(2)-Ge(1)	92.1(2)
C(16)-N(2)-Ge(1)	135.7(3)
C(24)-N(3)-C(9)	117.5(3)
C(24)-N(3)-Ge(1)	112.9(2)
C(9)-N(3)-Ge(1)	127.1(3)
C(24)-N(4)-C(29)	124.4(3)
N(3)-Ge(1)-N(1)	90.95(13)
N(3)-Ge(1)-N(2)	102.00(13)

N(1)-Ge(1)-N(2) 64.89(13)

Symmetry transformations used to generate equivalent atoms:

Table A16. Anisotropic displacement parameters ($\text{Å}^2 \times 10^3$) for L_2Ge . The anisotropic displacement factor exponent takes the form: $-2 \pi^2 [h^2 a^*{}^2 U_{11} + \dots + 2 h k a^* b^* U_{12}]$

	U11	U22	U33	U23	U13	U12
C(1)	27(3)	29(3)	28(2)	-7(2)	5(2)	-6(2)
C(2)	28(3)	37(3)	42(3)	-16(2)	13(2)	-4(2)
C(3)	31(3)	60(4)	44(3)	-21(3)	19(2)	-10(3)
C(4)	40(3)	58(3)	38(3)	-12(3)	19(2)	-18(3)
C(5)	36(3)	37(3)	32(3)	-8(2)	12(2)	-15(2)
C(6)	44(3)	37(3)	33(3)	5(2)	4(2)	-14(2)
C(7)	48(3)	27(3)	42(3)	3(2)	4(3)	-8(2)
C(8)	33(3)	22(2)	35(3)	1(2)	10(2)	-1(2)
C(9)	27(3)	23(2)	21(2)	-4(2)	6(2)	-6(2)
C(10)	28(3)	28(2)	30(2)	-12(2)	8(2)	-8(2)
C(11)	20(2)	22(2)	32(2)	5(2)	0(2)	1(2)
C(12)	21(3)	35(3)	35(3)	-2(2)	-1(2)	-3(2)
C(13)	26(3)	51(3)	40(3)	0(2)	-3(2)	-12(2)
C(14)	43(3)	45(3)	46(3)	-3(2)	11(2)	-20(2)
C(15)	26(3)	57(3)	64(3)	-4(3)	2(2)	8(2)
C(16)	23(3)	27(2)	26(2)	-5(2)	2(2)	-6(2)
C(17)	28(3)	27(2)	38(3)	-3(2)	5(2)	-4(2)
C(18)	44(3)	28(3)	48(3)	-13(2)	7(2)	-8(2)
C(19)	52(3)	45(3)	39(3)	-17(3)	14(2)	-15(2)
C(20)	46(3)	49(3)	27(3)	0(2)	4(2)	-15(2)
C(21)	30(3)	34(3)	29(3)	1(2)	4(2)	-6(2)
C(22)	40(3)	31(3)	47(3)	3(2)	-1(2)	4(2)
C(23)	64(4)	39(3)	40(3)	11(2)	2(3)	4(3)
C(24)	26(2)	14(2)	24(2)	2(2)	3(2)	1(2)
C(25)	26(2)	29(2)	23(2)	-2(2)	0(2)	-6(2)
C(26)	46(3)	31(3)	36(3)	-4(2)	3(2)	-12(2)
C(27)	35(3)	37(3)	37(3)	4(2)	-9(2)	-3(2)
C(28)	35(3)	44(3)	30(3)	-12(2)	2(2)	1(2)
C(29)	17(2)	35(3)	31(2)	-3(2)	4(2)	-3(2)
C(30)	19(3)	40(3)	33(3)	-4(2)	5(2)	0(2)
C(31)	35(3)	42(3)	45(3)	-13(2)	14(2)	0(2)
C(32)	35(3)	61(4)	34(3)	-11(3)	4(2)	-5(2)
C(33)	29(3)	53(3)	33(3)	4(2)	2(2)	-4(2)
C(34)	18(2)	38(3)	31(2)	-1(2)	3(2)	-3(2)
C(35)	40(3)	38(3)	49(3)	-3(2)	11(2)	1(2)
C(36)	43(3)	43(3)	39(3)	5(2)	11(2)	-4(2)
N(1)	21(2)	26(2)	29(2)	-5(2)	3(2)	-2(2)

N(2)	22(2)	22(2)	27(2)	2(2)	2(2)	1(2)
N(3)	18(2)	25(2)	28(2)	0(2)	4(2)	-2(2)
N(4)	23(2)	31(2)	23(2)	-2(2)	4(2)	-1(2)
Ge(1)	22(1)	23(1)	31(1)	0(1)	2(1)	-2(1)

A25. Crystal data and structure refinement of 1a.

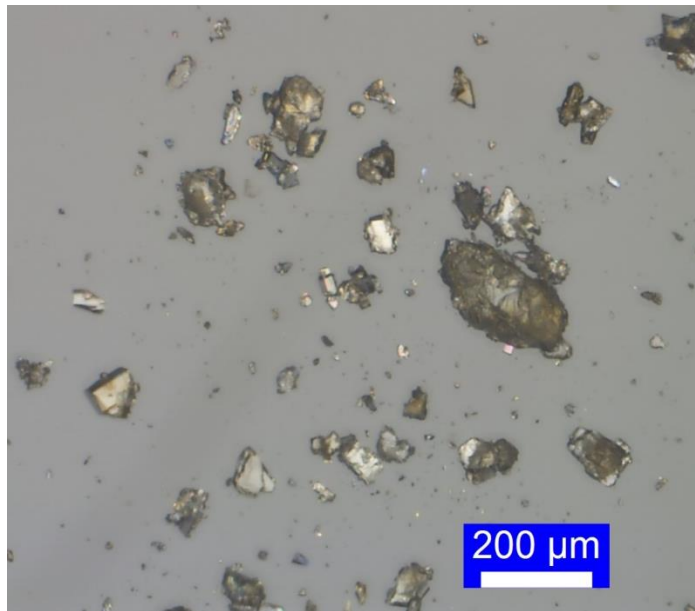


Figure S57. Sample of 1a.

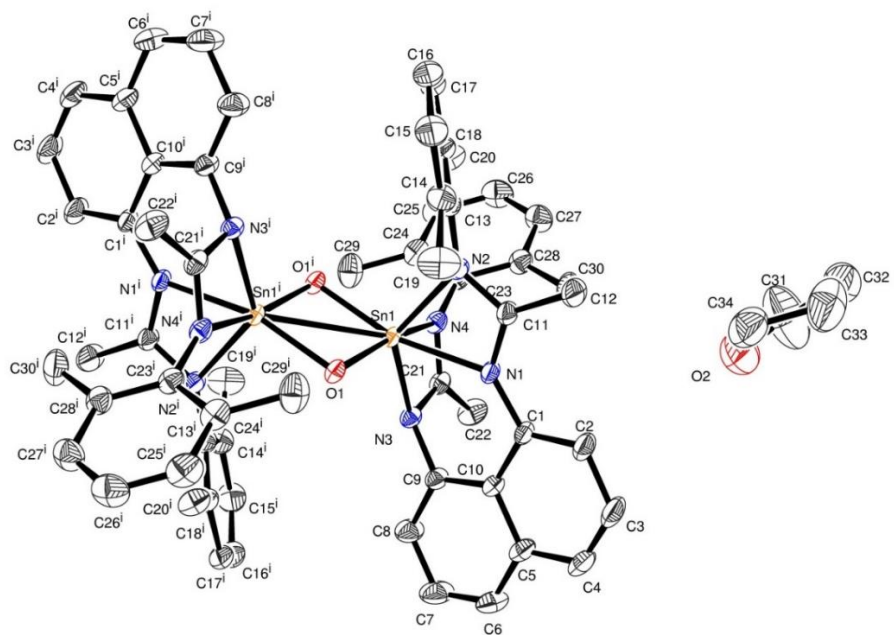


Figure S58. Asymmetric Unit of 1a.

Table A17. Crystal data and structure refinement for 1a.

Identification code	1a
Empirical formula	C60 H60 N8 O2 Sn2, 2(C4 H8 O)
Formula weight	1306.79
Temperature	193(2) K
Wavelength	0.71073 Å
Crystal system, space group	Triclinic, P -1
Unit cell dimensions	a = 11.0951(5) Å alpha = 88.337(2) deg. b = 11.8481(6) Å beta = 88.326(2) deg. c = 12.8106(6) Å gamma = 65.647(2) deg.
Volume	1533.27(13) Å^3
Z, Calculated density	1, 1.415 Mg/m^3
Absorption coefficient	0.870 mm^-1
F(000)	672
Crystal size	0.120 x 0.120 x 0.080 mm
Theta range for data collection	3.182 to 36.438 deg.
Limiting indices	-18<=h<=18, -19<=k<=19, -21<=l<=21
Reflections collected / unique	122943 / 14935 [R(int) = 0.0430]
Completeness to theta = 25.242	99.7 %
Refinement method	Full-matrix least-squares on F^2
Data / restraints / parameters	14935 / 0 / 376
Goodness-of-fit on F^2	1.061
Final R indices [I>2sigma(I)]	R1 = 0.0272, wR2 = 0.0652
R indices (all data)	R1 = 0.0361, wR2 = 0.0703
Largest diff. peak and hole	1.016 and -0.944 e.Å^-3

Table A18. Atomic coordinates (x 10^4) and equivalent isotropic displacement parameters (Å^2 x 10^3) for 1a. U(eq) is defined as one third of the trace of the orthogonalized Uij tensor.

	x	y	z	U(eq)
C(1)	1225(1)	5332(1)	8431(1)	22(1)
C(2)	581(1)	4715(2)	7943(1)	33(1)
C(3)	-758(2)	4974(2)	8162(2)	38(1)
C(4)	-1470(1)	5842(2)	8865(1)	34(1)
C(5)	-884(1)	6531(1)	9367(1)	28(1)
C(6)	-1641(2)	7429(2)	10105(2)	38(1)

C(7)	-1111(2)	8092(2)	10630(2)	43(1)
C(8)	205(2)	7926(2)	10406(1)	34(1)
C(9)	961(1)	7097(1)	9665(1)	23(1)
C(10)	470(1)	6319(1)	9142(1)	22(1)
C(11)	3519(1)	4161(1)	7727(1)	24(1)
C(12)	3330(2)	3412(2)	6877(2)	46(1)
C(13)	5954(1)	3202(1)	7614(1)	24(1)
C(14)	6330(2)	1970(1)	7966(1)	31(1)
C(15)	7575(2)	1088(2)	7666(1)	37(1)
C(16)	8441(2)	1419(2)	7069(1)	36(1)
C(17)	8087(1)	2646(2)	6775(1)	31(1)
C(18)	6842(1)	3554(1)	7034(1)	25(1)
C(19)	5448(2)	1609(2)	8691(2)	47(1)
C(20)	6454(2)	4881(2)	6702(2)	35(1)
C(21)	2328(1)	7708(1)	8523(1)	22(1)
C(22)	1220(2)	8870(1)	8143(1)	34(1)
C(23)	3877(1)	7715(1)	7170(1)	23(1)
C(24)	4677(2)	8352(1)	7317(1)	29(1)
C(25)	5098(2)	8821(2)	6435(2)	39(1)
C(26)	4741(2)	8659(2)	5440(2)	41(1)
C(27)	3956(2)	8027(2)	5305(1)	36(1)
C(28)	3512(1)	7541(1)	6167(1)	28(1)
C(29)	5065(2)	8512(2)	8401(2)	41(1)
C(30)	2698(2)	6815(2)	6002(1)	41(1)
C(31)	853(6)	3423(4)	4475(3)	112(2)
C(32)	1106(3)	2388(3)	3786(2)	74(1)
C(33)	1235(3)	1337(3)	4558(3)	86(1)
C(34)	1539(3)	1780(3)	5565(2)	65(1)
N(1)	2600(1)	4968(1)	8340(1)	21(1)
N(2)	4712(1)	4140(1)	7914(1)	23(1)
N(3)	2221(1)	7087(1)	9390(1)	20(1)
N(4)	3484(1)	7180(1)	8050(1)	22(1)
O(1)	4297(1)	4403(1)	10413(1)	20(1)
O(2)	883(2)	3071(2)	5526(2)	72(1)
Sn(1)	4040(1)	5497(1)	9137(1)	16(1)

Table A19. Bond lengths [Å] and angles [deg] for 1a.

C(1)-C(2)	1.3849(18)
C(1)-N(1)	1.4063(16)
C(1)-C(10)	1.4515(18)
C(2)-C(3)	1.409(2)
C(2)-H(2)	0.9500
C(3)-C(4)	1.354(3)
C(3)-H(3)	0.9500
C(4)-C(5)	1.414(2)
C(4)-H(4)	0.9500
C(5)-C(6)	1.417(2)
C(5)-C(10)	1.4388(18)

C(6)-C(7)	1.361(3)
C(6)-H(6)	0.9500
C(7)-C(8)	1.412(2)
C(7)-H(7)	0.9500
C(8)-C(9)	1.3772(19)
C(8)-H(8)	0.9500
C(9)-N(3)	1.4267(16)
C(9)-C(10)	1.4371(18)
C(11)-N(1)	1.3285(16)
C(11)-N(2)	1.3415(16)
C(11)-C(12)	1.497(2)
C(11)-Sn(1)	2.6612(12)
C(12)-H(12A)	0.9800
C(12)-H(12B)	0.9800
C(12)-H(12C)	0.9800
C(13)-C(18)	1.405(2)
C(13)-C(14)	1.407(2)
C(13)-N(2)	1.4186(16)
C(14)-C(15)	1.397(2)
C(14)-C(19)	1.508(3)
C(15)-C(16)	1.383(3)
C(15)-H(15)	0.9500
C(16)-C(17)	1.383(2)
C(16)-H(16)	0.9500
C(17)-C(18)	1.3949(19)
C(17)-H(17)	0.9500
C(18)-C(20)	1.501(2)
C(19)-H(19A)	0.9800
C(19)-H(19B)	0.9800
C(19)-H(19C)	0.9800
C(20)-H(20A)	0.9800
C(20)-H(20B)	0.9800
C(20)-H(20C)	0.9800
C(21)-N(4)	1.3113(17)
C(21)-N(3)	1.3439(17)
C(21)-C(22)	1.4978(18)
C(21)-Sn(1)	2.6374(12)
C(22)-H(22A)	0.9800
C(22)-H(22B)	0.9800
C(22)-H(22C)	0.9800
C(23)-C(24)	1.401(2)
C(23)-C(28)	1.404(2)
C(23)-N(4)	1.4213(17)
C(24)-C(25)	1.397(2)
C(24)-C(29)	1.505(2)
C(25)-C(26)	1.387(3)
C(25)-H(25)	0.9500
C(26)-C(27)	1.380(3)
C(26)-H(26)	0.9500
C(27)-C(28)	1.400(2)
C(27)-H(27)	0.9500
C(28)-C(30)	1.504(2)

C(29)-H(29A)	0.9800
C(29)-H(29B)	0.9800
C(29)-H(29C)	0.9800
C(30)-H(30A)	0.9800
C(30)-H(30B)	0.9800
C(30)-H(30C)	0.9800
C(31)-O(2)	1.395(4)
C(31)-C(32)	1.458(5)
C(31)-H(31A)	0.9900
C(31)-H(31B)	0.9900
C(32)-C(33)	1.530(5)
C(32)-H(32A)	0.9900
C(32)-H(32B)	0.9900
C(33)-C(34)	1.504(4)
C(33)-H(33A)	0.9900
C(33)-H(33B)	0.9900
C(34)-O(2)	1.397(3)
C(34)-H(34A)	0.9900
C(34)-H(34B)	0.9900
N(1)-Sn(1)	2.2236(10)
N(2)-Sn(1)	2.1644(11)
N(3)-Sn(1)	2.1423(10)
N(4)-Sn(1)	2.2742(10)
O(1)-Sn(1)#1	1.9996(8)
O(1)-Sn(1)	2.0079(9)
Sn(1)-Sn(1)#1	2.97787(19)
C(2)-C(1)-N(1)	122.61(12)
C(2)-C(1)-C(10)	118.62(12)
N(1)-C(1)-C(10)	118.51(10)
C(1)-C(2)-C(3)	121.84(15)
C(1)-C(2)-H(2)	119.1
C(3)-C(2)-H(2)	119.1
C(4)-C(3)-C(2)	120.95(14)
C(4)-C(3)-H(3)	119.5
C(2)-C(3)-H(3)	119.5
C(3)-C(4)-C(5)	120.05(13)
C(3)-C(4)-H(4)	120.0
C(5)-C(4)-H(4)	120.0
C(4)-C(5)-C(6)	119.19(13)
C(4)-C(5)-C(10)	120.64(14)
C(6)-C(5)-C(10)	120.16(14)
C(7)-C(6)-C(5)	121.41(14)
C(7)-C(6)-H(6)	119.3
C(5)-C(6)-H(6)	119.3
C(6)-C(7)-C(8)	119.61(15)
C(6)-C(7)-H(7)	120.2
C(8)-C(7)-H(7)	120.2
C(9)-C(8)-C(7)	120.89(15)
C(9)-C(8)-H(8)	119.6
C(7)-C(8)-H(8)	119.6
C(8)-C(9)-N(3)	117.66(12)

C(8)-C(9)-C(10)	121.30(12)
N(3)-C(9)-C(10)	120.95(11)
C(9)-C(10)-C(5)	116.42(12)
C(9)-C(10)-C(1)	125.86(11)
C(5)-C(10)-C(1)	117.71(12)
N(1)-C(11)-N(2)	110.50(11)
N(1)-C(11)-C(12)	127.95(12)
N(2)-C(11)-C(12)	121.42(12)
N(1)-C(11)-Sn(1)	56.50(6)
N(2)-C(11)-Sn(1)	54.00(6)
C(12)-C(11)-Sn(1)	174.81(11)
C(11)-C(12)-H(12A)	109.5
C(11)-C(12)-H(12B)	109.5
H(12A)-C(12)-H(12B)	109.5
C(11)-C(12)-H(12C)	109.5
H(12A)-C(12)-H(12C)	109.5
H(12B)-C(12)-H(12C)	109.5
C(18)-C(13)-C(14)	120.86(12)
C(18)-C(13)-N(2)	118.26(12)
C(14)-C(13)-N(2)	120.64(13)
C(15)-C(14)-C(13)	118.33(15)
C(15)-C(14)-C(19)	120.20(15)
C(13)-C(14)-C(19)	121.40(14)
C(16)-C(15)-C(14)	121.13(15)
C(16)-C(15)-H(15)	119.4
C(14)-C(15)-H(15)	119.4
C(15)-C(16)-C(17)	119.94(14)
C(15)-C(16)-H(16)	120.0
C(17)-C(16)-H(16)	120.0
C(16)-C(17)-C(18)	120.96(15)
C(16)-C(17)-H(17)	119.5
C(18)-C(17)-H(17)	119.5
C(17)-C(18)-C(13)	118.63(13)
C(17)-C(18)-C(20)	120.86(14)
C(13)-C(18)-C(20)	120.51(12)
C(14)-C(19)-H(19A)	109.5
C(14)-C(19)-H(19B)	109.5
H(19A)-C(19)-H(19B)	109.5
C(14)-C(19)-H(19C)	109.5
H(19A)-C(19)-H(19C)	109.5
H(19B)-C(19)-H(19C)	109.5
C(18)-C(20)-H(20A)	109.5
C(18)-C(20)-H(20B)	109.5
H(20A)-C(20)-H(20B)	109.5
C(18)-C(20)-H(20C)	109.5
H(20A)-C(20)-H(20C)	109.5
H(20B)-C(20)-H(20C)	109.5
N(4)-C(21)-N(3)	112.95(11)
N(4)-C(21)-C(22)	124.42(13)
N(3)-C(21)-C(22)	122.62(12)
N(4)-C(21)-Sn(1)	59.57(6)
N(3)-C(21)-Sn(1)	53.94(6)

C(22)-C(21)-Sn(1)	171.30(10)
C(21)-C(22)-H(22A)	109.5
C(21)-C(22)-H(22B)	109.5
H(22A)-C(22)-H(22B)	109.5
C(21)-C(22)-H(22C)	109.5
H(22A)-C(22)-H(22C)	109.5
H(22B)-C(22)-H(22C)	109.5
C(24)-C(23)-C(28)	121.39(13)
C(24)-C(23)-N(4)	119.17(12)
C(28)-C(23)-N(4)	119.36(12)
C(25)-C(24)-C(23)	118.07(15)
C(25)-C(24)-C(29)	121.70(15)
C(23)-C(24)-C(29)	120.23(14)
C(26)-C(25)-C(24)	121.11(16)
C(26)-C(25)-H(25)	119.4
C(24)-C(25)-H(25)	119.4
C(27)-C(26)-C(25)	120.25(15)
C(27)-C(26)-H(26)	119.9
C(25)-C(26)-H(26)	119.9
C(26)-C(27)-C(28)	120.55(16)
C(26)-C(27)-H(27)	119.7
C(28)-C(27)-H(27)	119.7
C(27)-C(28)-C(23)	118.63(14)
C(27)-C(28)-C(30)	119.79(14)
C(23)-C(28)-C(30)	121.55(13)
C(24)-C(29)-H(29A)	109.5
C(24)-C(29)-H(29B)	109.5
H(29A)-C(29)-H(29B)	109.5
C(24)-C(29)-H(29C)	109.5
H(29A)-C(29)-H(29C)	109.5
H(29B)-C(29)-H(29C)	109.5
C(28)-C(30)-H(30A)	109.5
C(28)-C(30)-H(30B)	109.5
H(30A)-C(30)-H(30B)	109.5
C(28)-C(30)-H(30C)	109.5
H(30A)-C(30)-H(30C)	109.5
H(30B)-C(30)-H(30C)	109.5
O(2)-C(31)-C(32)	112.0(3)
O(2)-C(31)-H(31A)	109.2
C(32)-C(31)-H(31A)	109.2
O(2)-C(31)-H(31B)	109.2
C(32)-C(31)-H(31B)	109.2
H(31A)-C(31)-H(31B)	107.9
C(31)-C(32)-C(33)	102.4(3)
C(31)-C(32)-H(32A)	111.3
C(33)-C(32)-H(32A)	111.3
C(31)-C(32)-H(32B)	111.3
C(33)-C(32)-H(32B)	111.3
H(32A)-C(32)-H(32B)	109.2
C(34)-C(33)-C(32)	102.9(2)
C(34)-C(33)-H(33A)	111.2
C(32)-C(33)-H(33A)	111.2

C(34)-C(33)-H(33B)	111.2
C(32)-C(33)-H(33B)	111.2
H(33A)-C(33)-H(33B)	109.1
O(2)-C(34)-C(33)	106.0(2)
O(2)-C(34)-H(34A)	110.5
C(33)-C(34)-H(34A)	110.5
O(2)-C(34)-H(34B)	110.5
C(33)-C(34)-H(34B)	110.5
H(34A)-C(34)-H(34B)	108.7
C(11)-N(1)-C(1)	132.08(11)
C(11)-N(1)-Sn(1)	93.61(7)
C(1)-N(1)-Sn(1)	134.30(8)
C(11)-N(2)-C(13)	126.28(11)
C(11)-N(2)-Sn(1)	95.91(8)
C(13)-N(2)-Sn(1)	134.66(8)
C(21)-N(3)-C(9)	118.61(10)
C(21)-N(3)-Sn(1)	95.58(8)
C(9)-N(3)-Sn(1)	127.19(8)
C(21)-N(4)-C(23)	123.45(11)
C(21)-N(4)-Sn(1)	90.62(8)
C(23)-N(4)-Sn(1)	145.85(9)
Sn(1)#1-O(1)-Sn(1)	95.98(4)
C(31)-O(2)-C(34)	106.4(3)
O(1)#1-Sn(1)-O(1)	84.01(4)
O(1)#1-Sn(1)-N(3)	117.25(4)
O(1)-Sn(1)-N(3)	106.26(4)
O(1)#1-Sn(1)-N(2)	103.51(4)
O(1)-Sn(1)-N(2)	101.24(4)
N(3)-Sn(1)-N(2)	132.38(4)
O(1)#1-Sn(1)-N(1)	163.46(4)
O(1)-Sn(1)-N(1)	97.84(4)
N(3)-Sn(1)-N(1)	78.15(4)
N(2)-Sn(1)-N(1)	59.97(4)
O(1)#1-Sn(1)-N(4)	93.43(4)
O(1)-Sn(1)-N(4)	162.99(4)
N(3)-Sn(1)-N(4)	60.07(4)
N(2)-Sn(1)-N(4)	95.71(4)
N(1)-Sn(1)-N(4)	89.39(4)
O(1)#1-Sn(1)-C(21)	109.70(4)
O(1)-Sn(1)-C(21)	136.53(4)
N(3)-Sn(1)-C(21)	30.47(4)
N(2)-Sn(1)-C(21)	114.25(4)
N(1)-Sn(1)-C(21)	80.27(4)
N(4)-Sn(1)-C(21)	29.81(4)
O(1)#1-Sn(1)-C(11)	133.59(4)
O(1)-Sn(1)-C(11)	100.72(4)
N(3)-Sn(1)-C(11)	105.72(4)
N(2)-Sn(1)-C(11)	30.09(4)
N(1)-Sn(1)-C(11)	29.88(4)
N(4)-Sn(1)-C(11)	93.23(4)
C(21)-Sn(1)-C(11)	98.20(4)
O(1)#1-Sn(1)-Sn(1)#1	42.11(3)

O(1)-Sn(1)-Sn(1)#1	41.90(2)
N(3)-Sn(1)-Sn(1)#1	119.75(3)
N(2)-Sn(1)-Sn(1)#1	106.75(3)
N(1)-Sn(1)-Sn(1)#1	137.37(3)
N(4)-Sn(1)-Sn(1)#1	133.24(3)
C(21)-Sn(1)-Sn(1)#1	135.70(3)
C(11)-Sn(1)-Sn(1)#1	126.04(3)

Symmetry transformations used to generate equivalent atoms: #1 -x+1,-y+1,-z+2

Table A20. Anisotropic displacement parameters ($\text{\AA}^2 \times 10^3$) for 1a. The anisotropic displacement factor exponent takes the form: $-2 \pi^2 [h^2 a^* a^* U_{11} + \dots + 2 h k a^* b^* U_{12}]$

	U11	U22	U33	U23	U13	U12
C(1)	16(1)	24(1)	25(1)	-1(1)	-5(1)	-9(1)
C(2)	23(1)	40(1)	39(1)	-10(1)	-5(1)	-16(1)
C(3)	26(1)	48(1)	46(1)	-4(1)	-9(1)	-22(1)
C(4)	19(1)	43(1)	43(1)	5(1)	-6(1)	-16(1)
C(5)	16(1)	31(1)	35(1)	3(1)	-2(1)	-9(1)
C(6)	20(1)	42(1)	48(1)	-4(1)	8(1)	-10(1)
C(7)	28(1)	42(1)	55(1)	-17(1)	15(1)	-10(1)
C(8)	26(1)	31(1)	42(1)	-13(1)	7(1)	-10(1)
C(9)	18(1)	21(1)	28(1)	-2(1)	0(1)	-6(1)
C(10)	15(1)	23(1)	26(1)	1(1)	-2(1)	-7(1)
C(11)	20(1)	26(1)	27(1)	-8(1)	-2(1)	-9(1)
C(12)	30(1)	60(1)	51(1)	-36(1)	2(1)	-19(1)
C(13)	19(1)	23(1)	26(1)	-7(1)	-2(1)	-5(1)
C(14)	31(1)	24(1)	34(1)	-5(1)	0(1)	-8(1)
C(15)	35(1)	24(1)	42(1)	-4(1)	-3(1)	-1(1)
C(16)	24(1)	33(1)	37(1)	-7(1)	-2(1)	3(1)
C(17)	19(1)	36(1)	30(1)	-5(1)	-2(1)	-5(1)
C(18)	18(1)	26(1)	27(1)	-4(1)	-3(1)	-5(1)
C(19)	48(1)	32(1)	58(1)	0(1)	12(1)	-15(1)
C(20)	25(1)	31(1)	46(1)	2(1)	0(1)	-10(1)
C(21)	19(1)	16(1)	28(1)	0(1)	-5(1)	-6(1)
C(22)	25(1)	22(1)	46(1)	9(1)	-5(1)	0(1)
C(23)	20(1)	21(1)	27(1)	6(1)	-3(1)	-7(1)
C(24)	29(1)	24(1)	37(1)	6(1)	-5(1)	-13(1)
C(25)	40(1)	35(1)	48(1)	11(1)	-1(1)	-22(1)
C(26)	47(1)	38(1)	39(1)	11(1)	5(1)	-20(1)
C(27)	41(1)	36(1)	29(1)	8(1)	-1(1)	-14(1)
C(28)	26(1)	29(1)	28(1)	7(1)	-4(1)	-10(1)
C(29)	53(1)	38(1)	43(1)	6(1)	-14(1)	-29(1)
C(30)	45(1)	54(1)	33(1)	8(1)	-13(1)	-30(1)
C(31)	195(5)	94(3)	72(2)	-11(2)	-7(3)	-84(3)
C(32)	53(1)	90(2)	66(2)	-21(2)	-8(1)	-14(1)
C(33)	64(2)	57(2)	122(3)	-37(2)	-28(2)	-6(1)

C(34)	43(1)	68(2)	77(2)	-8(1)	-9(1)	-15(1)
N(1)	16(1)	22(1)	24(1)	-4(1)	-4(1)	-7(1)
N(2)	17(1)	24(1)	26(1)	-8(1)	-1(1)	-6(1)
N(3)	17(1)	18(1)	25(1)	-2(1)	-1(1)	-6(1)
N(4)	18(1)	20(1)	25(1)	5(1)	-5(1)	-6(1)
O(1)	17(1)	22(1)	24(1)	3(1)	-5(1)	-10(1)
O(2)	74(1)	70(1)	71(1)	-24(1)	2(1)	-27(1)
Sn(1)	13(1)	16(1)	20(1)	0(1)	-4(1)	-5(1)

A26. Crystal data and structure refinement of 1b.

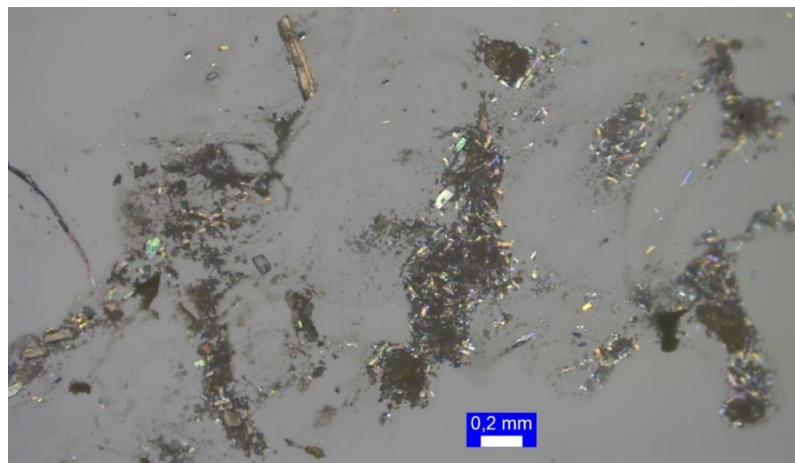


Figure S59. Sample of 1b.

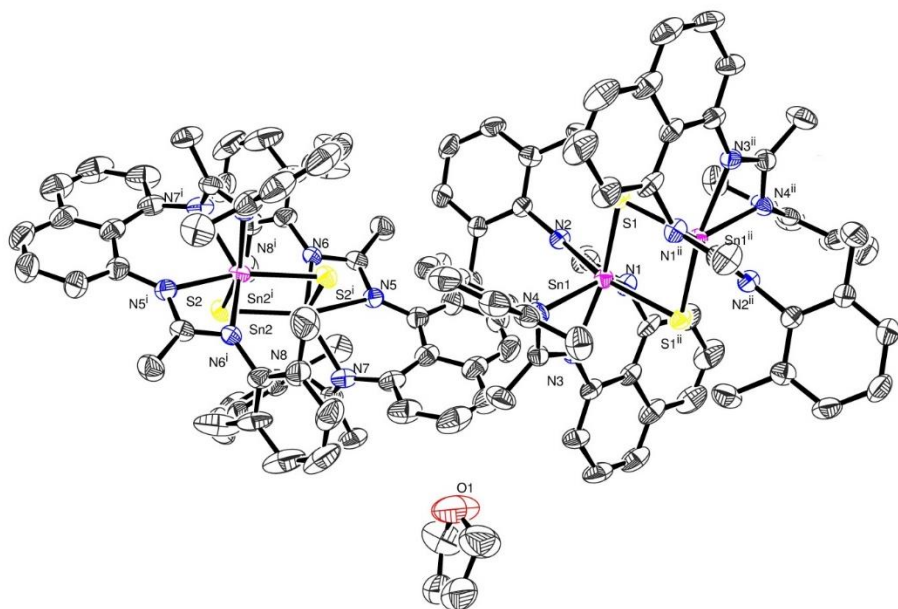


Figure S60. Asymmetric unit of 1b (Symmetry code : i = -x, -y, 1-z ; ii = -x, 1-y, 2-z).

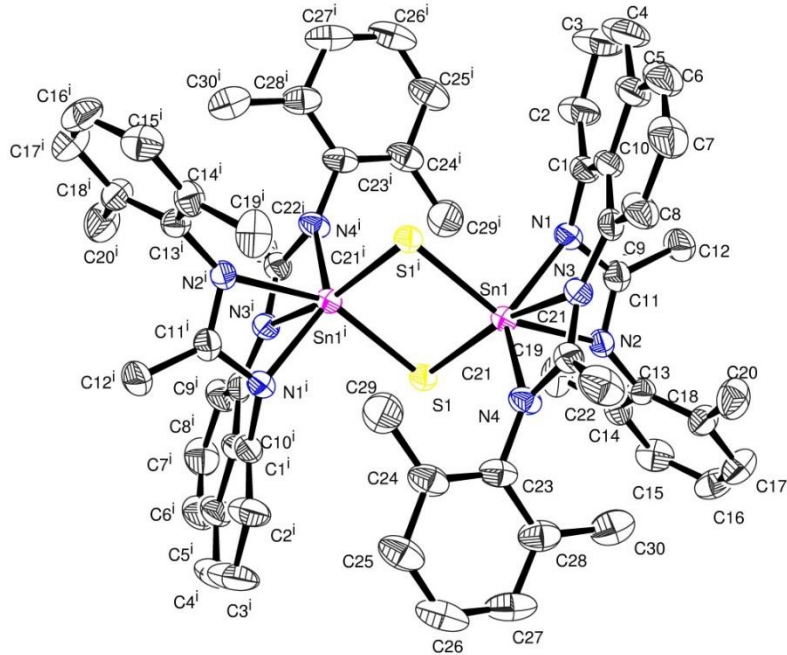


Figure S61. Compound 1b (Symmetry code : i= -x, 1-y, 2-z).

Table A21. Crystal data and structure refinement for 1b.

Identification code	1b
Empirical formula	C ₆₀ H ₆₀ N ₈ S ₂ Sn ₂ , C ₄ H ₈ O
Formula weight	1266.80
Temperature	193(2) K
Wavelength	0.71073 Å
Crystal system, space group	Triclinic, P -1
Unit cell dimensions	a = 12.269(5) Å alpha = 95.205(15) deg. b = 12.952(7) Å beta = 94.892(14) deg. c = 19.923(6) Å gamma = 110.382(19) deg.
Volume	2932(2) Å ³
Z, Calculated density	2, 1.435 Mg/m ³
Absorption coefficient	0.972 mm ⁻¹
F(000)	1296
Crystal size	0.100 x 0.080 x 0.060 mm
Theta range for data collection	2.837 to 28.722 deg.

Limiting indices	-16<=h<=16, -17<=k<=17, -26<=l<=26
Reflections collected / unique	75605 / 15114 [R(int) = 0.1174]
Completeness to theta = 25.242	99.9 %
Refinement method	Full-matrix least-squares on F^2
Data / restraints / parameters	15114 / 0 / 706
Goodness-of-fit on F^2	1.008
Final R indices [I>2sigma(I)]	R1 = 0.0515, wR2 = 0.0893
R indices (all data)	R1 = 0.1157, wR2 = 0.1092
Largest diff. peak and hole	0.687 and -0.593 e.A^-3

Table A22. Atomic coordinates (x 10^4) and equivalent isotropic displacement parameters (A^2 x 10^3) for 1b. U(eq) is defined as one third of the trace of the orthogonalized Uij tensor.

	x	y	z	U(eq)
C(1)	2592(4)	6749(4)	8920(2)	37(1)
C(2)	2884(5)	7875(4)	8972(3)	52(1)
C(3)	4065(5)	8594(5)	9071(3)	71(2)
C(4)	4919(5)	8150(5)	9100(3)	65(2)
C(5)	4674(4)	6991(5)	9059(3)	48(1)
C(6)	5589(4)	6578(5)	9095(3)	56(2)
C(7)	5369(4)	5471(5)	9085(3)	55(2)
C(8)	4211(4)	4720(4)	9051(3)	44(1)
C(9)	3262(4)	5068(4)	9008(2)	34(1)
C(10)	3473(4)	6245(4)	8993(2)	34(1)
C(11)	837(4)	5695(4)	8142(2)	33(1)
C(12)	1231(4)	6306(4)	7553(2)	47(1)
C(13)	-836(4)	4290(4)	7492(2)	31(1)
C(14)	-1886(4)	4487(4)	7392(2)	36(1)
C(15)	-2644(4)	3987(4)	6802(3)	45(1)
C(16)	-2363(5)	3323(4)	6313(3)	49(1)
C(17)	-1319(5)	3151(4)	6410(3)	48(1)
C(18)	-544(4)	3612(4)	7000(2)	36(1)
C(19)	-2172(5)	5265(5)	7905(3)	50(1)
C(20)	609(4)	3436(5)	7086(3)	53(1)
C(21)	1632(4)	3272(4)	9070(2)	33(1)
C(22)	2207(4)	2417(4)	9001(3)	54(2)
C(23)	-212(4)	1913(4)	9313(3)	35(1)
C(24)	-244(4)	1663(4)	9986(3)	41(1)
C(25)	-1004(4)	626(4)	10091(3)	50(1)
C(26)	-1696(4)	-134(4)	9560(4)	56(2)
C(27)	-1649(4)	105(4)	8906(3)	54(2)
C(28)	-914(4)	1137(4)	8765(3)	44(1)
C(29)	512(5)	2461(4)	10574(3)	56(2)
C(30)	-856(5)	1396(5)	8045(3)	59(2)

C(31)	2199(4)	3911(4)	5415(3)	41(1)
C(32)	2329(5)	4999(4)	5368(3)	54(1)
C(33)	2942(5)	5857(5)	5898(4)	69(2)
C(34)	3394(5)	5607(5)	6482(4)	66(2)
C(35)	3345(4)	4525(5)	6546(3)	54(2)
C(36)	3794(5)	4291(7)	7156(3)	72(2)
C(37)	3753(5)	3248(7)	7234(3)	77(2)
C(38)	3336(5)	2384(6)	6677(3)	66(2)
C(39)	2929(4)	2608(5)	6054(3)	43(1)
C(40)	2817(4)	3657(4)	5991(3)	43(1)
C(41)	648(4)	2940(4)	4426(2)	35(1)
C(42)	309(5)	3879(4)	4194(3)	54(1)
C(43)	-829(4)	1495(4)	3612(3)	44(1)
C(44)	-1937(5)	1388(5)	3776(3)	59(2)
C(45)	-2875(6)	970(6)	3285(4)	88(2)
C(46)	-2746(7)	594(6)	2632(4)	90(3)
C(47)	-1646(6)	666(5)	2467(3)	72(2)
C(48)	-672(5)	1126(4)	2961(3)	52(1)
C(49)	-2124(6)	1727(7)	4493(4)	92(3)
C(50)	537(6)	1232(6)	2779(3)	71(2)
C(51)	3373(4)	1988(4)	4987(3)	38(1)
C(52)	4675(4)	2597(5)	5127(3)	57(2)
C(53)	3345(4)	1555(4)	3769(3)	41(1)
C(54)	3623(4)	610(5)	3577(3)	56(2)
C(55)	4058(5)	543(6)	2963(4)	80(2)
C(56)	4220(5)	1373(8)	2554(4)	90(3)
C(57)	3967(5)	2293(6)	2752(3)	71(2)
C(58)	3542(4)	2424(5)	3366(3)	51(1)
C(59)	3487(5)	-271(5)	4043(4)	88(3)
C(60)	3339(5)	3469(5)	3601(3)	65(2)
C(61)	5681(8)	2215(8)	8124(5)	115(3)
C(62)	6549(9)	1870(10)	8452(5)	145(5)
C(63)	6224(7)	1656(6)	9147(6)	108(3)
C(64)	5219(8)	2057(8)	9169(4)	116(3)
N(1)	1386(3)	6079(3)	8778(2)	32(1)
N(2)	-56(3)	4756(3)	8109(2)	29(1)
N(3)	2106(3)	4357(3)	9033(2)	30(1)
N(4)	523(3)	2992(3)	9188(2)	32(1)
N(5)	1442(3)	3001(3)	4947(2)	35(1)
N(6)	167(3)	1905(3)	4119(2)	33(1)
N(7)	2683(3)	1793(3)	5474(2)	39(1)
N(8)	2808(3)	1605(3)	4370(2)	37(1)
S(1)	-1432(1)	4460(1)	9574(1)	30(1)
S(2)	268(1)	-759(1)	4290(1)	36(1)
Sn(1)	496(1)	4687(1)	9270(1)	26(1)
Sn(2)	1041(1)	1155(1)	4825(1)	30(1)
O(1)	4754(5)	2050(6)	8513(3)	126(2)

Table A23. Bond lengths [Å] and angles [deg] for 1b.

C(1)-C(2)	1.367(7)
C(1)-N(1)	1.419(5)
C(1)-C(10)	1.447(7)
C(2)-C(3)	1.409(7)
C(2)-H(2)	0.9500
C(3)-C(4)	1.359(9)
C(3)-H(3)	0.9500
C(4)-C(5)	1.417(8)
C(4)-H(4)	0.9500
C(5)-C(6)	1.401(8)
C(5)-C(10)	1.441(6)
C(6)-C(7)	1.361(8)
C(6)-H(6)	0.9500
C(7)-C(8)	1.406(7)
C(7)-H(7)	0.9500
C(8)-C(9)	1.387(6)
C(8)-H(8)	0.9500
C(9)-N(3)	1.404(5)
C(9)-C(10)	1.459(7)
C(11)-N(2)	1.315(5)
C(11)-N(1)	1.345(6)
C(11)-C(12)	1.496(6)
C(12)-H(12A)	0.9800
C(12)-H(12B)	0.9800
C(12)-H(12C)	0.9800
C(13)-C(14)	1.399(6)
C(13)-C(18)	1.408(6)
C(13)-N(2)	1.433(5)
C(14)-C(15)	1.385(6)
C(14)-C(19)	1.519(6)
C(15)-C(16)	1.385(7)
C(15)-H(15)	0.9500
C(16)-C(17)	1.376(7)
C(16)-H(16)	0.9500
C(17)-C(18)	1.390(6)
C(17)-H(17)	0.9500
C(18)-C(20)	1.507(6)
C(19)-H(19A)	0.9800
C(19)-H(19B)	0.9800
C(19)-H(19C)	0.9800
C(20)-H(20A)	0.9800
C(20)-H(20B)	0.9800
C(20)-H(20C)	0.9800
C(21)-N(4)	1.328(5)
C(21)-N(3)	1.332(5)
C(21)-C(22)	1.508(6)
C(22)-H(22A)	0.9800
C(22)-H(22B)	0.9800
C(22)-H(22C)	0.9800

C(23)-C(28)	1.408(7)
C(23)-C(24)	1.409(7)
C(23)-N(4)	1.433(5)
C(24)-C(25)	1.390(6)
C(24)-C(29)	1.492(7)
C(25)-C(26)	1.372(8)
C(25)-H(25)	0.9500
C(26)-C(27)	1.368(8)
C(26)-H(26)	0.9500
C(27)-C(28)	1.397(7)
C(27)-H(27)	0.9500
C(28)-C(30)	1.504(8)
C(29)-H(29A)	0.9800
C(29)-H(29B)	0.9800
C(29)-H(29C)	0.9800
C(30)-H(30A)	0.9800
C(30)-H(30B)	0.9800
C(30)-H(30C)	0.9800
C(31)-C(32)	1.376(7)
C(31)-N(5)	1.418(6)
C(31)-C(40)	1.446(7)
C(32)-C(33)	1.409(8)
C(32)-H(32)	0.9500
C(33)-C(34)	1.361(9)
C(33)-H(33)	0.9500
C(34)-C(35)	1.399(9)
C(34)-H(34)	0.9500
C(35)-C(36)	1.393(9)
C(35)-C(40)	1.433(7)
C(36)-C(37)	1.358(10)
C(36)-H(36)	0.9500
C(37)-C(38)	1.423(9)
C(37)-H(37)	0.9500
C(38)-C(39)	1.391(7)
C(38)-H(38)	0.9500
C(39)-C(40)	1.427(7)
C(39)-N(7)	1.427(6)
C(41)-N(6)	1.326(6)
C(41)-N(5)	1.339(6)
C(41)-C(42)	1.513(7)
C(42)-H(42A)	0.9800
C(42)-H(42B)	0.9800
C(42)-H(42C)	0.9800
C(43)-C(44)	1.388(7)
C(43)-C(48)	1.395(7)
C(43)-N(6)	1.426(6)
C(44)-C(45)	1.362(8)
C(44)-C(49)	1.516(9)
C(45)-C(46)	1.389(11)
C(45)-H(45)	0.9500
C(46)-C(47)	1.390(10)
C(46)-H(46)	0.9500

C(47)-C(48)	1.396(8)
C(47)-H(47)	0.9500
C(48)-C(50)	1.519(8)
C(49)-H(49A)	0.9800
C(49)-H(49B)	0.9800
C(49)-H(49C)	0.9800
C(50)-H(50A)	0.9800
C(50)-H(50B)	0.9800
C(50)-H(50C)	0.9800
C(51)-N(8)	1.319(6)
C(51)-N(7)	1.326(6)
C(51)-C(52)	1.503(6)
C(51)-Sn(2)	2.662(5)
C(52)-H(52A)	0.9800
C(52)-H(52B)	0.9800
C(52)-H(52C)	0.9800
C(53)-C(58)	1.405(7)
C(53)-C(54)	1.411(7)
C(53)-N(8)	1.422(6)
C(54)-C(55)	1.384(9)
C(54)-C(59)	1.509(9)
C(55)-C(56)	1.377(11)
C(55)-H(55)	0.9500
C(56)-C(57)	1.365(10)
C(56)-H(56)	0.9500
C(57)-C(58)	1.389(8)
C(57)-H(57)	0.9500
C(58)-C(60)	1.502(8)
C(59)-H(59A)	0.9800
C(59)-H(59B)	0.9800
C(59)-H(59C)	0.9800
C(60)-H(60A)	0.9800
C(60)-H(60B)	0.9800
C(60)-H(60C)	0.9800
C(61)-O(1)	1.396(9)
C(61)-C(62)	1.423(11)
C(61)-H(61A)	0.9900
C(61)-H(61B)	0.9900
C(62)-C(63)	1.498(13)
C(62)-H(62A)	0.9900
C(62)-H(62B)	0.9900
C(63)-C(64)	1.498(11)
C(63)-H(63A)	0.9900
C(63)-H(63B)	0.9900
C(64)-O(1)	1.378(9)
C(64)-H(64A)	0.9900
C(64)-H(64B)	0.9900
N(1)-Sn(1)	2.130(4)
N(2)-Sn(1)	2.374(3)
N(3)-Sn(1)	2.240(3)
N(4)-Sn(1)	2.198(4)
N(5)-Sn(2)	2.252(4)

N(6)-Sn(2)	2.189(4)
N(7)-Sn(2)	2.148(4)
N(8)-Sn(2)	2.327(4)
S(1)-Sn(1)	2.4172(14)
S(1)-Sn(1)#1	2.4585(13)
S(2)-Sn(2)	2.4271(17)
S(2)-Sn(2)#2	2.4546(13)
C(2)-C(1)-N(1)	117.6(5)
C(2)-C(1)-C(10)	121.9(4)
N(1)-C(1)-C(10)	120.5(4)
C(1)-C(2)-C(3)	121.0(6)
C(1)-C(2)-H(2)	119.5
C(3)-C(2)-H(2)	119.5
C(4)-C(3)-C(2)	118.9(6)
C(4)-C(3)-H(3)	120.6
C(2)-C(3)-H(3)	120.6
C(3)-C(4)-C(5)	122.8(5)
C(3)-C(4)-H(4)	118.6
C(5)-C(4)-H(4)	118.6
C(6)-C(5)-C(4)	120.5(5)
C(6)-C(5)-C(10)	120.4(5)
C(4)-C(5)-C(10)	119.1(5)
C(7)-C(6)-C(5)	121.1(5)
C(7)-C(6)-H(6)	119.4
C(5)-C(6)-H(6)	119.4
C(6)-C(7)-C(8)	120.2(5)
C(6)-C(7)-H(7)	119.9
C(8)-C(7)-H(7)	119.9
C(9)-C(8)-C(7)	121.8(5)
C(9)-C(8)-H(8)	119.1
C(7)-C(8)-H(8)	119.1
C(8)-C(9)-N(3)	123.2(4)
C(8)-C(9)-C(10)	118.9(4)
N(3)-C(9)-C(10)	117.7(4)
C(5)-C(10)-C(1)	116.1(4)
C(5)-C(10)-C(9)	117.4(4)
C(1)-C(10)-C(9)	126.5(4)
N(2)-C(11)-N(1)	112.8(4)
N(2)-C(11)-C(12)	125.4(4)
N(1)-C(11)-C(12)	121.8(4)
C(11)-C(12)-H(12A)	109.5
C(11)-C(12)-H(12B)	109.5
H(12A)-C(12)-H(12B)	109.5
C(11)-C(12)-H(12C)	109.5
H(12A)-C(12)-H(12C)	109.5
H(12B)-C(12)-H(12C)	109.5
C(14)-C(13)-C(18)	120.9(4)
C(14)-C(13)-N(2)	120.1(4)
C(18)-C(13)-N(2)	119.0(4)
C(15)-C(14)-C(13)	118.7(4)
C(15)-C(14)-C(19)	120.4(4)

C(13)-C(14)-C(19)	120.9(4)
C(16)-C(15)-C(14)	121.0(5)
C(16)-C(15)-H(15)	119.5
C(14)-C(15)-H(15)	119.5
C(17)-C(16)-C(15)	120.0(5)
C(17)-C(16)-H(16)	120.0
C(15)-C(16)-H(16)	120.0
C(16)-C(17)-C(18)	121.1(5)
C(16)-C(17)-H(17)	119.5
C(18)-C(17)-H(17)	119.5
C(17)-C(18)-C(13)	118.4(4)
C(17)-C(18)-C(20)	120.1(4)
C(13)-C(18)-C(20)	121.5(4)
C(14)-C(19)-H(19A)	109.5
C(14)-C(19)-H(19B)	109.5
H(19A)-C(19)-H(19B)	109.5
C(14)-C(19)-H(19C)	109.5
H(19A)-C(19)-H(19C)	109.5
H(19B)-C(19)-H(19C)	109.5
C(18)-C(20)-H(20A)	109.5
C(18)-C(20)-H(20B)	109.5
H(20A)-C(20)-H(20B)	109.5
C(18)-C(20)-H(20C)	109.5
H(20A)-C(20)-H(20C)	109.5
H(20B)-C(20)-H(20C)	109.5
N(4)-C(21)-N(3)	110.9(4)
N(4)-C(21)-C(22)	121.1(4)
N(3)-C(21)-C(22)	128.0(4)
C(21)-C(22)-H(22A)	109.5
C(21)-C(22)-H(22B)	109.5
H(22A)-C(22)-H(22B)	109.5
C(21)-C(22)-H(22C)	109.5
H(22A)-C(22)-H(22C)	109.5
H(22B)-C(22)-H(22C)	109.5
C(28)-C(23)-C(24)	121.4(4)
C(28)-C(23)-N(4)	119.5(4)
C(24)-C(23)-N(4)	119.1(4)
C(25)-C(24)-C(23)	117.5(5)
C(25)-C(24)-C(29)	120.1(5)
C(23)-C(24)-C(29)	122.4(4)
C(26)-C(25)-C(24)	121.6(6)
C(26)-C(25)-H(25)	119.2
C(24)-C(25)-H(25)	119.2
C(27)-C(26)-C(25)	120.8(5)
C(27)-C(26)-H(26)	119.6
C(25)-C(26)-H(26)	119.6
C(26)-C(27)-C(28)	120.7(5)
C(26)-C(27)-H(27)	119.6
C(28)-C(27)-H(27)	119.6
C(27)-C(28)-C(23)	118.1(5)
C(27)-C(28)-C(30)	120.7(5)
C(23)-C(28)-C(30)	121.2(5)

C(24)-C(29)-H(29A)	109.5
C(24)-C(29)-H(29B)	109.5
H(29A)-C(29)-H(29B)	109.5
C(24)-C(29)-H(29C)	109.5
H(29A)-C(29)-H(29C)	109.5
H(29B)-C(29)-H(29C)	109.5
C(28)-C(30)-H(30A)	109.5
C(28)-C(30)-H(30B)	109.5
H(30A)-C(30)-H(30B)	109.5
C(28)-C(30)-H(30C)	109.5
H(30A)-C(30)-H(30C)	109.5
H(30B)-C(30)-H(30C)	109.5
C(32)-C(31)-N(5)	123.8(5)
C(32)-C(31)-C(40)	119.0(5)
N(5)-C(31)-C(40)	117.1(4)
C(31)-C(32)-C(33)	121.8(6)
C(31)-C(32)-H(32)	119.1
C(33)-C(32)-H(32)	119.1
C(34)-C(33)-C(32)	119.6(6)
C(34)-C(33)-H(33)	120.2
C(32)-C(33)-H(33)	120.2
C(33)-C(34)-C(35)	121.1(6)
C(33)-C(34)-H(34)	119.4
C(35)-C(34)-H(34)	119.4
C(36)-C(35)-C(34)	119.8(6)
C(36)-C(35)-C(40)	120.0(6)
C(34)-C(35)-C(40)	120.2(6)
C(37)-C(36)-C(35)	121.1(6)
C(37)-C(36)-H(36)	119.4
C(35)-C(36)-H(36)	119.4
C(36)-C(37)-C(38)	120.6(6)
C(36)-C(37)-H(37)	119.7
C(38)-C(37)-H(37)	119.7
C(39)-C(38)-C(37)	119.3(6)
C(39)-C(38)-H(38)	120.4
C(37)-C(38)-H(38)	120.4
C(38)-C(39)-C(40)	120.4(5)
C(38)-C(39)-N(7)	118.8(5)
C(40)-C(39)-N(7)	120.8(4)
C(39)-C(40)-C(35)	117.5(5)
C(39)-C(40)-C(31)	125.3(5)
C(35)-C(40)-C(31)	117.2(5)
N(6)-C(41)-N(5)	110.2(4)
N(6)-C(41)-C(42)	122.6(4)
N(5)-C(41)-C(42)	127.3(4)
C(41)-C(42)-H(42A)	109.5
C(41)-C(42)-H(42B)	109.5
H(42A)-C(42)-H(42B)	109.5
C(41)-C(42)-H(42C)	109.5
H(42A)-C(42)-H(42C)	109.5
H(42B)-C(42)-H(42C)	109.5
C(44)-C(43)-C(48)	120.9(5)

C(44)-C(43)-N(6)	120.8(5)
C(48)-C(43)-N(6)	118.1(4)
C(45)-C(44)-C(43)	119.5(6)
C(45)-C(44)-C(49)	119.2(6)
C(43)-C(44)-C(49)	121.3(5)
C(44)-C(45)-C(46)	120.7(7)
C(44)-C(45)-H(45)	119.6
C(46)-C(45)-H(45)	119.6
C(45)-C(46)-C(47)	120.2(6)
C(45)-C(46)-H(46)	119.9
C(47)-C(46)-H(46)	119.9
C(46)-C(47)-C(48)	119.5(7)
C(46)-C(47)-H(47)	120.3
C(48)-C(47)-H(47)	120.3
C(43)-C(48)-C(47)	119.0(6)
C(43)-C(48)-C(50)	121.2(5)
C(47)-C(48)-C(50)	119.8(6)
C(44)-C(49)-H(49A)	109.5
C(44)-C(49)-H(49B)	109.5
H(49A)-C(49)-H(49B)	109.5
C(44)-C(49)-H(49C)	109.5
H(49A)-C(49)-H(49C)	109.5
H(49B)-C(49)-H(49C)	109.5
C(48)-C(50)-H(50A)	109.5
C(48)-C(50)-H(50B)	109.5
H(50A)-C(50)-H(50B)	109.5
C(48)-C(50)-H(50C)	109.5
H(50A)-C(50)-H(50C)	109.5
H(50B)-C(50)-H(50C)	109.5
N(8)-C(51)-N(7)	113.7(4)
N(8)-C(51)-C(52)	123.4(4)
N(7)-C(51)-C(52)	122.9(5)
N(8)-C(51)-Sn(2)	60.9(2)
N(7)-C(51)-Sn(2)	53.2(2)
C(52)-C(51)-Sn(2)	172.2(4)
C(51)-C(52)-H(52A)	109.5
C(51)-C(52)-H(52B)	109.5
H(52A)-C(52)-H(52B)	109.5
C(51)-C(52)-H(52C)	109.5
H(52A)-C(52)-H(52C)	109.5
H(52B)-C(52)-H(52C)	109.5
C(58)-C(53)-C(54)	121.6(5)
C(58)-C(53)-N(8)	119.5(5)
C(54)-C(53)-N(8)	118.9(5)
C(55)-C(54)-C(53)	117.7(6)
C(55)-C(54)-C(59)	121.7(6)
C(53)-C(54)-C(59)	120.5(5)
C(56)-C(55)-C(54)	121.2(7)
C(56)-C(55)-H(55)	119.4
C(54)-C(55)-H(55)	119.4
C(57)-C(56)-C(55)	120.5(6)
C(57)-C(56)-H(56)	119.8

C(55)-C(56)-H(56)	119.8
C(56)-C(57)-C(58)	121.5(7)
C(56)-C(57)-H(57)	119.2
C(58)-C(57)-H(57)	119.2
C(57)-C(58)-C(53)	117.5(6)
C(57)-C(58)-C(60)	121.3(6)
C(53)-C(58)-C(60)	121.2(5)
C(54)-C(59)-H(59A)	109.5
C(54)-C(59)-H(59B)	109.5
H(59A)-C(59)-H(59B)	109.5
C(54)-C(59)-H(59C)	109.5
H(59A)-C(59)-H(59C)	109.5
H(59B)-C(59)-H(59C)	109.5
C(58)-C(60)-H(60A)	109.5
C(58)-C(60)-H(60B)	109.5
H(60A)-C(60)-H(60B)	109.5
C(58)-C(60)-H(60C)	109.5
H(60A)-C(60)-H(60C)	109.5
H(60B)-C(60)-H(60C)	109.5
O(1)-C(61)-C(62)	109.7(9)
O(1)-C(61)-H(61A)	109.7
C(62)-C(61)-H(61A)	109.7
O(1)-C(61)-H(61B)	109.7
C(62)-C(61)-H(61B)	109.7
H(61A)-C(61)-H(61B)	108.2
C(61)-C(62)-C(63)	106.7(8)
C(61)-C(62)-H(62A)	110.4
C(63)-C(62)-H(62A)	110.4
C(61)-C(62)-H(62B)	110.4
C(63)-C(62)-H(62B)	110.4
H(62A)-C(62)-H(62B)	108.6
C(62)-C(63)-C(64)	101.4(7)
C(62)-C(63)-H(63A)	111.5
C(64)-C(63)-H(63A)	111.5
C(62)-C(63)-H(63B)	111.5
C(64)-C(63)-H(63B)	111.5
H(63A)-C(63)-H(63B)	109.3
O(1)-C(64)-C(63)	108.8(8)
O(1)-C(64)-H(64A)	109.9
C(63)-C(64)-H(64A)	109.9
O(1)-C(64)-H(64B)	109.9
C(63)-C(64)-H(64B)	109.9
H(64A)-C(64)-H(64B)	108.3
C(11)-N(1)-C(1)	123.0(4)
C(11)-N(1)-Sn(1)	99.0(3)
C(1)-N(1)-Sn(1)	125.9(3)
C(11)-N(2)-C(13)	120.9(4)
C(11)-N(2)-Sn(1)	88.9(3)
C(13)-N(2)-Sn(1)	150.1(3)
C(21)-N(3)-C(9)	132.6(4)
C(21)-N(3)-Sn(1)	93.9(3)
C(9)-N(3)-Sn(1)	132.2(3)

C(21)-N(4)-C(23)	125.3(4)
C(21)-N(4)-Sn(1)	95.9(3)
C(23)-N(4)-Sn(1)	138.0(3)
C(41)-N(5)-C(31)	131.7(4)
C(41)-N(5)-Sn(2)	93.7(3)
C(31)-N(5)-Sn(2)	134.5(3)
C(41)-N(6)-C(43)	125.7(4)
C(41)-N(6)-Sn(2)	97.0(3)
C(43)-N(6)-Sn(2)	135.1(3)
C(51)-N(7)-C(39)	119.4(4)
C(51)-N(7)-Sn(2)	97.2(3)
C(39)-N(7)-Sn(2)	123.8(3)
C(51)-N(8)-C(53)	125.2(4)
C(51)-N(8)-Sn(2)	89.4(3)
C(53)-N(8)-Sn(2)	145.3(3)
Sn(1)-S(1)-Sn(1)#1	87.92(4)
Sn(2)-S(2)-Sn(2)#2	87.14(4)
N(1)-Sn(1)-N(4)	131.38(14)
N(1)-Sn(1)-N(3)	77.63(14)
N(4)-Sn(1)-N(3)	59.16(13)
N(1)-Sn(1)-N(2)	58.65(13)
N(4)-Sn(1)-N(2)	99.06(13)
N(3)-Sn(1)-N(2)	91.81(12)
N(1)-Sn(1)-S(1)	118.91(10)
N(4)-Sn(1)-S(1)	103.69(10)
N(3)-Sn(1)-S(1)	162.73(10)
N(2)-Sn(1)-S(1)	93.17(9)
N(1)-Sn(1)-S(1)#1	96.05(10)
N(4)-Sn(1)-S(1)#1	105.19(10)
N(3)-Sn(1)-S(1)#1	90.90(10)
N(2)-Sn(1)-S(1)#1	153.19(9)
S(1)-Sn(1)-S(1)#1	92.08(4)
N(7)-Sn(2)-N(6)	132.85(15)
N(7)-Sn(2)-N(5)	77.24(15)
N(6)-Sn(2)-N(5)	58.93(14)
N(7)-Sn(2)-N(8)	59.18(14)
N(6)-Sn(2)-N(8)	97.54(14)
N(5)-Sn(2)-N(8)	84.40(13)
N(7)-Sn(2)-S(2)	120.77(12)
N(6)-Sn(2)-S(2)	100.09(10)
N(5)-Sn(2)-S(2)	158.57(10)
N(8)-Sn(2)-S(2)	95.04(10)
N(7)-Sn(2)-S(2)#2	98.24(11)
N(6)-Sn(2)-S(2)#2	102.43(10)
N(5)-Sn(2)-S(2)#2	95.94(10)
N(8)-Sn(2)-S(2)#2	156.87(11)
S(2)-Sn(2)-S(2)#2	92.86(4)
N(7)-Sn(2)-C(51)	29.63(14)
N(6)-Sn(2)-C(51)	116.03(15)
N(5)-Sn(2)-C(51)	77.16(14)
N(8)-Sn(2)-C(51)	29.71(14)
S(2)-Sn(2)-C(51)	112.22(11)

S(2)#2-Sn(2)-C(51)	127.86(12)
C(64)-O(1)-C(61)	105.8(6)

Symmetry transformations used to generate equivalent atoms: #1 -x,-y+1,-z+2 #2 -x,-y,-z+1

Table A24. Anisotropic displacement parameters ($\text{A}^2 \times 10^3$) for 1b. The anisotropic displacement factor exponent takes the form: $-2 \pi^2 [h^2 a^{*2} U_{11} + \dots + 2 h k a^* b^* U_{12}]$

	U11	U22	U33	U23	U13	U12
C(1)	28(2)	45(3)	24(2)	7(2)	-3(2)	-4(2)
C(2)	48(3)	34(3)	64(4)	13(3)	3(3)	0(2)
C(3)	54(4)	40(3)	94(5)	16(3)	-3(4)	-13(3)
C(4)	38(3)	57(4)	74(4)	18(3)	0(3)	-15(3)
C(5)	33(3)	55(3)	38(3)	11(2)	3(2)	-5(2)
C(6)	30(3)	73(4)	48(3)	9(3)	1(2)	-4(3)
C(7)	25(3)	83(5)	52(3)	7(3)	2(2)	14(3)
C(8)	25(2)	55(3)	48(3)	10(3)	7(2)	10(2)
C(9)	26(2)	49(3)	22(2)	3(2)	4(2)	7(2)
C(10)	28(2)	38(3)	27(2)	7(2)	2(2)	-1(2)
C(11)	38(3)	36(3)	29(2)	7(2)	7(2)	15(2)
C(12)	52(3)	48(3)	32(3)	14(2)	6(2)	5(3)
C(13)	30(2)	31(2)	30(2)	5(2)	2(2)	8(2)
C(14)	38(3)	41(3)	31(2)	11(2)	6(2)	17(2)
C(15)	35(3)	47(3)	52(3)	11(3)	-8(2)	16(2)
C(16)	52(3)	43(3)	41(3)	-4(2)	-16(2)	12(3)
C(17)	51(3)	50(3)	39(3)	-9(2)	-6(2)	22(3)
C(18)	35(2)	38(3)	34(3)	-2(2)	2(2)	13(2)
C(19)	55(3)	67(4)	43(3)	13(3)	9(3)	39(3)
C(20)	43(3)	68(4)	50(3)	-4(3)	9(3)	27(3)
C(21)	31(2)	33(3)	34(2)	4(2)	8(2)	10(2)
C(22)	38(3)	48(3)	86(4)	14(3)	21(3)	22(3)
C(23)	22(2)	26(2)	56(3)	4(2)	4(2)	10(2)
C(24)	35(3)	29(3)	64(3)	12(2)	10(2)	13(2)
C(25)	42(3)	37(3)	76(4)	24(3)	13(3)	15(2)
C(26)	33(3)	34(3)	99(5)	24(3)	6(3)	6(2)
C(27)	32(3)	30(3)	89(5)	-2(3)	-11(3)	6(2)
C(28)	31(3)	36(3)	62(4)	1(3)	-3(2)	11(2)
C(29)	77(4)	42(3)	52(3)	13(3)	11(3)	22(3)
C(30)	54(3)	50(3)	61(4)	-6(3)	-7(3)	11(3)
C(31)	34(3)	39(3)	45(3)	5(2)	10(2)	7(2)
C(32)	48(3)	37(3)	68(4)	4(3)	6(3)	8(3)
C(33)	54(4)	44(4)	97(5)	-10(4)	10(4)	6(3)
C(34)	41(3)	65(4)	71(4)	-18(4)	7(3)	0(3)
C(35)	31(3)	76(4)	47(3)	-3(3)	11(2)	10(3)
C(36)	57(4)	109(6)	42(4)	-5(4)	6(3)	24(4)
C(37)	60(4)	137(7)	30(3)	11(4)	-1(3)	31(4)

C(38)	63(4)	106(5)	38(3)	25(3)	1(3)	39(4)
C(39)	30(2)	60(3)	39(3)	16(3)	8(2)	13(2)
C(40)	31(3)	55(3)	39(3)	5(2)	10(2)	8(2)
C(41)	37(3)	38(3)	36(3)	16(2)	10(2)	17(2)
C(42)	66(4)	47(3)	57(4)	13(3)	2(3)	30(3)
C(43)	43(3)	44(3)	45(3)	13(2)	-7(2)	19(2)
C(44)	38(3)	81(4)	63(4)	36(3)	-4(3)	23(3)
C(45)	46(4)	106(6)	103(6)	51(5)	-16(4)	15(4)
C(46)	67(5)	72(5)	100(6)	27(4)	-44(5)	-5(4)
C(47)	87(5)	56(4)	60(4)	5(3)	-28(4)	19(4)
C(48)	62(4)	49(3)	44(3)	4(3)	-12(3)	25(3)
C(49)	61(4)	164(8)	86(5)	65(5)	29(4)	69(5)
C(50)	92(5)	85(5)	42(3)	-6(3)	5(3)	42(4)
C(51)	30(2)	41(3)	47(3)	8(2)	5(2)	17(2)
C(52)	27(3)	78(4)	59(4)	9(3)	5(2)	11(3)
C(53)	26(2)	49(3)	41(3)	-3(2)	7(2)	6(2)
C(54)	23(2)	48(3)	84(4)	-19(3)	2(3)	3(2)
C(55)	31(3)	91(5)	91(5)	-50(4)	14(3)	2(3)
C(56)	41(4)	147(8)	52(4)	-37(5)	10(3)	7(4)
C(57)	45(3)	104(6)	43(4)	7(4)	5(3)	1(4)
C(58)	35(3)	69(4)	41(3)	5(3)	8(2)	9(3)
C(59)	49(4)	41(4)	177(8)	10(4)	40(4)	14(3)
C(60)	69(4)	65(4)	64(4)	32(3)	24(3)	20(3)
C(61)	107(7)	126(8)	137(8)	25(6)	25(6)	68(6)
C(62)	118(8)	194(11)	127(9)	-94(8)	-55(7)	106(8)
C(63)	81(6)	44(4)	176(10)	15(5)	-34(6)	5(4)
C(64)	130(8)	159(9)	88(6)	13(6)	-8(6)	93(7)
N(1)	32(2)	29(2)	30(2)	7(2)	6(2)	5(2)
N(2)	27(2)	33(2)	25(2)	5(2)	5(2)	8(2)
N(3)	23(2)	33(2)	32(2)	1(2)	6(2)	7(2)
N(4)	28(2)	24(2)	45(2)	6(2)	10(2)	10(2)
N(5)	32(2)	32(2)	39(2)	10(2)	4(2)	10(2)
N(6)	34(2)	30(2)	36(2)	6(2)	2(2)	16(2)
N(7)	32(2)	55(3)	35(2)	16(2)	8(2)	17(2)
N(8)	34(2)	35(2)	44(2)	7(2)	13(2)	11(2)
S(1)	24(1)	32(1)	29(1)	3(1)	3(1)	6(1)
S(2)	37(1)	34(1)	40(1)	7(1)	13(1)	14(1)
Sn(1)	25(1)	24(1)	27(1)	4(1)	5(1)	6(1)
Sn(2)	26(1)	32(1)	35(1)	10(1)	6(1)	12(1)
O(1)	88(4)	234(8)	82(4)	11(4)	0(3)	92(5)

A27. Crystal data and structure refinement of 2a.

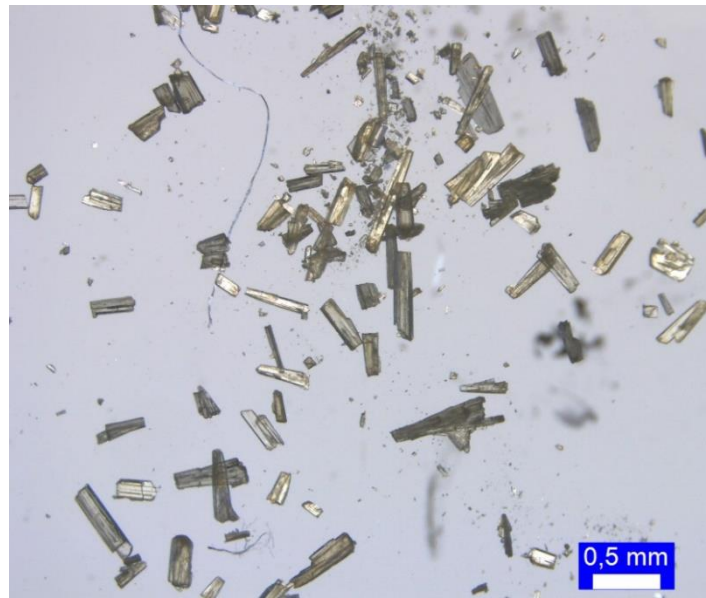


Figure S62. Sample of 2a.

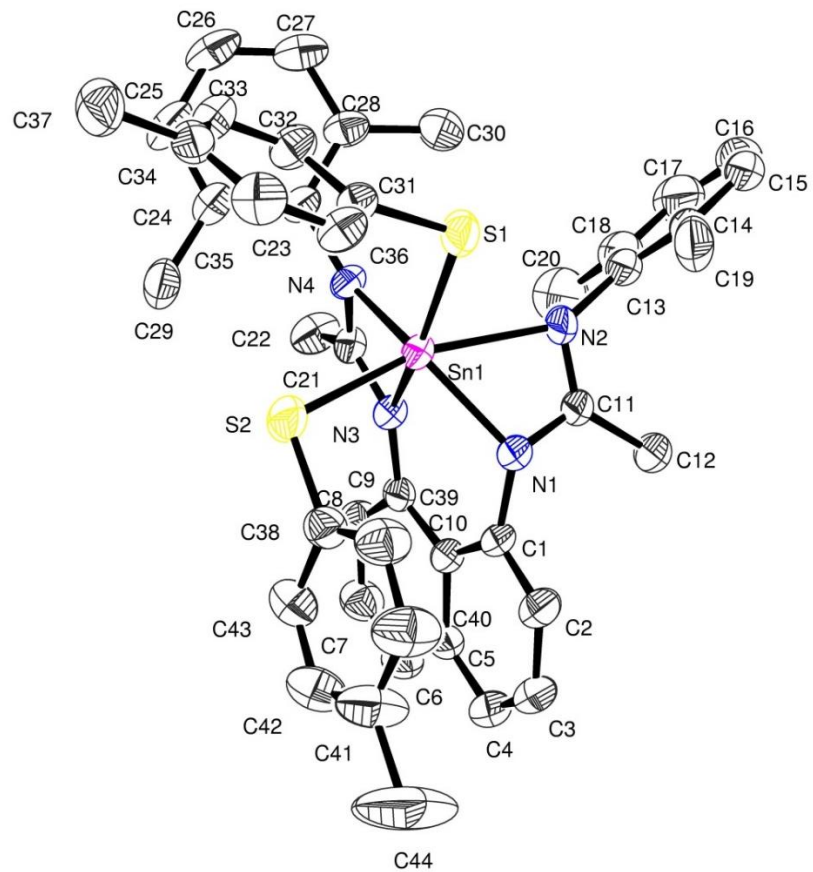


Figure S63. Asymmetric unit of 2a.

Table A25. Crystal data and structure refinement for 2a.

Identification code	2a
Empirical formula	C44 H44 N4 S2 Sn
Formula weight	811.64
Temperature	193(2) K
Wavelength	0.71073 Å
Crystal system, space group	Monoclinic, P 21/c
Unit cell dimensions	a = 19.655(17) Å alpha = 90 deg. b = 11.760(8) Å beta = 104.67(4) deg. c = 20.040(17) Å gamma = 90 deg.
Volume	4481(6) Å ³
Z, Calculated density	4, 1.203 Mg/m ³
Absorption coefficient	0.695 mm ⁻¹
F(000)	1672
Crystal size	0.120 x 0.060 x 0.060 mm
Theta range for data collection	2.723 to 29.596 deg.
Limiting indices	-26<=h<=27, -16<=k<=16, -27<=l<=27
Reflections collected / unique	124683 / 12518 [R(int) = 0.1184]
Completeness to theta = 25.242	99.5 %
Refinement method	Full-matrix least-squares on F ²
Data / restraints / parameters	12518 / 0 / 468
Goodness-of-fit on F ²	0.996
Final R indices [I>2sigma(I)]	R1 = 0.0473, wR2 = 0.1191
R indices (all data)	R1 = 0.0947, wR2 = 0.1422
Largest diff. peak and hole	0.537 and -0.874 e.Å ⁻³

Table A26. Atomic coordinates (x 10⁴) and equivalent isotropic displacement parameters (Å² x 10³) for 2a. U(eq) is defined as one third of the trace of the orthogonalized Uij tensor.

	x	y	z	U(eq)
C(1)	1960(2)	7174(3)	5651(2)	40(1)
C(2)	1523(2)	7951(3)	5862(2)	49(1)
C(3)	1459(2)	9075(3)	5605(2)	55(1)
C(4)	1823(2)	9403(3)	5142(2)	52(1)
C(5)	2296(2)	8642(3)	4937(2)	41(1)
C(6)	2675(2)	9027(3)	4466(2)	47(1)

C(7)	3132(2)	8320(3)	4261(2)	51(1)
C(8)	3244(2)	7209(3)	4523(2)	44(1)
C(9)	2893(2)	6784(3)	4991(2)	35(1)
C(10)	2384(2)	7498(3)	5205(2)	36(1)
C(11)	1506(2)	5294(3)	5435(2)	41(1)
C(12)	849(2)	5699(3)	4941(2)	63(1)
C(13)	1325(2)	3333(3)	5118(2)	53(1)
C(14)	865(2)	2741(3)	5436(3)	63(1)
C(15)	478(2)	1848(4)	5068(4)	84(2)
C(16)	538(3)	1553(4)	4422(4)	90(2)
C(17)	989(3)	2136(4)	4125(3)	89(2)
C(18)	1396(2)	3043(4)	4464(2)	66(1)
C(19)	777(2)	3073(4)	6129(3)	80(2)
C(20)	1857(3)	3691(4)	4121(2)	84(2)
C(21)	3498(2)	4900(3)	5253(2)	37(1)
C(22)	3888(2)	4762(3)	4700(2)	55(1)
C(23)	4033(2)	3193(3)	5890(2)	37(1)
C(24)	4737(2)	3402(3)	6228(2)	43(1)
C(25)	5187(2)	2466(4)	6404(2)	54(1)
C(26)	4948(2)	1369(4)	6262(2)	61(1)
C(27)	4251(2)	1182(3)	5937(2)	54(1)
C(28)	3778(2)	2082(3)	5743(2)	43(1)
C(29)	5011(2)	4575(3)	6449(2)	54(1)
C(30)	3014(2)	1866(3)	5398(2)	58(1)
C(31)	3336(2)	3378(3)	7696(2)	39(1)
C(32)	3925(2)	2785(3)	7626(2)	45(1)
C(33)	4500(2)	2663(3)	8181(2)	46(1)
C(34)	4512(2)	3111(3)	8825(2)	42(1)
C(35)	3921(2)	3687(3)	8889(2)	52(1)
C(36)	3335(2)	3834(3)	8335(2)	47(1)
C(37)	5143(2)	2959(4)	9431(2)	62(1)
C(38)	3226(2)	7381(3)	7131(2)	43(1)
C(39)	2722(2)	7433(3)	7504(2)	57(1)
C(40)	2420(3)	8455(4)	7605(2)	73(1)
C(41)	2608(3)	9444(4)	7331(3)	79(2)
C(42)	3103(3)	9390(4)	6958(2)	67(1)
C(43)	3412(2)	8391(3)	6857(2)	53(1)
C(44)	2222(4)	10570(5)	7417(4)	153(3)
N(1)	1928(1)	6031(2)	5877(1)	38(1)
N(2)	1743(1)	4257(2)	5488(2)	44(1)
N(3)	3053(1)	5725(2)	5316(1)	35(1)
N(4)	3544(1)	4119(2)	5747(1)	35(1)
S(1)	2568(1)	3477(1)	7001(1)	48(1)
S(2)	3685(1)	6111(1)	7058(1)	57(1)
Sn(1)	2816(1)	4955(1)	6249(1)	34(1)

Table A27. Bond lengths [Å] and angles [deg] for 2a.

C(1)-C(2)	1.391(5)
C(1)-C(10)	1.420(5)
C(1)-N(1)	1.425(4)
C(2)-C(3)	1.412(5)
C(2)-H(2)	0.9500
C(3)-C(4)	1.362(5)
C(3)-H(3)	0.9500
C(4)-C(5)	1.424(5)
C(4)-H(4)	0.9500
C(5)-C(6)	1.418(5)
C(5)-C(10)	1.442(4)
C(6)-C(7)	1.362(5)
C(6)-H(6)	0.9500
C(7)-C(8)	1.404(5)
C(7)-H(7)	0.9500
C(8)-C(9)	1.391(5)
C(8)-H(8)	0.9500
C(9)-N(3)	1.403(4)
C(9)-C(10)	1.451(5)
C(11)-N(2)	1.301(4)
C(11)-N(1)	1.361(4)
C(11)-C(12)	1.493(5)
C(12)-H(12A)	0.9800
C(12)-H(12B)	0.9800
C(12)-H(12C)	0.9800
C(13)-C(18)	1.394(6)
C(13)-C(14)	1.415(6)
C(13)-N(2)	1.448(5)
C(14)-C(15)	1.392(6)
C(14)-C(19)	1.494(7)
C(15)-C(16)	1.375(8)
C(15)-H(15)	0.9500
C(16)-C(17)	1.369(8)
C(16)-H(16)	0.9500
C(17)-C(18)	1.401(6)
C(17)-H(17)	0.9500
C(18)-C(20)	1.481(6)
C(19)-H(19A)	0.9800
C(19)-H(19B)	0.9800
C(19)-H(19C)	0.9800
C(20)-H(20A)	0.9800
C(20)-H(20B)	0.9800
C(20)-H(20C)	0.9800
C(21)-N(3)	1.334(4)
C(21)-N(4)	1.337(4)
C(21)-C(22)	1.506(5)
C(22)-H(22A)	0.9800
C(22)-H(22B)	0.9800
C(22)-H(22C)	0.9800

C(23)-C(24)	1.400(5)
C(23)-C(28)	1.405(5)
C(23)-N(4)	1.432(4)
C(24)-C(25)	1.400(5)
C(24)-C(29)	1.507(5)
C(25)-C(26)	1.378(6)
C(25)-H(25)	0.9500
C(26)-C(27)	1.377(6)
C(26)-H(26)	0.9500
C(27)-C(28)	1.398(5)
C(27)-H(27)	0.9500
C(28)-C(30)	1.506(5)
C(29)-H(29A)	0.9800
C(29)-H(29B)	0.9800
C(29)-H(29C)	0.9800
C(30)-H(30A)	0.9800
C(30)-H(30B)	0.9800
C(30)-H(30C)	0.9800
C(31)-C(36)	1.389(5)
C(31)-C(32)	1.389(5)
C(31)-S(1)	1.779(4)
C(32)-C(33)	1.378(5)
C(32)-H(32)	0.9500
C(33)-C(34)	1.389(5)
C(33)-H(33)	0.9500
C(34)-C(35)	1.380(5)
C(34)-C(37)	1.510(5)
C(35)-C(36)	1.393(5)
C(35)-H(35)	0.9500
C(36)-H(36)	0.9500
C(37)-H(37A)	0.9800
C(37)-H(37B)	0.9800
C(37)-H(37C)	0.9800
C(38)-C(39)	1.387(5)
C(38)-C(43)	1.395(5)
C(38)-S(2)	1.771(4)
C(39)-C(40)	1.378(5)
C(39)-H(39)	0.9500
C(40)-C(41)	1.377(6)
C(40)-H(40)	0.9500
C(41)-C(42)	1.369(6)
C(41)-C(44)	1.558(7)
C(42)-C(43)	1.362(6)
C(42)-H(42)	0.9500
C(43)-H(43)	0.9500
C(44)-H(44A)	0.9800
C(44)-H(44B)	0.9800
C(44)-H(44C)	0.9800
N(1)-Sn(1)	2.132(3)
N(2)-Sn(1)	2.411(3)
N(3)-Sn(1)	2.230(3)
N(4)-Sn(1)	2.180(3)

S(1)-Sn(1)	2.4297(15)
S(2)-Sn(1)	2.4483(16)
C(2)-C(1)-C(10)	121.4(3)
C(2)-C(1)-N(1)	116.2(3)
C(10)-C(1)-N(1)	122.3(3)
C(1)-C(2)-C(3)	120.6(4)
C(1)-C(2)-H(2)	119.7
C(3)-C(2)-H(2)	119.7
C(4)-C(3)-C(2)	120.0(3)
C(4)-C(3)-H(3)	120.0
C(2)-C(3)-H(3)	120.0
C(3)-C(4)-C(5)	120.7(3)
C(3)-C(4)-H(4)	119.6
C(5)-C(4)-H(4)	119.6
C(6)-C(5)-C(4)	118.9(3)
C(6)-C(5)-C(10)	120.7(3)
C(4)-C(5)-C(10)	120.4(3)
C(7)-C(6)-C(5)	120.3(3)
C(7)-C(6)-H(6)	119.9
C(5)-C(6)-H(6)	119.9
C(6)-C(7)-C(8)	120.6(3)
C(6)-C(7)-H(7)	119.7
C(8)-C(7)-H(7)	119.7
C(9)-C(8)-C(7)	122.0(3)
C(9)-C(8)-H(8)	119.0
C(7)-C(8)-H(8)	119.0
C(8)-C(9)-N(3)	122.8(3)
C(8)-C(9)-C(10)	119.2(3)
N(3)-C(9)-C(10)	117.8(3)
C(1)-C(10)-C(5)	116.7(3)
C(1)-C(10)-C(9)	126.1(3)
C(5)-C(10)-C(9)	117.2(3)
N(2)-C(11)-N(1)	113.5(3)
N(2)-C(11)-C(12)	125.8(3)
N(1)-C(11)-C(12)	120.7(3)
C(11)-C(12)-H(12A)	109.5
C(11)-C(12)-H(12B)	109.5
H(12A)-C(12)-H(12B)	109.5
C(11)-C(12)-H(12C)	109.5
H(12A)-C(12)-H(12C)	109.5
H(12B)-C(12)-H(12C)	109.5
C(18)-C(13)-C(14)	122.0(4)
C(18)-C(13)-N(2)	119.0(4)
C(14)-C(13)-N(2)	118.9(4)
C(15)-C(14)-C(13)	117.3(5)
C(15)-C(14)-C(19)	120.8(5)
C(13)-C(14)-C(19)	121.9(4)
C(16)-C(15)-C(14)	121.6(5)
C(16)-C(15)-H(15)	119.2
C(14)-C(15)-H(15)	119.2
C(17)-C(16)-C(15)	120.1(5)

C(17)-C(16)-H(16)	120.0
C(15)-C(16)-H(16)	120.0
C(16)-C(17)-C(18)	121.6(6)
C(16)-C(17)-H(17)	119.2
C(18)-C(17)-H(17)	119.2
C(13)-C(18)-C(17)	117.5(5)
C(13)-C(18)-C(20)	122.0(4)
C(17)-C(18)-C(20)	120.5(5)
C(14)-C(19)-H(19A)	109.5
C(14)-C(19)-H(19B)	109.5
H(19A)-C(19)-H(19B)	109.5
C(14)-C(19)-H(19C)	109.5
H(19A)-C(19)-H(19C)	109.5
H(19B)-C(19)-H(19C)	109.5
C(18)-C(20)-H(20A)	109.5
C(18)-C(20)-H(20B)	109.5
H(20A)-C(20)-H(20B)	109.5
C(18)-C(20)-H(20C)	109.5
H(20A)-C(20)-H(20C)	109.5
H(20B)-C(20)-H(20C)	109.5
N(3)-C(21)-N(4)	110.6(3)
N(3)-C(21)-C(22)	128.0(3)
N(4)-C(21)-C(22)	121.3(3)
C(21)-C(22)-H(22A)	109.5
C(21)-C(22)-H(22B)	109.5
H(22A)-C(22)-H(22B)	109.5
C(21)-C(22)-H(22C)	109.5
H(22A)-C(22)-H(22C)	109.5
H(22B)-C(22)-H(22C)	109.5
C(24)-C(23)-C(28)	121.4(3)
C(24)-C(23)-N(4)	119.7(3)
C(28)-C(23)-N(4)	118.6(3)
C(25)-C(24)-C(23)	118.0(3)
C(25)-C(24)-C(29)	119.4(3)
C(23)-C(24)-C(29)	122.5(3)
C(26)-C(25)-C(24)	121.5(4)
C(26)-C(25)-H(25)	119.3
C(24)-C(25)-H(25)	119.3
C(27)-C(26)-C(25)	119.6(3)
C(27)-C(26)-H(26)	120.2
C(25)-C(26)-H(26)	120.2
C(26)-C(27)-C(28)	121.5(4)
C(26)-C(27)-H(27)	119.2
C(28)-C(27)-H(27)	119.2
C(27)-C(28)-C(23)	118.0(4)
C(27)-C(28)-C(30)	121.1(3)
C(23)-C(28)-C(30)	121.0(3)
C(24)-C(29)-H(29A)	109.5
C(24)-C(29)-H(29B)	109.5
H(29A)-C(29)-H(29B)	109.5
C(24)-C(29)-H(29C)	109.5
H(29A)-C(29)-H(29C)	109.5

H(29B)-C(29)-H(29C)	109.5
C(28)-C(30)-H(30A)	109.5
C(28)-C(30)-H(30B)	109.5
H(30A)-C(30)-H(30B)	109.5
C(28)-C(30)-H(30C)	109.5
H(30A)-C(30)-H(30C)	109.5
H(30B)-C(30)-H(30C)	109.5
C(36)-C(31)-C(32)	118.8(3)
C(36)-C(31)-S(1)	119.8(3)
C(32)-C(31)-S(1)	121.2(3)
C(33)-C(32)-C(31)	120.3(3)
C(33)-C(32)-H(32)	119.9
C(31)-C(32)-H(32)	119.9
C(32)-C(33)-C(34)	122.0(3)
C(32)-C(33)-H(33)	119.0
C(34)-C(33)-H(33)	119.0
C(35)-C(34)-C(33)	117.1(3)
C(35)-C(34)-C(37)	121.6(4)
C(33)-C(34)-C(37)	121.3(4)
C(34)-C(35)-C(36)	122.2(3)
C(34)-C(35)-H(35)	118.9
C(36)-C(35)-H(35)	118.9
C(31)-C(36)-C(35)	119.6(3)
C(31)-C(36)-H(36)	120.2
C(35)-C(36)-H(36)	120.2
C(34)-C(37)-H(37A)	109.5
C(34)-C(37)-H(37B)	109.5
H(37A)-C(37)-H(37B)	109.5
C(34)-C(37)-H(37C)	109.5
H(37A)-C(37)-H(37C)	109.5
H(37B)-C(37)-H(37C)	109.5
C(39)-C(38)-C(43)	118.0(3)
C(39)-C(38)-S(2)	122.0(3)
C(43)-C(38)-S(2)	119.7(3)
C(40)-C(39)-C(38)	120.7(4)
C(40)-C(39)-H(39)	119.7
C(38)-C(39)-H(39)	119.7
C(41)-C(40)-C(39)	120.6(4)
C(41)-C(40)-H(40)	119.7
C(39)-C(40)-H(40)	119.7
C(42)-C(41)-C(40)	118.6(4)
C(42)-C(41)-C(44)	122.2(5)
C(40)-C(41)-C(44)	119.1(5)
C(43)-C(42)-C(41)	121.7(4)
C(43)-C(42)-H(42)	119.1
C(41)-C(42)-H(42)	119.1
C(42)-C(43)-C(38)	120.3(4)
C(42)-C(43)-H(43)	119.8
C(38)-C(43)-H(43)	119.8
C(41)-C(44)-H(44A)	109.5
C(41)-C(44)-H(44B)	109.5
H(44A)-C(44)-H(44B)	109.5

C(41)-C(44)-H(44C)	109.5
H(44A)-C(44)-H(44C)	109.5
H(44B)-C(44)-H(44C)	109.5
C(11)-N(1)-C(1)	117.5(3)
C(11)-N(1)-Sn(1)	99.1(2)
C(1)-N(1)-Sn(1)	124.9(2)
C(11)-N(2)-C(13)	121.1(3)
C(11)-N(2)-Sn(1)	88.3(2)
C(13)-N(2)-Sn(1)	150.6(2)
C(21)-N(3)-C(9)	132.6(3)
C(21)-N(3)-Sn(1)	93.8(2)
C(9)-N(3)-Sn(1)	132.8(2)
C(21)-N(4)-C(23)	125.9(3)
C(21)-N(4)-Sn(1)	95.9(2)
C(23)-N(4)-Sn(1)	137.4(2)
C(31)-S(1)-Sn(1)	105.59(12)
C(38)-S(2)-Sn(1)	103.78(13)
N(1)-Sn(1)-N(4)	132.96(11)
N(1)-Sn(1)-N(3)	78.01(11)
N(4)-Sn(1)-N(3)	59.72(10)
N(1)-Sn(1)-N(2)	58.27(11)
N(4)-Sn(1)-N(2)	97.20(12)
N(3)-Sn(1)-N(2)	86.71(11)
N(1)-Sn(1)-S(1)	111.48(9)
N(4)-Sn(1)-S(1)	102.83(8)
N(3)-Sn(1)-S(1)	158.14(7)
N(2)-Sn(1)-S(1)	82.44(9)
N(1)-Sn(1)-S(2)	105.90(9)
N(4)-Sn(1)-S(2)	97.26(9)
N(3)-Sn(1)-S(2)	94.06(9)
N(2)-Sn(1)-S(2)	163.67(8)
S(1)-Sn(1)-S(2)	101.67(7)

Symmetry transformations used to generate equivalent atoms:

Table A28. Anisotropic displacement parameters ($\text{Å}^2 \times 10^3$) for 2a. The anisotropic displacement factor exponent takes the form: $-2 \pi^2 [h^2 a^* a^* U_{11} + \dots + 2 h k a^* b^* U_{12}]$

	U11	U22	U33	U23	U13	U12
C(1)	29(2)	30(2)	57(2)	10(2)	2(2)	6(1)
C(2)	40(2)	42(2)	66(3)	9(2)	13(2)	8(2)
C(3)	43(2)	38(2)	86(3)	7(2)	17(2)	11(2)
C(4)	44(2)	35(2)	72(3)	11(2)	8(2)	7(2)
C(5)	37(2)	32(2)	49(2)	5(1)	-1(2)	-2(1)
C(6)	52(2)	36(2)	50(2)	10(2)	4(2)	-1(2)
C(7)	57(2)	46(2)	50(2)	8(2)	14(2)	-6(2)
C(8)	47(2)	39(2)	44(2)	4(2)	7(2)	0(2)

C(9)	30(2)	32(2)	37(2)	3(1)	-5(1)	-3(1)
C(10)	30(2)	32(2)	41(2)	5(1)	-1(1)	2(1)
C(11)	27(2)	34(2)	55(2)	11(2)	-1(2)	0(1)
C(12)	37(2)	42(2)	91(3)	18(2)	-17(2)	1(2)
C(13)	34(2)	36(2)	74(3)	6(2)	-13(2)	1(2)
C(14)	30(2)	36(2)	107(4)	20(2)	-10(2)	0(2)
C(15)	39(2)	42(2)	151(5)	13(3)	-16(3)	-1(2)
C(16)	58(3)	46(3)	139(5)	-4(3)	-29(3)	-3(2)
C(17)	71(3)	59(3)	107(4)	-11(3)	-34(3)	4(3)
C(18)	55(3)	52(2)	70(3)	4(2)	-20(2)	2(2)
C(19)	37(2)	78(3)	118(5)	32(3)	9(3)	-8(2)
C(20)	91(4)	89(4)	57(3)	-1(3)	-8(3)	-2(3)
C(21)	29(2)	37(2)	42(2)	-1(1)	2(1)	1(1)
C(22)	61(3)	55(2)	54(2)	9(2)	22(2)	16(2)
C(23)	36(2)	37(2)	36(2)	0(1)	6(1)	10(1)
C(24)	37(2)	50(2)	39(2)	0(2)	7(2)	12(2)
C(25)	44(2)	70(3)	44(2)	1(2)	6(2)	27(2)
C(26)	69(3)	55(2)	57(3)	4(2)	14(2)	34(2)
C(27)	76(3)	37(2)	53(2)	3(2)	21(2)	15(2)
C(28)	54(2)	36(2)	40(2)	-2(2)	12(2)	10(2)
C(29)	33(2)	65(2)	60(2)	-9(2)	5(2)	3(2)
C(30)	56(3)	42(2)	73(3)	-14(2)	9(2)	-2(2)
C(31)	37(2)	37(2)	41(2)	7(1)	6(2)	2(1)
C(32)	48(2)	49(2)	36(2)	1(2)	8(2)	11(2)
C(33)	39(2)	54(2)	44(2)	9(2)	12(2)	12(2)
C(34)	41(2)	41(2)	41(2)	10(2)	3(2)	-4(2)
C(35)	64(3)	55(2)	35(2)	-4(2)	13(2)	1(2)
C(36)	48(2)	46(2)	48(2)	1(2)	14(2)	14(2)
C(37)	55(3)	70(3)	49(2)	12(2)	-5(2)	-8(2)
C(38)	45(2)	40(2)	42(2)	-5(2)	7(2)	-2(2)
C(39)	69(3)	48(2)	58(3)	12(2)	27(2)	2(2)
C(40)	99(4)	57(3)	81(3)	0(2)	55(3)	8(2)
C(41)	117(4)	39(2)	91(4)	-6(2)	45(3)	5(3)
C(42)	87(3)	42(2)	75(3)	8(2)	24(3)	-10(2)
C(43)	58(2)	48(2)	54(2)	-1(2)	16(2)	-11(2)
C(44)	228(9)	47(3)	225(9)	-10(4)	133(7)	29(4)
N(1)	30(1)	32(1)	49(2)	8(1)	3(1)	2(1)
N(2)	28(1)	39(2)	56(2)	10(1)	-4(1)	-3(1)
N(3)	30(1)	33(1)	39(2)	4(1)	3(1)	3(1)
N(4)	31(1)	32(1)	39(2)	2(1)	4(1)	7(1)
S(1)	35(1)	54(1)	51(1)	14(1)	0(1)	-2(1)
S(2)	41(1)	51(1)	66(1)	-16(1)	-10(1)	4(1)
Sn(1)	26(1)	33(1)	38(1)	2(1)	1(1)	4(1)

A28. Crystal data and structure refinement of 3b.

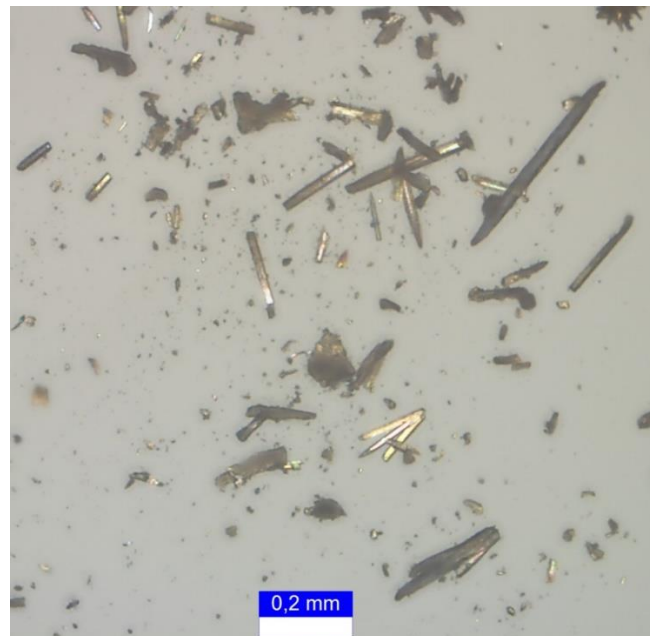


Figure S64. Sample of 3b.

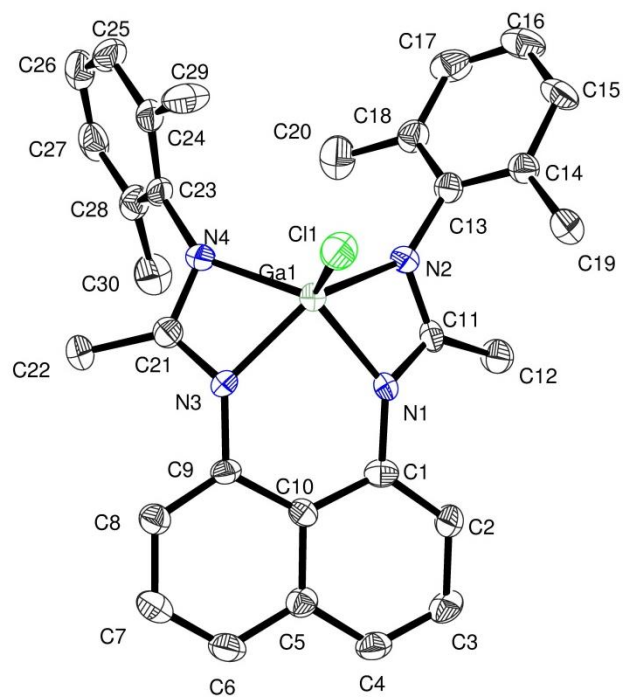


Figure S65. Asymmetric Unit of 3b.

Table A29. Crystal data and structure refinement for 3b.

Identification code	3b
Empirical formula	C30 H30 Cl Ga N4
Formula weight	551.75
Temperature	193(2) K
Wavelength	0.71073 Å
Crystal system, space group	Monoclinic, P 21/c
Unit cell dimensions	a = 10.208(2) Å alpha = 90 deg. b = 19.494(4) Å beta = 90.929(7) deg. c = 13.220(3) Å gamma = 90 deg.
Volume	2630.4(10) Å^3
Z, Calculated density	4, 1.393 Mg/m^3
Absorption coefficient	1.174 mm^-1
F(000)	1144
Crystal size	0.100 x 0.040 x 0.040 mm
Theta range for data collection	3.255 to 24.147 deg.
Limiting indices	-11<=h<=11, -22<=k<=21, -15<=l<=15
Reflections collected / unique	26145 / 4150 [R(int) = 0.1436]
Completeness to theta = 25.242	98.7 %
Refinement method	Full-matrix least-squares on F^2
Data / restraints / parameters	4150 / 0 / 331
Goodness-of-fit on F^2	1.010
Final R indices [I>2sigma(I)]	R1 = 0.0502, wR2 = 0.0863
R indices (all data)	R1 = 0.1078, wR2 = 0.1079
Largest diff. peak and hole	0.447 and -0.523 e.Å^-3

Table A30. Atomic coordinates (x 10^4) and equivalent isotropic displacement parameters (Å^2 x 10^3) for 3b. U(eq) is defined as one third of the trace of the orthogonalized Uij tensor.

	x	y	z	U(eq)
C(1)	794(5)	4090(2)	5502(3)	24(1)
C(2)	-495(5)	4091(3)	5177(4)	29(1)
C(3)	-864(5)	4177(2)	4165(4)	30(1)
C(4)	81(5)	4279(2)	3470(4)	31(1)
C(5)	1417(5)	4316(2)	3747(4)	26(1)

C(6)	2352(5)	4442(3)	2991(4)	33(1)
C(7)	3651(5)	4491(3)	3232(4)	34(1)
C(8)	4072(5)	4419(2)	4234(4)	27(1)
C(9)	3212(5)	4270(2)	5002(3)	23(1)
C(10)	1825(5)	4219(2)	4782(3)	21(1)
C(11)	580(5)	3659(2)	7257(4)	24(1)
C(12)	-697(5)	3284(3)	7223(4)	34(1)
C(13)	1038(5)	3471(2)	9078(4)	26(1)
C(14)	121(5)	3868(2)	9593(4)	26(1)
C(15)	-103(5)	3716(3)	10601(4)	36(1)
C(16)	541(6)	3193(3)	11090(4)	43(2)
C(17)	1426(6)	2799(3)	10565(4)	40(2)
C(18)	1695(5)	2930(3)	9559(4)	31(1)
C(19)	-607(5)	4450(3)	9077(4)	35(1)
C(20)	2662(5)	2501(3)	9001(4)	46(2)
C(21)	4693(5)	3837(2)	6356(4)	26(1)
C(22)	5883(5)	3640(3)	5775(4)	33(1)
C(23)	5439(5)	3287(3)	7938(4)	28(1)
C(24)	6011(5)	3565(3)	8807(4)	32(1)
C(25)	6882(5)	3166(3)	9366(4)	40(2)
C(26)	7205(5)	2516(3)	9069(4)	43(2)
C(27)	6589(5)	2231(3)	8240(4)	40(2)
C(28)	5671(5)	2600(3)	7668(4)	32(1)
C(29)	5666(6)	4275(3)	9151(4)	46(2)
C(30)	4939(6)	2248(3)	6824(4)	45(2)
N(1)	1147(4)	4005(2)	6526(3)	24(1)
N(2)	1397(4)	3646(2)	8065(3)	25(1)
N(3)	3659(4)	4180(2)	6006(3)	24(1)
N(4)	4550(4)	3696(2)	7342(3)	25(1)
Cl(1)	2899(1)	5202(1)	8016(1)	35(1)
Ga(1)	2771(1)	4185(1)	7328(1)	24(1)

Table A31. Bond lengths [Å] and angles [deg] for 3b.

C(1)-C(2)	1.378(6)
C(1)-N(1)	1.406(6)
C(1)-C(10)	1.452(6)
C(2)-C(3)	1.394(6)
C(2)-H(2)	0.9500
C(3)-C(4)	1.359(6)
C(3)-H(3)	0.9500
C(4)-C(5)	1.408(7)
C(4)-H(4)	0.9500
C(5)-C(6)	1.414(6)
C(5)-C(10)	1.437(6)
C(6)-C(7)	1.362(7)
C(6)-H(6)	0.9500
C(7)-C(8)	1.393(7)
C(7)-H(7)	0.9500
C(8)-C(9)	1.384(6)

C(8)-H(8)	0.9500
C(9)-N(3)	1.408(6)
C(9)-C(10)	1.445(6)
C(11)-N(1)	1.320(5)
C(11)-N(2)	1.345(6)
C(11)-C(12)	1.494(6)
C(11)-Ga(1)	2.462(5)
C(12)-H(12A)	0.9800
C(12)-H(12B)	0.9800
C(12)-H(12C)	0.9800
C(13)-C(18)	1.397(7)
C(13)-C(14)	1.399(6)
C(13)-N(2)	1.435(6)
C(14)-C(15)	1.388(6)
C(14)-C(19)	1.513(7)
C(15)-C(16)	1.370(7)
C(15)-H(15)	0.9500
C(16)-C(17)	1.382(7)
C(16)-H(16)	0.9500
C(17)-C(18)	1.386(7)
C(17)-H(17)	0.9500
C(18)-C(20)	1.498(7)
C(19)-H(19A)	0.9800
C(19)-H(19B)	0.9800
C(19)-H(19C)	0.9800
C(20)-H(20A)	0.9800
C(20)-H(20B)	0.9800
C(20)-H(20C)	0.9800
C(21)-N(3)	1.327(6)
C(21)-N(4)	1.342(6)
C(21)-C(22)	1.498(6)
C(21)-Ga(1)	2.458(5)
C(22)-H(22A)	0.9800
C(22)-H(22B)	0.9800
C(22)-H(22C)	0.9800
C(23)-C(24)	1.391(7)
C(23)-C(28)	1.407(7)
C(23)-N(4)	1.433(6)
C(24)-C(25)	1.385(7)
C(24)-C(29)	1.501(7)
C(25)-C(26)	1.368(8)
C(25)-H(25)	0.9500
C(26)-C(27)	1.373(8)
C(26)-H(26)	0.9500
C(27)-C(28)	1.395(7)
C(27)-H(27)	0.9500
C(28)-C(30)	1.499(7)
C(29)-H(29A)	0.9800
C(29)-H(29B)	0.9800
C(29)-H(29C)	0.9800
C(30)-H(30A)	0.9800
C(30)-H(30B)	0.9800

C(30)-H(30C)	0.9800
N(1)-Ga(1)	1.984(4)
N(2)-Ga(1)	2.017(4)
N(3)-Ga(1)	1.981(4)
N(4)-Ga(1)	2.051(4)
Cl(1)-Ga(1)	2.1828(14)
C(2)-C(1)-N(1)	121.9(4)
C(2)-C(1)-C(10)	119.6(4)
N(1)-C(1)-C(10)	118.3(4)
C(1)-C(2)-C(3)	122.7(5)
C(1)-C(2)-H(2)	118.6
C(3)-C(2)-H(2)	118.6
C(4)-C(3)-C(2)	118.9(5)
C(4)-C(3)-H(3)	120.5
C(2)-C(3)-H(3)	120.5
C(3)-C(4)-C(5)	121.8(5)
C(3)-C(4)-H(4)	119.1
C(5)-C(4)-H(4)	119.1
C(4)-C(5)-C(6)	119.1(5)
C(4)-C(5)-C(10)	120.3(4)
C(6)-C(5)-C(10)	120.5(4)
C(7)-C(6)-C(5)	120.8(5)
C(7)-C(6)-H(6)	119.6
C(5)-C(6)-H(6)	119.6
C(6)-C(7)-C(8)	119.9(5)
C(6)-C(7)-H(7)	120.0
C(8)-C(7)-H(7)	120.0
C(9)-C(8)-C(7)	122.0(5)
C(9)-C(8)-H(8)	119.0
C(7)-C(8)-H(8)	119.0
C(8)-C(9)-N(3)	121.3(4)
C(8)-C(9)-C(10)	119.9(4)
N(3)-C(9)-C(10)	118.8(4)
C(5)-C(10)-C(9)	116.7(4)
C(5)-C(10)-C(1)	116.5(4)
C(9)-C(10)-C(1)	126.8(4)
N(1)-C(11)-N(2)	108.5(4)
N(1)-C(11)-C(12)	128.4(5)
N(2)-C(11)-C(12)	122.9(4)
N(1)-C(11)-Ga(1)	53.5(2)
N(2)-C(11)-Ga(1)	55.0(2)
C(12)-C(11)-Ga(1)	175.4(4)
C(11)-C(12)-H(12A)	109.5
C(11)-C(12)-H(12B)	109.5
H(12A)-C(12)-H(12B)	109.5
C(11)-C(12)-H(12C)	109.5
H(12A)-C(12)-H(12C)	109.5
H(12B)-C(12)-H(12C)	109.5
C(18)-C(13)-C(14)	121.1(5)
C(18)-C(13)-N(2)	118.4(4)
C(14)-C(13)-N(2)	120.3(4)

C(15)-C(14)-C(13)	118.1(5)
C(15)-C(14)-C(19)	120.4(5)
C(13)-C(14)-C(19)	121.6(4)
C(16)-C(15)-C(14)	121.8(5)
C(16)-C(15)-H(15)	119.1
C(14)-C(15)-H(15)	119.1
C(15)-C(16)-C(17)	119.3(5)
C(15)-C(16)-H(16)	120.4
C(17)-C(16)-H(16)	120.4
C(16)-C(17)-C(18)	121.4(5)
C(16)-C(17)-H(17)	119.3
C(18)-C(17)-H(17)	119.3
C(17)-C(18)-C(13)	118.4(5)
C(17)-C(18)-C(20)	120.7(5)
C(13)-C(18)-C(20)	120.9(5)
C(14)-C(19)-H(19A)	109.5
C(14)-C(19)-H(19B)	109.5
H(19A)-C(19)-H(19B)	109.5
C(14)-C(19)-H(19C)	109.5
H(19A)-C(19)-H(19C)	109.5
H(19B)-C(19)-H(19C)	109.5
C(18)-C(20)-H(20A)	109.5
C(18)-C(20)-H(20B)	109.5
H(20A)-C(20)-H(20B)	109.5
C(18)-C(20)-H(20C)	109.5
H(20A)-C(20)-H(20C)	109.5
H(20B)-C(20)-H(20C)	109.5
N(3)-C(21)-N(4)	110.1(4)
N(3)-C(21)-C(22)	126.7(4)
N(4)-C(21)-C(22)	123.2(5)
N(3)-C(21)-Ga(1)	53.5(2)
N(4)-C(21)-Ga(1)	56.6(2)
C(22)-C(21)-Ga(1)	178.5(4)
C(21)-C(22)-H(22A)	109.5
C(21)-C(22)-H(22B)	109.5
H(22A)-C(22)-H(22B)	109.5
C(21)-C(22)-H(22C)	109.5
H(22A)-C(22)-H(22C)	109.5
H(22B)-C(22)-H(22C)	109.5
C(24)-C(23)-C(28)	120.7(5)
C(24)-C(23)-N(4)	119.4(5)
C(28)-C(23)-N(4)	119.9(5)
C(25)-C(24)-C(23)	118.7(5)
C(25)-C(24)-C(29)	120.5(5)
C(23)-C(24)-C(29)	120.8(5)
C(26)-C(25)-C(24)	121.5(6)
C(26)-C(25)-H(25)	119.3
C(24)-C(25)-H(25)	119.3
C(25)-C(26)-C(27)	119.7(6)
C(25)-C(26)-H(26)	120.2
C(27)-C(26)-H(26)	120.2
C(26)-C(27)-C(28)	121.3(5)

C(26)-C(27)-H(27)	119.4
C(28)-C(27)-H(27)	119.4
C(27)-C(28)-C(23)	117.9(5)
C(27)-C(28)-C(30)	119.3(5)
C(23)-C(28)-C(30)	122.7(5)
C(24)-C(29)-H(29A)	109.5
C(24)-C(29)-H(29B)	109.5
H(29A)-C(29)-H(29B)	109.5
C(24)-C(29)-H(29C)	109.5
H(29A)-C(29)-H(29C)	109.5
H(29B)-C(29)-H(29C)	109.5
C(28)-C(30)-H(30A)	109.5
C(28)-C(30)-H(30B)	109.5
H(30A)-C(30)-H(30B)	109.5
C(28)-C(30)-H(30C)	109.5
H(30A)-C(30)-H(30C)	109.5
H(30B)-C(30)-H(30C)	109.5
C(11)-N(1)-C(1)	131.0(4)
C(11)-N(1)-Ga(1)	94.2(3)
C(1)-N(1)-Ga(1)	133.8(3)
C(11)-N(2)-C(13)	125.6(4)
C(11)-N(2)-Ga(1)	91.9(3)
C(13)-N(2)-Ga(1)	139.9(3)
C(21)-N(3)-C(9)	129.4(4)
C(21)-N(3)-Ga(1)	93.9(3)
C(9)-N(3)-Ga(1)	133.3(3)
C(21)-N(4)-C(23)	124.7(4)
C(21)-N(4)-Ga(1)	90.3(3)
C(23)-N(4)-Ga(1)	144.7(3)
N(3)-Ga(1)-N(1)	85.32(15)
N(3)-Ga(1)-N(2)	139.06(16)
N(1)-Ga(1)-N(2)	65.43(16)
N(3)-Ga(1)-N(4)	65.69(15)
N(1)-Ga(1)-N(4)	130.88(15)
N(2)-Ga(1)-N(4)	112.06(16)
N(3)-Ga(1)-Cl(1)	110.32(12)
N(1)-Ga(1)-Cl(1)	115.30(11)
N(2)-Ga(1)-Cl(1)	107.98(12)
N(4)-Ga(1)-Cl(1)	111.79(12)
N(3)-Ga(1)-C(21)	32.59(15)
N(1)-Ga(1)-C(21)	109.82(16)
N(2)-Ga(1)-C(21)	132.52(16)
N(4)-Ga(1)-C(21)	33.10(15)
Cl(1)-Ga(1)-C(21)	115.20(12)
N(3)-Ga(1)-C(11)	113.13(16)
N(1)-Ga(1)-C(11)	32.32(15)
N(2)-Ga(1)-C(11)	33.11(15)
N(4)-Ga(1)-C(11)	127.61(16)
Cl(1)-Ga(1)-C(11)	116.26(11)
C(21)-Ga(1)-C(11)	126.69(16)

Symmetry transformations used to generate equivalent atoms:

Table A32. Anisotropic displacement parameters ($\text{A}^2 \times 10^3$) for 3b. The anisotropic displacement factor exponent takes the form: $-2 \pi^2 [h^2 a^{*2} U_{11} + \dots + 2 h k a^* b^* U_{12}]$

	U11	U22	U33	U23	U13	U12
C(1)	30(3)	21(3)	22(3)	-4(2)	-4(2)	-4(2)
C(2)	20(3)	38(3)	29(3)	-1(3)	1(2)	-4(3)
C(3)	25(3)	32(3)	31(3)	-10(3)	-10(3)	-4(3)
C(4)	34(3)	34(3)	23(3)	-3(3)	-7(3)	5(3)
C(5)	26(3)	26(3)	24(3)	-4(2)	-3(2)	-1(2)
C(6)	40(4)	38(3)	20(3)	2(2)	-1(3)	2(3)
C(7)	41(4)	37(3)	23(3)	3(3)	6(3)	0(3)
C(8)	27(3)	30(3)	24(3)	-1(2)	1(2)	-2(2)
C(9)	23(3)	28(3)	18(3)	0(2)	-4(2)	-2(2)
C(10)	25(3)	18(3)	19(3)	-3(2)	2(2)	0(2)
C(11)	19(3)	27(3)	25(3)	-6(3)	6(3)	-2(2)
C(12)	29(3)	41(3)	33(3)	2(3)	2(3)	-10(3)
C(13)	21(3)	30(3)	26(3)	1(3)	1(2)	-7(3)
C(14)	26(3)	28(3)	25(3)	1(2)	1(3)	-4(3)
C(15)	44(4)	45(4)	20(3)	-1(3)	8(3)	-12(3)
C(16)	57(4)	46(4)	25(3)	7(3)	1(3)	-13(3)
C(17)	47(4)	38(4)	35(3)	16(3)	-7(3)	-6(3)
C(18)	28(3)	30(3)	33(3)	6(3)	0(3)	1(3)
C(19)	35(3)	42(3)	29(3)	-3(3)	7(3)	2(3)
C(20)	42(4)	40(4)	58(4)	15(3)	9(3)	4(3)
C(21)	24(3)	29(3)	25(3)	-3(2)	0(3)	-6(3)
C(22)	25(3)	45(3)	30(3)	-2(3)	7(3)	3(3)
C(23)	19(3)	39(4)	25(3)	11(3)	1(3)	3(3)
C(24)	21(3)	44(4)	29(3)	8(3)	4(3)	1(3)
C(25)	28(3)	57(4)	34(3)	19(3)	-5(3)	-2(3)
C(26)	29(3)	55(4)	46(4)	29(3)	9(3)	8(3)
C(27)	35(4)	42(4)	42(4)	16(3)	14(3)	5(3)
C(28)	25(3)	33(3)	39(3)	4(3)	1(3)	-5(3)
C(29)	54(4)	55(4)	30(3)	0(3)	-15(3)	4(3)
C(30)	47(4)	39(4)	51(4)	1(3)	6(3)	2(3)
N(1)	19(2)	33(3)	20(2)	4(2)	5(2)	1(2)
N(2)	24(2)	32(3)	20(2)	4(2)	1(2)	-1(2)
N(3)	18(2)	33(2)	21(2)	1(2)	-2(2)	4(2)
N(4)	25(3)	30(3)	19(2)	-1(2)	0(2)	3(2)
Cl(1)	33(1)	35(1)	36(1)	-7(1)	-3(1)	3(1)
Ga(1)	19(1)	30(1)	21(1)	0(1)	1(1)	0(1)

A29. Crystal data and structure refinement of 3c.



Figure S66. Sample of 3c.

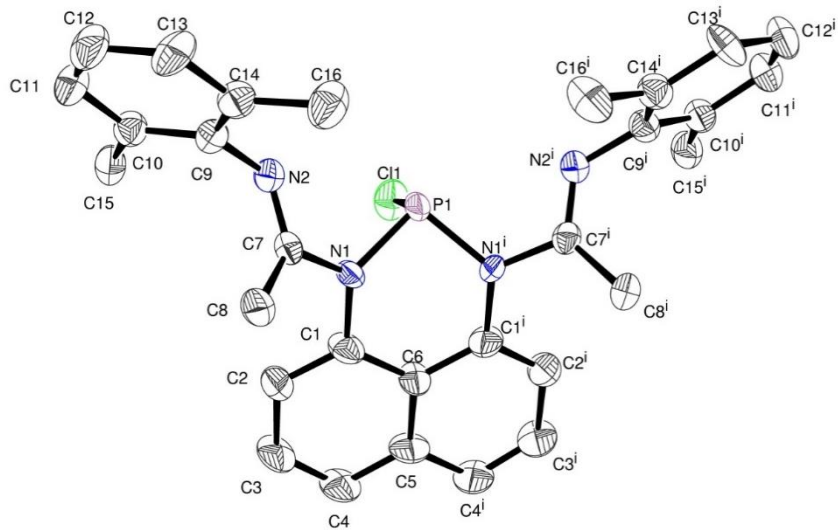


Figure S67. Compound 3c.

Table A33. Crystal data and structure refinement for 3c.

Identification code	3c
Empirical formula	C ₃₀ H ₃₀ ClN ₄ P
Formula weight	513.00
Temperature	193(2) K

Wavelength	0.71073 Å
Crystal system, space group	Orthorhombic, P m n 21
Unit cell dimensions	a = 24.654(7) Å alpha = 90 deg. b = 9.373(3) Å beta = 90 deg. c = 5.8749(18) Å gamma = 90 deg.
Volume	1357.6(7) Å ³
Z, Calculated density	2, 1.255 Mg/m ³
Absorption coefficient	0.225 mm ⁻¹
F(000)	540
Crystal size	0.200 x 0.200 x 0.200 mm
Theta range for data collection	2.325 to 24.525 deg.
Limiting indices	-28<=h<=28, -10<=k<=10, -6<=l<=6
Reflections collected / unique	30903 / 2301 [R(int) = 0.2318]
Completeness to theta = 25.242	99.4 %
Refinement method	Full-matrix least-squares on F ²
Data / restraints / parameters	2301 / 1 / 172
Goodness-of-fit on F ²	1.073
Final R indices [I>2sigma(I)]	R1 = 0.0817, wR2 = 0.1887
R indices (all data)	R1 = 0.1280, wR2 = 0.2250
Absolute structure parameter	0.07(11)
Largest diff. peak and hole	1.307 and -0.529 e.Å ⁻³

Table A34. Atomic coordinates (x 10⁴) and equivalent isotropic displacement parameters (Å² x 10³) for 3c. U(eq) is defined as one third of the trace of the orthogonalized Uij tensor.

	x	y	z	U(eq)
C(1)	5511(4)	7365(9)	4926(18)	39(2)
C(2)	5986(4)	8075(10)	4550(20)	46(3)
C(3)	5976(4)	9548(10)	4280(20)	49(3)
C(4)	5502(4)	10278(10)	4260(20)	47(3)
C(5)	5000	9559(13)	4410(30)	45(4)
C(6)	5000	8064(13)	4820(30)	35(3)
C(7)	5983(3)	5160(9)	6163(16)	29(2)
C(8)	6268(4)	5820(11)	8209(19)	42(3)
C(9)	6508(4)	3081(9)	6169(17)	32(2)
C(10)	7018(3)	3082(10)	5041(17)	34(2)
C(11)	7415(4)	2169(11)	5840(20)	46(3)
C(12)	7330(4)	1298(12)	7710(20)	50(3)

C(13)	6830(4)	1298(11)	8712(19)	47(3)
C(14)	6410(4)	2186(10)	8028(17)	37(2)
C(15)	7114(4)	4037(11)	3080(20)	44(3)
C(16)	5867(4)	2149(12)	9140(20)	52(3)
N(1)	5512(3)	5857(7)	5309(12)	28(2)
P(1)	5000	4762(3)	4477(7)	35(1)
Cl(1)	5000	5218(4)	972(6)	48(1)
N(2)	6087(3)	3963(8)	5247(14)	35(2)

Table A35. Bond lengths [Å] and angles [deg] for 3c.

C(1)-C(2)	1.367(13)
C(1)-C(6)	1.420(11)
C(1)-N(1)	1.431(11)
C(2)-C(3)	1.390(13)
C(2)-H(2)	0.9500
C(3)-C(4)	1.355(14)
C(3)-H(3)	0.9500
C(4)-C(5)	1.412(11)
C(4)-H(4)	0.9500
C(5)-C(6)	1.422(17)
C(7)-N(2)	1.271(11)
C(7)-N(1)	1.424(11)
C(7)-C(8)	1.524(14)
C(8)-H(8A)	0.9800
C(8)-H(8B)	0.9800
C(8)-H(8C)	0.9800
C(9)-C(14)	1.399(14)
C(9)-C(10)	1.421(12)
C(9)-N(2)	1.432(11)
C(10)-C(11)	1.382(13)
C(10)-C(15)	1.478(15)
C(11)-C(12)	1.384(17)
C(11)-H(11)	0.9500
C(12)-C(13)	1.366(15)
C(12)-H(12)	0.9500
C(13)-C(14)	1.388(13)
C(13)-H(13)	0.9500
C(14)-C(16)	1.490(13)
C(15)-H(15A)	0.9800
C(15)-H(15B)	0.9800
C(15)-H(15C)	0.9800
C(16)-H(16A)	0.9800
C(16)-H(16B)	0.9800
C(16)-H(16C)	0.9800
N(1)-P(1)	1.699(7)
P(1)-Cl(1)	2.103(5)
C(2)-C(1)-C(6)	121.9(9)
C(2)-C(1)-N(1)	120.3(8)

C(6)-C(1)-N(1)	117.7(8)
C(1)-C(2)-C(3)	119.1(9)
C(1)-C(2)-H(2)	120.4
C(3)-C(2)-H(2)	120.4
C(4)-C(3)-C(2)	121.2(9)
C(4)-C(3)-H(3)	119.4
C(2)-C(3)-H(3)	119.4
C(3)-C(4)-C(5)	121.0(9)
C(3)-C(4)-H(4)	119.5
C(5)-C(4)-H(4)	119.5
C(4)-C(5)-C(4)#1	122.5(12)
C(4)-C(5)-C(6)	118.7(6)
C(4)#1-C(5)-C(6)	118.7(6)
C(1)-C(6)-C(1)#1	124.8(11)
C(1)-C(6)-C(5)	117.5(5)
C(1)#1-C(6)-C(5)	117.5(5)
N(2)-C(7)-N(1)	114.9(8)
N(2)-C(7)-C(8)	126.8(8)
N(1)-C(7)-C(8)	117.9(8)
C(7)-C(8)-H(8A)	109.5
C(7)-C(8)-H(8B)	109.5
H(8A)-C(8)-H(8B)	109.5
C(7)-C(8)-H(8C)	109.5
H(8A)-C(8)-H(8C)	109.5
H(8B)-C(8)-H(8C)	109.5
C(14)-C(9)-C(10)	121.2(8)
C(14)-C(9)-N(2)	121.1(8)
C(10)-C(9)-N(2)	117.6(8)
C(11)-C(10)-C(9)	117.8(9)
C(11)-C(10)-C(15)	121.8(9)
C(9)-C(10)-C(15)	120.3(8)
C(10)-C(11)-C(12)	121.9(9)
C(10)-C(11)-H(11)	119.0
C(12)-C(11)-H(11)	119.0
C(13)-C(12)-C(11)	118.5(10)
C(13)-C(12)-H(12)	120.7
C(11)-C(12)-H(12)	120.7
C(12)-C(13)-C(14)	123.3(10)
C(12)-C(13)-H(13)	118.4
C(14)-C(13)-H(13)	118.4
C(13)-C(14)-C(9)	117.2(9)
C(13)-C(14)-C(16)	121.9(9)
C(9)-C(14)-C(16)	120.8(8)
C(10)-C(15)-H(15A)	109.5
C(10)-C(15)-H(15B)	109.5
H(15A)-C(15)-H(15B)	109.5
C(10)-C(15)-H(15C)	109.5
H(15A)-C(15)-H(15C)	109.5
H(15B)-C(15)-H(15C)	109.5
C(14)-C(16)-H(16A)	109.5
C(14)-C(16)-H(16B)	109.5
H(16A)-C(16)-H(16B)	109.5

C(14)-C(16)-H(16C)	109.5
H(16A)-C(16)-H(16C)	109.5
H(16B)-C(16)-H(16C)	109.5
C(7)-N(1)-C(1)	120.7(7)
C(7)-N(1)-P(1)	115.5(5)
C(1)-N(1)-P(1)	123.4(6)
N(1)#1-P(1)-N(1)	96.0(5)
N(1)#1-P(1)-Cl(1)	99.1(3)
N(1)-P(1)-Cl(1)	99.1(3)
C(7)-N(2)-C(9)	119.7(8)

Symmetry transformations used to generate equivalent atoms: #1 -x+1,y,z

Table A36. Anisotropic displacement parameters ($\text{Å}^2 \times 10^3$) for 3c. The anisotropic displacement factor exponent takes the form: $-2 \pi^2 [h^2 a^* a^* U_{11} + \dots + 2 h k a^* b^* U_{12}]$

	U11	U22	U33	U23	U13	U12
C(1)	41(6)	25(5)	50(7)	8(5)	-5(5)	-6(4)
C(2)	34(5)	35(5)	69(8)	1(6)	3(6)	-6(4)
C(3)	50(7)	30(5)	67(7)	18(6)	4(6)	-14(5)
C(4)	58(7)	23(5)	61(7)	14(5)	-2(6)	-6(5)
C(5)	57(9)	20(6)	57(9)	9(7)	0	0
C(6)	33(7)	25(7)	46(9)	16(6)	0	0
C(7)	24(5)	31(5)	31(5)	3(5)	1(4)	-5(4)
C(8)	29(5)	42(6)	56(7)	-6(5)	-9(5)	-2(5)
C(9)	30(5)	33(5)	32(5)	-1(5)	0(4)	3(4)
C(10)	32(5)	35(5)	37(6)	3(4)	0(4)	1(4)
C(11)	32(6)	48(6)	57(7)	-2(6)	-1(6)	11(5)
C(12)	35(6)	52(7)	61(7)	-1(6)	-11(6)	17(5)
C(13)	48(7)	44(6)	49(7)	15(5)	-3(5)	23(5)
C(14)	38(5)	36(5)	36(6)	1(5)	-2(5)	3(5)
C(15)	29(5)	49(6)	54(6)	1(6)	4(5)	2(5)
C(16)	48(7)	52(6)	57(7)	17(6)	15(6)	11(5)
N(1)	23(4)	23(4)	38(5)	-1(3)	-6(3)	-4(3)
P(1)	19(2)	22(2)	66(3)	3(2)	0	0
Cl(1)	40(2)	66(2)	38(2)	-9(2)	0	0
N(2)	26(4)	33(4)	48(5)	-1(4)	-3(4)	2(3)

A30. Crystal data and structure refinement of 3d.

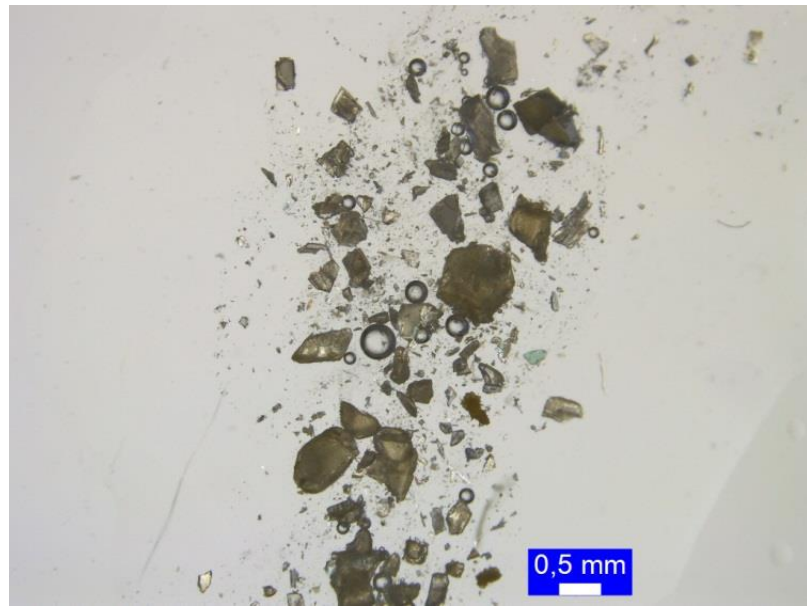


Figure S68. Sample of 3d.

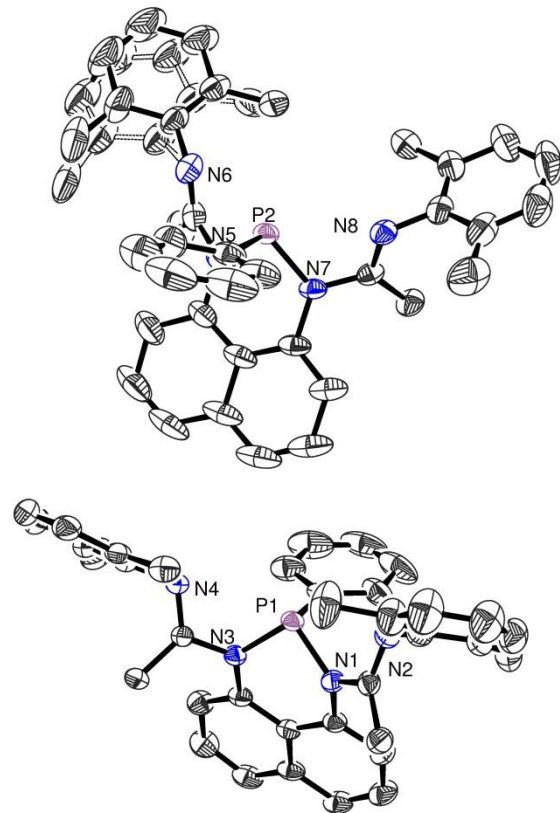


Figure S69. Asymmetric unit of 3d.

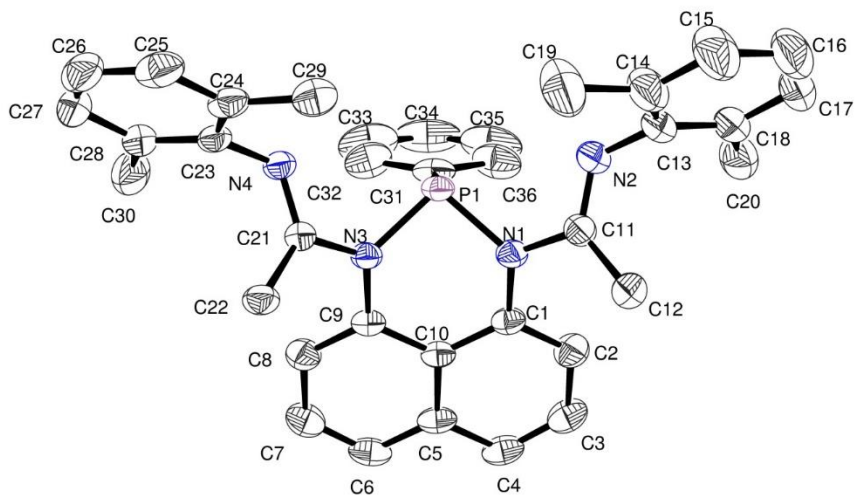


Figure S70. Compound 3d.

Table A37. Crystal data and structure refinement for 3d.

Identification code	3d
Empirical formula	C ₃₆ H ₃₅ N ₄ P
Formula weight	554.65
Temperature	193(2) K
Wavelength	0.71073 Å
Crystal system, space group	Triclinic, P -1
Unit cell dimensions	a = 14.874(2) Å alpha = 88.252(5) deg. b = 15.358(3) Å beta = 89.683(5) deg. c = 17.869(3) Å gamma = 65.830(5) deg.
Volume	3722.2(11) Å ³
Z, Calculated density	4, 0.990 Mg/m ³
Absorption coefficient	0.099 mm ⁻¹
F(000)	1176
Crystal size	0.400 x 0.280 x 0.200 mm
Theta range for data collection	2.481 to 29.872 deg.
Limiting indices	-20<=h<=20, -21<=k<=21, -25<=l<=25
Reflections collected / unique	232160 / 21313 [R(int) = 0.0700]
Completeness to theta = 25.242	99.5 %
Refinement method	Full-matrix least-squares on F ²
Data / restraints / parameters	21313 / 291 / 823

Goodness-of-fit on F^2	1.020
Final R indices [I>2sigma(I)]	R1 = 0.0565, wR2 = 0.1619
R indices (all data)	R1 = 0.0794, wR2 = 0.1800
Largest diff. peak and hole	0.432 and -0.266 e.Å^-3

Table A38. Atomic coordinates ($\times 10^4$) and equivalent isotropic displacement parameters ($\text{Å}^2 \times 10^3$) for 3d. U(eq) is defined as one third of the trace of the orthogonalized U_{ij} tensor.

	x	y	z	U(eq)
C(1)	6834(1)	6364(1)	5601(1)	31(1)
C(2)	6932(1)	7080(1)	5997(1)	41(1)
C(3)	7290(1)	6906(1)	6742(1)	47(1)
C(4)	7574(1)	6023(1)	7081(1)	42(1)
C(5)	7555(1)	5252(1)	6673(1)	36(1)
C(6)	7930(1)	4316(1)	6996(1)	44(1)
C(7)	7977(1)	3564(1)	6588(1)	47(1)
C(8)	7623(1)	3713(1)	5841(1)	40(1)
C(9)	7196(1)	4622(1)	5520(1)	31(1)
C(10)	7177(1)	5420(1)	5921(1)	30(1)
C(11)	5798(1)	7468(1)	4609(1)	34(1)
C(12)	5007(1)	8086(1)	5129(1)	41(1)
C(13)	5200(2)	8561(1)	3604(1)	47(1)
C(14)	4421(2)	8550(2)	3171(1)	62(1)
C(15)	3776(2)	9403(2)	2831(2)	81(1)
C(16)	3891(2)	10247(2)	2912(2)	78(1)
C(17)	4679(2)	10241(1)	3326(1)	64(1)
C(18)	5345(2)	9403(1)	3676(1)	51(1)
C(19)	4307(2)	7621(2)	3070(2)	83(1)
C(20)	6220(2)	9393(2)	4106(1)	61(1)
C(21)	6476(1)	4113(1)	4478(1)	29(1)
C(22)	5847(1)	3760(1)	4960(1)	38(1)
C(23)	6279(1)	3326(1)	3437(1)	34(1)
C(24)	5395(1)	3763(1)	3032(1)	39(1)
C(25)	5055(2)	3174(2)	2647(1)	51(1)
C(26)	5576(2)	2205(2)	2653(1)	59(1)
C(27)	6459(2)	1784(2)	3042(1)	56(1)
C(28)	6828(1)	2337(1)	3441(1)	43(1)
C(29)	4841(1)	4829(1)	3003(1)	45(1)
C(30)	7807(2)	1893(1)	3849(1)	63(1)
C(31)	8139(1)	5391(1)	4168(1)	41(1)
C(32)	8808(1)	4457(2)	4067(1)	57(1)
C(33)	9811(2)	4256(2)	3995(2)	82(1)
C(34)	10131(2)	4966(3)	4009(1)	87(1)
C(35)	9472(2)	5895(3)	4091(1)	84(1)
C(36)	8464(2)	6119(2)	4171(1)	60(1)
C(37)	8380(1)	3302(2)	383(1)	47(1)

C(38)	8391(2)	2439(2)	655(1)	69(1)
C(39)	8116(2)	2351(2)	1400(2)	84(1)
C(40)	7801(2)	3104(2)	1843(1)	76(1)
C(41)	7732(1)	4012(2)	1589(1)	61(1)
C(42)	7369(2)	4805(2)	2048(1)	71(1)
C(43)	7256(2)	5684(2)	1785(1)	70(1)
C(44)	7502(2)	5821(2)	1032(1)	57(1)
C(45)	7908(1)	5051(1)	572(1)	42(1)
C(46)	8020(1)	4122(2)	832(1)	46(1)
C(47)	9319(1)	2603(1)	-763(1)	47(1)
C(48)	10203(2)	1850(2)	-363(2)	64(1)
C(57)	8407(1)	5948(1)	-401(1)	36(1)
C(58)	9048(1)	6234(1)	103(1)	46(1)
C(59)	8438(1)	6995(1)	-1363(1)	44(1)
C(60)	9299(1)	6695(1)	-1788(1)	48(1)
C(61)	9578(2)	7390(2)	-2107(1)	69(1)
C(62)	9015(3)	8343(2)	-2006(2)	86(1)
C(63)	8160(3)	8632(2)	-1602(2)	82(1)
C(64)	7838(2)	7972(1)	-1277(1)	63(1)
C(65)	9910(1)	5657(2)	-1904(1)	51(1)
C(66)	6892(2)	8274(2)	-859(2)	89(1)
C(67)	6849(1)	4634(2)	-866(1)	47(1)
C(68)	6112(2)	5543(2)	-812(1)	62(1)
C(69)	5122(2)	5695(3)	-875(1)	86(1)
C(70)	4887(2)	4928(3)	-1001(1)	92(1)
C(71)	5608(2)	4032(3)	-1064(2)	90(1)
C(72)	6594(2)	3868(2)	-1005(1)	66(1)
N(1)	6434(1)	6545(1)	4864(1)	32(1)
N(2)	5898(1)	7688(1)	3925(1)	42(1)
N(3)	6803(1)	4768(1)	4783(1)	29(1)
N(4)	6681(1)	3909(1)	3793(1)	32(1)
N(5)	8682(1)	3386(1)	-358(1)	41(1)
N(6)	9139(1)	2633(1)	-1465(1)	51(1)
C(49)	9816(2)	1990(2)	-1977(1)	51(1)
C(50)	9677(3)	1167(2)	-2158(2)	80(1)
C(51)	10303(4)	574(3)	-2693(3)	103(1)
C(52)	11020(3)	789(3)	-3045(2)	98(1)
C(53)	11123(3)	1616(2)	-2874(2)	75(1)
C(54)	10529(2)	2218(2)	-2333(1)	52(1)
C(55)	8858(4)	965(3)	-1787(3)	118(2)
C(56)	10632(2)	3118(2)	-2164(2)	56(1)
C(49')	9815(13)	1742(10)	-1708(13)	68(2)
C(50')	9652(15)	895(11)	-1696(13)	80(3)
C(51')	10368(16)	143(13)	-2071(14)	95(3)
C(52')	10995(19)	326(15)	-2546(15)	93(3)
C(53')	11101(17)	1166(13)	-2626(13)	85(3)
C(54')	10496(16)	1881(13)	-2165(12)	69(2)
C(55')	8878(19)	803(17)	-1184(17)	103(5)
C(56')	10666(19)	2735(14)	-2144(14)	69(4)
N(7)	8181(1)	5175(1)	-172(1)	35(1)
N(8)	8117(1)	6305(1)	-1057(1)	38(1)
P(1)	6821(1)	5675(1)	4189(1)	29(1)

Table A39. Bond lengths [Å] and angles [deg] for 3d.

C(1)-C(2)	1.383(2)
C(1)-N(1)	1.4207(18)
C(1)-C(10)	1.426(2)
C(2)-C(3)	1.413(2)
C(2)-H(2)	0.9500
C(3)-C(4)	1.366(3)
C(3)-H(3)	0.9500
C(4)-C(5)	1.419(2)
C(4)-H(4)	0.9500
C(5)-C(6)	1.416(2)
C(5)-C(10)	1.4347(19)
C(6)-C(7)	1.363(3)
C(6)-H(6)	0.9500
C(7)-C(8)	1.415(2)
C(7)-H(7)	0.9500
C(8)-C(9)	1.381(2)
C(8)-H(8)	0.9500
C(9)-N(3)	1.4175(17)
C(9)-C(10)	1.429(2)
C(11)-N(2)	1.282(2)
C(11)-N(1)	1.4071(19)
C(11)-C(12)	1.509(2)
C(12)-H(12A)	0.9800
C(12)-H(12B)	0.9800
C(12)-H(12C)	0.9800
C(13)-C(14)	1.403(3)
C(13)-C(18)	1.406(3)
C(13)-N(2)	1.422(2)
C(14)-C(15)	1.390(3)
C(14)-C(19)	1.520(3)
C(15)-C(16)	1.388(4)
C(15)-H(15)	0.9500
C(16)-C(17)	1.387(4)
C(16)-H(16)	0.9500
C(17)-C(18)	1.394(3)
C(17)-H(17)	0.9500
C(18)-C(20)	1.509(3)
C(19)-H(19A)	0.9800
C(19)-H(19B)	0.9800
C(19)-H(19C)	0.9800
C(20)-H(20A)	0.9800
C(20)-H(20B)	0.9800
C(20)-H(20C)	0.9800
C(21)-N(4)	1.2762(18)
C(21)-N(3)	1.4081(18)
C(21)-C(22)	1.513(2)

C(22)-H(22A)	0.9800
C(22)-H(22B)	0.9800
C(22)-H(22C)	0.9800
C(23)-C(28)	1.399(2)
C(23)-C(24)	1.400(2)
C(23)-N(4)	1.4294(19)
C(24)-C(25)	1.401(2)
C(24)-C(29)	1.501(3)
C(25)-C(26)	1.366(3)
C(25)-H(25)	0.9500
C(26)-C(27)	1.383(3)
C(26)-H(26)	0.9500
C(27)-C(28)	1.398(3)
C(27)-H(27)	0.9500
C(28)-C(30)	1.511(3)
C(29)-H(29A)	0.9800
C(29)-H(29B)	0.9800
C(29)-H(29C)	0.9800
C(30)-H(30A)	0.9800
C(30)-H(30B)	0.9800
C(30)-H(30C)	0.9800
C(31)-C(32)	1.387(3)
C(31)-C(36)	1.388(3)
C(31)-P(1)	1.8268(16)
C(32)-C(33)	1.401(3)
C(32)-H(32)	0.9500
C(33)-C(34)	1.356(5)
C(33)-H(33)	0.9500
C(34)-C(35)	1.373(5)
C(34)-H(34)	0.9500
C(35)-C(36)	1.401(3)
C(35)-H(35)	0.9500
C(36)-H(36)	0.9500
C(37)-C(38)	1.390(3)
C(37)-N(5)	1.415(2)
C(37)-C(46)	1.421(3)
C(38)-C(39)	1.410(3)
C(38)-H(38)	0.9500
C(39)-C(40)	1.338(4)
C(39)-H(39)	0.9500
C(40)-C(41)	1.417(4)
C(40)-H(40)	0.9500
C(41)-C(42)	1.402(4)
C(41)-C(46)	1.442(2)
C(42)-C(43)	1.359(4)
C(42)-H(42)	0.9500
C(43)-C(44)	1.425(3)
C(43)-H(43)	0.9500
C(44)-C(45)	1.381(3)
C(44)-H(44)	0.9500
C(45)-N(7)	1.4183(19)
C(45)-C(46)	1.430(3)

C(47)-N(6)	1.279(2)
C(47)-N(5)	1.408(2)
C(47)-C(48)	1.514(3)
C(48)-H(48A)	0.9800
C(48)-H(48B)	0.9800
C(48)-H(48C)	0.9800
C(57)-N(8)	1.278(2)
C(57)-N(7)	1.409(2)
C(57)-C(58)	1.513(2)
C(58)-H(58A)	0.9800
C(58)-H(58B)	0.9800
C(58)-H(58C)	0.9800
C(59)-C(60)	1.399(3)
C(59)-C(64)	1.410(3)
C(59)-N(8)	1.423(2)
C(60)-C(61)	1.399(3)
C(60)-C(65)	1.498(3)
C(61)-C(62)	1.373(4)
C(61)-H(61)	0.9500
C(62)-C(63)	1.373(5)
C(62)-H(62)	0.9500
C(63)-C(64)	1.398(4)
C(63)-H(63)	0.9500
C(64)-C(66)	1.493(4)
C(65)-H(65A)	0.9800
C(65)-H(65B)	0.9800
C(65)-H(65C)	0.9800
C(66)-H(66A)	0.9800
C(66)-H(66B)	0.9800
C(66)-H(66C)	0.9800
C(67)-C(68)	1.383(3)
C(67)-C(72)	1.406(3)
C(67)-P(2)	1.8276(18)
C(68)-C(69)	1.398(3)
C(68)-H(68)	0.9500
C(69)-C(70)	1.384(5)
C(69)-H(69)	0.9500
C(70)-C(71)	1.362(5)
C(70)-H(70)	0.9500
C(71)-C(72)	1.387(3)
C(71)-H(71)	0.9500
C(72)-H(72)	0.9500
N(1)-P(1)	1.7412(13)
N(3)-P(1)	1.7352(12)
N(5)-P(2)	1.7418(15)
N(6)-C(49')	1.406(13)
N(6)-C(49)	1.434(3)
C(49)-C(54)	1.391(4)
C(49)-C(50)	1.408(4)
C(50)-C(51)	1.401(5)
C(50)-C(55)	1.520(6)
C(51)-C(52)	1.383(6)

C(51)-H(51)	0.9500
C(52)-C(53)	1.384(5)
C(52)-H(52)	0.9500
C(53)-C(54)	1.395(3)
C(53)-H(53)	0.9500
C(54)-C(56)	1.491(4)
C(55)-H(55A)	0.9800
C(55)-H(55B)	0.9800
C(55)-H(55C)	0.9800
C(56)-H(56A)	0.9800
C(56)-H(56B)	0.9800
C(56)-H(56C)	0.9800
C(49')-C(54')	1.377(16)
C(49')-C(50')	1.418(15)
C(50')-C(51')	1.395(15)
C(50')-C(55')	1.514(17)
C(51')-C(52')	1.365(18)
C(51')-H(51')	0.9500
C(52')-C(53')	1.366(17)
C(52')-H(52')	0.9500
C(53')-C(54')	1.389(15)
C(53')-H(53')	0.9500
C(54')-C(56')	1.436(16)
C(55')-H(55D)	0.9800
C(55')-H(55E)	0.9800
C(55')-H(55F)	0.9800
C(56')-H(56D)	0.9800
C(56')-H(56E)	0.9800
C(56')-H(56F)	0.9800
N(7)-P(2)	1.7316(13)
C(2)-C(1)-N(1)	120.82(14)
C(2)-C(1)-C(10)	119.88(14)
N(1)-C(1)-C(10)	119.24(12)
C(1)-C(2)-C(3)	120.46(16)
C(1)-C(2)-H(2)	119.8
C(3)-C(2)-H(2)	119.8
C(4)-C(3)-C(2)	121.09(15)
C(4)-C(3)-H(3)	119.5
C(2)-C(3)-H(3)	119.5
C(3)-C(4)-C(5)	120.02(14)
C(3)-C(4)-H(4)	120.0
C(5)-C(4)-H(4)	120.0
C(6)-C(5)-C(4)	120.46(14)
C(6)-C(5)-C(10)	119.98(15)
C(4)-C(5)-C(10)	119.54(15)
C(7)-C(6)-C(5)	120.57(14)
C(7)-C(6)-H(6)	119.7
C(5)-C(6)-H(6)	119.7
C(6)-C(7)-C(8)	120.29(16)
C(6)-C(7)-H(7)	119.9
C(8)-C(7)-H(7)	119.9

C(9)-C(8)-C(7)	120.89(16)
C(9)-C(8)-H(8)	119.6
C(7)-C(8)-H(8)	119.6
C(8)-C(9)-N(3)	120.50(13)
C(8)-C(9)-C(10)	120.13(13)
N(3)-C(9)-C(10)	119.34(13)
C(1)-C(10)-C(9)	123.30(12)
C(1)-C(10)-C(5)	118.73(13)
C(9)-C(10)-C(5)	117.93(14)
N(2)-C(11)-N(1)	116.28(14)
N(2)-C(11)-C(12)	125.10(15)
N(1)-C(11)-C(12)	118.40(13)
C(11)-C(12)-H(12A)	109.5
C(11)-C(12)-H(12B)	109.5
H(12A)-C(12)-H(12B)	109.5
C(11)-C(12)-H(12C)	109.5
H(12A)-C(12)-H(12C)	109.5
H(12B)-C(12)-H(12C)	109.5
C(14)-C(13)-C(18)	121.07(17)
C(14)-C(13)-N(2)	119.13(16)
C(18)-C(13)-N(2)	119.61(18)
C(15)-C(14)-C(13)	118.2(2)
C(15)-C(14)-C(19)	121.5(2)
C(13)-C(14)-C(19)	120.24(18)
C(16)-C(15)-C(14)	121.5(2)
C(16)-C(15)-H(15)	119.2
C(14)-C(15)-H(15)	119.2
C(17)-C(16)-C(15)	119.5(2)
C(17)-C(16)-H(16)	120.2
C(15)-C(16)-H(16)	120.2
C(16)-C(17)-C(18)	120.9(2)
C(16)-C(17)-H(17)	119.5
C(18)-C(17)-H(17)	119.5
C(17)-C(18)-C(13)	118.7(2)
C(17)-C(18)-C(20)	120.79(18)
C(13)-C(18)-C(20)	120.53(17)
C(14)-C(19)-H(19A)	109.5
C(14)-C(19)-H(19B)	109.5
H(19A)-C(19)-H(19B)	109.5
C(14)-C(19)-H(19C)	109.5
H(19A)-C(19)-H(19C)	109.5
H(19B)-C(19)-H(19C)	109.5
C(18)-C(20)-H(20A)	109.5
C(18)-C(20)-H(20B)	109.5
H(20A)-C(20)-H(20B)	109.5
C(18)-C(20)-H(20C)	109.5
H(20A)-C(20)-H(20C)	109.5
H(20B)-C(20)-H(20C)	109.5
N(4)-C(21)-N(3)	117.03(12)
N(4)-C(21)-C(22)	124.59(13)
N(3)-C(21)-C(22)	118.20(12)
C(21)-C(22)-H(22A)	109.5

C(21)-C(22)-H(22B)	109.5
H(22A)-C(22)-H(22B)	109.5
C(21)-C(22)-H(22C)	109.5
H(22A)-C(22)-H(22C)	109.5
H(22B)-C(22)-H(22C)	109.5
C(28)-C(23)-C(24)	121.63(15)
C(28)-C(23)-N(4)	118.81(15)
C(24)-C(23)-N(4)	119.27(14)
C(23)-C(24)-C(25)	117.83(17)
C(23)-C(24)-C(29)	120.81(14)
C(25)-C(24)-C(29)	121.34(17)
C(26)-C(25)-C(24)	121.32(19)
C(26)-C(25)-H(25)	119.3
C(24)-C(25)-H(25)	119.3
C(25)-C(26)-C(27)	120.30(17)
C(25)-C(26)-H(26)	119.9
C(27)-C(26)-H(26)	119.9
C(26)-C(27)-C(28)	120.79(19)
C(26)-C(27)-H(27)	119.6
C(28)-C(27)-H(27)	119.6
C(27)-C(28)-C(23)	118.10(18)
C(27)-C(28)-C(30)	121.50(18)
C(23)-C(28)-C(30)	120.38(16)
C(24)-C(29)-H(29A)	109.5
C(24)-C(29)-H(29B)	109.5
H(29A)-C(29)-H(29B)	109.5
C(24)-C(29)-H(29C)	109.5
H(29A)-C(29)-H(29C)	109.5
H(29B)-C(29)-H(29C)	109.5
C(28)-C(30)-H(30A)	109.5
C(28)-C(30)-H(30B)	109.5
H(30A)-C(30)-H(30B)	109.5
C(28)-C(30)-H(30C)	109.5
H(30A)-C(30)-H(30C)	109.5
H(30B)-C(30)-H(30C)	109.5
C(32)-C(31)-C(36)	119.91(18)
C(32)-C(31)-P(1)	119.67(14)
C(36)-C(31)-P(1)	120.05(16)
C(31)-C(32)-C(33)	119.3(2)
C(31)-C(32)-H(32)	120.3
C(33)-C(32)-H(32)	120.3
C(34)-C(33)-C(32)	120.8(3)
C(34)-C(33)-H(33)	119.6
C(32)-C(33)-H(33)	119.6
C(33)-C(34)-C(35)	120.3(2)
C(33)-C(34)-H(34)	119.9
C(35)-C(34)-H(34)	119.9
C(34)-C(35)-C(36)	120.4(3)
C(34)-C(35)-H(35)	119.8
C(36)-C(35)-H(35)	119.8
C(31)-C(36)-C(35)	119.3(3)
C(31)-C(36)-H(36)	120.3

C(35)-C(36)-H(36)	120.3
C(38)-C(37)-N(5)	120.3(2)
C(38)-C(37)-C(46)	120.48(18)
N(5)-C(37)-C(46)	119.11(16)
C(37)-C(38)-C(39)	120.1(3)
C(37)-C(38)-H(38)	120.0
C(39)-C(38)-H(38)	120.0
C(40)-C(39)-C(38)	120.6(2)
C(40)-C(39)-H(39)	119.7
C(38)-C(39)-H(39)	119.7
C(39)-C(40)-C(41)	121.9(2)
C(39)-C(40)-H(40)	119.0
C(41)-C(40)-H(40)	119.0
C(42)-C(41)-C(40)	121.6(2)
C(42)-C(41)-C(46)	119.6(2)
C(40)-C(41)-C(46)	118.7(2)
C(43)-C(42)-C(41)	121.11(18)
C(43)-C(42)-H(42)	119.4
C(41)-C(42)-H(42)	119.4
C(42)-C(43)-C(44)	120.5(2)
C(42)-C(43)-H(43)	119.7
C(44)-C(43)-H(43)	119.7
C(45)-C(44)-C(43)	120.2(2)
C(45)-C(44)-H(44)	119.9
C(43)-C(44)-H(44)	119.9
C(44)-C(45)-N(7)	120.64(18)
C(44)-C(45)-C(46)	120.20(16)
N(7)-C(45)-C(46)	119.11(15)
C(37)-C(46)-C(45)	123.82(14)
C(37)-C(46)-C(41)	117.97(19)
C(45)-C(46)-C(41)	118.19(19)
N(6)-C(47)-N(5)	115.93(17)
N(6)-C(47)-C(48)	125.21(19)
N(5)-C(47)-C(48)	118.58(18)
C(47)-C(48)-H(48A)	109.5
C(47)-C(48)-H(48B)	109.5
H(48A)-C(48)-H(48B)	109.5
C(47)-C(48)-H(48C)	109.5
H(48A)-C(48)-H(48C)	109.5
H(48B)-C(48)-H(48C)	109.5
N(8)-C(57)-N(7)	116.39(14)
N(8)-C(57)-C(58)	124.66(16)
N(7)-C(57)-C(58)	118.67(14)
C(57)-C(58)-H(58A)	109.5
C(57)-C(58)-H(58B)	109.5
H(58A)-C(58)-H(58B)	109.5
C(57)-C(58)-H(58C)	109.5
H(58A)-C(58)-H(58C)	109.5
H(58B)-C(58)-H(58C)	109.5
C(60)-C(59)-C(64)	121.40(19)
C(60)-C(59)-N(8)	119.61(16)
C(64)-C(59)-N(8)	118.82(19)

C(59)-C(60)-C(61)	118.4(2)
C(59)-C(60)-C(65)	121.09(16)
C(61)-C(60)-C(65)	120.5(2)
C(62)-C(61)-C(60)	120.7(3)
C(62)-C(61)-H(61)	119.7
C(60)-C(61)-H(61)	119.7
C(63)-C(62)-C(61)	120.6(2)
C(63)-C(62)-H(62)	119.7
C(61)-C(62)-H(62)	119.7
C(62)-C(63)-C(64)	121.4(2)
C(62)-C(63)-H(63)	119.3
C(64)-C(63)-H(63)	119.3
C(63)-C(64)-C(59)	117.5(3)
C(63)-C(64)-C(66)	122.1(2)
C(59)-C(64)-C(66)	120.4(2)
C(60)-C(65)-H(65A)	109.5
C(60)-C(65)-H(65B)	109.5
H(65A)-C(65)-H(65B)	109.5
C(60)-C(65)-H(65C)	109.5
H(65A)-C(65)-H(65C)	109.5
H(65B)-C(65)-H(65C)	109.5
C(64)-C(66)-H(66A)	109.5
C(64)-C(66)-H(66B)	109.5
H(66A)-C(66)-H(66B)	109.5
C(64)-C(66)-H(66C)	109.5
H(66A)-C(66)-H(66C)	109.5
H(66B)-C(66)-H(66C)	109.5
C(68)-C(67)-C(72)	119.26(19)
C(68)-C(67)-P(2)	120.49(16)
C(72)-C(67)-P(2)	119.72(17)
C(67)-C(68)-C(69)	120.4(3)
C(67)-C(68)-H(68)	119.8
C(69)-C(68)-H(68)	119.8
C(70)-C(69)-C(68)	119.3(3)
C(70)-C(69)-H(69)	120.3
C(68)-C(69)-H(69)	120.3
C(71)-C(70)-C(69)	120.7(2)
C(71)-C(70)-H(70)	119.6
C(69)-C(70)-H(70)	119.6
C(70)-C(71)-C(72)	120.7(3)
C(70)-C(71)-H(71)	119.6
C(72)-C(71)-H(71)	119.6
C(71)-C(72)-C(67)	119.5(3)
C(71)-C(72)-H(72)	120.2
C(67)-C(72)-H(72)	120.2
C(11)-N(1)-C(1)	121.74(12)
C(11)-N(1)-P(1)	115.80(10)
C(1)-N(1)-P(1)	121.96(10)
C(11)-N(2)-C(13)	119.13(15)
C(21)-N(3)-C(9)	120.53(12)
C(21)-N(3)-P(1)	117.10(9)
C(9)-N(3)-P(1)	122.03(10)

C(21)-N(4)-C(23)	119.03(12)
C(47)-N(5)-C(37)	123.32(15)
C(47)-N(5)-P(2)	114.58(12)
C(37)-N(5)-P(2)	121.45(13)
C(47)-N(6)-C(49')	103.7(10)
C(47)-N(6)-C(49)	122.66(18)
C(54)-C(49)-C(50)	121.2(2)
C(54)-C(49)-N(6)	120.7(2)
C(50)-C(49)-N(6)	117.8(3)
C(51)-C(50)-C(49)	117.5(3)
C(51)-C(50)-C(55)	122.6(3)
C(49)-C(50)-C(55)	119.9(3)
C(52)-C(51)-C(50)	121.8(3)
C(52)-C(51)-H(51)	119.1
C(50)-C(51)-H(51)	119.1
C(51)-C(52)-C(53)	119.7(3)
C(51)-C(52)-H(52)	120.2
C(53)-C(52)-H(52)	120.2
C(52)-C(53)-C(54)	120.5(3)
C(52)-C(53)-H(53)	119.8
C(54)-C(53)-H(53)	119.8
C(49)-C(54)-C(53)	119.4(3)
C(49)-C(54)-C(56)	120.6(2)
C(53)-C(54)-C(56)	120.0(3)
C(50)-C(55)-H(55A)	109.5
C(50)-C(55)-H(55B)	109.5
H(55A)-C(55)-H(55B)	109.5
C(50)-C(55)-H(55C)	109.5
H(55A)-C(55)-H(55C)	109.5
H(55B)-C(55)-H(55C)	109.5
C(54)-C(56)-H(56A)	109.5
C(54)-C(56)-H(56B)	109.5
H(56A)-C(56)-H(56B)	109.5
C(54)-C(56)-H(56C)	109.5
H(56A)-C(56)-H(56C)	109.5
H(56B)-C(56)-H(56C)	109.5
C(54')-C(49')-N(6)	108.9(12)
C(54')-C(49')-C(50')	123.2(13)
N(6)-C(49')-C(50')	125.1(13)
C(51')-C(50')-C(49')	114.0(14)
C(51')-C(50')-C(55')	125.0(15)
C(49')-C(50')-C(55')	119.9(13)
C(52')-C(51')-C(50')	119.4(17)
C(52')-C(51')-H(51')	120.3
C(50')-C(51')-H(51')	120.3
C(51')-C(52')-C(53')	126.4(17)
C(51')-C(52')-H(52')	116.8
C(53')-C(52')-H(52')	116.8
C(52')-C(53')-C(54')	114.3(16)
C(52')-C(53')-H(53')	122.8
C(54')-C(53')-H(53')	122.8
C(49')-C(54')-C(53')	121.1(15)

C(49')-C(54')-C(56')	121.6(14)
C(53')-C(54')-C(56')	117.2(16)
C(50')-C(55')-H(55D)	109.5
C(50')-C(55')-H(55E)	109.5
H(55D)-C(55')-H(55E)	109.5
C(50')-C(55')-H(55F)	109.5
H(55D)-C(55')-H(55F)	109.5
H(55E)-C(55')-H(55F)	109.5
C(54')-C(56')-H(56D)	109.5
C(54')-C(56')-H(56E)	109.5
H(56D)-C(56')-H(56E)	109.5
C(54')-C(56')-H(56F)	109.5
H(56D)-C(56')-H(56F)	109.5
H(56E)-C(56')-H(56F)	109.5
C(57)-N(7)-C(45)	122.64(13)
C(57)-N(7)-P(2)	115.12(10)
C(45)-N(7)-P(2)	121.95(12)
C(57)-N(8)-C(59)	119.18(14)
N(3)-P(1)-N(1)	94.96(6)
N(3)-P(1)-C(31)	100.91(7)
N(1)-P(1)-C(31)	100.64(7)
N(7)-P(2)-N(5)	95.30(7)
N(7)-P(2)-C(67)	101.39(8)
N(5)-P(2)-C(67)	100.83(8)

Symmetry transformations used to generate equivalent atoms:

Table A40. Anisotropic displacement parameters ($\text{Å}^2 \times 10^3$) for 3d. The anisotropic displacement factor exponent takes the form: $-2 \pi^2 [h^2 a^* a^* U_{11} + \dots + 2 h k a^* b^* U_{12}]$

	U11	U22	U33	U23	U13	U12
C(1)	32(1)	42(1)	24(1)	-3(1)	0(1)	-19(1)
C(2)	47(1)	46(1)	37(1)	-6(1)	-5(1)	-25(1)
C(3)	49(1)	61(1)	36(1)	-13(1)	-6(1)	-27(1)
C(4)	38(1)	66(1)	27(1)	-8(1)	-4(1)	-24(1)
C(5)	29(1)	56(1)	24(1)	-2(1)	0(1)	-19(1)
C(6)	40(1)	64(1)	26(1)	8(1)	-6(1)	-20(1)
C(7)	48(1)	50(1)	38(1)	12(1)	-11(1)	-16(1)
C(8)	44(1)	41(1)	32(1)	4(1)	-5(1)	-14(1)
C(9)	29(1)	40(1)	23(1)	0(1)	0(1)	-15(1)
C(10)	26(1)	41(1)	24(1)	-1(1)	1(1)	-16(1)
C(11)	42(1)	35(1)	31(1)	1(1)	-5(1)	-20(1)
C(12)	45(1)	39(1)	39(1)	-3(1)	0(1)	-17(1)
C(13)	68(1)	38(1)	33(1)	6(1)	-5(1)	-21(1)
C(14)	88(2)	49(1)	52(1)	13(1)	-25(1)	-32(1)
C(15)	103(2)	60(1)	77(2)	20(1)	-44(2)	-30(1)
C(16)	110(2)	47(1)	68(2)	18(1)	-31(1)	-23(1)

C(17)	97(2)	40(1)	54(1)	7(1)	-9(1)	-28(1)
C(18)	72(1)	42(1)	40(1)	4(1)	0(1)	-26(1)
C(19)	117(2)	61(1)	83(2)	19(1)	-52(2)	-48(2)
C(20)	73(1)	51(1)	66(1)	3(1)	0(1)	-33(1)
C(21)	30(1)	31(1)	26(1)	-1(1)	2(1)	-13(1)
C(22)	46(1)	47(1)	30(1)	-5(1)	10(1)	-27(1)
C(23)	44(1)	40(1)	23(1)	-6(1)	9(1)	-23(1)
C(24)	43(1)	56(1)	28(1)	-8(1)	9(1)	-29(1)
C(25)	56(1)	80(1)	35(1)	-11(1)	6(1)	-45(1)
C(26)	86(2)	71(1)	44(1)	-19(1)	12(1)	-56(1)
C(27)	89(2)	46(1)	45(1)	-12(1)	13(1)	-38(1)
C(28)	60(1)	41(1)	33(1)	-5(1)	8(1)	-24(1)
C(29)	39(1)	56(1)	39(1)	-4(1)	1(1)	-17(1)
C(30)	74(1)	41(1)	61(1)	-5(1)	-6(1)	-10(1)
C(31)	36(1)	68(1)	23(1)	1(1)	3(1)	-28(1)
C(32)	39(1)	79(1)	49(1)	-12(1)	10(1)	-21(1)
C(33)	37(1)	129(2)	64(1)	-14(2)	14(1)	-17(1)
C(34)	47(1)	178(3)	47(1)	2(2)	9(1)	-58(2)
C(35)	74(2)	157(3)	56(1)	16(2)	0(1)	-85(2)
C(36)	60(1)	93(2)	47(1)	9(1)	1(1)	-53(1)
C(37)	47(1)	66(1)	37(1)	13(1)	-3(1)	-33(1)
C(38)	83(2)	80(2)	62(1)	21(1)	-2(1)	-53(1)
C(39)	95(2)	113(2)	65(2)	38(2)	-5(1)	-68(2)
C(40)	63(1)	130(2)	47(1)	34(1)	0(1)	-55(2)
C(41)	42(1)	118(2)	29(1)	13(1)	-1(1)	-39(1)
C(42)	44(1)	140(2)	28(1)	1(1)	4(1)	-39(1)
C(43)	48(1)	120(2)	34(1)	-23(1)	5(1)	-26(1)
C(44)	47(1)	84(2)	33(1)	-14(1)	5(1)	-20(1)
C(45)	33(1)	68(1)	23(1)	-2(1)	-1(1)	-20(1)
C(46)	33(1)	81(1)	28(1)	10(1)	-3(1)	-29(1)
C(47)	51(1)	41(1)	54(1)	2(1)	-2(1)	-25(1)
C(48)	66(1)	47(1)	75(2)	12(1)	-12(1)	-21(1)
C(57)	36(1)	39(1)	28(1)	-5(1)	-5(1)	-11(1)
C(58)	55(1)	50(1)	35(1)	-1(1)	-16(1)	-23(1)
C(59)	55(1)	42(1)	37(1)	5(1)	-20(1)	-21(1)
C(60)	53(1)	54(1)	43(1)	13(1)	-20(1)	-30(1)
C(61)	79(2)	78(2)	68(1)	26(1)	-22(1)	-52(1)
C(62)	120(2)	63(2)	92(2)	30(1)	-33(2)	-56(2)
C(63)	115(2)	42(1)	84(2)	16(1)	-37(2)	-30(1)
C(64)	85(2)	41(1)	55(1)	3(1)	-26(1)	-16(1)
C(65)	44(1)	61(1)	49(1)	9(1)	-5(1)	-24(1)
C(66)	94(2)	53(1)	86(2)	-7(1)	0(2)	5(1)
C(67)	41(1)	80(1)	27(1)	3(1)	-4(1)	-31(1)
C(68)	45(1)	90(2)	42(1)	8(1)	-4(1)	-19(1)
C(69)	44(1)	140(3)	53(1)	16(2)	-6(1)	-18(2)
C(70)	53(1)	189(4)	47(1)	16(2)	-12(1)	-64(2)
C(71)	72(2)	164(3)	65(2)	3(2)	-12(1)	-81(2)
C(72)	63(1)	101(2)	54(1)	-1(1)	-8(1)	-54(1)
N(1)	39(1)	35(1)	24(1)	0(1)	-4(1)	-18(1)
N(2)	56(1)	38(1)	32(1)	3(1)	-3(1)	-21(1)
N(3)	34(1)	34(1)	22(1)	0(1)	0(1)	-16(1)
N(4)	36(1)	36(1)	25(1)	-4(1)	4(1)	-17(1)

N(5)	47(1)	48(1)	35(1)	5(1)	-2(1)	-26(1)
N(6)	57(1)	45(1)	53(1)	-9(1)	-3(1)	-23(1)
C(49)	66(1)	35(1)	46(1)	-8(1)	-4(1)	-15(1)
C(50)	109(2)	49(1)	86(2)	-18(1)	4(2)	-37(1)
C(51)	139(3)	56(2)	110(3)	-41(2)	10(2)	-33(2)
C(52)	122(3)	66(2)	88(2)	-41(2)	24(2)	-18(2)
C(53)	86(2)	61(2)	61(2)	-20(1)	14(1)	-13(1)
C(54)	59(1)	43(1)	43(1)	-9(1)	-2(1)	-11(1)
C(55)	162(4)	93(3)	141(4)	-42(3)	27(3)	-91(3)
C(56)	68(2)	53(2)	48(1)	-11(1)	13(1)	-25(2)
C(49')	80(4)	51(4)	70(5)	-15(4)	-3(4)	-20(4)
C(50')	100(5)	55(4)	84(5)	-28(4)	-5(4)	-29(4)
C(51')	118(5)	63(4)	100(5)	-32(4)	0(5)	-30(4)
C(52')	115(5)	63(4)	90(5)	-32(4)	6(4)	-22(4)
C(53')	99(4)	62(4)	78(4)	-28(4)	7(4)	-16(4)
C(54')	81(4)	54(4)	63(4)	-19(4)	-2(4)	-18(4)
C(55')	137(11)	75(9)	125(12)	-42(9)	16(8)	-68(8)
C(56')	82(8)	49(8)	59(8)	-1(7)	26(7)	-9(7)
N(7)	38(1)	48(1)	22(1)	-3(1)	-1(1)	-18(1)
N(8)	43(1)	40(1)	30(1)	0(1)	-9(1)	-16(1)
P(1)	34(1)	37(1)	20(1)	0(1)	-1(1)	-18(1)
P(2)	38(1)	46(1)	23(1)	-1(1)	0(1)	-21(1)

A31. Crystal data and structure refinement of L₂Al₂.

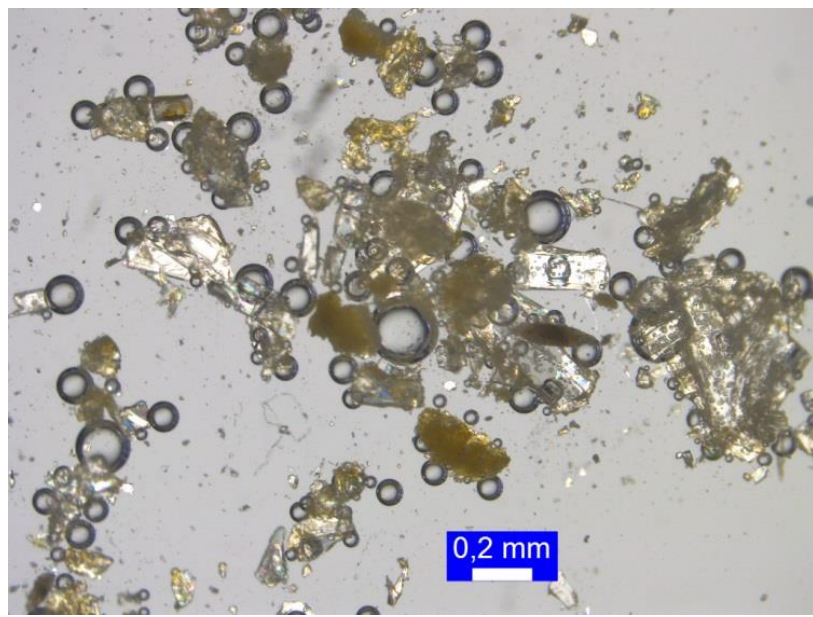


Figure S71. Sample of L₂Al₂.

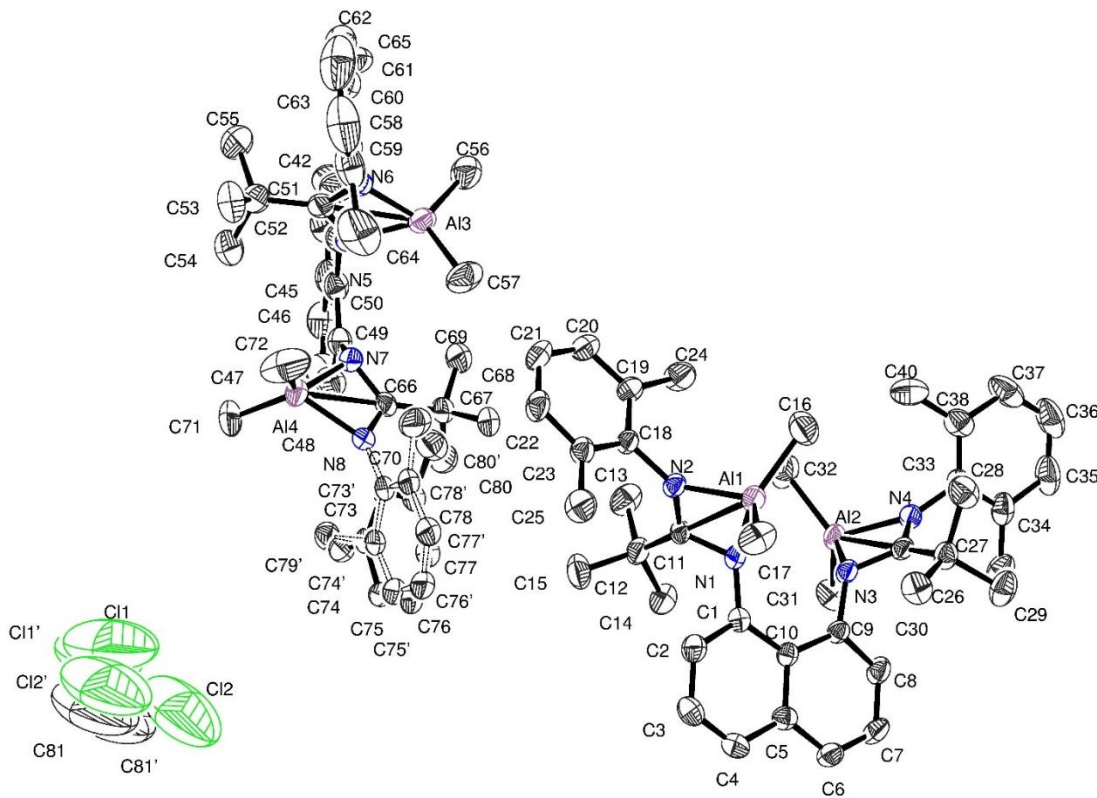


Figure S72. Asymmetric Unit of L_2Al_2 .

Table A41. Crystal data and structure refinement for L_2Al_2 .

Identification code	L_2Al_2
Empirical formula	$2(\text{C40 H54 Al2 N4}) \cdot \text{C H2 Cl2}$
Formula weight	1374.58
Temperature	193(2) K
Wavelength	0.71073 Å
Crystal system, space group	Triclinic, P -1
Unit cell dimensions	$a = 13.6197(8)$ Å $\alpha = 97.990(2)$ deg. $b = 16.5022(10)$ Å $\beta = 90.083(2)$ deg. $c = 18.7841(12)$ Å $\gamma = 93.983(2)$ deg.
Volume	41705.4 Å ³
Z, Calculated density	2, 1.095 Mg/m ³
Absorption coefficient	0.164 mm ⁻¹
F(000)	1476
Crystal size	0.200 x 0.200 x 0.200 mm
Theta range for data collection	2.499 to 25.365 deg.

Limiting indices	-16<=h<=16, -19<=k<=19, -22<=l<=22
Reflections collected / unique	91796 / 15233 [R(int) = 0.0721]
Completeness to theta = 25.242	99.8 %
Refinement method	Full-matrix least-squares on F^2
Data / restraints / parameters	15233 / 373 / 984
Goodness-of-fit on F^2	1.025
Final R indices [I>2sigma(I)]	R1 = 0.0746, wR2 = 0.2087
R indices (all data)	R1 = 0.1051, wR2 = 0.2388
Largest diff. peak and hole	3.084 and -0.760 e.A^-3

Table A42. Atomic coordinates (x 10^4) and equivalent isotropic displacement parameters (A^2 x 10^3) for L₂Al₂. U(eq) is defined as one third of the trace of the orthogonalized Uij tensor.

	x	y	z	U(eq)
C(1)	2613(2)	9164(2)	4831(2)	29(1)
C(2)	2679(3)	8708(2)	5395(2)	40(1)
C(3)	2742(3)	9061(2)	6115(2)	45(1)
C(4)	2686(3)	9889(2)	6287(2)	41(1)
C(5)	2547(2)	10385(2)	5740(2)	31(1)
C(6)	2452(2)	11235(2)	5943(2)	37(1)
C(7)	2347(3)	11737(2)	5442(2)	41(1)
C(8)	2313(3)	11407(2)	4718(2)	38(1)
C(9)	2356(2)	10581(2)	4480(2)	28(1)
C(10)	2506(2)	10028(2)	4993(2)	26(1)
C(11)	3209(2)	8091(2)	3978(2)	28(1)
C(12)	4311(2)	8143(2)	4144(2)	37(1)
C(13)	4875(3)	7925(2)	3440(2)	53(1)
C(14)	4704(3)	9018(2)	4469(2)	45(1)
C(15)	4563(3)	7534(2)	4656(2)	57(1)
C(16)	1047(3)	8129(3)	2691(2)	59(1)
C(17)	521(3)	7814(3)	4379(2)	55(1)
C(18)	2954(2)	6661(2)	3304(2)	30(1)
C(19)	3240(2)	6514(2)	2585(2)	34(1)
C(20)	3458(2)	5723(2)	2296(2)	41(1)
C(21)	3359(3)	5087(2)	2697(2)	44(1)
C(22)	3014(3)	5227(2)	3392(2)	42(1)
C(23)	2805(2)	6012(2)	3712(2)	35(1)
C(24)	3300(3)	7174(2)	2105(2)	53(1)
C(25)	2410(3)	6132(2)	4463(2)	52(1)
C(26)	1647(2)	10658(2)	3315(2)	29(1)
C(27)	541(2)	10696(2)	3480(2)	36(1)
C(28)	-53(3)	10245(3)	2822(2)	50(1)

C(29)	237(3)	11583(2)	3618(2)	52(1)
C(30)	241(3)	10258(2)	4122(2)	45(1)
C(31)	4308(3)	11393(3)	3523(2)	54(1)
C(32)	3888(3)	9652(3)	2413(2)	59(1)
C(33)	1724(2)	11205(2)	2138(2)	36(1)
C(34)	1726(3)	12062(2)	2175(2)	45(1)
C(35)	1388(3)	12383(3)	1578(2)	63(1)
C(36)	1088(3)	11888(3)	960(3)	69(1)
C(37)	1133(3)	11049(3)	913(2)	63(1)
C(38)	1465(3)	10690(2)	1498(2)	45(1)
C(39)	2115(3)	12639(2)	2817(2)	51(1)
C(40)	1553(3)	9782(3)	1413(2)	61(1)
C(41)	8569(3)	3615(2)	874(2)	49(1)
C(42)	8763(3)	3300(3)	178(2)	65(1)
C(43)	9668(4)	3480(4)	-154(3)	78(2)
C(44)	10369(4)	3970(3)	219(3)	72(1)
C(45)	10219(3)	4319(3)	938(2)	59(1)
C(46)	10986(3)	4824(3)	1320(3)	70(1)
C(47)	10883(3)	5146(3)	2014(3)	74(1)
C(48)	9989(3)	5005(3)	2353(2)	58(1)
C(49)	9191(3)	4560(2)	2008(2)	44(1)
C(50)	9293(3)	4162(2)	1286(2)	45(1)
C(51)	7175(3)	2653(2)	1036(2)	42(1)
C(52)	7684(3)	1887(3)	1204(2)	53(1)
C(53)	6970(4)	1357(3)	1618(3)	73(1)
C(54)	8575(4)	2153(3)	1702(3)	71(1)
C(55)	8018(4)	1359(3)	523(3)	84(2)
C(56)	6565(4)	4214(3)	-122(2)	66(1)
C(57)	5618(3)	4511(3)	1506(3)	70(1)
C(58)	5482(3)	2031(2)	677(2)	44(1)
C(59)	4741(3)	1925(3)	1184(2)	62(1)
C(60)	3987(4)	1315(4)	994(4)	87(2)
C(61)	3948(4)	837(4)	332(5)	98(2)
C(62)	4637(4)	980(3)	-159(3)	76(1)
C(63)	5409(3)	1582(2)	-8(2)	50(1)
C(64)	4759(4)	2469(4)	1896(3)	96(2)
C(65)	6092(4)	1761(3)	-601(2)	62(1)
C(66)	8032(2)	5201(2)	2834(2)	35(1)
C(67)	7979(3)	6047(2)	2572(2)	41(1)
C(68)	6955(3)	6357(2)	2726(2)	50(1)
C(69)	8148(3)	5995(3)	1760(2)	56(1)
C(70)	8734(3)	6692(2)	2969(2)	56(1)
C(71)	9320(5)	3588(4)	3593(3)	108(2)
C(72)	6931(6)	3137(3)	3266(3)	104(2)
Al(1)	1499(1)	8057(1)	3663(1)	34(1)
Al(2)	3359(1)	10534(1)	3068(1)	35(1)
Al(3)	6416(1)	3859(1)	820(1)	44(1)
Al(4)	8084(1)	3888(1)	3214(1)	53(1)
N(1)	2615(2)	8733(1)	4124(1)	29(1)
N(2)	2678(2)	7455(1)	3619(1)	29(1)
C(73)	7417(5)	5501(10)	4094(6)	38(1)
C(74)	8137(5)	5849(5)	4613(4)	40(1)

C(75)	7818(7)	6293(4)	5250(3)	47(1)
C(76)	6835(7)	6359(4)	5375(3)	48(2)
C(77)	6130(6)	5981(4)	4885(4)	48(2)
C(78)	6417(5)	5553(4)	4237(4)	44(1)
C(79)	9206(5)	5710(5)	4512(5)	52(2)
C(80)	5623(5)	5133(5)	3717(4)	56(2)
C(73')	7269(11)	5430(30)	4075(14)	40(2)
C(74')	7835(12)	5886(15)	4646(10)	42(2)
C(75')	7349(15)	6276(11)	5243(8)	46(2)
C(76')	6344(15)	6204(10)	5246(8)	49(3)
C(77')	5787(12)	5706(11)	4717(8)	48(2)
C(78')	6249(11)	5313(12)	4122(8)	42(2)
C(79')	8933(12)	5898(13)	4655(12)	48(4)
C(80')	5632(12)	4766(14)	3547(10)	60(4)
N(3)	2302(2)	10326(1)	3726(1)	31(1)
N(4)	2110(2)	10871(2)	2736(1)	31(1)
N(5)	7604(2)	3426(2)	1134(2)	45(1)
N(6)	6240(2)	2679(2)	829(1)	39(1)
N(7)	8308(2)	4510(2)	2416(2)	38(1)
N(8)	7756(2)	5008(2)	3469(1)	36(1)
Cl(1)	2725(8)	1180(9)	8148(5)	263(3)
C(81)	2038(12)	1111(14)	8958(9)	229(3)
Cl(2)	964(5)	1711(5)	8828(3)	224(3)
Cl(1')	3217(11)	1271(14)	8214(8)	243(4)
C(81')	2326(16)	1450(30)	8927(15)	232(3)
Cl(2')	1182(9)	815(8)	8849(4)	234(3)

Table A43. Bond lengths [Å] and angles [deg] for L₂Al₂.

C(1)-C(2)	1.389(4)
C(1)-N(1)	1.417(4)
C(1)-C(10)	1.434(4)
C(2)-C(3)	1.395(5)
C(2)-H(2)	0.9500
C(3)-C(4)	1.367(5)
C(3)-H(3)	0.9500
C(4)-C(5)	1.419(5)
C(4)-H(4)	0.9500
C(5)-C(6)	1.417(4)
C(5)-C(10)	1.444(4)
C(6)-C(7)	1.352(5)
C(6)-H(6)	0.9500
C(7)-C(8)	1.393(5)
C(7)-H(7)	0.9500
C(8)-C(9)	1.380(4)
C(8)-H(8)	0.9500
C(9)-N(3)	1.421(4)
C(9)-C(10)	1.439(4)

C(11)-N(2)	1.333(4)
C(11)-N(1)	1.375(4)
C(11)-C(12)	1.527(4)
C(11)-Al(1)	2.396(3)
C(12)-C(15)	1.539(5)
C(12)-C(13)	1.542(5)
C(12)-C(14)	1.546(4)
C(13)-H(13A)	0.9800
C(13)-H(13B)	0.9800
C(13)-H(13C)	0.9800
C(14)-H(14A)	0.9800
C(14)-H(14B)	0.9800
C(14)-H(14C)	0.9800
C(15)-H(15A)	0.9800
C(15)-H(15B)	0.9800
C(15)-H(15C)	0.9800
C(16)-Al(1)	1.948(4)
C(16)-H(16A)	0.9800
C(16)-H(16B)	0.9800
C(16)-H(16C)	0.9800
C(17)-Al(1)	1.956(4)
C(17)-H(17A)	0.9800
C(17)-H(17B)	0.9800
C(17)-H(17C)	0.9800
C(18)-C(19)	1.398(4)
C(18)-C(23)	1.406(4)
C(18)-N(2)	1.437(4)
C(19)-C(20)	1.395(4)
C(19)-C(24)	1.507(5)
C(20)-C(21)	1.373(5)
C(20)-H(20)	0.9500
C(21)-C(22)	1.383(5)
C(21)-H(21)	0.9500
C(22)-C(23)	1.398(4)
C(22)-H(22)	0.9500
C(23)-C(25)	1.502(5)
C(24)-H(24A)	0.9800
C(24)-H(24B)	0.9800
C(24)-H(24C)	0.9800
C(25)-H(25A)	0.9800
C(25)-H(25B)	0.9800
C(25)-H(25C)	0.9800
C(26)-N(4)	1.335(4)
C(26)-N(3)	1.369(4)
C(26)-C(27)	1.542(4)
C(26)-Al(2)	2.395(3)
C(27)-C(30)	1.532(5)
C(27)-C(29)	1.536(5)
C(27)-C(28)	1.547(5)
C(28)-H(28A)	0.9800
C(28)-H(28B)	0.9800
C(28)-H(28C)	0.9800

C(29)-H(29A)	0.9800
C(29)-H(29B)	0.9800
C(29)-H(29C)	0.9800
C(30)-H(30A)	0.9800
C(30)-H(30B)	0.9800
C(30)-H(30C)	0.9800
C(31)-Al(2)	1.954(4)
C(31)-H(31A)	0.9800
C(31)-H(31B)	0.9800
C(31)-H(31C)	0.9800
C(32)-Al(2)	1.949(4)
C(32)-H(32A)	0.9800
C(32)-H(32B)	0.9800
C(32)-H(32C)	0.9800
C(33)-C(38)	1.403(5)
C(33)-C(34)	1.407(5)
C(33)-N(4)	1.433(4)
C(34)-C(35)	1.395(5)
C(34)-C(39)	1.500(6)
C(35)-C(36)	1.368(7)
C(35)-H(35)	0.9500
C(36)-C(37)	1.381(7)
C(36)-H(36)	0.9500
C(37)-C(38)	1.406(5)
C(37)-H(37)	0.9500
C(38)-C(40)	1.497(6)
C(39)-H(39A)	0.9800
C(39)-H(39B)	0.9800
C(39)-H(39C)	0.9800
C(40)-H(40A)	0.9800
C(40)-H(40B)	0.9800
C(40)-H(40C)	0.9800
C(41)-C(42)	1.372(5)
C(41)-N(5)	1.432(5)
C(41)-C(50)	1.438(5)
C(42)-C(43)	1.414(6)
C(42)-H(42)	0.9500
C(43)-C(44)	1.337(7)
C(43)-H(43)	0.9500
C(44)-C(45)	1.414(6)
C(44)-H(44)	0.9500
C(45)-C(46)	1.418(7)
C(45)-C(50)	1.445(5)
C(46)-C(47)	1.349(7)
C(46)-H(46)	0.9500
C(47)-C(48)	1.395(6)
C(47)-H(47)	0.9500
C(48)-C(49)	1.377(5)
C(48)-H(48)	0.9500
C(49)-N(7)	1.431(5)
C(49)-C(50)	1.433(5)
C(51)-N(6)	1.336(4)

C(51)-N(5)	1.354(5)
C(51)-C(52)	1.552(5)
C(51)-Al(3)	2.389(4)
C(52)-C(54)	1.532(6)
C(52)-C(55)	1.533(6)
C(52)-C(53)	1.546(6)
C(53)-H(53A)	0.9800
C(53)-H(53B)	0.9800
C(53)-H(53C)	0.9800
C(54)-H(54A)	0.9800
C(54)-H(54B)	0.9800
C(54)-H(54C)	0.9800
C(55)-H(55A)	0.9800
C(55)-H(55B)	0.9800
C(55)-H(55C)	0.9800
C(56)-Al(3)	1.945(5)
C(56)-H(56A)	0.9800
C(56)-H(56B)	0.9800
C(56)-H(56C)	0.9800
C(57)-Al(3)	1.944(4)
C(57)-H(57A)	0.9800
C(57)-H(57B)	0.9800
C(57)-H(57C)	0.9800
C(58)-C(63)	1.392(5)
C(58)-C(59)	1.407(5)
C(58)-N(6)	1.433(5)
C(59)-C(60)	1.396(8)
C(59)-C(64)	1.503(8)
C(60)-C(61)	1.375(9)
C(60)-H(60)	0.9500
C(61)-C(62)	1.350(9)
C(61)-H(61)	0.9500
C(62)-C(63)	1.396(6)
C(62)-H(62)	0.9500
C(63)-C(65)	1.500(6)
C(64)-H(64A)	0.9800
C(64)-H(64B)	0.9800
C(64)-H(64C)	0.9800
C(65)-H(65A)	0.9800
C(65)-H(65B)	0.9800
C(65)-H(65C)	0.9800
C(66)-N(8)	1.326(4)
C(66)-N(7)	1.368(4)
C(66)-C(67)	1.549(4)
C(66)-Al(4)	2.381(3)
C(67)-C(68)	1.533(5)
C(67)-C(69)	1.533(5)
C(67)-C(70)	1.540(5)
C(68)-H(68A)	0.9800
C(68)-H(68B)	0.9800
C(68)-H(68C)	0.9800
C(69)-H(69A)	0.9800

C(69)-H(69B)	0.9800
C(69)-H(69C)	0.9800
C(70)-H(70A)	0.9800
C(70)-H(70B)	0.9800
C(70)-H(70C)	0.9800
C(71)-Al(4)	1.948(6)
C(71)-H(71A)	0.9800
C(71)-H(71B)	0.9800
C(71)-H(71C)	0.9800
C(72)-Al(4)	1.943(6)
C(72)-H(72A)	0.9800
C(72)-H(72B)	0.9800
C(72)-H(72C)	0.9800
Al(1)-N(2)	1.942(3)
Al(1)-N(1)	1.948(3)
Al(2)-N(3)	1.942(3)
Al(2)-N(4)	1.954(3)
Al(3)-N(5)	1.938(3)
Al(3)-N(6)	1.948(3)
Al(4)-N(8)	1.928(3)
Al(4)-N(7)	1.945(3)
C(73)-C(78)	1.395(7)
C(73)-C(74)	1.415(7)
C(73)-N(8)	1.429(7)
C(74)-C(75)	1.401(7)
C(74)-C(79)	1.498(8)
C(75)-C(76)	1.369(9)
C(75)-H(75)	0.9500
C(76)-C(77)	1.384(9)
C(76)-H(76)	0.9500
C(77)-C(78)	1.391(7)
C(77)-H(77)	0.9500
C(78)-C(80)	1.519(8)
C(79)-H(79A)	0.9800
C(79)-H(79B)	0.9800
C(79)-H(79C)	0.9800
C(80)-H(80A)	0.9800
C(80)-H(80B)	0.9800
C(80)-H(80C)	0.9800
C(73')-C(78')	1.394(10)
C(73')-C(74')	1.413(9)
C(73')-N(8)	1.440(15)
C(74')-C(75')	1.403(10)
C(74')-C(79')	1.495(11)
C(75')-C(76')	1.367(12)
C(75')-H(75')	0.9500
C(76')-C(77')	1.386(12)
C(76')-H(76')	0.9500
C(77')-C(78')	1.388(10)
C(77')-H(77')	0.9500
C(78')-C(80')	1.519(11)
C(79')-H(79D)	0.9800

C(79')-H(79E)	0.9800
C(79')-H(79F)	0.9800
C(80')-H(80D)	0.9800
C(80')-H(80E)	0.9800
C(80')-H(80F)	0.9800
Cl(1)-C(81)	1.800(14)
C(81)-Cl(2)	1.858(17)
C(81)-H(81A)	0.9900
C(81)-H(81B)	0.9900
Cl(1')-C(81')	1.816(16)
C(81')-Cl(2')	1.810(16)
C(81')-H(81C)	0.9900
C(81')-H(81D)	0.9900
C(2)-C(1)-N(1)	117.2(3)
C(2)-C(1)-C(10)	118.8(3)
N(1)-C(1)-C(10)	123.9(3)
C(1)-C(2)-C(3)	123.1(3)
C(1)-C(2)-H(2)	118.5
C(3)-C(2)-H(2)	118.5
C(4)-C(3)-C(2)	119.5(3)
C(4)-C(3)-H(3)	120.3
C(2)-C(3)-H(3)	120.3
C(3)-C(4)-C(5)	120.4(3)
C(3)-C(4)-H(4)	119.8
C(5)-C(4)-H(4)	119.8
C(6)-C(5)-C(4)	118.7(3)
C(6)-C(5)-C(10)	120.9(3)
C(4)-C(5)-C(10)	120.5(3)
C(7)-C(6)-C(5)	120.9(3)
C(7)-C(6)-H(6)	119.6
C(5)-C(6)-H(6)	119.6
C(6)-C(7)-C(8)	119.2(3)
C(6)-C(7)-H(7)	120.4
C(8)-C(7)-H(7)	120.4
C(9)-C(8)-C(7)	123.3(3)
C(9)-C(8)-H(8)	118.4
C(7)-C(8)-H(8)	118.4
C(8)-C(9)-N(3)	117.4(3)
C(8)-C(9)-C(10)	119.4(3)
N(3)-C(9)-C(10)	123.2(2)
C(1)-C(10)-C(9)	126.2(3)
C(1)-C(10)-C(5)	117.5(3)
C(9)-C(10)-C(5)	116.3(3)
N(2)-C(11)-N(1)	108.5(3)
N(2)-C(11)-C(12)	126.7(3)
N(1)-C(11)-C(12)	124.6(3)
N(2)-C(11)-Al(1)	54.09(15)
N(1)-C(11)-Al(1)	54.39(15)
C(12)-C(11)-Al(1)	176.7(2)
C(11)-C(12)-C(15)	111.6(3)
C(11)-C(12)-C(13)	109.2(3)

C(15)-C(12)-C(13)	107.7(3)
C(11)-C(12)-C(14)	112.2(3)
C(15)-C(12)-C(14)	109.3(3)
C(13)-C(12)-C(14)	106.7(3)
C(12)-C(13)-H(13A)	109.5
C(12)-C(13)-H(13B)	109.5
H(13A)-C(13)-H(13B)	109.5
C(12)-C(13)-H(13C)	109.5
H(13A)-C(13)-H(13C)	109.5
H(13B)-C(13)-H(13C)	109.5
C(12)-C(14)-H(14A)	109.5
C(12)-C(14)-H(14B)	109.5
H(14A)-C(14)-H(14B)	109.5
C(12)-C(14)-H(14C)	109.5
H(14A)-C(14)-H(14C)	109.5
H(14B)-C(14)-H(14C)	109.5
C(12)-C(15)-H(15A)	109.5
C(12)-C(15)-H(15B)	109.5
H(15A)-C(15)-H(15B)	109.5
C(12)-C(15)-H(15C)	109.5
H(15A)-C(15)-H(15C)	109.5
H(15B)-C(15)-H(15C)	109.5
Al(1)-C(16)-H(16A)	109.5
Al(1)-C(16)-H(16B)	109.5
H(16A)-C(16)-H(16B)	109.5
Al(1)-C(16)-H(16C)	109.5
H(16A)-C(16)-H(16C)	109.5
H(16B)-C(16)-H(16C)	109.5
Al(1)-C(17)-H(17A)	109.5
Al(1)-C(17)-H(17B)	109.5
H(17A)-C(17)-H(17B)	109.5
Al(1)-C(17)-H(17C)	109.5
H(17A)-C(17)-H(17C)	109.5
H(17B)-C(17)-H(17C)	109.5
C(19)-C(18)-C(23)	120.8(3)
C(19)-C(18)-N(2)	121.2(3)
C(23)-C(18)-N(2)	117.6(3)
C(20)-C(19)-C(18)	118.9(3)
C(20)-C(19)-C(24)	118.6(3)
C(18)-C(19)-C(24)	122.5(3)
C(21)-C(20)-C(19)	121.0(3)
C(21)-C(20)-H(20)	119.5
C(19)-C(20)-H(20)	119.5
C(20)-C(21)-C(22)	119.7(3)
C(20)-C(21)-H(21)	120.2
C(22)-C(21)-H(21)	120.2
C(21)-C(22)-C(23)	121.5(3)
C(21)-C(22)-H(22)	119.2
C(23)-C(22)-H(22)	119.2
C(22)-C(23)-C(18)	117.9(3)
C(22)-C(23)-C(25)	119.7(3)
C(18)-C(23)-C(25)	122.4(3)

C(19)-C(24)-H(24A)	109.5
C(19)-C(24)-H(24B)	109.5
H(24A)-C(24)-H(24B)	109.5
C(19)-C(24)-H(24C)	109.5
H(24A)-C(24)-H(24C)	109.5
H(24B)-C(24)-H(24C)	109.5
C(23)-C(25)-H(25A)	109.5
C(23)-C(25)-H(25B)	109.5
H(25A)-C(25)-H(25B)	109.5
C(23)-C(25)-H(25C)	109.5
H(25A)-C(25)-H(25C)	109.5
H(25B)-C(25)-H(25C)	109.5
N(4)-C(26)-N(3)	108.7(3)
N(4)-C(26)-C(27)	127.0(3)
N(3)-C(26)-C(27)	124.0(3)
N(4)-C(26)-Al(2)	54.65(15)
N(3)-C(26)-Al(2)	54.15(15)
C(27)-C(26)-Al(2)	177.4(2)
C(30)-C(27)-C(29)	109.2(3)
C(30)-C(27)-C(26)	112.2(3)
C(29)-C(27)-C(26)	112.0(3)
C(30)-C(27)-C(28)	106.7(3)
C(29)-C(27)-C(28)	108.0(3)
C(26)-C(27)-C(28)	108.4(3)
C(27)-C(28)-H(28A)	109.5
C(27)-C(28)-H(28B)	109.5
H(28A)-C(28)-H(28B)	109.5
C(27)-C(28)-H(28C)	109.5
H(28A)-C(28)-H(28C)	109.5
H(28B)-C(28)-H(28C)	109.5
C(27)-C(29)-H(29A)	109.5
C(27)-C(29)-H(29B)	109.5
H(29A)-C(29)-H(29B)	109.5
C(27)-C(29)-H(29C)	109.5
H(29A)-C(29)-H(29C)	109.5
H(29B)-C(29)-H(29C)	109.5
C(27)-C(30)-H(30A)	109.5
C(27)-C(30)-H(30B)	109.5
H(30A)-C(30)-H(30B)	109.5
C(27)-C(30)-H(30C)	109.5
H(30A)-C(30)-H(30C)	109.5
H(30B)-C(30)-H(30C)	109.5
Al(2)-C(31)-H(31A)	109.5
Al(2)-C(31)-H(31B)	109.5
H(31A)-C(31)-H(31B)	109.5
Al(2)-C(31)-H(31C)	109.5
H(31A)-C(31)-H(31C)	109.5
H(31B)-C(31)-H(31C)	109.5
Al(2)-C(32)-H(32A)	109.5
Al(2)-C(32)-H(32B)	109.5
H(32A)-C(32)-H(32B)	109.5
Al(2)-C(32)-H(32C)	109.5

H(32A)-C(32)-H(32C)	109.5
H(32B)-C(32)-H(32C)	109.5
C(38)-C(33)-C(34)	120.7(3)
C(38)-C(33)-N(4)	120.1(3)
C(34)-C(33)-N(4)	118.7(3)
C(35)-C(34)-C(33)	118.3(4)
C(35)-C(34)-C(39)	119.2(4)
C(33)-C(34)-C(39)	122.4(3)
C(36)-C(35)-C(34)	121.7(4)
C(36)-C(35)-H(35)	119.2
C(34)-C(35)-H(35)	119.2
C(35)-C(36)-C(37)	119.8(4)
C(35)-C(36)-H(36)	120.1
C(37)-C(36)-H(36)	120.1
C(36)-C(37)-C(38)	121.0(4)
C(36)-C(37)-H(37)	119.5
C(38)-C(37)-H(37)	119.5
C(33)-C(38)-C(37)	118.2(4)
C(33)-C(38)-C(40)	122.4(3)
C(37)-C(38)-C(40)	119.4(4)
C(34)-C(39)-H(39A)	109.5
C(34)-C(39)-H(39B)	109.5
H(39A)-C(39)-H(39B)	109.5
C(34)-C(39)-H(39C)	109.5
H(39A)-C(39)-H(39C)	109.5
H(39B)-C(39)-H(39C)	109.5
C(38)-C(40)-H(40A)	109.5
C(38)-C(40)-H(40B)	109.5
H(40A)-C(40)-H(40B)	109.5
C(38)-C(40)-H(40C)	109.5
H(40A)-C(40)-H(40C)	109.5
H(40B)-C(40)-H(40C)	109.5
C(42)-C(41)-N(5)	116.9(4)
C(42)-C(41)-C(50)	119.7(4)
N(5)-C(41)-C(50)	123.1(3)
C(41)-C(42)-C(43)	122.3(4)
C(41)-C(42)-H(42)	118.8
C(43)-C(42)-H(42)	118.8
C(44)-C(43)-C(42)	119.5(4)
C(44)-C(43)-H(43)	120.2
C(42)-C(43)-H(43)	120.2
C(43)-C(44)-C(45)	121.3(4)
C(43)-C(44)-H(44)	119.4
C(45)-C(44)-H(44)	119.4
C(44)-C(45)-C(46)	119.6(4)
C(44)-C(45)-C(50)	120.5(4)
C(46)-C(45)-C(50)	119.9(4)
C(47)-C(46)-C(45)	121.3(4)
C(47)-C(46)-H(46)	119.3
C(45)-C(46)-H(46)	119.3
C(46)-C(47)-C(48)	119.2(4)
C(46)-C(47)-H(47)	120.4

C(48)-C(47)-H(47)	120.4
C(49)-C(48)-C(47)	123.0(4)
C(49)-C(48)-H(48)	118.5
C(47)-C(48)-H(48)	118.5
C(48)-C(49)-N(7)	116.3(3)
C(48)-C(49)-C(50)	119.4(3)
N(7)-C(49)-C(50)	124.3(3)
C(49)-C(50)-C(41)	126.5(3)
C(49)-C(50)-C(45)	116.9(4)
C(41)-C(50)-C(45)	116.6(3)
N(6)-C(51)-N(5)	108.7(3)
N(6)-C(51)-C(52)	126.9(3)
N(5)-C(51)-C(52)	124.2(3)
N(6)-C(51)-Al(3)	54.61(18)
N(5)-C(51)-Al(3)	54.17(18)
C(52)-C(51)-Al(3)	177.8(3)
C(54)-C(52)-C(55)	109.2(4)
C(54)-C(52)-C(53)	106.4(4)
C(55)-C(52)-C(53)	108.9(4)
C(54)-C(52)-C(51)	109.9(3)
C(55)-C(52)-C(51)	112.4(3)
C(53)-C(52)-C(51)	109.7(3)
C(52)-C(53)-H(53A)	109.5
C(52)-C(53)-H(53B)	109.5
H(53A)-C(53)-H(53B)	109.5
C(52)-C(53)-H(53C)	109.5
H(53A)-C(53)-H(53C)	109.5
H(53B)-C(53)-H(53C)	109.5
C(52)-C(54)-H(54A)	109.5
C(52)-C(54)-H(54B)	109.5
H(54A)-C(54)-H(54B)	109.5
C(52)-C(54)-H(54C)	109.5
H(54A)-C(54)-H(54C)	109.5
H(54B)-C(54)-H(54C)	109.5
C(52)-C(55)-H(55A)	109.5
C(52)-C(55)-H(55B)	109.5
H(55A)-C(55)-H(55B)	109.5
C(52)-C(55)-H(55C)	109.5
H(55A)-C(55)-H(55C)	109.5
H(55B)-C(55)-H(55C)	109.5
Al(3)-C(56)-H(56A)	109.5
Al(3)-C(56)-H(56B)	109.5
H(56A)-C(56)-H(56B)	109.5
Al(3)-C(56)-H(56C)	109.5
H(56A)-C(56)-H(56C)	109.5
H(56B)-C(56)-H(56C)	109.5
Al(3)-C(57)-H(57A)	109.5
Al(3)-C(57)-H(57B)	109.5
H(57A)-C(57)-H(57B)	109.5
Al(3)-C(57)-H(57C)	109.5
H(57A)-C(57)-H(57C)	109.5
H(57B)-C(57)-H(57C)	109.5

C(63)-C(58)-C(59)	120.1(4)
C(63)-C(58)-N(6)	119.4(3)
C(59)-C(58)-N(6)	119.9(4)
C(60)-C(59)-C(58)	117.8(5)
C(60)-C(59)-C(64)	121.8(5)
C(58)-C(59)-C(64)	120.4(4)
C(61)-C(60)-C(59)	121.9(5)
C(61)-C(60)-H(60)	119.0
C(59)-C(60)-H(60)	119.0
C(62)-C(61)-C(60)	119.2(5)
C(62)-C(61)-H(61)	120.4
C(60)-C(61)-H(61)	120.4
C(61)-C(62)-C(63)	121.9(6)
C(61)-C(62)-H(62)	119.1
C(63)-C(62)-H(62)	119.1
C(58)-C(63)-C(62)	118.8(4)
C(58)-C(63)-C(65)	122.2(3)
C(62)-C(63)-C(65)	118.9(4)
C(59)-C(64)-H(64A)	109.5
C(59)-C(64)-H(64B)	109.5
H(64A)-C(64)-H(64B)	109.5
C(59)-C(64)-H(64C)	109.5
H(64A)-C(64)-H(64C)	109.5
H(64B)-C(64)-H(64C)	109.5
C(63)-C(65)-H(65A)	109.5
C(63)-C(65)-H(65B)	109.5
H(65A)-C(65)-H(65B)	109.5
C(63)-C(65)-H(65C)	109.5
H(65A)-C(65)-H(65C)	109.5
H(65B)-C(65)-H(65C)	109.5
N(8)-C(66)-N(7)	108.7(3)
N(8)-C(66)-C(67)	126.6(3)
N(7)-C(66)-C(67)	124.5(3)
N(8)-C(66)-Al(4)	54.01(16)
N(7)-C(66)-Al(4)	54.80(16)
C(67)-C(66)-Al(4)	178.6(2)
C(68)-C(67)-C(69)	107.7(3)
C(68)-C(67)-C(70)	107.3(3)
C(69)-C(67)-C(70)	108.9(3)
C(68)-C(67)-C(66)	109.3(3)
C(69)-C(67)-C(66)	111.8(3)
C(70)-C(67)-C(66)	111.6(3)
C(67)-C(68)-H(68A)	109.5
C(67)-C(68)-H(68B)	109.5
H(68A)-C(68)-H(68B)	109.5
C(67)-C(68)-H(68C)	109.5
H(68A)-C(68)-H(68C)	109.5
H(68B)-C(68)-H(68C)	109.5
C(67)-C(69)-H(69A)	109.5
C(67)-C(69)-H(69B)	109.5
H(69A)-C(69)-H(69B)	109.5
C(67)-C(69)-H(69C)	109.5

H(69A)-C(69)-H(69C)	109.5
H(69B)-C(69)-H(69C)	109.5
C(67)-C(70)-H(70A)	109.5
C(67)-C(70)-H(70B)	109.5
H(70A)-C(70)-H(70B)	109.5
C(67)-C(70)-H(70C)	109.5
H(70A)-C(70)-H(70C)	109.5
H(70B)-C(70)-H(70C)	109.5
Al(4)-C(71)-H(71A)	109.5
Al(4)-C(71)-H(71B)	109.5
H(71A)-C(71)-H(71B)	109.5
Al(4)-C(71)-H(71C)	109.5
H(71A)-C(71)-H(71C)	109.5
H(71B)-C(71)-H(71C)	109.5
Al(4)-C(72)-H(72A)	109.5
Al(4)-C(72)-H(72B)	109.5
H(72A)-C(72)-H(72B)	109.5
Al(4)-C(72)-H(72C)	109.5
H(72A)-C(72)-H(72C)	109.5
H(72B)-C(72)-H(72C)	109.5
N(2)-Al(1)-N(1)	68.76(10)
N(2)-Al(1)-C(16)	109.38(16)
N(1)-Al(1)-C(16)	123.15(16)
N(2)-Al(1)-C(17)	116.99(16)
N(1)-Al(1)-C(17)	110.37(15)
C(16)-Al(1)-C(17)	118.43(19)
N(2)-Al(1)-C(11)	33.76(10)
N(1)-Al(1)-C(11)	35.01(10)
C(16)-Al(1)-C(11)	122.56(16)
C(17)-Al(1)-C(11)	118.58(15)
N(3)-Al(2)-C(32)	121.91(16)
N(3)-Al(2)-C(31)	110.39(15)
C(32)-Al(2)-C(31)	116.6(2)
N(3)-Al(2)-N(4)	68.71(11)
C(32)-Al(2)-N(4)	113.20(17)
C(31)-Al(2)-N(4)	117.48(15)
N(3)-Al(2)-C(26)	34.86(10)
C(32)-Al(2)-C(26)	124.88(17)
C(31)-Al(2)-C(26)	118.44(15)
N(4)-Al(2)-C(26)	33.87(10)
N(5)-Al(3)-C(57)	120.32(18)
N(5)-Al(3)-C(56)	111.99(18)
C(57)-Al(3)-C(56)	116.5(2)
N(5)-Al(3)-N(6)	68.45(13)
C(57)-Al(3)-N(6)	114.85(19)
C(56)-Al(3)-N(6)	116.06(16)
N(5)-Al(3)-C(51)	34.50(13)
C(57)-Al(3)-C(51)	125.11(19)
C(56)-Al(3)-C(51)	118.37(16)
N(6)-Al(3)-C(51)	33.98(12)
N(8)-Al(4)-C(72)	110.6(2)
N(8)-Al(4)-N(7)	68.85(12)

C(72)-Al(4)-N(7)	122.5(2)
N(8)-Al(4)-C(71)	117.1(2)
C(72)-Al(4)-C(71)	117.4(3)
N(7)-Al(4)-C(71)	111.3(2)
N(8)-Al(4)-C(66)	33.82(11)
C(72)-Al(4)-C(66)	123.7(2)
N(7)-Al(4)-C(66)	35.06(11)
C(71)-Al(4)-C(66)	118.6(2)
C(11)-N(1)-C(1)	118.8(2)
C(11)-N(1)-Al(1)	90.60(18)
C(1)-N(1)-Al(1)	124.7(2)
C(11)-N(2)-C(18)	131.0(3)
C(11)-N(2)-Al(1)	92.14(18)
C(18)-N(2)-Al(1)	136.8(2)
C(78)-C(73)-C(74)	120.7(5)
C(78)-C(73)-N(8)	121.8(5)
C(74)-C(73)-N(8)	116.9(6)
C(75)-C(74)-C(73)	118.1(5)
C(75)-C(74)-C(79)	120.1(5)
C(73)-C(74)-C(79)	121.7(5)
C(76)-C(75)-C(74)	120.5(5)
C(76)-C(75)-H(75)	119.7
C(74)-C(75)-H(75)	119.7
C(75)-C(76)-C(77)	121.3(5)
C(75)-C(76)-H(76)	119.3
C(77)-C(76)-H(76)	119.3
C(76)-C(77)-C(78)	119.8(6)
C(76)-C(77)-H(77)	120.1
C(78)-C(77)-H(77)	120.1
C(77)-C(78)-C(73)	119.4(6)
C(77)-C(78)-C(80)	118.4(5)
C(73)-C(78)-C(80)	122.2(5)
C(74)-C(79)-H(79A)	109.5
C(74)-C(79)-H(79B)	109.5
H(79A)-C(79)-H(79B)	109.5
C(74)-C(79)-H(79C)	109.5
H(79A)-C(79)-H(79C)	109.5
H(79B)-C(79)-H(79C)	109.5
C(78)-C(80)-H(80A)	109.5
C(78)-C(80)-H(80B)	109.5
H(80A)-C(80)-H(80B)	109.5
C(78)-C(80)-H(80C)	109.5
H(80A)-C(80)-H(80C)	109.5
H(80B)-C(80)-H(80C)	109.5
C(78')-C(73')-C(74')	121.2(10)
C(78')-C(73')-N(8)	118.8(11)
C(74')-C(73')-N(8)	119.7(10)
C(75')-C(74')-C(73')	119.0(10)
C(75')-C(74')-C(79')	119.4(11)
C(73')-C(74')-C(79')	121.4(10)
C(76')-C(75')-C(74')	118.3(11)
C(76')-C(75')-H(75')	120.8

C(74')-C(75')-H(75')	120.8
C(75')-C(76')-C(77')	122.9(10)
C(75')-C(76')-H(76')	118.5
C(77')-C(76')-H(76')	118.5
C(76')-C(77')-C(78')	119.6(11)
C(76')-C(77')-H(77')	120.2
C(78')-C(77')-H(77')	120.2
C(77')-C(78')-C(73')	118.5(10)
C(77')-C(78')-C(80')	119.2(11)
C(73')-C(78')-C(80')	122.3(10)
C(74')-C(79')-H(79D)	109.5
C(74')-C(79')-H(79E)	109.5
H(79D)-C(79')-H(79E)	109.5
C(74')-C(79')-H(79F)	109.5
H(79D)-C(79')-H(79F)	109.5
H(79E)-C(79')-H(79F)	109.5
C(78')-C(80')-H(80D)	109.5
C(78')-C(80')-H(80E)	109.5
H(80D)-C(80')-H(80E)	109.5
C(78')-C(80')-H(80F)	109.5
H(80D)-C(80')-H(80F)	109.5
H(80E)-C(80')-H(80F)	109.5
C(26)-N(3)-C(9)	119.8(2)
C(26)-N(3)-Al(2)	90.99(18)
C(9)-N(3)-Al(2)	124.0(2)
C(26)-N(4)-C(33)	129.3(3)
C(26)-N(4)-Al(2)	91.48(19)
C(33)-N(4)-Al(2)	139.2(2)
C(51)-N(5)-C(41)	121.9(3)
C(51)-N(5)-Al(3)	91.3(2)
C(41)-N(5)-Al(3)	124.5(3)
C(51)-N(6)-C(58)	130.0(3)
C(51)-N(6)-Al(3)	91.4(2)
C(58)-N(6)-Al(3)	138.6(2)
C(66)-N(7)-C(49)	118.8(3)
C(66)-N(7)-Al(4)	90.1(2)
C(49)-N(7)-Al(4)	126.1(2)
C(66)-N(8)-C(73)	131.1(8)
C(66)-N(8)-C(73')	134(2)
C(66)-N(8)-Al(4)	92.2(2)
C(73)-N(8)-Al(4)	136.6(8)
C(73')-N(8)-Al(4)	133(2)
Cl(1)-C(81)-Cl(2)	102.5(11)
Cl(1)-C(81)-H(81A)	111.3
Cl(2)-C(81)-H(81A)	111.3
Cl(1)-C(81)-H(81B)	111.3
Cl(2)-C(81)-H(81B)	111.3
H(81A)-C(81)-H(81B)	109.2
Cl(2')-C(81')-Cl(1')	117.8(15)
Cl(2')-C(81')-H(81C)	107.9
Cl(1')-C(81')-H(81C)	107.9
Cl(2')-C(81')-H(81D)	107.9

Cl(1')-C(81')-H(81D)	107.9
H(81C)-C(81')-H(81D)	107.2

Symmetry transformations used to generate equivalent atoms:

Table A44. Anisotropic displacement parameters ($\text{Å}^2 \times 10^3$) for L_2Al_2 . The anisotropic displacement factor exponent takes the form: $-2 \pi^2 [h^2 a^{*2} U_{11} + \dots + 2 h k a^* b^* U_{12}]$

	U11	U22	U33	U23	U13	U12
C(1)	28(2)	29(2)	31(2)	7(1)	0(1)	2(1)
C(2)	51(2)	29(2)	41(2)	9(1)	0(2)	6(1)
C(3)	60(2)	46(2)	34(2)	18(2)	-1(2)	9(2)
C(4)	48(2)	47(2)	28(2)	6(1)	-1(1)	7(2)
C(5)	29(2)	35(2)	30(2)	3(1)	3(1)	2(1)
C(6)	39(2)	38(2)	34(2)	-2(1)	4(1)	7(1)
C(7)	51(2)	26(2)	45(2)	-4(1)	7(2)	9(1)
C(8)	48(2)	27(2)	41(2)	8(1)	7(2)	10(1)
C(9)	31(2)	27(1)	27(2)	5(1)	7(1)	4(1)
C(10)	22(1)	28(1)	30(2)	5(1)	4(1)	3(1)
C(11)	34(2)	24(1)	27(2)	7(1)	1(1)	6(1)
C(12)	35(2)	28(2)	48(2)	1(1)	-5(1)	5(1)
C(13)	33(2)	51(2)	72(3)	-7(2)	5(2)	3(2)
C(14)	32(2)	37(2)	64(2)	0(2)	-3(2)	1(1)
C(15)	53(2)	42(2)	77(3)	12(2)	-28(2)	7(2)
C(16)	59(2)	51(2)	65(3)	11(2)	-21(2)	3(2)
C(17)	42(2)	54(2)	64(3)	-6(2)	9(2)	-4(2)
C(18)	32(2)	23(1)	34(2)	3(1)	-2(1)	4(1)
C(19)	35(2)	30(2)	37(2)	2(1)	2(1)	0(1)
C(20)	39(2)	37(2)	43(2)	-5(2)	3(1)	4(1)
C(21)	42(2)	28(2)	59(2)	-3(2)	1(2)	8(1)
C(22)	48(2)	24(2)	56(2)	10(1)	-4(2)	4(1)
C(23)	38(2)	29(2)	39(2)	8(1)	-1(1)	3(1)
C(24)	76(3)	45(2)	38(2)	10(2)	13(2)	6(2)
C(25)	70(3)	41(2)	47(2)	17(2)	10(2)	3(2)
C(26)	38(2)	23(1)	28(2)	4(1)	4(1)	6(1)
C(27)	34(2)	38(2)	37(2)	10(1)	7(1)	10(1)
C(28)	35(2)	69(3)	48(2)	12(2)	4(2)	8(2)
C(29)	47(2)	51(2)	61(2)	15(2)	21(2)	18(2)
C(30)	40(2)	54(2)	44(2)	17(2)	10(2)	1(2)
C(31)	46(2)	68(3)	50(2)	17(2)	-2(2)	-3(2)
C(32)	71(3)	61(2)	52(2)	16(2)	25(2)	31(2)
C(33)	34(2)	47(2)	29(2)	16(1)	8(1)	9(1)
C(34)	42(2)	47(2)	51(2)	23(2)	13(2)	15(2)
C(35)	62(3)	73(3)	66(3)	43(2)	15(2)	27(2)
C(36)	63(3)	103(4)	55(3)	46(3)	5(2)	24(3)
C(37)	49(2)	110(4)	33(2)	20(2)	1(2)	7(2)
C(38)	41(2)	62(2)	34(2)	11(2)	7(1)	4(2)

C(39)	62(2)	35(2)	60(2)	13(2)	15(2)	11(2)
C(40)	71(3)	69(3)	39(2)	-3(2)	7(2)	-2(2)
C(41)	39(2)	62(2)	45(2)	2(2)	5(2)	16(2)
C(42)	53(2)	85(3)	53(2)	-10(2)	10(2)	14(2)
C(43)	68(3)	113(4)	53(3)	1(3)	24(2)	24(3)
C(44)	52(3)	97(4)	70(3)	21(3)	26(2)	22(3)
C(45)	43(2)	71(3)	70(3)	21(2)	13(2)	20(2)
C(46)	32(2)	84(3)	96(4)	19(3)	7(2)	6(2)
C(47)	36(2)	91(4)	93(4)	4(3)	-8(2)	2(2)
C(48)	39(2)	71(3)	64(3)	3(2)	-11(2)	7(2)
C(49)	34(2)	48(2)	52(2)	9(2)	-2(2)	11(2)
C(50)	35(2)	53(2)	50(2)	11(2)	5(2)	15(2)
C(51)	45(2)	51(2)	28(2)	-1(1)	6(1)	13(2)
C(52)	54(2)	57(2)	49(2)	-1(2)	0(2)	21(2)
C(53)	72(3)	70(3)	84(3)	31(3)	-6(3)	20(2)
C(54)	64(3)	73(3)	78(3)	11(2)	-17(2)	22(2)
C(55)	104(4)	82(3)	66(3)	-9(3)	2(3)	51(3)
C(56)	83(3)	49(2)	66(3)	12(2)	2(2)	5(2)
C(57)	51(2)	76(3)	76(3)	-22(2)	5(2)	19(2)
C(58)	38(2)	51(2)	46(2)	19(2)	1(2)	5(2)
C(59)	49(2)	82(3)	66(3)	43(2)	16(2)	16(2)
C(60)	48(3)	96(4)	135(5)	74(4)	14(3)	2(3)
C(61)	60(3)	61(3)	180(7)	46(4)	-15(4)	-12(3)
C(62)	74(3)	44(2)	108(4)	11(2)	-28(3)	-4(2)
C(63)	56(2)	39(2)	54(2)	9(2)	-7(2)	2(2)
C(64)	87(4)	156(6)	58(3)	39(3)	39(3)	41(4)
C(65)	86(3)	57(2)	40(2)	-4(2)	2(2)	3(2)
C(66)	29(2)	35(2)	40(2)	5(1)	-12(1)	3(1)
C(67)	52(2)	34(2)	40(2)	10(1)	-5(2)	5(2)
C(68)	65(2)	43(2)	47(2)	12(2)	-7(2)	18(2)
C(69)	72(3)	51(2)	48(2)	17(2)	-1(2)	12(2)
C(70)	69(3)	37(2)	60(2)	10(2)	-8(2)	-5(2)
C(71)	164(6)	96(4)	73(3)	6(3)	-27(4)	90(4)
C(72)	186(7)	56(3)	63(3)	6(2)	38(4)	-32(4)
Al(1)	32(1)	29(1)	41(1)	1(1)	-4(1)	5(1)
Al(2)	35(1)	38(1)	33(1)	10(1)	8(1)	12(1)
Al(3)	42(1)	43(1)	44(1)	-5(1)	-1(1)	8(1)
Al(4)	90(1)	34(1)	40(1)	7(1)	-1(1)	20(1)
N(1)	33(1)	23(1)	33(1)	4(1)	-2(1)	6(1)
N(2)	35(1)	23(1)	31(1)	4(1)	2(1)	3(1)
C(73)	54(3)	28(3)	33(2)	7(2)	-6(2)	12(3)
C(74)	60(3)	24(2)	38(2)	8(2)	-9(3)	11(3)
C(75)	75(4)	28(2)	38(2)	3(2)	-13(3)	9(3)
C(76)	74(4)	33(3)	39(3)	8(2)	-4(3)	18(3)
C(77)	63(3)	42(3)	41(3)	10(2)	-4(3)	15(3)
C(78)	55(3)	40(3)	38(3)	10(2)	-4(2)	13(2)
C(79)	55(3)	39(4)	59(4)	1(3)	-24(3)	5(3)
C(80)	49(3)	72(5)	47(4)	8(3)	0(3)	12(3)
C(73')	59(4)	30(5)	32(4)	8(4)	-9(4)	14(4)
C(74')	64(4)	27(4)	37(4)	9(3)	-9(4)	10(5)
C(75')	67(5)	33(4)	40(4)	5(3)	-6(4)	13(5)
C(76')	70(5)	37(5)	42(5)	7(4)	-1(5)	17(5)

C(77')	64(5)	45(5)	38(5)	10(4)	-1(4)	15(4)
C(78')	57(4)	38(5)	34(4)	9(4)	-4(4)	18(4)
C(79')	65(6)	31(7)	48(7)	4(6)	-12(6)	0(7)
C(80')	42(6)	70(9)	64(8)	-17(7)	-10(6)	23(7)
N(3)	40(1)	24(1)	29(1)	6(1)	6(1)	10(1)
N(4)	35(1)	32(1)	29(1)	8(1)	6(1)	8(1)
N(5)	39(2)	53(2)	40(2)	-6(1)	2(1)	11(1)
N(6)	39(2)	46(2)	33(1)	2(1)	3(1)	6(1)
N(7)	38(2)	36(1)	39(2)	2(1)	-4(1)	7(1)
N(8)	43(2)	33(1)	31(1)	2(1)	-7(1)	6(1)
Cl(1)	333(8)	279(6)	141(4)	-59(4)	-43(5)	-45(7)
C(81)	276(7)	267(6)	127(4)	-2(5)	-90(5)	-56(6)
Cl(2)	247(5)	253(6)	170(3)	61(4)	-116(3)	-66(5)
Cl(1')	285(8)	275(7)	142(5)	-33(5)	-86(5)	-52(8)
C(81')	278(7)	266(6)	131(4)	-6(5)	-88(5)	-61(6)
Cl(2')	277(7)	264(7)	138(4)	-2(5)	-96(4)	-77(6)

A32. Crystal data and structure refinement of L₂Al₂I₄.

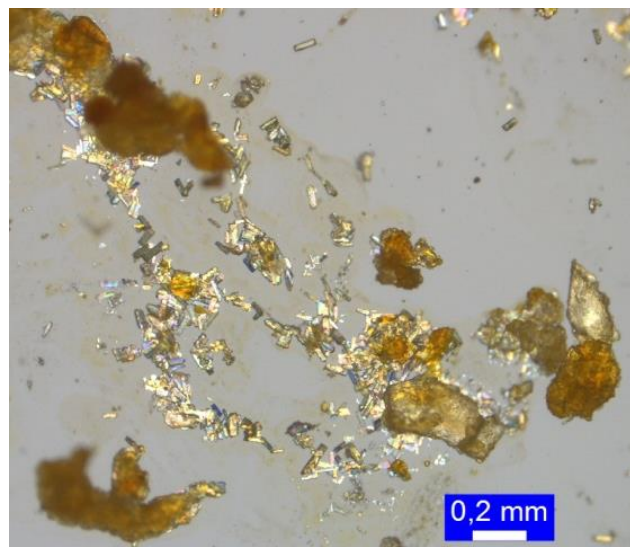


Figure S73. Sample of L₂Al₂I₄.

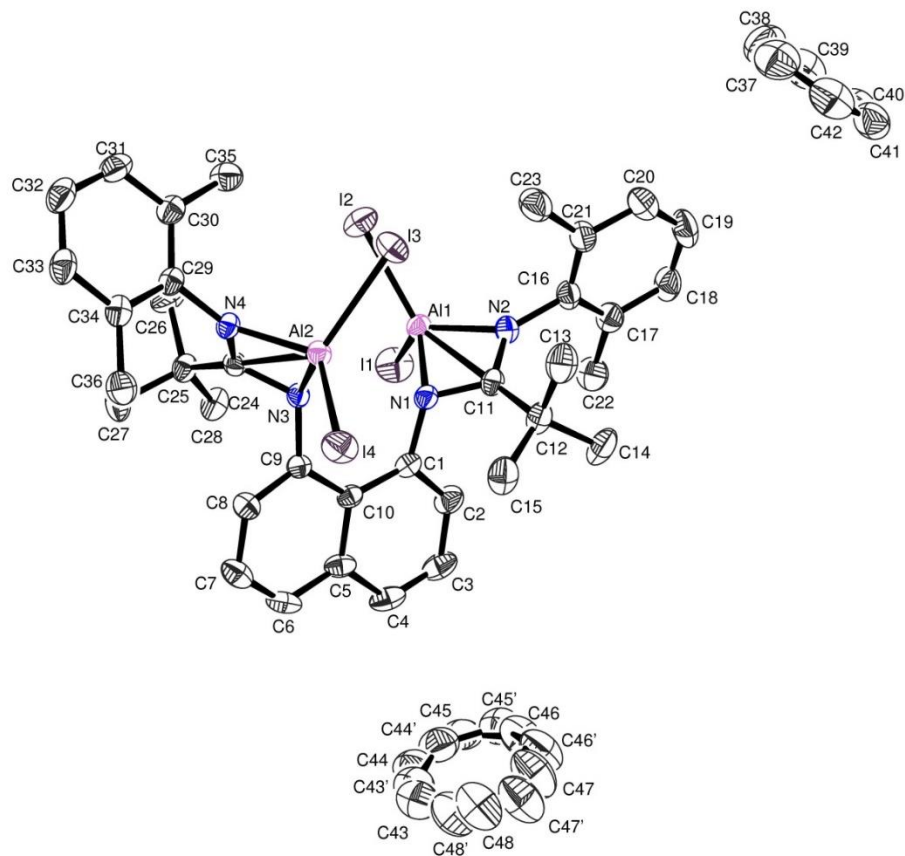


Figure S74. Asymmetric Unit of $\text{L}_2\text{Al}_2\text{I}_4$.

Table A45. Crystal data and structure refinement for $\text{L}_2\text{Al}_2\text{I}_4$.

Identification code	$\text{L}_2\text{Al}_2\text{I}_4$
Empirical formula	$\text{C}_{36}\text{H}_{42}\text{Al}_2\text{I}_4\text{N}_4, 2(\text{C}_6\text{H}_6)$
Formula weight	1248.51
Temperature	193(2) K
Wavelength	0.71073 Å
Crystal system, space group	Monoclinic, P 21/c
Unit cell dimensions	$a = 13.0156(3)$ Å $\alpha = 90$ deg. $b = 13.0496(3)$ Å $\beta = 98.3060(10)$ deg. $c = 29.8921(7)$ Å $\gamma = 90$ deg.
Volume	5023.9(2) Å ³
Z, Calculated density	4, 1.651 Mg/m ³
Absorption coefficient	2.551 mm ⁻¹
F(000)	2432
Crystal size	0.140 x 0.080 x 0.060 mm

Theta range for data collection	2.589 to 33.217 deg.
Limiting indices	-20<=h<=20, -20<=k<=20, -45<=l<=45
Reflections collected / unique	104161 / 19179 [R(int) = 0.0501]
Completeness to theta = 25.242	99.6 %
Refinement method	Full-matrix least-squares on F^2
Data / restraints / parameters	19179 / 222 / 589
Goodness-of-fit on F^2	1.026
Final R indices [$I > 2\sigma(I)$]	R1 = 0.0411, wR2 = 0.0758
R indices (all data)	R1 = 0.0847, wR2 = 0.0890
Largest diff. peak and hole	1.137 and -1.111 e. \AA^{-3}

Table A46. Atomic coordinates ($\times 10^4$) and equivalent isotropic displacement parameters ($\text{\AA}^2 \times 10^3$) for $\text{L}_2\text{Al}_2\text{I}_4$. U(eq) is defined as one third of the trace of the orthogonalized U_{ij} tensor.

	x	y	z	U(eq)
Al(1)	6466(1)	8207(1)	6486(1)	27(1)
Al(2)	8086(1)	4881(1)	6435(1)	24(1)
C(1)	6627(2)	6937(2)	7321(1)	27(1)
C(2)	5947(2)	7393(2)	7574(1)	36(1)
C(3)	6067(3)	7317(3)	8045(1)	43(1)
C(4)	6896(3)	6818(2)	8267(1)	38(1)
C(5)	7662(2)	6383(2)	8028(1)	30(1)
C(6)	8527(3)	5901(2)	8278(1)	35(1)
C(7)	9249(3)	5417(2)	8063(1)	36(1)
C(8)	9120(2)	5421(2)	7591(1)	29(1)
C(9)	8335(2)	5948(2)	7330(1)	23(1)
C(10)	7537(2)	6429(2)	7541(1)	24(1)
C(11)	5359(2)	6893(2)	6649(1)	26(1)
C(12)	4685(2)	5965(2)	6742(1)	35(1)
C(13)	4426(3)	5384(3)	6289(1)	50(1)
C(14)	3673(3)	6282(3)	6904(1)	51(1)
C(15)	5260(3)	5210(3)	7084(1)	45(1)
C(16)	4146(2)	7829(2)	6056(1)	31(1)
C(17)	3412(2)	8454(2)	6223(1)	36(1)
C(18)	2488(2)	8678(3)	5942(1)	43(1)
C(19)	2301(3)	8303(3)	5505(1)	49(1)
C(20)	3050(3)	7724(3)	5339(1)	46(1)
C(21)	3992(2)	7484(3)	5609(1)	37(1)
C(22)	3607(3)	8927(3)	6690(1)	46(1)
C(23)	4795(3)	6890(3)	5401(1)	49(1)
C(24)	9343(2)	6084(2)	6722(1)	23(1)
C(25)	10128(2)	6927(2)	6897(1)	28(1)
C(26)	10414(3)	7536(3)	6489(1)	44(1)

C(27)	11128(2)	6465(3)	7153(1)	41(1)
C(28)	9673(2)	7705(2)	7201(1)	35(1)
C(29)	10287(2)	5199(2)	6151(1)	26(1)
C(30)	10318(2)	5655(2)	5729(1)	31(1)
C(31)	11129(3)	5395(3)	5494(1)	38(1)
C(32)	11877(2)	4690(3)	5667(1)	41(1)
C(33)	11813(2)	4224(3)	6073(1)	37(1)
C(35)	9516(3)	6419(2)	5519(1)	38(1)
C(36)	10946(3)	3873(3)	6751(1)	39(1)
C(37)	1037(4)	7988(4)	4237(2)	72(1)
C(42)	226(4)	7538(3)	4406(2)	67(1)
C(41)	-527(4)	8124(4)	4546(1)	64(1)
C(40)	-474(4)	9176(4)	4525(1)	61(1)
C(39)	335(4)	9626(3)	4357(2)	69(1)
C(38)	1086(4)	9047(4)	4207(2)	76(1)
C(34)	11022(2)	4455(2)	6324(1)	30(1)
C(43)	6359(8)	6056(8)	9558(3)	68(2)
C(44)	6415(7)	7087(8)	9488(3)	63(2)
C(45)	5594(9)	7634(7)	9288(3)	65(2)
C(46)	4666(9)	7139(10)	9160(4)	77(2)
C(47)	4541(8)	6079(10)	9246(4)	87(2)
C(48)	5422(10)	5546(7)	9450(4)	80(2)
C(43')	6402(12)	6476(15)	9529(6)	69(2)
C(44')	5980(13)	7358(12)	9346(6)	68(2)
C(45')	4997(15)	7490(11)	9161(6)	66(2)
C(46')	4389(11)	6633(15)	9158(5)	78(3)
C(47')	4751(14)	5692(12)	9379(6)	84(2)
C(48')	5814(15)	5607(12)	9544(6)	78(2)
I(1)	6783(1)	9801(1)	6946(1)	53(1)
I(2)	7436(1)	8253(1)	5829(1)	44(1)
I(3)	7038(1)	4873(1)	5666(1)	38(1)
I(4)	7773(1)	3252(1)	6834(1)	41(1)
N(1)	6374(2)	7015(2)	6839(1)	26(1)
N(2)	5110(2)	7634(2)	6347(1)	28(1)
N(3)	8371(2)	5978(2)	6853(1)	22(1)
N(4)	9442(2)	5397(2)	6402(1)	23(1)

Table A47. Bond lengths [Å] and angles [deg] for L₂Al₂I₄.

Al(1)-N(1)	1.894(2)
Al(1)-N(2)	1.906(2)
Al(1)-C(11)	2.336(3)
Al(1)-I(2)	2.4847(9)
Al(1)-I(1)	2.4949(9)
Al(2)-N(3)	1.901(2)
Al(2)-N(4)	1.905(2)
Al(2)-C(24)	2.339(3)
Al(2)-I(3)	2.4987(8)
Al(2)-I(4)	2.4996(8)

C(1)-C(2)	1.378(4)
C(1)-C(10)	1.431(4)
C(1)-N(1)	1.434(3)
C(2)-C(3)	1.398(4)
C(2)-H(2)	0.9500
C(3)-C(4)	1.350(5)
C(3)-H(3)	0.9500
C(4)-C(5)	1.427(4)
C(4)-H(4)	0.9500
C(5)-C(6)	1.407(4)
C(5)-C(10)	1.442(4)
C(6)-C(7)	1.367(5)
C(6)-H(6)	0.9500
C(7)-C(8)	1.396(4)
C(7)-H(7)	0.9500
C(8)-C(9)	1.376(4)
C(8)-H(8)	0.9500
C(9)-N(3)	1.433(3)
C(9)-C(10)	1.436(4)
C(11)-N(2)	1.331(3)
C(11)-N(1)	1.371(3)
C(11)-C(12)	1.544(4)
C(12)-C(14)	1.525(4)
C(12)-C(15)	1.534(4)
C(12)-C(13)	1.547(5)
C(13)-H(13A)	0.9800
C(13)-H(13B)	0.9800
C(13)-H(13C)	0.9800
C(14)-H(14A)	0.9800
C(14)-H(14B)	0.9800
C(14)-H(14C)	0.9800
C(15)-H(15A)	0.9800
C(15)-H(15B)	0.9800
C(15)-H(15C)	0.9800
C(16)-C(21)	1.396(4)
C(16)-C(17)	1.402(4)
C(16)-N(2)	1.442(4)
C(17)-C(18)	1.396(4)
C(17)-C(22)	1.513(5)
C(18)-C(19)	1.382(5)
C(18)-H(18)	0.9500
C(19)-C(20)	1.382(5)
C(19)-H(19)	0.9500
C(20)-C(21)	1.404(4)
C(20)-H(20)	0.9500
C(21)-C(23)	1.505(5)
C(22)-H(22A)	0.9800
C(22)-H(22B)	0.9800
C(22)-H(22C)	0.9800
C(23)-H(23A)	0.9800
C(23)-H(23B)	0.9800
C(23)-H(23C)	0.9800

C(24)-N(4)	1.330(3)
C(24)-N(3)	1.385(3)
C(24)-C(25)	1.540(4)
C(25)-C(27)	1.534(4)
C(25)-C(28)	1.537(4)
C(25)-C(26)	1.545(4)
C(26)-H(26A)	0.9800
C(26)-H(26B)	0.9800
C(26)-H(26C)	0.9800
C(27)-H(27A)	0.9800
C(27)-H(27B)	0.9800
C(27)-H(27C)	0.9800
C(28)-H(28A)	0.9800
C(28)-H(28B)	0.9800
C(28)-H(28C)	0.9800
C(29)-C(30)	1.401(4)
C(29)-C(34)	1.408(4)
C(29)-N(4)	1.441(3)
C(30)-C(31)	1.392(4)
C(30)-C(35)	1.512(4)
C(31)-C(32)	1.384(5)
C(31)-H(31)	0.9500
C(32)-C(33)	1.370(5)
C(32)-H(32)	0.9500
C(33)-C(34)	1.393(4)
C(33)-H(33)	0.9500
C(35)-H(35C)	0.9800
C(35)-H(35B)	0.9800
C(35)-H(35A)	0.9800
C(36)-C(34)	1.503(4)
C(36)-H(36A)	0.9800
C(36)-H(36C)	0.9800
C(36)-H(36B)	0.9800
C(37)-C(42)	1.367(7)
C(37)-C(38)	1.387(7)
C(37)-H(37)	0.9500
C(42)-C(41)	1.355(7)
C(42)-H(42)	0.9500
C(41)-C(40)	1.376(6)
C(41)-H(41)	0.9500
C(40)-C(39)	1.363(7)
C(40)-H(40)	0.9500
C(39)-C(38)	1.361(7)
C(39)-H(39)	0.9500
C(38)-H(38)	0.9500
C(43)-C(44)	1.365(11)
C(43)-C(48)	1.386(12)
C(43)-H(43)	0.9500
C(44)-C(45)	1.351(11)
C(44)-H(44)	0.9500
C(45)-C(46)	1.374(13)
C(45)-H(45)	0.9500

C(46)-C(47)	1.421(14)
C(46)-H(46)	0.9500
C(47)-C(48)	1.403(12)
C(47)-H(47)	0.9500
C(48)-H(48)	0.9500
C(43')-C(44')	1.356(16)
C(43')-C(48')	1.373(15)
C(43')-H(43')	0.9500
C(44')-C(45')	1.330(16)
C(44')-H(44')	0.9500
C(45')-C(46')	1.369(16)
C(45')-H(45')	0.9500
C(46')-C(47')	1.442(16)
C(46')-H(46')	0.9500
C(47')-C(48')	1.404(16)
C(47')-H(47')	0.9500
C(48')-H(48')	0.9500
N(1)-Al(1)-N(2)	70.66(10)
N(1)-Al(1)-C(11)	35.93(10)
N(2)-Al(1)-C(11)	34.74(9)
N(1)-Al(1)-I(2)	122.74(8)
N(2)-Al(1)-I(2)	113.38(8)
C(11)-Al(1)-I(2)	125.58(7)
N(1)-Al(1)-I(1)	113.30(8)
N(2)-Al(1)-I(1)	121.40(8)
C(11)-Al(1)-I(1)	123.66(7)
I(2)-Al(1)-I(1)	110.74(3)
N(3)-Al(2)-N(4)	70.93(9)
N(3)-Al(2)-C(24)	36.29(9)
N(4)-Al(2)-C(24)	34.65(9)
N(3)-Al(2)-I(3)	129.53(8)
N(4)-Al(2)-I(3)	109.88(7)
C(24)-Al(2)-I(3)	126.83(7)
N(3)-Al(2)-I(4)	110.92(7)
N(4)-Al(2)-I(4)	122.78(8)
C(24)-Al(2)-I(4)	123.35(7)
I(3)-Al(2)-I(4)	109.33(3)
C(2)-C(1)-C(10)	120.2(3)
C(2)-C(1)-N(1)	116.6(3)
C(10)-C(1)-N(1)	123.3(2)
C(1)-C(2)-C(3)	122.3(3)
C(1)-C(2)-H(2)	118.8
C(3)-C(2)-H(2)	118.8
C(4)-C(3)-C(2)	119.6(3)
C(4)-C(3)-H(3)	120.2
C(2)-C(3)-H(3)	120.2
C(3)-C(4)-C(5)	120.9(3)
C(3)-C(4)-H(4)	119.6
C(5)-C(4)-H(4)	119.6
C(6)-C(5)-C(4)	118.4(3)
C(6)-C(5)-C(10)	121.4(3)

C(4)-C(5)-C(10)	120.2(3)
C(7)-C(6)-C(5)	120.5(3)
C(7)-C(6)-H(6)	119.7
C(5)-C(6)-H(6)	119.7
C(6)-C(7)-C(8)	118.9(3)
C(6)-C(7)-H(7)	120.6
C(8)-C(7)-H(7)	120.6
C(9)-C(8)-C(7)	123.1(3)
C(9)-C(8)-H(8)	118.5
C(7)-C(8)-H(8)	118.5
C(8)-C(9)-N(3)	116.7(2)
C(8)-C(9)-C(10)	119.6(2)
N(3)-C(9)-C(10)	123.7(2)
C(1)-C(10)-C(9)	127.2(2)
C(1)-C(10)-C(5)	116.6(2)
C(9)-C(10)-C(5)	116.2(2)
N(2)-C(11)-N(1)	108.8(2)
N(2)-C(11)-C(12)	127.1(2)
N(1)-C(11)-C(12)	123.7(2)
N(2)-C(11)-Al(1)	54.70(14)
N(1)-C(11)-Al(1)	54.16(13)
C(12)-C(11)-Al(1)	175.5(2)
C(14)-C(12)-C(15)	108.8(3)
C(14)-C(12)-C(11)	112.5(3)
C(15)-C(12)-C(11)	112.9(3)
C(14)-C(12)-C(13)	108.8(3)
C(15)-C(12)-C(13)	107.0(3)
C(11)-C(12)-C(13)	106.6(3)
C(12)-C(13)-H(13A)	109.5
C(12)-C(13)-H(13B)	109.5
H(13A)-C(13)-H(13B)	109.5
C(12)-C(13)-H(13C)	109.5
H(13A)-C(13)-H(13C)	109.5
H(13B)-C(13)-H(13C)	109.5
C(12)-C(14)-H(14A)	109.5
C(12)-C(14)-H(14B)	109.5
H(14A)-C(14)-H(14B)	109.5
C(12)-C(14)-H(14C)	109.5
H(14A)-C(14)-H(14C)	109.5
H(14B)-C(14)-H(14C)	109.5
C(12)-C(15)-H(15A)	109.5
C(12)-C(15)-H(15B)	109.5
H(15A)-C(15)-H(15B)	109.5
C(12)-C(15)-H(15C)	109.5
H(15A)-C(15)-H(15C)	109.5
H(15B)-C(15)-H(15C)	109.5
C(21)-C(16)-C(17)	121.2(3)
C(21)-C(16)-N(2)	120.8(3)
C(17)-C(16)-N(2)	117.8(3)
C(18)-C(17)-C(16)	118.6(3)
C(18)-C(17)-C(22)	119.0(3)
C(16)-C(17)-C(22)	122.3(3)

C(19)-C(18)-C(17)	121.0(3)
C(19)-C(18)-H(18)	119.5
C(17)-C(18)-H(18)	119.5
C(20)-C(19)-C(18)	119.7(3)
C(20)-C(19)-H(19)	120.1
C(18)-C(19)-H(19)	120.1
C(19)-C(20)-C(21)	121.2(3)
C(19)-C(20)-H(20)	119.4
C(21)-C(20)-H(20)	119.4
C(16)-C(21)-C(20)	118.1(3)
C(16)-C(21)-C(23)	123.3(3)
C(20)-C(21)-C(23)	118.5(3)
C(17)-C(22)-H(22A)	109.5
C(17)-C(22)-H(22B)	109.5
H(22A)-C(22)-H(22B)	109.5
C(17)-C(22)-H(22C)	109.5
H(22A)-C(22)-H(22C)	109.5
H(22B)-C(22)-H(22C)	109.5
C(21)-C(23)-H(23A)	109.5
C(21)-C(23)-H(23B)	109.5
H(23A)-C(23)-H(23B)	109.5
C(21)-C(23)-H(23C)	109.5
H(23A)-C(23)-H(23C)	109.5
H(23B)-C(23)-H(23C)	109.5
N(4)-C(24)-N(3)	108.8(2)
N(4)-C(24)-C(25)	126.7(2)
N(3)-C(24)-C(25)	124.3(2)
N(4)-C(24)-Al(2)	54.50(13)
N(3)-C(24)-Al(2)	54.36(13)
C(25)-C(24)-Al(2)	176.59(19)
C(27)-C(25)-C(28)	109.6(2)
C(27)-C(25)-C(24)	111.2(2)
C(28)-C(25)-C(24)	112.3(2)
C(27)-C(25)-C(26)	108.2(3)
C(28)-C(25)-C(26)	106.5(3)
C(24)-C(25)-C(26)	108.8(2)
C(25)-C(26)-H(26A)	109.5
C(25)-C(26)-H(26B)	109.5
H(26A)-C(26)-H(26B)	109.5
C(25)-C(26)-H(26C)	109.5
H(26A)-C(26)-H(26C)	109.5
H(26B)-C(26)-H(26C)	109.5
C(25)-C(27)-H(27A)	109.5
C(25)-C(27)-H(27B)	109.5
H(27A)-C(27)-H(27B)	109.5
C(25)-C(27)-H(27C)	109.5
H(27A)-C(27)-H(27C)	109.5
H(27B)-C(27)-H(27C)	109.5
C(25)-C(28)-H(28A)	109.5
C(25)-C(28)-H(28B)	109.5
H(28A)-C(28)-H(28B)	109.5
C(25)-C(28)-H(28C)	109.5

H(28A)-C(28)-H(28C)	109.5
H(28B)-C(28)-H(28C)	109.5
C(30)-C(29)-C(34)	121.1(3)
C(30)-C(29)-N(4)	121.1(2)
C(34)-C(29)-N(4)	117.5(2)
C(31)-C(30)-C(29)	118.3(3)
C(31)-C(30)-C(35)	118.7(3)
C(29)-C(30)-C(35)	123.0(3)
C(32)-C(31)-C(30)	121.2(3)
C(32)-C(31)-H(31)	119.4
C(30)-C(31)-H(31)	119.4
C(33)-C(32)-C(31)	119.8(3)
C(33)-C(32)-H(32)	120.1
C(31)-C(32)-H(32)	120.1
C(32)-C(33)-C(34)	121.6(3)
C(32)-C(33)-H(33)	119.2
C(34)-C(33)-H(33)	119.2
C(30)-C(35)-H(35C)	109.5
C(30)-C(35)-H(35B)	109.5
H(35C)-C(35)-H(35B)	109.5
C(30)-C(35)-H(35A)	109.5
H(35C)-C(35)-H(35A)	109.5
H(35B)-C(35)-H(35A)	109.5
C(34)-C(36)-H(36A)	109.5
C(34)-C(36)-H(36C)	109.5
H(36A)-C(36)-H(36C)	109.5
C(34)-C(36)-H(36B)	109.5
H(36A)-C(36)-H(36B)	109.5
H(36C)-C(36)-H(36B)	109.5
C(42)-C(37)-C(38)	119.8(5)
C(42)-C(37)-H(37)	120.1
C(38)-C(37)-H(37)	120.1
C(41)-C(42)-C(37)	120.2(4)
C(41)-C(42)-H(42)	119.9
C(37)-C(42)-H(42)	119.9
C(42)-C(41)-C(40)	120.3(4)
C(42)-C(41)-H(41)	119.8
C(40)-C(41)-H(41)	119.8
C(39)-C(40)-C(41)	119.6(4)
C(39)-C(40)-H(40)	120.2
C(41)-C(40)-H(40)	120.2
C(38)-C(39)-C(40)	120.7(4)
C(38)-C(39)-H(39)	119.6
C(40)-C(39)-H(39)	119.6
C(39)-C(38)-C(37)	119.4(5)
C(39)-C(38)-H(38)	120.3
C(37)-C(38)-H(38)	120.3
C(33)-C(34)-C(29)	117.9(3)
C(33)-C(34)-C(36)	119.6(3)
C(29)-C(34)-C(36)	122.4(3)
C(44)-C(43)-C(48)	120.2(9)
C(44)-C(43)-H(43)	119.9

C(48)-C(43)-H(43)	119.9
C(45)-C(44)-C(43)	122.1(9)
C(45)-C(44)-H(44)	118.9
C(43)-C(44)-H(44)	118.9
C(44)-C(45)-C(46)	118.8(9)
C(44)-C(45)-H(45)	120.6
C(46)-C(45)-H(45)	120.6
C(45)-C(46)-C(47)	121.8(9)
C(45)-C(46)-H(46)	119.1
C(47)-C(46)-H(46)	119.1
C(48)-C(47)-C(46)	117.0(9)
C(48)-C(47)-H(47)	121.5
C(46)-C(47)-H(47)	121.5
C(43)-C(48)-C(47)	119.9(9)
C(43)-C(48)-H(48)	120.0
C(47)-C(48)-H(48)	120.0
C(44')-C(43')-C(48')	121.2(13)
C(44')-C(43')-H(43')	119.4
C(48')-C(43')-H(43')	119.4
C(45')-C(44')-C(43')	126.0(14)
C(45')-C(44')-H(44')	117.0
C(43')-C(44')-H(44')	117.0
C(44')-C(45')-C(46')	114.6(14)
C(44')-C(45')-H(45')	122.7
C(46')-C(45')-H(45')	122.7
C(45')-C(46')-C(47')	122.9(13)
C(45')-C(46')-H(46')	118.5
C(47')-C(46')-H(46')	118.6
C(48')-C(47')-C(46')	117.9(13)
C(48')-C(47')-H(47')	121.1
C(46')-C(47')-H(47')	121.0
C(43')-C(48')-C(47')	116.7(13)
C(43')-C(48')-H(48')	121.6
C(47')-C(48')-H(48')	121.6
C(11)-N(1)-C(1)	118.4(2)
C(11)-N(1)-Al(1)	89.91(17)
C(1)-N(1)-Al(1)	126.53(18)
C(11)-N(2)-C(16)	130.0(2)
C(11)-N(2)-Al(1)	90.57(17)
C(16)-N(2)-Al(1)	139.5(2)
C(24)-N(3)-C(9)	116.6(2)
C(24)-N(3)-Al(2)	89.36(15)
C(9)-N(3)-Al(2)	126.95(17)
C(24)-N(4)-C(29)	130.9(2)
C(24)-N(4)-Al(2)	90.86(16)
C(29)-N(4)-Al(2)	138.27(18)

Symmetry transformations used to generate equivalent atoms:

Table A48. Anisotropic displacement parameters ($\text{\AA}^2 \times 10^3$) for $\text{L}_2\text{Al}_2\text{I}_4$. The anisotropic displacement factor exponent takes the form: $-2 \pi^2 [h^2 a^{*2} U_{11} + \dots + 2 h k a^* b^* U_{12}]$

	U11	U22	U33	U23	U13	U12
Al(1)	26(1)	27(1)	30(1)	2(1)	5(1)	-1(1)
Al(2)	24(1)	24(1)	25(1)	-2(1)	2(1)	-2(1)
C(1)	29(1)	26(1)	27(1)	0(1)	9(1)	-1(1)
C(2)	36(2)	38(2)	38(2)	-1(1)	14(1)	7(1)
C(3)	52(2)	43(2)	40(2)	-2(1)	26(2)	4(2)
C(4)	57(2)	34(2)	27(1)	-4(1)	19(1)	-5(2)
C(5)	43(2)	23(1)	24(1)	0(1)	9(1)	-4(1)
C(6)	54(2)	31(2)	20(1)	4(1)	0(1)	-5(1)
C(7)	41(2)	29(1)	33(2)	4(1)	-7(1)	0(1)
C(8)	30(1)	29(1)	29(1)	1(1)	1(1)	2(1)
C(9)	25(1)	22(1)	22(1)	-1(1)	3(1)	-3(1)
C(10)	27(1)	21(1)	23(1)	0(1)	7(1)	-3(1)
C(11)	22(1)	27(1)	31(1)	-2(1)	7(1)	3(1)
C(12)	27(1)	33(2)	46(2)	4(1)	10(1)	0(1)
C(13)	42(2)	43(2)	64(2)	-4(2)	6(2)	-15(2)
C(14)	35(2)	50(2)	72(2)	18(2)	26(2)	5(2)
C(15)	37(2)	31(2)	68(2)	14(2)	7(2)	-1(1)
C(16)	24(1)	31(1)	37(2)	5(1)	2(1)	1(1)
C(17)	33(2)	31(2)	43(2)	7(1)	6(1)	5(1)
C(18)	29(2)	41(2)	58(2)	11(2)	6(1)	10(1)
C(19)	30(2)	49(2)	64(2)	11(2)	-9(2)	4(2)
C(20)	43(2)	50(2)	41(2)	1(2)	-5(1)	-1(2)
C(21)	30(2)	41(2)	39(2)	-1(1)	1(1)	-1(1)
C(22)	43(2)	45(2)	52(2)	-2(2)	10(2)	17(2)
C(23)	43(2)	66(2)	38(2)	-10(2)	1(1)	10(2)
C(24)	22(1)	23(1)	24(1)	1(1)	3(1)	4(1)
C(25)	26(1)	28(1)	32(1)	-6(1)	6(1)	-5(1)
C(26)	50(2)	40(2)	45(2)	-10(1)	20(2)	-21(2)
C(27)	26(2)	45(2)	50(2)	-16(2)	-2(1)	0(1)
C(28)	33(2)	29(2)	44(2)	-13(1)	11(1)	-6(1)
C(29)	24(1)	26(1)	29(1)	-7(1)	7(1)	-2(1)
C(30)	31(1)	31(1)	31(1)	-7(1)	8(1)	-3(1)
C(31)	41(2)	45(2)	32(2)	-5(1)	15(1)	-5(1)
C(32)	33(2)	50(2)	45(2)	-11(2)	15(1)	-1(1)
C(33)	27(2)	40(2)	45(2)	-8(1)	9(1)	6(1)
C(35)	43(2)	37(2)	33(2)	3(1)	8(1)	3(1)
C(36)	36(2)	38(2)	44(2)	4(1)	5(1)	12(1)
C(37)	86(3)	69(3)	59(3)	-16(2)	11(2)	8(3)
C(42)	90(3)	41(2)	63(3)	-2(2)	-10(2)	-8(2)
C(41)	61(3)	66(3)	60(3)	20(2)	-7(2)	-10(2)
C(40)	63(3)	67(3)	51(2)	3(2)	-3(2)	15(2)
C(39)	87(3)	45(2)	68(3)	2(2)	-11(3)	-10(2)
C(38)	81(3)	77(3)	72(3)	-1(3)	22(3)	-25(3)
C(34)	26(1)	28(1)	36(2)	-7(1)	5(1)	-1(1)

C(43)	78(4)	64(4)	61(3)	-2(4)	11(3)	19(4)
C(44)	65(4)	70(4)	58(4)	14(3)	23(3)	19(3)
C(45)	74(4)	74(4)	51(3)	18(3)	18(3)	21(3)
C(46)	85(4)	73(5)	69(3)	-6(4)	-6(4)	18(4)
C(47)	92(4)	73(4)	85(4)	-14(4)	-24(3)	6(4)
C(48)	89(5)	65(4)	80(4)	-14(3)	-10(4)	15(4)
C(43')	73(4)	74(5)	61(4)	2(4)	13(3)	13(4)
C(44')	73(5)	74(4)	61(4)	9(4)	22(4)	10(4)
C(45')	75(5)	66(5)	61(4)	0(4)	17(4)	11(4)
C(46')	85(5)	66(6)	74(5)	8(5)	-19(4)	3(4)
C(47')	92(5)	65(5)	83(5)	-3(4)	-23(4)	2(4)
C(48')	84(5)	68(4)	77(5)	-1(4)	-6(4)	13(4)
I(1)	69(1)	38(1)	52(1)	-14(1)	7(1)	-10(1)
I(2)	48(1)	43(1)	45(1)	7(1)	22(1)	0(1)
I(3)	39(1)	41(1)	30(1)	-4(1)	-6(1)	-1(1)
I(4)	49(1)	31(1)	42(1)	7(1)	1(1)	-9(1)
N(1)	23(1)	28(1)	27(1)	2(1)	6(1)	3(1)
N(2)	23(1)	28(1)	31(1)	0(1)	3(1)	2(1)
N(3)	20(1)	24(1)	23(1)	-2(1)	3(1)	0(1)
N(4)	21(1)	23(1)	26(1)	-3(1)	5(1)	0(1)

A33. Crystal data and structure refinement of 4a.

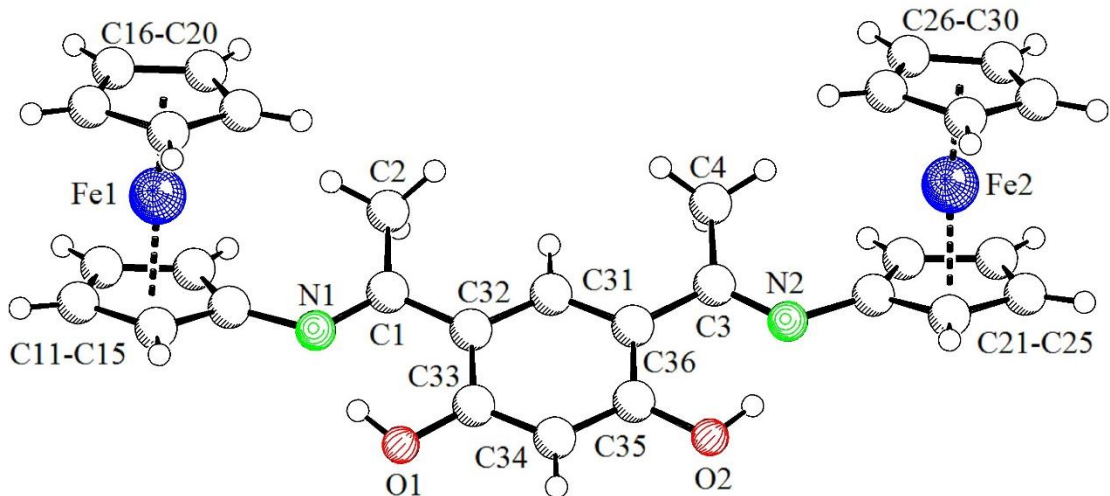


Figure S75. Compound 4a.

Table A49. Sample and crystal data for 4a.

Identification code	4a	
Chemical formula	C ₃₀ H ₂₈ Fe ₂ N ₂ O ₂	
Formula weight	560.24 g/mol	
Temperature	173(2) K	
Wavelength	0.71073 Å	
Crystal size	0.020 x 0.100 x 0.330 mm	
Crystal habit	red plate	
Crystal system	monoclinic	
Space group	P 1 21/n 1	
Unit cell dimensions	a = 7.5164(2) Å b = 16.1852(4) Å c = 18.8959(6) Å	a = 90° b = 93.9080(10)° g = 90°
Volume	2293.42(11) Å ³	
Z	4	
Density (calculated)	1.623 g/cm ³	
Absorption coefficient	1.299 mm ⁻¹	
F(000)	1160	

Table A50. Data collection and structure refinement for 4a

Theta range for data collection	4.09 to 25.00°
Index ranges	-8<=h<=8, -18<=k<=19, -22<=l<=22
Reflections collected	7165
Independent reflections	3850 [R(int) = 0.0552]
Absorption correction	multi-scan
Max. and min. transmission	0.9740 and 0.6740
Structure solution technique	direct methods
Structure solution program	SHELXL-2014/7 (Sheldrick, 2014)
Refinement method	Full-matrix least-squares on F ²
Refinement program	SHELXL-2014/7 (Sheldrick, 2014)
Function minimized	S w(F ₀ ² - F _c ²) ²
Data / restraints / parameters	3850 / 2 / 333
Goodness-of-fit on F²	1.099
D/smax	0.001
Final R indices	3414 data; I>2s(I) R1 = 0.0638, wR2 = 0.1703 all data R1 = 0.0708, wR2 = 0.1771
Weighting scheme	w=1/[s ² (F ₀ ²)+(0.0762P) ² +5.3520P]where P=(F ₀ ² +2F _c ²)/3
Largest diff. peak and hole	0.474 and -0.686 eÅ ⁻³
R.M.S. deviation from mean	0.125 eÅ ⁻³

Table A51. Bond lengths (Å) for 4a.

Fe1-C13	2.043(5)	Fe1-C15	2.048(5)
Fe1-C18	2.049(4)	Fe1-C19	2.050(5)
Fe1-C17	2.056(5)	Fe1-C12	2.057(5)
Fe1-C16	2.058(5)	Fe1-C20	2.058(5)
Fe1-C11	2.059(5)	Fe1-C14	2.063(5)
O1-C33	1.320(5)	O1-H1	0.86(2)
N1-C1	1.298(5)	N1-C11	1.409(6)
C1-C32	1.454(6)	C1-C2	1.507(6)
C2-H2A	0.98	C2-H2B	0.98
C2-H2C	0.98	Fe2-C28	2.035(5)
Fe2-C23	2.042(5)	Fe2-C24	2.045(5)
Fe2-C29	2.046(4)	Fe2-C25	2.046(4)
Fe2-C30	2.052(5)	Fe2-C27	2.056(5)
Fe2-C22	2.060(5)	Fe2-C26	2.060(5)
Fe2-C21	2.070(4)	O2-C35	1.340(6)
O2-H2	0.88(2)	N2-C3	1.300(6)
N2-C21	1.425(6)	C3-C36	1.463(6)
C3-C4	1.504(6)	C4-H4A	0.98
C4-H4B	0.98	C4-H4C	0.98
C11-C15	1.432(6)	C11-C12	1.438(6)
C12-C13	1.424(7)	C12-H12	0.95
C13-C14	1.429(7)	C13-H13	0.95
C14-C15	1.409(6)	C14-H14	0.95
C15-H15	0.95	C16-C20	1.428(7)
C16-C17	1.434(7)	C16-H16	0.95
C17-C18	1.413(7)	C17-H17	0.95
C18-C19	1.422(7)	C18-H18	0.95
C19-C20	1.432(7)	C19-H19	0.95
C20-H20	0.95	C21-C25	1.427(7)
C21-C22	1.447(6)	C22-C23	1.416(6)
C22-H22	0.95	C23-C24	1.417(7)
C23-H23	0.95	C24-C25	1.423(7)
C24-H24	0.95	C25-H25	0.95
C26-C27	1.410(8)	C26-C30	1.428(7)
C26-H26	0.95	C27-C28	1.436(8)
C27-H27	0.95	C28-C29	1.391(7)
C28-H28	0.95	C29-C30	1.429(7)
C29-H29	0.95	C30-H30	0.95
C31-C36	1.391(6)	C31-C32	1.396(6)
C31-H31	0.95	C32-C33	1.437(6)
C33-C34	1.389(6)	C34-C35	1.401(6)
C34-H34	0.95	C35-C36	1.426(6)

Table A52. Bond angles ($^{\circ}$) for 4a.

C13-Fe1-C15	68.09(19)	C13-Fe1-C18	159.5(2)
C15-Fe1-C18	108.94(19)	C13-Fe1-C19	158.2(2)
C15-Fe1-C19	123.30(19)	C18-Fe1-C19	40.6(2)
C13-Fe1-C17	123.3(2)	C15-Fe1-C17	124.0(2)
C18-Fe1-C17	40.3(2)	C19-Fe1-C17	68.3(2)
C13-Fe1-C12	40.63(18)	C15-Fe1-C12	68.50(19)
C18-Fe1-C12	159.0(2)	C19-Fe1-C12	122.07(19)
C17-Fe1-C12	158.5(2)	C13-Fe1-C16	107.1(2)
C15-Fe1-C16	159.6(2)	C18-Fe1-C16	68.2(2)
C19-Fe1-C16	68.6(2)	C17-Fe1-C16	40.8(2)
C12-Fe1-C16	121.6(2)	C13-Fe1-C20	122.1(2)
C15-Fe1-C20	158.9(2)	C18-Fe1-C20	68.2(2)
C19-Fe1-C20	40.8(2)	C17-Fe1-C20	68.3(2)
C12-Fe1-C20	106.3(2)	C16-Fe1-C20	40.6(2)
C13-Fe1-C11	68.47(18)	C15-Fe1-C11	40.83(18)
C18-Fe1-C11	123.49(19)	C19-Fe1-C11	107.00(18)
C17-Fe1-C11	159.7(2)	C12-Fe1-C11	40.89(18)
C16-Fe1-C11	157.79(19)	C20-Fe1-C11	121.90(19)
C13-Fe1-C14	40.74(19)	C15-Fe1-C14	40.10(18)
C18-Fe1-C14	123.9(2)	C19-Fe1-C14	159.3(2)
C17-Fe1-C14	108.7(2)	C12-Fe1-C14	68.47(19)
C16-Fe1-C14	123.5(2)	C20-Fe1-C14	158.9(2)
C11-Fe1-C14	68.31(18)	C33-O1-H1	107.(4)
C1-N1-C11	127.1(4)	N1-C1-C32	118.4(4)
N1-C1-C2	122.6(4)	C32-C1-C2	119.0(4)
C1-C2-H2A	109.5	C1-C2-H2B	109.5
H2A-C2-H2B	109.5	C1-C2-H2C	109.5
H2A-C2-H2C	109.5	H2B-C2-H2C	109.5
C28-Fe2-C23	105.2(2)	C28-Fe2-C24	120.2(2)
C23-Fe2-C24	40.6(2)	C28-Fe2-C29	39.9(2)
C23-Fe2-C29	116.85(19)	C24-Fe2-C29	102.8(2)
C28-Fe2-C25	157.00(19)	C23-Fe2-C25	68.42(19)
C24-Fe2-C25	40.71(19)	C29-Fe2-C25	121.65(19)
C28-Fe2-C30	68.0(2)	C23-Fe2-C30	152.4(2)
C24-Fe2-C30	118.1(2)	C29-Fe2-C30	40.82(19)
C25-Fe2-C30	106.9(2)	C28-Fe2-C27	41.1(2)
C23-Fe2-C27	125.5(2)	C24-Fe2-C27	159.3(2)
C29-Fe2-C27	68.0(2)	C25-Fe2-C27	159.8(2)
C30-Fe2-C27	67.9(2)	C28-Fe2-C22	121.8(2)
C23-Fe2-C22	40.38(18)	C24-Fe2-C22	68.22(19)
C29-Fe2-C22	153.6(2)	C25-Fe2-C22	68.56(18)
C30-Fe2-C22	165.37(19)	C27-Fe2-C22	111.3(2)
C28-Fe2-C26	68.3(2)	C23-Fe2-C26	163.7(2)
C24-Fe2-C26	155.7(2)	C29-Fe2-C26	68.4(2)
C25-Fe2-C26	123.4(2)	C30-Fe2-C26	40.7(2)

C27-Fe2-C26	40.1(2)	C22-Fe2-C26	129.3(2)
C28-Fe2-C21	159.6(2)	C23-Fe2-C21	68.41(19)
C24-Fe2-C21	68.32(19)	C29-Fe2-C21	160.5(2)
C25-Fe2-C21	40.56(18)	C30-Fe2-C21	126.7(2)
C27-Fe2-C21	125.9(2)	C22-Fe2-C21	41.02(18)
C26-Fe2-C21	112.2(2)	C35-O2-H2	107.(4)
C3-N2-C21	125.8(4)	N2-C3-C36	117.2(4)
N2-C3-C4	123.0(4)	C36-C3-C4	119.9(4)
C3-C4-H4A	109.5	C3-C4-H4B	109.5
H4A-C4-H4B	109.5	C3-C4-H4C	109.5
H4A-C4-H4C	109.5	H4B-C4-H4C	109.5
N1-C11-C15	131.3(4)	N1-C11-C12	121.3(4)
C15-C11-C12	107.2(4)	N1-C11-Fe1	130.5(3)
C15-C11-Fe1	69.2(3)	C12-C11-Fe1	69.5(3)
C13-C12-C11	107.5(4)	C13-C12-Fe1	69.1(3)
C11-C12-Fe1	69.6(3)	C13-C12-H12	126.2
C11-C12-H12	126.2	Fe1-C12-H12	126.6
C12-C13-C14	108.7(4)	C12-C13-Fe1	70.2(3)
C14-C13-Fe1	70.4(3)	C12-C13-H13	125.7
C14-C13-H13	125.7	Fe1-C13-H13	125.3
C15-C14-C13	107.5(4)	C15-C14-Fe1	69.4(3)
C13-C14-Fe1	68.9(3)	C15-C14-H14	126.2
C13-C14-H14	126.2	Fe1-C14-H14	127.1
C14-C15-C11	109.0(4)	C14-C15-Fe1	70.5(3)
C11-C15-Fe1	70.0(3)	C14-C15-H15	125.5
C11-C15-H15	125.5	Fe1-C15-H15	125.6
C20-C16-C17	107.7(4)	C20-C16-Fe1	69.7(3)
C17-C16-Fe1	69.6(3)	C20-C16-H16	126.1
C17-C16-H16	126.1	Fe1-C16-H16	126.1
C18-C17-C16	107.9(4)	C18-C17-Fe1	69.6(3)
C16-C17-Fe1	69.6(3)	C18-C17-H17	126.0
C16-C17-H17	126.0	Fe1-C17-H17	126.3
C17-C18-C19	108.9(4)	C17-C18-Fe1	70.2(3)
C19-C18-Fe1	69.7(3)	C17-C18-H18	125.6
C19-C18-H18	125.6	Fe1-C18-H18	126.1
C18-C19-C20	107.6(4)	C18-C19-Fe1	69.7(3)
C20-C19-Fe1	69.9(3)	C18-C19-H19	126.2
C20-C19-H19	126.2	Fe1-C19-H19	125.8
C16-C20-C19	108.0(4)	C16-C20-Fe1	69.7(3)
C19-C20-Fe1	69.3(3)	C16-C20-H20	126.0
C19-C20-H20	126.0	Fe1-C20-H20	126.6
N2-C21-C25	121.7(4)	N2-C21-C22	130.4(4)
C25-C21-C22	107.2(4)	N2-C21-Fe2	134.5(3)
C25-C21-Fe2	68.8(2)	C22-C21-Fe2	69.1(3)
C23-C22-C21	107.7(4)	C23-C22-Fe2	69.1(3)
C21-C22-Fe2	69.9(3)	C23-C22-H22	126.1

C21-C22-H22	126.1	Fe2-C22-H22	126.4
C22-C23-C24	108.7(4)	C22-C23-Fe2	70.5(3)
C24-C23-Fe2	69.8(3)	C22-C23-H23	125.6
C24-C23-H23	125.6	Fe2-C23-H23	125.6
C23-C24-C25	108.0(4)	C23-C24-Fe2	69.6(3)
C25-C24-Fe2	69.7(3)	C23-C24-H24	126.0
C25-C24-H24	126.0	Fe2-C24-H24	126.3
C24-C25-C21	108.4(4)	C24-C25-Fe2	69.6(3)
C21-C25-Fe2	70.6(2)	C24-C25-H25	125.8
C21-C25-H25	125.8	Fe2-C25-H25	125.5
C27-C26-C30	107.8(5)	C27-C26-Fe2	69.8(3)
C30-C26-Fe2	69.4(3)	C27-C26-H26	126.1
C30-C26-H26	126.1	Fe2-C26-H26	126.3
C26-C27-C28	107.7(5)	C26-C27-Fe2	70.1(3)
C28-C27-Fe2	68.7(3)	C26-C27-H27	126.1
C28-C27-H27	126.1	Fe2-C27-H27	126.6
C29-C28-C27	108.5(5)	C29-C28-Fe2	70.5(3)
C27-C28-Fe2	70.2(3)	C29-C28-H28	125.7
C27-C28-H28	125.7	Fe2-C28-H28	125.2
C28-C29-C30	108.2(5)	C28-C29-Fe2	69.7(3)
C30-C29-Fe2	69.8(3)	C28-C29-H29	125.9
C30-C29-H29	125.9	Fe2-C29-H29	126.2
C26-C30-C29	107.7(4)	C26-C30-Fe2	70.0(3)
C29-C30-Fe2	69.4(3)	C26-C30-H30	126.1
C29-C30-H30	126.1	Fe2-C30-H30	126.1
C36-C31-C32	124.5(4)	C36-C31-H31	117.8
C32-C31-H31	117.8	C31-C32-C33	117.6(4)
C31-C32-C1	121.5(4)	C33-C32-C1	120.9(4)
O1-C33-C34	120.1(4)	O1-C33-C32	120.9(4)
C34-C33-C32	119.0(4)	C33-C34-C35	122.0(4)
C33-C34-H34	119.0	C35-C34-H34	119.0
O2-C35-C34	119.2(4)	O2-C35-C36	120.9(4)
C34-C35-C36	120.0(4)	C31-C36-C35	116.9(4)
C31-C36-C3	121.7(4)	C35-C36-C3	121.4(4)

Table A53. Torsion angles ($^{\circ}$) for 4a.

C11-N1-C1-C32	-176.5(4)	C11-N1-C1-C2	2.2(7)
C21-N2-C3-C36	176.1(4)	C21-N2-C3-C4	-5.5(7)
C1-N1-C11-C15	32.2(7)	C1-N1-C11-C12	-154.0(4)
C1-N1-C11-Fe1	-65.1(6)	N1-C11-C12-C13	-175.4(4)
C15-C11-C12-C13	-0.2(5)	Fe1-C11-C12-C13	58.9(3)
N1-C11-C12-Fe1	125.7(4)	C15-C11-C12-Fe1	-59.1(3)
C11-C12-C13-C14	0.9(5)	Fe1-C12-C13-C14	60.1(3)
C11-C12-C13-Fe1	-59.2(3)	C12-C13-C14-C15	-1.3(5)
Fe1-C13-C14-C15	58.8(3)	C12-C13-C14-Fe1	-60.0(3)
C13-C14-C15-C11	1.2(5)	Fe1-C14-C15-C11	59.6(3)
C13-C14-C15-Fe1	-58.5(3)	N1-C11-C15-C14	173.9(4)
C12-C11-C15-C14	-0.6(5)	Fe1-C11-C15-C14	-60.0(3)
N1-C11-C15-Fe1	-126.1(5)	C12-C11-C15-Fe1	59.3(3)
C20-C16-C17-C18	0.3(6)	Fe1-C16-C17-C18	-59.3(3)
C20-C16-C17-Fe1	59.5(3)	C16-C17-C18-C19	0.1(5)
Fe1-C17-C18-C19	-59.2(3)	C16-C17-C18-Fe1	59.3(3)
C17-C18-C19-C20	-0.5(5)	Fe1-C18-C19-C20	-59.9(3)
C17-C18-C19-Fe1	59.5(3)	C17-C16-C20-C19	-0.6(5)
Fe1-C16-C20-C19	58.9(3)	C17-C16-C20-Fe1	-59.4(3)
C18-C19-C20-C16	0.6(5)	Fe1-C19-C20-C16	-59.1(3)
C18-C19-C20-Fe1	59.8(3)	C3-N2-C21-C25	158.1(4)
C3-N2-C21-C22	-32.9(8)	C3-N2-C21-Fe2	67.4(6)
N2-C21-C22-C23	-169.7(4)	C25-C21-C22-C23	0.5(5)
Fe2-C21-C22-C23	59.0(3)	N2-C21-C22-Fe2	131.3(5)
C25-C21-C22-Fe2	-58.5(3)	C21-C22-C23-C24	0.1(5)
Fe2-C22-C23-C24	59.6(3)	C21-C22-C23-Fe2	-59.5(3)
C22-C23-C24-C25	-0.7(5)	Fe2-C23-C24-C25	59.3(3)
C22-C23-C24-Fe2	-60.0(3)	C23-C24-C25-C21	1.0(5)
Fe2-C24-C25-C21	60.2(3)	C23-C24-C25-Fe2	-59.2(3)
N2-C21-C25-C24	170.3(4)	C22-C21-C25-C24	-0.9(5)
Fe2-C21-C25-C24	-59.6(3)	N2-C21-C25-Fe2	-130.1(4)
C22-C21-C25-Fe2	58.7(3)	C30-C26-C27-C28	0.6(6)
Fe2-C26-C27-C28	-58.6(4)	C30-C26-C27-Fe2	59.2(3)
C26-C27-C28-C29	-0.9(6)	Fe2-C27-C28-C29	-60.3(3)
C26-C27-C28-Fe2	59.5(4)	C27-C28-C29-C30	0.8(5)
Fe2-C28-C29-C30	-59.4(3)	C27-C28-C29-Fe2	60.2(3)
C27-C26-C30-C29	-0.1(6)	Fe2-C26-C30-C29	59.3(3)
C27-C26-C30-Fe2	-59.5(4)	C28-C29-C30-C26	-0.4(5)
Fe2-C29-C30-C26	-59.7(3)	C28-C29-C30-Fe2	59.3(3)
C36-C31-C32-C33	-1.5(6)	C36-C31-C32-C1	178.6(4)
N1-C1-C32-C31	176.9(4)	C2-C1-C32-C31	-1.7(6)
N1-C1-C32-C33	-2.9(6)	C2-C1-C32-C33	178.4(4)
C31-C32-C33-O1	-176.9(4)	C1-C32-C33-O1	3.0(6)
C31-C32-C33-C34	1.7(6)	C1-C32-C33-C34	-178.5(4)
O1-C33-C34-C35	176.4(4)	C32-C33-C34-C35	-2.2(7)

C33-C34-C35-O2	-178.4(4)	C33-C34-C35-C36	2.4(7)
C32-C31-C36-C35	1.7(6)	C32-C31-C36-C3	-179.5(4)
O2-C35-C36-C31	178.7(4)	C34-C35-C36-C31	-2.1(6)
O2-C35-C36-C3	-0.1(7)	C34-C35-C36-C3	179.1(4)
N2-C3-C36-C31	-177.8(4)	C4-C3-C36-C31	3.7(6)
N2-C3-C36-C35	1.0(6)	C4-C3-C36-C35	-177.6(4)

Table A54. Hydrogen bond distances (\AA) and angles ($^\circ$) for 4a.

	Donor-H	Acceptor-H	Donor-Acceptor	Angle
O1-H1…N1	0.86(2)	1.76(3)	2.521(5)	148.(5)
O2-H2…N2	0.88(2)	1.70(3)	2.507(5)	151.(6)

A34. Crystal data and structure refinement of 4b.

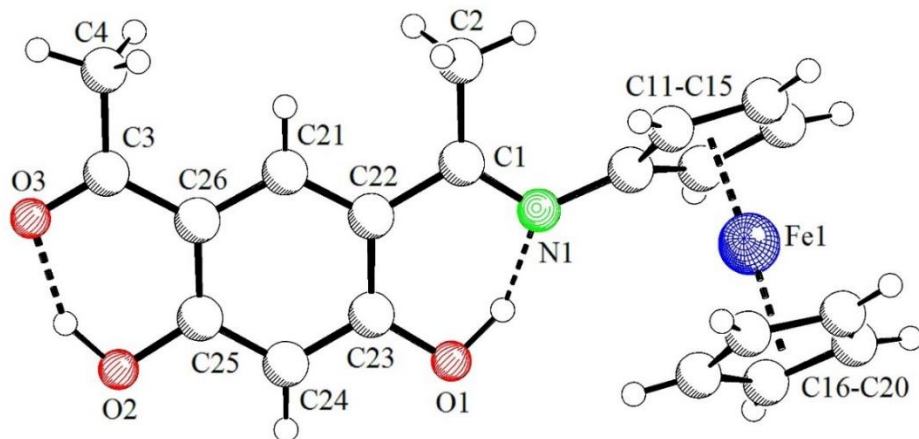


Figure S76. Compound 4b.

Table A55. Sample and crystal data for 4b.

Identification code	4b
Chemical formula	$\text{C}_{20}\text{H}_{19}\text{FeNO}_3$
Formula weight	377.21 g/mol
Temperature	173(2) K
Wavelength	0.71073 \AA
Crystal size	0.020 x 0.020 x 0.060 mm
Crystal habit	orange needle
Crystal system	triclinic
Space group	P -1
Unit cell dimensions	$a = 7.3038(4) \text{\AA}$ $a = 70.193(4)^\circ$ $b = 9.7641(8) \text{\AA}$ $b = 77.772(4)^\circ$ $c = 12.7298(10) \text{\AA}$ $g = 77.567(3)^\circ$
Volume	824.51(11) \AA^3

Z	2
Density (calculated)	1.519 g/cm ³
Absorption coefficient	0.934 mm ⁻¹
F(000)	392

Table A56 . Data collection and structure refinement for 4b.

Theta range for data collection	4.15 to 25.00°
Index ranges	-7<=h<=8, -11<=k<=10, -15<=l<=15
Reflections collected	3967
Independent reflections	2842 [R(int) = 0.0447]
Absorption correction	multi-scan
Max. and min. transmission	0.9820 and 0.9460
Structure solution technique	direct methods
Structure solution program	SHELXL-2014/7 (Sheldrick, 2014)
Refinement method	Full-matrix least-squares on F ²
Refinement program	SHELXL-2014/7 (Sheldrick, 2014)
Function minimized	S w(F _o ² - F _c ²) ²
Data / restraints / parameters	2842 / 197 / 282
Goodness-of-fit on F²	1.111
Final R indices	2393 data; I>2s(I) R1 = 0.0651, wR2 = 0.1306 all data R1 = 0.0823, wR2 = 0.1428
Weighting scheme	w=1/[s ² (F _o ²)+3.5808P]where P=(F _o ² +2F _c ²)/3
Largest diff. peak and hole	0.360 and -0.374 eÅ ⁻³
R.M.S. deviation from mean	0.088 eÅ ⁻³

Table A57. Bond lengths (Å) for 4b.

N1-C1	1.294(6)	N1-C11	1.419(6)
C2-C1	1.494(7)	C2-H2A	0.98
C2-H2B	0.98	C2-H2C	0.98
C1-C22	1.480(7)	C22-C21	1.383(7)
C22-C23	1.426(7)	C23-O1	1.325(6)
C23-C24	1.392(7)	C24-C25	1.388(7)
C24-H24	0.95	C25-O2	1.357(6)
C25-C26	1.421(7)	C26-C21	1.407(7)
C26-C3	1.461(7)	C21-H21	0.95
C3-O3	1.240(6)	C3-C4	1.498(7)
C4-H4A	0.98	C4-H4B	0.98
C4-H4C	0.98	O1-H1	1.02(8)
O2-H2	1.03(8)	C11-C12	1.419(7)
C11-C15	1.423(7)	C11-Fe1	2.045(5)
C12-C13	1.413(7)	C12-Fe1	2.037(5)
C12-H12	0.95	C13-C14	1.398(8)
C13-Fe1	2.041(5)	C13-H13	0.95
C14-C15	1.418(8)	C14-Fe1	2.028(5)
C14-H14	0.95	C15-Fe1	2.040(5)
C15-H15	0.95	Fe1-C16A	2.026(11)
Fe1-C19	2.033(10)	Fe1-C20A	2.034(12)
Fe1-C19A	2.035(12)	Fe1-C18	2.036(9)
Fe1-C20	2.041(10)	Fe1-C17	2.042(8)
Fe1-C16	2.044(9)	C16-C17	1.412(11)
C16-C20	1.417(12)	C16-H16	0.95
C17-C18	1.424(11)	C17-H17	0.95
C18-C19	1.416(12)	C18-H18	0.95
C19-C20	1.429(11)	C19-H19	0.95
C20-H20	0.95	C16A-C17A	1.408(13)
C16A-C20A	1.422(13)	C16A-H16A	0.95
C17A-C18A	1.414(13)	C17A-H17A	0.95
C18A-C19A	1.413(13)	C18A-H18A	0.95
C19A-C20A	1.430(13)	C19A-H19A	0.95
C20A-H20A	0.95		

Table A58. Bond angles ($^{\circ}$) for 4b.

C1-N1-C11	122.3(4)	C1-C2-H2A	109.5
C1-C2-H2B	109.5	H2A-C2-H2B	109.5
C1-C2-H2C	109.5	H2A-C2-H2C	109.5
H2B-C2-H2C	109.5	N1-C1-C22	116.3(4)
N1-C1-C2	123.9(5)	C22-C1-C2	119.8(4)
C21-C22-C23	118.8(4)	C21-C22-C1	120.6(4)
C23-C22-C1	120.5(4)	O1-C23-C24	118.2(5)
O1-C23-C22	122.1(5)	C24-C23-C22	119.8(5)
C25-C24-C23	120.4(5)	C25-C24-H24	119.8
C23-C24-H24	119.8	O2-C25-C24	118.2(5)
O2-C25-C26	120.5(5)	C24-C25-C26	121.3(5)
C21-C26-C25	117.1(4)	C21-C26-C3	122.3(5)
C25-C26-C3	120.5(4)	C22-C21-C26	122.6(4)
C22-C21-H21	118.7	C26-C21-H21	118.7
O3-C3-C26	120.3(5)	O3-C3-C4	119.4(5)
C26-C3-C4	120.2(4)	C3-C4-H4A	109.5
C3-C4-H4B	109.5	H4A-C4-H4B	109.5
C3-C4-H4C	109.5	H4A-C4-H4C	109.5
H4B-C4-H4C	109.5	C23-O1-H1	103.(4)
C25-O2-H2	105.(4)	C12-C11-N1	128.4(5)
C12-C11-C15	108.2(4)	N1-C11-C15	123.4(4)
C12-C11-Fe1	69.4(3)	N1-C11-Fe1	124.7(3)
C15-C11-Fe1	69.4(3)	C13-C12-C11	108.1(5)
C13-C12-Fe1	69.9(3)	C11-C12-Fe1	70.0(3)
C13-C12-H12	126.0	C11-C12-H12	126.0
Fe1-C12-H12	125.8	C14-C13-C12	107.7(5)
C14-C13-Fe1	69.4(3)	C12-C13-Fe1	69.6(3)
C14-C13-H13	126.2	C12-C13-H13	126.2
Fe1-C13-H13	126.4	C13-C14-C15	109.6(5)
C13-C14-Fe1	70.4(3)	C15-C14-Fe1	70.1(3)
C13-C14-H14	125.2	C15-C14-H14	125.2
Fe1-C14-H14	125.9	C14-C15-C11	106.6(5)
C14-C15-Fe1	69.2(3)	C11-C15-Fe1	69.8(3)
C14-C15-H15	126.7	C11-C15-H15	126.7
Fe1-C15-H15	125.9	C16A-Fe1-C14	145.6(6)
C14-Fe1-C19	128.4(5)	C16A-Fe1-C20A	41.0(4)
C14-Fe1-C20A	169.2(6)	C16A-Fe1-C19A	68.5(6)
C14-Fe1-C19A	128.3(6)	C20A-Fe1-C19A	41.2(4)
C14-Fe1-C18	111.2(4)	C19-Fe1-C18	40.7(4)
C16A-Fe1-C12	115.2(6)	C14-Fe1-C12	67.8(2)
C19-Fe1-C12	153.8(4)	C20A-Fe1-C12	119.6(6)
C19A-Fe1-C12	148.3(5)	C18-Fe1-C12	162.3(5)
C16A-Fe1-C15	172.8(5)	C14-Fe1-C15	40.8(2)
C19-Fe1-C15	108.8(5)	C20A-Fe1-C15	132.1(6)
C19A-Fe1-C15	104.9(6)	C18-Fe1-C15	123.0(5)

C12-Fe1-C15	68.7(2)	C16A-Fe1-C13	118.4(5)
C14-Fe1-C13	40.2(2)	C19-Fe1-C13	164.9(4)
C20A-Fe1-C13	150.5(6)	C19A-Fe1-C13	167.8(6)
C18-Fe1-C13	127.2(4)	C12-Fe1-C13	40.5(2)
C15-Fe1-C13	68.6(2)	C14-Fe1-C20	162.9(4)
C19-Fe1-C20	41.1(4)	C18-Fe1-C20	69.5(5)
C12-Fe1-C20	117.0(4)	C15-Fe1-C20	123.5(5)
C13-Fe1-C20	153.0(4)	C14-Fe1-C17	123.6(4)
C19-Fe1-C17	68.1(5)	C18-Fe1-C17	40.9(3)
C12-Fe1-C17	123.7(4)	C15-Fe1-C17	158.9(5)
C13-Fe1-C17	108.6(3)	C20-Fe1-C17	68.8(5)
C14-Fe1-C16	156.5(4)	C19-Fe1-C16	67.8(5)
C18-Fe1-C16	68.5(4)	C12-Fe1-C16	104.9(4)
C15-Fe1-C16	159.6(5)	C13-Fe1-C16	119.9(4)
C20-Fe1-C16	40.6(4)	C17-Fe1-C16	40.4(3)
C17-C16-C20	109.3(9)	C17-C16-Fe1	69.7(5)
C20-C16-Fe1	69.6(5)	C17-C16-H16	125.4
C20-C16-H16	125.4	Fe1-C16-H16	126.9
C16-C17-C18	108.1(8)	C16-C17-Fe1	69.9(5)
C18-C17-Fe1	69.3(5)	C16-C17-H17	125.9
C18-C17-H17	125.9	Fe1-C17-H17	126.4
C19-C18-C17	106.9(9)	C19-C18-Fe1	69.5(6)
C17-C18-Fe1	69.8(5)	C19-C18-H18	126.5
C17-C18-H18	126.5	Fe1-C18-H18	125.7
C18-C19-C20	109.5(10)	C18-C19-Fe1	69.7(6)
C20-C19-Fe1	69.8(6)	C18-C19-H19	125.3
C20-C19-H19	125.3	Fe1-C19-H19	126.8
C16-C20-C19	106.2(10)	C16-C20-Fe1	69.8(5)
C19-C20-Fe1	69.2(6)	C16-C20-H20	126.9
C19-C20-H20	126.9	Fe1-C20-H20	125.7
C17A-C16A-C20A	108.3(11)	C17A-C16A-Fe1	70.9(6)
C20A-C16A-Fe1	69.8(7)	C17A-C16A-H16A	125.8
C20A-C16A-H16A	125.8	Fe1-C16A-H16A	125.1
C16A-C17A-C18A	109.0(11)	C16A-C17A-Fe1	68.7(6)
C18A-C17A-Fe1	70.2(6)	C16A-C17A-H17A	125.5
C18A-C17A-H17A	125.5	Fe1-C17A-H17A	127.1
C19A-C18A-C17A	107.0(11)	C19A-C18A-Fe1	68.8(6)
C17A-C18A-Fe1	69.6(6)	C19A-C18A-H18A	126.5
C17A-C18A-H18A	126.5	Fe1-C18A-H18A	126.6
C18A-C19A-C20A	109.2(12)	C18A-C19A-Fe1	70.9(6)
C20A-C19A-Fe1	69.4(7)	C18A-C19A-H19A	125.4
C20A-C19A-H19A	125.4	Fe1-C19A-H19A	125.9
C16A-C20A-C19A	106.5(11)	C16A-C20A-Fe1	69.2(6)
C19A-C20A-Fe1	69.5(7)	C16A-C20A-H20A	126.7
C19A-C20A-H20A	126.7	Fe1-C20A-H20A	126.2

Table A59. Torsion angles ($^{\circ}$) for 4b.

C11-N1-C1-C22	-176.7(4)	C11-N1-C1-C2	3.4(7)
N1-C1-C22-C21	179.5(4)	C2-C1-C22-C21	-0.6(7)
N1-C1-C22-C23	1.7(7)	C2-C1-C22-C23	-178.3(4)
C21-C22-C23-O1	179.3(4)	C1-C22-C23-O1	-2.9(7)
C21-C22-C23-C24	0.2(7)	C1-C22-C23-C24	178.0(4)
O1-C23-C24-C25	-178.7(5)	C22-C23-C24-C25	0.4(7)
C23-C24-C25-O2	-179.9(4)	C23-C24-C25-C26	-0.9(8)
O2-C25-C26-C21	179.8(4)	C24-C25-C26-C21	0.8(7)
O2-C25-C26-C3	-0.8(7)	C24-C25-C26-C3	-179.8(5)
C23-C22-C21-C26	-0.3(7)	C1-C22-C21-C26	-178.1(4)
C25-C26-C21-C22	-0.2(7)	C3-C26-C21-C22	-179.6(4)
C21-C26-C3-O3	179.4(5)	C25-C26-C3-O3	0.1(7)
C21-C26-C3-C4	-0.5(7)	C25-C26-C3-C4	-179.9(5)
C1-N1-C11-C12	56.5(7)	C1-N1-C11-C15	-126.6(5)
C1-N1-C11-Fe1	146.6(4)	N1-C11-C12-C13	178.3(5)
C15-C11-C12-C13	1.0(6)	Fe1-C11-C12-C13	59.7(4)
N1-C11-C12-Fe1	118.5(5)	C15-C11-C12-Fe1	-58.7(3)
C11-C12-C13-C14	-0.6(6)	Fe1-C12-C13-C14	59.2(4)
C11-C12-C13-Fe1	-59.8(3)	C12-C13-C14-C15	0.0(6)
Fe1-C13-C14-C15	59.3(4)	C12-C13-C14-Fe1	-59.3(4)
C13-C14-C15-C11	0.6(6)	Fe1-C14-C15-C11	60.1(3)
C13-C14-C15-Fe1	-59.5(4)	C12-C11-C15-C14	-1.0(6)
N1-C11-C15-C14	-178.4(4)	Fe1-C11-C15-C14	-59.7(3)
C12-C11-C15-Fe1	58.7(3)	N1-C11-C15-Fe1	-118.7(5)
C20-C16-C17-C18	-0.5(12)	Fe1-C16-C17-C18	-59.0(7)
C20-C16-C17-Fe1	58.4(8)	C16-C17-C18-C19	-0.6(12)
Fe1-C17-C18-C19	-59.9(8)	C16-C17-C18-Fe1	59.3(7)
C17-C18-C19-C20	1.5(15)	Fe1-C18-C19-C20	-58.5(9)
C17-C18-C19-Fe1	60.1(8)	C17-C16-C20-C19	1.4(14)
Fe1-C16-C20-C19	60.0(9)	C17-C16-C20-Fe1	-58.5(7)
C18-C19-C20-C16	-1.8(15)	Fe1-C19-C20-C16	-60.4(8)
C18-C19-C20-Fe1	58.5(9)	C20A-C16A-C17A-C18A	1.2(16)
Fe1-C16A-C17A-C18A	-58.8(10)	C20A-C16A-C17A-Fe1	60.0(10)
C16A-C17A-C18A-C19A	-1.0(16)	Fe1-C17A-C18A-C19A	-58.9(10)
C16A-C17A-C18A-Fe1	57.9(9)	C17A-C18A-C19A-C20A	0.4(18)
Fe1-C18A-C19A-C20A	-59.0(11)	C17A-C18A-C19A-Fe1	59.4(10)
C17A-C16A-C20A-C19A	-1.0(17)	Fe1-C16A-C20A-C19A	59.7(11)
C17A-C16A-C20A-Fe1	-60.7(10)	C18A-C19A-C20A-C16A	0.4(19)
Fe1-C19A-C20A-C16A	-59.6(10)	C18A-C19A-C20A-Fe1	59.9(11)

Table A60. Hydrogen bond distances (\AA) and angles ($^\circ$) for 4b.

	Donor-H	Acceptor-H	Donor-Acceptor	Angle
C2-H2A…O2	0.98	2.64	3.486(7)	144.0
O1-H1…N1	1.02(8)	1.55(7)	2.502(5)	153.(7)
O2-H2…O3	1.03(8)	1.59(8)	2.535(6)	150.(7)